Morven North Offshore Wind Array Project

Environmental Impact Assessment Report

Volume 3, Annex 7.1: Physical Processes Shared Technical Report

MVCNS-J1201-RPS-10036
May 2026

B01

Document status

Version	Purpose of document	Authored by	Checker	Approved by	Date
FINAL	Application	TTRPSEL	TTRPSEL	MvOWL	May 2026

Prepared by:	Prepared for:
TTRPSEL	**Morven Offshore Wind Limited**

Table of contents

List of tables

List of figures

1 Introduction

1.1.1.1 The Morven North Offshore Wind Array Project (hereafter “Morven North”) and the Morven South Offshore Wind Array Project (hereafter “Morven South”) are both located within the Morven Option Lease Agreement Site (hereafter “Morven Site”) in Scottish offshore waters (Figure 1.1). Morven North is located approximately 61km from the Aberdeenshire coast (at its closest point) and Morven South is located approximately 86km from the Aberdeenshire coast (at its closest point). Each project will comprise wind turbines, Offshore Substation Platforms (OSPs), associated foundations, inter-array and interconnector cables and cable protection. Consent for the offshore export cables of Morven North and Morven South will be sought separately.

1.1.1.2 As shown in Figure 1.1, Morven North is situated northwest of Morven South. The external boundaries of the projects correspond with the boundaries of the Morven Site.

1.1.1.3 This Physical Processes Shared Technical Report presents baseline characterisation of physical processes, potential environmental changes due to the presence of infrastructure and potential changes during construction for both Morven North and Morven South.

1.1.1.4 Consent for Morven North and Morven South will be sought separately, aided by the development of a separate Environmental Impact Assessment (EIA) and Habitats Regulations Appraisal (HRA) for each project. To enable the assessment of cumulative effects, modelling has been undertaken for Morven North and Morven South (as separate projects) but also for the Morven Site (both projects). The modelling outcomes for both Morven North and Morven South are therefore reported in this Physical Processes Shared Technical Report.

1.1.1.5 The information from this Physical Processes Shared Technical Report provides the physical processes modelling to inform the assessment of the likely significant effects of Morven North and Morven South on physical processes receptors. This report accompanies the Environmental Impact Assessment (EIA) provided in Volume 2, Chapter 7: Physical Processes of the respective EIA Reports for Morven North and Morven South to support the respective consent applications.

1.1.1.6 The aim of this Physical Processes Shared Technical Report is to:

- characterise the physical processes baseline environment relating to hydrography and sedimentology within and surrounding Morven North and Morven South;
- identify environmental variations to the baseline arising from the presence of Morven North, Morven South and also with the combined presence of Morven North and Morven South;
- identify environmental variations during construction due to Morven North and Morven South.

1.1.1.7 The physical processes modelling presented in this technical report relates to the Morven North Boundary and Morven South Boundary, as described in Volume 1, Chapter 3: Project Description, of the Morven North Environmental Impact Assessment (EIA) Report and Morven South EIA Report respectively.

1.1.1.8 For the purposes of this Physical Processes Technical Report physical processes are defined as encompassing the following elements:

- bathymetry;
- tidal elevations and currents;
- waves;
- water column processes;
- seabed substrate and geology;
- sediment transport;
- suspended sediments.

1.1.1.9 Throughout the remainder of this technical report, the elements listed above are collectively referred to as “physical processes”.

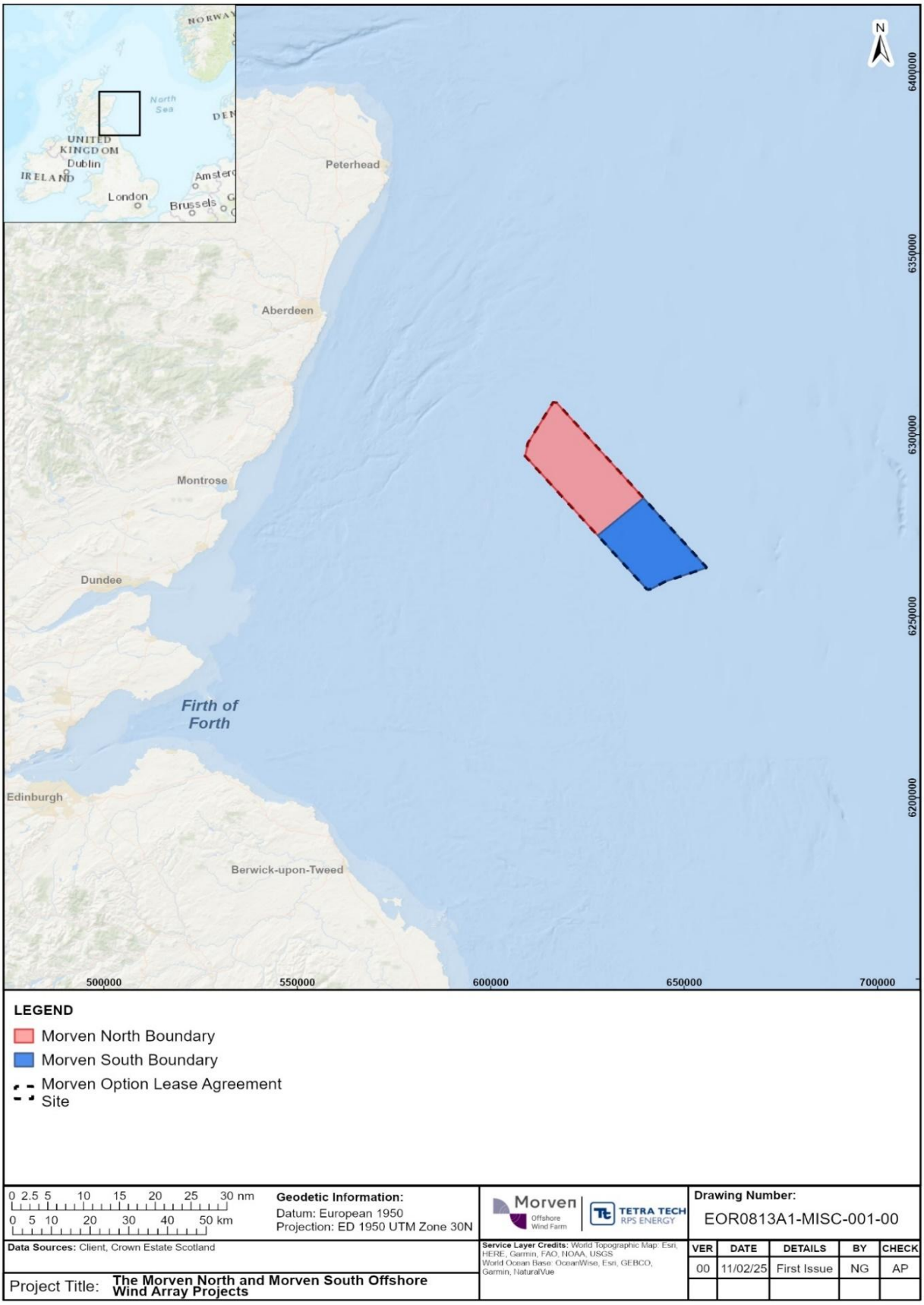

Figure 1.1: The boundaries of Morven North and Morven South within the Morven Option Lease Agreement Site

2 Study areas

2.1.1.1 Three study areas have been defined for physical processes for the purpose of this technical report:

- The Morven North Physical Processes Study Area;
- The Morven South Physical Processes Study Area;
- The Morven North and Morven South Regional Physical Processes Study Area (hereafter the "Regional Physical Processes Study Area").

2.1.1.2 The study areas specified for physical processes are shown in Figure 2.1 and defined as follows:

- The Morven North Physical Processes Study Area includes the Morven North Boundary, plus one spring tidal excursion from the Morven North Boundary;
- The Morven South Physical Processes Study Area includes the Morven South Boundary, plus one spring tidal excursion from the Morven South Boundary;
- The Regional Physical Processes Study Area includes the Morven North Boundary and Morven South Boundary, plus one spring tidal excursion from the Morven North Boundary and Morven South Boundary.

2.1.1.3 One spring tidal excursion of between circa 5km and 14km from the Morven North Boundary and Morven South Boundary was identified through interim numerical modelling techniques and is defined as the distance that suspended sediment is transported due to tidal currents before being carried back on the returning tide.

2.1.1.4 The Physical Processes Study Areas encompass the entire water column, including the seabed that may be influenced by changes to physical processes due to Morven North, Morven South or Morven North and Morven South together. It is however noted that although the Physical Processes Study Areas form the focus for the assessment, the numerical model domain for all three study areas is not limited to this region. The modelling study would therefore also identify potential impacts beyond the Physical Processes Study Areas. The modelling domain includes all banks within the Firth of Forth Bank Complex Marine Protected Area (MPA), which is located to the east of the Morven North Boundary and Morven South Boundary and is within the Morven North Physical Processes Study Area, as shown in Figure 2.1.

2.1.1.5 The study areas for physical processes for the Morven Option Lease Agreement Site (hereafter, "Morven Site") were presented to and agreed during the scoping process for the Morven Option Lease Agreement Site. The underlying principles used to define the study area(s) for Morven North and Morven South have not changed, other than the limits have been applied relative to each project, rather than the Morven Site. The study areas for Morven North and Morven South for physical processes were presented to the Marine Directorate Licencing Operations Team (MD-LOT) via a "Targeted Consultation Exercise" undertaken in Quarter 1 2025.

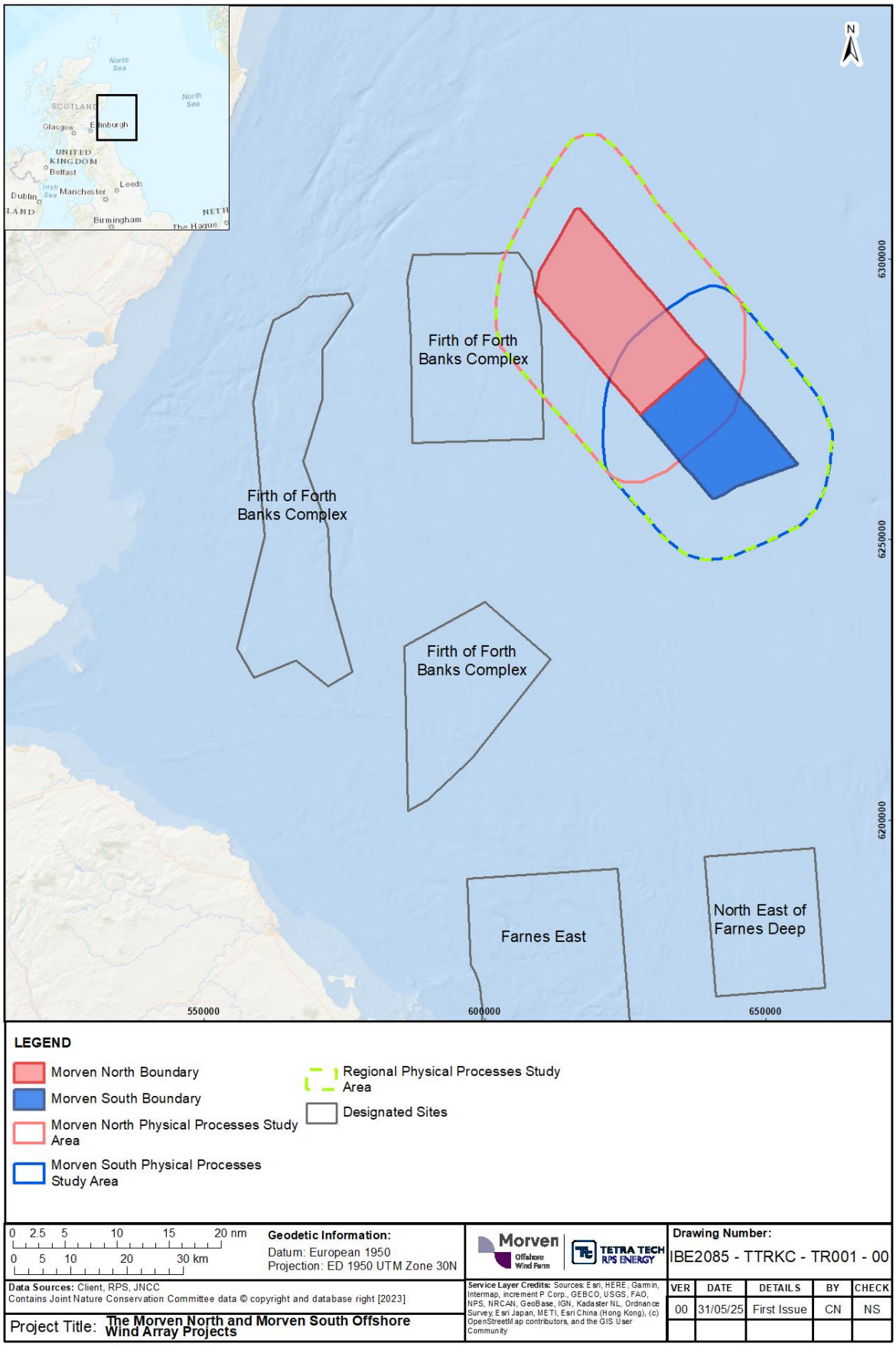

Figure 2.1: Physical Processes Study Areas for Morven North and Morven South Offshore Wind Array Projects

3 Methodology

3.1 Numerical modelling

3.1.1.1 Numerical modelling techniques were used to describe tide, wave and sediment transport regimes. The MIKE suite of software was employed, as a single model mesh could be used to simulate these processes both individually and when considered together. The extents of the model domain are shown in Figure 3.1.

3.1.1.2 The MIKE suite of models is a widely used industry standard modelling suite developed by the Danish Hydraulic Institute (DHI). It has been approved for use by industry and government bodies including the Scottish Environmental Protection Agency (SEPA). The MIKE suite is a modular system that contains a number of different but complementary modules encompassing different physical processes: these are summarised in Table 3.1 and described in further detail within the relevant sections of this report.

3.1.1.3 Following the establishment of baseline conditions, a number of scenarios were modelled to determine the environmental variations arising from the construction and presence of Morven North, Morven South and with Morven North and Morven South considered together. These are outlined in Table 3.2 and are based on the maximum design scenario (MDS) for physical processes, as further detailed in Volume 1, Chapter 7: Physical Processes, of the Morven North and Morven South EIA Reports.

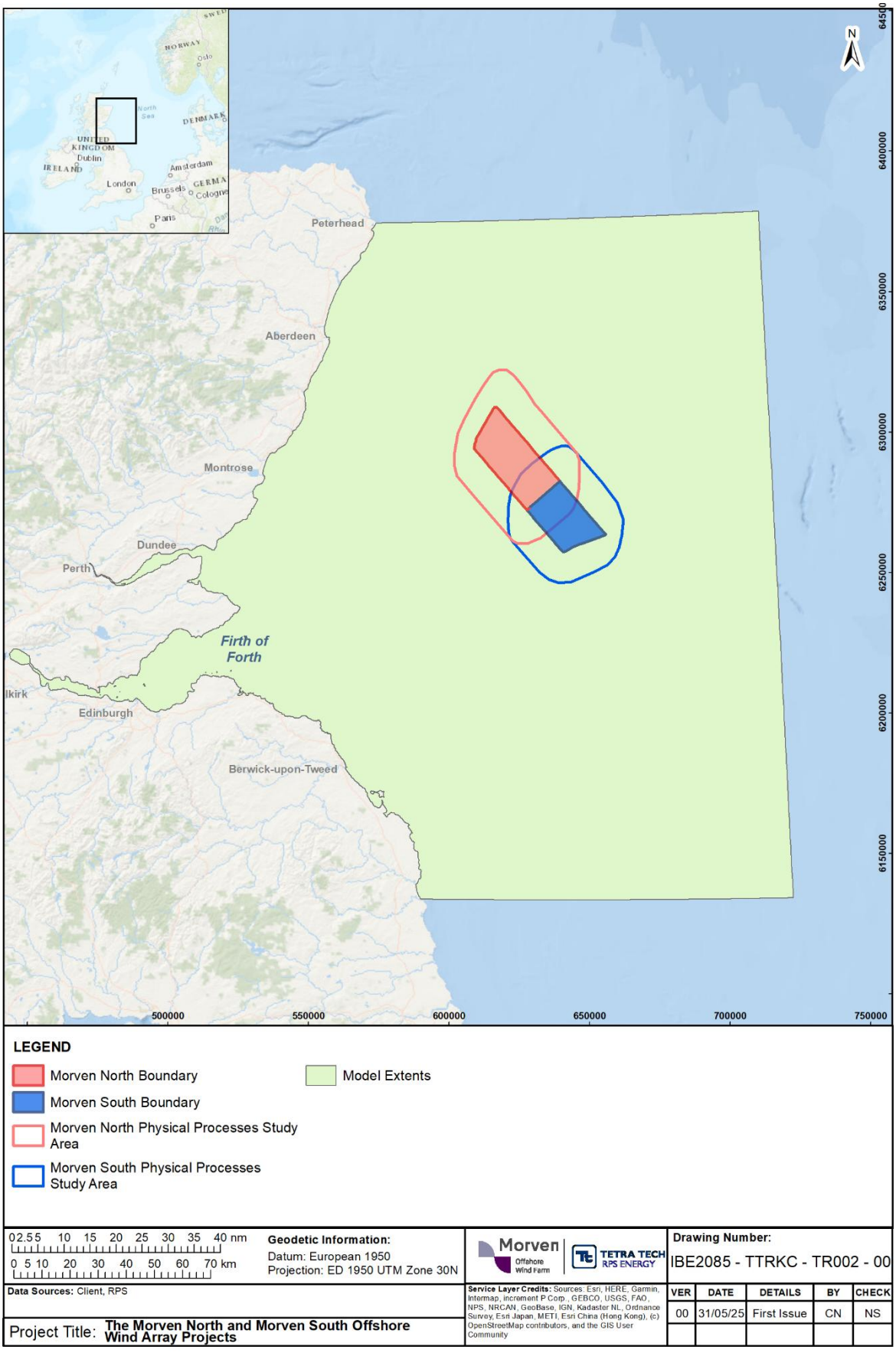

Figure 3.1: Extent of model domain for Morven North and Morven South physical processes modelling

Table 3.1: Mike suite of models relevant to Morven North and Morven South physical processes modelling

Simulation	Model	Description
Baseline and post-construction tidal flow	MIKE21 Flow Model (FM) modelling system	The FM Module is a flexible mesh, 2-dimensional, depth averaged hydrodynamic model which simulates the water level variations and flows in response to a variety of forcing functions in lakes, estuaries and coastal areas. The water levels and flows are resolved on a mesh when provided with bathymetry, bed resistance coefficient, wind field, hydrodynamic boundary conditions, etc.
Baseline and post-construction wave climate	MIKE21 Spectral Wave (SW)	The wave modelling was undertaken using the spectral wave model, MIKE21 SW. The waves were computed on the same grid as the tidal flows. The model resolves the wave field by simulating wind generation of waves within the model domain and the propagation of externally generated swell waves through the domain. The model setup ensured that the detail of both locally generated wind waves and swell conditions from further afield were captured.
Baseline and post-construction littoral currents	MIKE21 FM and SW	The MIKE suite facilitates the coupling of models. The depth averaged hydrodynamic model, used for the tidal modelling, coupled with the spectral wave model, provides a full wave climate incorporating the impact of water levels and currents on waves and wave breaking. Using this, the littoral currents (i.e. those currents driven by tidal, wave and meteorological forces) were examined.
Post-construction water column processes	MIKE 3 FM	The MIKE 3 Flow Model is a 3-dimensional flexible mesh modelling system, which incorporates an unstructured mesh in the horizontal domain, with a structured mesh in the vertical domain. This facilitated the analysis of temperature and salinity variation through the water column, to support the assessment of the impact to seasonal stratification.
Baseline and post-construction sediment transport	MIKE21 Sand Transport (ST)	This module enables assessment of bed sediment transport rates and initial rates of bed level change for non-cohesive sediment resulting from currents or combined wave current flows. Sediment transport was facilitated over the model domain and allowed the sediment transport pattern within the Physical Processes Study Areas to be determined. The model combines inputs from both the hydrodynamic model and, if required, the wave propagation model. It uses sediment size and gradation to determine the bed level changes and sediment transport rates.
Sandwave clearance, foundation installation and cable installation	MIKE21 Mud Transport (MT)	The MIKE MT module allows the modelling of erosion, transport and deposition of both cohesive and non-cohesive/granular sediments, (i.e. is not limited to mud transport). This model is suited to sediment releases in the water column and allows sediment sources which may vary spatially and temporally. A sample of representative locations were selected for each relevant construction activity to cover the range of conditions across the Morven North Boundary and Morven South Boundary, both in terms of water depth and tidal currents.

Table 3.2: Summary of modelled environmental variation scenarios for Morven North and Morven South

Variation/Activity	Description	Parameter modelled
Hydrography Section 5.2	Models configured to take account of the presence of Morven North, Morven South or Morven North and Morven South together to quantify: • changes to tidal currents; • changes to wave climate; • changes to littoral currents; • changes to water column processes. Monopile and gravity base foundations accounted for as 'pier' structures within the modelling, with scour and cable protection represented within the post-construction model mesh. Note potential changes to water column processes as a result of cable protection or cable crossings have not been accounted for in the model due to the water depth within the Morven North Boundary and Morven South Boundary which deemed this infrastructure as having no potential impact on seasonal stratification.	Morven North: • 96 wind turbine monopile installations represented by pier structures 15m in diameter and scour protection 2.5m in height and 67.5m in diameter. • Four High Voltage Alternating Current (HVAC) collector Offshore Substation Platforms (OSPs) with gravity base foundations represented by pier structures of varying diameter between 17m and 67m and scour protection 4m in height and 227m in diameter. • One bridge-linked HVDC (High Voltage Direct Current) converter OSP with gravity base foundations, each represented by six pier structures of 45m x 45m to account for the overall 180m x 240m dimensions at the surface and 195m x 255m at the bed of each foundation. Scour protection of 4m in height included for each HVDC installation, with a width of 245m and length of 30m. Note, there will be a maximum of one bridge-linked HVDC converter OSP within the Morven Site, however the modelling has incorporated one HVDC OSP within both the Morven North Boundary and Morven South Boundary, in order to provide a representation of potential impact due to each separate project. • Cable protection to a height of 3m and width of 10m along 42.4km and 48.4km of the inter-array cables and interconnector cables respectively, in addition to five inter-array cable crossings and five interconnector cable crossings with a height of 4m, width of 36m and length of 80m. Morven South: • 95 wind turbine monopile installations represented by pier structures 15m in diameter and

Variation/Activity	Description	Parameter modelled
		scour protection 2.5m in height and 67.5m in diameter. • Four HVAC collector OSPs with gravity base foundations represented by pier structures of varying diameter between 17m and 67m and scour protection 4m in height and 227m in diameter. • One bridge-linked HVDC converter OSP with gravity base foundations, each represented by six pier structures of 45m x 45m to account for the overall 180m x 240m dimensions at the surface and 195m x 255m at the bed of each foundation. Scour protection of 4m in height included for each HVDC installation, with a width of 245m and length of 305m. Note, there will be a maximum of one bridge-linked HVDC converter OSP within the Morven Site, however the modelling has incorporated one HVDC OSP within both the Morven North Boundary and Morven South Boundary, in order to provide a representation of potential impact due to each separate project. • Cable protection to a height of 3m and width of 10m along 42.0km and 26.4km of the inter-array and interconnector cables respectively, in addition to five inter-array cable crossings and five interconnector cable crossings with a height of 4m, width of 36m and length of 80m.
Sedimentology Section 5.3	Models configured to take account of the presence of Morven North, Morven South or Morven North and Morven South together to quantify: • changes to sediment transport characteristics.	As above.
Seabed features clearance for foundations Section 6.2.2	Sample dredging operation: • dredging and disposal is undertaken in a cycle along sample routes.	Sample sandwave clearance operation modelled for the bridge-linked HVDC OSPs within both the Morven North Boundary and Morven South Boundary. Sample clearance is undertaken to an average depth of 3m in a north south orientation with a dredging rate of 20,000m^3/h with a spill of 3% and material

Variation/Activity	Description	Parameter modelled
		released through the water column, prior to being dumped at the northerly or southerly ends of the clearance area.
Seabed features clearance for cables Section 6.2.3	Sample dredging operation: • dredging is undertaken in a cycle along sample routes.	Sample sandwave clearance operations modelled for two representative interconnector cables within both the Morven North Boundary and Morven South Boundary. Sample clearance is undertaken to an average depth of 3m in various orientations with a dredging rate of 20,000m^3/h and material released through the water column. 100% of material is considered to be disturbed within the 20m wide clearance corridors during the dredging process, with no specific dumping process for this activity incorporated into the modelling.
Augured pile installation Section 6.3.1	Three sample locations are presented with the Morven North Boundary and the Morven South Boundary: • piles are 16m in diameter to be drilled to a maximum depth of 64m. • three adjacent operations occurring simultaneously.	Sample augured pile installation for three wind turbine monopile locations, with drilling undertaken at 1.5m/h over a 43 hour period. 14,358m^3 of material is mobilised per pile which is released through the water column.
Inter-array cabling Section 6.3.2	Trenching is undertaken along two sample inter-array cable routes within the Morven North Boundary and two sample interconnector cable routes within the Morven South Boundary. Each sample route is circa 5km, with a burial depth of 3m and trench width of 3m.	• Dredge trenching is undertaken at 200m/h; • the routes are trenched over a period of 15 hours; • circa 21,885m^3 material is released through the water column.

3.2 Data sources

3.2.1.1 Information on the physical environment within the Physical Processes Study Areas and beyond to the extent of the model domain was collected through a detailed desktop review of existing studies and datasets. These are summarised in Table 3.3.

Table 3.3: Summary of key data sources for Morven North and Morven South

Title	Source	Year	Author
European Centre for Medium-range Weather Forecast (ECMWF) European Wave Model	ECMWF – Wave Data	2025	ECMWF

Title	Source	Year	Author
United Kingdom Hydrographic Office (UKHO) - Published Charts and Tide tables	Charts 1409 0:200000 and 273 0:200000 incorporating tidal diamonds with current stream data	2024	UKHO
Joint Nature Conservation Committee (JNCC) Marine Protected Area (MPA) Mapper	JNCC MPA	2023	JNCC
Scottish Shelf Model 3.02 – 27 Year Reanalysis. Scottish Shelf Waters Reanalysis Service (SSW-RS)	Marine Scotland	2022	Barton *et al*.
European Marine Observation and Data Network (EMODnet) seafloor geomorphology	EMODnet – Seafloor geomorphology	2021	EMODnet
Atlas of United Kingdom (UK) Marine Renewable Energy Resources • Annual mean significant wave height (m) • Annual mean wave power (kW/m) • Mean spring tidal range (m)	Atlas of UK Marine Renewable Energy Resources	2017	ABP Marine Environmental Research (ABPmer),
British Geographical Survey (BGS) Seabed Geology Layers	Marine Scotland	2017	BGS
European Marine Observation and Data Network (EMODnet) seabed substrate map (250 k scale)	EMODnet – Seabed Substrate	2016	EMODnet
Monthly average non-algal Suspended Particulate Matter (SPM) concentrations on the UK shelf waters	Cefas Climatology Data	2016	Cefas
Suspended Sediment Climatologies around the UK	Cefas Climatology Report	2016	Cefas
Marine Environmental Data Information Network (MEDIN) including Admiralty Marine Data Portal	Admiralty Marine Data Portal - bathymetry data	2003-2009	MEDIN

3.3 Site specific surveys

3.3.1.1 A summary of the pre-construction site investigation surveys undertaken of relevance to physical processes and utilised within the modelling study is outlined in Table 3.4.

Table 3.4: Summary of surveys undertaken to inform physical processes relating to Morven North and Morven South

Title	Extent of survey	Overview of survey	Survey contractor	Date	Reference to further information
Geophysical survey	Morven North Boundary and Morven South Boundary	Geophysical survey to establish bathymetry, seabed geology, morphology and sediments	Gardline and XOcean	April – August 2022	Gardline, 2022
Metocean survey	Morven North Boundary and Morven South Boundary	Metocean survey to establish wave and current data at a location within the Morven North Boundary and a location within the Morven South Boundary (Figure 4.7). Three metocean devices were deployed in the vicinity of each survey area, consisting of a light detection and ranging (LiDAR) buoy, wavebuoy and subsea mooring.	Partrac	October 2022 – April 2024	Partrac, 2024
Benthic subtidal survey	Morven North Boundary and Morven South Boundary	Seabed imagery and grab sampling with particle size analysis	Gardline	April – August 2022	Gardline, 2023

4 Baseline characterisation

4.1.1.1 This section outlines the numerical modelling undertaken in order to determine the baseline conditions. It describes the physical processes in terms of sea state and sediment transport regimes.

4.2 Bathymetry

4.2.1.1 Geophysical data collected in 2022 indicates that the water depth across the Morven North Boundary ranges between 64[1]m to 75m, relative to Lowest Astronomical Tide (LAT), with depths ranging from 64m to 76m across the Morven South Boundary, as shown in Figure 4.1. A maximum depth of 75m was recorded close to the southwestern edge of the Morven North Boundary, with the shallowest depths located towards the centre in a region of megaripples.

4.2.1.2 Within the Morven South Boundary, a maximum depth of 76m was recorded at the southeastern edge, with the shallowest areas located in the centre. There were gentle undulations in the seabed, with a general gradient of <1° throughout the Morven North Boundary and Morven South Boundary. A sandbank crossed the southeastern part of the Morven South Boundary, measuring 4m high and approximately 4km at its widest point.

4.2.1.3 Further shoals, influenced by seabed currents, were present across the Morven North Boundary and Morven South Boundary, most dominant within the Morven North Boundary. These typically had gradients of <1° and are thought to be both accumulations of surficial sediments and associated with the underlying geology. One discrete feature within the Morven South Boundary rises 2m above the seabed, with gradients up to 8° on its flanks. The seabed across much of the Morven North Boundary was dominated by megaripples, extending within the Morven South Boundary to a lesser extent and with less definition. The megaripples were typically 0.5m above the seabed and had wavelengths of 15m to 50m, generally orientated from west to east. Figure 4.2 shows a sample area of well-defined megaripples within the Morven North Boundary.

4.2.1.4 The model domain had full bathymetric coverage and was populated using a combination of data sources. The site specific geophysical survey undertaken in 2022 and the resulting bathymetry data was used to construct the model mesh. The survey data provided to LAT vertical datum was converted to model Mean Sea Level (MSL) datum using reference values published by Admiralty. Where additional data was required for the model domain beyond the survey area, bathymetry data was sourced from the MEDIN portal as illustrated in Figure 4.3. Data was extracted to MSL datum at the finest resolution available in the vicinity of the Regional Physical Processes Study Area, with resolution decreasing toward the outer model boundaries and with distance from the Regional Physical Processes Study Area.

[1] Following review of bathymetric data, 64m LAT has been taken as the shallowest point within the Morven North Boundary for physical processes throughout this chapter, which is the shallowest point reflecting seabed substrate. Note this differs from the shallowest point stated within other chapters of the EIA, due to the presence of a shipwreck, which raises the seabed level further and is of relevance to other topics.

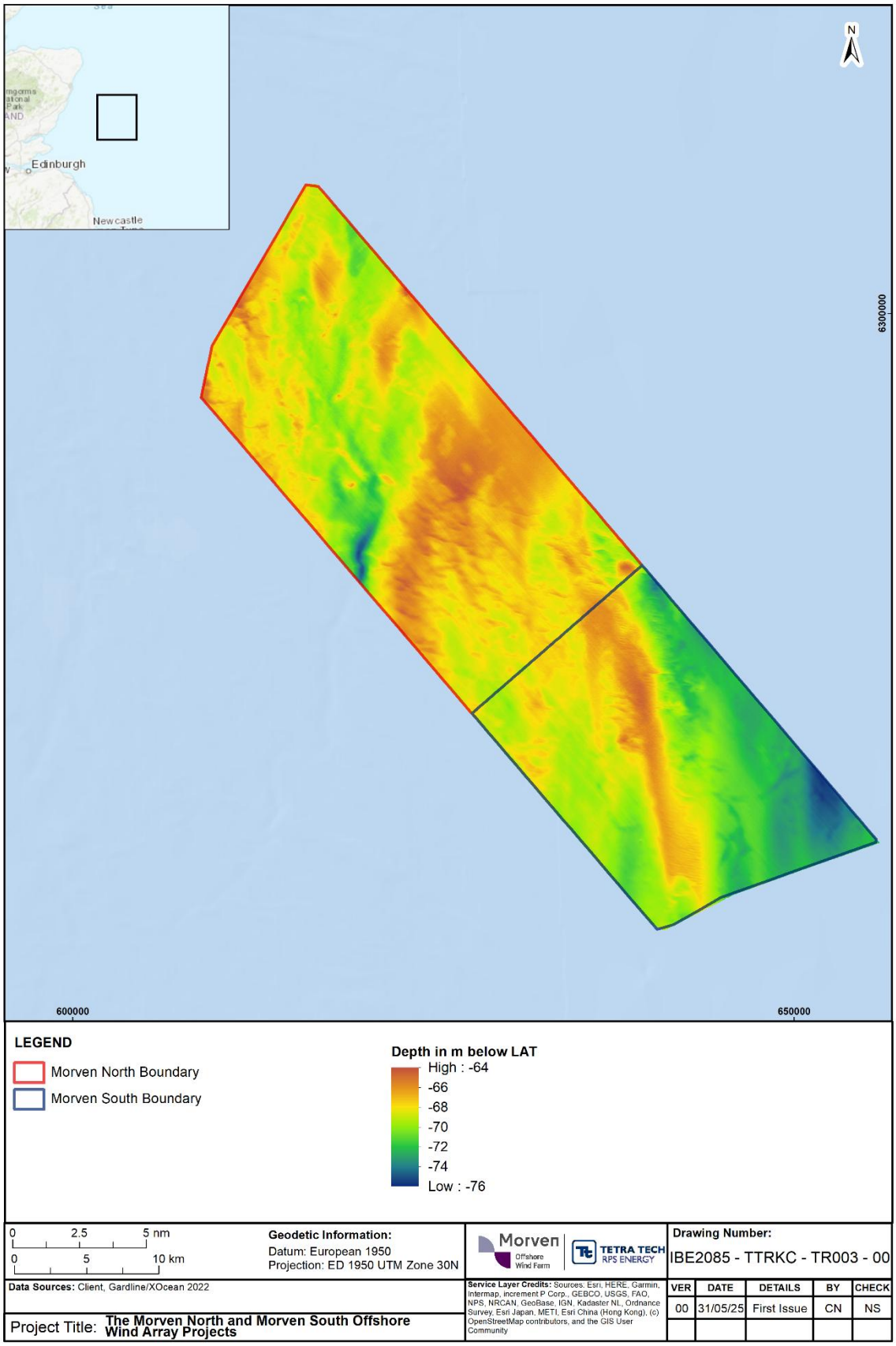

Figure 4.1: Bathymetric data as captured by site specific survey for Morven North and Morven South (Gardline/XOcean, 2022)

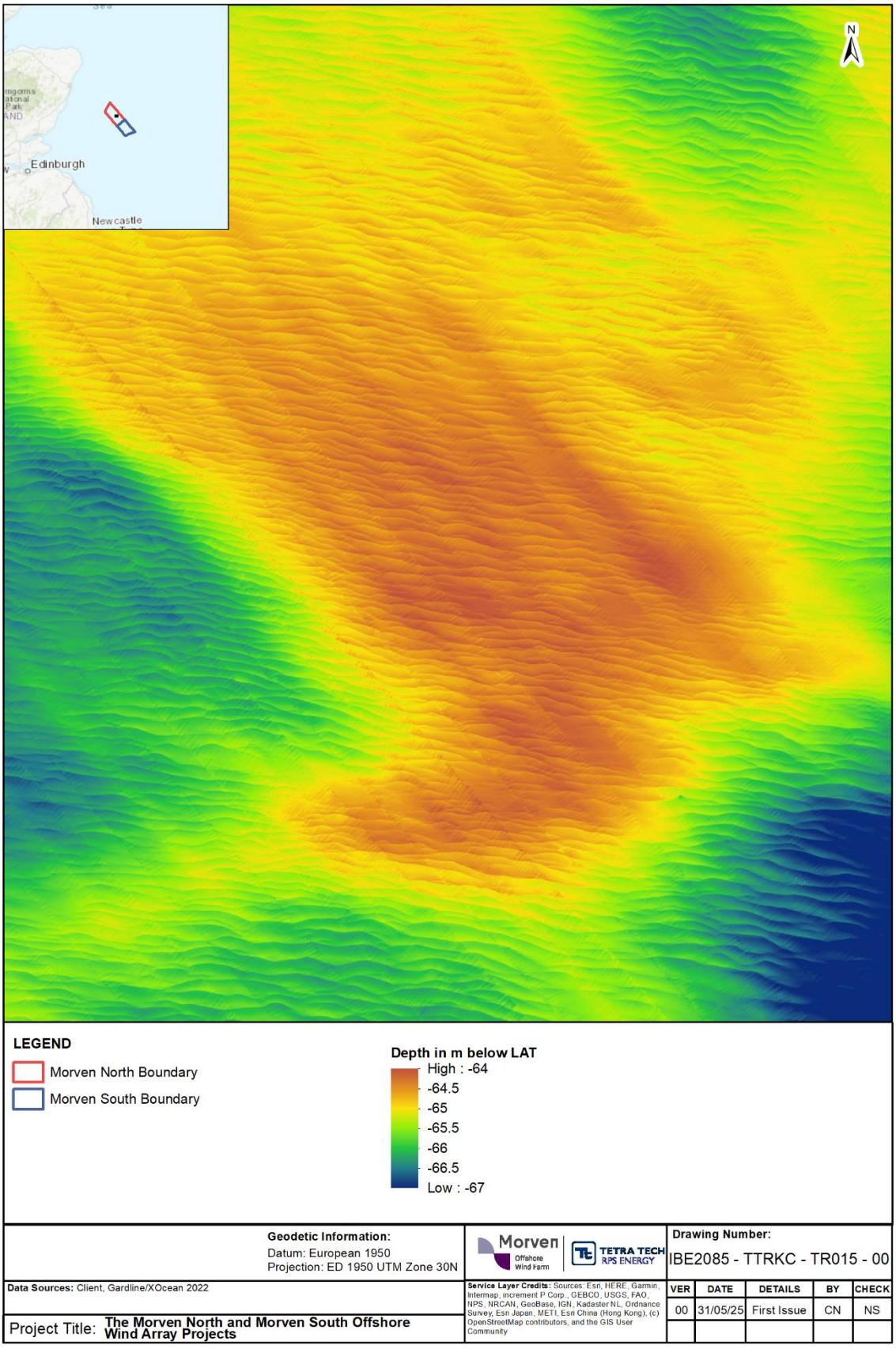

Figure 4.2: Bathymetric data from site specific survey showing areas of megaripples within the Morven North Boundary (Gardline/XOcean 2022)

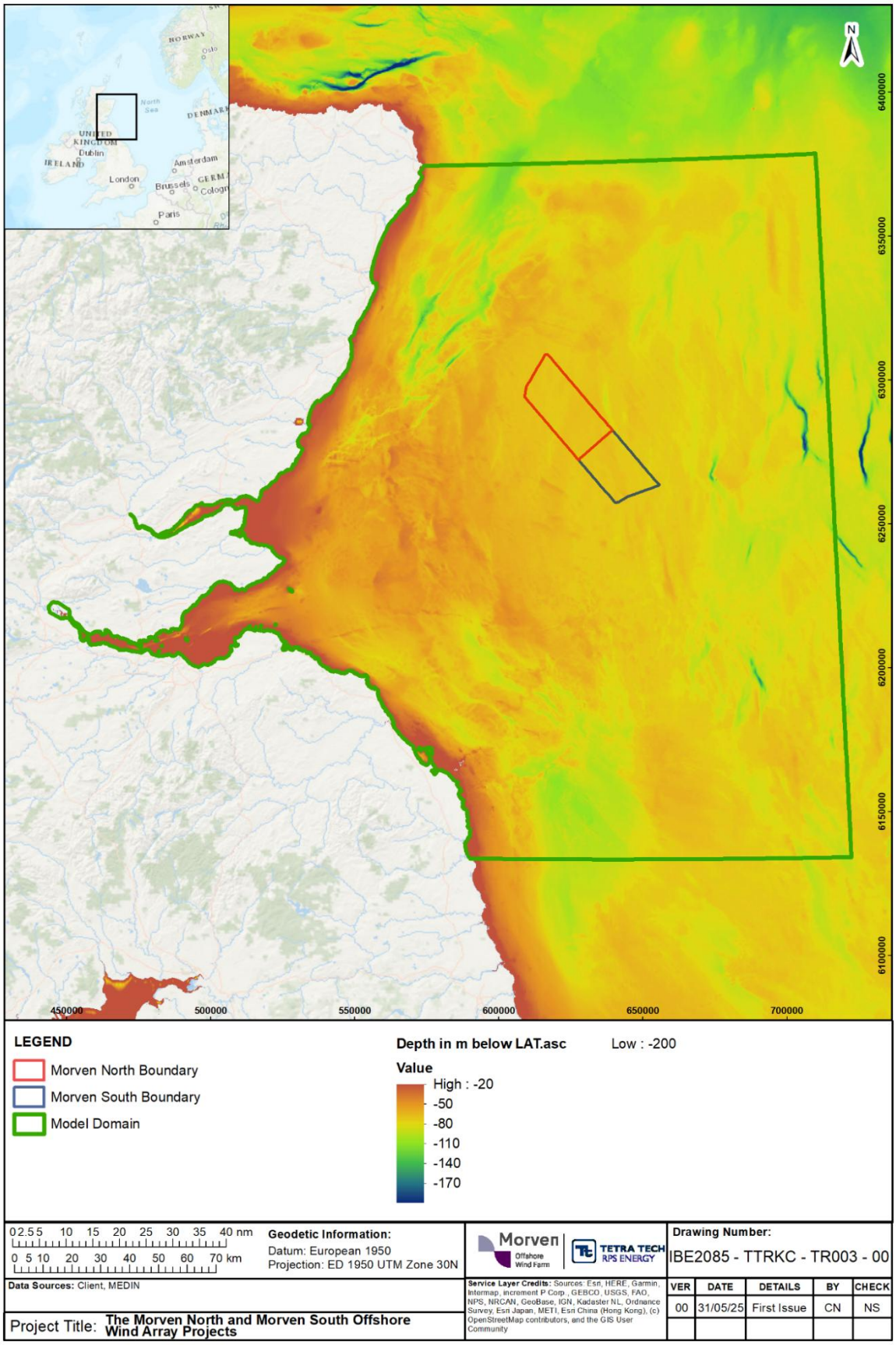

Figure 4.3: Bathymetric data from Marine Environmental Data Information Network Portal within the Morven physical processes model domain

4.2.1.5 The resolution of the model bathymetry was designed to reflect variations in water depth and bed forms for the accurate simulation of tidal currents, as shown in Figure 4.4. Additional model resolution was also included to incorporate the presence of Morven North and Morven South. This enabled the same cell arrangement to be used for the baseline and post-construction assessment, thereby avoiding the introduction of any numerical mesh effects into the assessment. Note an arbitrary but representative layout was selected to define the presence and quantity of scour and cable protection within the Morven North Boundary and Morven South Boundary, as defined by the MDS for the impacts related to the presence of the infrastructure, as presented within the physical processes Chapters (Volume 2, Chapter 7: Physical Processes, of the Morven North and Morven South EIA Reports).

4.2.1.6 Across the Morven North Boundary and Morven South Boundary, the mesh resolution varied between circa 60m down to 6m in order that the influence of scour and cable protection on the tidal flow and sediment transport for Morven North and Morven South could be quantified. With increasing distance from the Regional Physical Processes Study Area, the cell size was increased but maintained at a level which retained model accuracy. Figure 4.5 illustrates the mesh resolution with an inset of the mesh within the Morven North Boundary. The triangular mesh is represented by the black mesh structure within this figure, where the higher resolution meshing can be seen as darker clusters in the vicinity of the Morven North Boundary and Morven South Boundary and around the individual foundations, cable protection and cable crossings. Figure 4.6 shows an example of the mesh structure surrounding one wind turbine monopile foundation within the Morven North Boundary.

4.2.1.7 The extent of the domain was designed to provide the basis for a model which could be utilised for tide, wave and sediment transport modelling. The focus of the study is one tidal excursion from Morven North and Morven South to quantify any changes due to the infrastructure however a larger domain is required to develop wave fields and ensure that tidal currents are simulated. The model extends north, south and offshore beyond the adjacent banks to ensure that any influence on the Firth of Forth Banks Complex MPA is included in the detailed model. Throughout this report, for reference, the Firth of Forth Banks Complex MPA is represented by a grey outline within the appropriate figures.

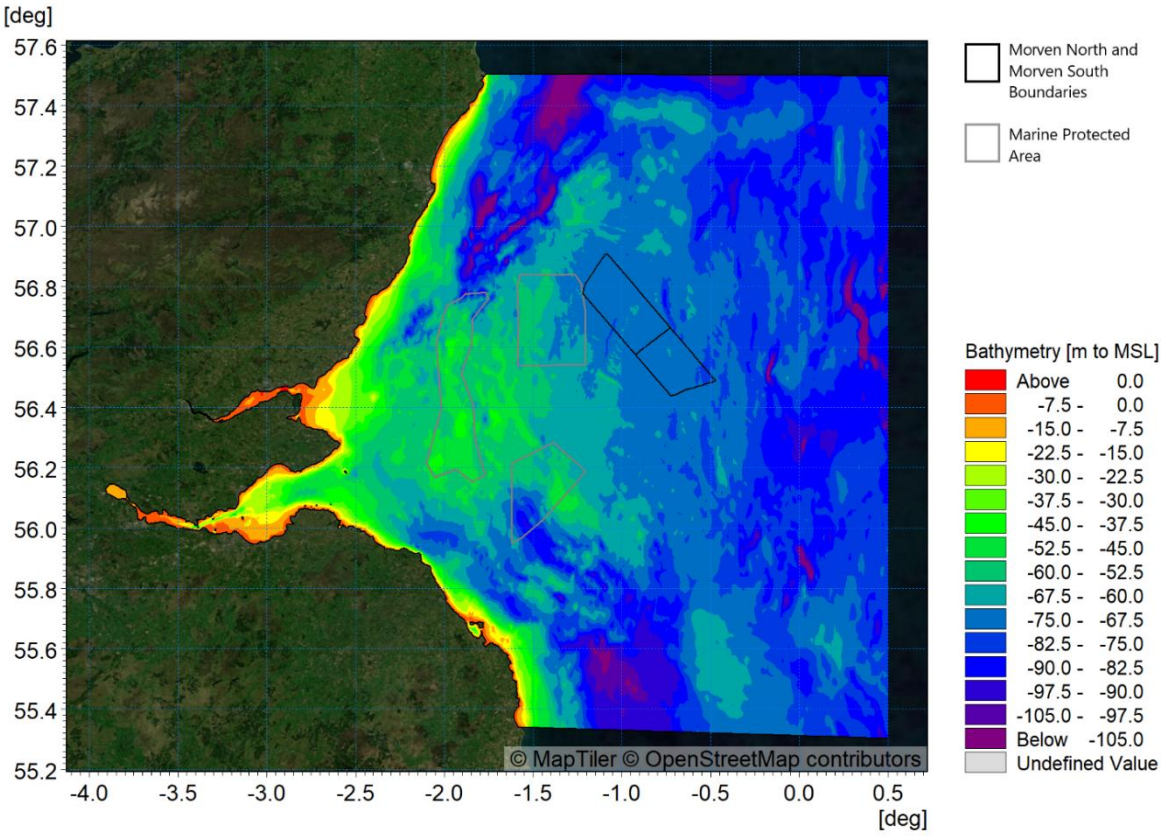

Figure 4.4: Model bathymetry as viewed within the modelling software for the Morven North and Morven South physical processes modelling

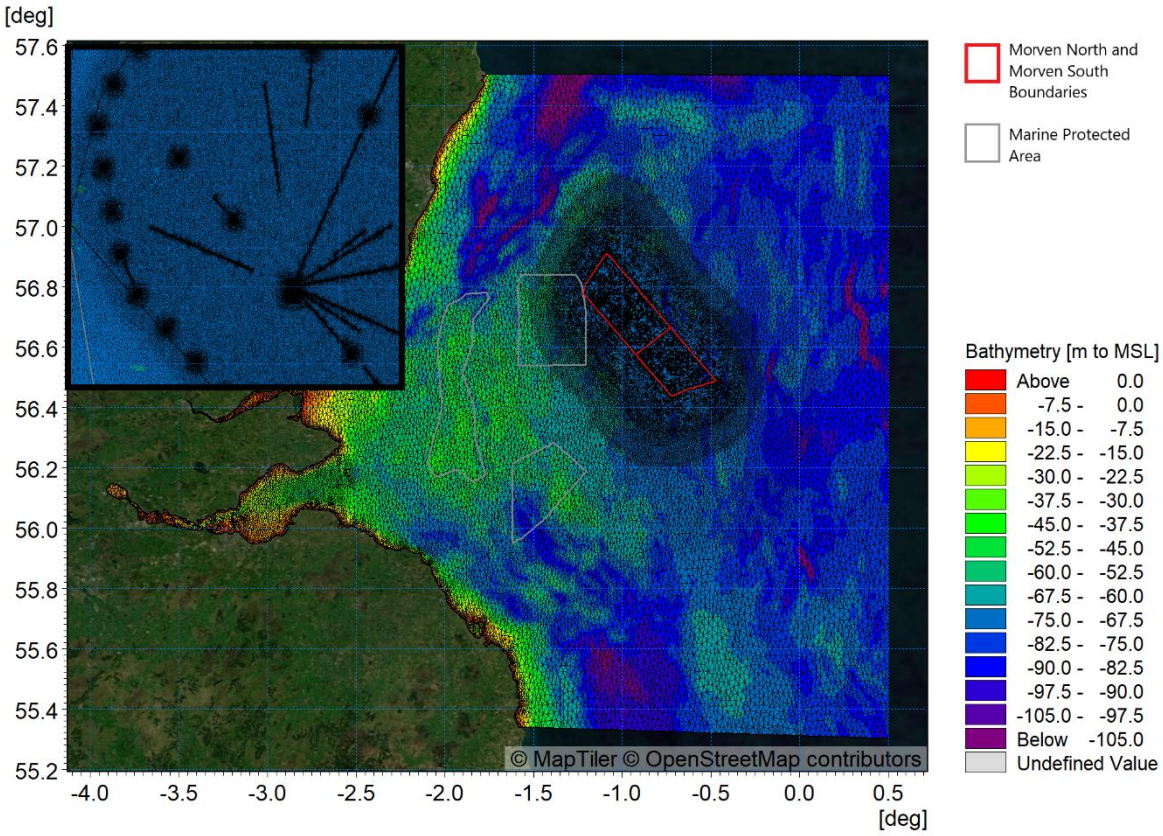

Figure 4.5: Model mesh with inset map to demonstrate the detailed representation of Morven North infrastructure

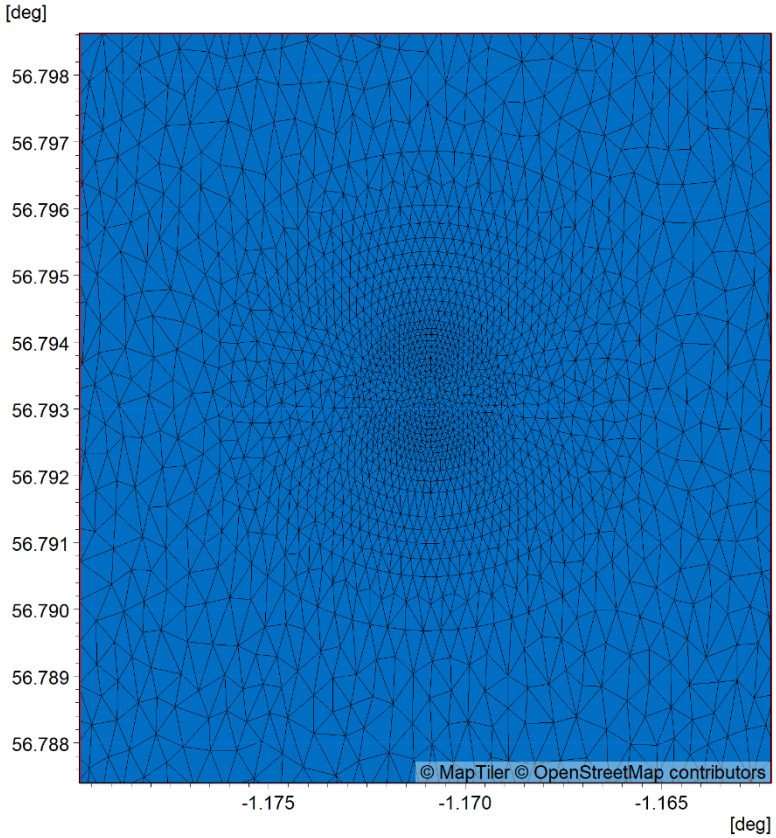

Figure 4.6: Model mesh surrounding a single wind turbine monopile foundation within the Morven North Boundary

4.3 Hydrography

4.3.1.1 The UKHO states that the mean tidal range at the Standard Port of Montrose is 3.0m whilst the Standard Ports of Aberdeen and Leith are subject to a mean tidal range of 2.75m and 3.6m respectively. The tidal characteristics for these sites are shown in Table 4.1 in metres referenced to Chart Datum (CD), whilst the locations of these ports relative to the Regional Physical Processes Study Area are shown in Figure 4.7. The Atlas of UK Marine Renewable Energy Resources reports mean spring tidal ranges between approximately 2.5m to 2.8m across the Morven North Boundary and 2.4m to 2.7m across the Morven South Boundary (ABPmer, 2017).

Table 4.1: Tidal Levels at Standard Ports closest to Morven North and Morven South

Tidal Level (m CD)	Aberdeen	Montrose	Leith
Lowest Astronomical Tide (LAT)	0.0	0.2	-0.1
Mean Low Water Springs (MLWS)	0.6	0.8	0.8
Mean Low Water Neaps (MLWN)	1.6	1.9	2.0
Mean Sea Level (MSL)	2.6	2.9	3.2
Mean High Water Neaps (MHWN)	3.4	3.8	4.4
Mean High Water Springs (MHWS)	4.3	4.9	5.6
Highest Astronomical Tide (HAT)	4.8	5.6	6.3

4.3.1.2 The tidal flow simulations which form the basis of the study were undertaken using the MIKE21 FM modelling system. The FM Module is a 2-dimensional, depth averaged hydrodynamic model which simulates the water level variations and flows in response to a variety of forcing functions in lakes, estuaries and coastal areas. The water levels and flows are resolved on a mesh covering the area of interest when provided with bathymetry, bed resistance coefficient, eddy viscosity coefficient, and hydrodynamic boundary conditions.

4.3.1.3 The tidal model was driven using boundary conditions extracted from the DHI global tidal model which is based on the DTU10 ocean model developed by the National Space Institute of Denmark. These boundaries were fully defined “flather” boundaries for which both surface elevation and current vectors are specified. A single baseline model was calibrated to represent the Regional Physical Processes Study Area, using the following data sources:

- Partrac metocean data collected for Morven North and Morven South;
- Admiralty tidal harmonics;
- Admiralty tidal diamonds.

4.3.1.4 A large amount of hydrometric data was available across the model domain; with the principal sources used for model calibration illustrated in Figure 4.7 and calibration plots presented in the subsequent figures. Within Figure 4.7, tidal stream data points are presented, with the numbering related to the Admiralty Chart number and the lettering related to the tidal diamond within that particular chart. For example, the site 1409G relates to the tidal diamond “G” from the Admiralty Chart number 1409. Figure 4.7 also presents the Admiralty Standard and Secondary Ports where Admiralty Tidal Predictions have been made for the purpose of model calibration, along with the two site specific metocean data points surveyed by Partrac.

4.3.1.5 Figure 4.8 and Figure 4.9 show the comparison of the modelled (red) and Admiralty tidal levels predicted from harmonic analysis (black) during a selected period in 2023 and 2024 respectively. The model correlated well through both spring and neap tidal phases.

4.3.1.6 Figure 4.10 through to Figure 4.25 show the measured data during the Partrac campaign at a number of locations across the Regional Physical Processes Study Area for both spring and neap tidal states.

Figure 4.10 to Figure 4.13 show comparison of current speed and direction for spring and neap tides respectively at monitoring point A (within the Morven North Boundary) during May 2023, whilst Figure 4.14 to Figure 4.17 show a further comparison at the same location during September 2023. Figure 4.18 to Figure 4.25 show the same periods at the second monitoring point B, located within the Morven South Boundary. In each case four traces are included from the monitored data, these being representative of near-surface, mid depth and near-bed flow conditions, along with a depth averaged condition, comparable to the trace produced by the depth averaged Two-dimensional (2D) model (shown in red). The plots show that whilst there is a range of current speeds and directions within the water column, the modelled depth averaged values are representative of the average currents.

4.3.1.7 Figure 4.26 to Figure 4.37 relate to Admiralty tidal diamonds for locations within the domain and compare tidal current speed and direction from Admiralty tidal diamonds with the modelled values at the corresponding location within the model domain. This data is published in a generalised format (i.e. there are 14 sets of hourly current speed data each referenced to high water Leith for spring and neap tides and a single set of current direction values). These values therefore do not relate to a known time period or specific tidal range. The Admiralty data (shown by points) generally correlate well with the modelled current directions and current speeds. It is noted that at some of the tidal stream locations (notably 273A, 1409E and 1409G), the Admiralty current direction is opposing the direction simulated by the model. However, the site specific data recorded by Partrac shows the variation in current direction throughout the water column, for example in Figure 4.21 where the Partrac near-surface current directions are opposing the current directions within the remainder of the water column. This corroborates the difference in direction observed by the Admiralty data at some of these locations, in comparison to the depth averaged output from the model. These datasets are typically used as a cross reference as current speeds are not consistent across all neap or spring tides due to the varying tidal range. Generally, the field data supporting the diamonds was collected using drogues which often measure higher surface current speeds than those simulated in a depth averaged model. It is important to note that the field measurements behind the Admiralty tidal diamonds may have been collected at different times and under different sea and meteorological conditions and thus are considered secondary to site specific metocean survey data.

4.3.1.8 The calibration data demonstrates that the numerical model representatively simulates the tidal currents in the region. This includes the representation of the skew tide where peak flood and ebb flows are typically one to two hours prior to high and low water respectively. Figure 4.38 illustrates tidal patterns during peak flood on a spring tide whilst Figure 4.39 illustrates the ebb tide. These points in the tidal cycle are used as reference for the assessment of potential impacts and changes to tidal flows due to Morven North and Morven South. The period selected for the comparative study represents a spring tide on the upper end of the range experienced in the region; this was to ensure the study included the greatest variation in tidal conditions (i.e. water depth and current speed). Residual tidal flows and how they drive sediment transport regimes are examined in Section 4.8.

4.3.1.9 Figure 4.38 and Figure 4.39 illustrate current speeds up to 0.66m/s during peak flood and 0.70m/s during peak ebb within the Morven North Boundary. Peak current speeds are shown to be lower within the Morven South Boundary at 0.59m/s and 0.61m/s during peak flood and peak ebb respectively. The Atlas of UK Marine Renewable Energy Resources also indicates spring peak current speeds of circa up to circa 0.6m/s across the Morven North Boundary and Morven South Boundary (ABPmer, 2017).

4.3.1.10 The site specific survey undertaken by Partrac between October 2022 and November 2023 recorded maximum current speeds up to 1.0m/s within the Morven North Boundary, with mean current speeds of 0.26m/s. Near-surface current speeds were recorded up to a maximum 0.99m/s, with mean near-surface current speeds of 0.28m/s. Near-bed current speeds were recorded up to a maximum 0.63m/s, with mean near-bed current speeds of 0.22m/s.

4.3.1.11 Within the Morven South Boundary, maximum current speeds up to 0.88m/s were recorded, with mean current speeds of 0.24m/s. Near-surface current speeds were recorded up to a maximum 0.85m/s, with mean near-surface current speeds of 0.25m/s. Near-bed current speeds were recorded up to a maximum 0.61 m/s, with mean near-bed current speeds of 0.21m/s.

4.3.1.12 Current directions at both sites aligned predominantly in a north northeast to south southwest orientation.

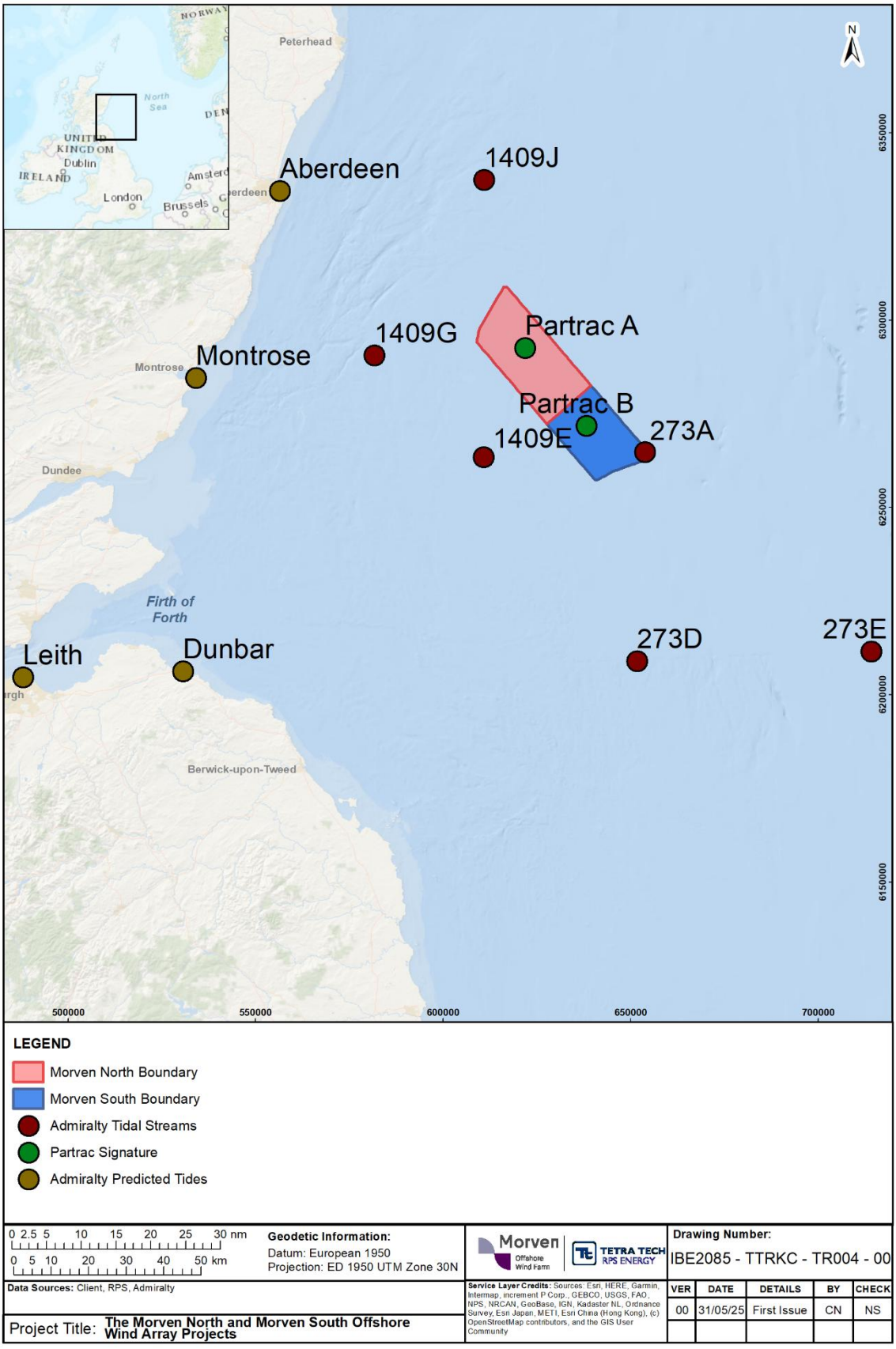

Figure 4.7: Location of selected calibration datasets relevant to the Morven North and Morven South hydrodynamics modelling

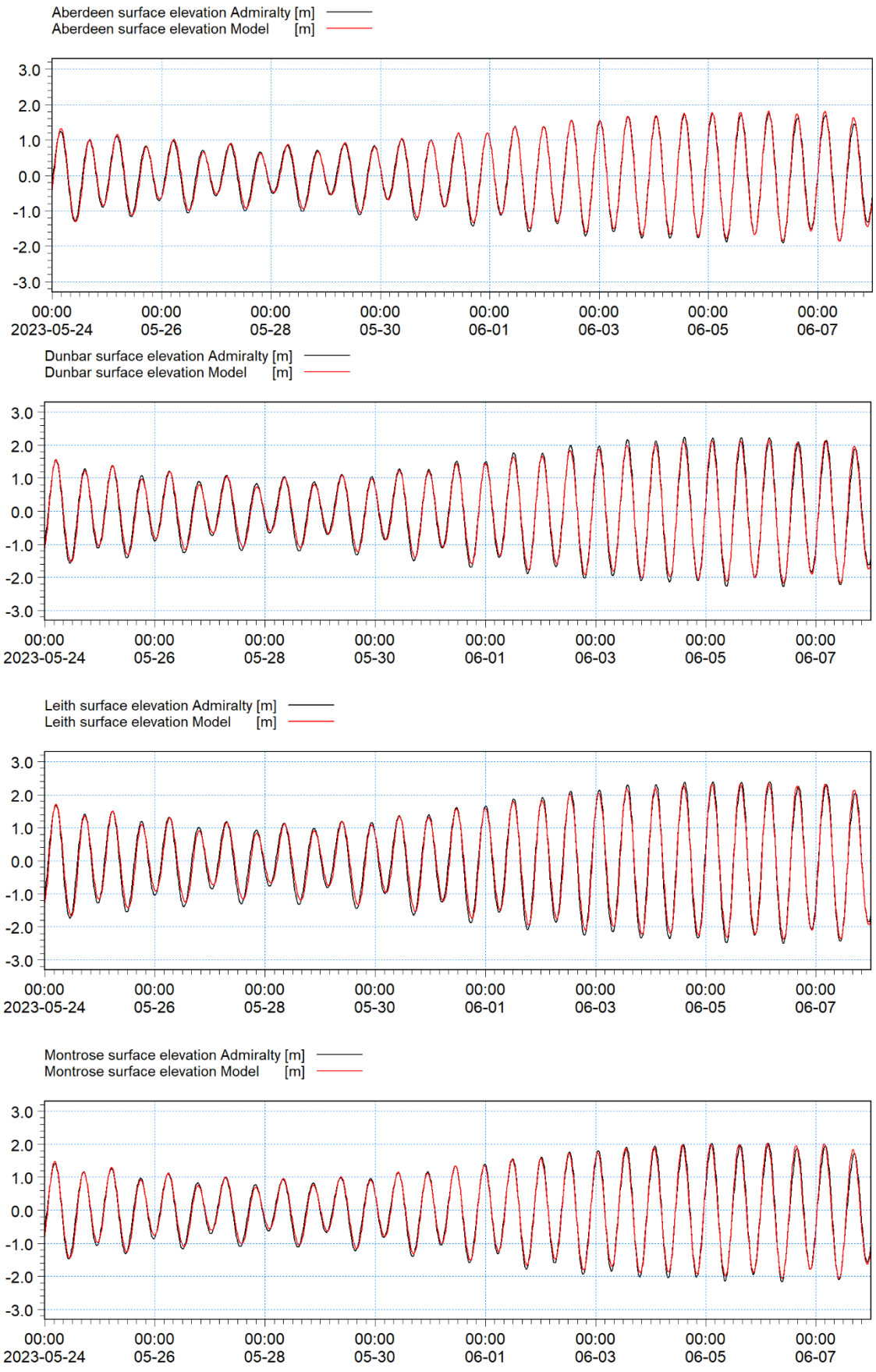

Figure 4.8: Comparison of model and Admiralty harmonics – 2023

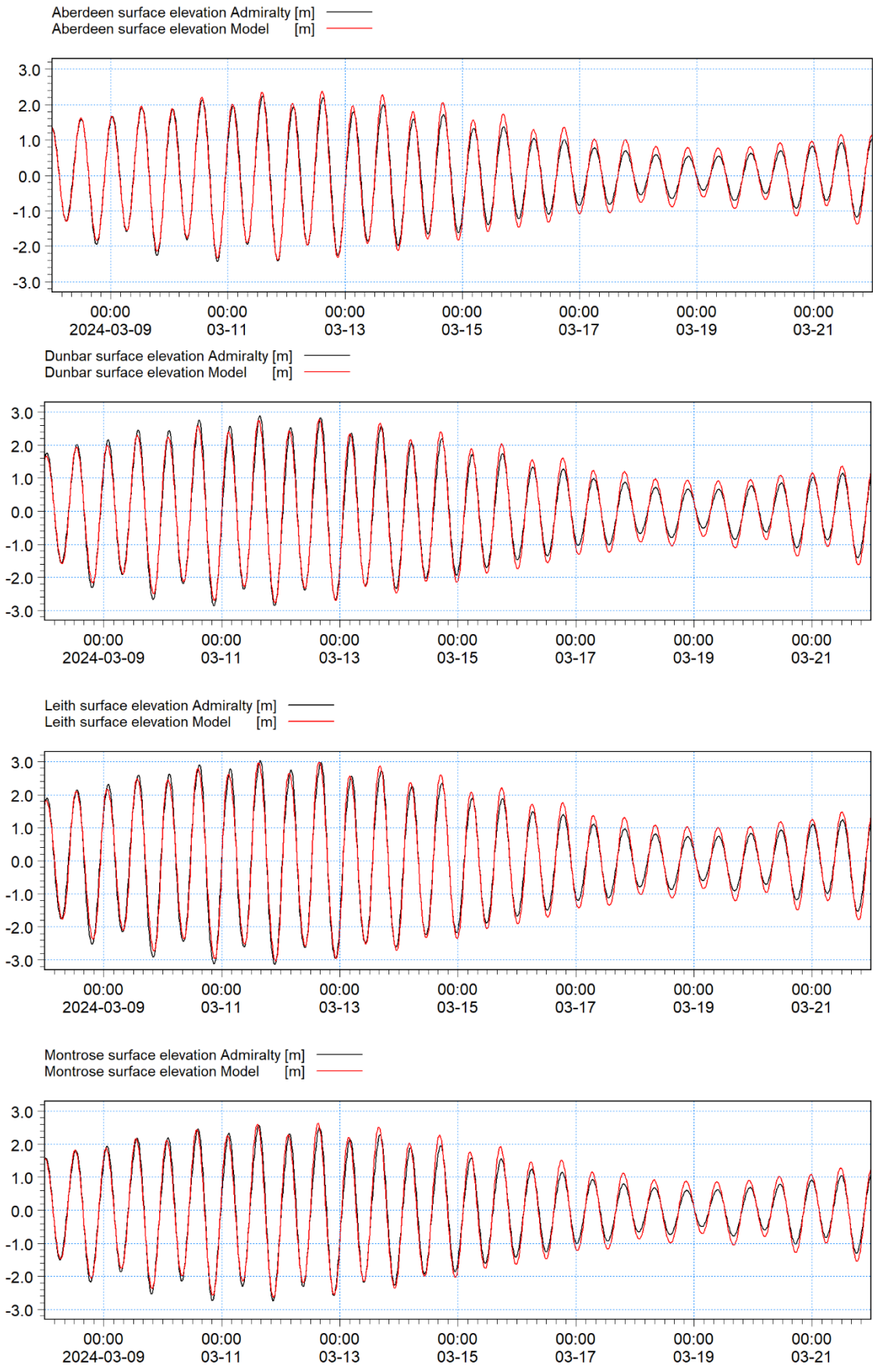

Figure 4.9: Comparison of model and Admiralty harmonics - 2024

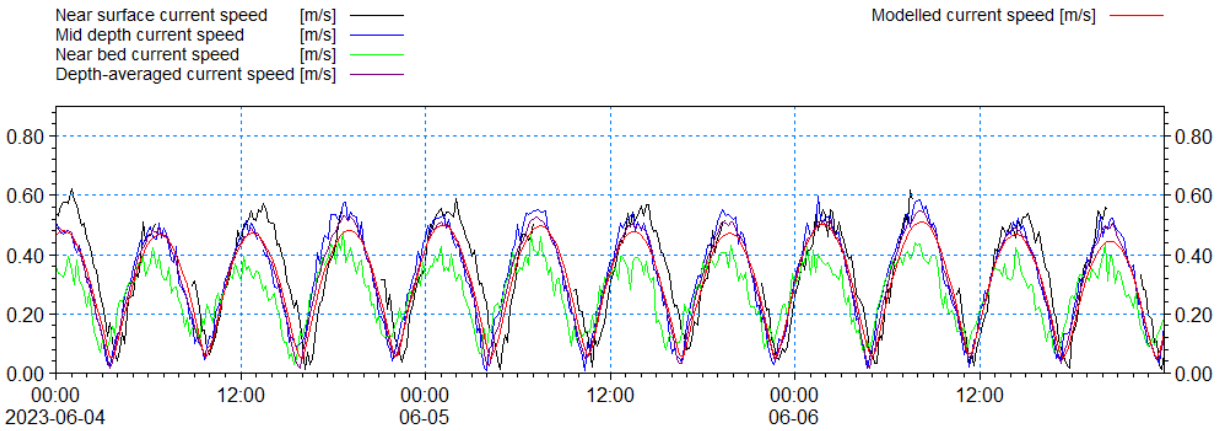

Figure 4.10: Comparison of model and recorded data - May 2023– Partrac Location A – current speed spring

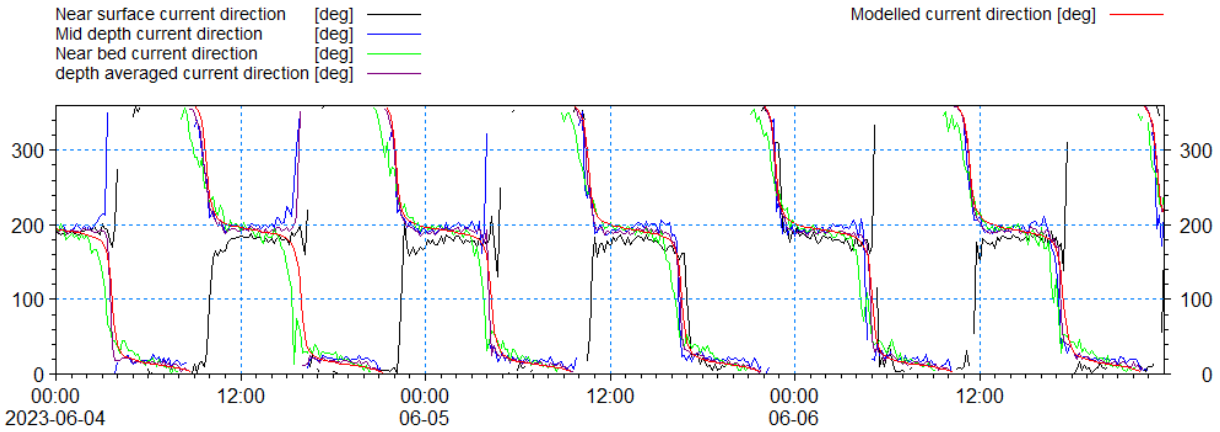

Figure 4.11: Comparison of model and recorded data - May 2023 – Partrac Location A – current direction spring

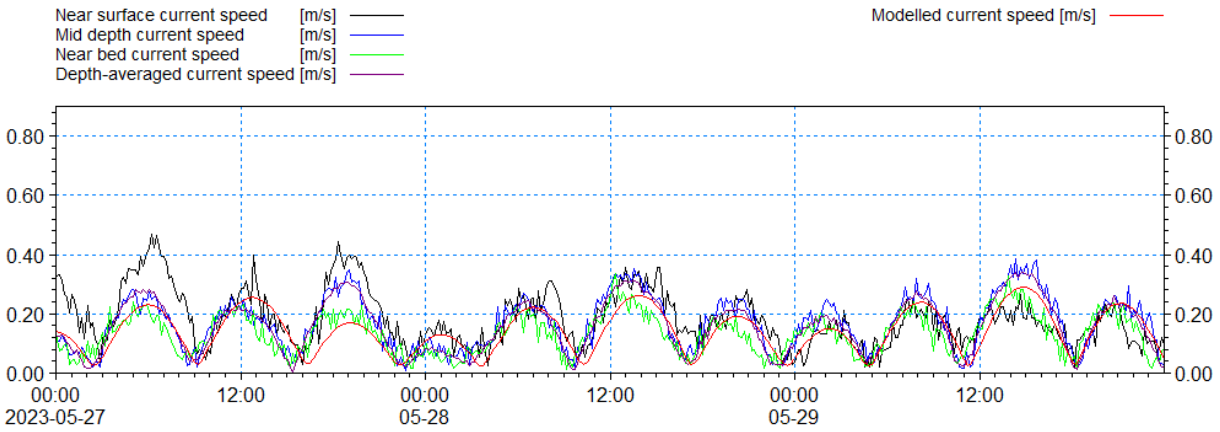

Figure 4.12: Comparison of model and recorded data - May 2023 – Partrac Location A – current speed neap

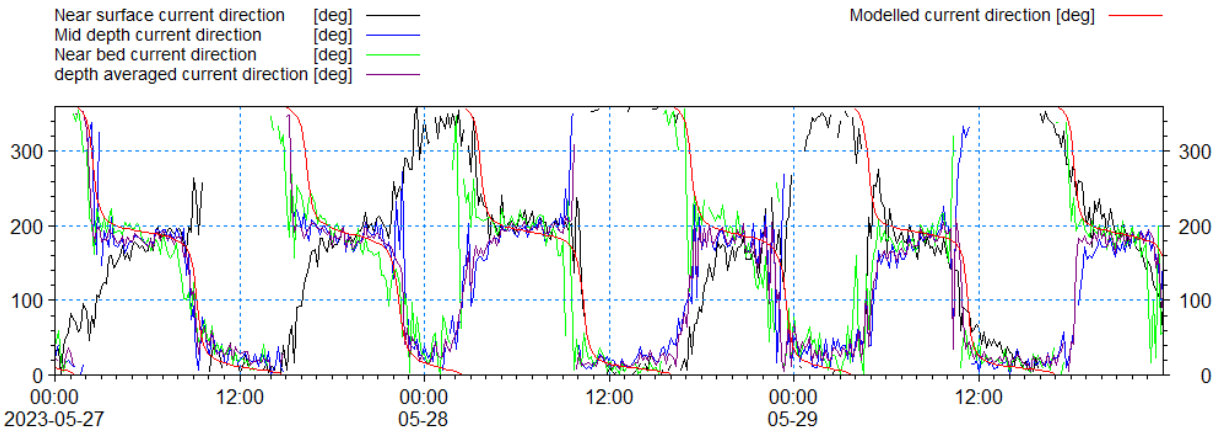

Figure 4.13: Comparison of model and recorded data - May 2023 – Partrac Location A – current direction neap

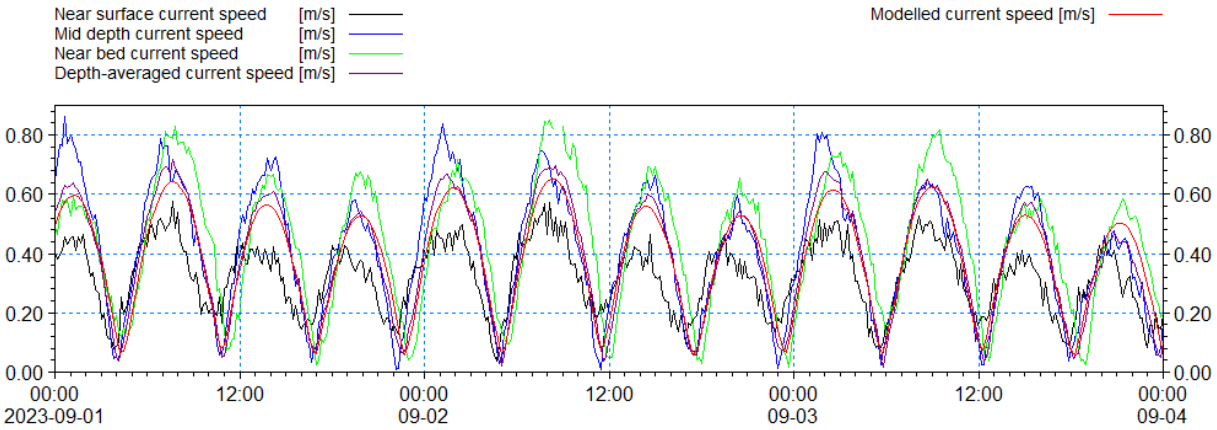

Figure 4.14: Comparison of model and recorded data - September 2023 – Partrac Location A – current speed spring

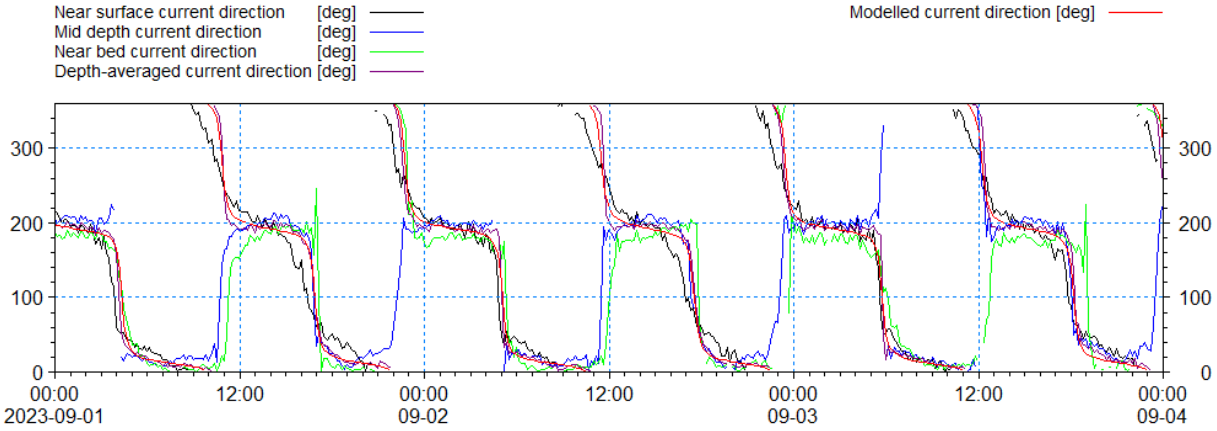

Figure 4.15: Comparison of model and recorded data - September 2023 – Partrac Location A – current direction spring

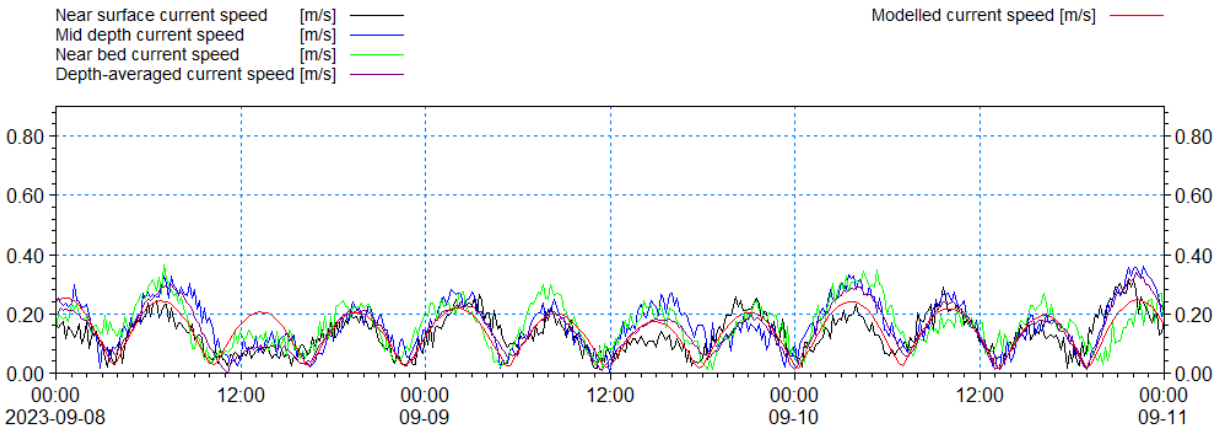

Figure 4.16: Comparison of model and recorded data - September 2023 – Partrac Location A – current speed neap

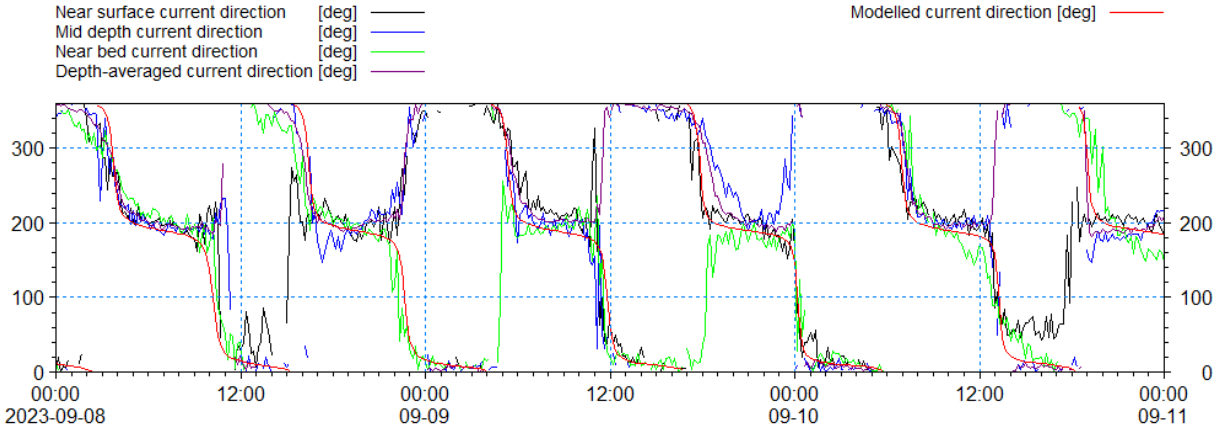

Figure 4.17: Comparison of model and recorded data - September 2023 – Partrac Location A – current direction neap

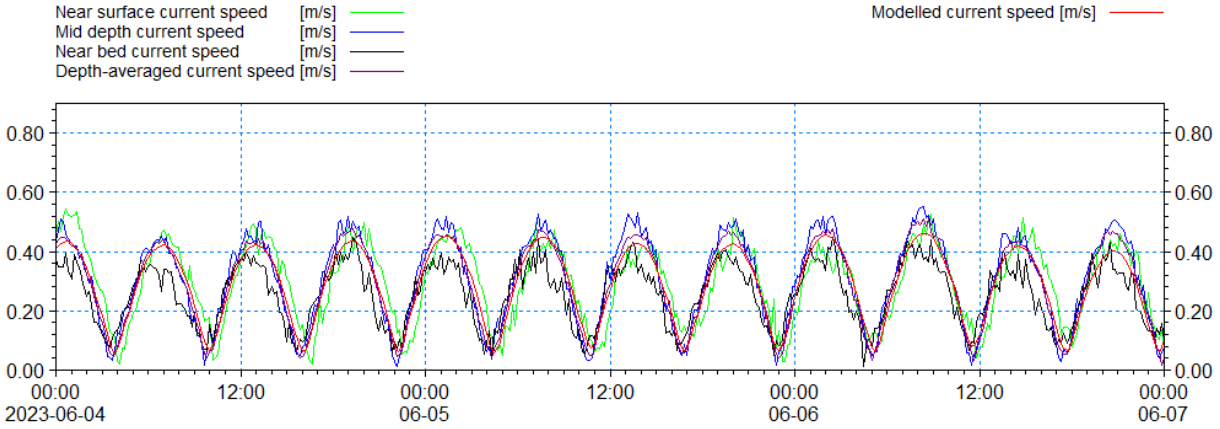

Figure 4.18: Comparison of model and recorded data – May 2023 – Partrac Location B – current speed spring

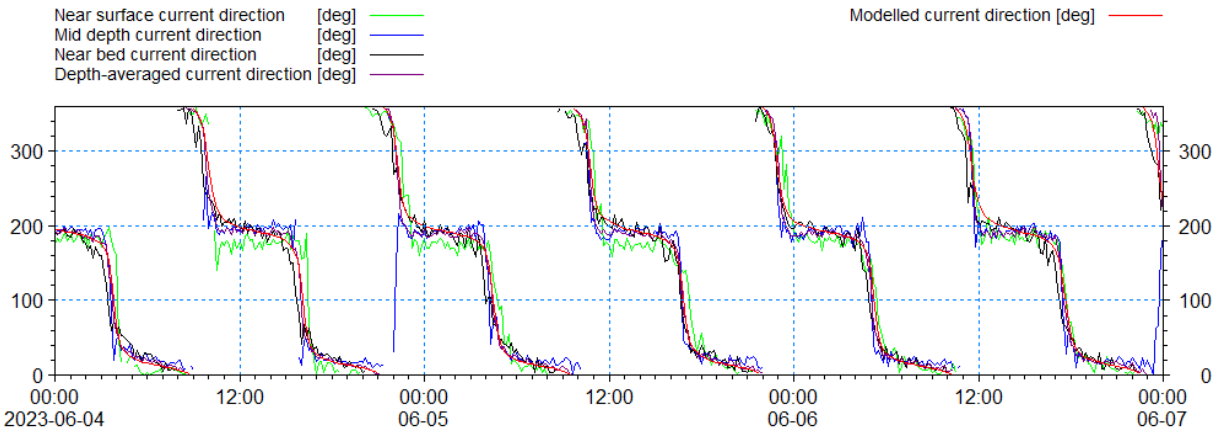

Figure 4.19: Comparison of model and recorded data – May 2023 – Partrac Location B – current direction spring

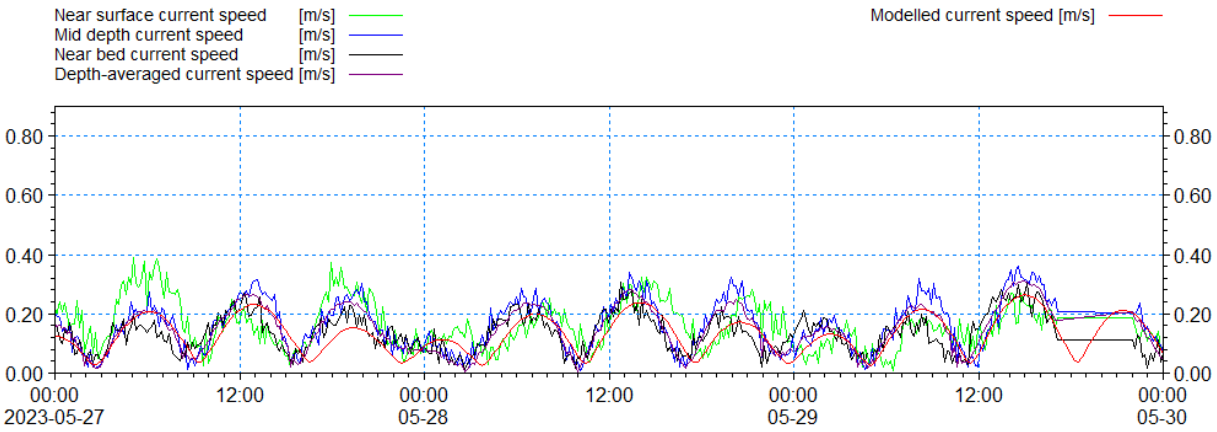

Figure 4.20: Comparison of model and recorded data – May 2023 – Partrac Location B – current speed neap

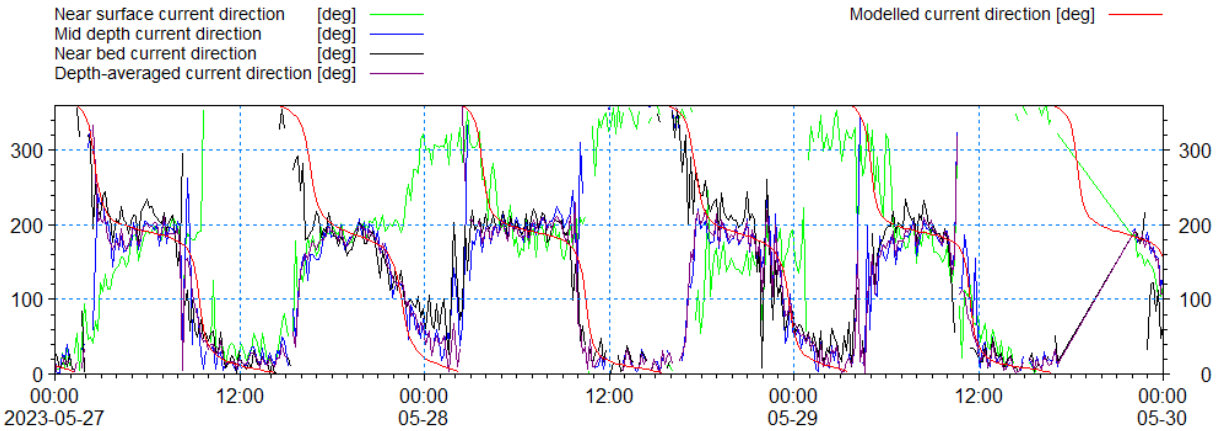

Figure 4.21: Comparison of model and recorded data – May 2023 – Partrac Location B – current direction neap

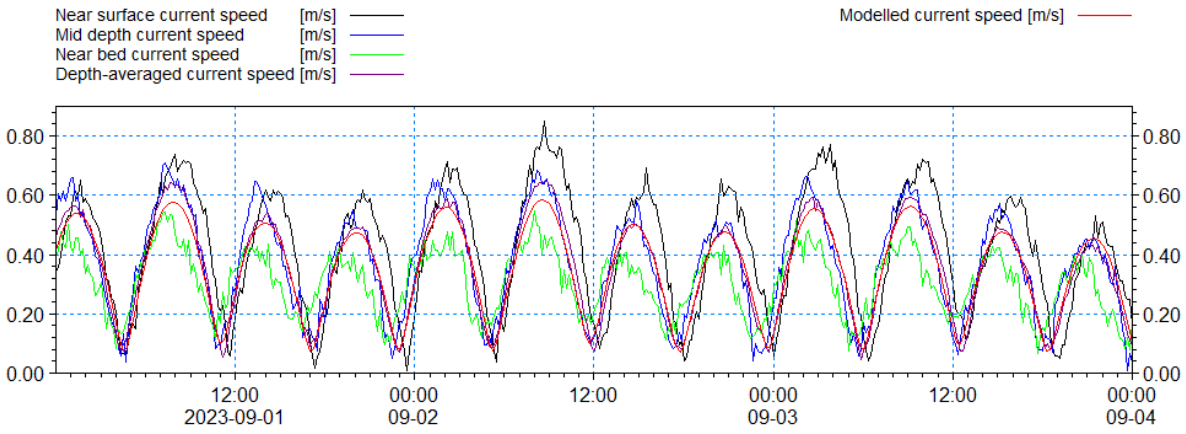

Figure 4.22: Comparison of model and recorded data – September 2023 – Partrac Location B – current speed spring

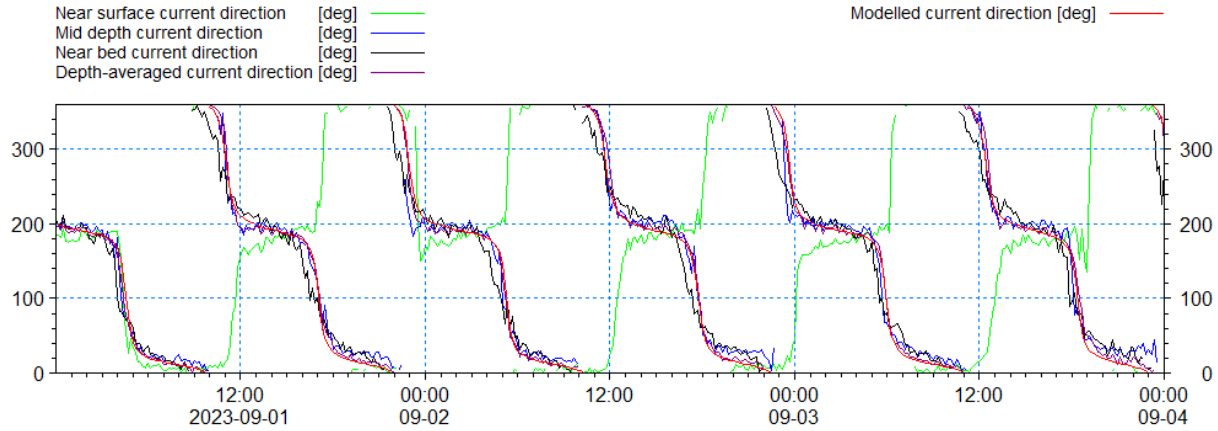

Figure 4.23: Comparison of model and recorded data – September 2023 – Partrac Location B – current direction spring

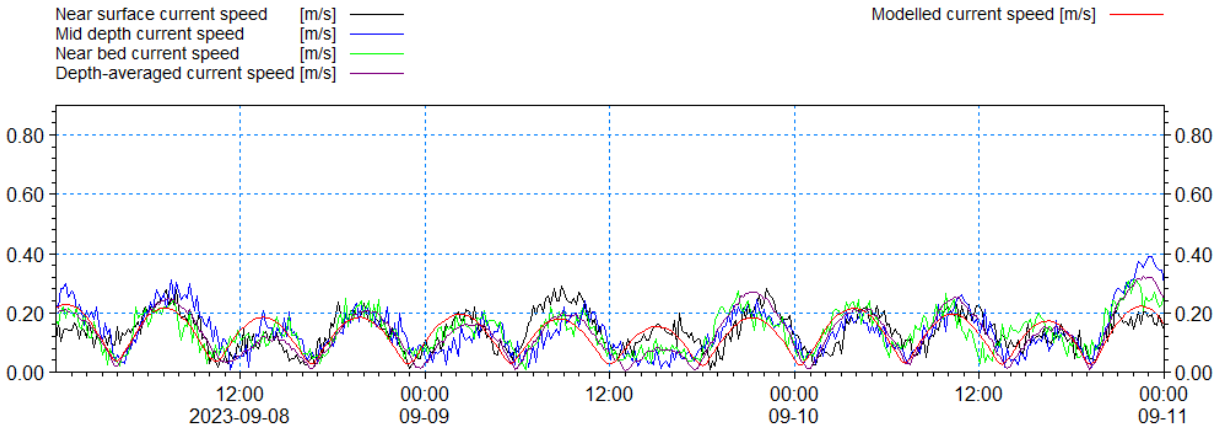

Figure 4.24: Comparison of model and recorded data – September 2023 – Partrac Location B – current speed neap

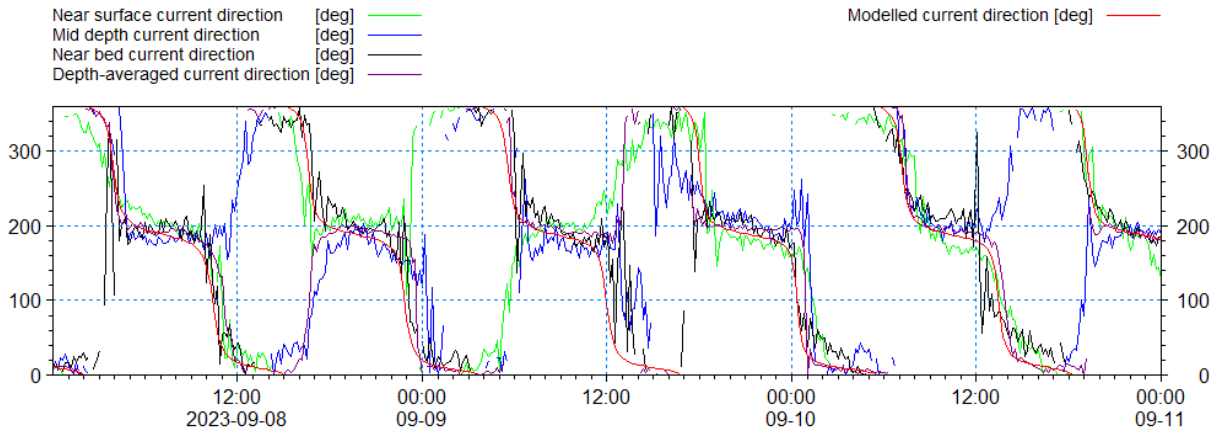

Figure 4.25: Comparison of model and recorded data – September 2023 – Partrac Location B – current direction neap

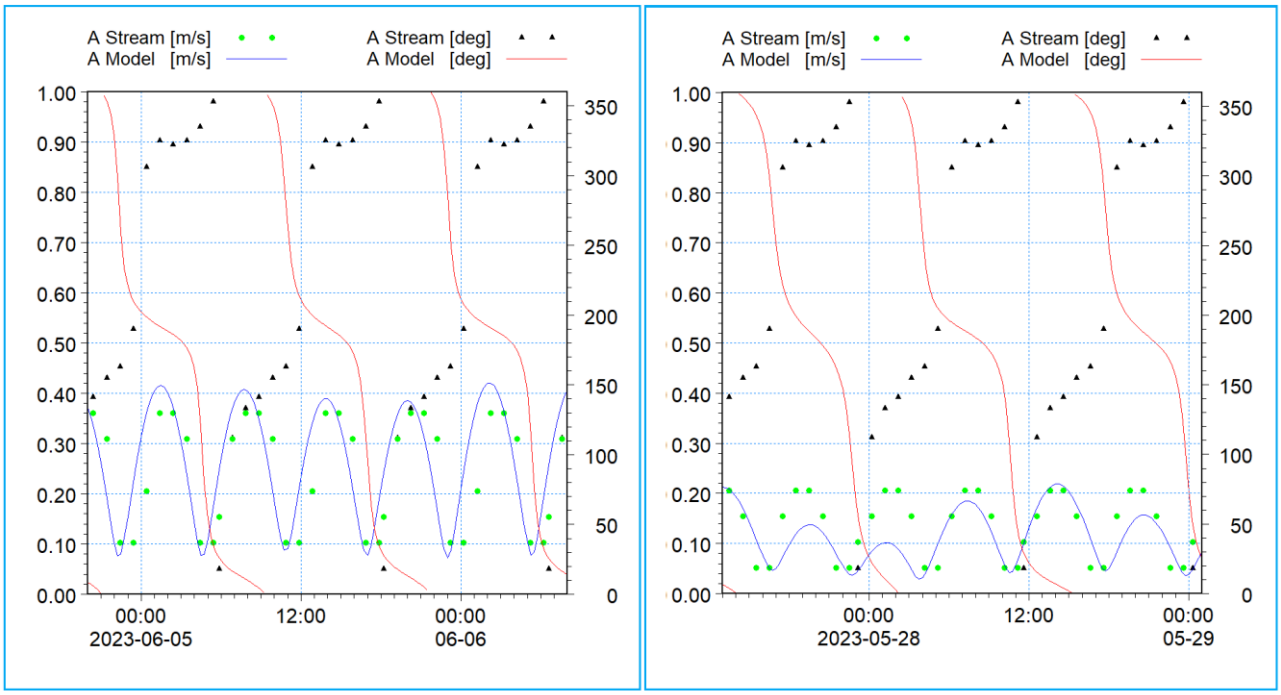

Figure 4.26: Comparison of model simulation 2023/Admiralty Diamond Location 273A (spring left, neap right)

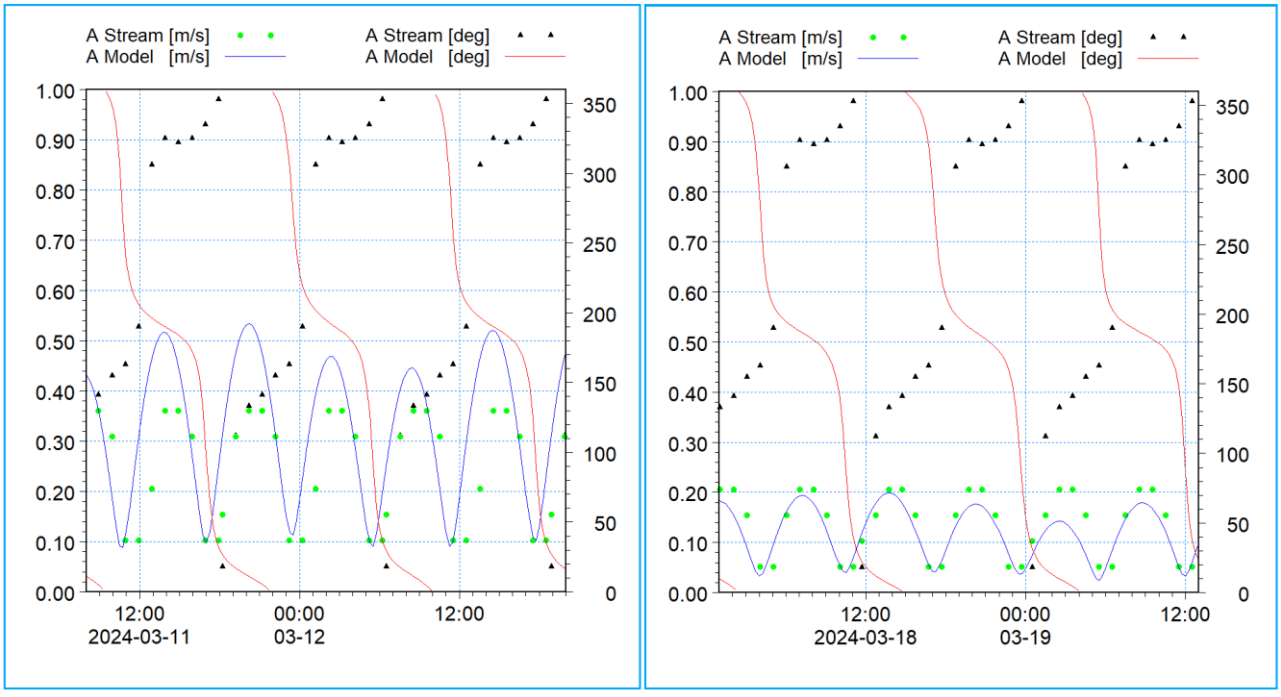

Figure 4.27: Comparison of model simulation 2024/Admiralty Diamond Location 273A (spring left, neap right)

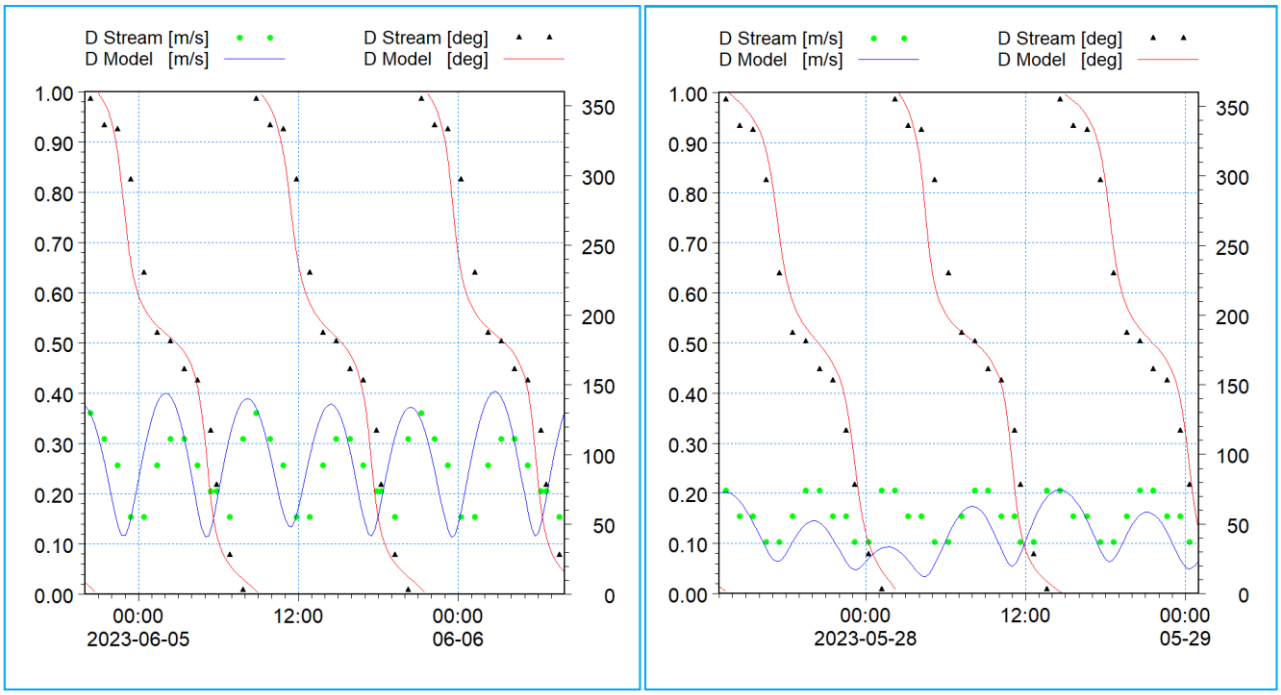

Figure 4.28: Comparison of current speed and direction from model simulation 2023/Admiralty Diamond Location 273D (spring left, neap right)

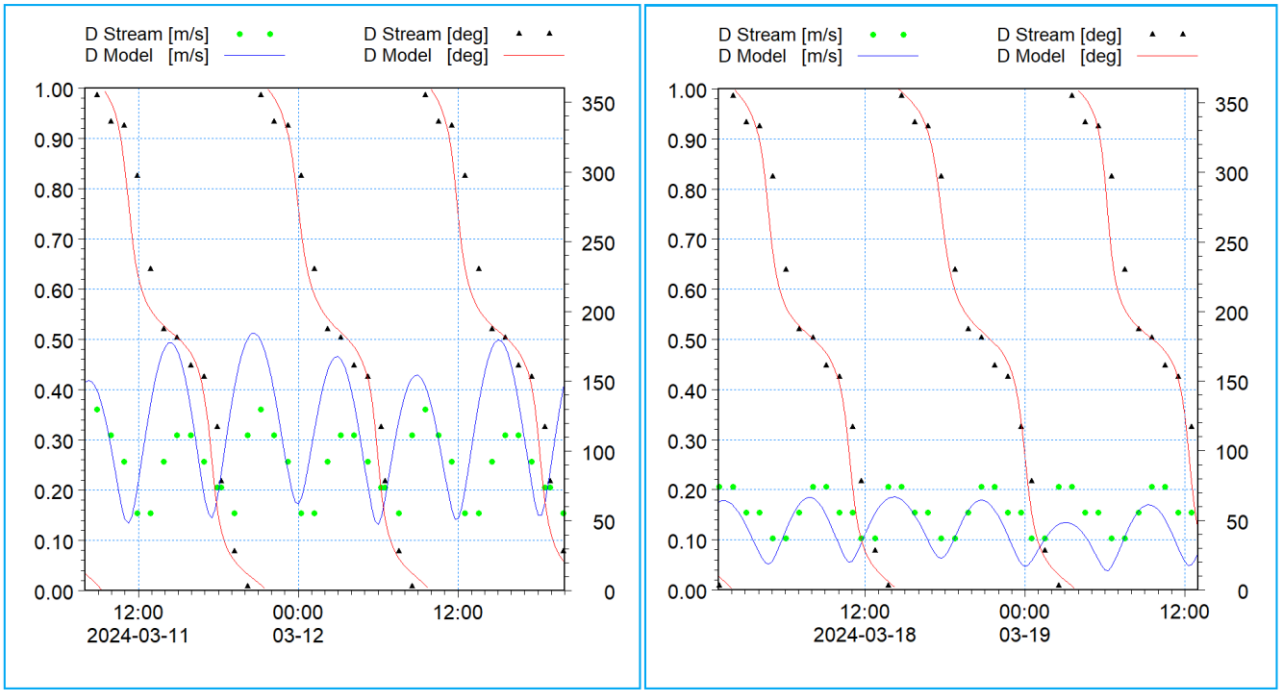

Figure 4.29: Comparison of current speed and direction from model simulation 2024/Admiralty Diamond Location 273D (spring left, neap right)

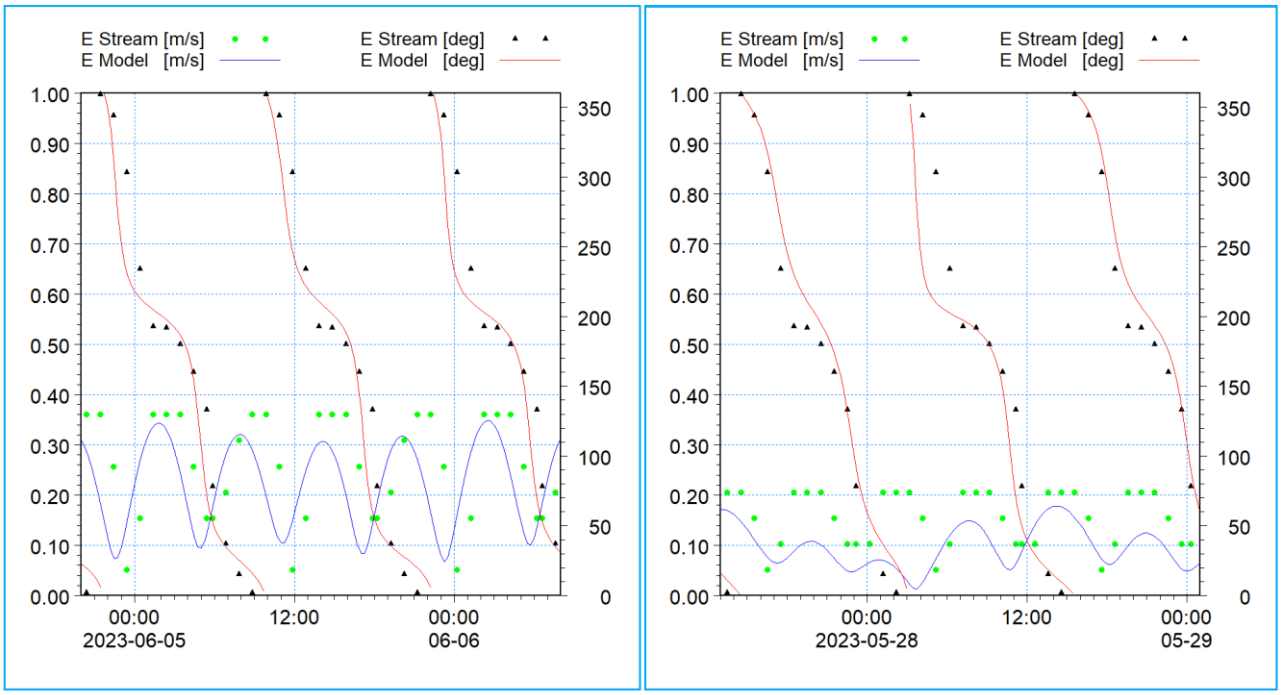

Figure 4.30: Comparison of current speed and direction from model simulation 2023/Admiralty Diamond Location 273E (spring left, neap right)

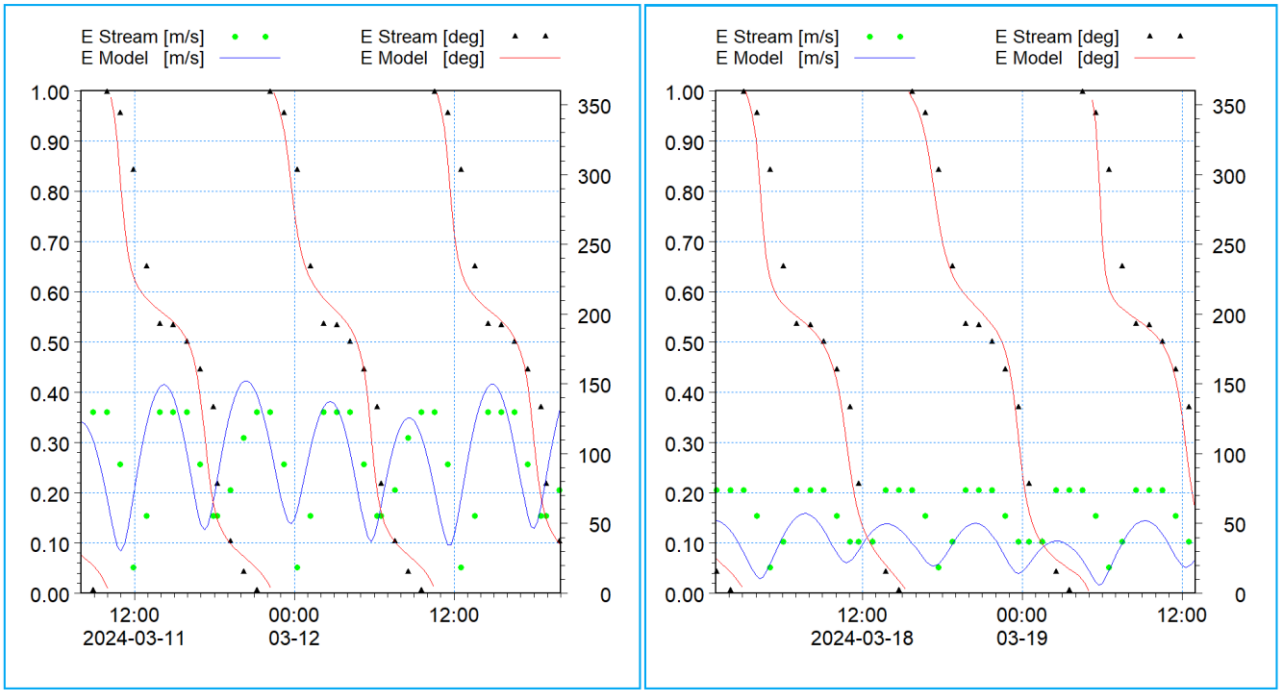

Figure 4.31: Comparison of current speed and direction from model simulation 2024/Admiralty Diamond Location 273E (spring left, neap right)

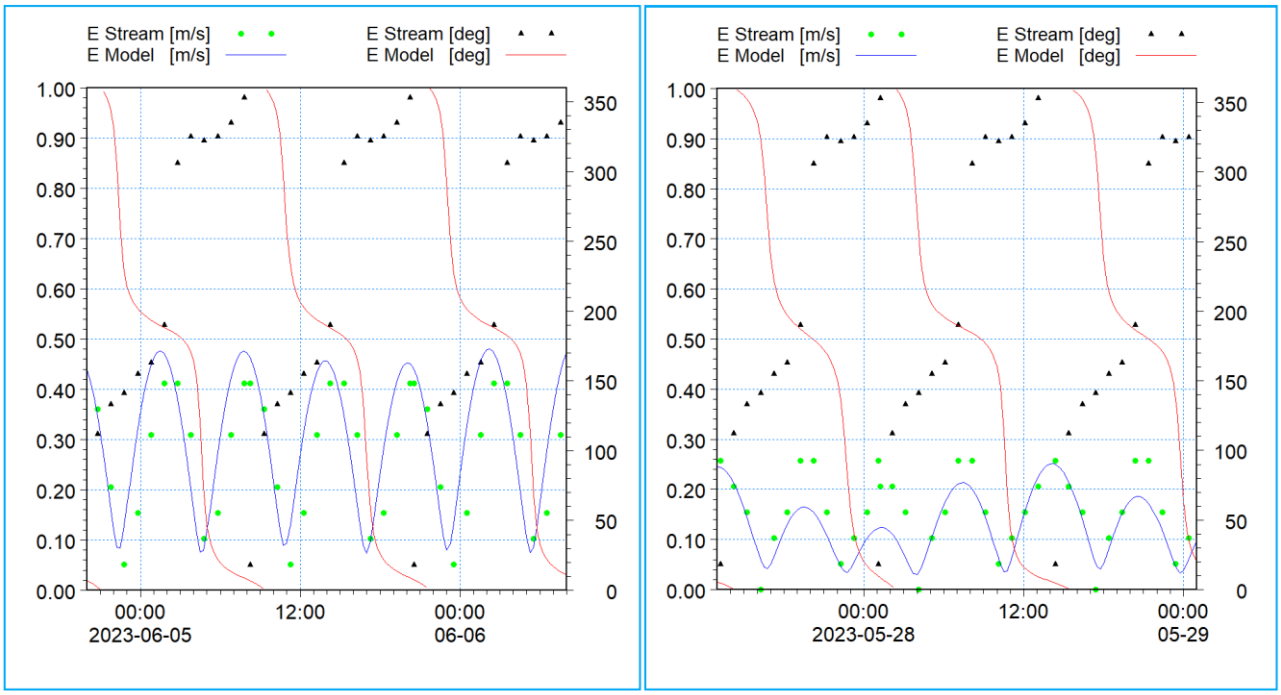

Figure 4.32: Comparison of current speed and direction from model simulation 2023/Admiralty Diamond Location 1409E (spring left, neap right)

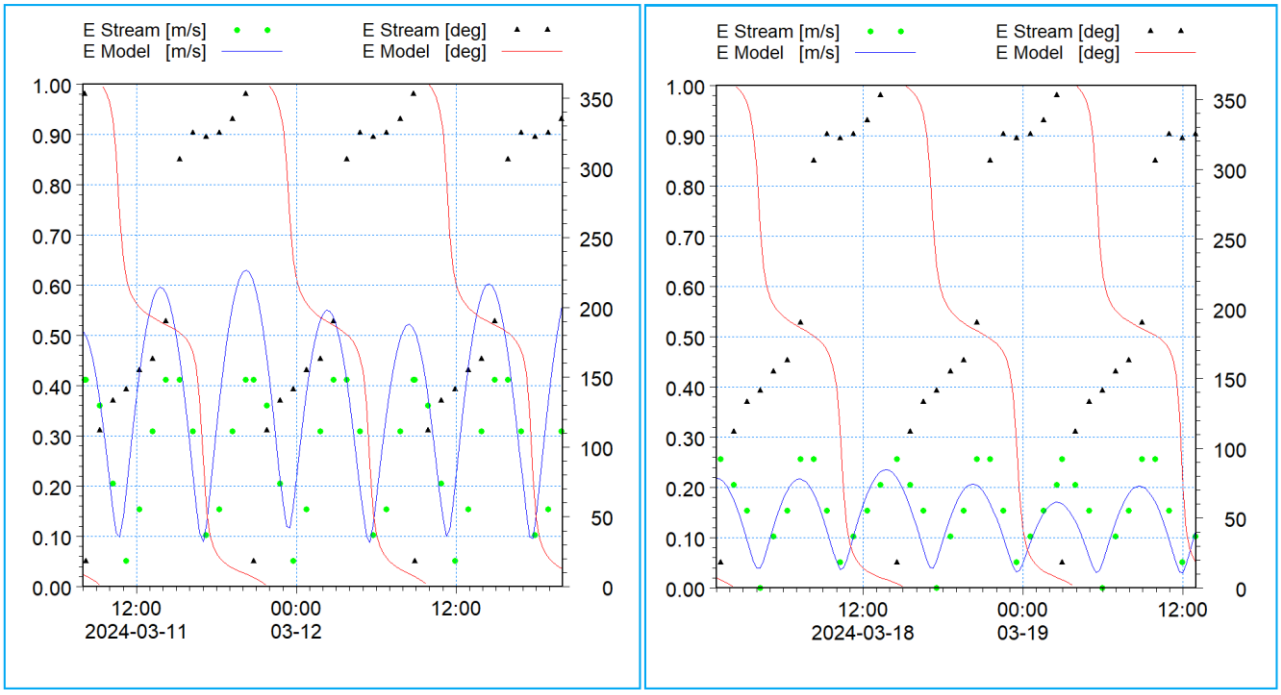

Figure 4.33: Comparison of current speed and direction from model simulation 2024/Admiralty Diamond Location 1409E (spring left, neap right)

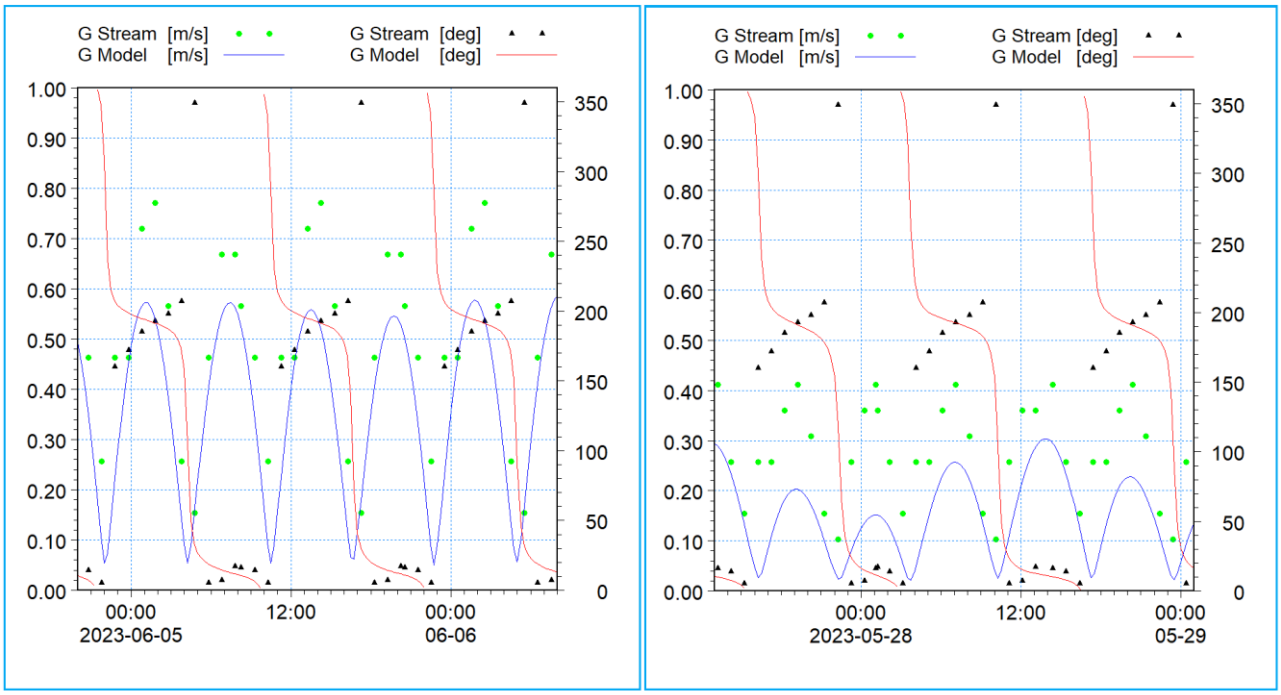

Figure 4.34: Comparison of current speed and direction from model simulation 2023/Admiralty Diamond Location 1409G (spring left, neap right)

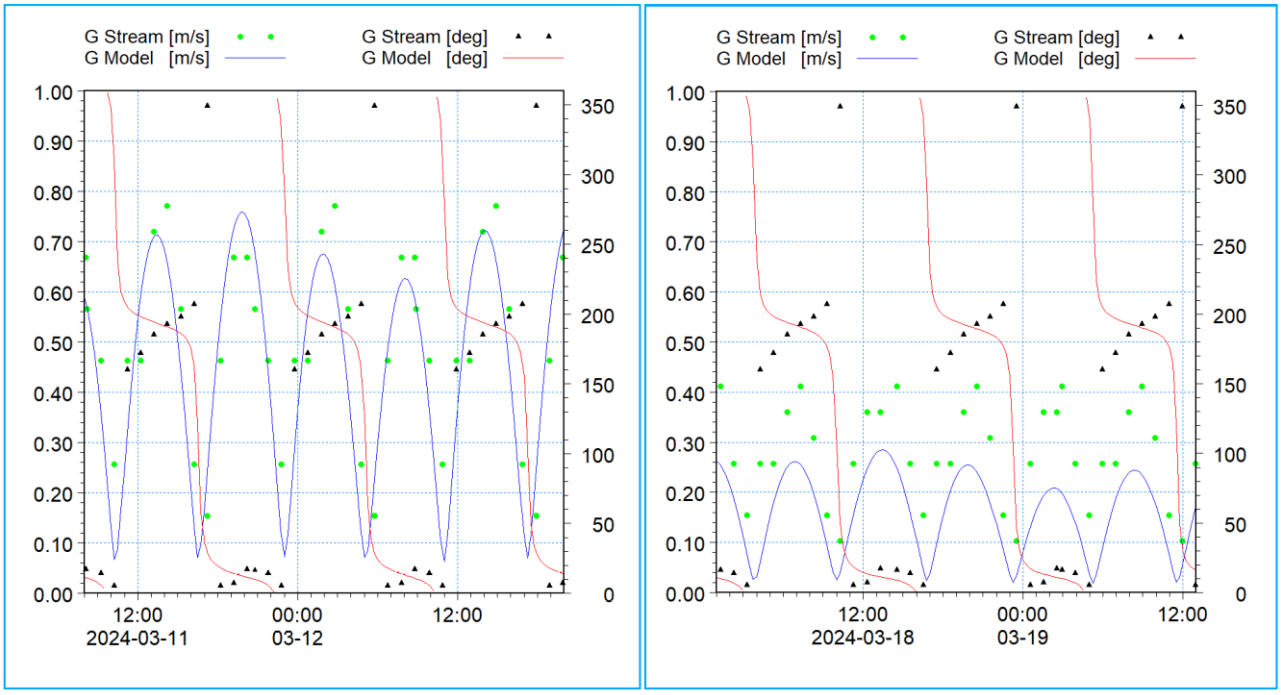

Figure 4.35: Comparison of current speed and direction from model simulation 2024/Admiralty Diamond Location 1409G (spring left, neap right)

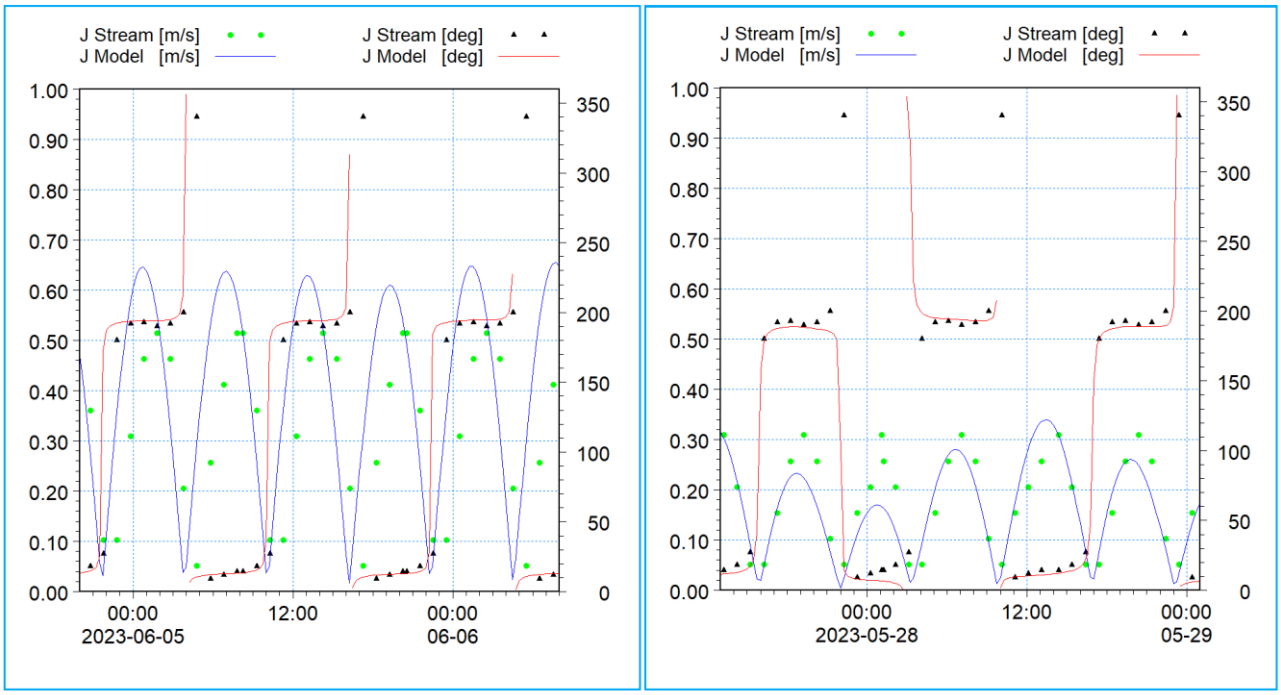

Figure 4.36: Comparison of current speed and direction from model simulation 2023/Admiralty Diamond Location 1409J (spring left, neap right)

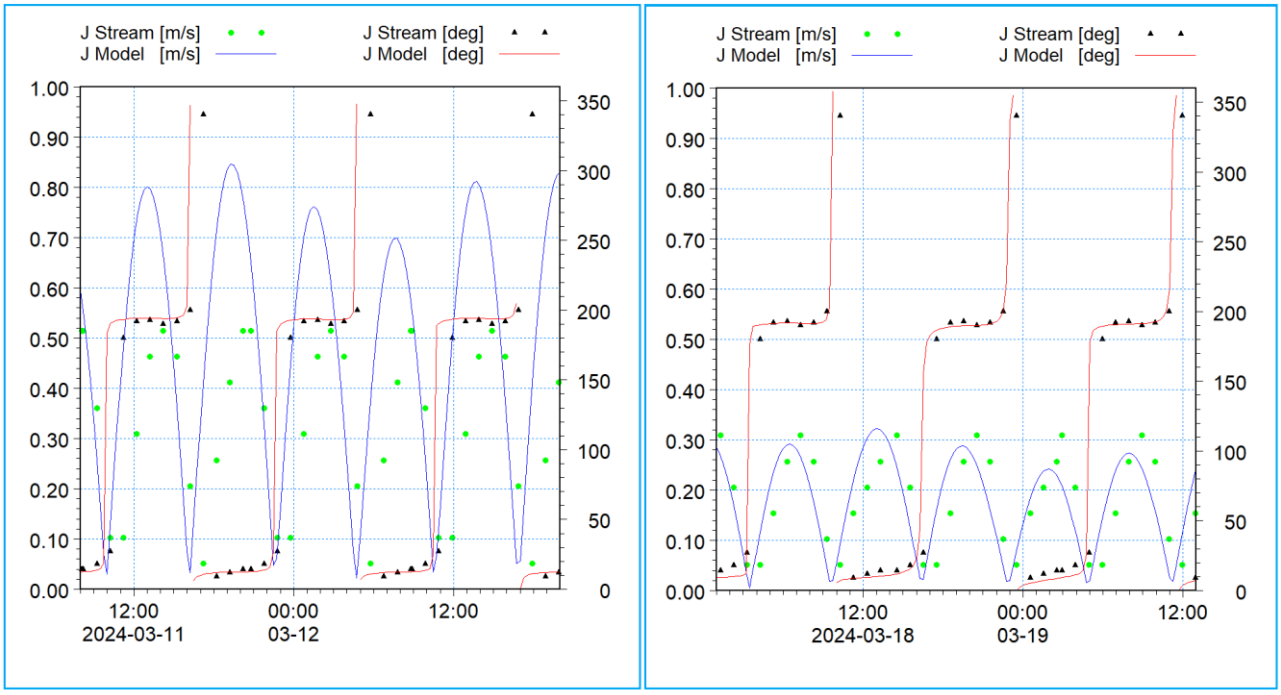

Figure 4.37: Comparison of current speed and direction from model simulation 2024/Admiralty Diamond Location 1409J (spring left, neap right)

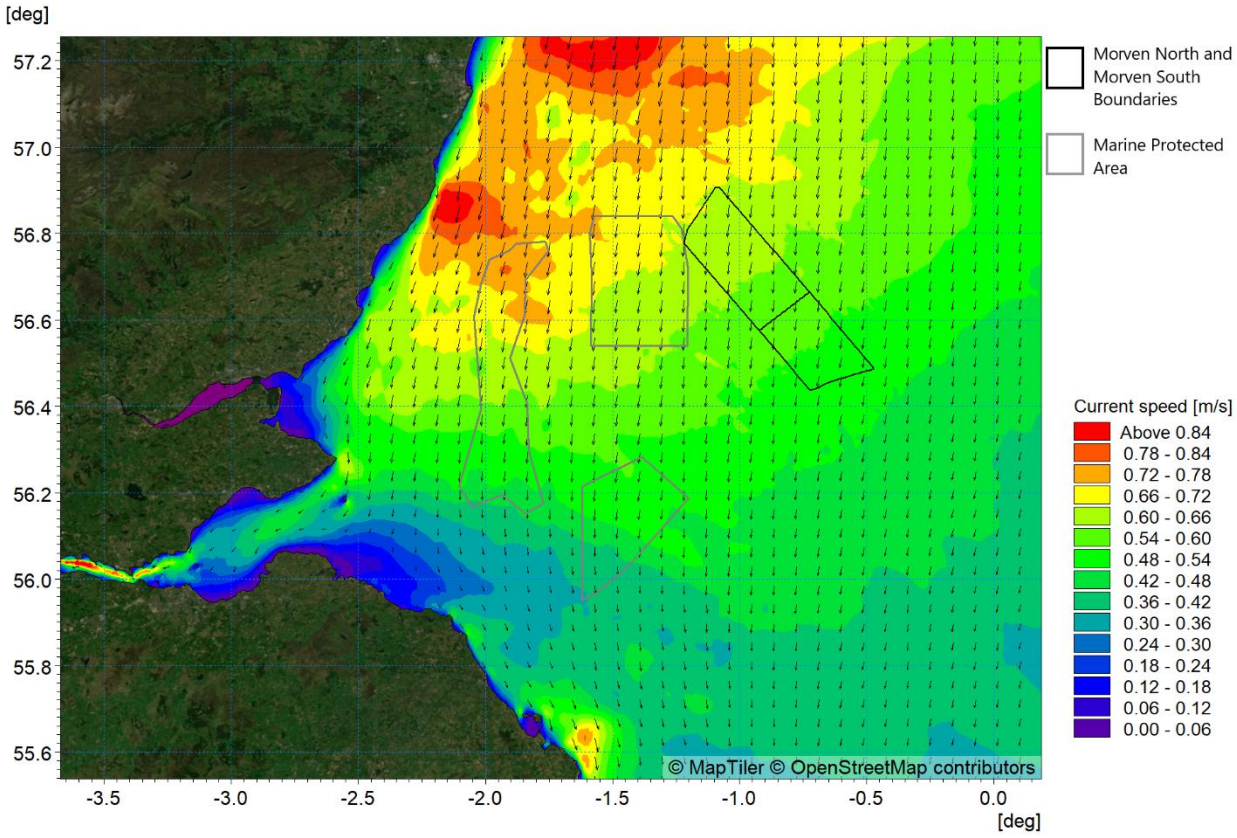

Figure 4.38: Tidal flow patterns – peak flood (high water -1 hour)

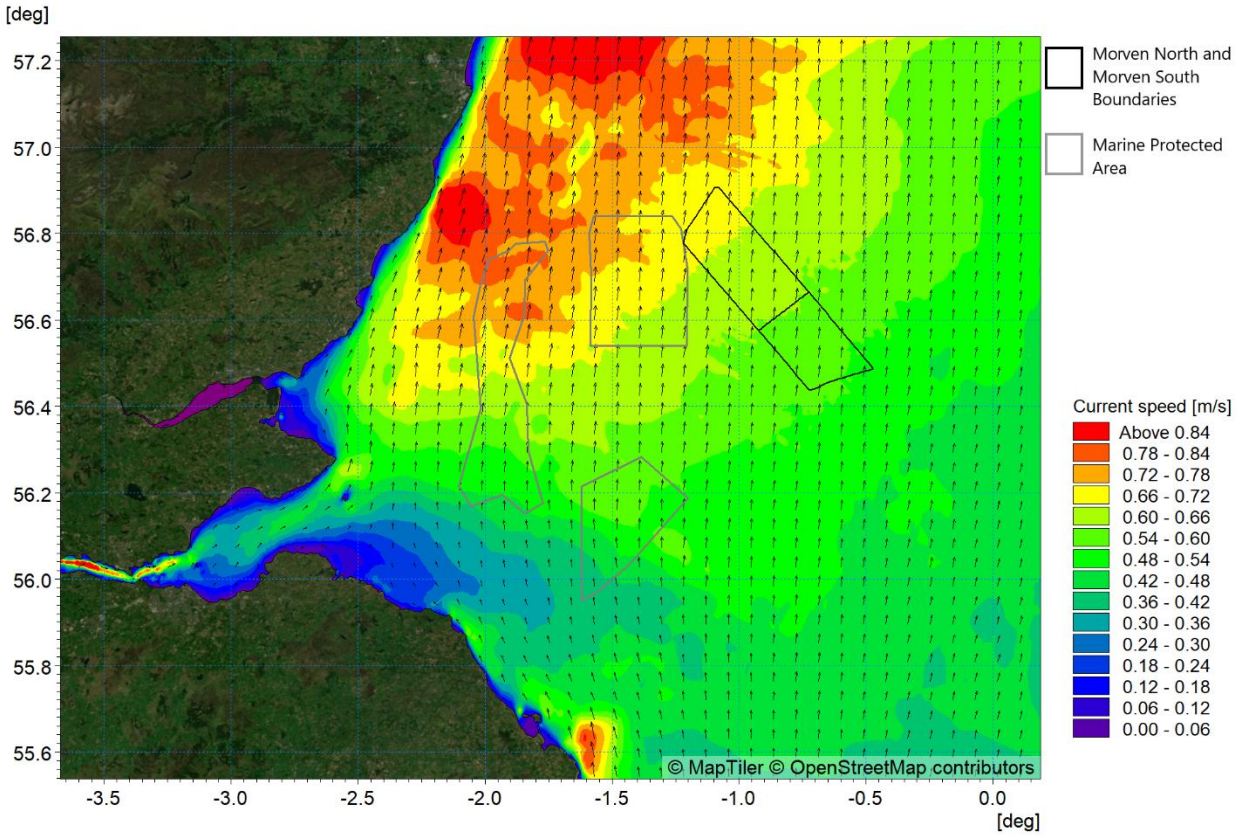

Figure 4.39: Tidal flow patterns – peak ebb (low water -1 hour)

4.4 Wave climate

4.4.1.1 In the North Sea, the propagation of tidal waves (as well as the dominant residual circulation) generally follows cyclonic patterns (Vindenes *et al.*, 2018). Strong winds can occur in the North Sea however, wave heights vary greatly due to water depth and fetch limitations (Royal Haskoning DHV, 2012). Annual mean significant wave height ranged from approximately 1.75m to 1.91m across the Morven North Boundary and 1.81m to 1.95m across the Morven South Boundary. Annual mean wave power ranged from approximately 13.8kW/m to 16.7kW/m across the Morven North Boundary and 14.8kW/m to 17.5kW/m across the Morven South Boundary (ABPmer, 2017).

4.4.1.2 The site specific metocean survey undertaken by Partrac deployed two Waverider buoys, one within the Morven North Boundary and one within the Morven South Boundary (as depicted in Figure 4.40). The Morven North Waverider was deployed between October 2022 and November 2023, whilst the Morven South Waverider was deployed between October 2022 and April 2024. The maximum spectral significant wave height (Hm0) recorded at the Morven North Waverider was 10.09m, with peak wave periods (Tp) up to 18.18 seconds, whilst the maximum Hm0 at the Morven South Waverider was 9.95m and Tp up to 20.00 seconds. The most significant storm during the deployment was Storm Babet from the east as recorded at both locations during October 2023. The dominant wave sectors in both the Morven North Boundary and Morven South Boundary were from the north northeast and north.

4.4.1.3 In addition to the data collected during the Partrac field study, longer term data was used in order to evaluate the baseline wave climate for more extreme events to enable assessment of Morven North and Morven South over a wider range of conditions. For this assessment, twenty-five years of ECMWF wave data was used.

4.4.1.4 In order to evaluate the potential changes in wave climate due to Morven North and Morven South, a comparative study was carried out. This meant that baseline wave climate was required; due to the comparative nature of the assessment, a full metocean study was not essential, however representative sea-states were required.

4.4.1.5 An analysis was undertaken to determine the offshore conditions for which waves reach the site from all directions. Twenty-five years of ECMWF data were obtained for multiple locations on the northern, eastern and southern boundaries of the model domain. The wave roses for these sites are presented in Figure 4.41 overlain on the model domain at the locations to which they relate. Extreme value analysis using peak over threshold was undertaken for the principal sectors to determine the 1 in 1 and 1 in 20 year offshore wave climate. These were then used as boundary conditions within the wave modelling to determine the resultant wave climate at the site and across the Regional Physical Processes Study Area.

4.4.1.6 In addition to boundary wave data, it was necessary to analyse the wind field to include the contribution of local wind seas. For this, a representative point was identified and utilised from the ECMWF 15 year dataset for the relevant sectors, as the variation in wind speed was found to have consistency across the domain. The wind rose for this period is presented in Figure 4.42. This was analysed on the same sectoral basis as the wave data to give an indication of the return period wind speed.

4.4.1.7 The wave modelling was undertaken using the spectral wave model, MIKE21 SW, to provide a full wave climate and wave breaking across the Physical Processes Study Area. The model used a quasi-stationary formulation which meant that for each event the wave field fully established over a number of numerical iterations until convergence was reached. The waves were computed on the same grid as the tidal flows. The model resolves the wave field by simulating wind generation of waves within the model domain and the propagation of externally generated swell waves through the domain. The model setup ensured that the detail of both locally generated wind waves and swell conditions from further afield were captured.

4.4.1.8 The resulting magnitude of the waves transformed from offshore correlate with those recorded during the Partrac measurement campaign. Data from the two Waverider Buoy datasets were compared with data produced from the model during Storm Babet in October 2023, where the most extreme wave climate was captured within both the Morven North Boundary and Morven South

Boundary. The location of the two buoys (Partrac North and Partrac South) are shown in Figure 4.40 and model validation plots for significant wave height, Tp and Mean Wave Direction (MWD) are presented in Figure 4.43, Figure 4.44 and Figure 4.45 respectively. The figures demonstrate that the modelled storm event correlates well with the recorded data, taking account of the spatial and temporal resolution of atmospheric and wave data input to the model.

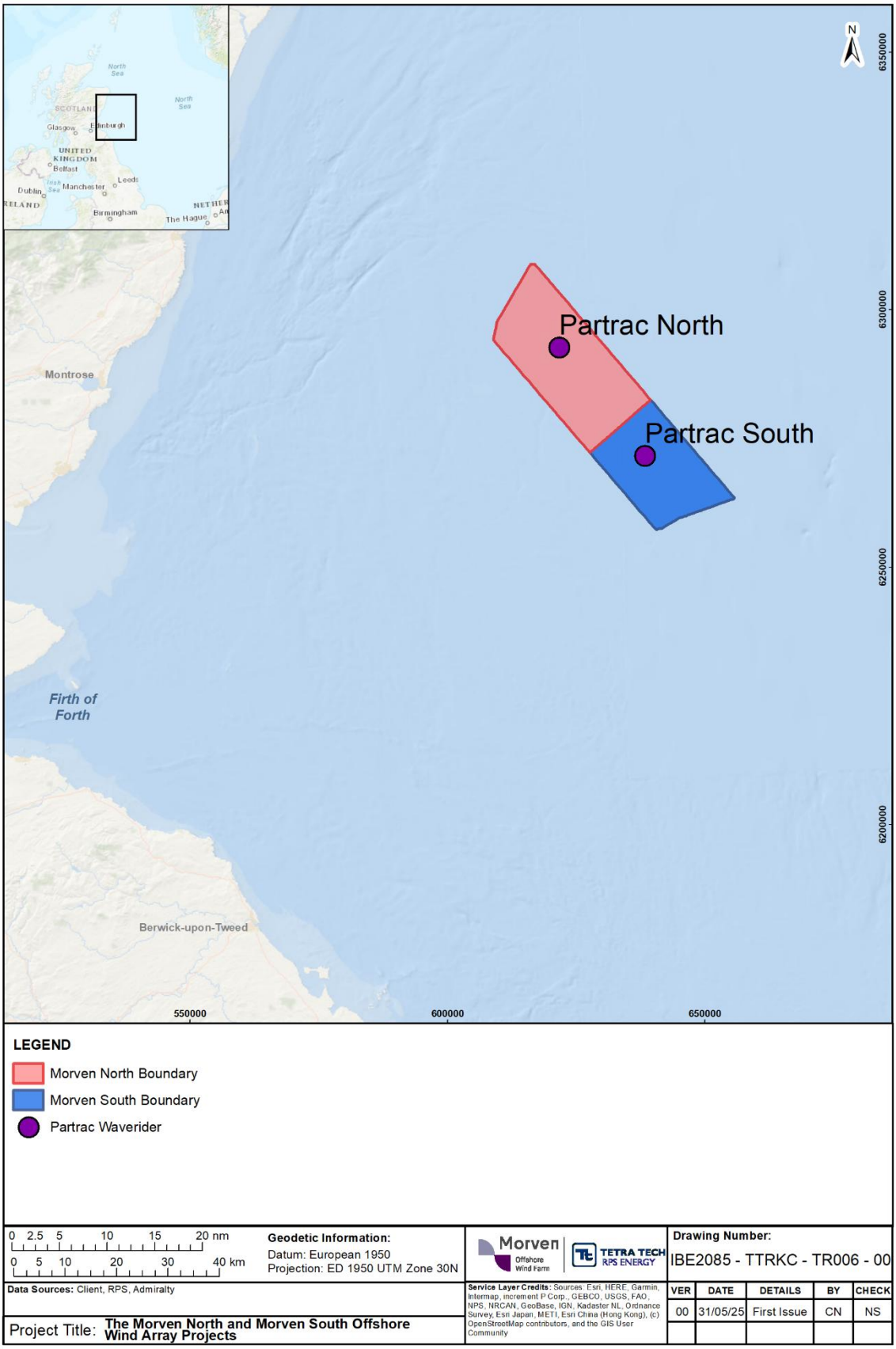

Figure 4.40: Location of selected wave calibration datasets related to Morven North and Morven South physical processes modelling

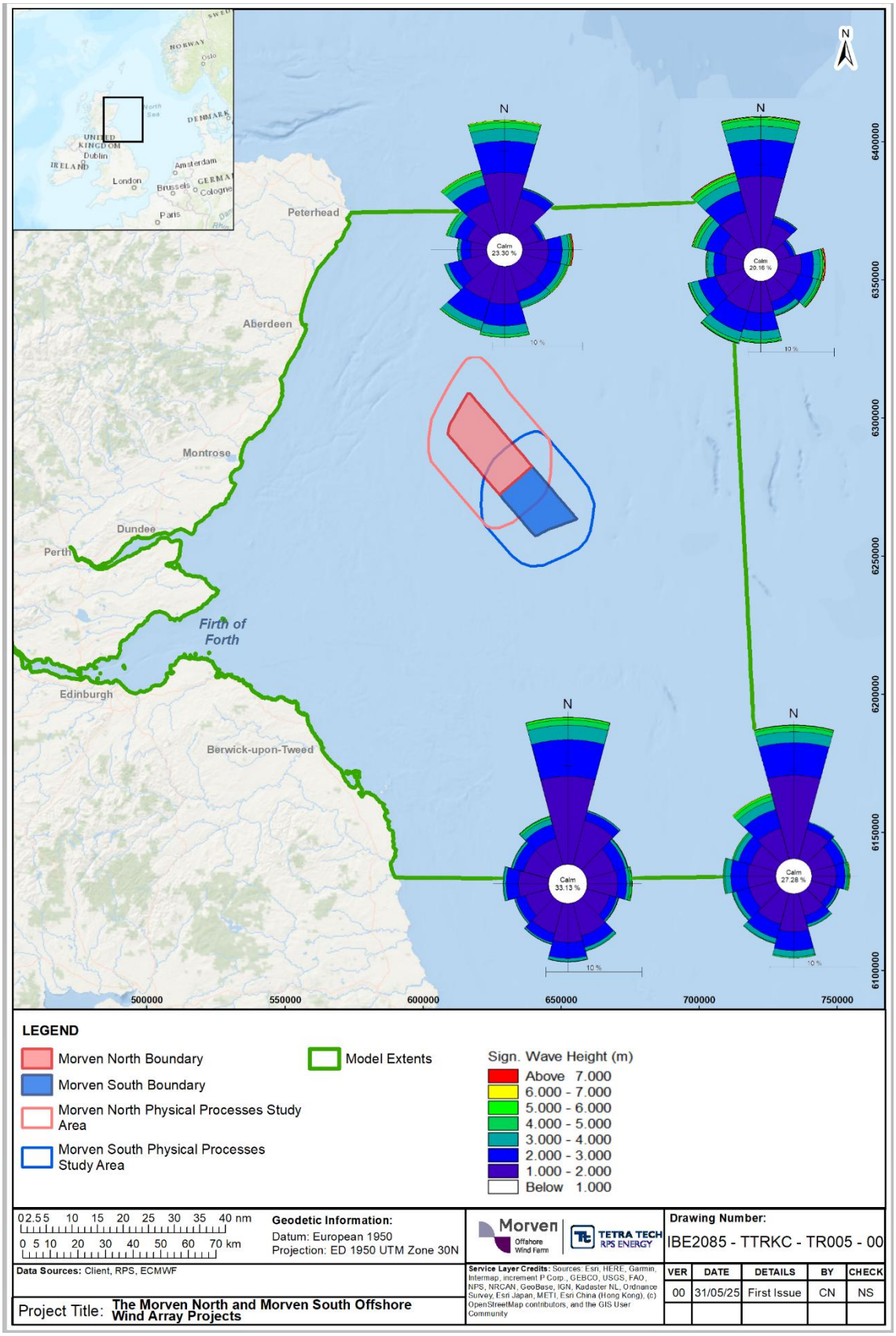

Figure 4.41: Wave roses for model boundaries – 25 year European Centre for Medium-Range Weather Forecast dataset (relating to Morven North and Morven South physical processes modelling)

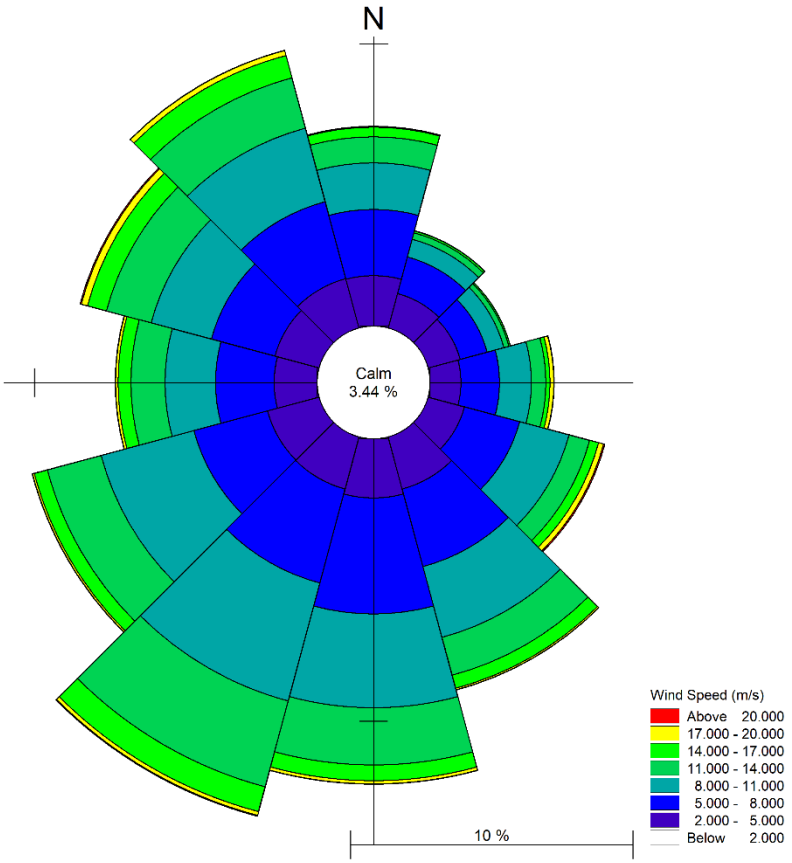

Figure 4.42: Wind roses applied to model – 15 year European Centre for Medium-Range Weather Forecast dataset (related to Morven North and Morven South physical processes modelling)

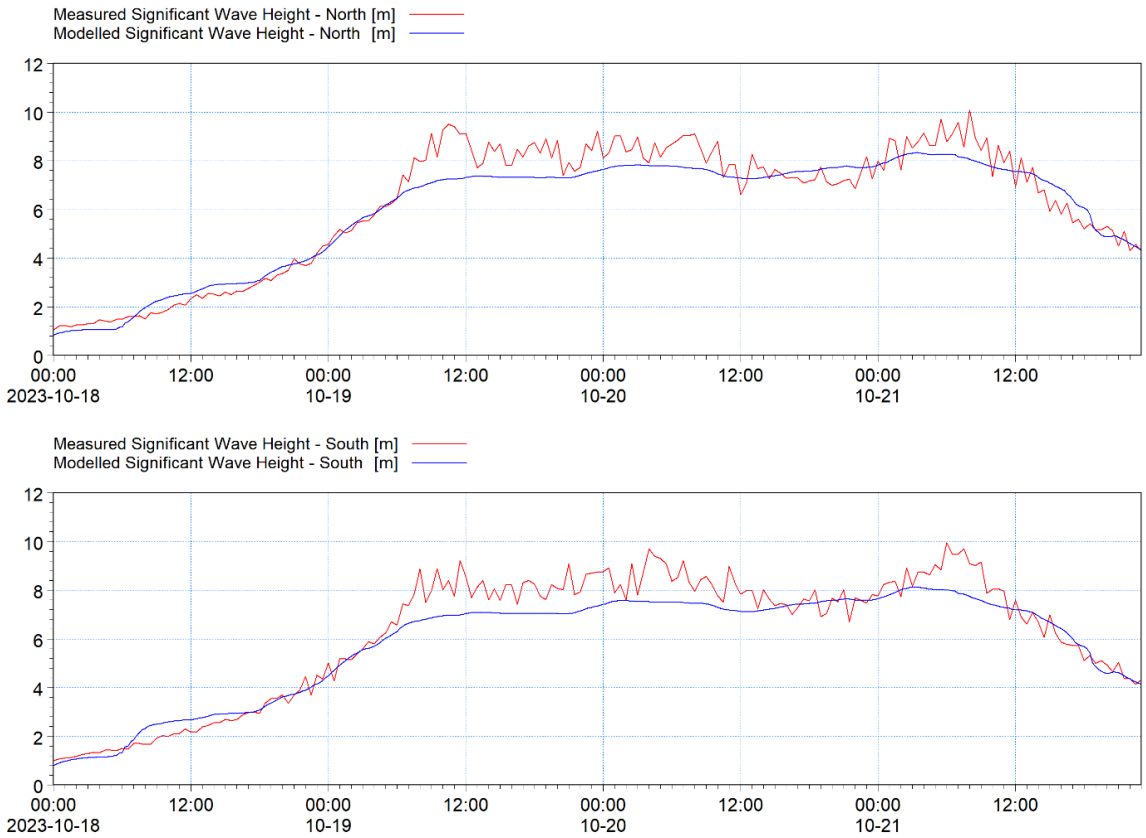

Figure 4.43: Comparison of model and recorded data - October 2023– Partrac North and South – Spectral significant wave height

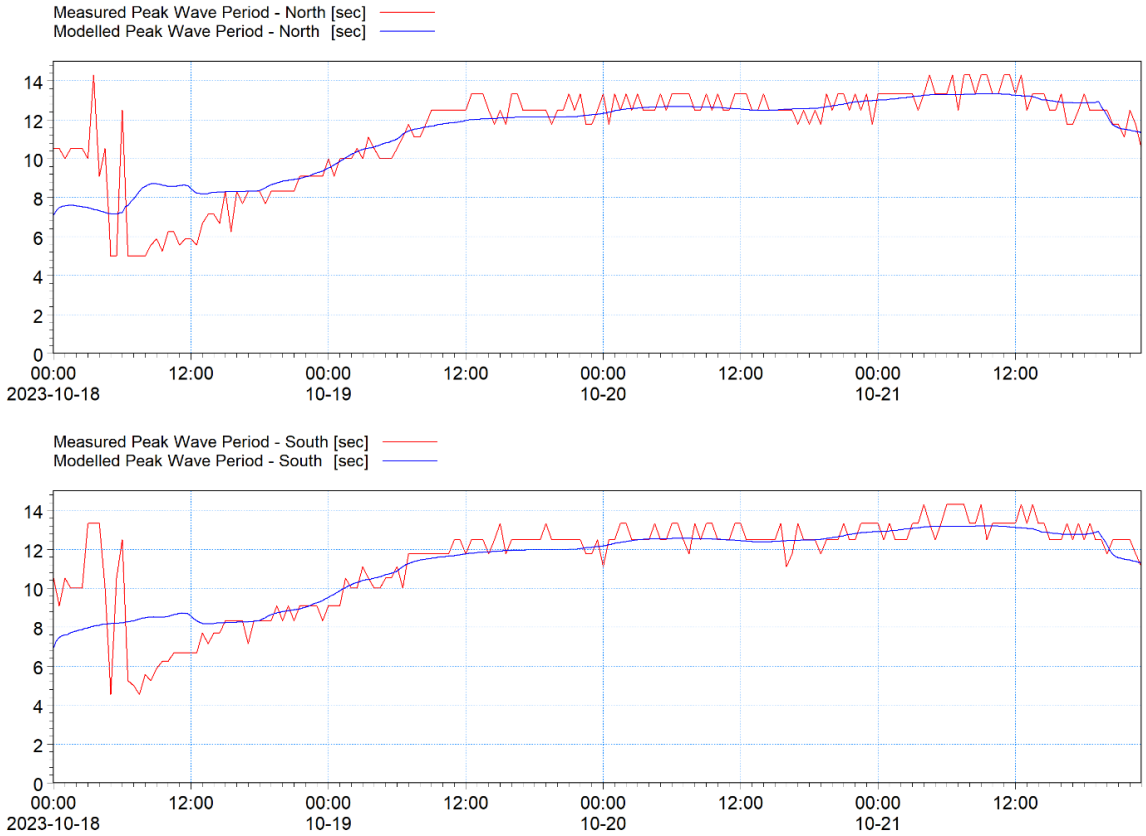

Figure 4.44: Comparison of model and recorded data - October 2023– Partrac North and South – Peak wave period

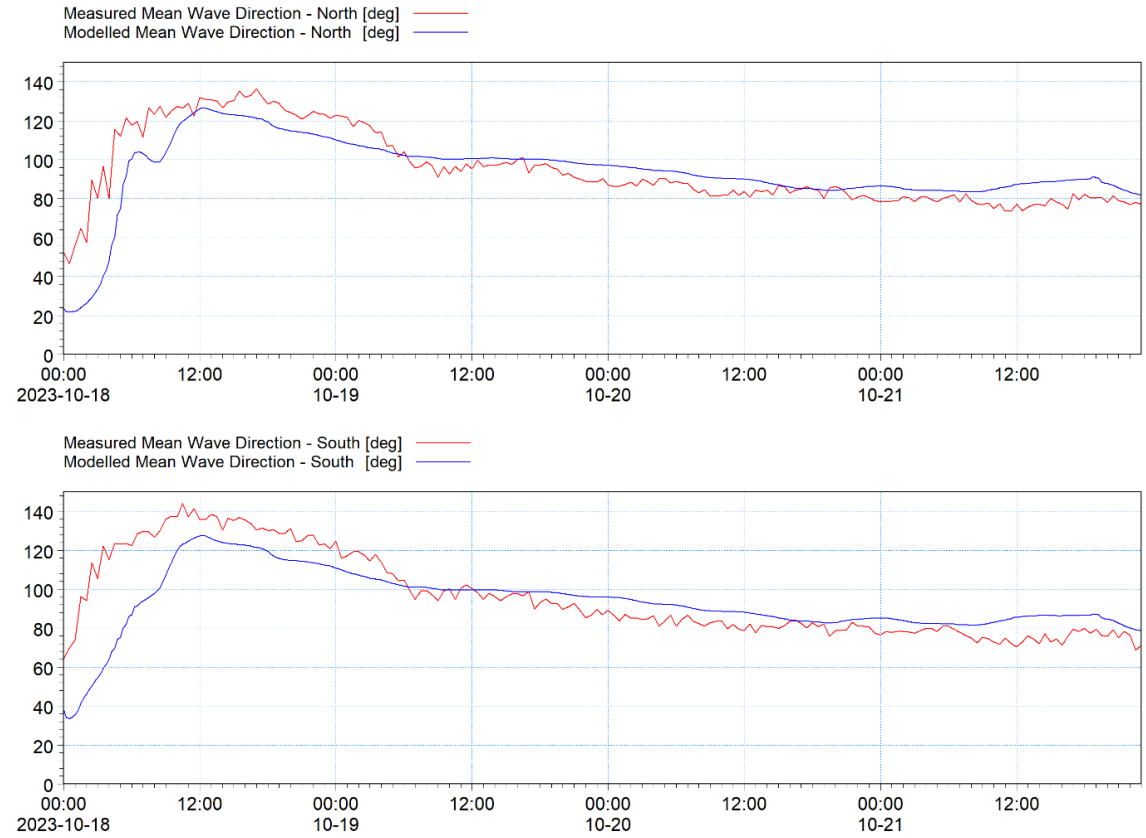

Figure 4.45: Comparison of model and recorded data - October 2023– Partrac North and South – Mean Wave Direction

4.4.1.9 The following set of figures (Figure 4.46 to Figure 4.50) show the wave climate for five 1 in 1 year return period events; from a northerly (000°), northeasterly (045°), easterly (090°), southeasterly (135°) and southerly (180°) direction. These sectors were selected to be representative of the different characteristics of the wave climate and also for sectors for which Morven North and Morven South may potentially affect marine processes along the coastline. Although the modelling was undertaken throughout the tidal cycle, the variation in wave climate throughout the cycle was limited, therefore the figures presented relate to Mean Sea Level(MSL) mid flood tide. Figure 4.48 shows the waves approaching from the east and demonstrates, as shown by the ECMWF wave roses in Figure 4.41, the largest waves approach from this sector, although the majority of waves approach from the north.

4.4.1.10 A second set of figures are presented relating to the 1 in 20 year return period. Figure 4.51 to Figure 4.55 present the data for the same sectors and tidal height as the 1 in 1 year return period. They have been presented to ensure that the baseline for more extreme conditions is established for assessment of the potential effect of Morven North and Morven South on wave climate.

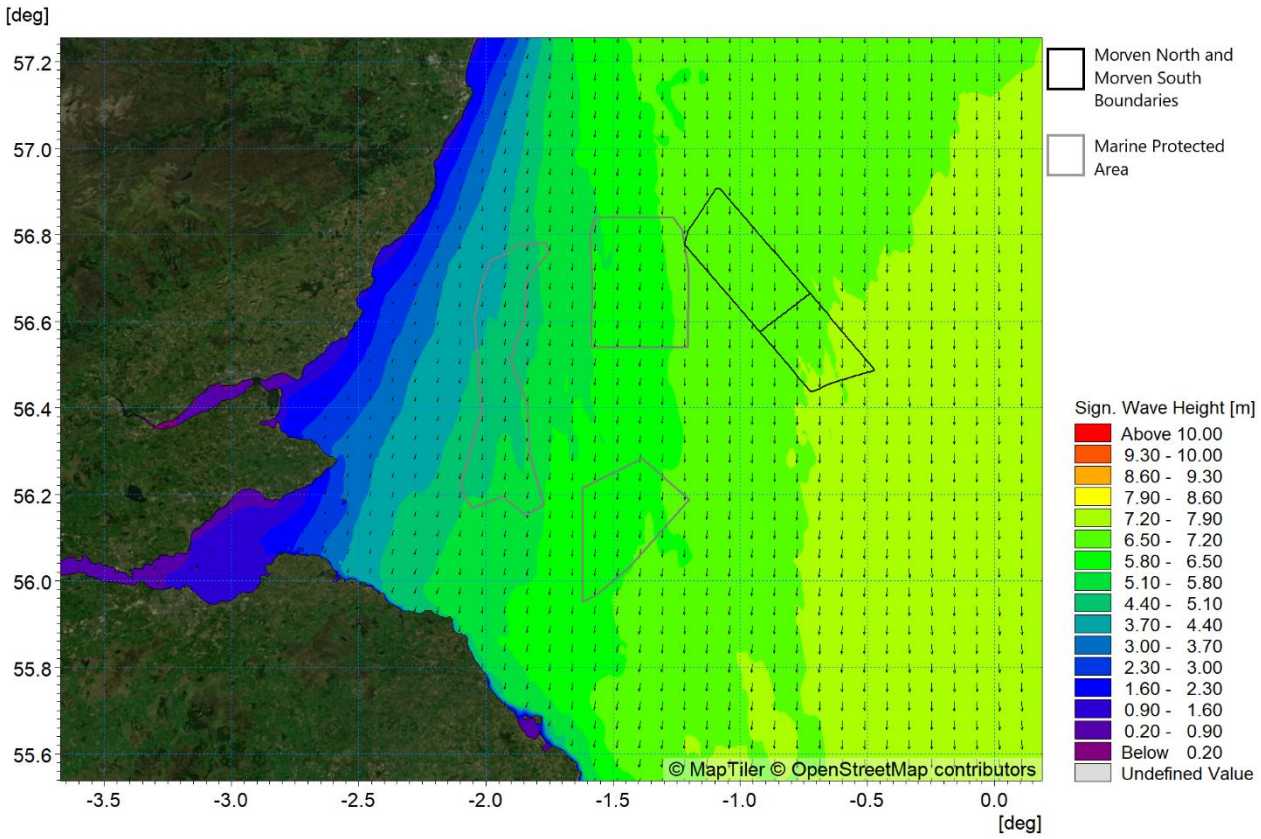

Figure 4.46: Wave climate 1:1 year storm from 000° at mid-tide

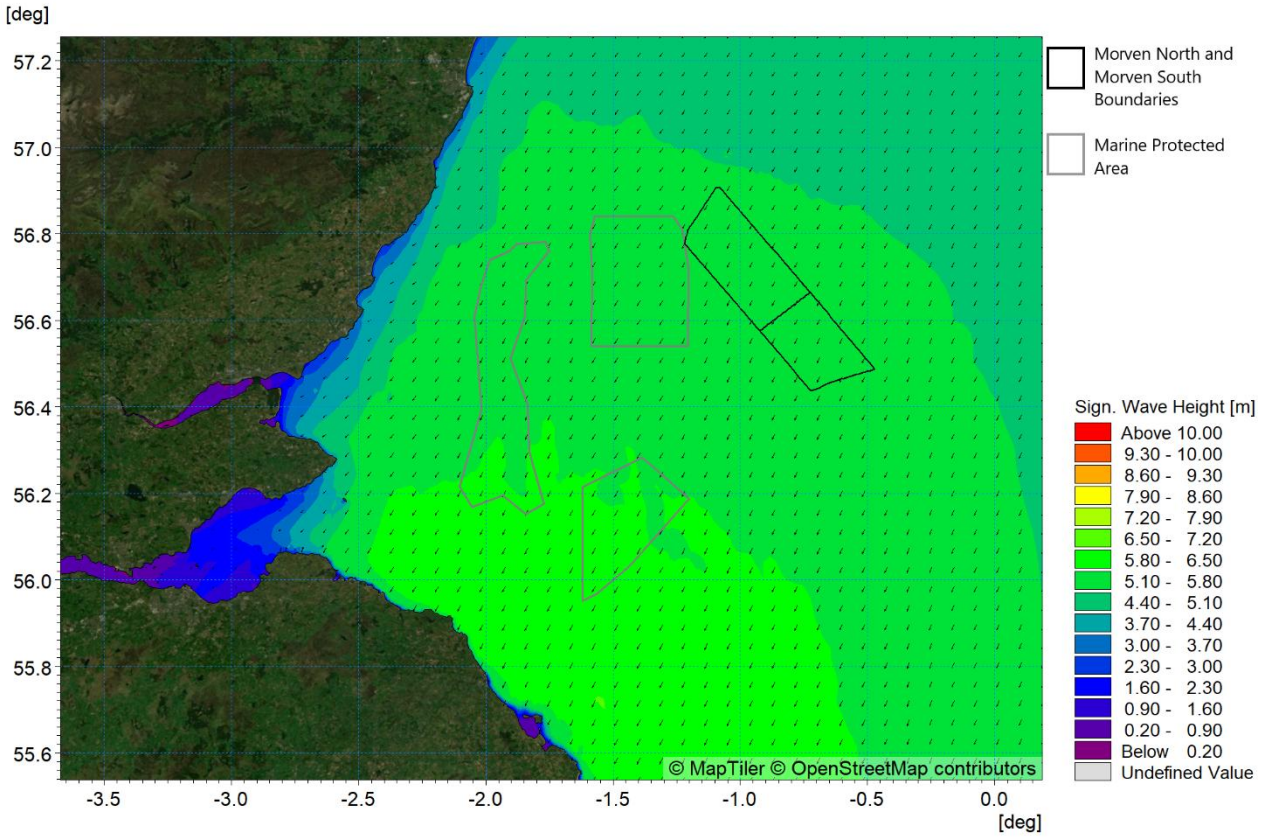

Figure 4.47: Wave climate 1:1 year storm from 045° at mid-tide

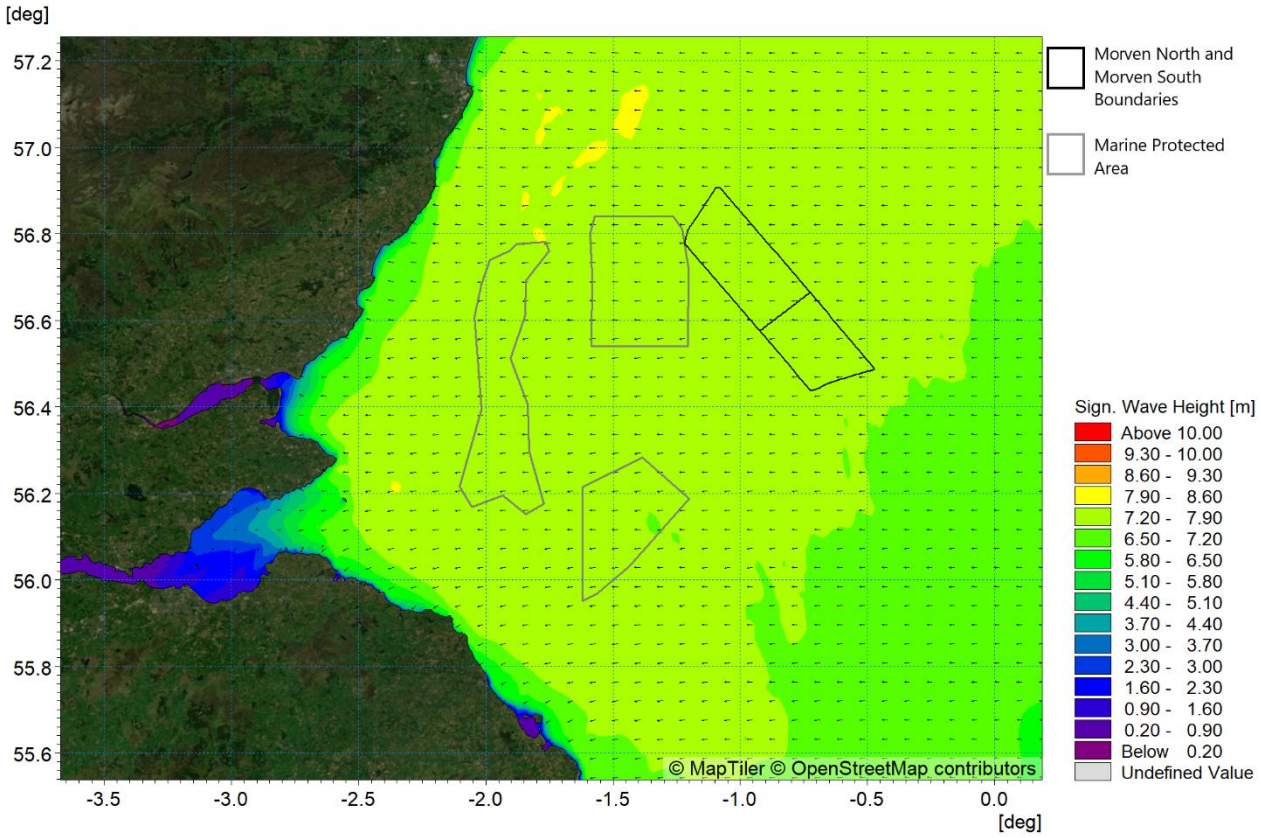

Figure 4.48: Wave climate 1:1 year storm from 090° at mid-tide

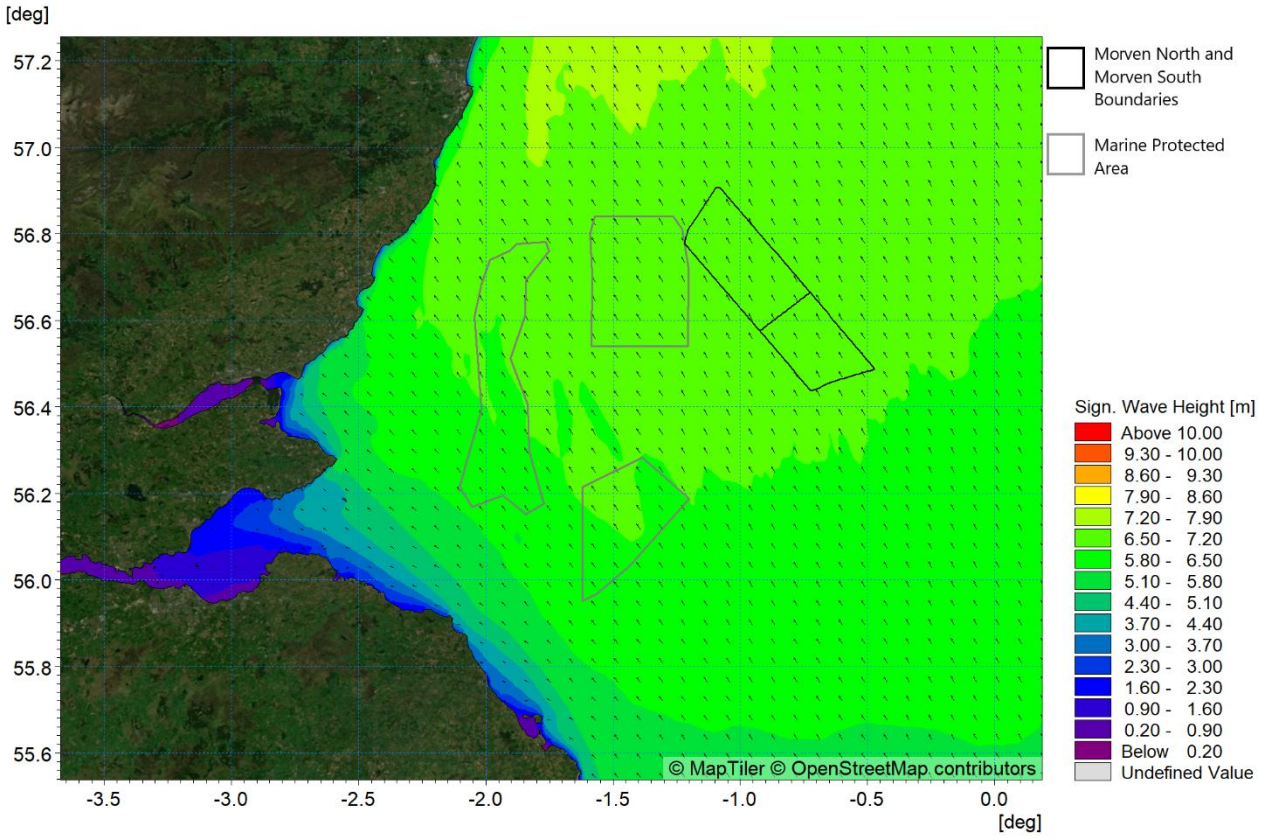

Figure 4.49: Wave climate 1:1 year storm from 135° at mid-tide

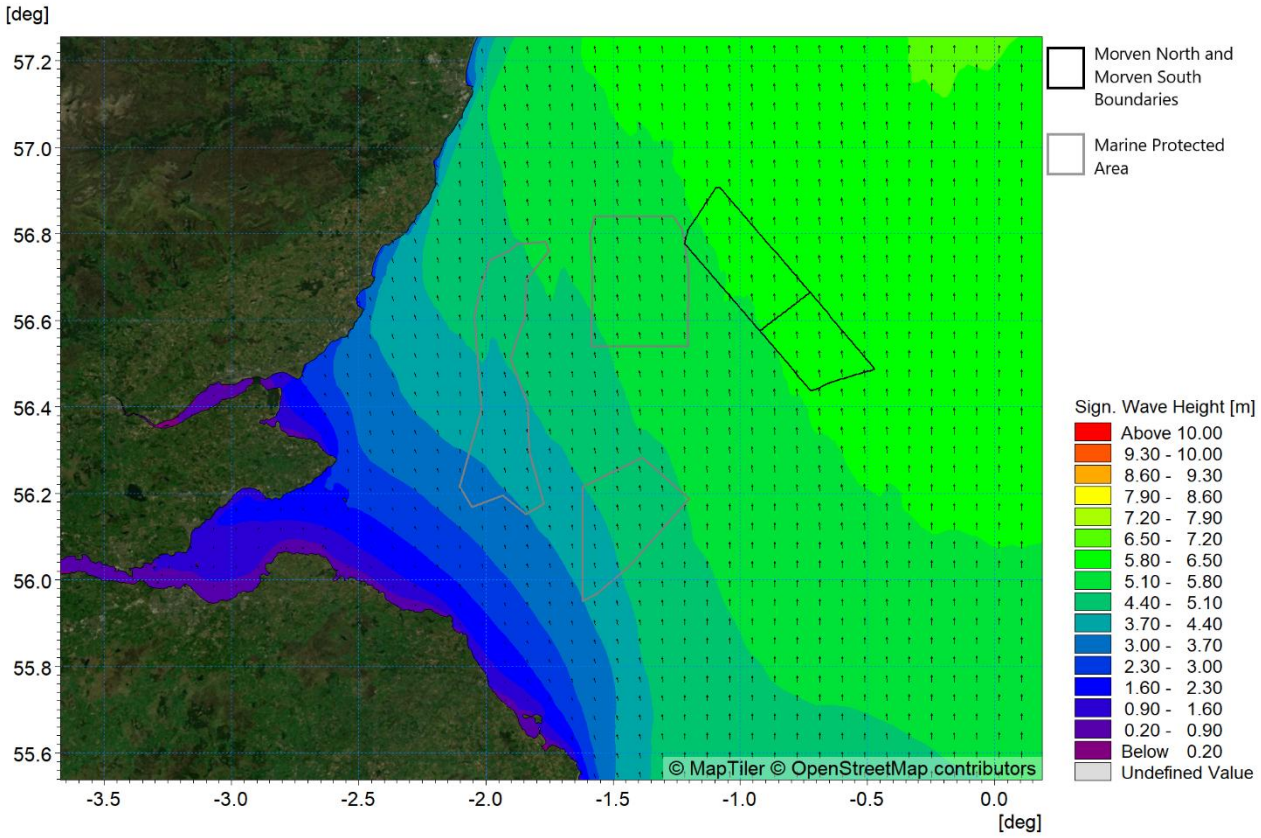

Figure 4.50: Wave climate 1:1 year storm from 180° at mid-tide

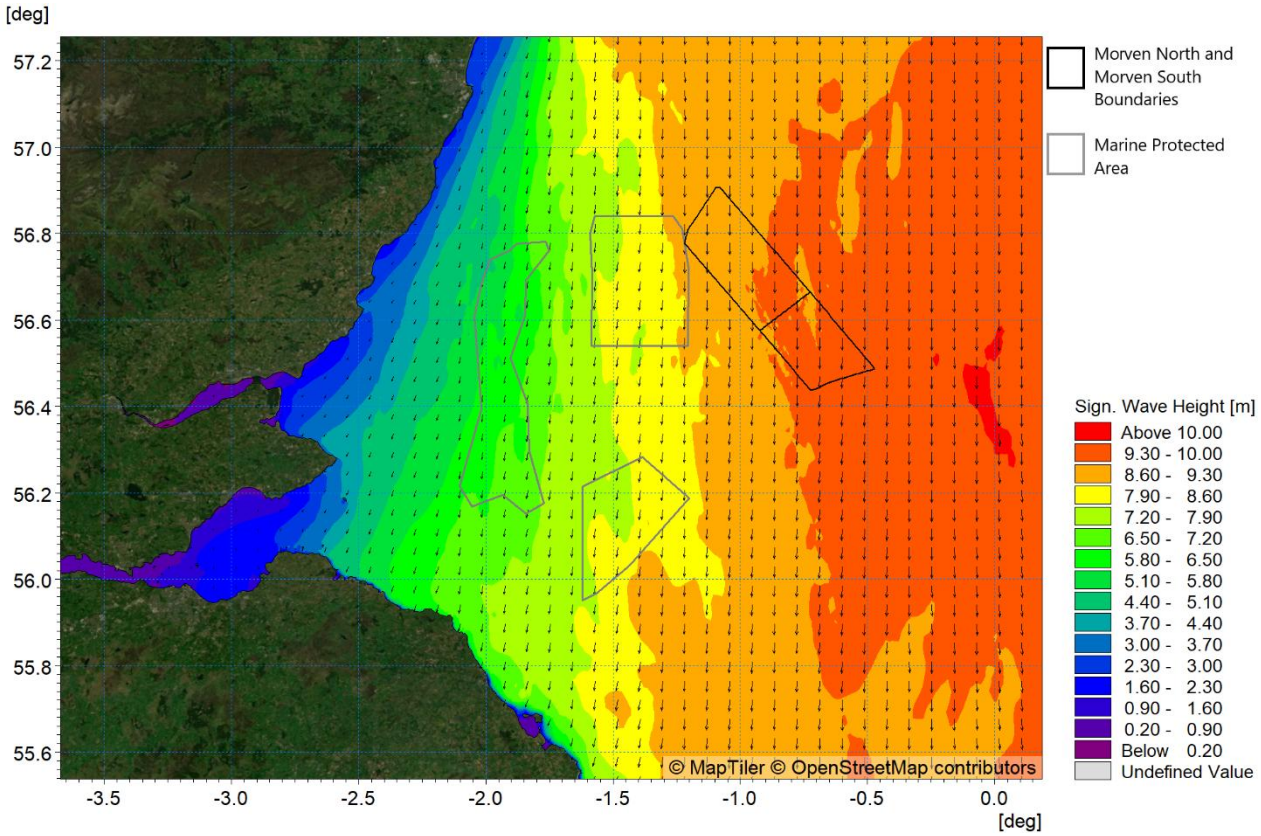

Figure 4.51: Wave climate 1:20 year storm from 000° at mid-tide

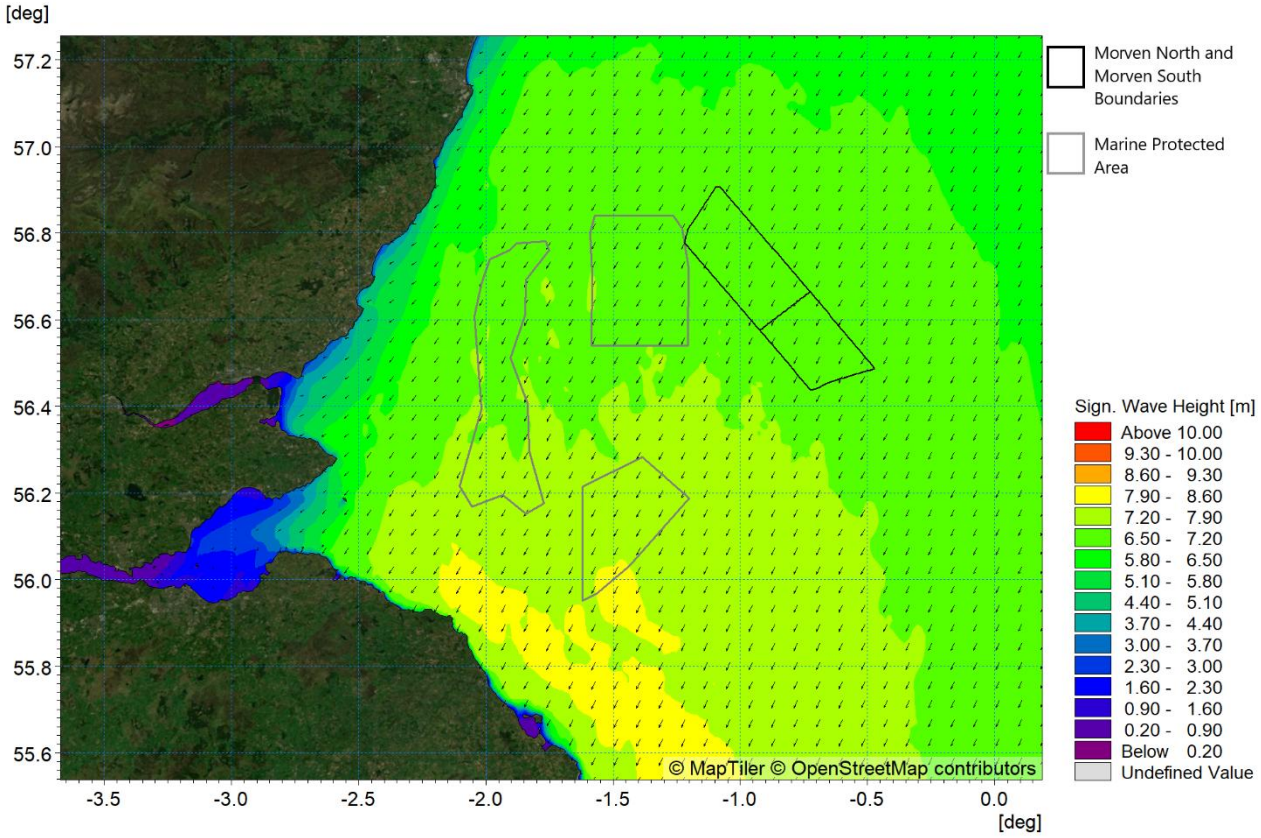

Figure 4.52: Wave climate 1:20 year storm from 045° at mid-tide

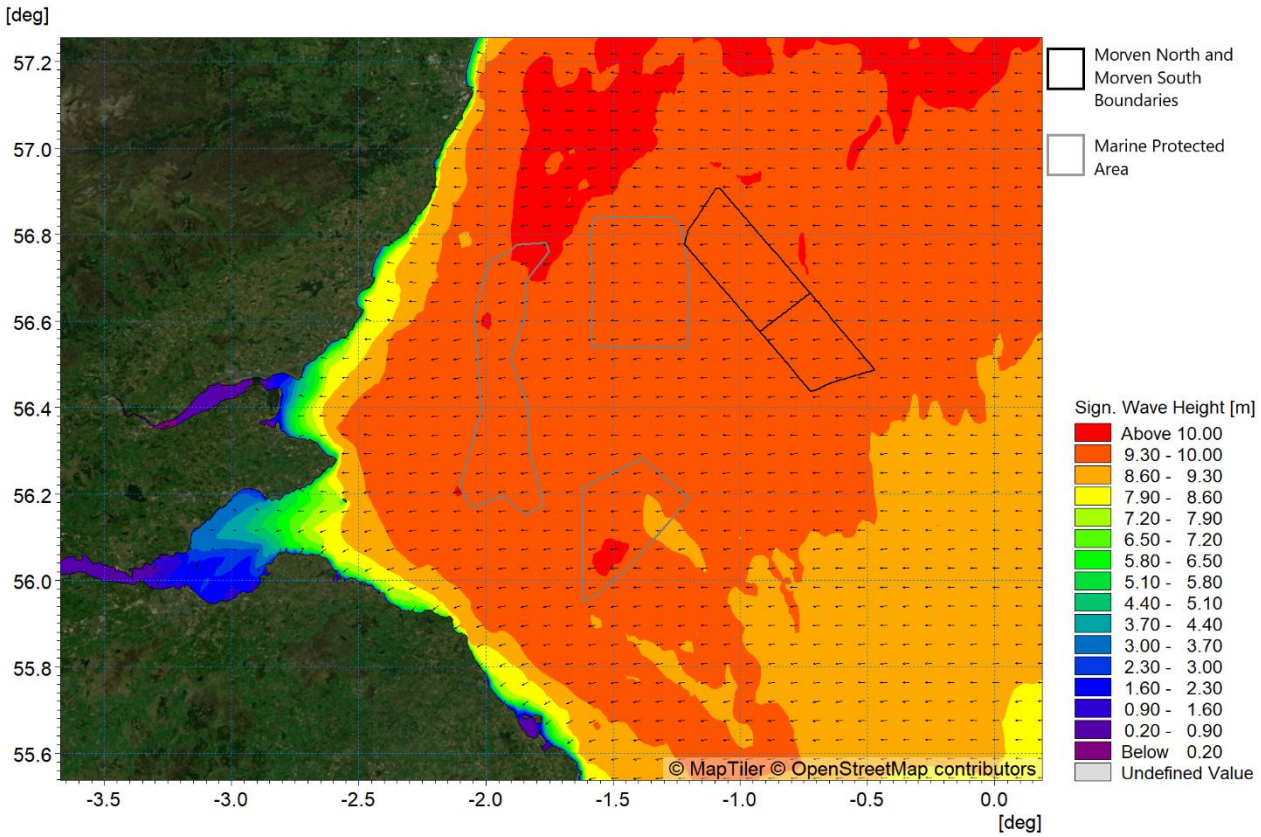

Figure 4.53: Wave climate 1:20 year storm from 090° at mid-tide

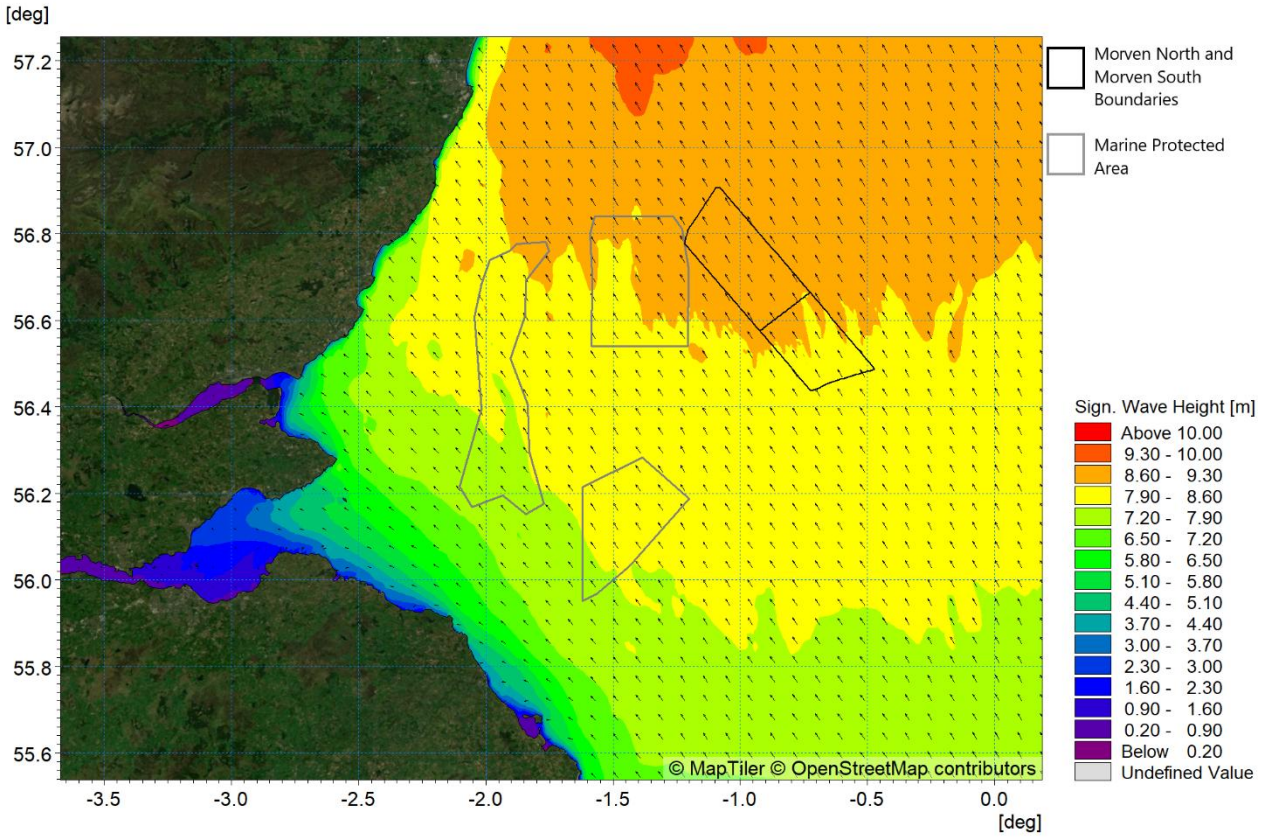

Figure 4.54: Wave climate 1:20 year storm from 135° at mid-tide

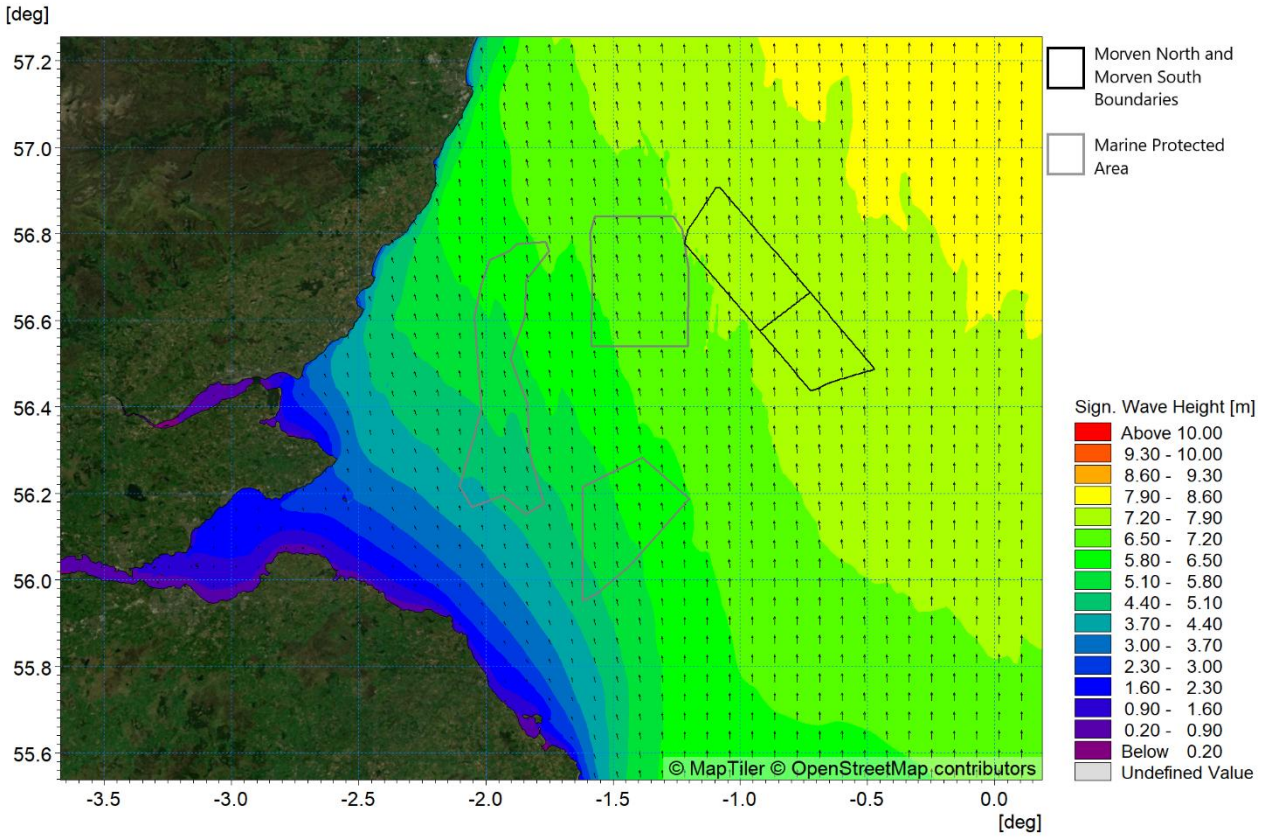

Figure 4.55: Wave climate 1:20 year storm from 180° at mid-tide

4.5 Littoral currents

4.5.1.1 A range of tidal and wave conditions were modelled independently, as presented under Sections 4.3 and 4.4 respectively, however the MIKE suite also facilitates the coupling of models. The depth averaged hydrodynamic model, used for the tidal modelling, coupled with the spectral wave model, provides a full wave climate incorporating the impact of water levels and currents on waves and wave breaking. For completeness, this has been used to provide a sample of the littoral currents (i.e. those currents driven by tidal, wave and meteorological forces) for examination. Currents in the Regional Physical Processes Study Area are primarily tide driven, with a residual component driven by storms. The modelled scenario was chosen based on the dominant wave direction from the north.

4.5.1.2 The 1 in 1 year storm from the dominant 000° sector was simulated with the inclusion of large spring tides to include a wide range of tidal conditions and the resulting peak flood and peak ebb currents are presented in Figure 4.56 and Figure 4.57 respectively. These correspond with the (calm) tidal plots presented in Figure 4.38 and Figure 4.39 in terms of tidal state. As expected, the presence of the northerly waves travelling southwards increase the currents on the flood tide whilst reducing them on the ebb.

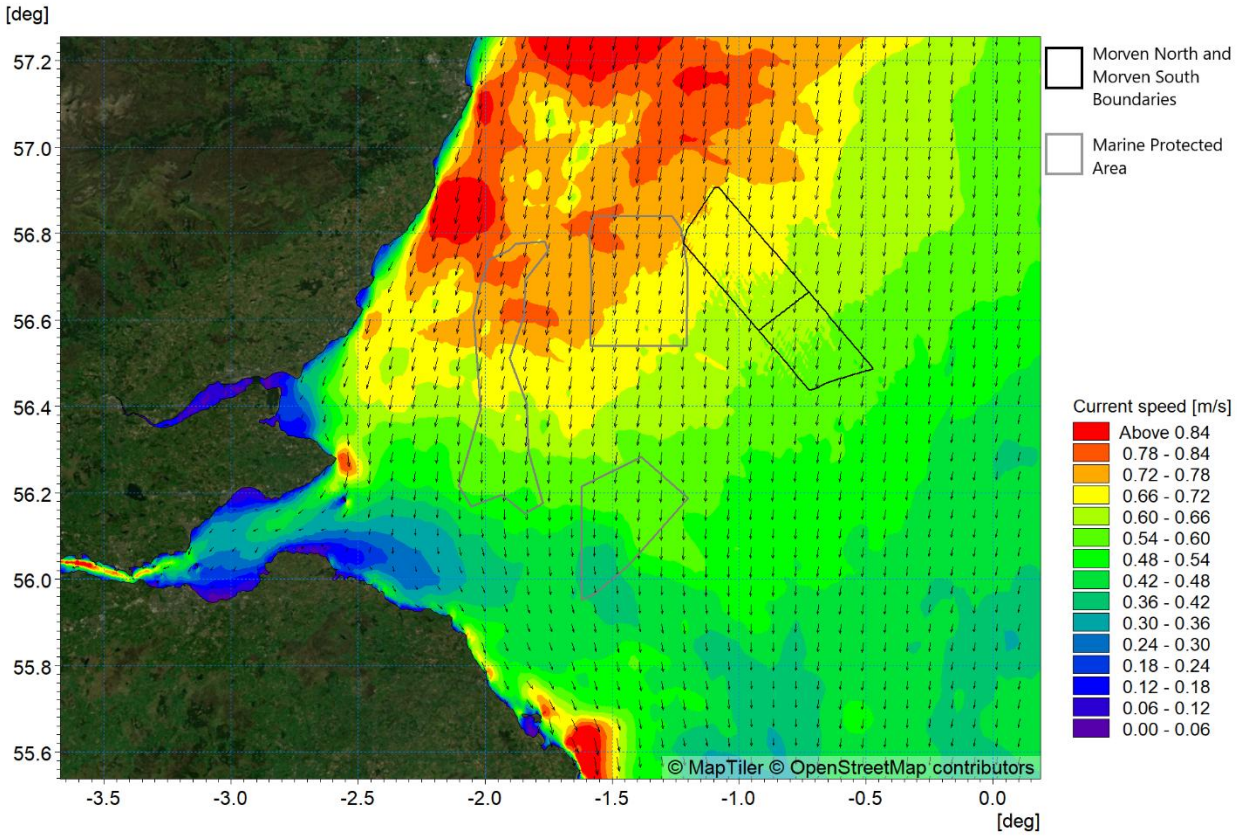

Figure 4.56: Littoral current 1:1 year storm from 000° - flood tide (high water – 1 hour)

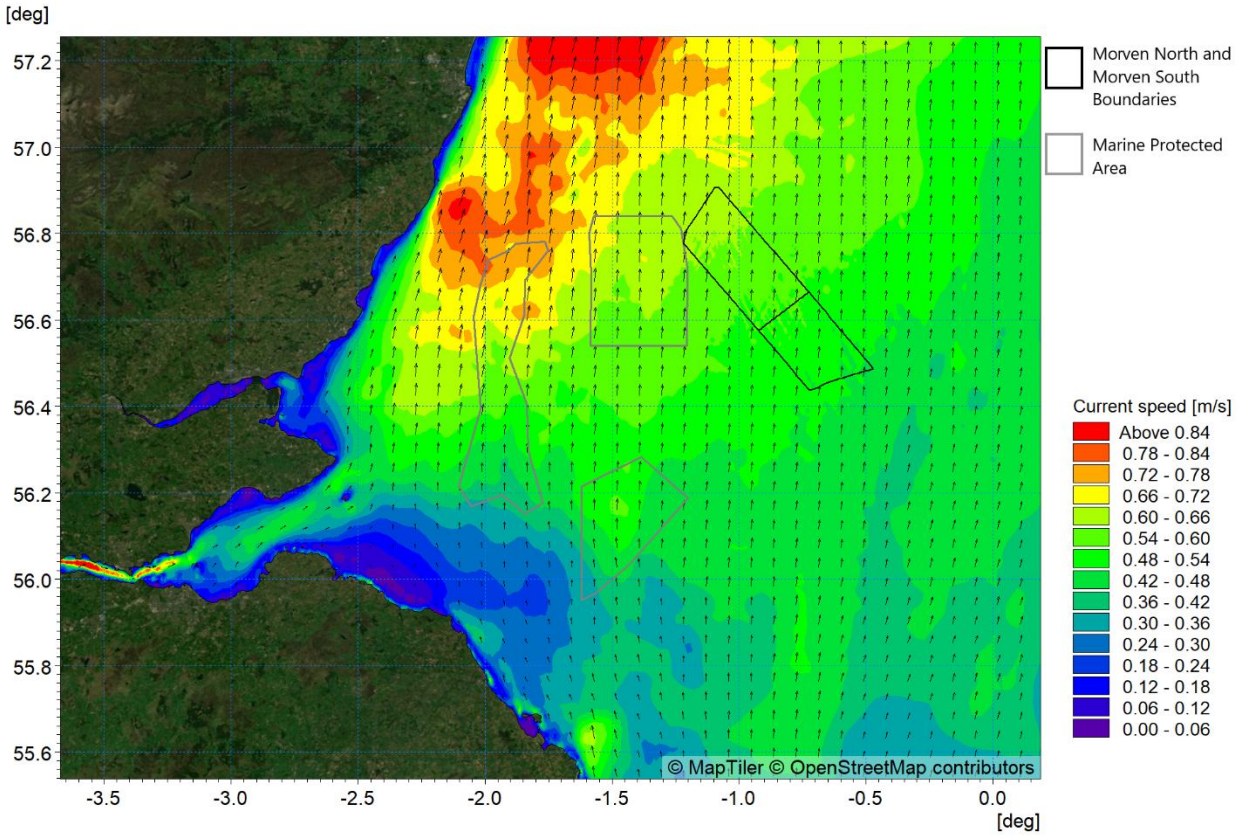

Figure 4.57: Littoral current 1:1 year storm from 000° - ebb tide (low water – 1 hour)

4.6 Water column processes

4.6.1.1 According to the results from the site specific survey undertaken by Partrac between October 2022 and May 2024, seasonal stratification is evident within the Morven North Boundary and the Morven South Boundary (Partrac, 2024). The degree of baseline seasonal stratification has been assessed using available desktop data sources (Note potential changes to seasonal stratification due to the infrastructure were assessed using a modelling study, as outlined in Section 5.2.4).

4.6.1.2 The Partrac study included Conductivity Temperature Depth (CTD) measurements at the locations shown in Figure 4.40. CTD profile data was available on a number of days throughout the campaign at two points (Partrac North and Partrac South) within the Morven North Boundary and Morven South Boundary respectively. Figure 4.58 and Figure 4.59 show the profiles for temperature and salinity over a range of dates from October 2022 to May 2024 at Partrac North, and Partrac South, respectively. Both figures show a consistent temperature and salinity profile throughout the water column during the months of October through to February, with a small difference between surface and bed temperatures and salinities in early May 2024, towards the onset of stratification. At Partrac North, where data is available on 30 May 2023, the thermocline was located from circa 12m to 17m depth, with uncertainty in the position of the halocline due to the range of available salinity data. In August 2023, the thermocline was seen to deepen to between circa 26m to 32m at Partrac North or circa 26m to 28m at Partrac South. In each case, the warmer surface layer can be clearly observed above the thermocline, with the cooler deeper layer positioned below the thermocline, and thus evidence of seasonal stratification within the Morven North Boundary and Morven South Boundary is presented.

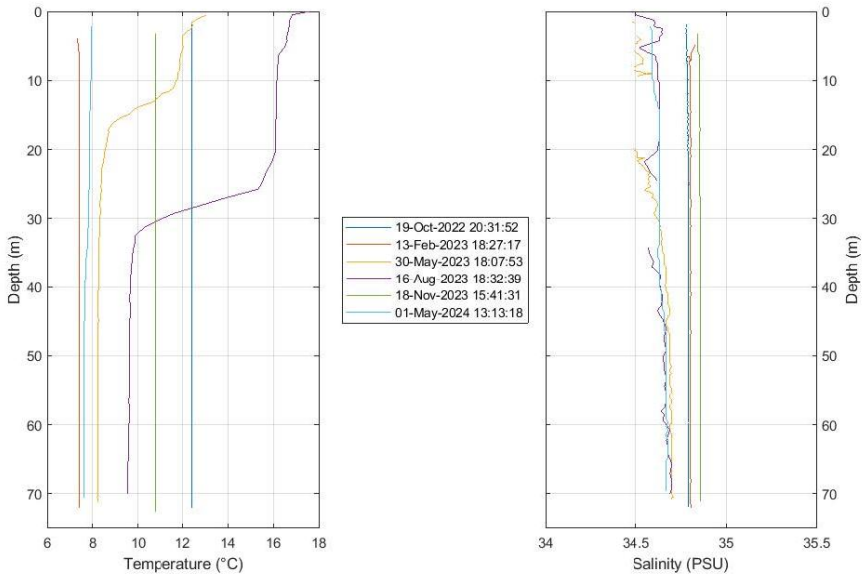

Figure 4.58: Partrac North Conductivity Temperature Depth Profile – temperature and salinity profiles (Partrac, 2024)

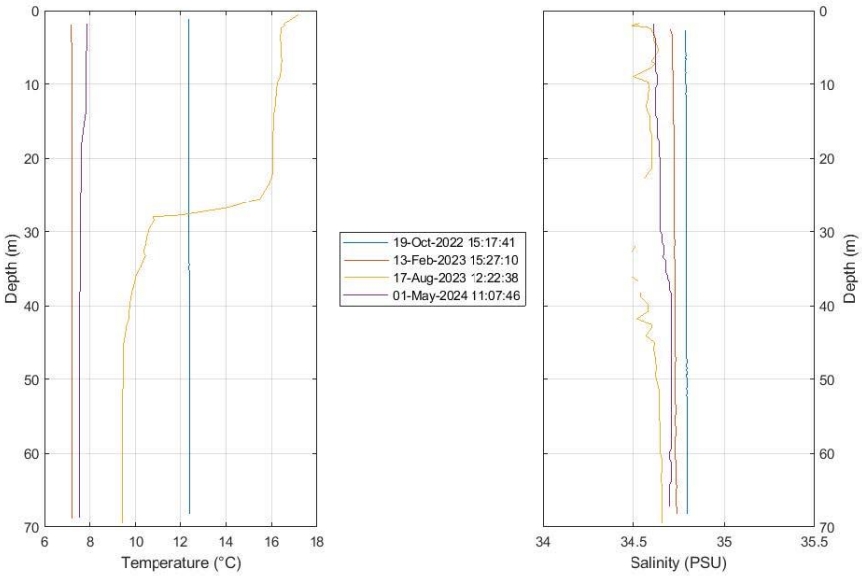

Figure 4.59: Partrac South Conductivity Temperature Depth Profile – temperature and salinity profiles (Partrac, 2024)

4.6.1.3 The SSW-RS (Barton *et al*., 2022) provides a 27 year reanalysis dataset (1993 to 2019) of the Scottish Shelf Model (De Dominicis *et al*., 2018), which covers the Scottish continental shelf waters. This dataset was the focus of the baseline assessment, which provides 20 vertical layers of temperature and salinity data as daily average or hourly values over the 27-year period. A typical year was extracted from the dataset following an analysis of daily average temperature values at a central test point (56° 39.72000' N, 00° 52.50000'W) during the stratified period over the last 10 years. The test point is located centrally within the Morven Site and is represented by a 'T' within Figure 4.60. It was noted from the data that it is the variation in near-surface and near-bed temperatures which is most apparent compared to salinity differences, and ultimately the dominant and most critical factor of the stratification. 2016 was selected as a typical year for further assessment, with onset of seasonal stratification occurring from April and peaking on 02 August, before decaying rapidly in late summer and early autumn, as shown in Figure 4.61.

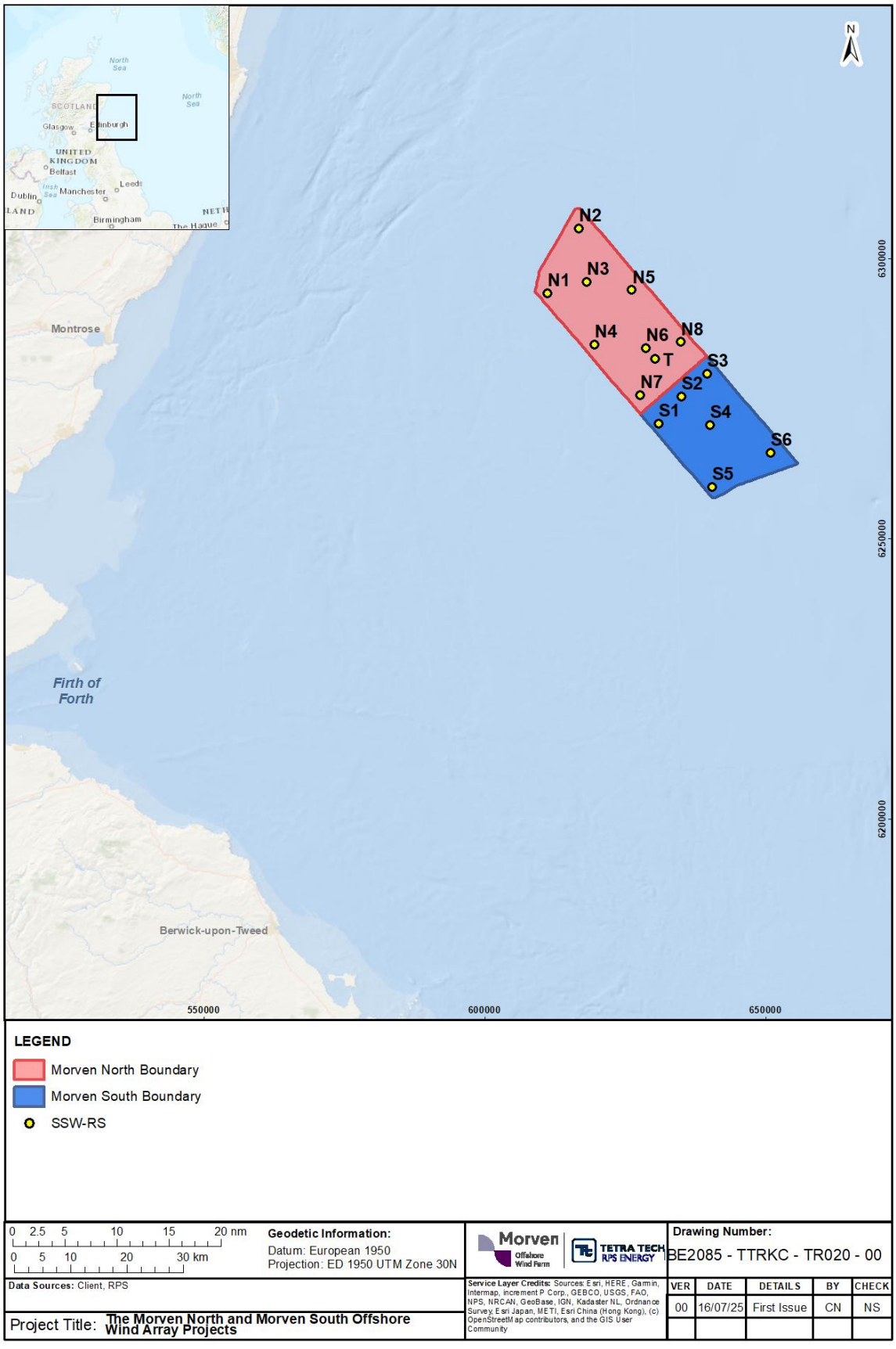

Figure 4.60: Scottish Shelf Waters Reanalysis Service Stratification analysis points within the Morven North Boundary and Morven South Boundary

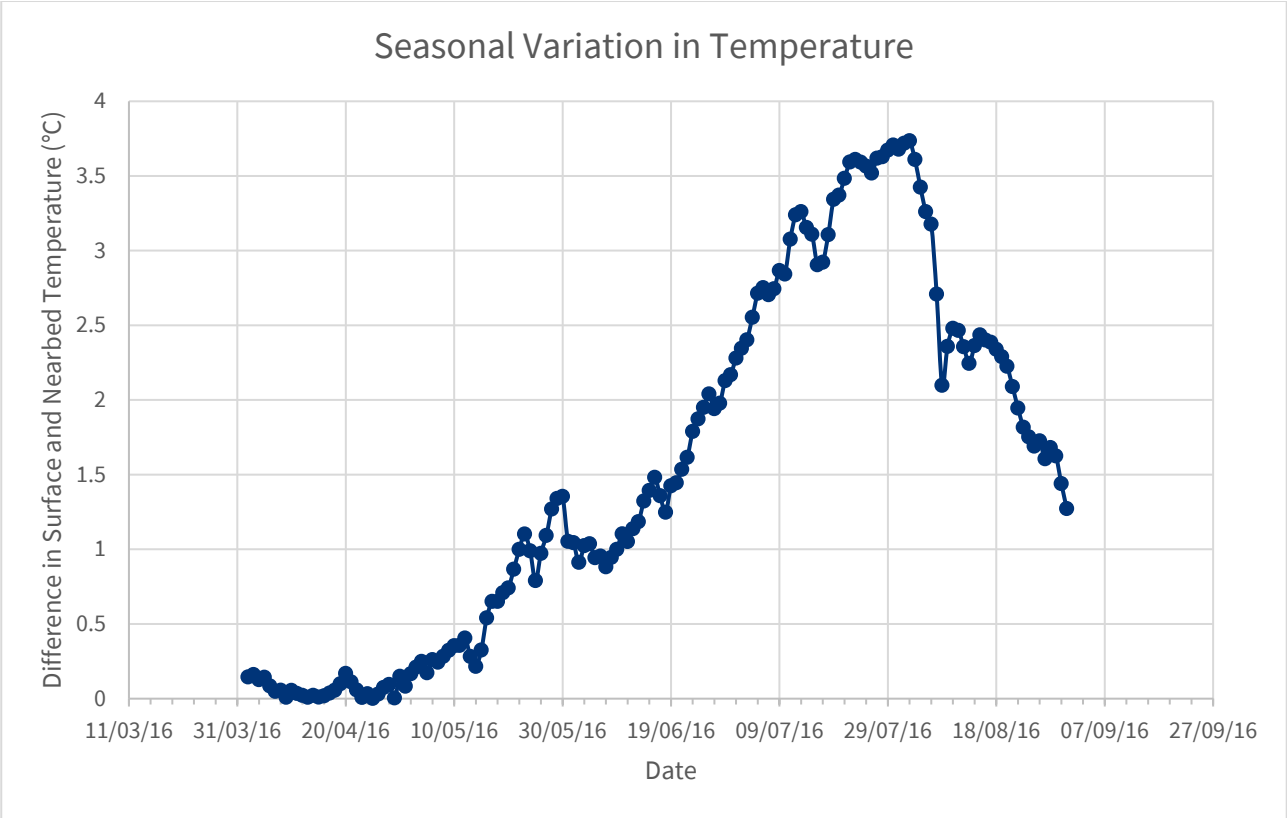

Figure 4.61: Seasonal variation in temperature (near-surface minus near-bed) at 56° 39.72000' N, 00° 52.50000'W (Barton *et al.*, 2022)

4.6.1.4 Following selection of a typical year of stratification, assessment of the spatial temperature variation at the peak on 02 August 2016 across the Morven North Boundary and Morven South Boundary was undertaken to ensure the optimum representation for further assessment. Eight points within the Morven North Boundary were analysed (N1 to N8) with a further six points within the Morven South Boundary (S1 to S6), as shown in Figure 4.60. The difference between near-surface and near-bed values is greatest within the Morven South Boundary compared to within the Morven North Boundary.

4.6.1.5 Within the Morven North Boundary, the greatest stratification occurred in the south with differences between near-surface and near-bed temperatures up to 3.92°C at point N8, as shown in Figure 4.62 by the SSW-RS data on 02 August 2016. The least stratified area within the Morven North Boundary is in the north at point N2, with a temperature difference of 1.98°C.

4.6.1.6 Within the Morven South Boundary, the greatest stratification occurred in the south with differences between near-surface and near-bed temperatures up to 4.62°C at point S6, as shown in Figure 4.62 by the SSW-RS data on 02 August 2016. The least stratified area within the Morven South Boundary is in the north at point S1, with a temperature difference of 3.73°C.

4.6.1.7 A single location was selected for further assessment, based on the most representative of the average stratification based on temperature across the Morven North Boundary and Morven South Boundary. Points N6 and N7 were closest to the average value across the site, both with a difference between near-surface and near-bed temperature of 3.56°C. Point N6 was selected for further assessment due to its central position relative to the Morven North Boundary and Morven South Boundary.

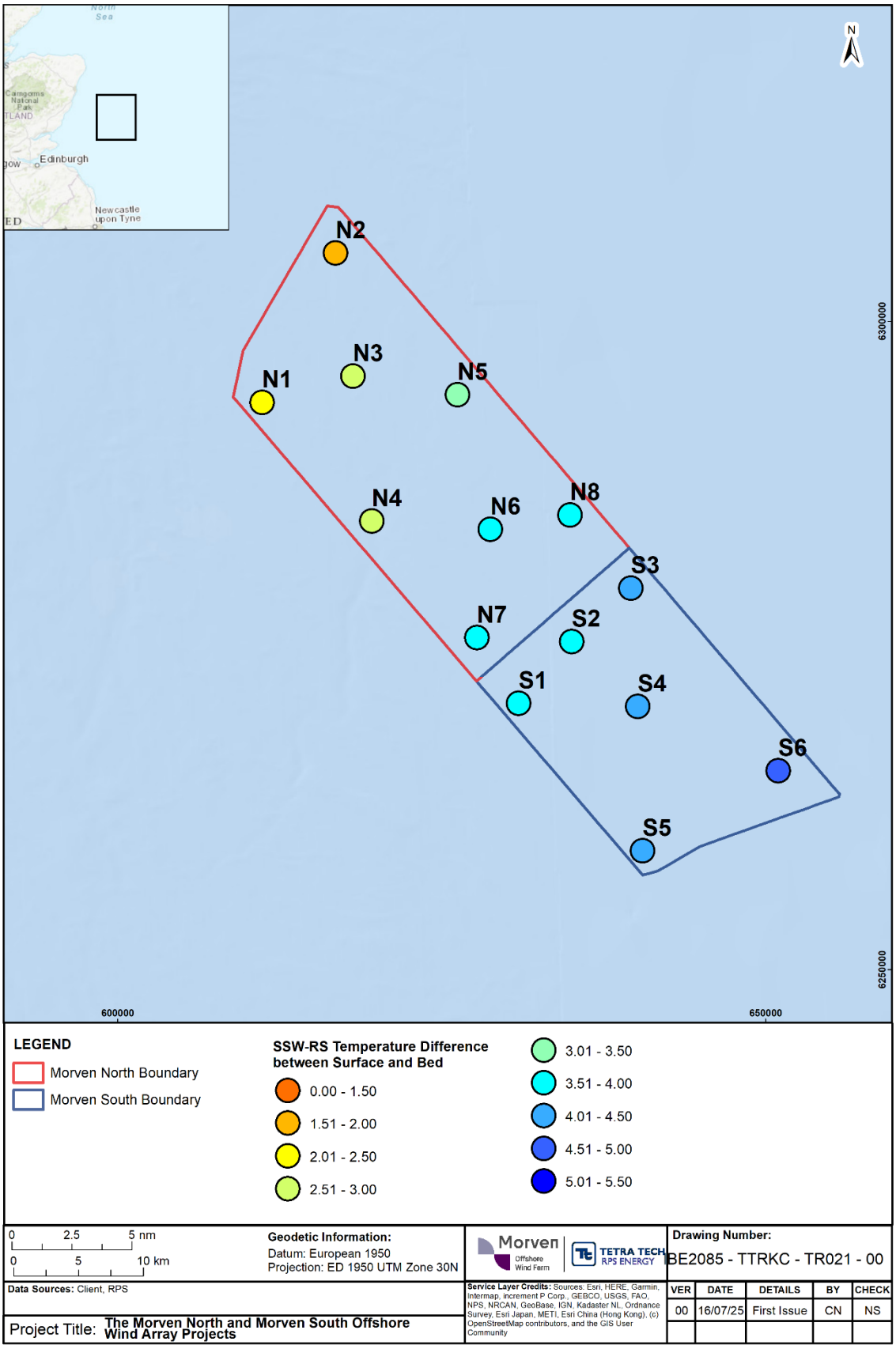

Figure 4.62: Temperature differences (near-surface minus near-bed) – Scottish Shelf Waters Reanalysis Service daily value 02 August 2016 (Barton *et al.*, 2022)

4.6.1.8 At point N6, the variation in temperature through the water column has been shown for 02 August 2016 in Figure 4.63. According to the 2022 geophysical survey by Gardline, the depth at point N6 is 67m relative to LAT. Therefore, each of the 20 vertical layers within the SSW-RS dataset is estimated to be 3.35m in depth. The position of the thermocline during this peak stratification is clearly seen to occur between a depth of 10.1m and 20.1m. Below 20.1m water depth, the temperature remains relatively constant, where the cooler deeper layer is observed. The warmer layer, situated above the thermocline occurs between 0m and 10.1m water depth.

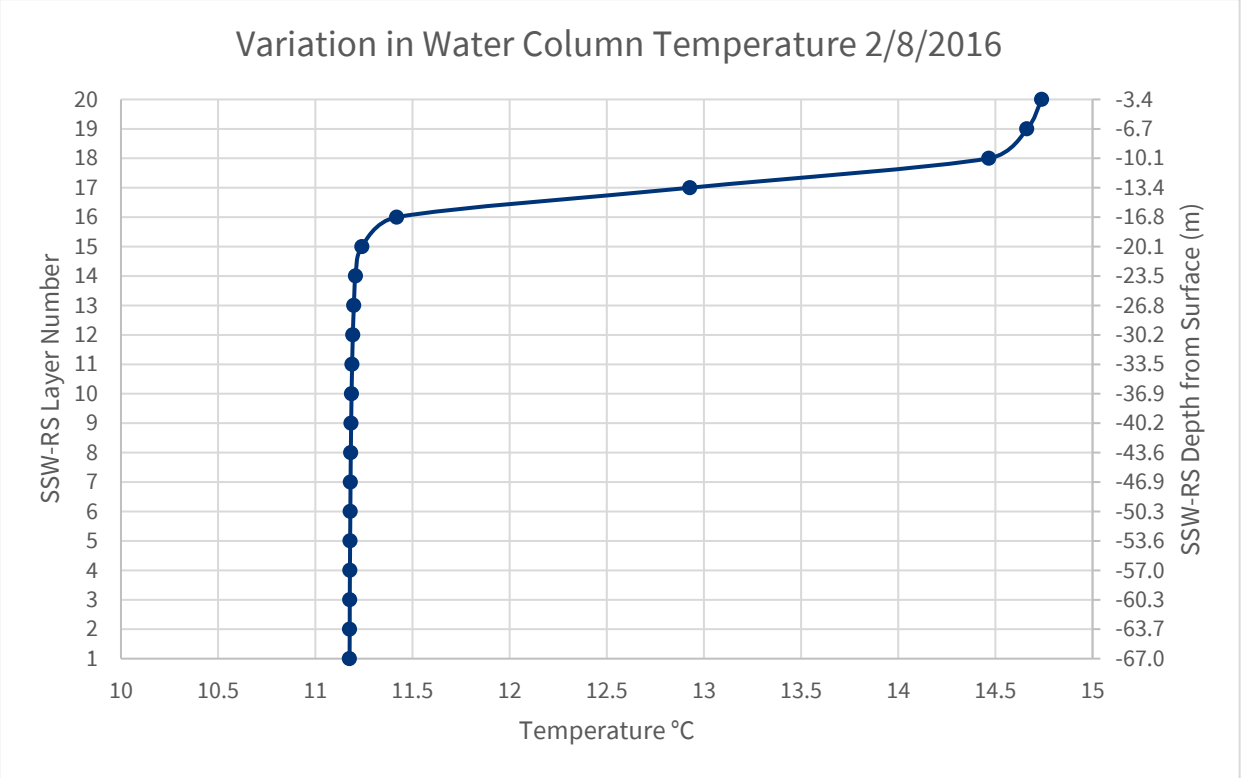

Figure 4.63: Variation in water column temperature at N6 on 02 August 2016 (Barton *et al.*, 2022)

4.6.1.9 In order to further understand seasonal variation in the baseline stratification, the position of the thermocline from March to October has been analysed using the SSW-RS data on the 2nd of each month, in line with the August data in Figure 4.63. The corresponding figures for these months are shown in Figure 4.64 to Figure 4.71. In March 2016, there is negligible difference in near-surface and near-bed temperatures prior to the onset of seasonal stratification, as shown in Figure 4.64, whilst Figure 4.65 marks the commencement of seasonal stratification with a weak and shallow thermocline at circa 6.7m depth. The thermocline deepens as the onset progresses through May, with a more marked difference between near-surface and near-bed temperature in the month of June, with the thermocline evident between circa 20.1m and 30.2m. As surface temperatures rise through July and August, as shown in Figure 4.68 and Figure 4.69, the position of the thermocline is closer to the surface layer, between 10.1m and 20.1m. The temperature difference between near-surface and near-bed layers decreases in September 2016, as shown in Figure 4.70 and by October 2016, the waters become fully mixed (Figure 4.71).

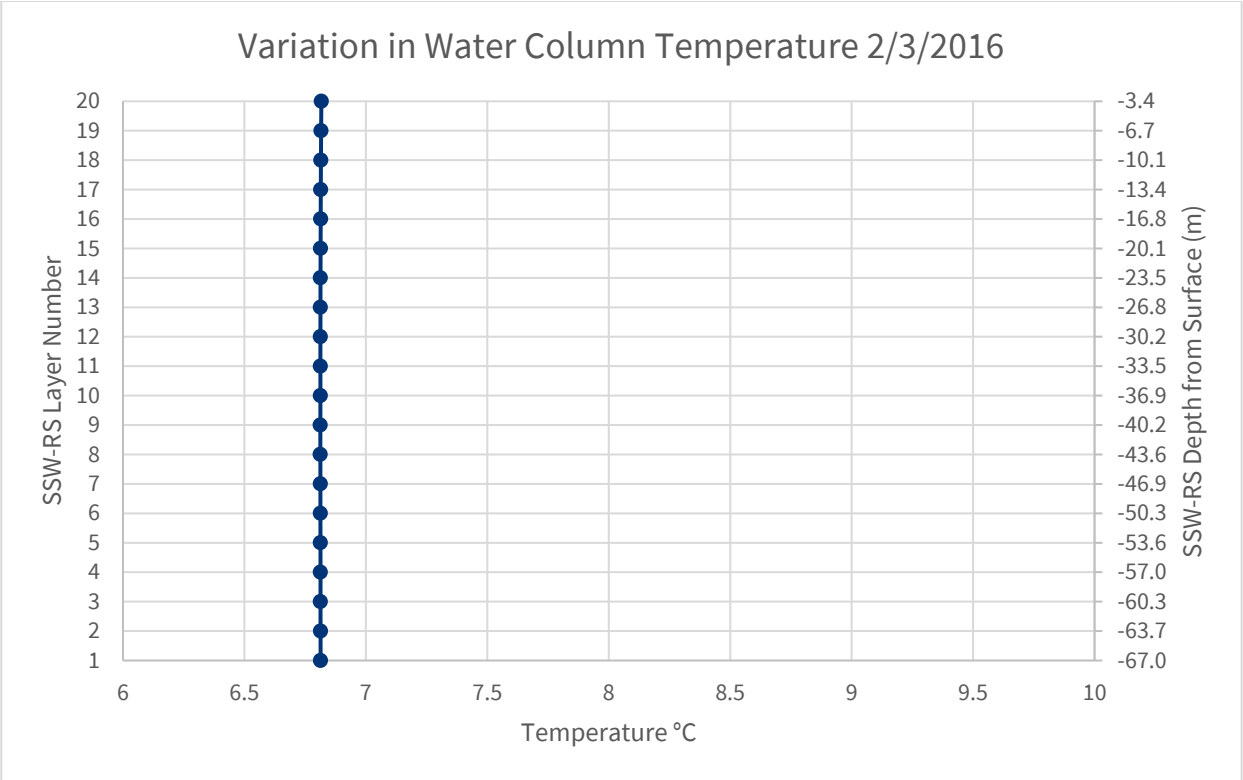

Figure 4.64: Variation in water column temperature at N6 on 02 March 2016 (Barton *et al.*, 2022)

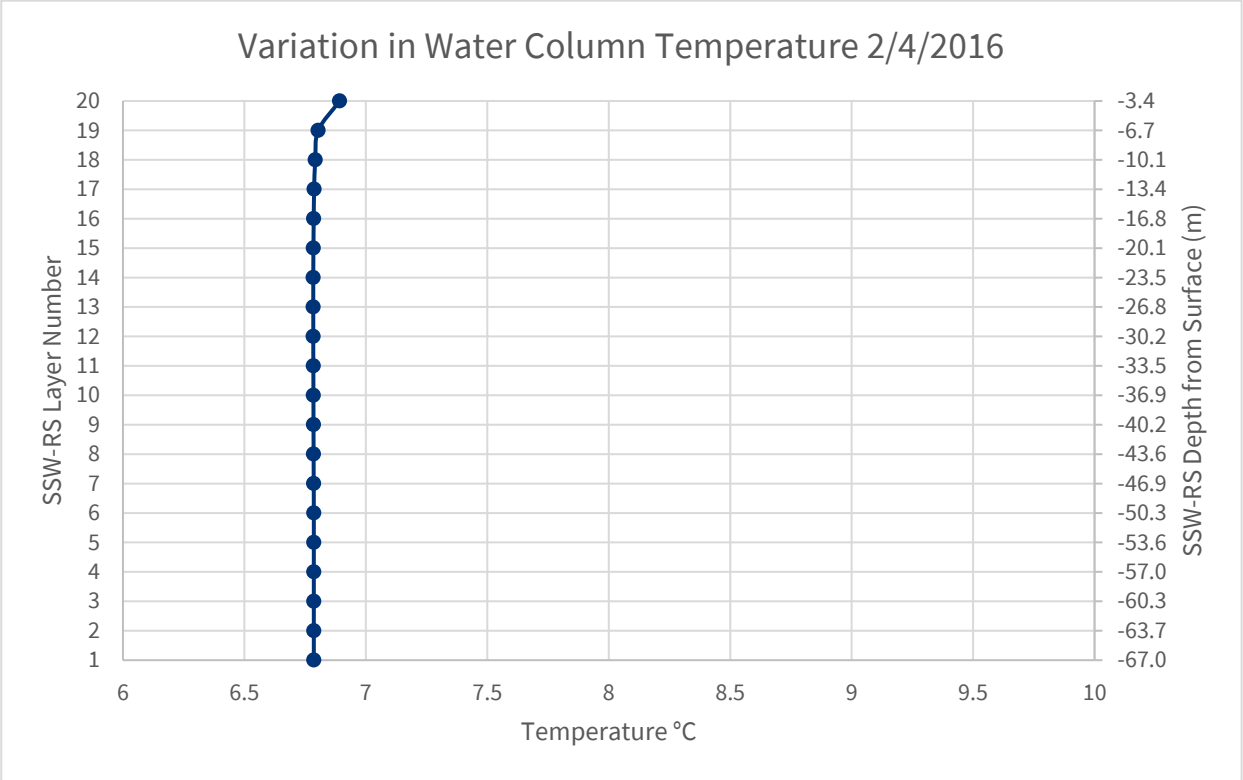

Figure 4.65: Variation in water column temperature at N6 on 02 April 2016 (Barton *et al.*, 2022)

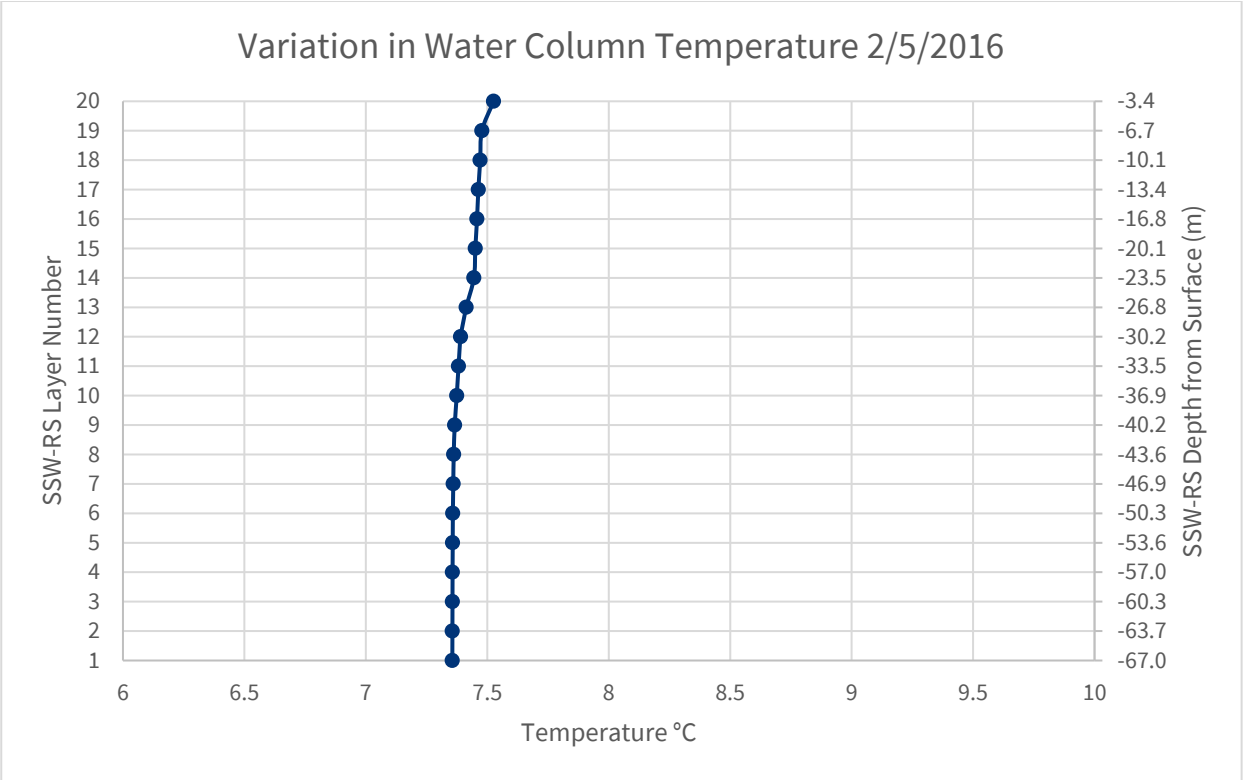

Figure 4.66: Variation in water column temperature at N6 on 02 May 2016 (Barton *et al.*, 2022)

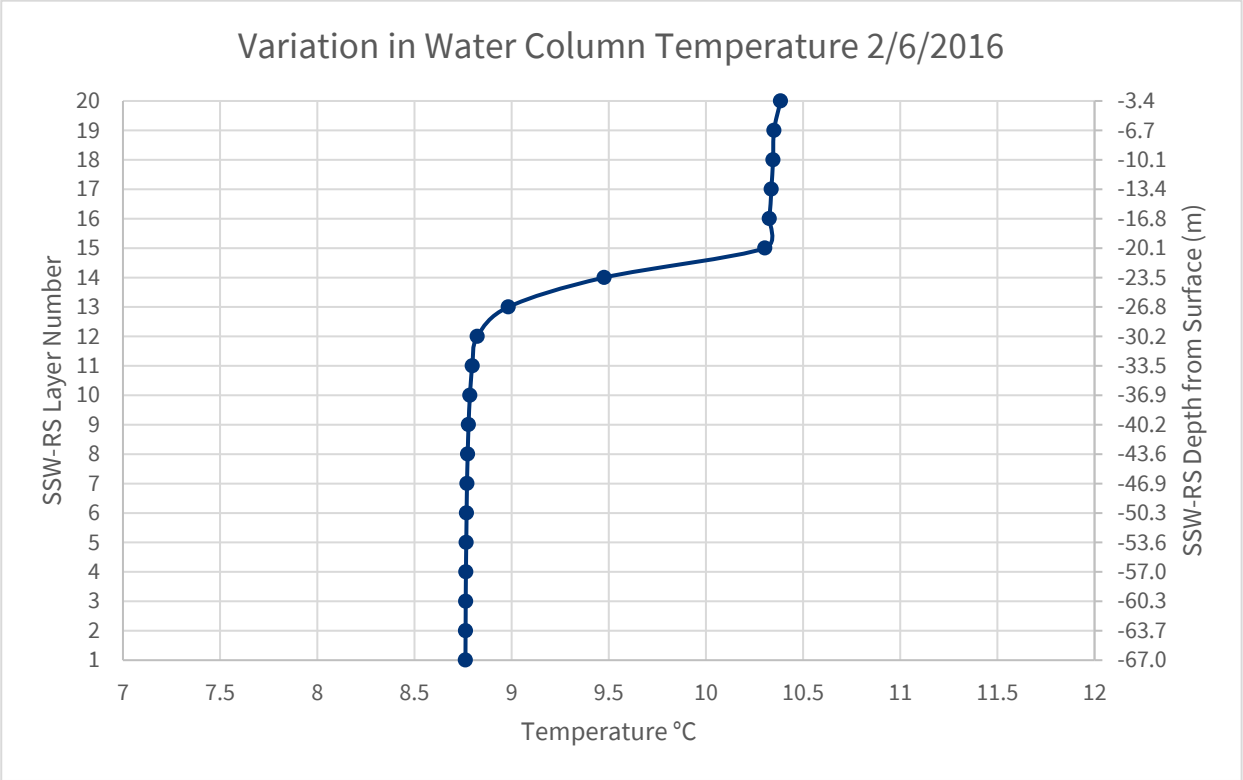

Figure 4.67: Variation in water column temperature at N6 on 02 June 2016 (Barton *et al.*, 2022)

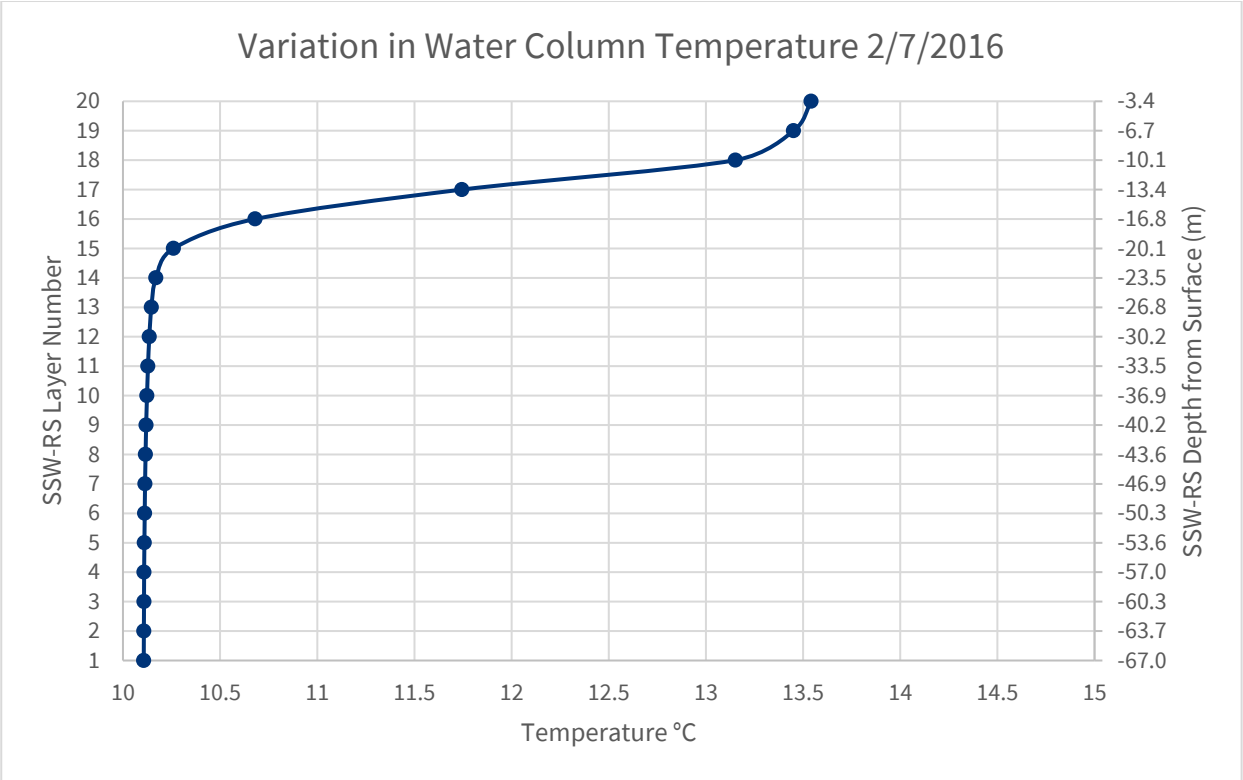

Figure 4.68: Variation in water column temperature at N6 on 02 July 2016 (Barton *et al.*, 2022)

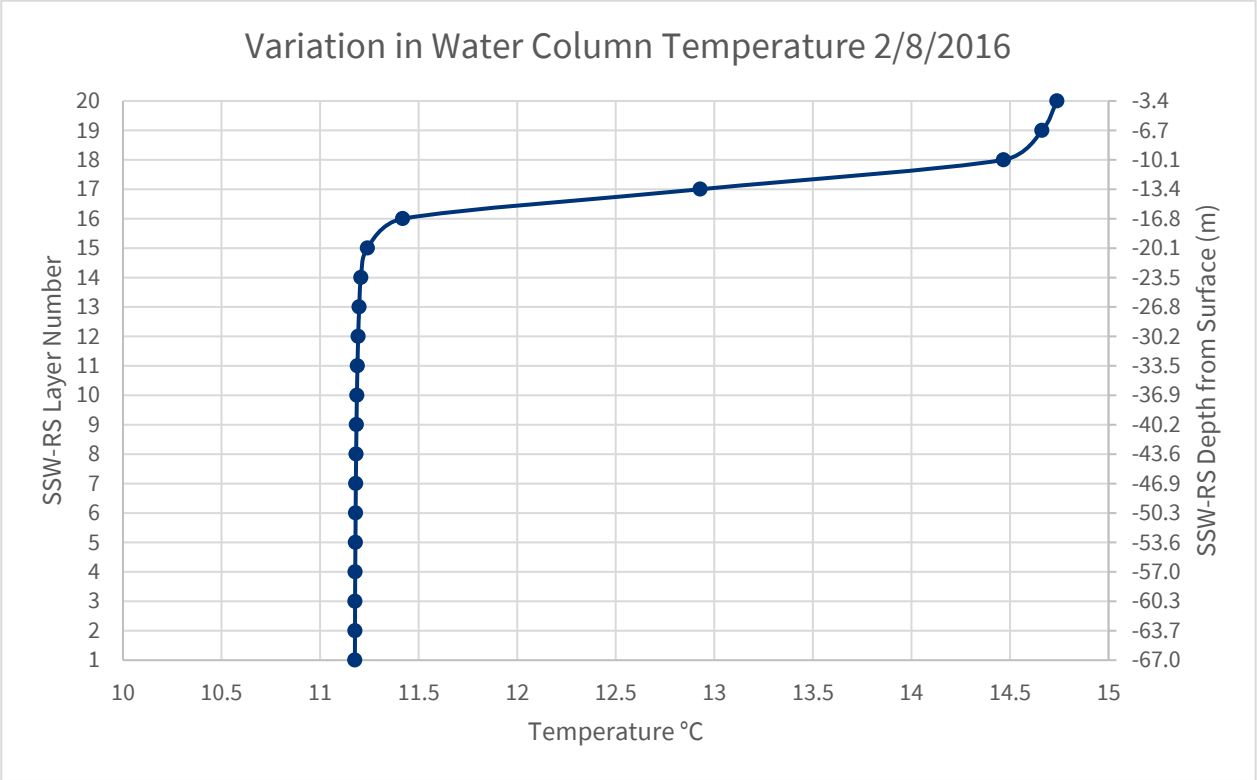

Figure 4.69: Variation in water column temperature at N6 on 02 August 2016 (Barton *et al.*, 2022)

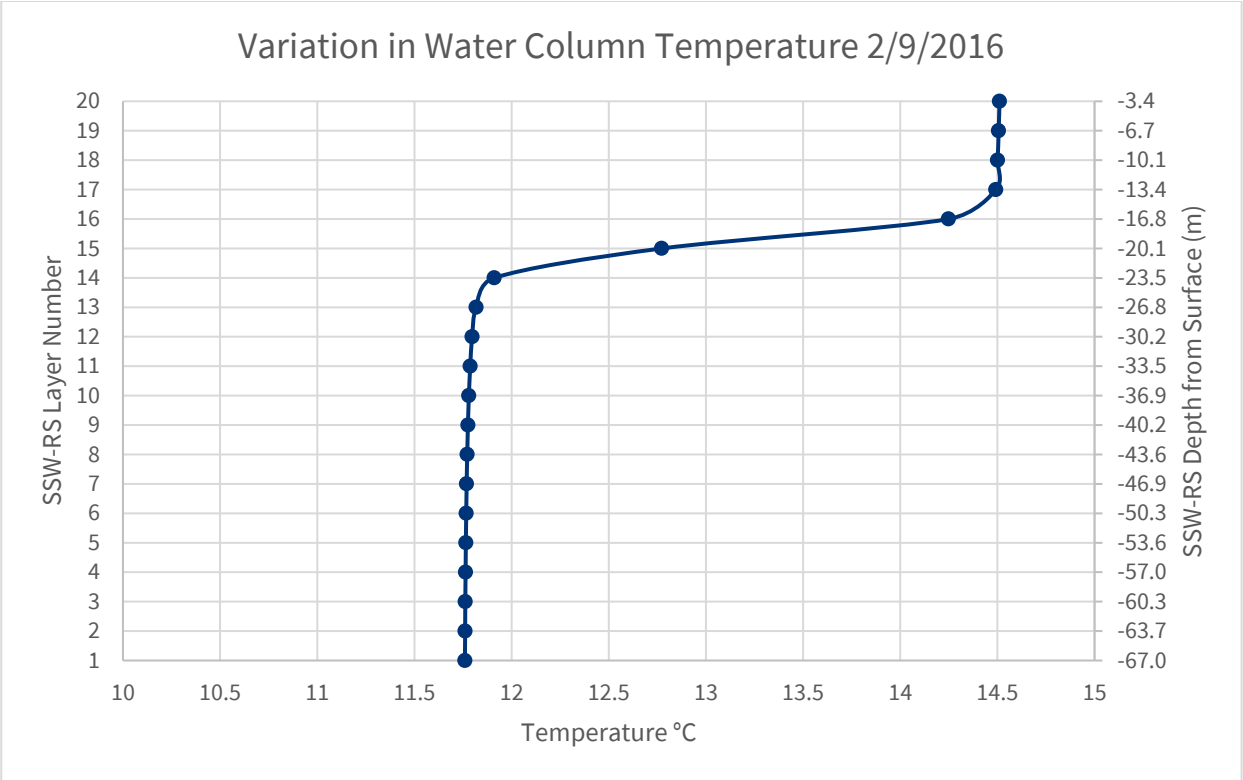

Figure 4.70: Variation in water column temperature at N6 on 02 September 2016 (Barton *et al.*, 2022)

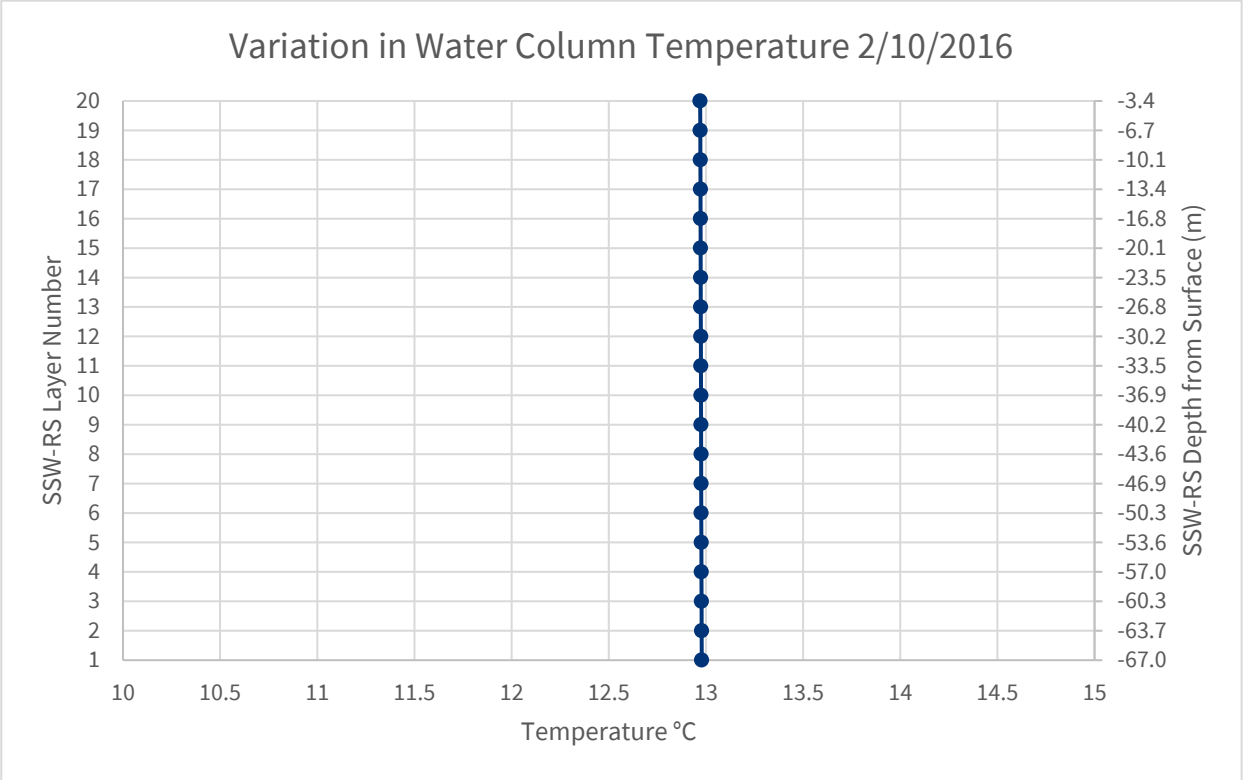

Figure 4.71: Variation in water column temperature at N6 on 02 October 2016 (Barton *et al.*, 2022)

4.7 Geology and seabed substrate

4.7.1.1 Information on the geology within the Morven North Boundary and Morven South Boundary allows for an understanding of the origin and stability of the seabed, and the geology which will be encountered during the construction of wind turbines and foundations, OSPs and foundations, inter-array cables, interconnector cables and associated infrastructure.

4.7.1.2 Offshore marine bedrock data (scale 1:250,000) provided by the BGS illustrates that the Morven North Boundary and Morven South Boundary are dominated by chalk (upper Cretaceous, Cenomanian to Maastrichtian) (Marine Scotland, 2017). Seafloor geomorphology data available on EMODnet (Figure 4.72) shows the presence of a channel within the Morven North Boundary and moraine landforms within the Morven South Boundary (EMODnet, 2021).

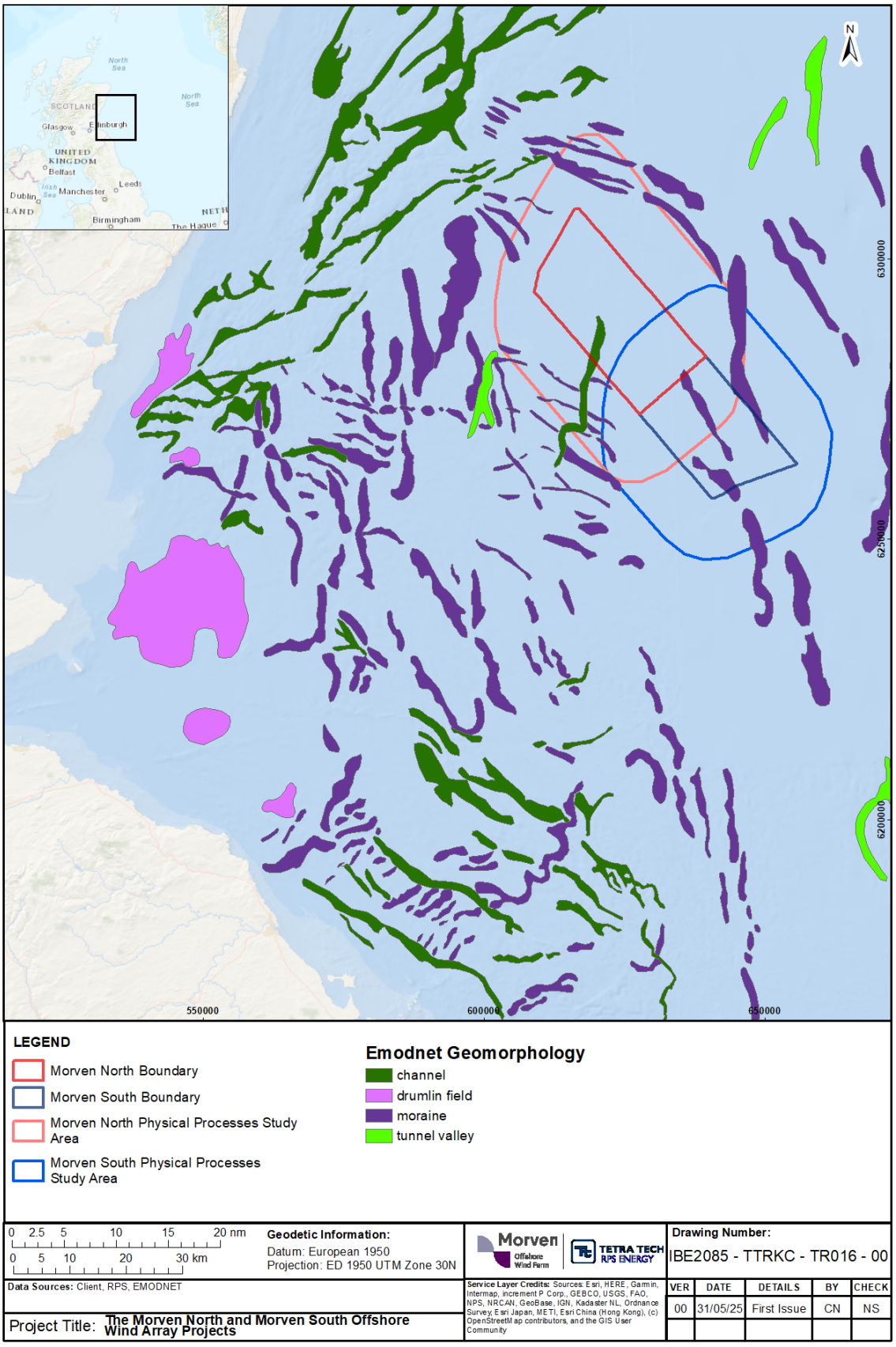

Figure 4.72: Seafloor geomorphology in vicinity of Morven North and Morven South (EMODnet, 2021)

4.7.1.3 There was no sub-seabed interpretation undertaken as part of the site specific geophysical survey scope of works (SoW). However, detailed imaging of the surficial Holocene sediments, as well as information on the Quaternary sediments circa 50m below the seabed and imaging of sub-cropping Palaeozoic and Mesozoic soils were collected using an Innomar Sub Bottom Profiler (SBP) and 2D Ultra High Resolution Seismic (UHRS) system. The predominant Holocene seabed sediment was fine to coarse sand with gravel and shell material, and seabed sediments were relatively homogenous within the Morven North Boundary and Morven South Boundary survey, as shown in Figure 4.73. This correlates with the megaripples that dominate much of the seabed. There were numerous higher Side Scan Sonar (SSS) reflectivity areas throughout the Morven North Boundary and Morven South Boundary, which were comprised of medium sand with shells, shell fragments and occasional gravels, pebbles and cobbles.

4.7.1.4 As expected, the surveyed surficial sands and gravelly sands were relatively thin, as numerous boulders and cobbles were present, particularly in the troughs between megaripples. A total of 32,687 boulders were interpreted from the SSS and Multibeam Echo Sounder (MBES) data across the Morven Site, with 27,400 boulders and 5,287 boulders located within the Morven North Boundary and Morven South Boundary respectively. Boulders were most common in the northwest and eastern areas of the Morven Site where the underlying geology formed broad seabed shoals. Within the Morven North Boundary, the boulder density was the highest in the northwest and southeastern corners, with the Morven South Boundary exhibiting increased boulder density in the northeast corner and central regions, although there is notably less boulder presence within the Morven South Boundary than within the Morven North Boundary. Across the Morven Site, there were 245 items of debris identified from the SSS data as well as 94 items of linear debris (such as fishing lines). The largest debris item measured 9.0m by 2.5m by 1.1m. It is likely that additional boulders and debris are present across the Morven North Boundary and Morven South Boundary as 100% sonar coverage was not acquired.

4.7.1.5 Figure 4.74 depicts the 250k scale mapping of seabed substrate using the Folk16 classification as available from EMODnet over the model domain. Within the Regional Physical Processes Study Area, the dominant classification is sand, with some slightly gravelly sand within the Morven North Physical Processes Study Area (EMODnet, 2016). There are also some small pockets of gravelly sand, sandy gravel and gravelly mud within the Morven North Physical Processes Study Area. This homogenous substrate predominantly comprised of sand is corroborated by the site specific seabed survey shown in Figure 4.73.

4.7.1.6 The Morven South Physical Processes Study Area is shown to be very homogenous, with sand as the dominant substrate, along with some small areas of slightly gravelly sand and gravelly sand (EMODnet, 2016). The Folk16 data from EMODnet was used within the modelling study to define the seabed substrate for the purpose of sediment transport modelling.

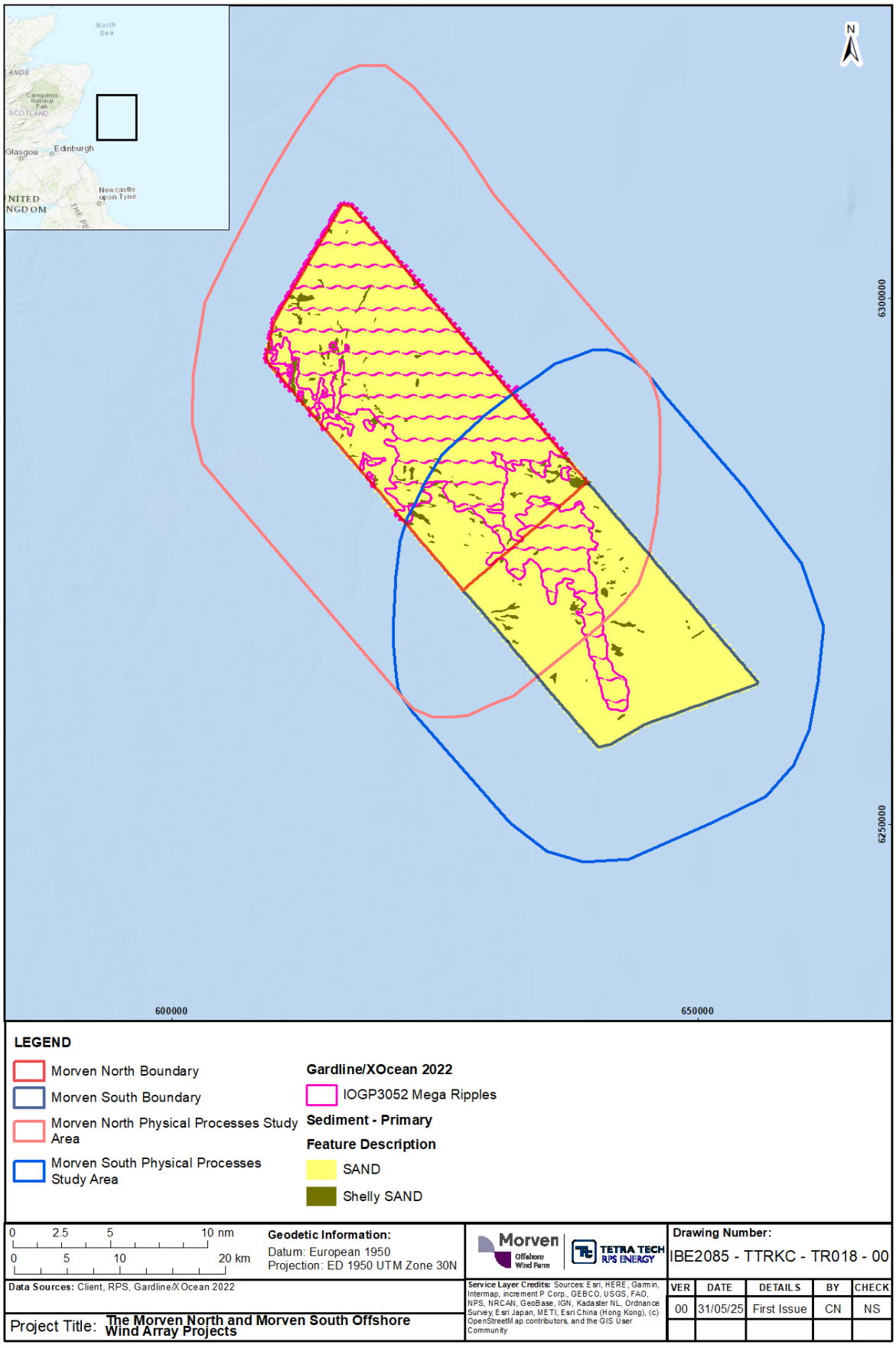

Figure 4.73: Seabed substrate in vicinity of Morven North and Morven South (Gardline/XOcean 2022)

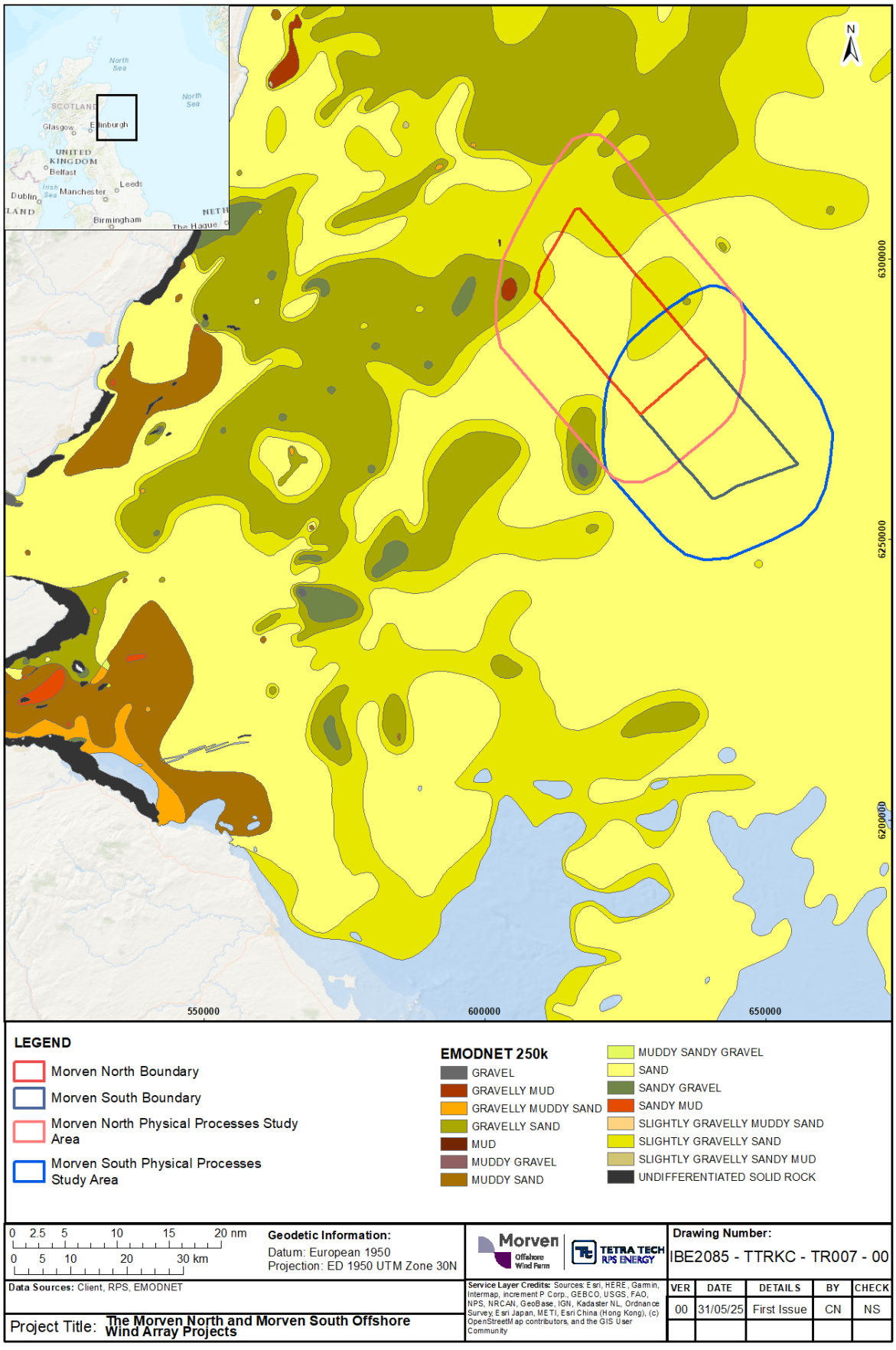

Figure 4.74: Seabed substrate in vicinity of Morven North, Morven South and wider model domain (EMODnet 2016)

4.8 Sediment transport

4.8.1.1 The MIKE21 Sediment Transport module enables assessment of bed sediment transport rates and initial rates of bed level change for non-cohesive sediment resulting from currents or combined wave current flows. It was used to determine the sediment transport pattern within the model domain. The model combines inputs from both the hydrodynamic model and, if required, the wave propagation model. It used sediment characteristics provided by the EMODnet seabed substrate data as presented previously in Section 4.7 to determine the sediment transport characteristics.

4.8.1.2 The model domain was set up with a layer of mobile bed material as described by the survey data. In areas where sediment is present an initial layer depth was set to 3m to ensure that sediment was not exhausted during the simulated events. Two sediment transport scenarios were examined, one relating to calm conditions and a second relating to the 1 in 1 year return period event from 000°. In each case the evaluations were undertaken over the course of two spring tides. These simulations included a period for the hydrodynamics and wave fields to stabilise and develop across the domain prior to sediment transport being enabled (i.e. a “warm-up” period).

4.8.1.3 For each scenario three aspects were examined:

- residual current, which is the net flow over the course of the tidal cycle. This is effectively the driving force of the sediment transport;
- potential sediment transport over this period;
- rate of change of the bed during flood and ebb tides. This provides information for a “snapshot” in time to enable the process to be illustrated.

4.8.1.4 For the tidal current alone, the residual current is presented in Figure 4.75. It is characterised by low residual current speeds of up to 0.008m/s within the Morven North Boundary and 0.007m/s within the Morven South Boundary, generally flowing in a northwesterly direction. These low residual current speeds are borne out by the low transport rates shown in Figure 4.76. The transport plot includes a log scale palette as the values within the Morven North Boundary and Morven South Boundary are several orders of magnitude smaller than those within the Firth of Forth and towards the coastline. Potential sediment transport over the course of one day or two tidal cycles reached up to a maximum of 0.09m^3/d/m within the Morven North Boundary under calm conditions. Similarly, rates of up to 0.01m^3/d/m were determined within the Morven South Boundary.

4.8.1.5 The sediment transport process is more clearly illustrated by the rate of bed level change plots presented in Figure 4.77 and Figure 4.78, where the bed levels are reduced at certain locations, during the flood tide and increase to the same degree on the return tide. This corresponds with the sand ripples that are evident within the Morven North Boundary. A log scale was also applied in these figures to encompass the range of values towards the coastline. At peak flood currents these changes reach a maximum of circa 10mm per day (i.e. the change in bed level should this peak current condition persist for one day) within the Morven North Boundary, or 7mm per day during peak ebb currents.

4.8.1.6 Bed level change is notably less within the Morven South Boundary, with a maximum of 1mm during flood currents and generally less than 1mm during ebb currents. The majority of the area within the Morven North Boundary and Morven South Boundary are subject to less than 1mm rate of bed level change per day under both flood and ebb peak current flows, indicating that although the bed is mobile, the area, particularly within the south of the Morven North Boundary and the entirety of the Morven South Boundary is stable.

4.8.1.7 When a storm approaches from the north, the flood tide currents are enhanced by the wave climate. This is reflected in an increase in the residual currents and thus an increase in the sediment transport capacity on the flood tide as illustrated in Figure 4.79 and Figure 4.80. Residual current speeds of up to 0.07m/s are seen to occur within both the Morven North Boundary and the Morven South Boundary, flowing south southwest. Similarly, the figures showing the changes in bed level peak tide indicate rates of change for both flood and ebb tide, Figure 4.81 and Figure 4.82. It is however noticeable that the increases and decreases in bed levels remain largely in opposition during the storm event indicating that tidal factors remain dominant under these circumstances. Under storm

conditions, it can be seen that the mobility of the bed within the entire Morven North Boundary and Morven South Boundary is affected.

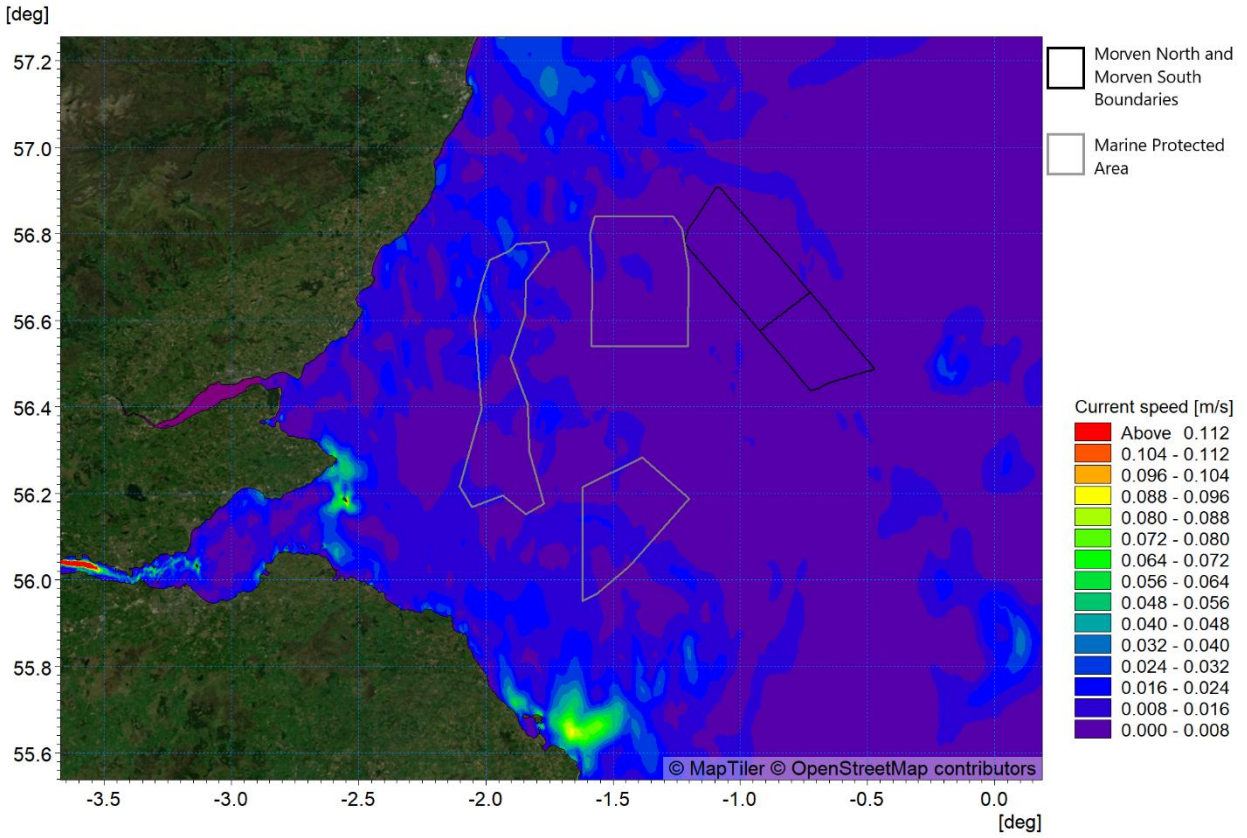

Figure 4.75: Residual current spring tide

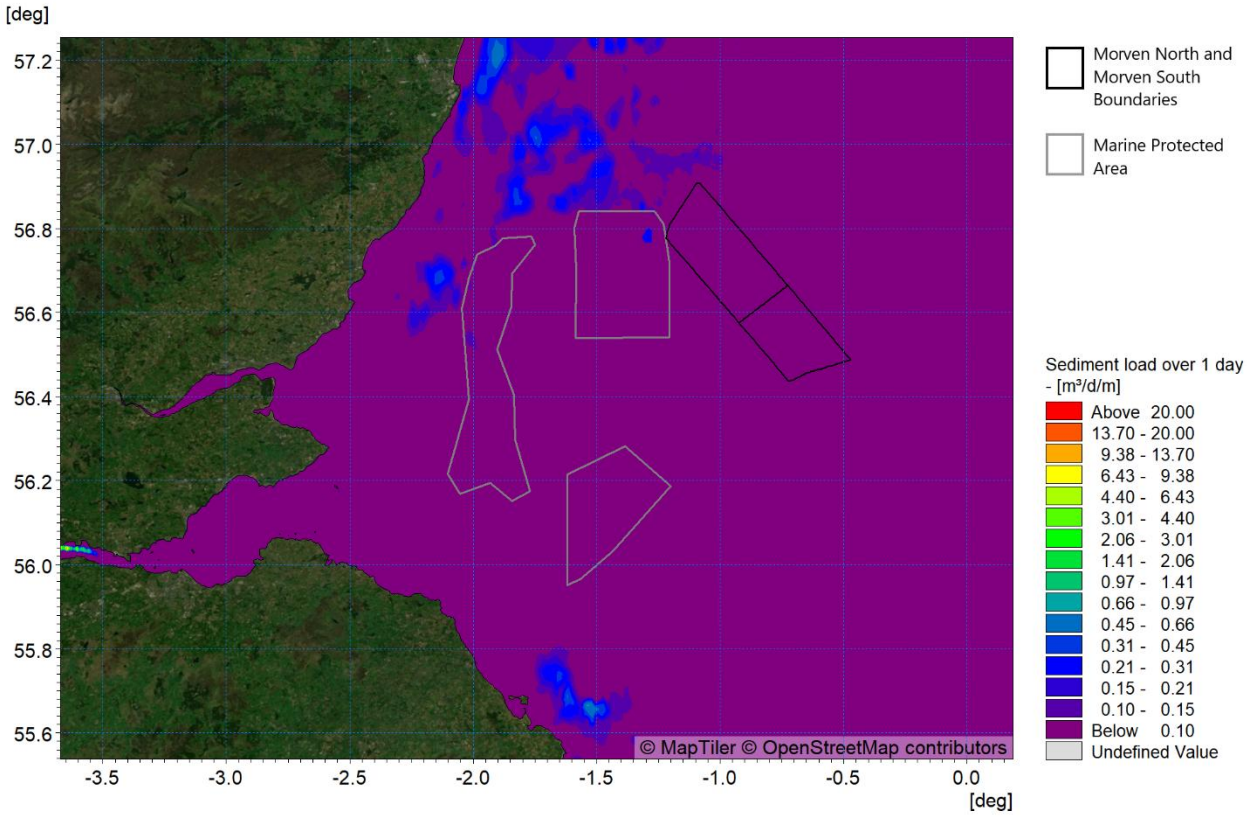

Figure 4.76: Potential sediment transport over the course of one day (two tide cycles)

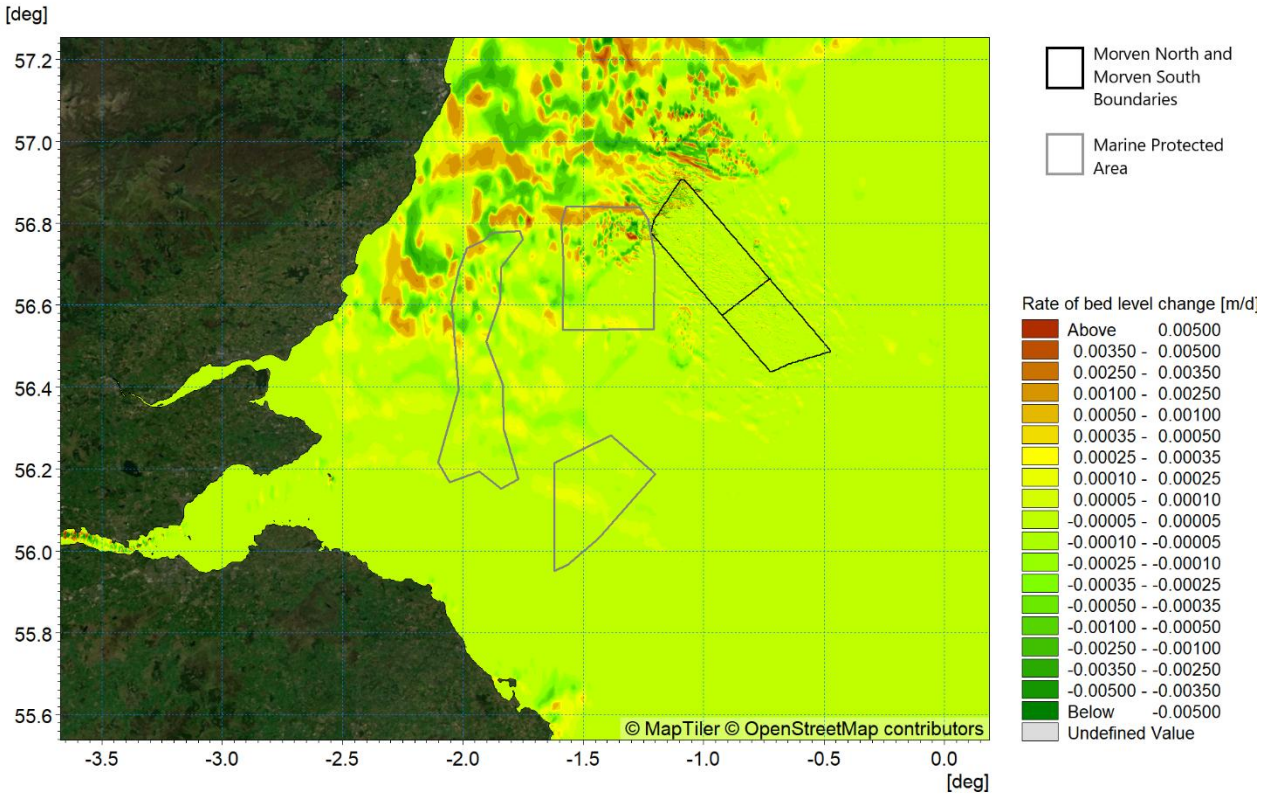

Figure 4.77: Rate of bed level change – peak flood tide

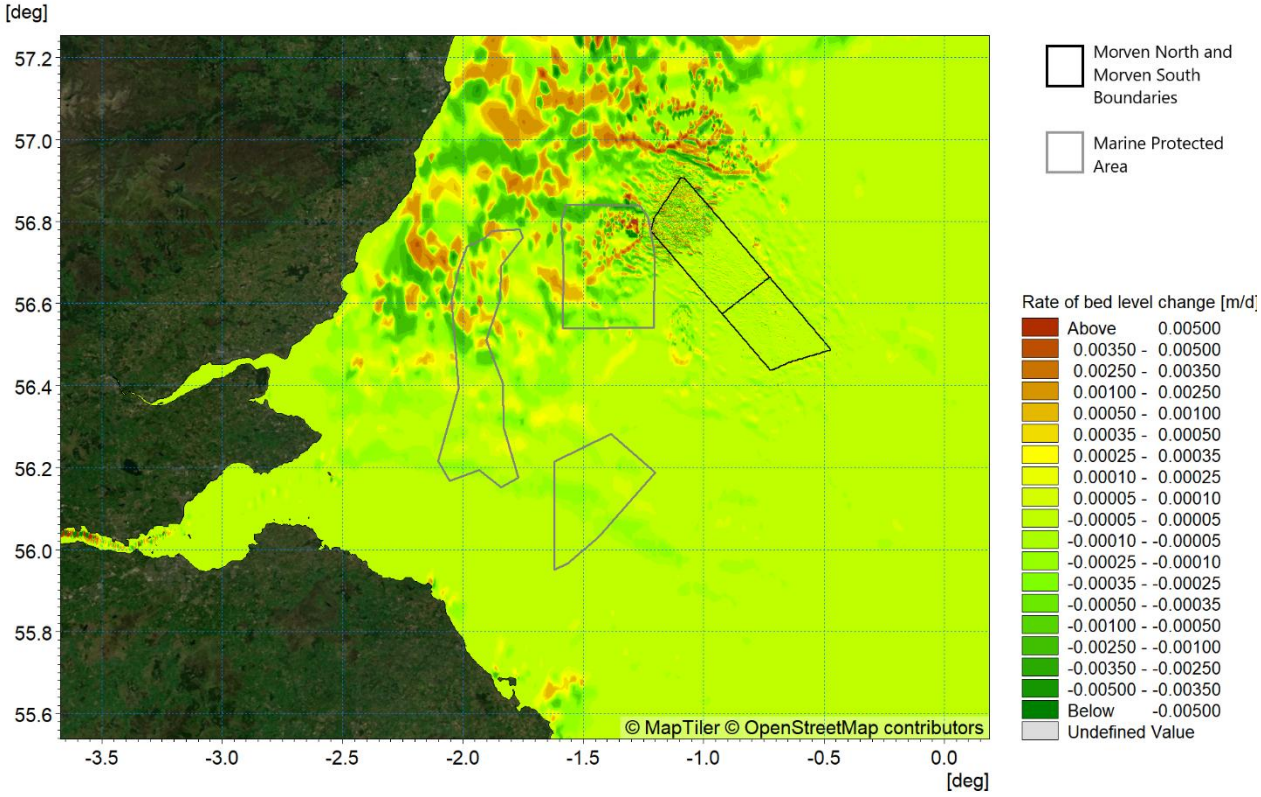

Figure 4.78: Rate of bed level change – peak ebb tide

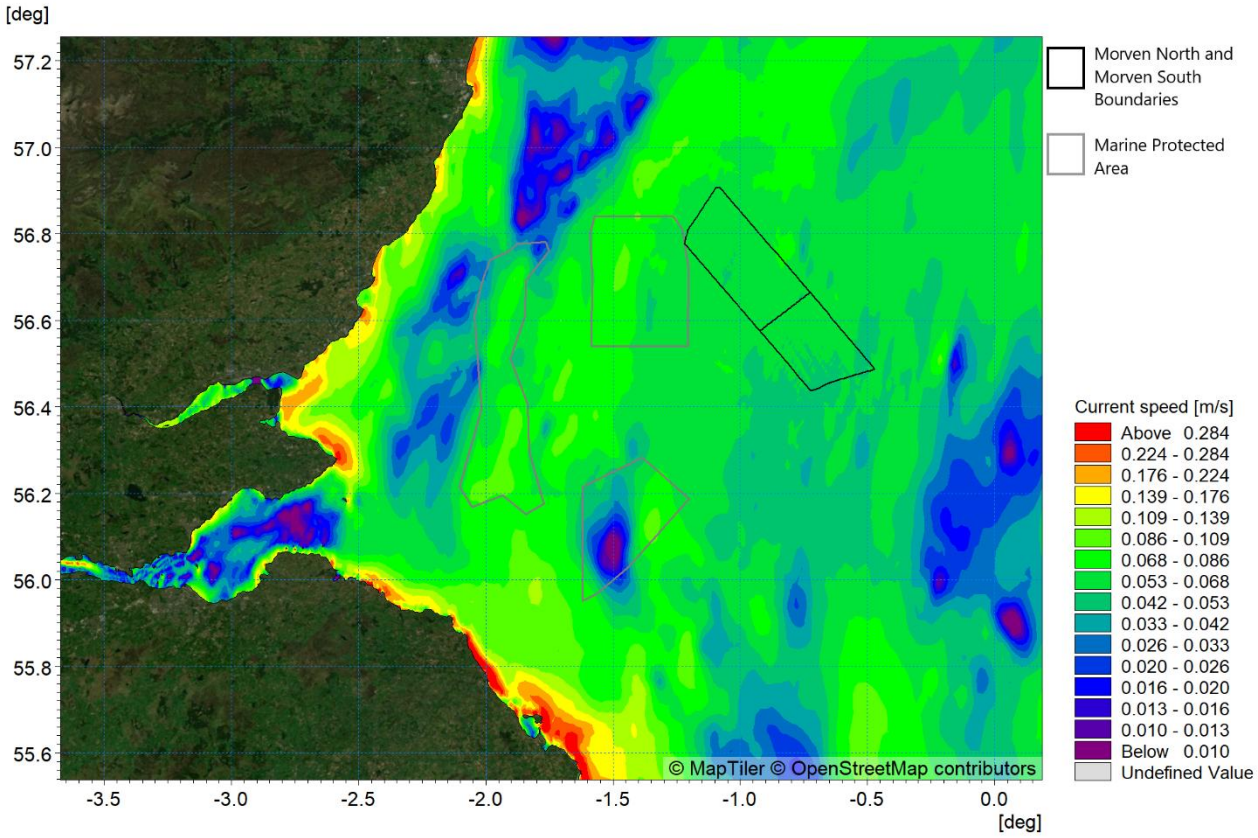

Figure 4.79: Residual current spring tide with 1:1 year storm from 000°

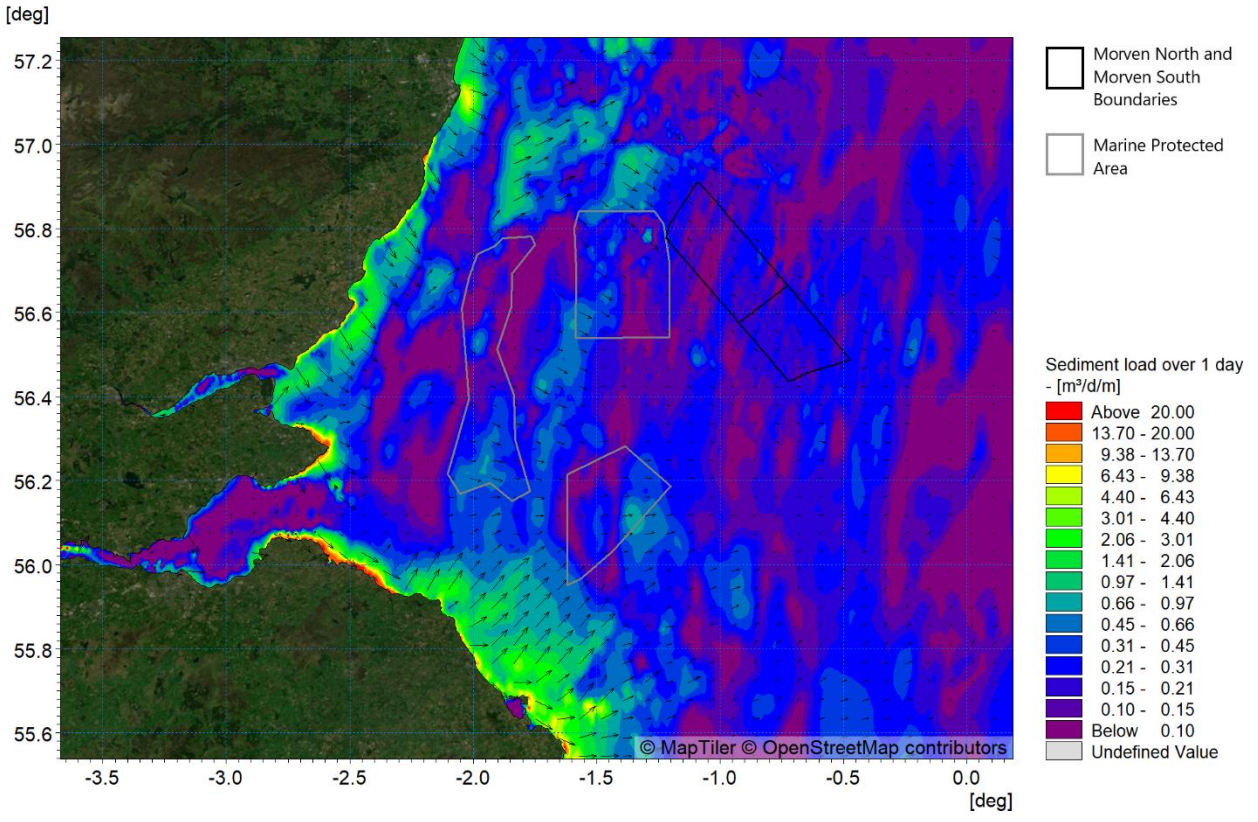

Figure 4.80: Potential sediment transport over the course of one day with 1:1 year storm from 000°

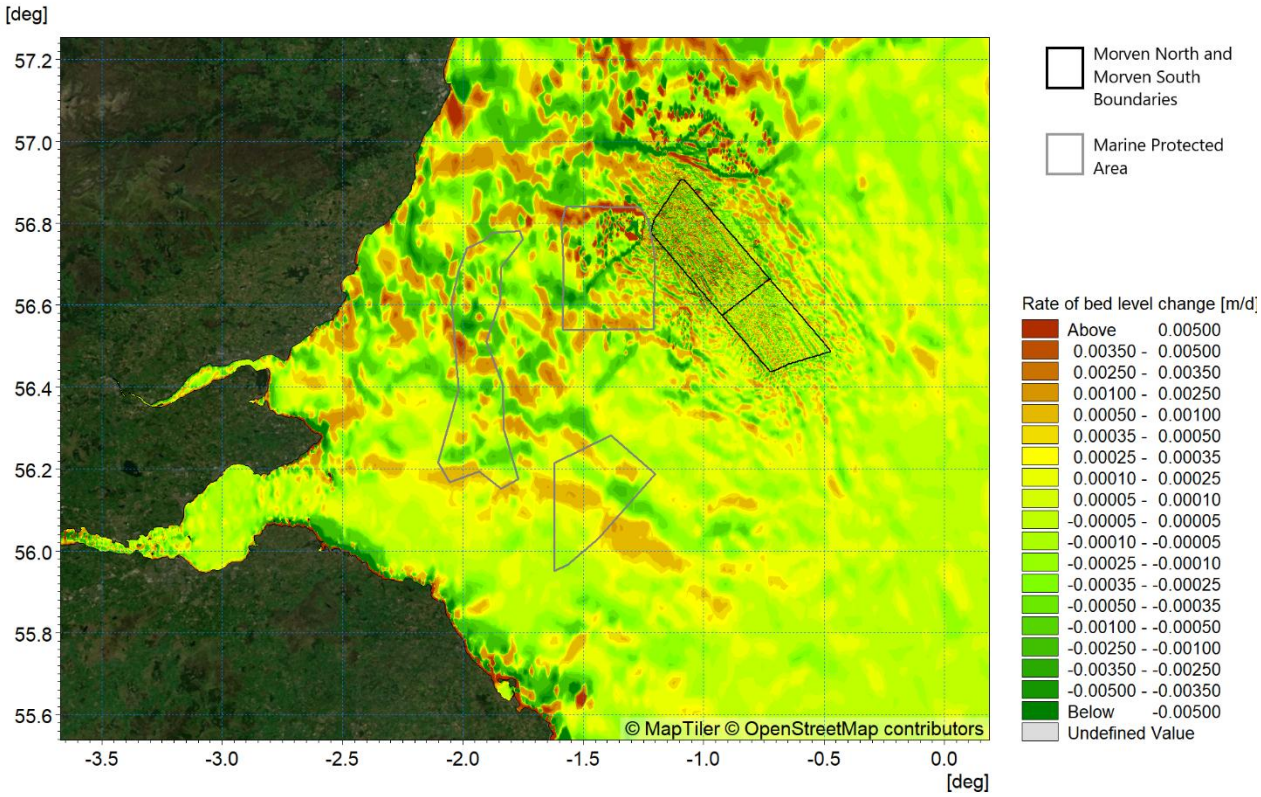

Figure 4.81: Rate of bed level change – peak flood tide with 1:1 year storm from 000°

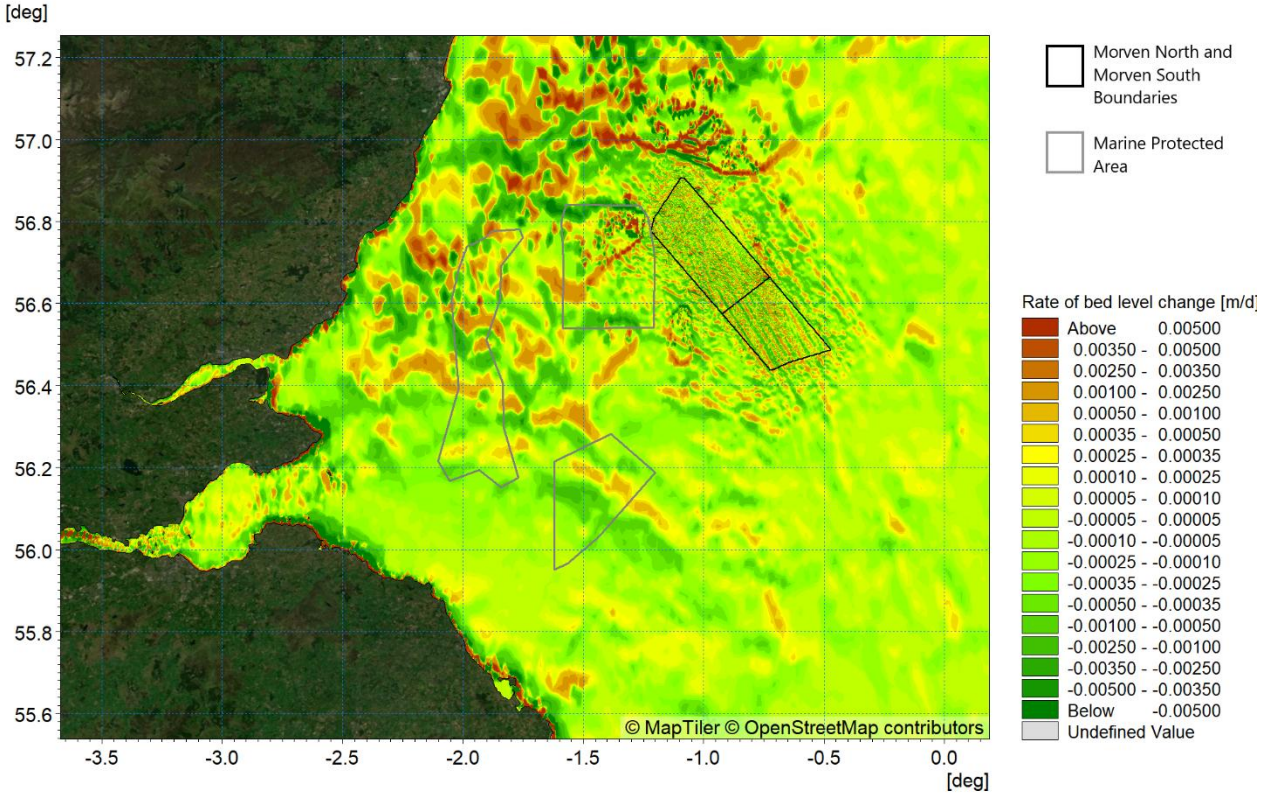

Figure 4.82: Rate of bed level change – peak ebb tide with 1:1 year storm from 000°

4.9 Suspended sediments

4.9.1.1 The principal mechanisms governing Suspended Sediment Concentrations (SSC) in the water column are tidal currents, with fluctuations observed across the spring-neap cycle and across the different tidal stages (high water, peak ebb, low water, peak flood). It is key to note that SSC can also be temporarily elevated by wave-driven currents during storm events. During high-energy storm events, levels of SSC can rise considerably, both near-bed and extending into the water column. Following storm events, SSC levels will gradually decrease to baseline conditions, regulated by the ambient regional tidal regimes. The seasonal nature and frequency of storm events supports a broadly seasonal pattern for SSC levels.

4.9.1.2 Turbidity data was collected by Partrac at one location within the Morven North Boundary and one location within the Morven South Boundary, in line with the current data collected during the same survey, as shown in Figure 4.7. The data collected from November 2022 to November 2023 suggests that generally turbidity levels are low, particularly within the Morven South Boundary. Figure 4.83 shows the turbidity data collected at the site within the Morven North Boundary, whilst Figure 4.84 shows the turbidity within the Morven South Boundary. In both cases, turbidity was at a maximum during the winter periods, corresponding with peak storm season. During storms, wave-driven currents can elevate SSC temporarily. SSC levels can rise significantly, compared to baseline levels, and then gradually decrease to baseline conditions after the storm. Therefore, SSC levels follow a broadly seasonal pattern due to the seasonal nature and frequency of storms. Elevated SSCs during storm events are less significant in deeper water, as the degree of wave penetration is lower than that of shallower water.

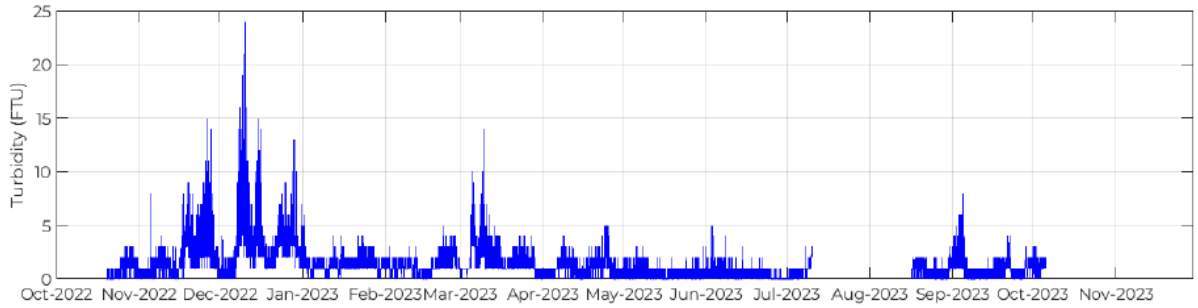

Figure 4.83: Partrac North Conductivity Temperature Depth (Morven North)– turbidity data (Partrac, 2024)

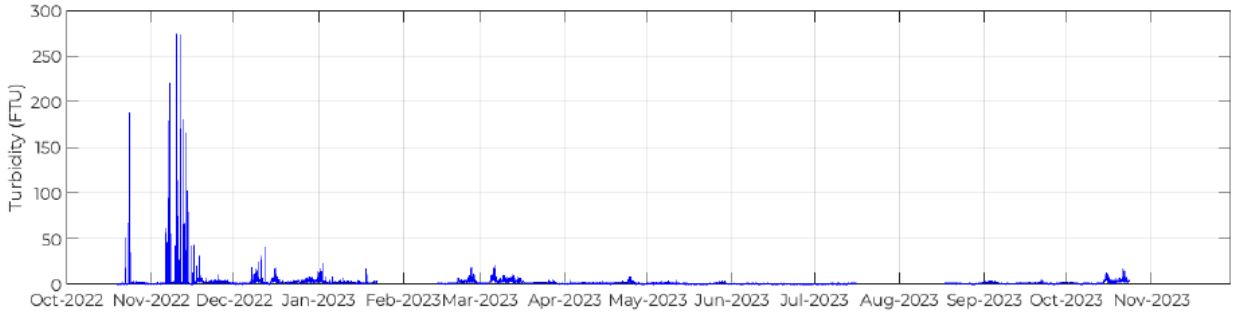

Figure 4.84: Partrac South Conductivity Temperature Depth (Morven South) – turbidity data (Partrac, 2024)

4.9.1.3 For more generalised conditions the Cefas Climatology Report 2016 (Cefas, 2016) and associated dataset provides the spatial distribution of average non-algal Suspended Particulate Matter (SPM) for the majority of the United Kingdom Continental Shelf (UKCS). Between 1998 and 2015, the

greatest plumes are associated with large rivers such as those that discharge into the Thames Estuary, The Wash and Liverpool Bay, which show mean values of SPM above 30mg/l. Within the Morven North Boundary and Morven South Boundary and surrounding waters, mean SPM levels were estimated to be between 0mg/l to 1mg/l from 1998 to 2015, with higher levels typically observed in winter months (e.g. up to 3mg/l) (Cefas, 2016). Figure 4.85 provides an overview of SPM levels in this period from 1998 to 2015 within the Firth of Forth and North Sea area in the vicinity of the Regional Physical Processes Study Area.

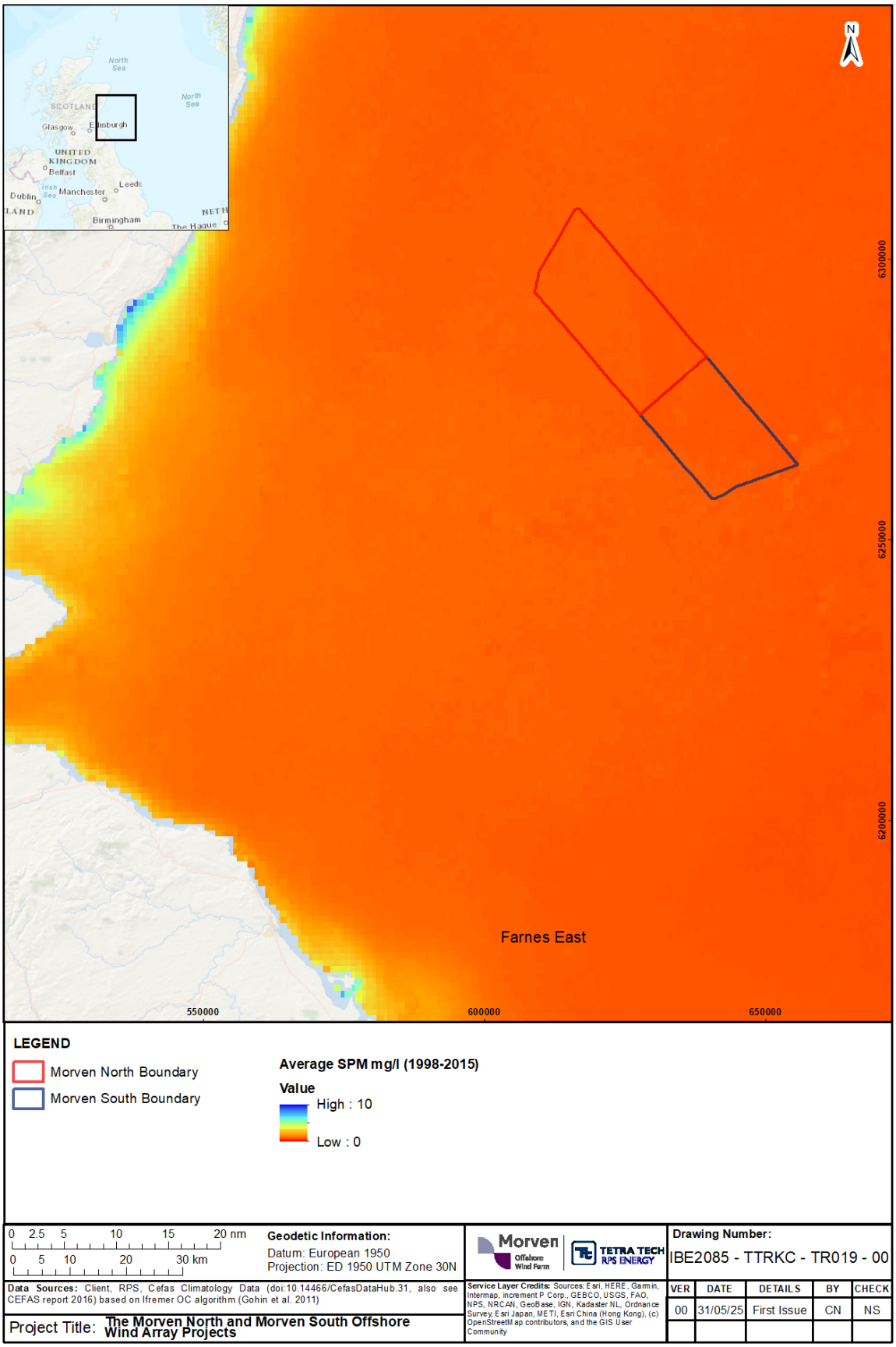

Figure 4.85: Distribution of average non-algal Suspended Particulate Matter in the vicinity of Morven North and Morven South (Cefas, 2016)

5 Potential environmental changes

5.1 Overview

5.1.1.1 The potential changes to the baseline hydrographic conditions as a result of the presence of Morven North and Morven South are quantified in the following sections. Furthermore, the potential changes are quantified as a result of the combined presence of Morven North and Morven South.

5.1.1.2 These changes relate to the presence of the infrastructure within the water column and seabed and are therefore associated with wind turbine foundations and OSP foundations along with cable and scour protection. The potential changes to sea state and sediment transport regimes were established by repeating the modelling undertaken in the previous section with the inclusion of either Morven North, Morven South or Morven North and South together.

5.1.1.3 The modelling was undertaken using an indicative layout which included the following changes for Morven North in line with the MDS for physical processes:

- Monopile foundations 15m in diameter relating to 96 wind turbine installations;
- Scour protection 2.5m in height and 67.5m in diameter with a total footprint of 3,578m^2 per wind turbine;
- Four HVAC collector OSP installations with circular footprint gravity base foundations, each with a diameter of 17m at the surface and 67m at the bed, with a caisson diameter of 51m;
- Scour protection 4.0m in height and 227m in diameter with a total footprint of 40,471m^2 per HVAC collector OSP;
- One bridge-linked HVDC converter OSP installation with two rectangular footprint gravity base foundations, each with dimensions of 180m x 240m at the surface and 195m x 255m at the bed. Note, there will be a maximum of one bridge-linked HVDC converter OSP within the Morven Site, however the modelling has incorporated one HVDC OSP within both the Morven North Boundary and Morven South Boundary, in order to provide a representation of potential impact due to each separate project;
- Scour protection 4.0m in height, 245m in width and 305m in length, with a total footprint of 74,725m^2 per foundation for the HVDC converter OSP;
- Cable protection along 42.4km of the inter-array cables, with a height of up to 3m and up to 10m width;
- Cable protection along 48.4km of the interconnector cables, with a height of up to 3m and up to 10m width;
- Cable crossings at five inter-array locations and five interconnector locations, each with a height of up to 4m, a width of up to 36m and a length of up to 80m.

5.1.1.4 Similarly, the indicative layout used within the modelling for Morven South included the following changes in line with the MDS for physical processes:

- Monopile foundations 15m in diameter relating to 95 wind turbine installations;
- Scour protection 2.5m in height and 67.5m in diameter with a total footprint of 3,578m^2 per wind turbine;
- Four HVAC collector OSP installations with circular footprint gravity base foundations, each with a diameter of 17m at the surface and 67m at the bed, with a caisson diameter of 51m;
- Scour protection 4.0m in height and 227m in diameter with a total footprint of 40,471m^2 per HVAC collector OSP;
- One bridge-linked HVDC converter OSP installation with two rectangular footprint gravity base foundations, each with dimensions of 180m x 240m at the surface and 195m x 255m at the bed. Note, there will be a maximum of one bridge-linked HVDC converter OSP within the Morven Site, however the modelling has incorporated one HVDC converter OSP within both the Morven North Boundary and Morven South Boundary, in order to provide a representation of potential impact due to each separate project.
- Scour protection 4.0m in height, 245m in width and 305m in length, with a total footprint of 74,725m^2 per foundation for the HVDC converter OSP;

- Cable protection along 42.0km of the inter-array cables, with a height of up to 3m and up to 10m width;
- Cable protection along 26.4km of the interconnector cables, with a height of up to 3m and up to 10m width;
- Cable crossings at five inter-array locations and five interconnector locations, each with a height of up to 4m, a width of up to 36m and a length of up to 80m.

5.1.1.5 It should be noted that the scale of the model mesh meant that the general flow and sediment patterns around the structures could be observed on the wider scale. However, the localised nature of the scour meant that a detailed assessment of the effectiveness of the scour protection proposed at each foundation location was not undertaken as this was not the purpose of the computational modelling. The scour protection does not have implications on the global scale and is restricted to reducing sediment erosion in the vicinity of the foundations; there would be larger implications if scour protection were not provided (Whitehouse *et al.*, 2006).

5.1.1.6 The methodology implemented for the modelling used parameters selected from the Project Description outlined in Volume 1, Chapter 3: Project Description, of the Morven North and Morven South EIA Reports, to ascertain the most influential and likely scenario for each physical processes' aspect under examination. The indicative layout used within the modelling study is presented in Figure 5.1, showing the definition between the infrastructure associated with Morven North and the infrastructure associated with Morven South. These layouts are indicative and have been considered for physical processes modelling purposes only, and the final layout designs of Morven North and Morven South will be subject to revision post consent, at the detailed design stage. When both Morven North and Morven South were considered together, the infrastructure from both Morven North and Morven South as outlined was included within the modelling. As noted within paragraphs 5.1.1.3 and 5.1.1.4, the modelling has incorporated one HVDC OSP within both the Morven North Boundary and Morven South Boundary, in order to provide a representation of potential impact due to each separate project, however there will be a maximum of one bridge-linked HVDC converter OSP within the Morven Site. Figure 5.2 provides a more detailed view of the infrastructure representation within the Morven North Boundary, whilst Figure 5.3 provides the detail of the infrastructure within the Morven South Boundary.

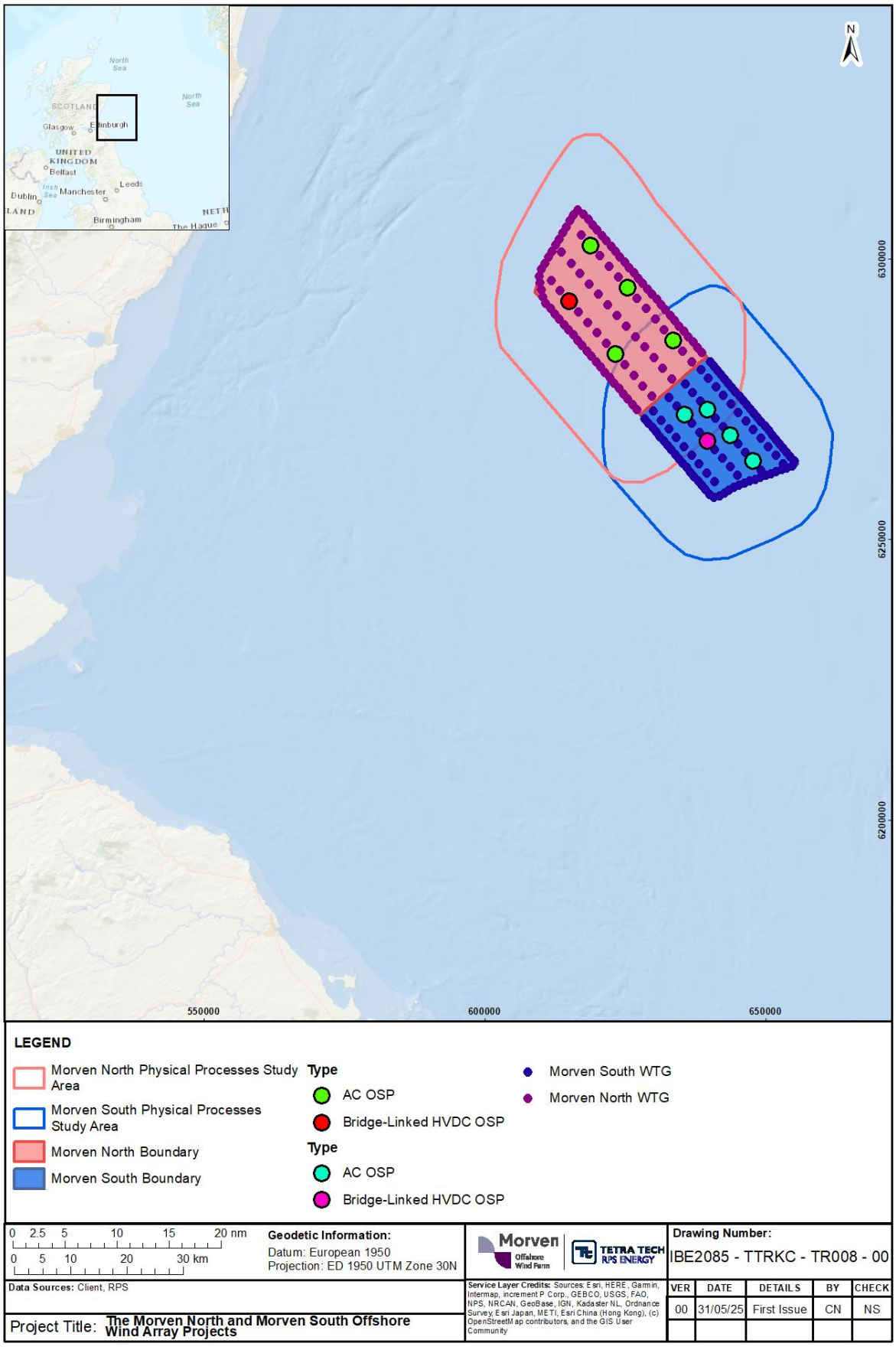

Figure 5.1: Indicative layout for Morven North and Morven South physical processes modelling

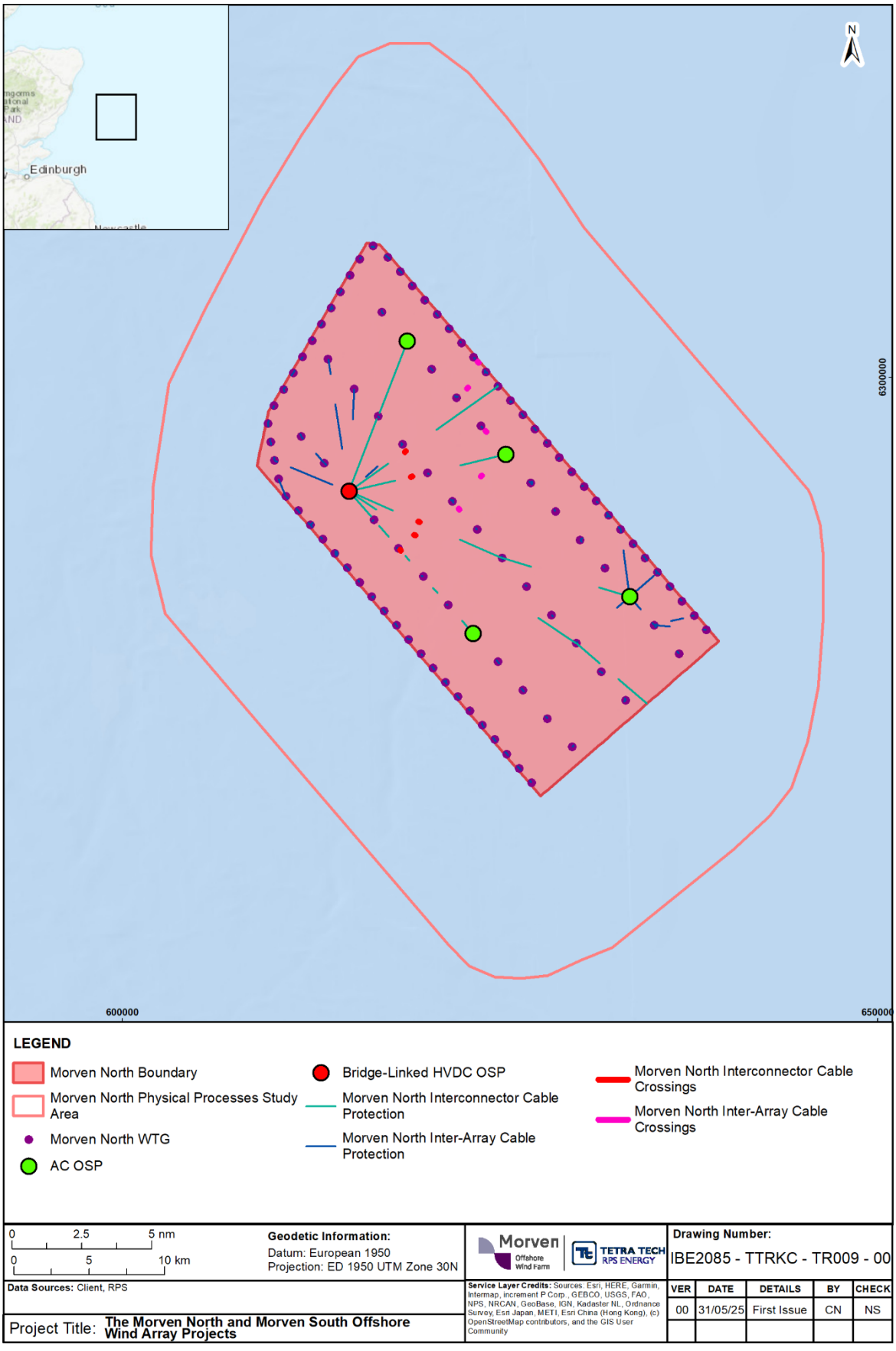

Figure 5.2: Indicative layout for Morven North physical processes modelling including cable protection/crossings

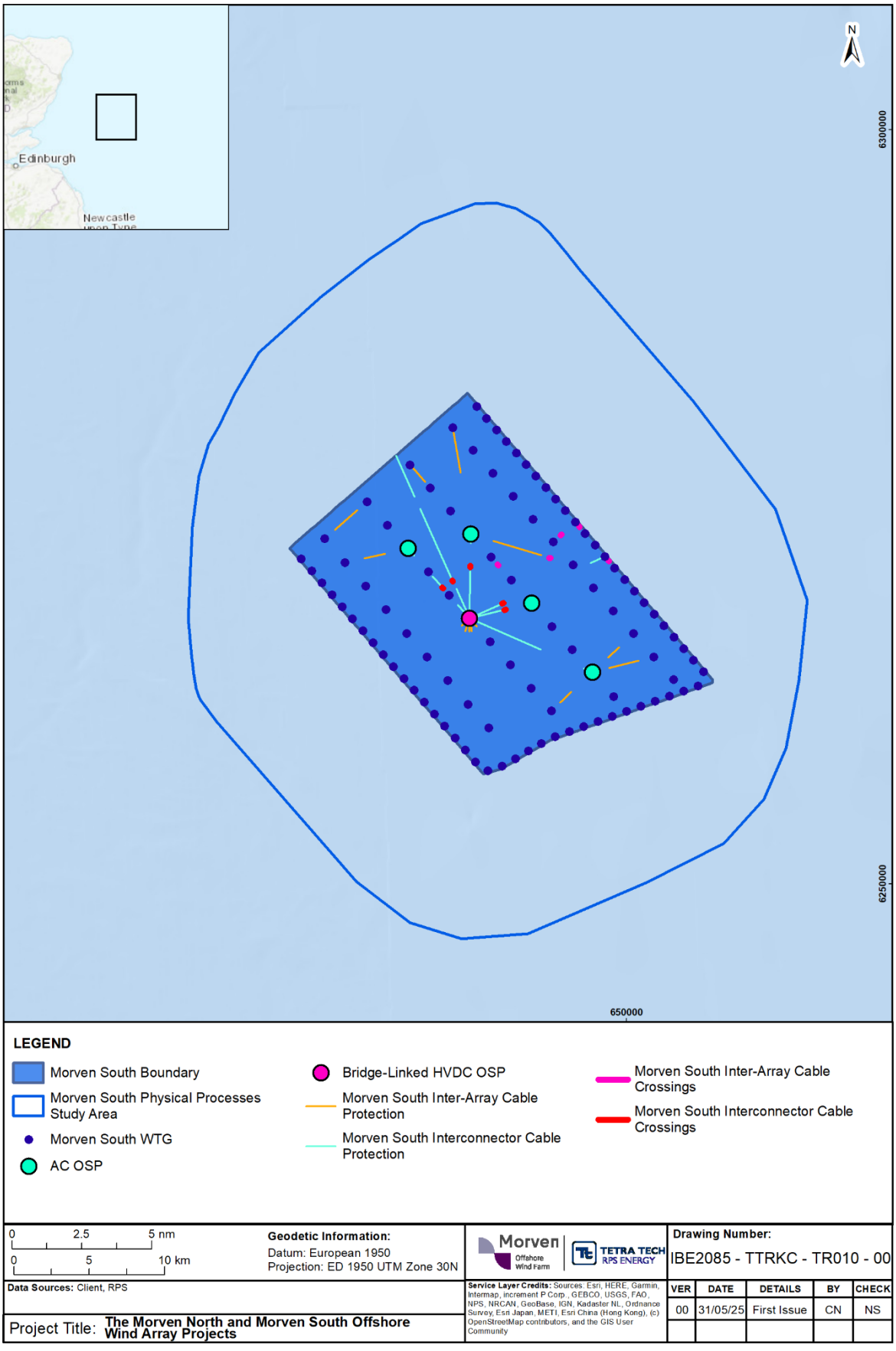

Figure 5.3: Indicative layout for Morven South physical processes modelling including cable protection/crossings

5.2 Post-construction hydrography

5.2.1 Tidal flow

5.2.1.1 The baseline spring tide simulation was repeated for Morven North with the addition of 112 structures (i.e. 96 monopile wind turbine foundations, four circular gravity base AC OSP foundations and one rectangular HVDC OSP comprised of two gravity base foundations). As noted previously, there will be a maximum of one bridge-linked HVDC converter OSP within the Morven Site, however the modelling has incorporated one HVDC converter OSP within both the Morven North Boundary and Morven South Boundary, in order to provide a representation of potential impact due to each separate project. The wind turbine foundations were represented by pier structures, which were 15m in diameter, whilst the HVAC collector OSP foundations were represented by pier structures of variable width through the water column, ranging from 17m at the surface to 67m at the bed. The bridge-linked HVDC converter OSP was comprised of two gravity base foundations sited adjacent to each other as defined in the MDS, each conceptualised within the model by six pier structures of 45m width and 45m length within the water column. This method was selected to adequately represent the sub grid losses due to the anticipated shape of these foundations, which will not obstruct the water column over the entire horizontal scale of the foundation structures, but which will allow water to penetrate through gaps within these structures. The model bathymetry was also amended to take account of scour and cable protection, noting that full scour protection allowance was incorporated for each of the bridge-linked HVDC converter OSP foundations, given their adjacent siting. This scenario represented the largest obstruction to tidal flow within the Morven North Boundary.

5.2.1.2 In addition, the baseline spring tide simulation was repeated for Morven South with the addition of 111 structures (i.e. 95 monopile wind turbine foundations, four circular gravity base HVAC collector OSP foundations and one rectangular gravity base HVDC converter OSP foundation, represented by twelve pier structures within the water column). The infrastructure was represented in the same way as per the Morven North modelling, with pier dimensions in line with paragraph 5.2.1.1 as per the Project Description (Volume 1, Chapter 3) for Morven South. The bathymetry was also amended to take account of scour and cable protection. This scenario represented the largest obstruction to tidal flow within the Morven South Boundary.

5.2.1.3 Finally, the baseline spring tide simulation was repeated for the combined presence of Morven North and Morven South, with the addition of 223 structures (i.e. 191 monopile wind turbine foundations, eight circular gravity base HVAC collector OSP foundations and two rectangular gravity base HVDC converter OSP foundations, each represented by twelve pier structures within the water column). Scour and cable protection were represented within the model bathymetry as per the individual Morven North and Morven South modelling campaigns. This scenario represented the largest obstruction to tidal flow within the Morven North Boundary and Morven South Boundary with the presence of Morven North and Morven South considered together.

5.2.1.4 The following figures show the same mid flood and mid ebb steps from the simulation as were presented in Figure 4.38 and Figure 4.39 respectively, but with the Morven North and Morven South infrastructure in place, as shown in Figure 5.4 and Figure 5.8 for peak flood and ebb respectively. Due to the limited magnitude of the changes, difference plots have also been provided for Morven North (Figure 5.6 and Figure 5.10), Morven South (Figure 5.7 and Figure 5.11) and Morven North and Morven South together (Figure 5.5 and Figure 5.9). These difference plots show the proposed infrastructure minus the baseline condition, therefore increases in current speed will be positive. A log scale has been introduced to accentuate the values for clarity. The same procedure for calculating differences and plotting figures has been implemented throughout this report.

Morven North

5.2.1.5 Peak current speeds during flood tide are seen to increase by up to 0.07m/s to the southwest of the bridge-linked HVDC converter OSP gravity base foundations within the Morven North Boundary, with a reduction in the order of 0.3m/s in the immediate vicinity of the pier structures, extending circa 90m to 100m in the lee of each structure, reducing to less than 0.01m/s within 4km (less than 2% of baseline current speeds of 0.63m/s). At the exposed frontage of these structures, a reduction in

current speed of up to 0.06m/s is seen to occur. The converse occurs during the peak current speeds on the ebb tide, whereby an increase in current speeds of up to 0.04m/s is observed to the northeast of the structures, adjacent to the decreased area in the lee of the pier structures. Reductions in current speed of up to 0.4m/s are observed in the immediate vicinity of the piers, reducing to less than 0.01m/s within circa 5km (less than 2% of baseline current speeds of 0.66m/s). The tidal wakes produced by the four circular OSP gravity base foundations and 96 monopile wind turbine foundations are seen to increase and decrease the current speeds by a notably lesser amount than the bridge-linked HVDC converter OSP gravity base foundations, due to their size and obstruction within the water column. There is no change in magnitude of current speed outside of the Morven North Physical Processes Study Area.

Morven South

5.2.1.6 A similar magnitude of impact to Morven North (paragraph 5.2.1.5), is observed in the vicinity of the bridge-linked HVDC converter OSP gravity base foundations within the Morven South Boundary, with peak current speeds during flood tide seen to increase by up to 0.07m/s to the southwest of the structures. Reductions are seen to occur by up to 0.3m/s but are limited to the immediate vicinity of the pier structures, with a return to less than 0.01m/s difference within 3km of the structures. This is a difference less than 2% of baseline current speeds of 0.54m/s). Peak ebb flows incur an increase of up to 0.05m/s to the northeast of the structures, with decreases of up to 0.3m/s in the immediate vicinity of the structures, reducing to less than 0.01m/s within circa 4km (less than 2% of baseline current speeds of 0.57m/s). There is no change in magnitude of current speed outside of the Morven South Physical Processes Study Area.

Morven North and Morven South

5.2.1.7 Modelled magnitudes of change in current speeds are not seen to increase with Morven North and Morven South infrastructure in place simultaneously, due to minimum spacing between turbines and locations of the bridge-linked HVDC converter OSP gravity base foundations. Lower baseline current speeds were observed within the results within the Morven South Boundary compared to the Morven North Boundary.

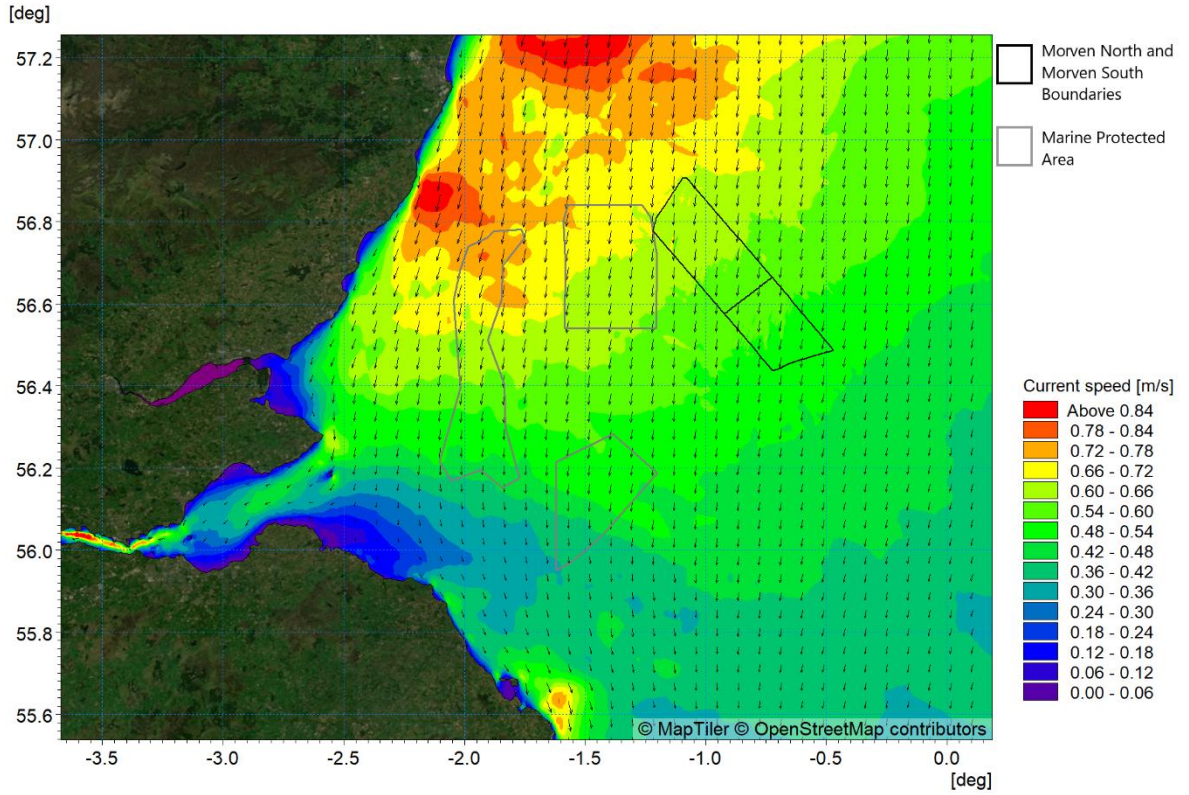

Figure 5.4: Post-construction (Morven North and Morven South) tidal flow patterns – peak flood (HW-1 hour)

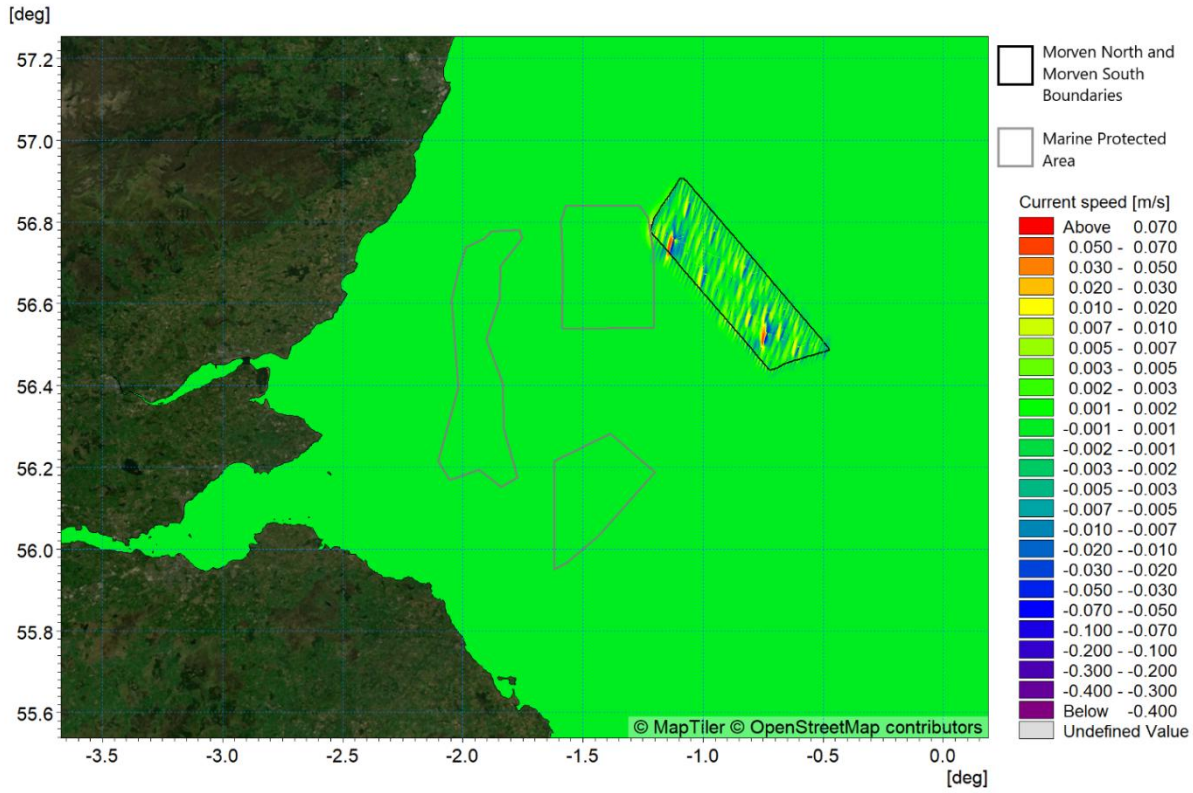

Figure 5.5: Change in tidal flow (post-construction Morven North and Morven South minus baseline) – peak flood (high water - 1 hour)

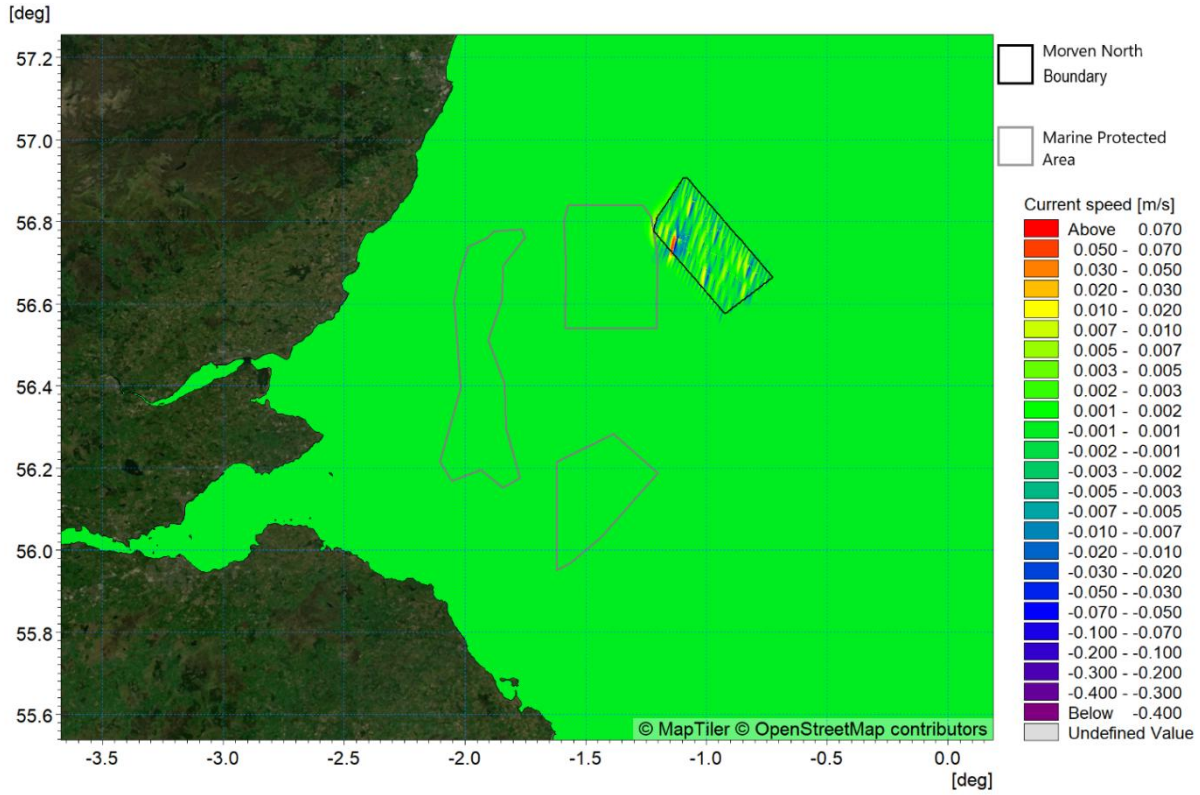

Figure 5.6: Change in tidal flow (post-construction Morven North minus baseline) – peak flood (high water - 1 hour)

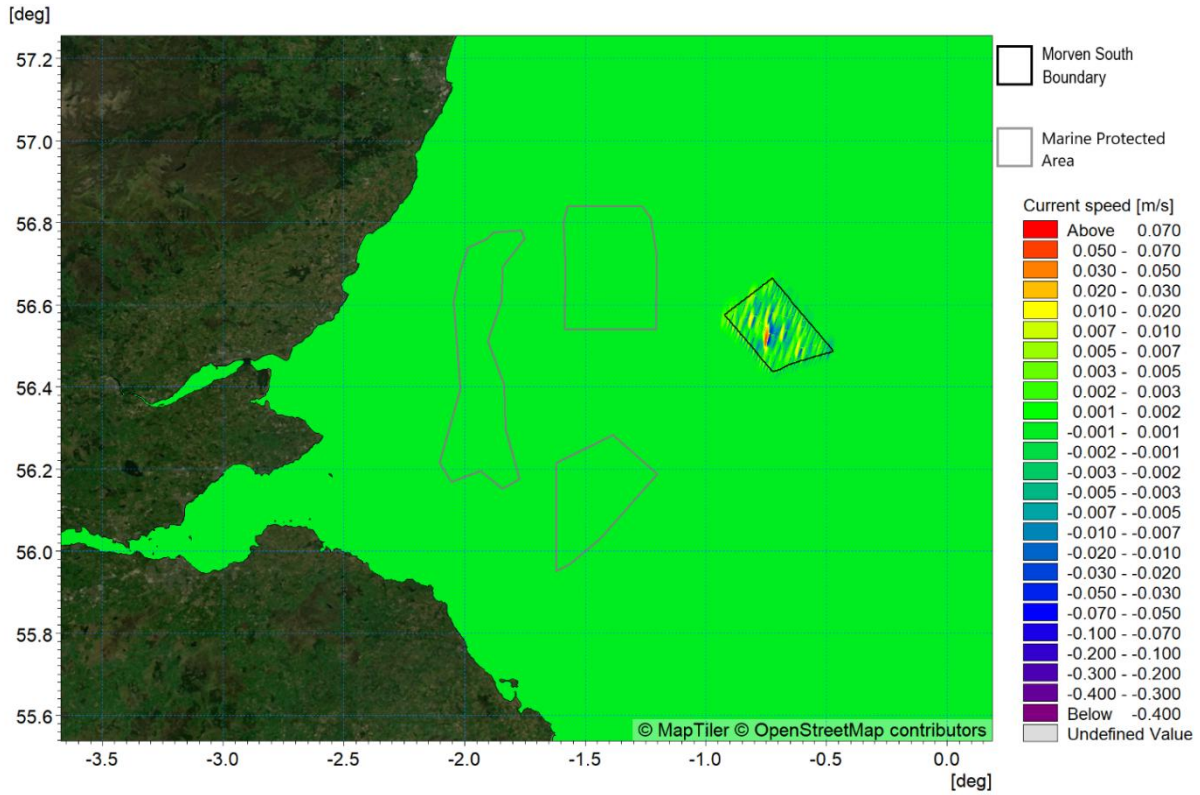

Figure 5.7: Change in tidal flow (post-construction Morven South minus baseline) – peak flood (high water - 1 hour)

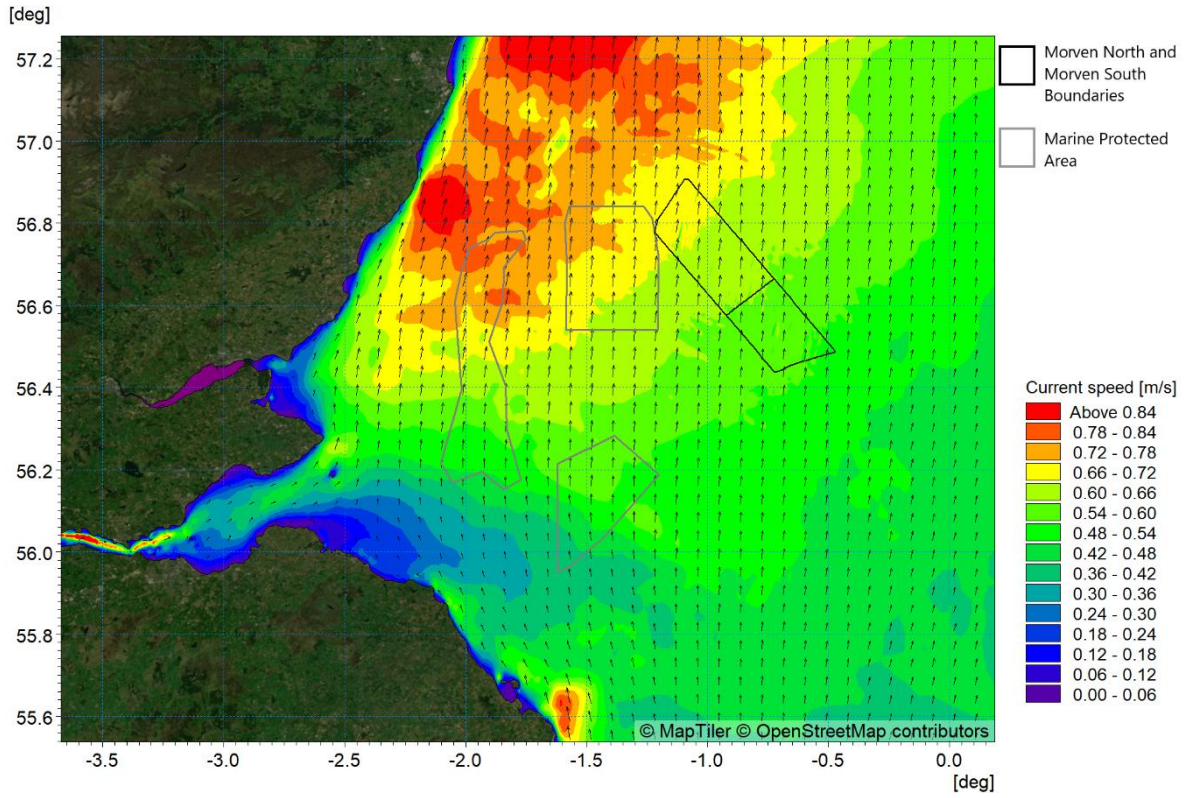

Figure 5.8: Post-construction (Morven North and Morven South) tidal flow patterns – peak ebb (low water - 1 hour)

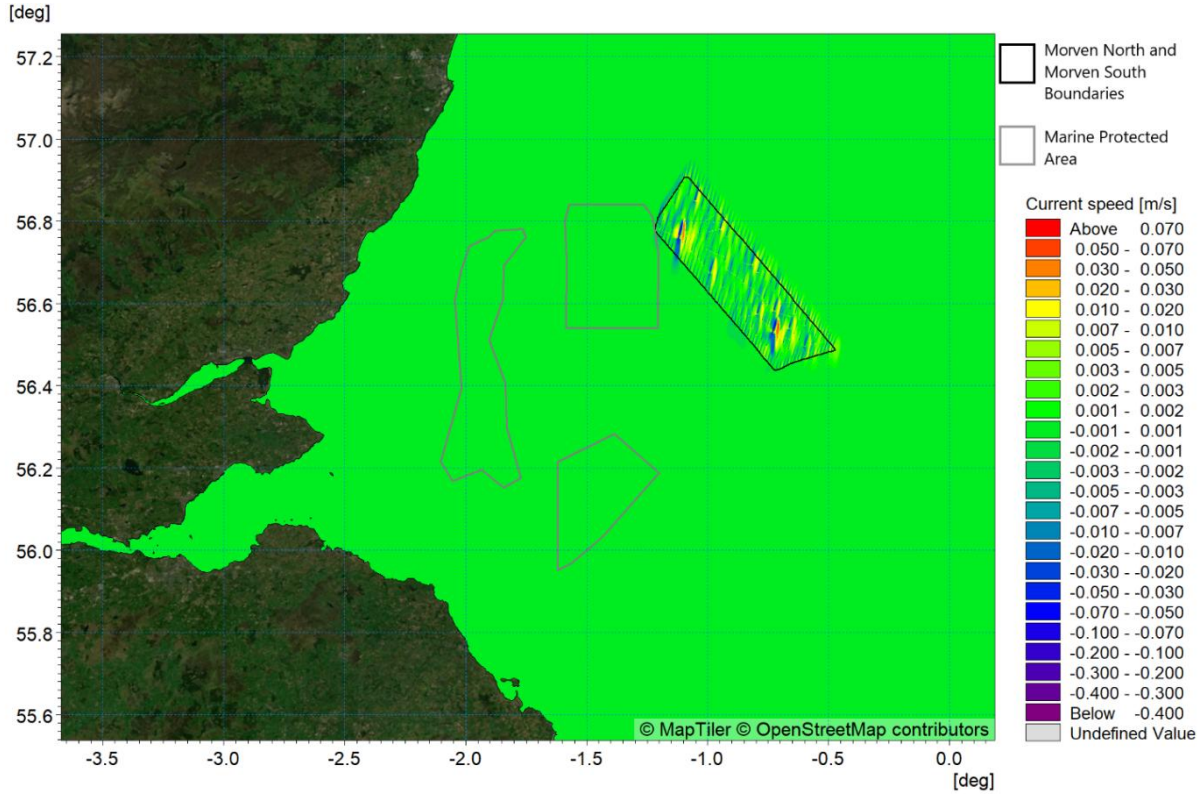

Figure 5.9: Change in tidal flow (post-construction Morven North and Morven South minus baseline) – peak ebb (low water - 1 hour)

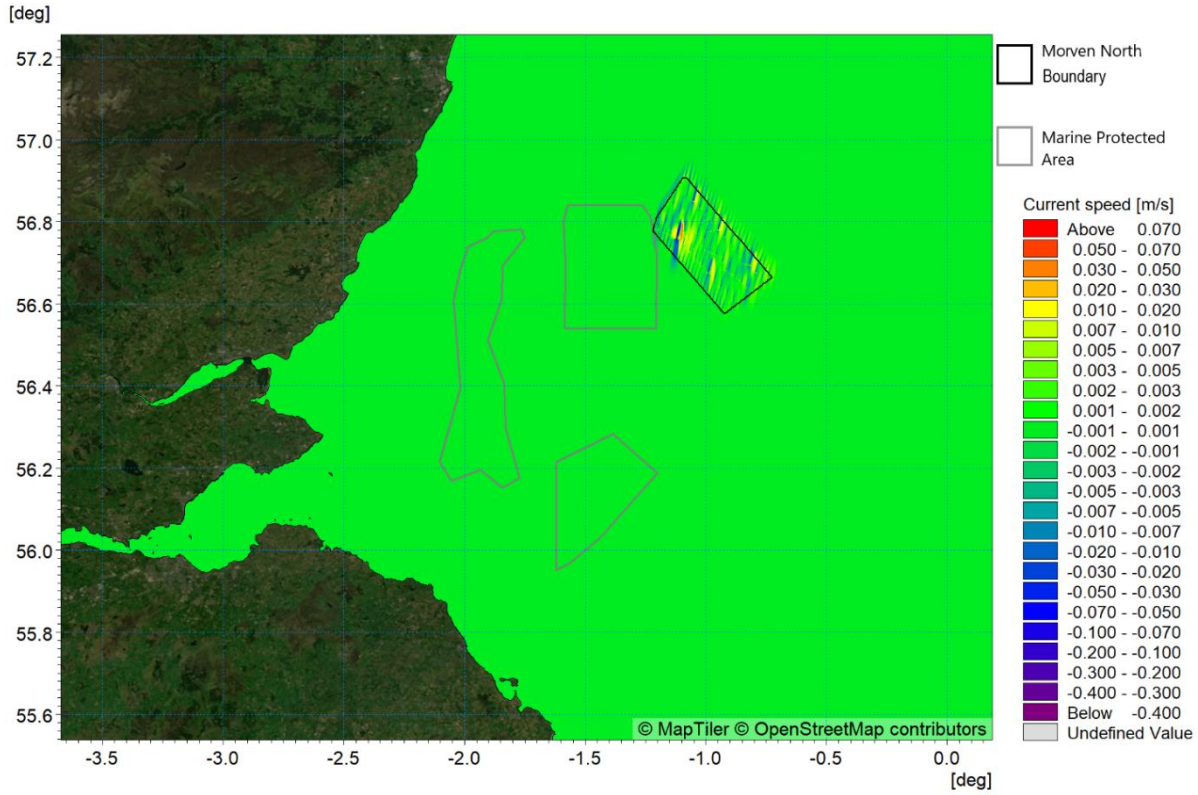

Figure 5.10: Change in tidal flow (post-construction Morven North minus baseline) – peak ebb (low water - 1 hour)

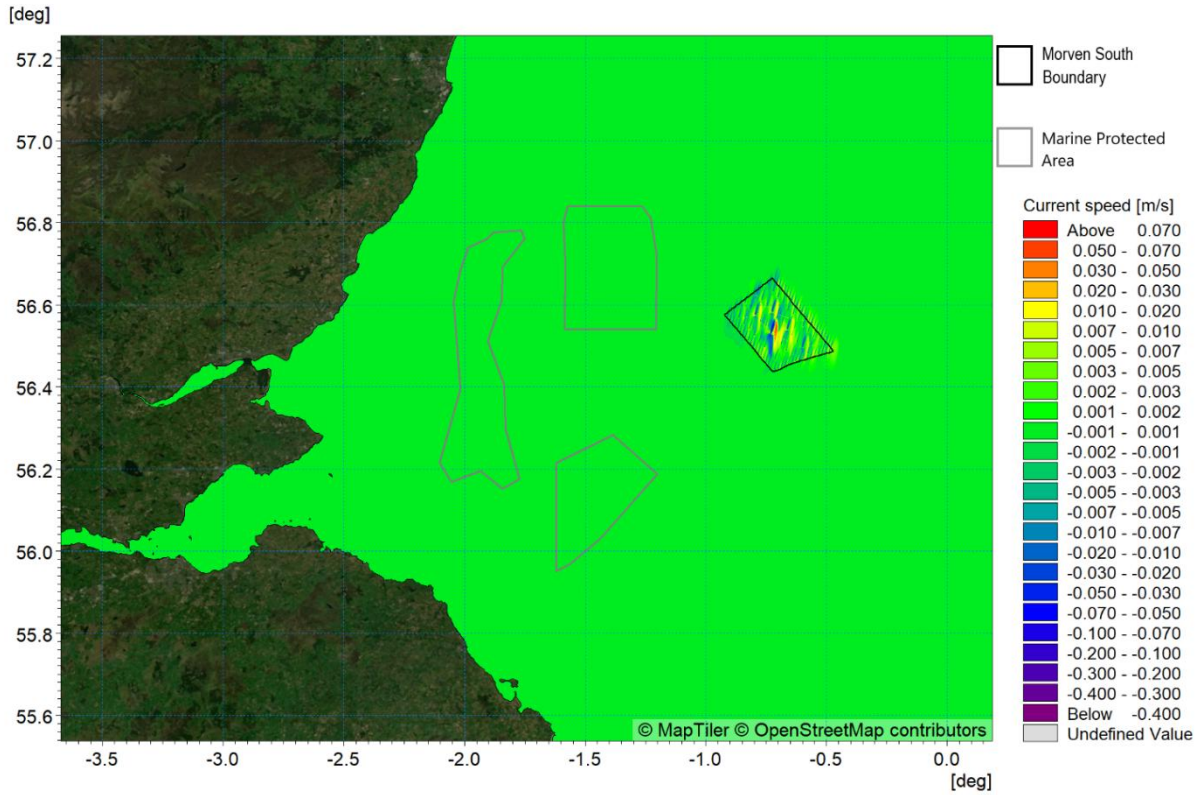

Figure 5.11: Change in tidal flow (post-construction Morven South minus baseline) – peak ebb (low water - 1 hour)

5.2.2 Wave climate

5.2.2.1 Using the same principle as for the tidal modelling, the wave climate modelling was repeated with the inclusion of the Morven North infrastructure, Morven South infrastructure and with the combined presence of the Morven North and Morven South infrastructure. Changes were found to be indiscernible from the baseline scenario by visual inspection of the significant wave height plots, therefore difference plots have been provided and a log scale was employed to highlight the variation.

5.2.2.2 The presence of both Morven North and Morven South was seen to have the greatest influence when storms approached from the southerly sector. The 1 in 1 year storm for the 180° direction for the MSL condition is presented in Figure 5.12 and corresponds to the baseline plot in Figure 4.50. The change in wave climate is presented in Figure 5.13, Figure 5.14 and Figure 5.15 due to Morven North, Morven South and Morven North and Morven South together respectively.

5.2.2.3 A similar pattern was observed between the 1 in 1 and 1 in 20 year return period storms from each direction therefore, for brevity, only the 1 in 20 year results are presented for the additional storm directions. The more severe 1 in 20 year storm event results are presented in Figure 5.16 to Figure 5.35 for the five principal directions which effect the Physical Processes Study Area (000°, 045°, 090°, 135°, 180°). In each case, the post-construction wave climate is followed by the difference plots of Morven North and Morven South together, Morven North and finally Morven South.

Morven North

5.2.2.4 For the 1 in 1 year storm, the changes within the Morven North Boundary are seen as reductions in the lee of the site and increases where the waves are deflected by the structures. These changes represent increases up to 0.35m and decreases up to 0.8m in the vicinity of the bridge-linked HVDC converter OSP gravity base foundations within the Morven North Boundary or up to circa 14% of baseline significant wave height. Notably smaller changes to the wave climate are incurred by the HVAC collector gravity base OSP foundations and wind turbine foundations.

5.2.2.5 It is apparent where the wave field interacts with either a wind turbine structure or a protection feature which reduces the water depth, the origin of the changes between baseline and post construction simulations are focussed on these locations. In the case of the 1 in 20 year storms, the changes are seen to follow the same pattern, with decreases in the lee of the infrastructure and increases either side. However, it is noted that the changes are not considerably increased from the more frequent return period scenario, for example for the 180° storm, increases are observed up to circa 0.4m, with decreases of up to 0.9m in the lee of the bridge-linked HVDC converter OSP gravity base foundations within the Morven North Boundary. This is relative to the baseline wave heights which are increased for the greater return period events giving rise to a less marked overall impact on wave climate.

Morven South

5.2.2.6 For the 1 in 1 year storm, the changes within the Morven South Boundary are seen as reductions in the lee of the site and increases where the waves are deflected by the structures. These changes represent increases up to 0.2m and decreases up to 0.8m in the vicinity of the bridge-linked HVDC converter OSP gravity base foundations within the Morven South Boundary or up to circa 14% of baseline significant wave height. Notably smaller changes to the wave climate are incurred by the HVAC collect gravity base OSP foundations and wind turbine foundations.

5.2.2.7 As for Morven North (paragraph 5.2.2.5), the 1 in 20 year storms follow the same pattern as the 1 in year storms, with decreases in the lee of the infrastructure and increases either side. It is noted that these changes are not considerably increased from the more frequent return period scenario.

Morven North and Morven South

5.2.2.8 The peak changes discussed under paragraphs 5.2.2.4 and 5.2.2.6 were unaffected when the Morven North and Morven South infrastructure was modelled together, however there was some accumulation of differences within the Morven North Boundary, when the Morven South

infrastructure was included together with the Morven North infrastructure from this southerly direction.

5.2.2.9 Note some modelled differences are observed beyond the Morven North Boundary and Morven South Boundary, however, these are limited in magnitude, for example for the northerly dominant storm, up to a maximum of circa 0.1m within 20km of the Morven Site, gradually reducing to baseline beyond this. This applies to both 1 in 1 year and 1 in 20 year storms from the North, with the less severe storm producing a marginally smaller extent of change. There is not anticipated to be any change to coastal wave climates due to the Morven North and Morven South infrastructure when present simultaneously.

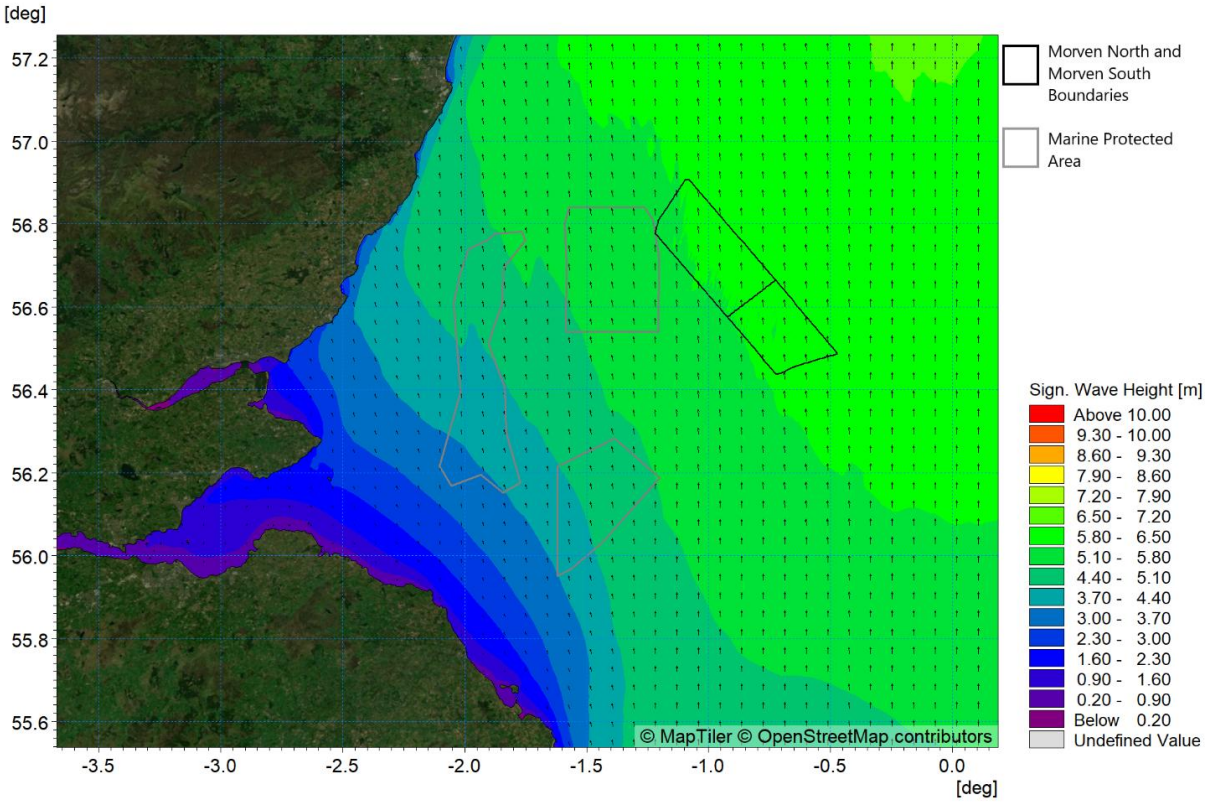

Figure 5.12: Post-construction (Morven North and Morven South) wave climate 1:1 year storm from 180° at mid-tide

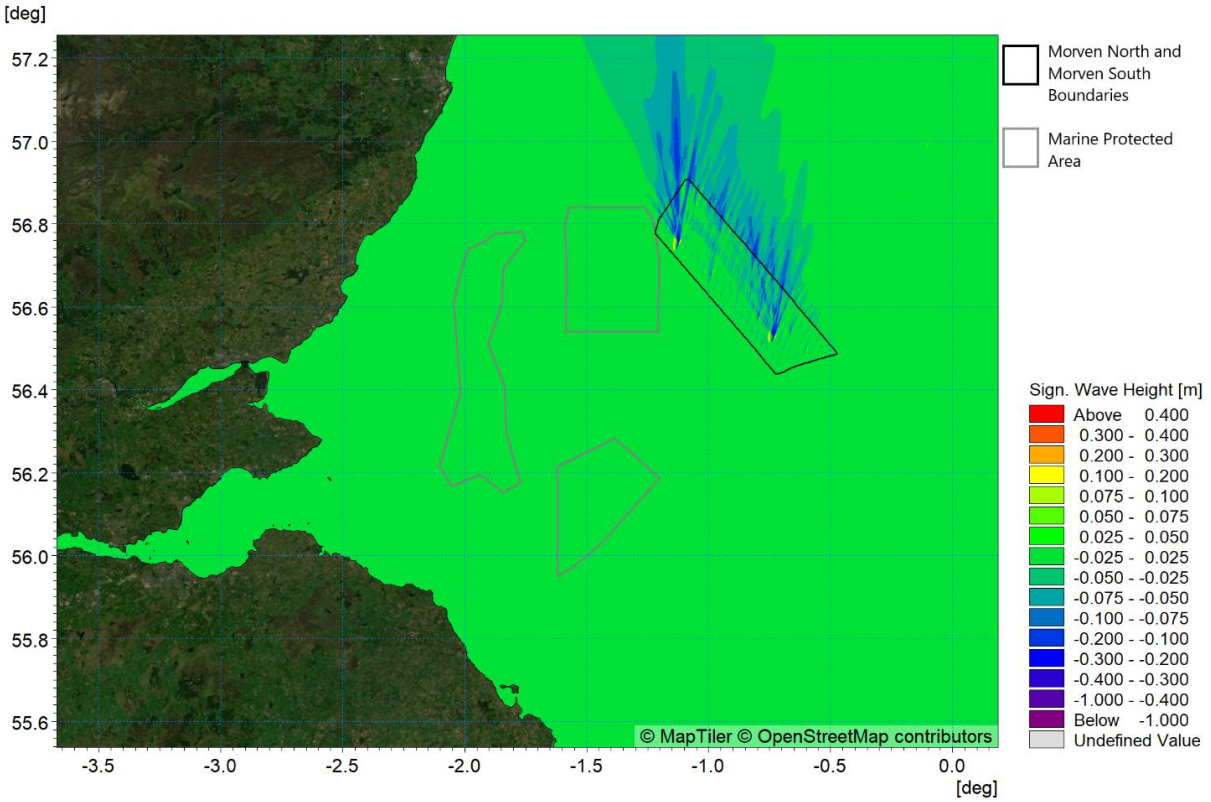

Figure 5.13: Change in wave climate (Morven North and Morven South) 1:1 year storm from 180° (post-construction minus baseline)

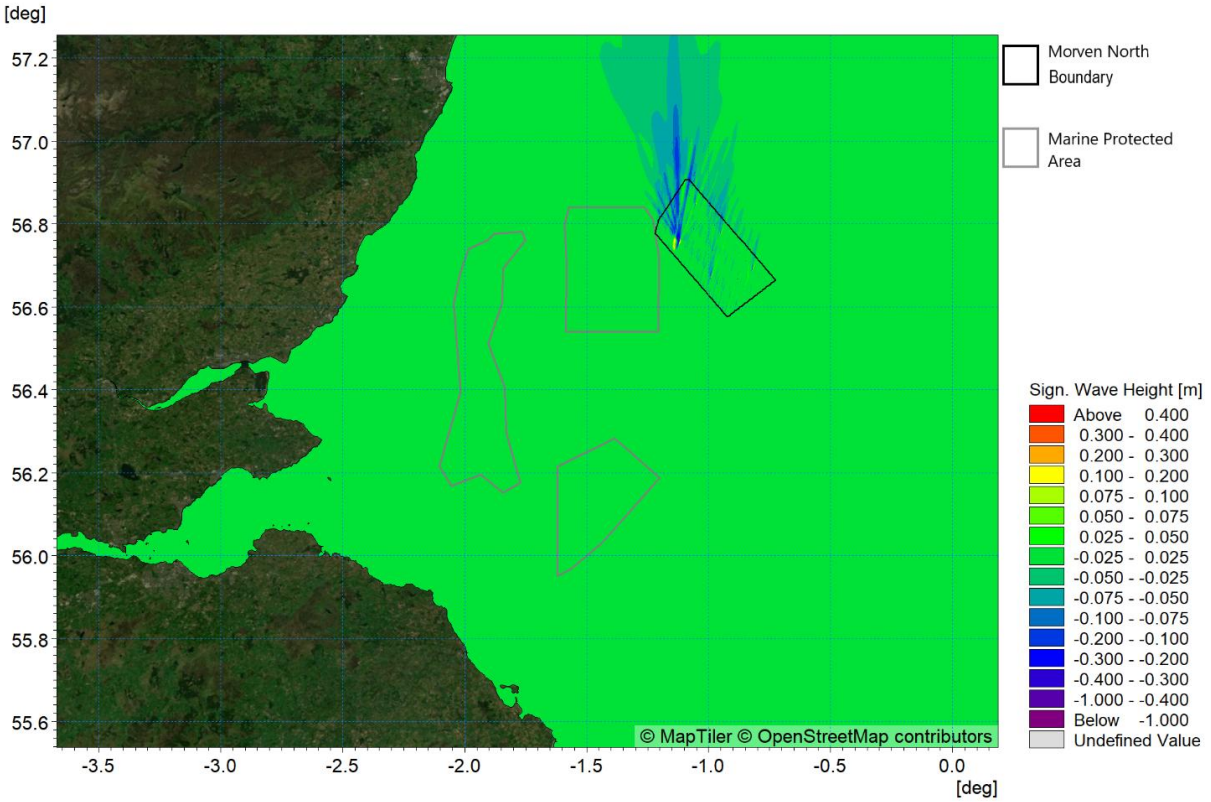

Figure 5.14: Change in wave climate (Morven North) 1:1 year storm from 180° (post-construction minus baseline)

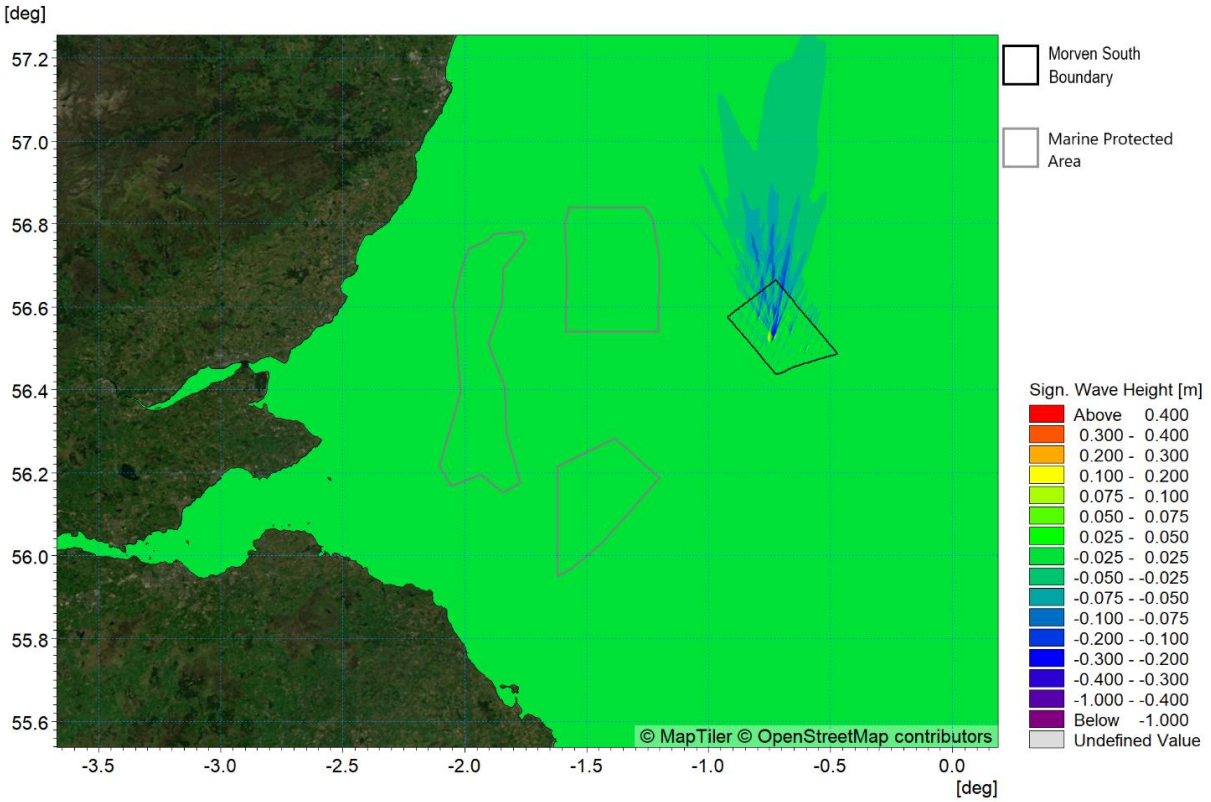

Figure 5.15: Change in wave climate (Morven South) 1:1 year storm from 180° (post-construction minus baseline)

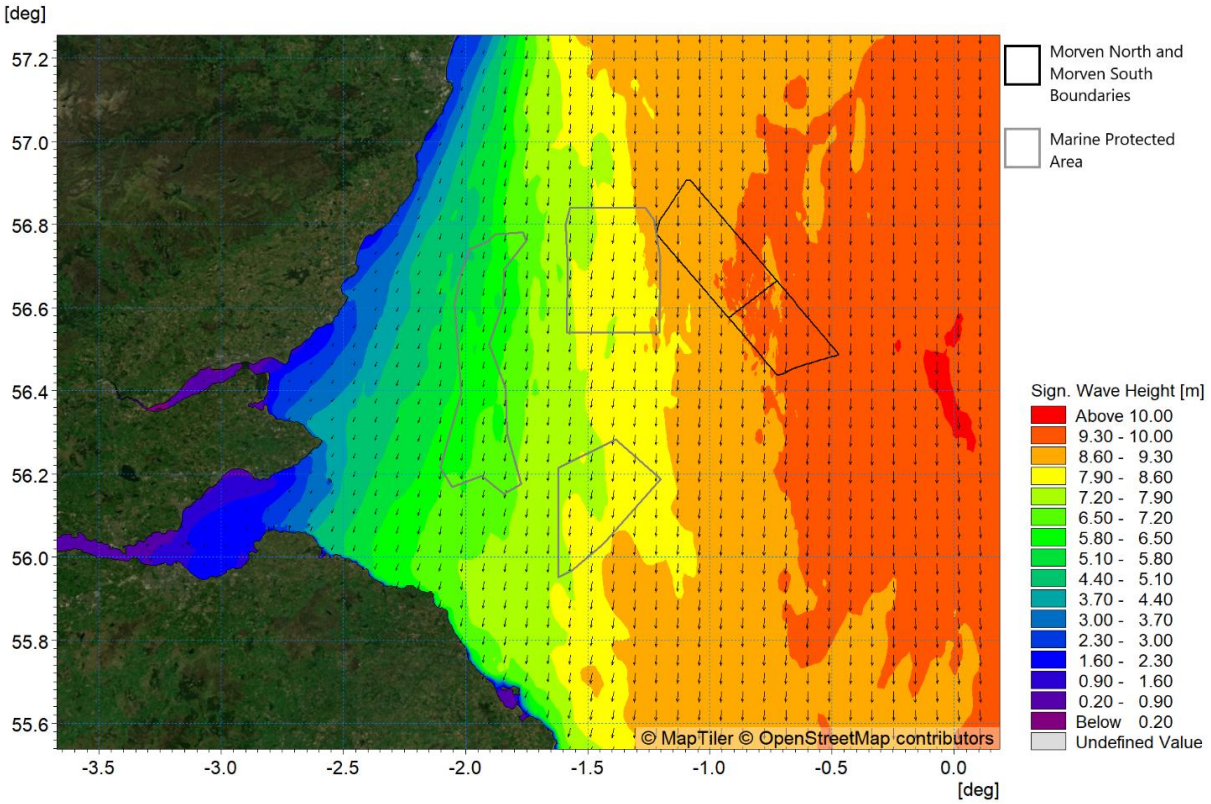

Figure 5.16: Post-construction (Morven North and Morven South) wave climate 1:20 year storm from 000° at mid-tide

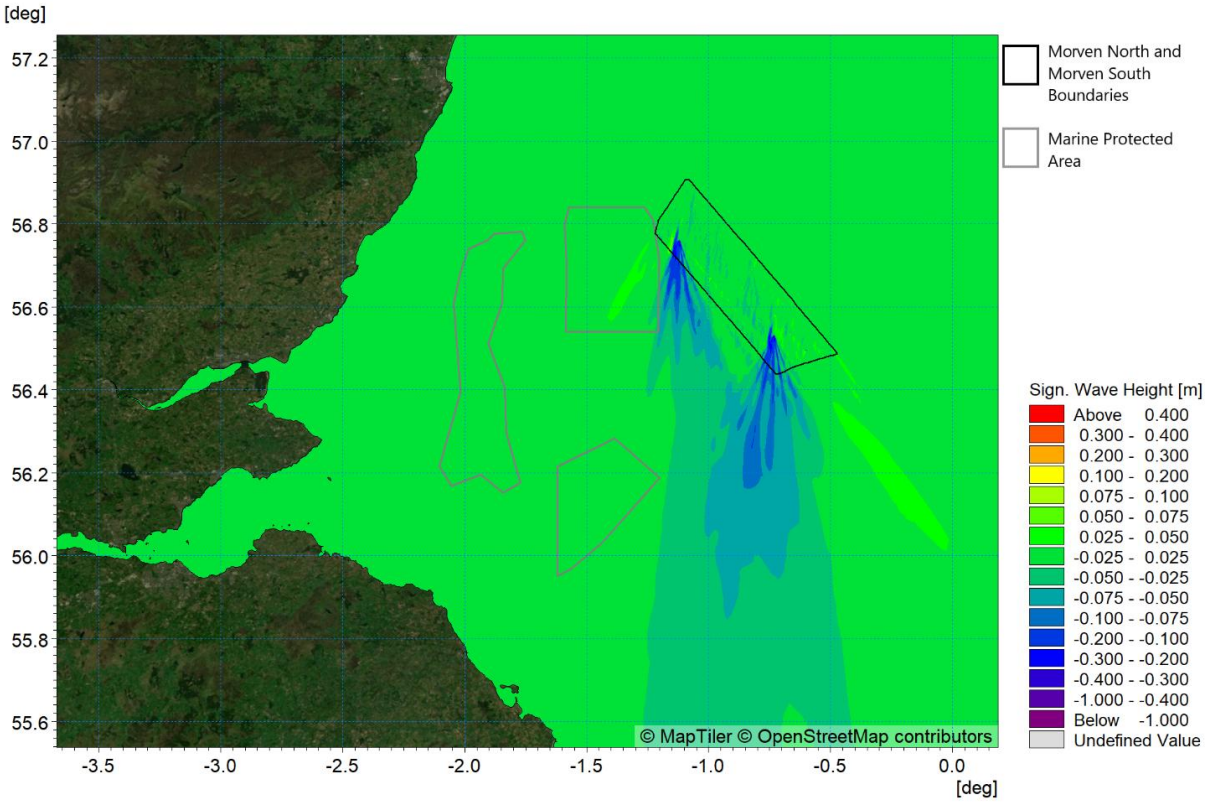

Figure 5.17: Change in wave climate (Morven North and Morven South) 1:20 year storm from 000° (post-construction minus baseline)

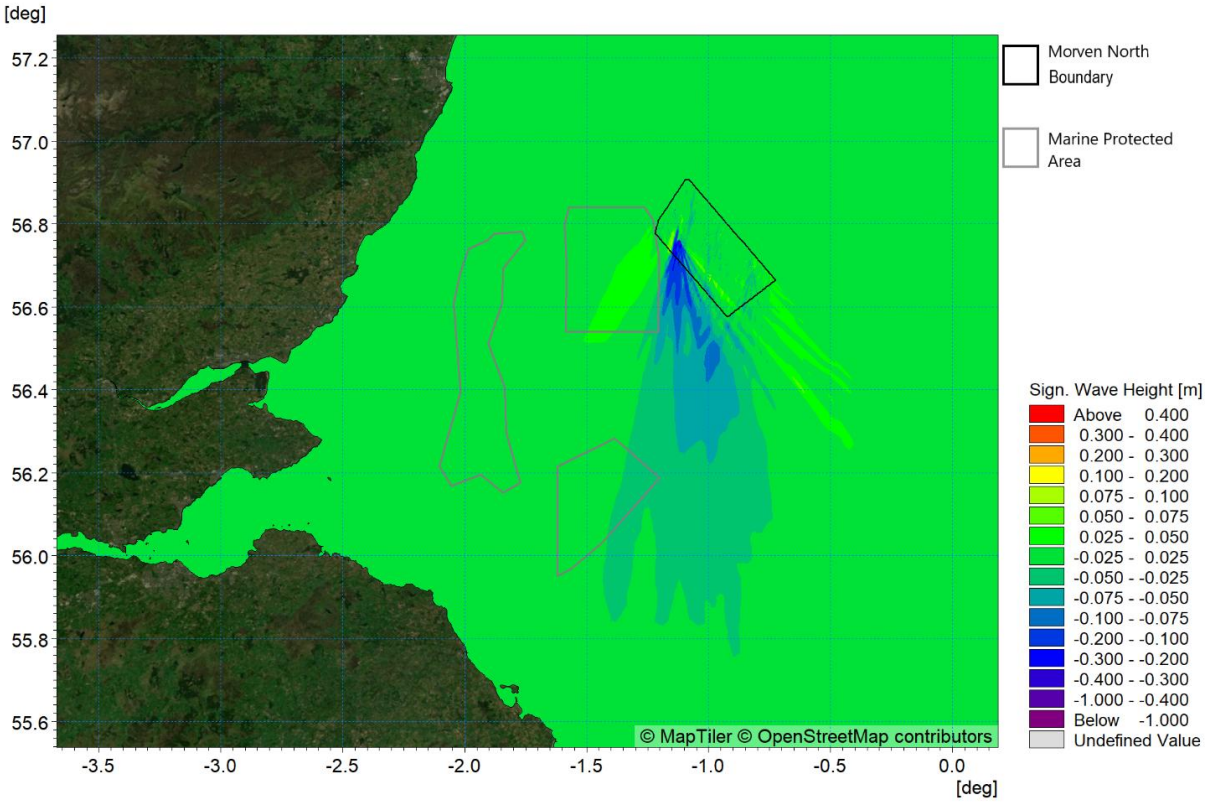

Figure 5.18: Change in wave climate (Morven North) 1:20 year storm from 000° (post-construction minus baseline)

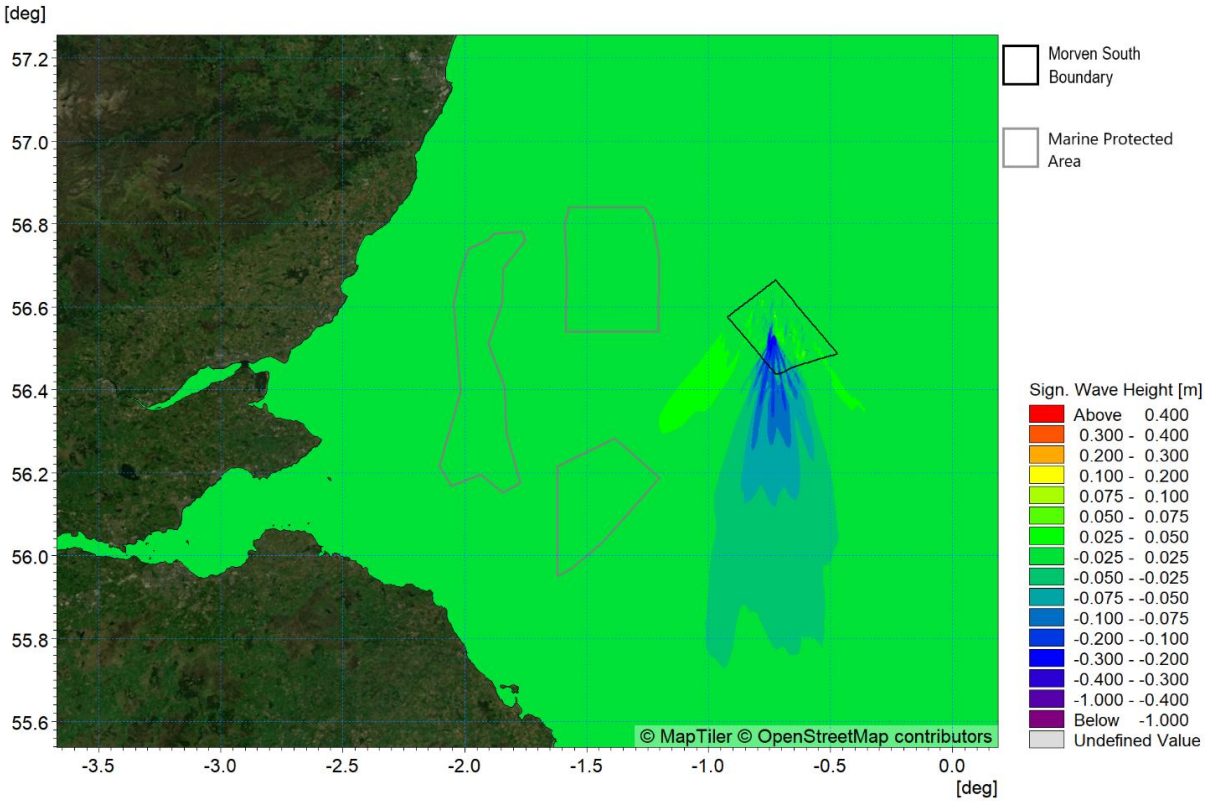

Figure 5.19: Change in wave climate (Morven South) 1:20 year storm from 000° (post-construction minus baseline)

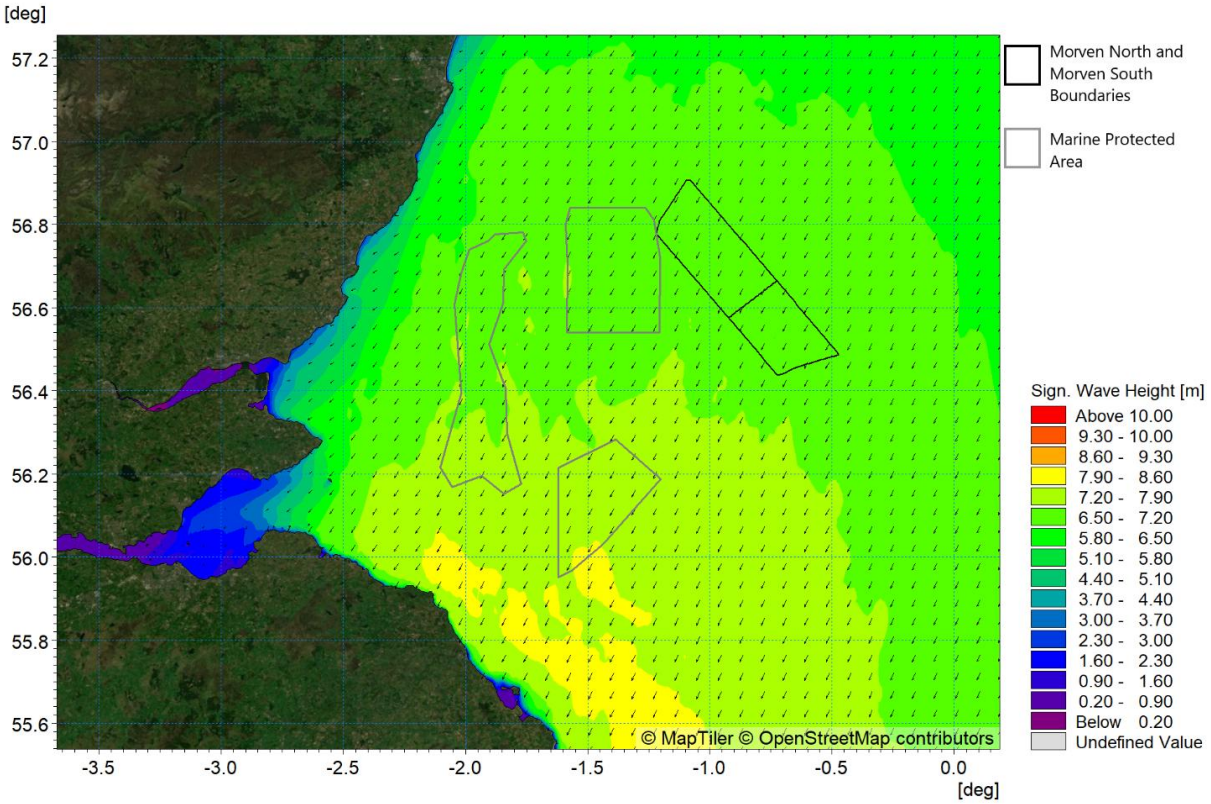

Figure 5.20: Post-construction (Morven North and Morven South) wave climate 1:20 year storm from 045° at mid-tide

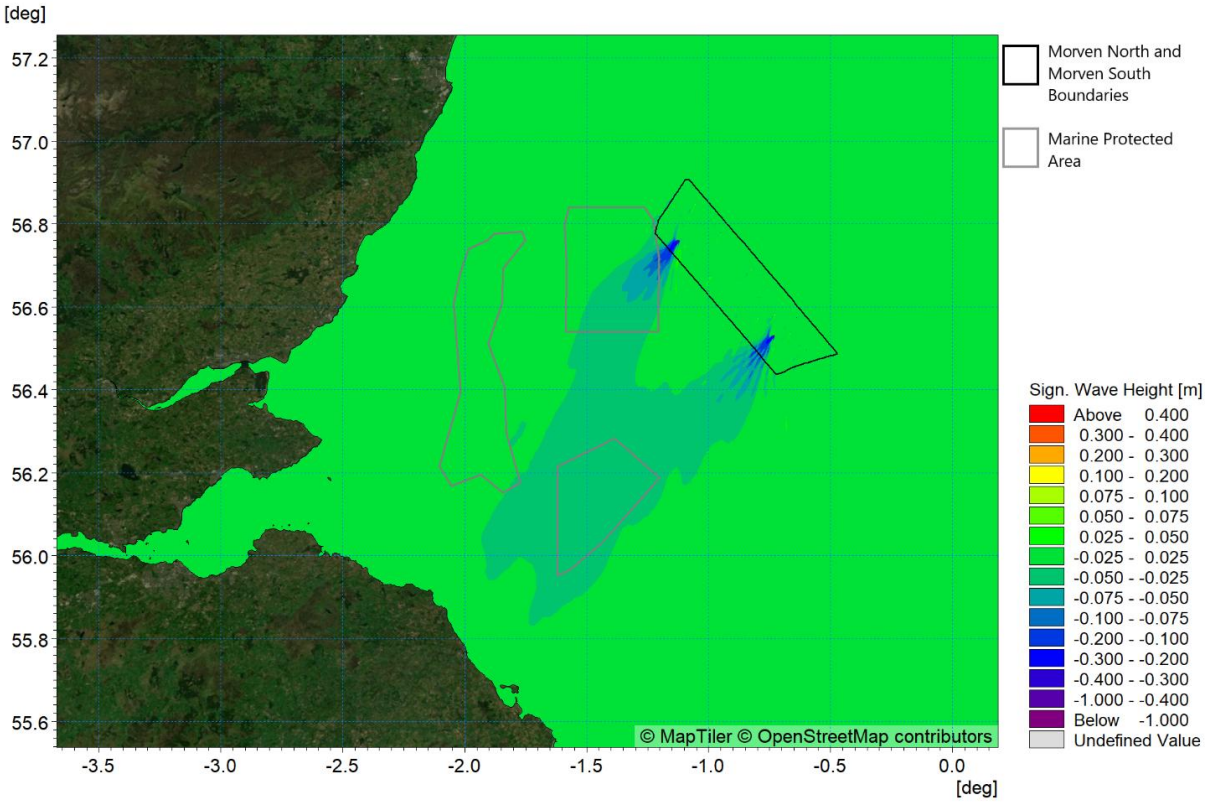

Figure 5.21: Change in wave climate (Morven North and Morven South) 1:20 year storm from 045° (post-construction minus baseline)

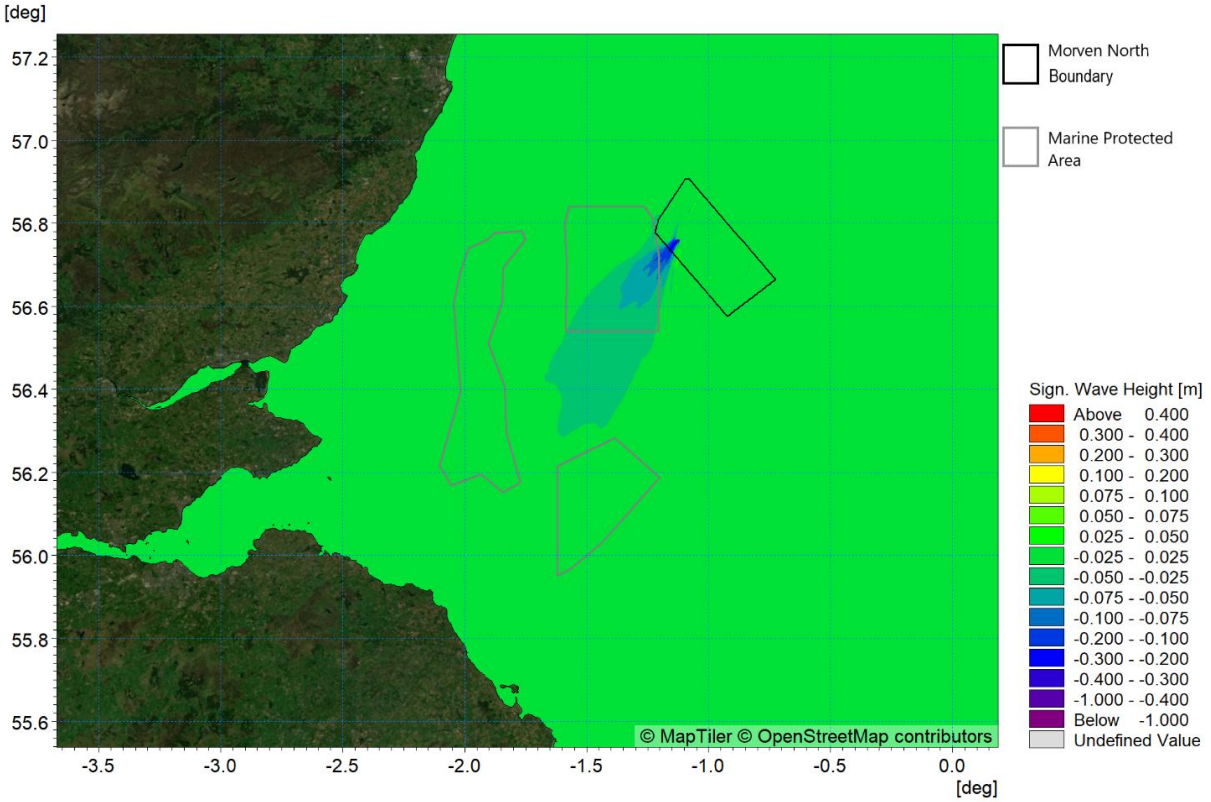

Figure 5.22: Change in wave climate (Morven North) 1:20 year storm from 045° (post-construction minus baseline)

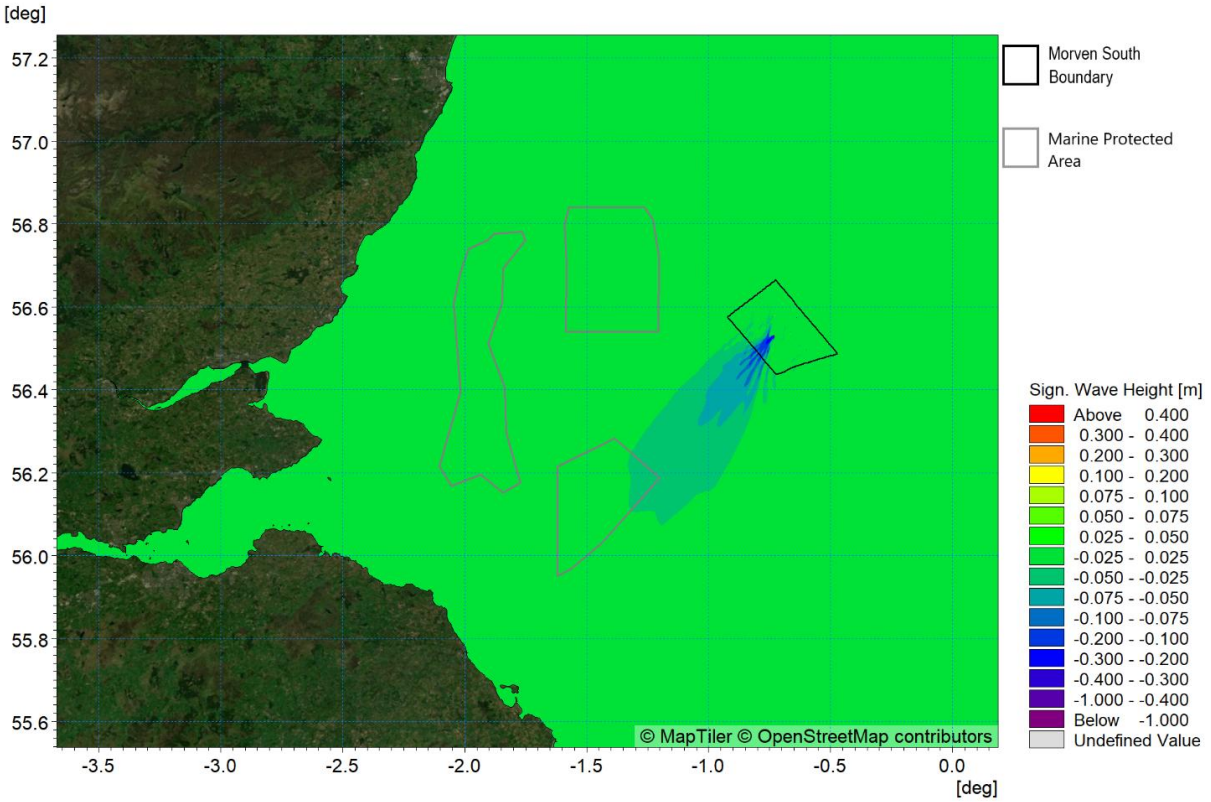

Figure 5.23: Change in wave climate (Morven South) 1:20 year storm from 045° (post-construction minus baseline)

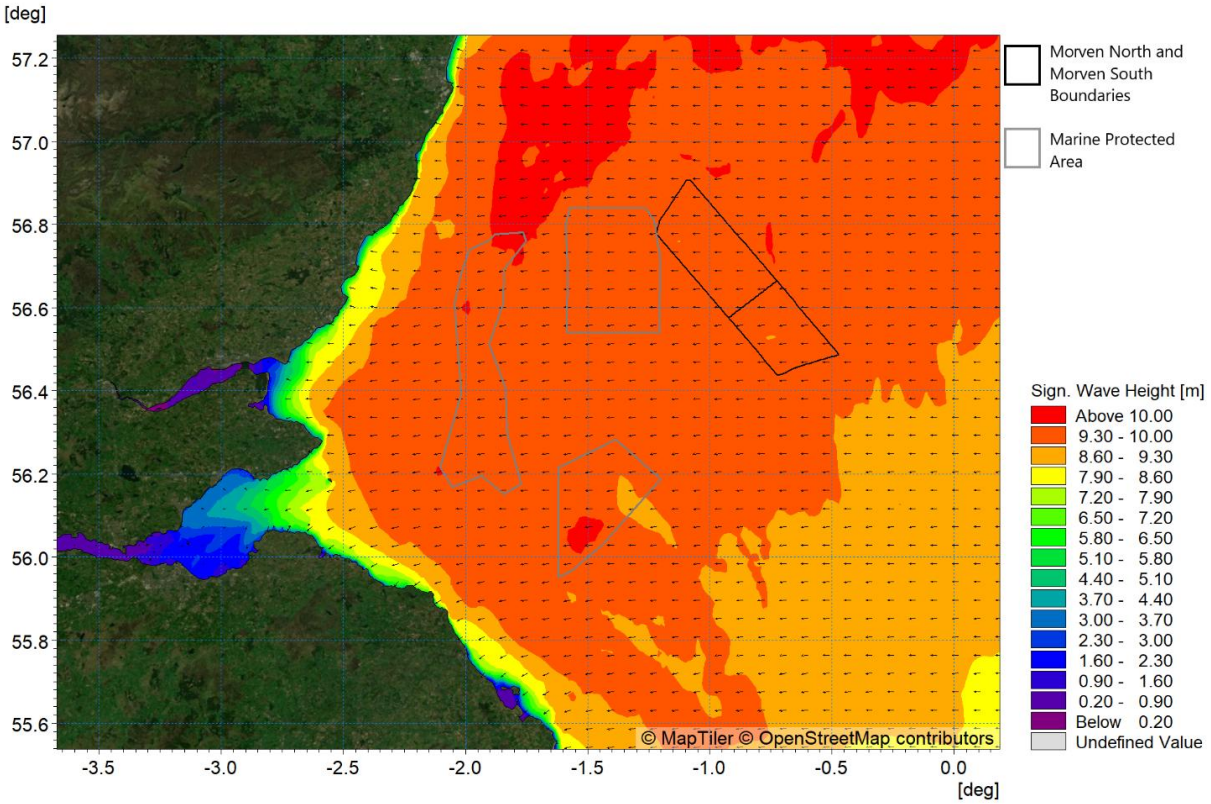

Figure 5.24: Post-construction (Morven North and Morven South) wave climate 1:20 year storm from 090° at mid-tide

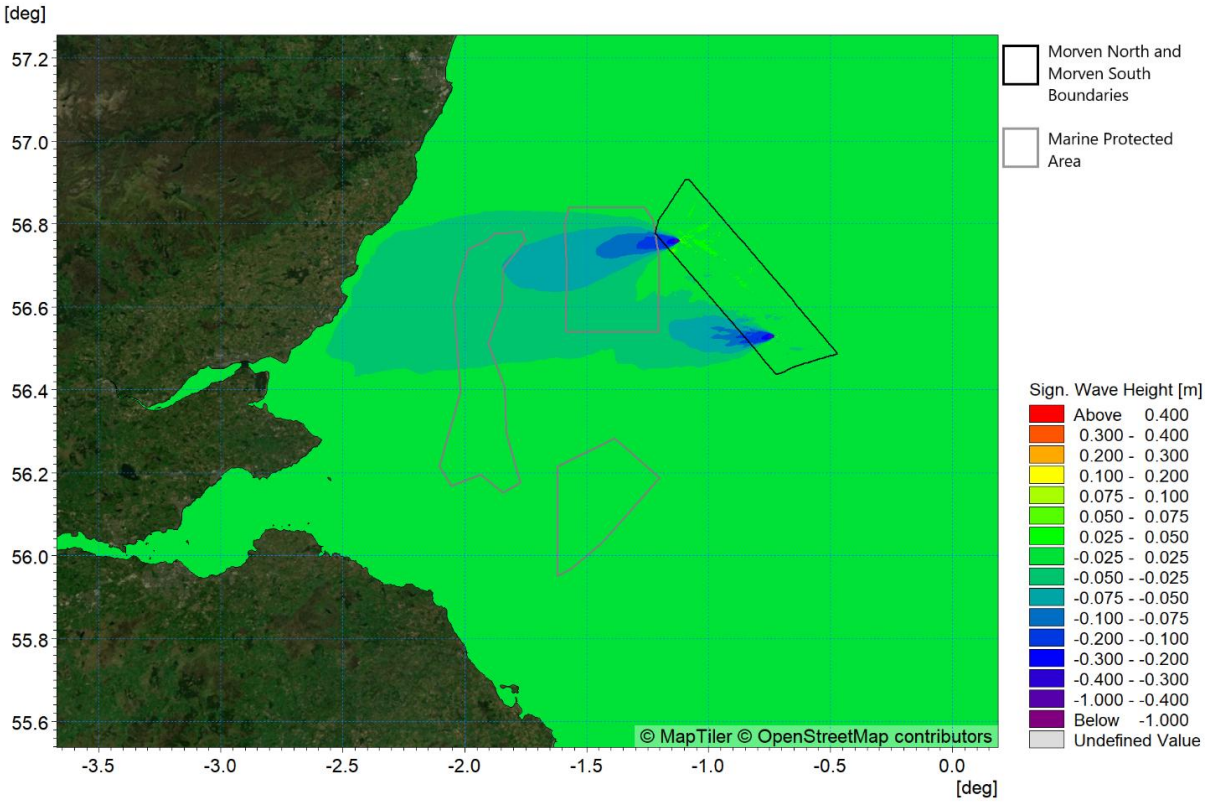

Figure 5.25: Change in wave climate (Morven North and Morven South) 1:20 year storm from 090° (post-construction minus baseline)

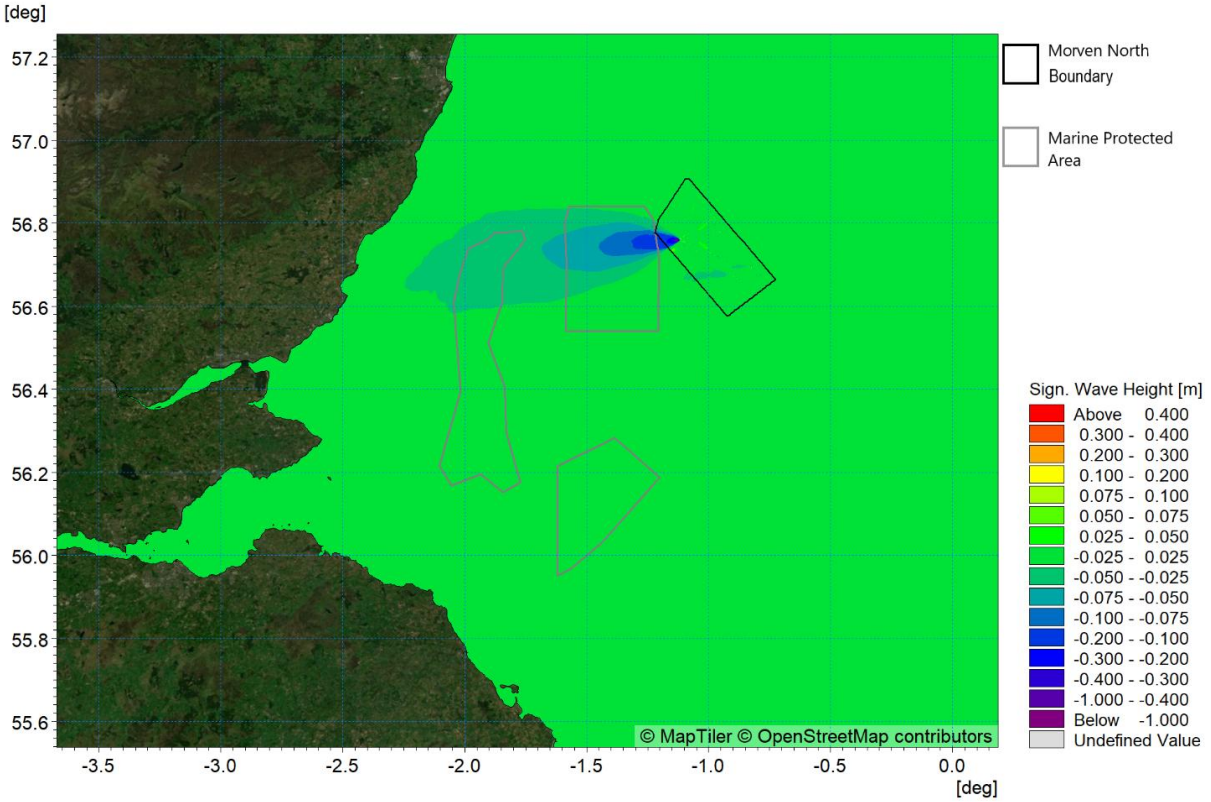

Figure 5.26: Change in wave climate (Morven North) 1:20 year storm from 090° (post-construction minus baseline)

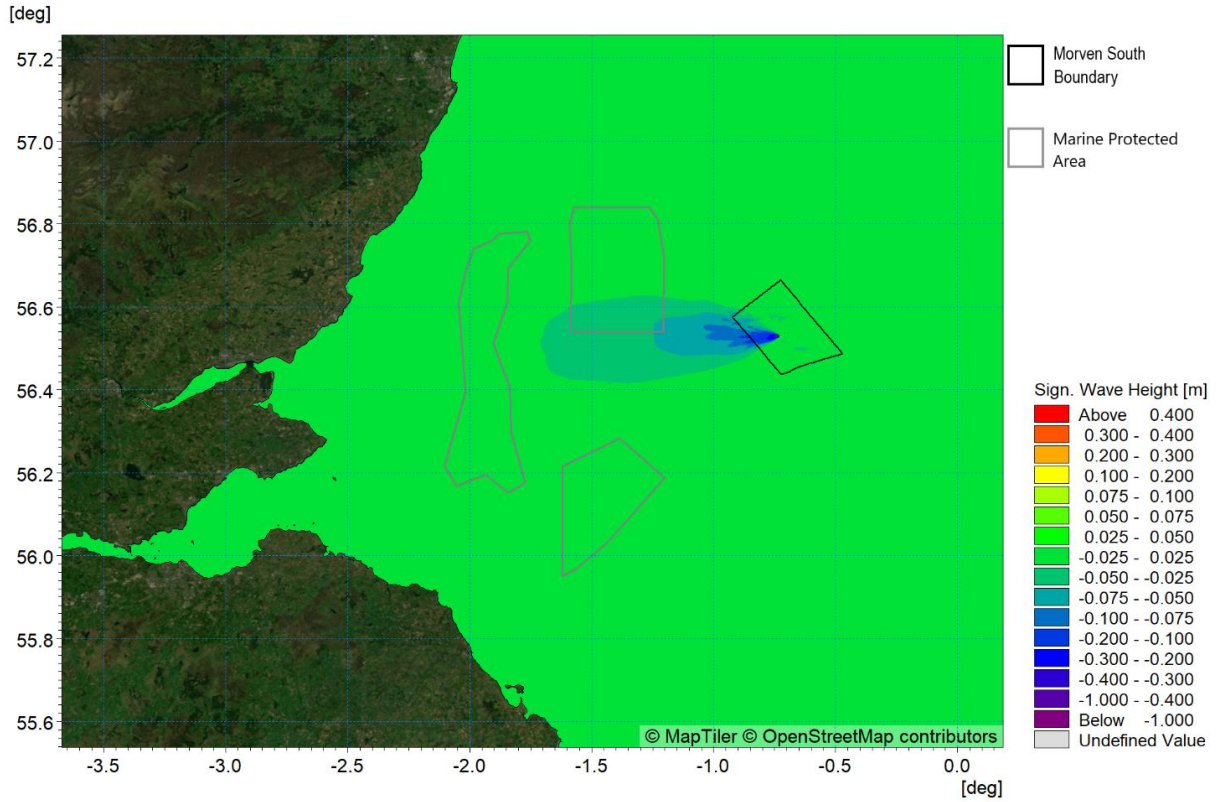

Figure 5.27: Change in wave climate (Morven South) 1:20 year storm from 090° (post-construction minus baseline)

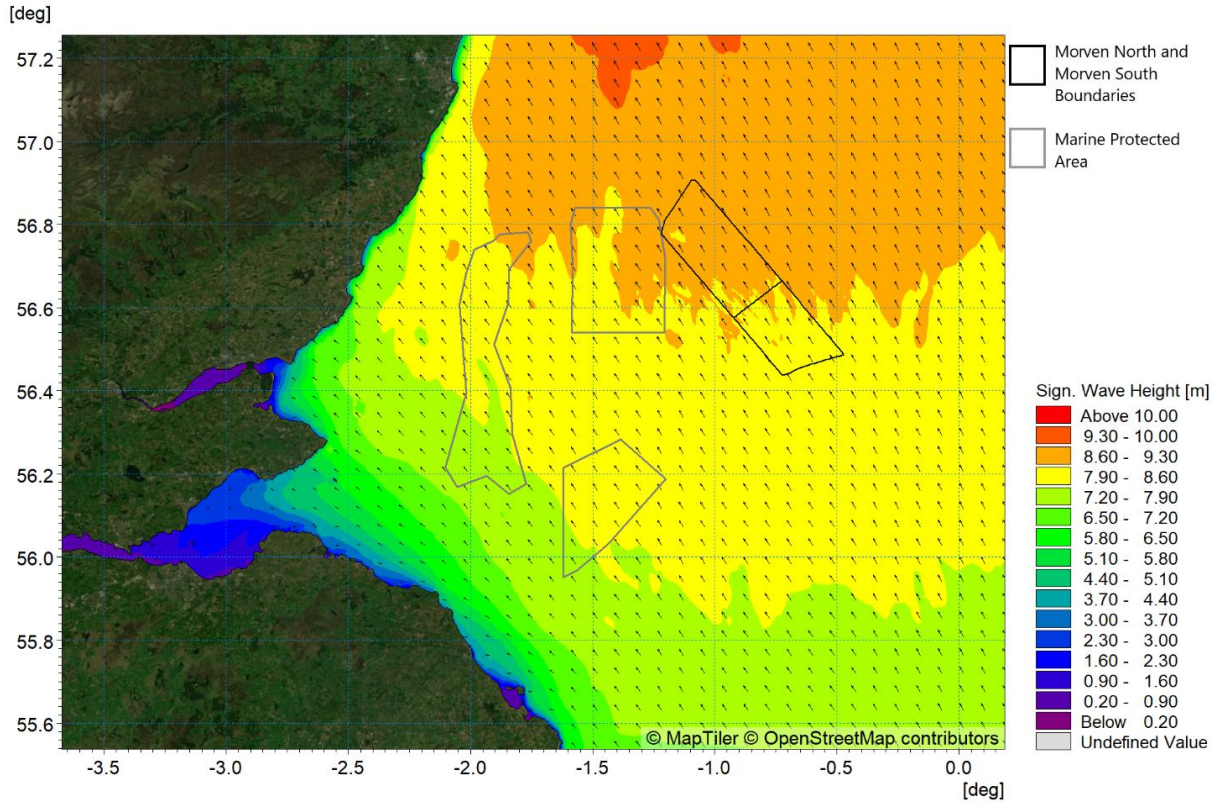

Figure 5.28: Post-construction (Morven North and Morven South) wave climate 1:20 year storm from 135° at mid-tide

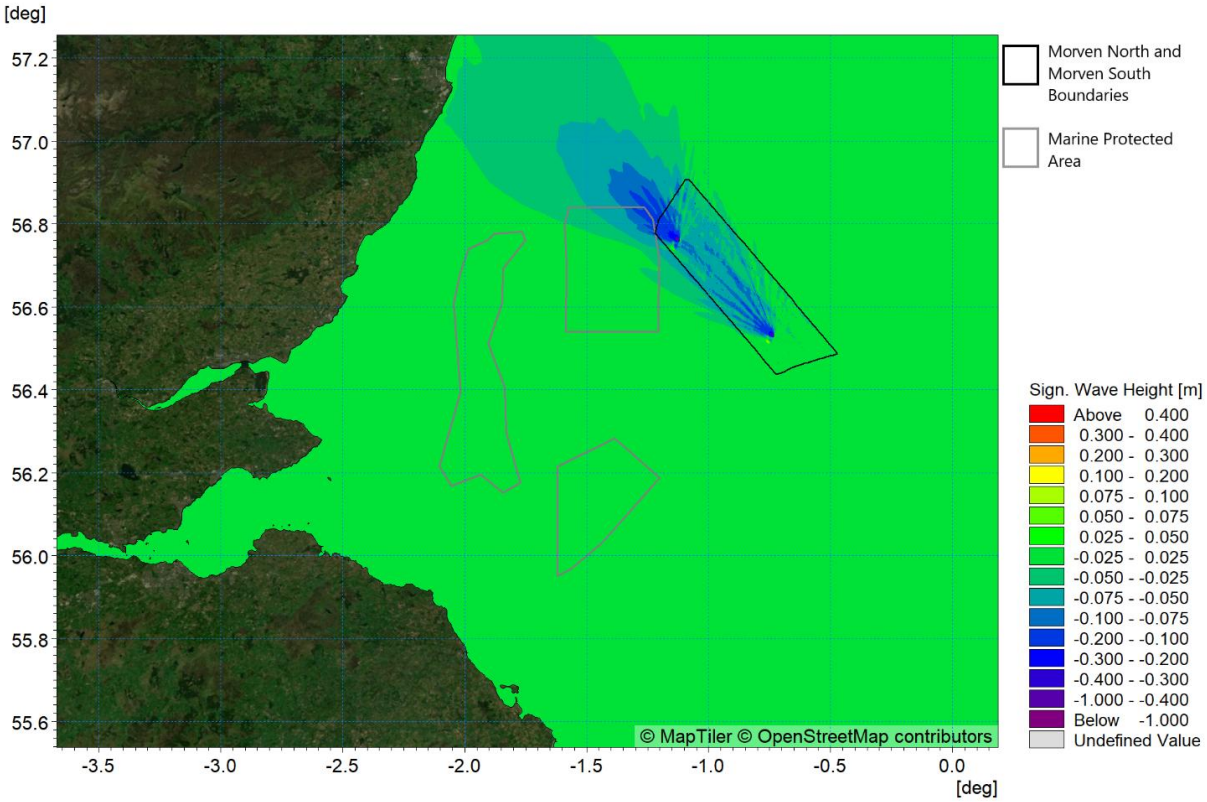

Figure 5.29: Change in wave climate (Morven North and Morven South) 1:20 year storm from 135° (post-construction minus baseline)

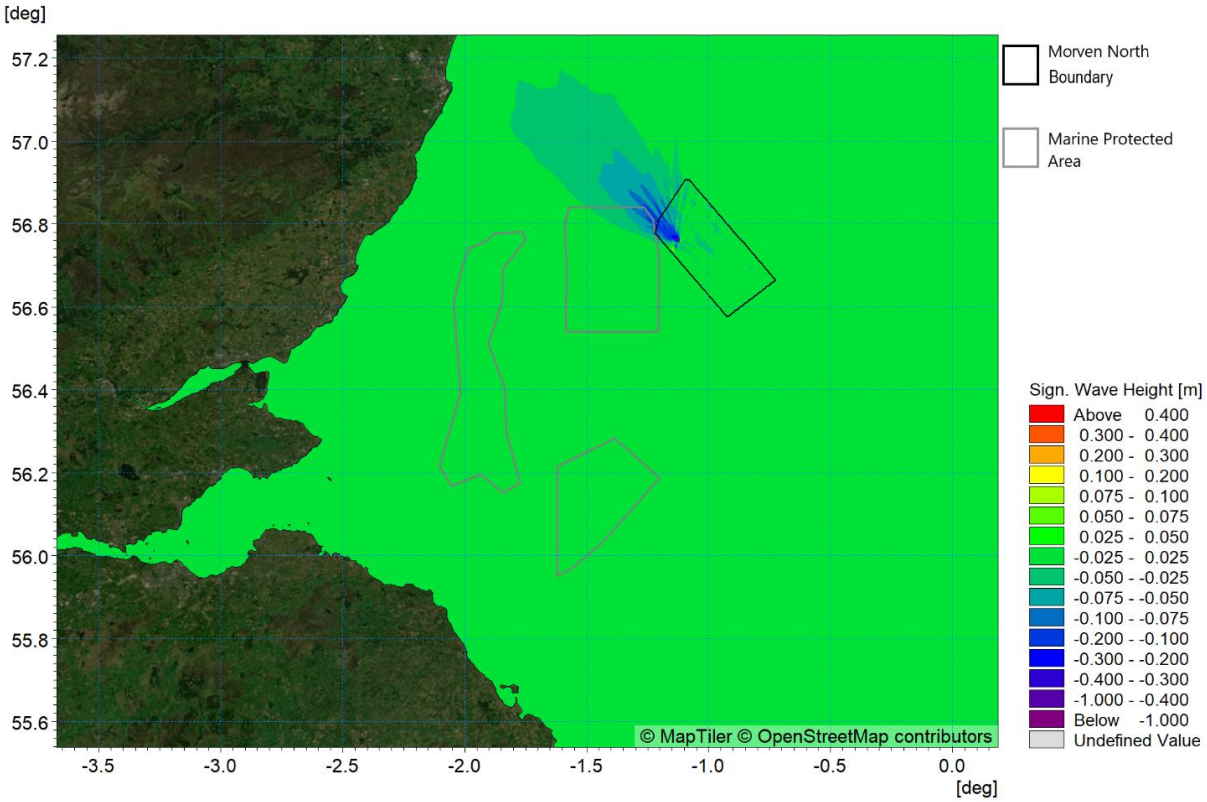

Figure 5.30: Change in wave climate (Morven North) 1:20 year storm from 135° (post-construction minus baseline)

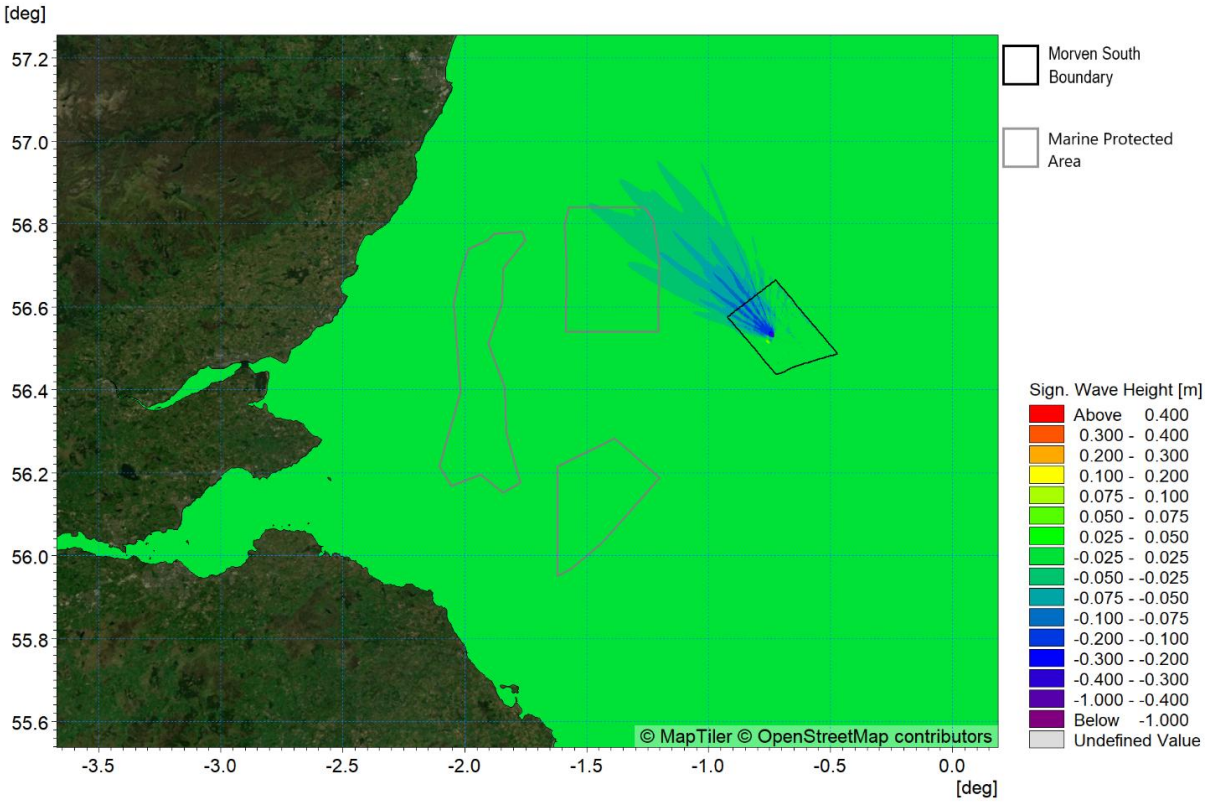

Figure 5.31: Change in wave climate (Morven South) 1:20 year storm from 135° (post-construction minus baseline)

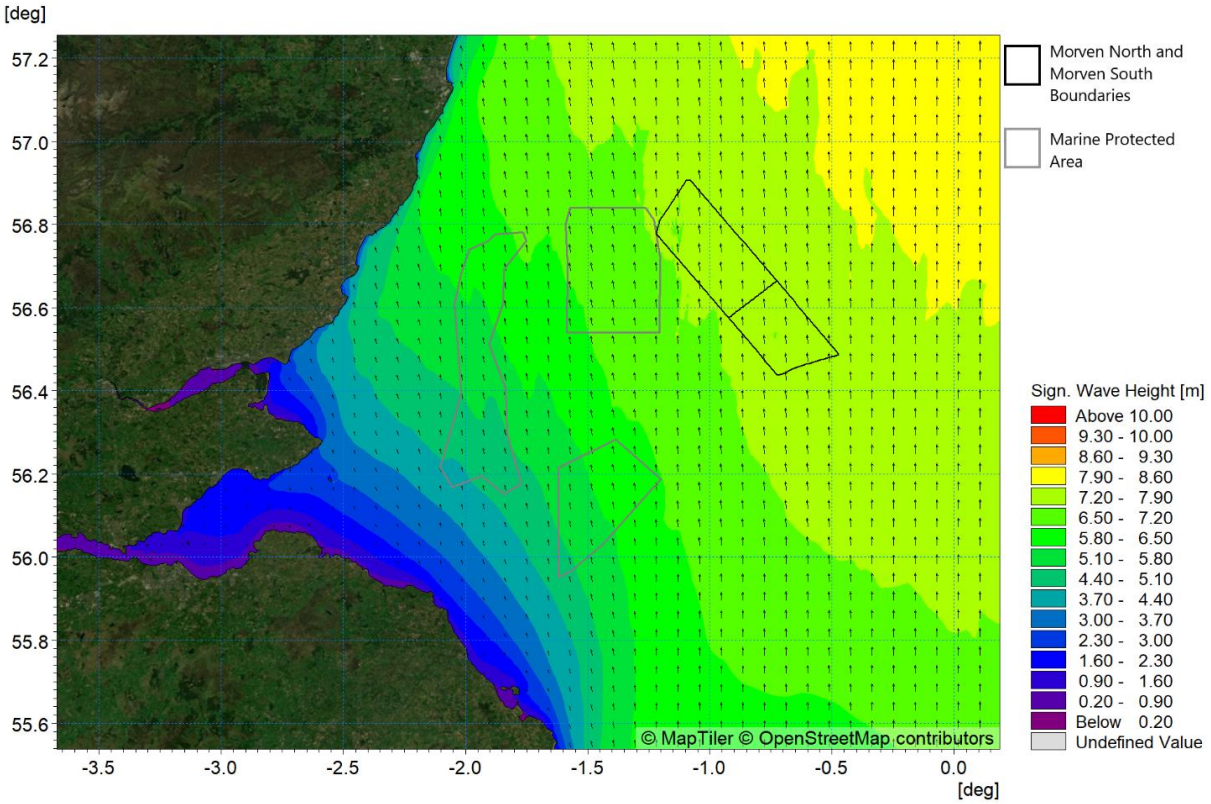

Figure 5.32: Post-construction (Morven North and Morven South) wave climate 1:20 year storm from 180° at mid-tide

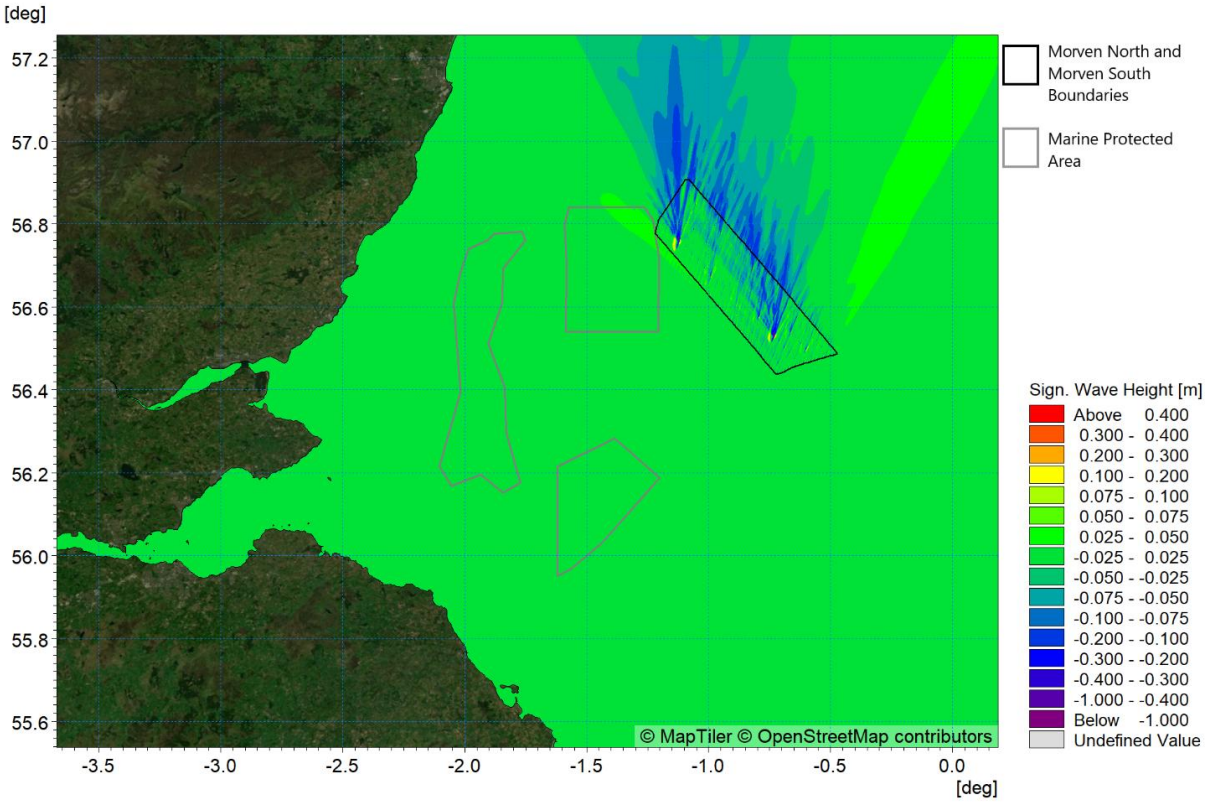

Figure 5.33: Change in wave climate (Morven North and Morven South) 1:20 year storm from 180° (post-construction minus baseline)

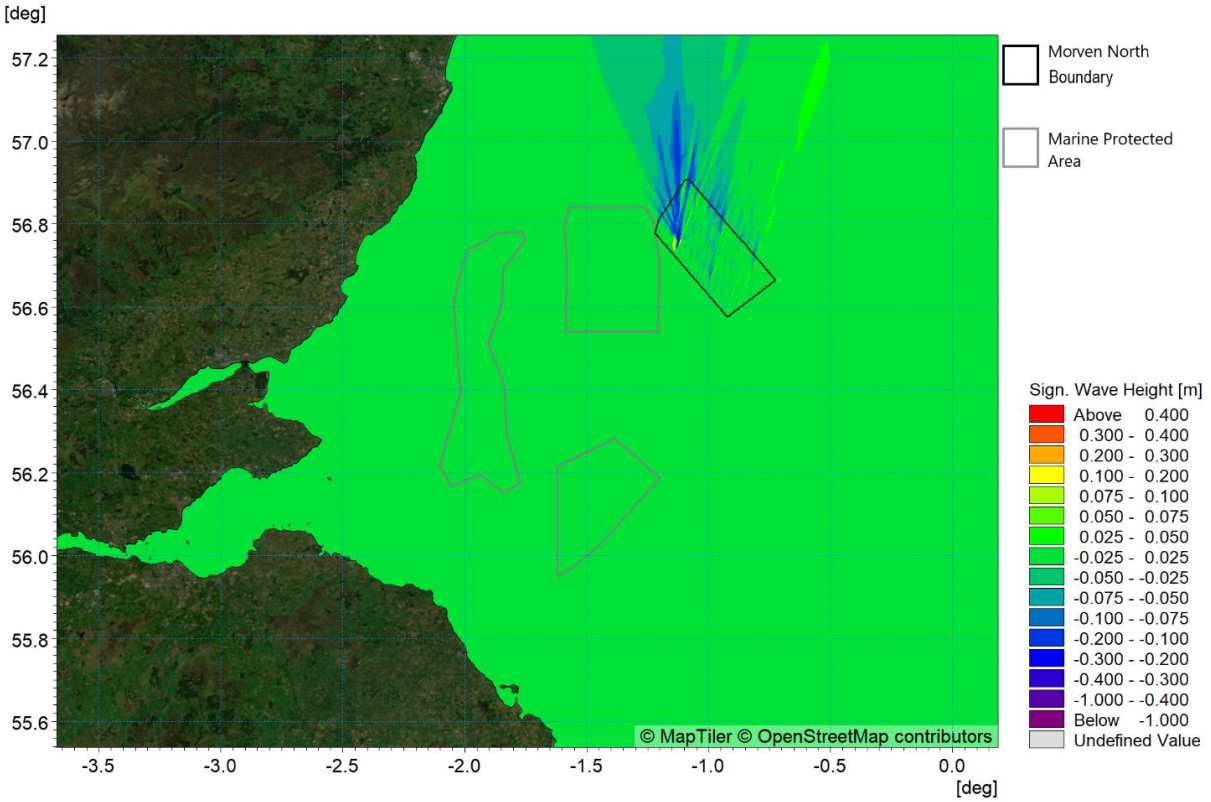

Figure 5.34: Change in wave climate (Morven North) 1:20 year storm from 180° (post-construction minus baseline)

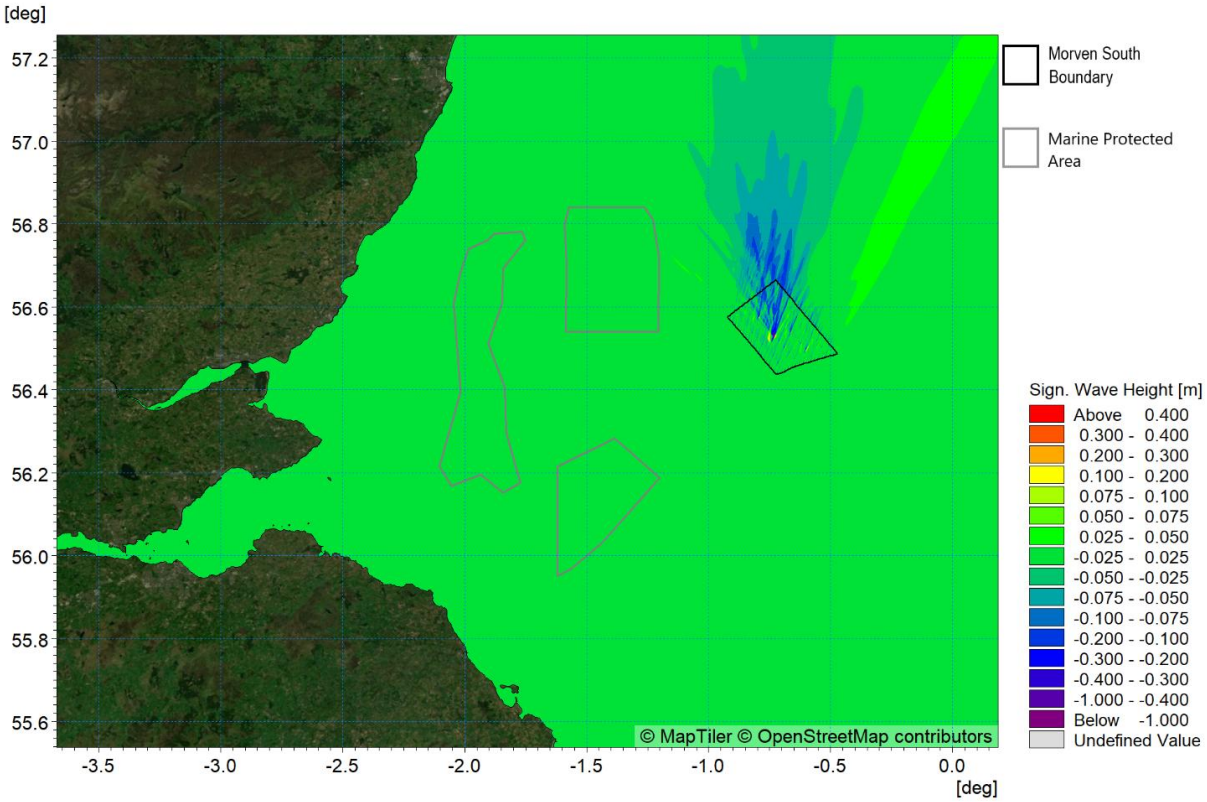

Figure 5.35: Change in wave climate (Morven South) 1:20 year storm from 180° (post-construction minus baseline)

5.2.3 Littoral currents

5.2.3.1 The previous sections established the magnitude of the changes in tidal currents and wave conditions individually however sediment transport regimes are driven by a combination of these factors. Although the modelling has demonstrated that the principal contribution to baseline sediment transport comes from tidal currents, for the sake of completeness, the influence on littoral currents due to Morven North and Morven South was examined.

5.2.3.2 The baseline coupled tide and wave modelling was extended to include the Morven North, Morven South and with Morven North and Morven South infrastructure for the 1 in 1 year storm from 000°. The baseline littoral currents for mid flood and mid ebb were presented in Figure 4.56 and Figure 4.57 respectively. The post-construction littoral currents are shown in Figure 5.36 and Figure 5.40 for Morven North and Morven South together, for the flood and ebb tides respectively. The corresponding changes for the flood tide are presented in Figure 5.37, Figure 5.38 and Figure 5.39 for Morven North and Morven South together, Morven North or Morven South respectively, whilst Figure 5.41, Figure 5.42 and Figure 5.43 show the corresponding information during the ebb tide.

Morven North

5.2.3.3 During the flood tide the influence of the wave climate is in concert with the tidal current and the tidal flow in the lee of each of the structures is further reduced. During the ebb tide, the tidal flow is in opposition to the wave climate and the resultant littoral current is reduced in magnitude.

5.2.3.4 The presence of the structures has a limited influence on the wave induced reduction in flow and there is little difference between changes in littoral current magnitude and the tidal flows alone due to the installation. For example, during the 1 in 1 year storm from 000°, within the Morven North Boundary, the bridge-linked HVDC converter OSP gravity base foundations have incurred an increase of up to 0.09m/s to the southwest of the structures during flood tide, whilst decreasing by up to 0.3m/s in the lee. This increase equates to circa 50% of the baseline littoral currents in this area. The

decrease in littoral currents is reduced to zero by circa 5km from the structures and is therefore confined to the Morven North Physical Processes Study Area.

Morven South

5.2.3.5 During the flood tide the influence of the wave climate is in concert with the tidal current and the tidal flow in the lee of each of the structures is further reduced. During the ebb tide, the tidal flow is in opposition to the wave climate and the resultant littoral current is reduced in magnitude.

5.2.3.6 The presence of the structures has a limited influence on the wave induced reduction in flow. During the 1 in 1 year storm from 000°, within the Morven South Boundary, the bridge-linked HVDC converter OSP gravity base foundations have incurred an increase of up to 0.16m/s to the southwest of the structures during flood tide, whilst decreasing by up to 0.3m/s in the lee. This increase equates to circa 60% of the baseline littoral currents in this area. The decrease in littoral currents is reduced to zero by circa 6km from the structures and is therefore confined to the Morven South Physical Processes Study Area.

Morven North and Morven South

5.2.3.7 Peak changes as a result of the presence of the Morven North and Morven South infrastructure are in line with the results outlined for Morven North and Morven South independently, as outlined in the previous sections. The change in littoral currents is limited to the Regional Physical Processes Study Area.

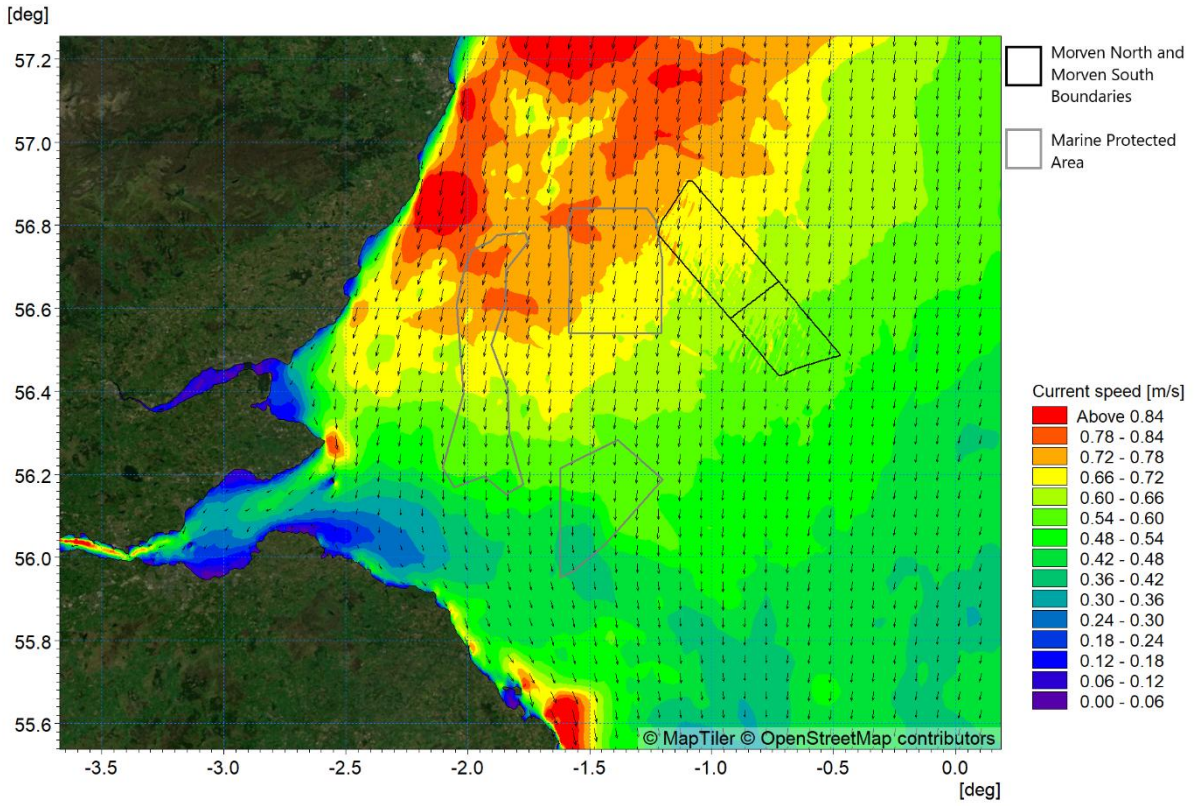

Figure 5.36: Post-construction (Morven North and Morven South) littoral current 1:1 year storm from 000° - flood tide (high water – 1 hour)

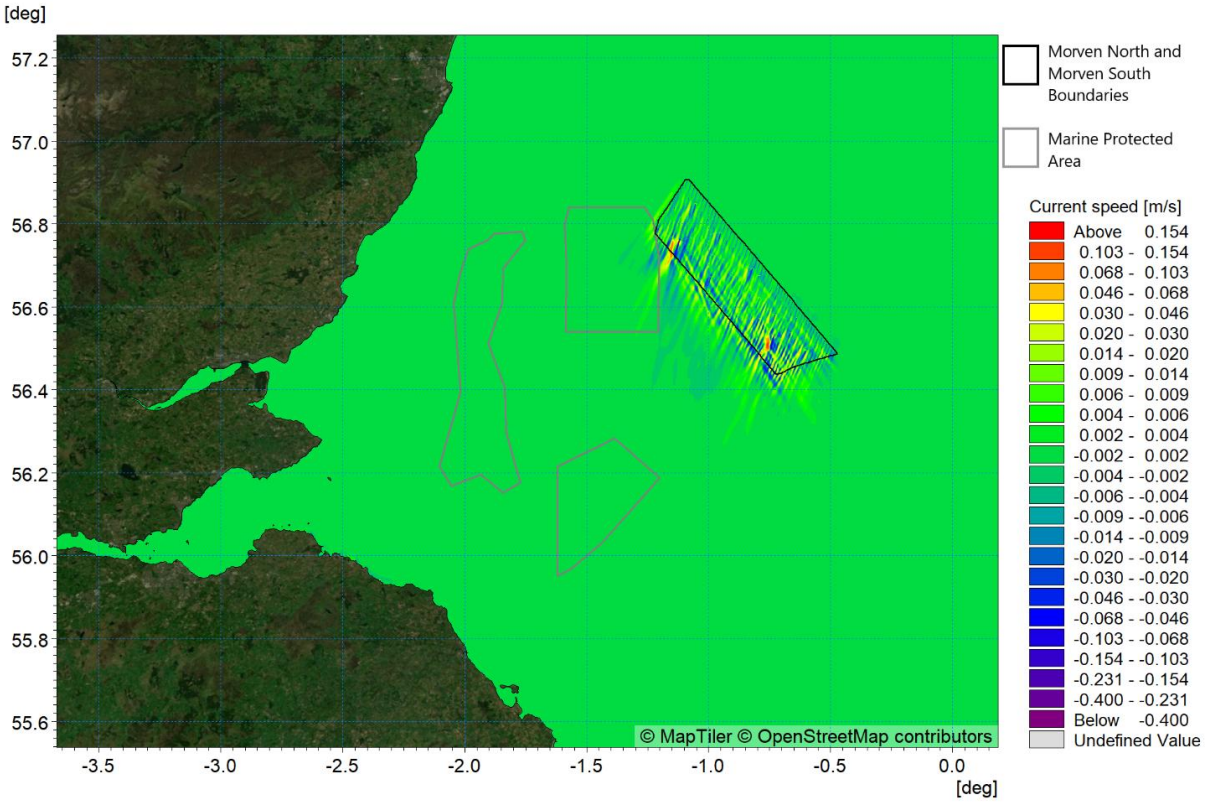

Figure 5.37: Change in littoral current 1:1 year storm from 000° - flood tide (post-construction Morven North and Morven South minus baseline)

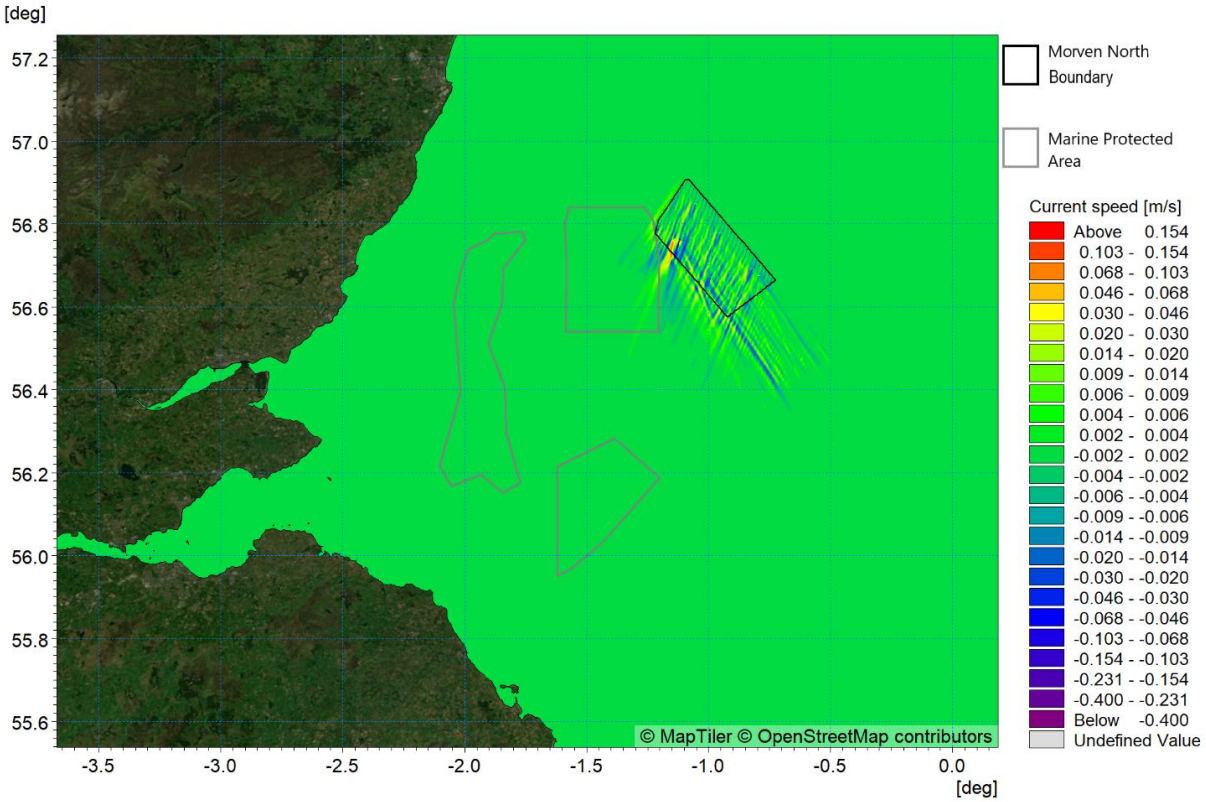

Figure 5.38: Change in littoral current 1:1 year storm from 000° - flood tide (post-construction Morven North minus baseline)

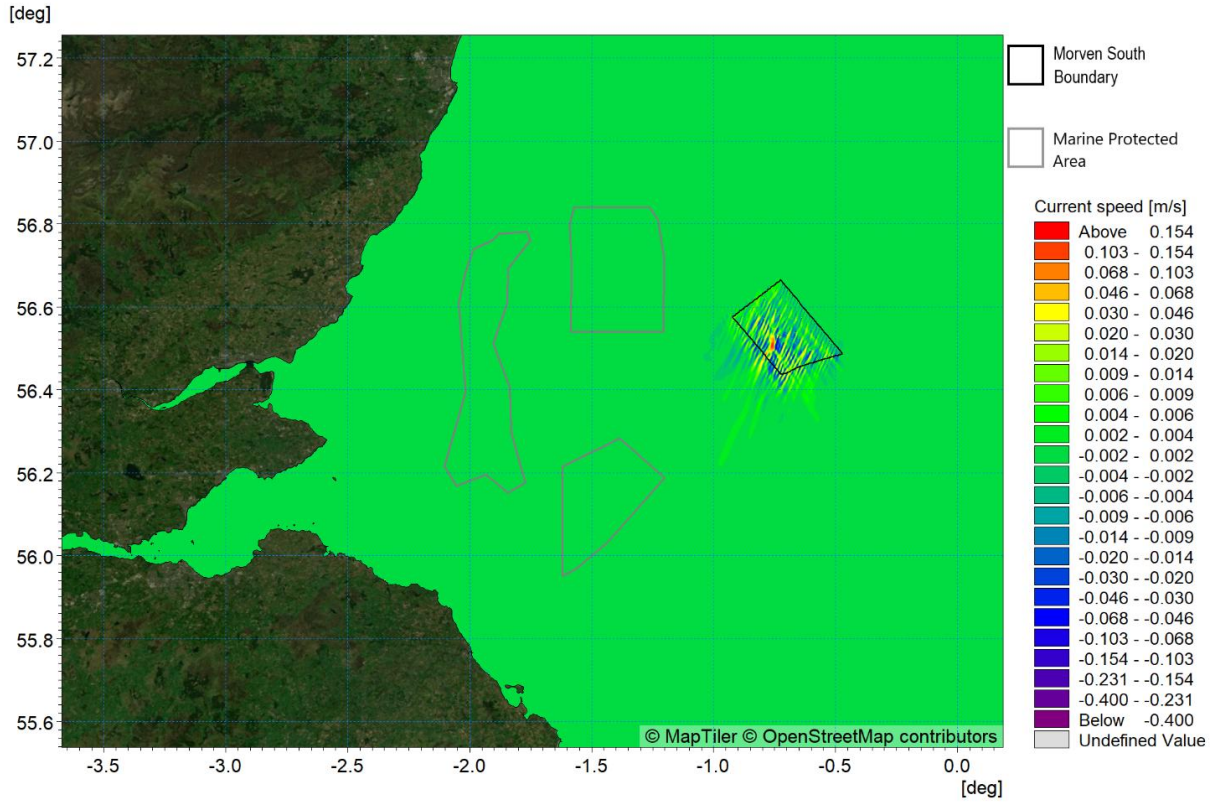

Figure 5.39: Change in littoral current 1:1 year storm from 000° - flood tide (post-construction Morven South minus baseline)

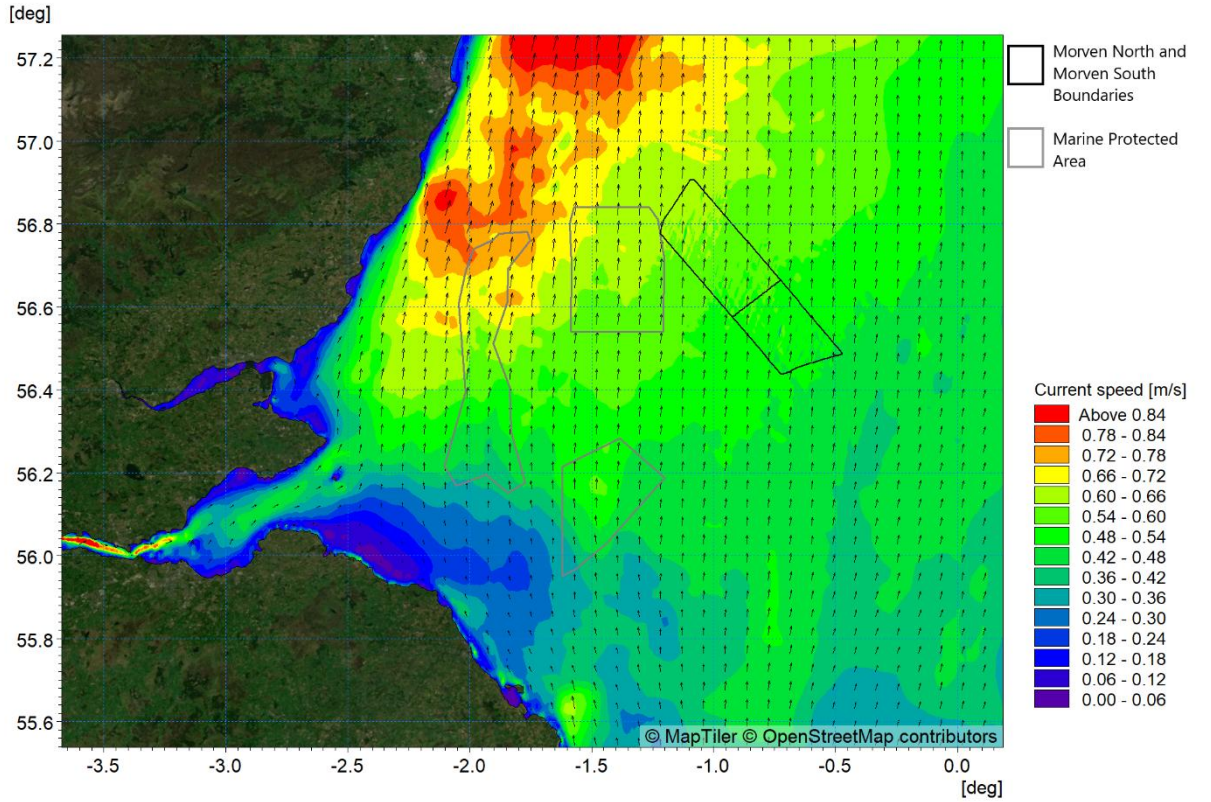

Figure 5.40: Post-construction (Morven North and Morven South) littoral current 1:1 year storm from 000° - ebb tide (low water – 1 hour)

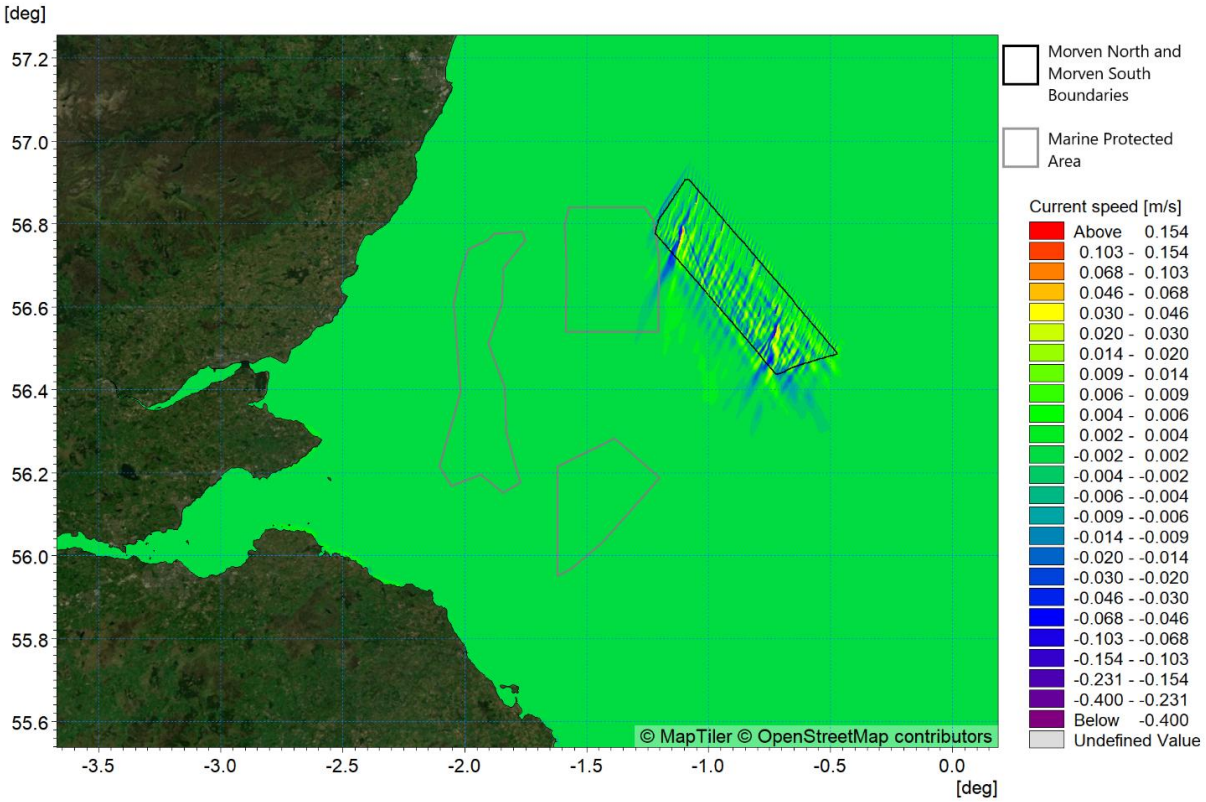

Figure 5.41: Change in littoral current 1:1 year storm from 000° - ebb tide (post-construction Morven North and Morven South minus baseline)

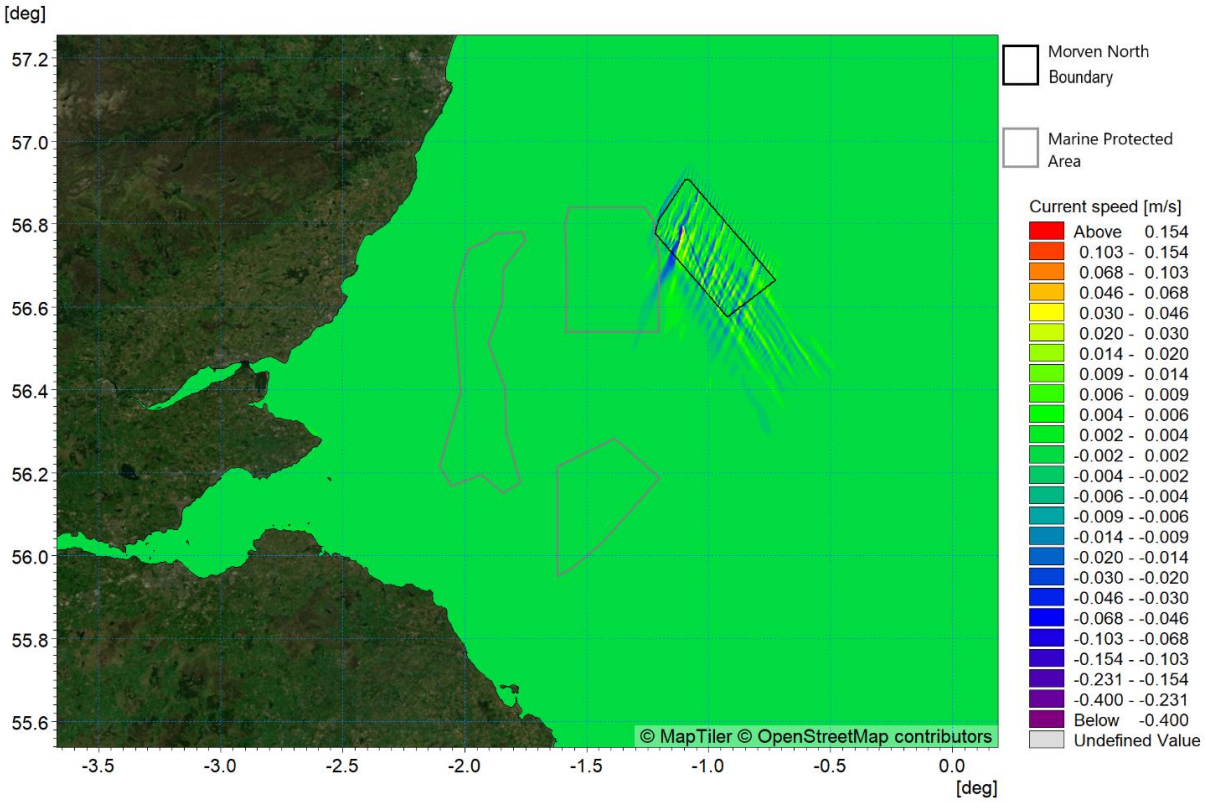

Figure 5.42: Change in littoral current 1:1 year storm from 000° - ebb tide (post-construction Morven North minus Baseline)

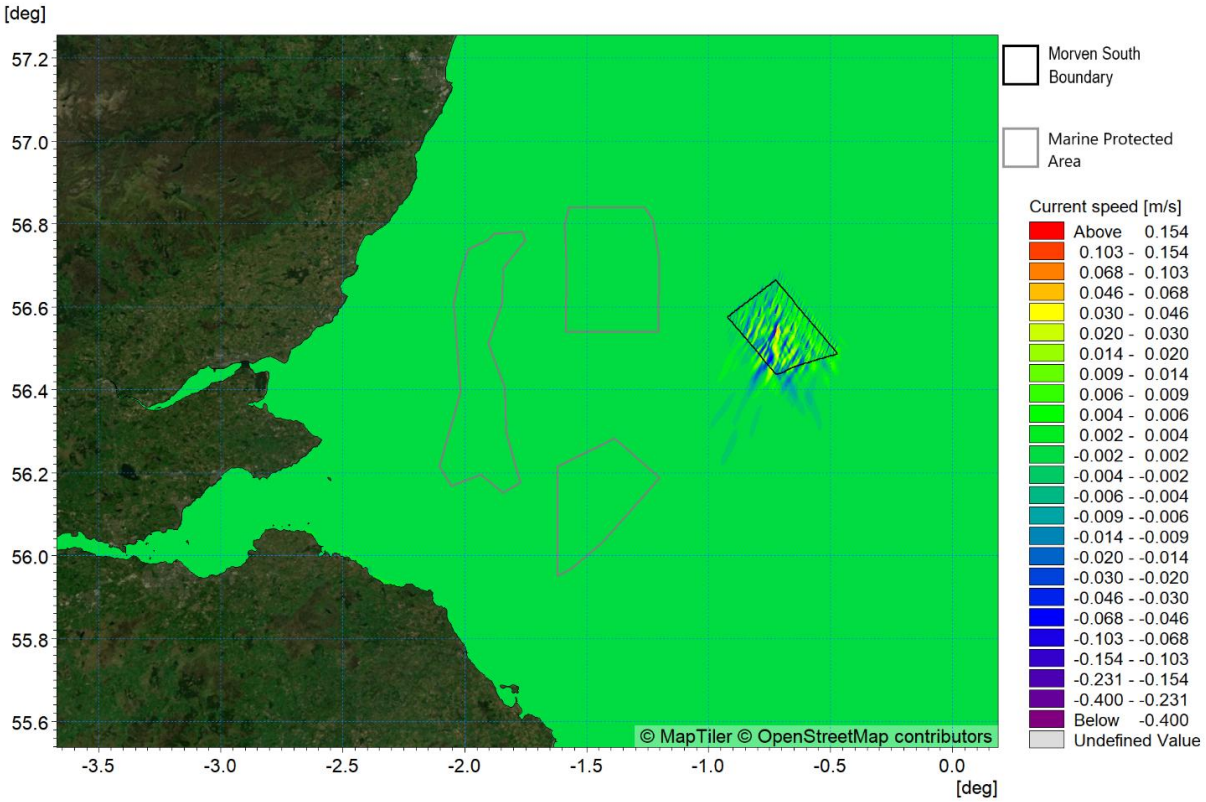

Figure 5.43: Change in littoral current 1:1 year storm from 000° - ebb tide (post-construction Morven South minus baseline)

5.2.4 Water column processes

5.2.4.1 Potential changes to seasonal stratification due to the combined presence of Morven North and Morven South were assessed using a high level three-dimensional (3D) numerical model, following consultation with MD-LOT and Marine Directorate – Science, Evidence, Data and Digital (MD-SEDD). This high level modelling was computationally intensive and thus, as agreed with MD-LOT, the relevant proposed infrastructure from Morven North and Morven South was represented together within each simulation. Due to the scale of potential impacts and the limited interaction of these impacts between Morven North and Morven South (as seen in the changes figures within this section), no independent modelling was deemed necessary for Morven North or Morven South.

5.2.4.2 The modelling was undertaken using the MIKE 3 Flow Model flexible mesh system. The hydrodynamic module is based on the numerical solution of the 3D incompressible Reynolds averaged Navier-Stokes equations invoking the assumptions of Boussinesq and of hydrostatic pressure. Thus, the model consists of continuity, momentum, temperature, salinity and density equations and is closed by a turbulent closure scheme.

5.2.4.3 The two-dimensional (2D) model developed for the baseline and post-construction tidal flows, wave climate, littoral currents and sedimentology as shown in Figure 4.5 was adapted and converted to a smaller extents 3D model covering the Regional Physical Processes Study Area. The extent of the model domain is shown in Figure 5.44. The MIKE 3 Flow Model FM was utilised to determine the impact of the combined presence of Morven North and Morven South infrastructure within the water column, by introducing a series of vertical layers defining current velocities, salinity and temperature. As per the 2D modelling, the MIKE 3 Flow Model was used to simulate both baseline and post-construction conditions to provide a comparative study of relevant variables through the water column within the Regional Physical Processes Study Area.

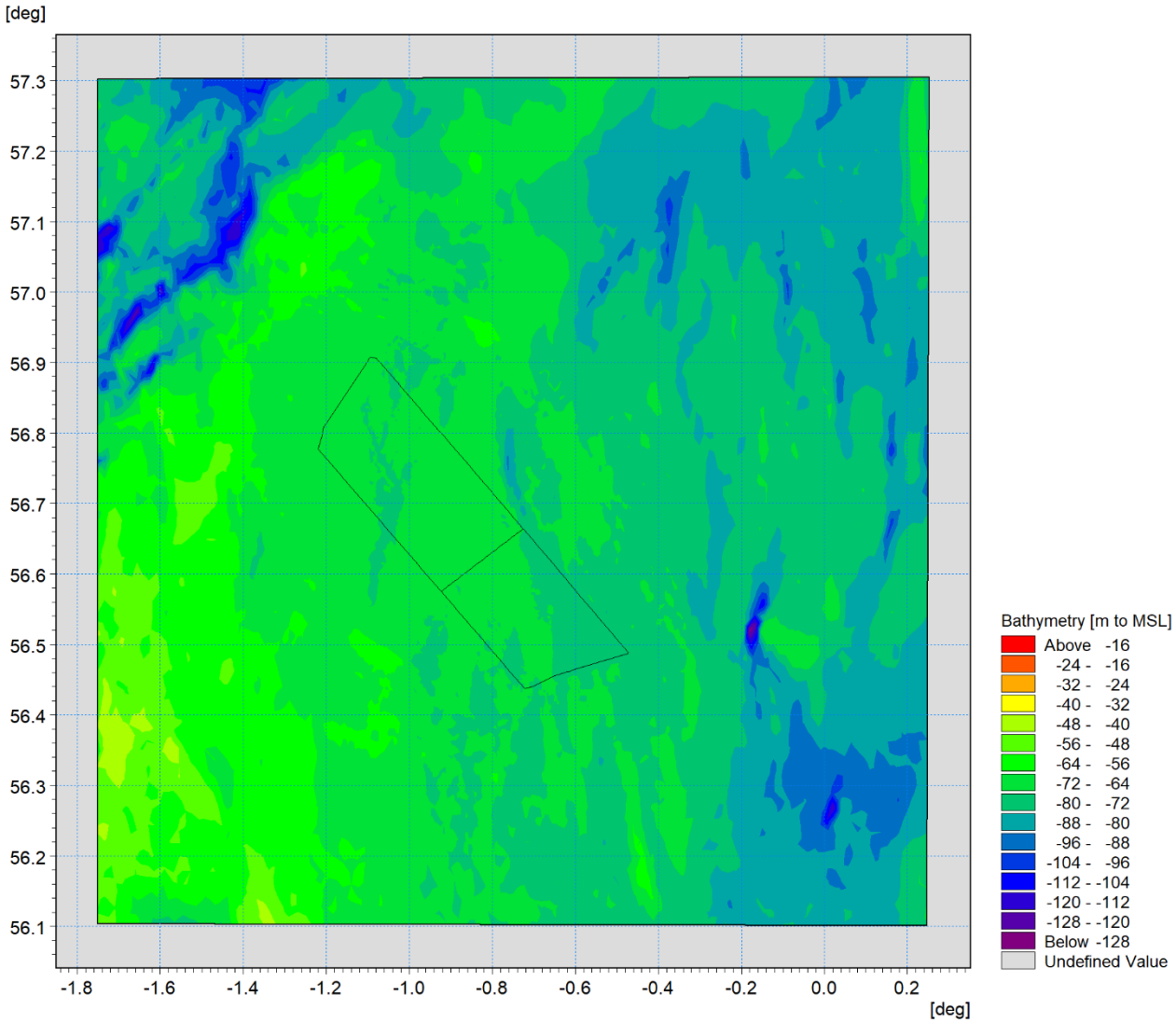

Figure 5.44: Model bathymetry as viewed within the modelling software for the Morven North and Morven South stratification modelling

5.2.4.4 The post-construction simulations were undertaken using the same bathymetry and mesh structure as the baseline simulations, with the addition of the combined MDS infrastructure for Morven North and Morven South to assess the impact on seasonal stratification. The MDS included the foundations and scour protection for Morven North and Morven South, as outlined in paragraphs 5.1.1.3 and 5.1.1.4 respectively, minus the inclusion of cable protection and cable crossings. The infrastructure was included within the modelling as sub-grid structures with pile dimensions and arrangements as outlined within the MDS. As noted previously, there will be a maximum of one bridge-linked HVDC converter OSP within the Morven Site, however the modelling has accounted for one HVDC converter OSP within both the Morven North Boundary and Morven South Boundary, in order to provide a representation of potential impact due to each separate project. The sub-grid structure technique allowed the flow past a structure to be modelled by considering the upstream and downstream water level. Pier structures were used to represent the MDS foundations, which captured the increasing resistance imposed by the structures and introduced turbulence production in their lee. This current induced drag force as calculated on each pier, allowed the effect on the flow due to the piers to be accurately simulated.

5.2.4.5 The inclusion of sub-grid structures allowed the modelling to be undertaken without resolving individual foundations and allowing a more efficient mesh structure in their vicinity. Investigative

simulations, including mesh independence testing, determined that model cell sizes were required to be in the order of 10m to adequately represent the effects in the vicinity of the structures.

5.2.4.6 The model was driven using boundary conditions extracted from the SSW-RS (Barton *et al*., 2022), the same dataset analysed to determine the baseline environment for water column processes, as discussed in Section 4.6. The hindcast model provides three-dimensional currents, temperature and salinity data, which were extracted and used to provide 3D boundary conditions for modelling. The number of 3D layers required was determined following a sensitivity analysis, the outcome of which demonstrated the need for the full 20 layers provided by the SSW-RS model to be included in the model in order to capture the disturbance due to the presence of infrastructure at the thermocline.

5.2.4.7 Simulations were undertaken to allow the assessment of the impact on seasonal stratification during two key periods within a typical year; the onset of stratification in Spring and peak stratification in Summer. The typical year of 2016 was selected, as outlined in the baseline assessment under paragraph 0. For each period, simulations were undertaken for both baseline conditions and with infrastructure in place over a full spring neap tidal cycle, in addition to a period of model warm-up. The onset of stratification was simulated from 25 April to 8 May 2016, whilst peak stratification was simulated from 24 July to 8 August 2016.

5.2.4.8 Initial investigative simulations determined that due to the subtlety of the potential changes on stratification associated with the infrastructure, it was important to isolate the effect being examined and create an idealised situation, so this effect may be clearly observed. For this reason, temperature and salinity values varied through the water column, but remained constant over the domain of the model and over the duration of the modelling. By adopting this approach, it was ensured that the modelling process did not introduce ambiguity into the determination of the cause of changes to water column mixing, as background temperature and salinity were constant. Therefore, any changes between baseline and post-construction simulations may be directly attributed to the infrastructure in this comparative assessment.

5.2.4.9 Temperature and salinity values were selected from the SSW-RS dataset at a point N6 on 30 April 2018 and 01 August 2016 for the onset and peak simulation periods respectively. The selection criteria for N6 is described under paragraph 4.6.1.7, in line with the baseline description. The onset temperature and salinity data was selected based on a weak, yet present thermocline from the daily SSW-RS data, whilst the peak period temperature and salinity data was selected based on the maximum temperature stratification values observed in the hourly data at 20:00 on 01 August 2016. The selected temperature and salinity values were applied as initial conditions and boundary conditions within the modelling.

5.2.4.10 Figure 5.45 shows the variation in water column temperature at point N6 on 30 April 2016, whilst Figure 5.46 shows the corresponding variation in water column salinity. The data shows the presence of a cooler layer below a depth of circa 23.5m, with the formation of a thermocline separating the cooler layer from the warmer surface layer which reaches a depth of circa 6.7m. There is negligible difference in salinity within the water column during this period.

5.2.4.11 Figure 5.47 shows the variation in water column temperature at point N6 on 01 August 2016, whilst Figure 5.48 shows the corresponding variation in water column salinity. The data clearly shows the presence of the thermocline between 10.1m depth and 16.8m, with a warmer layer from 10.1m to the surface and the cooler layer from 16.8m to the seabed. A similar pattern is observed in the salinity data, with depths below 16.8m remaining relatively consistent in terms of Practical Salinity Units (PSU).

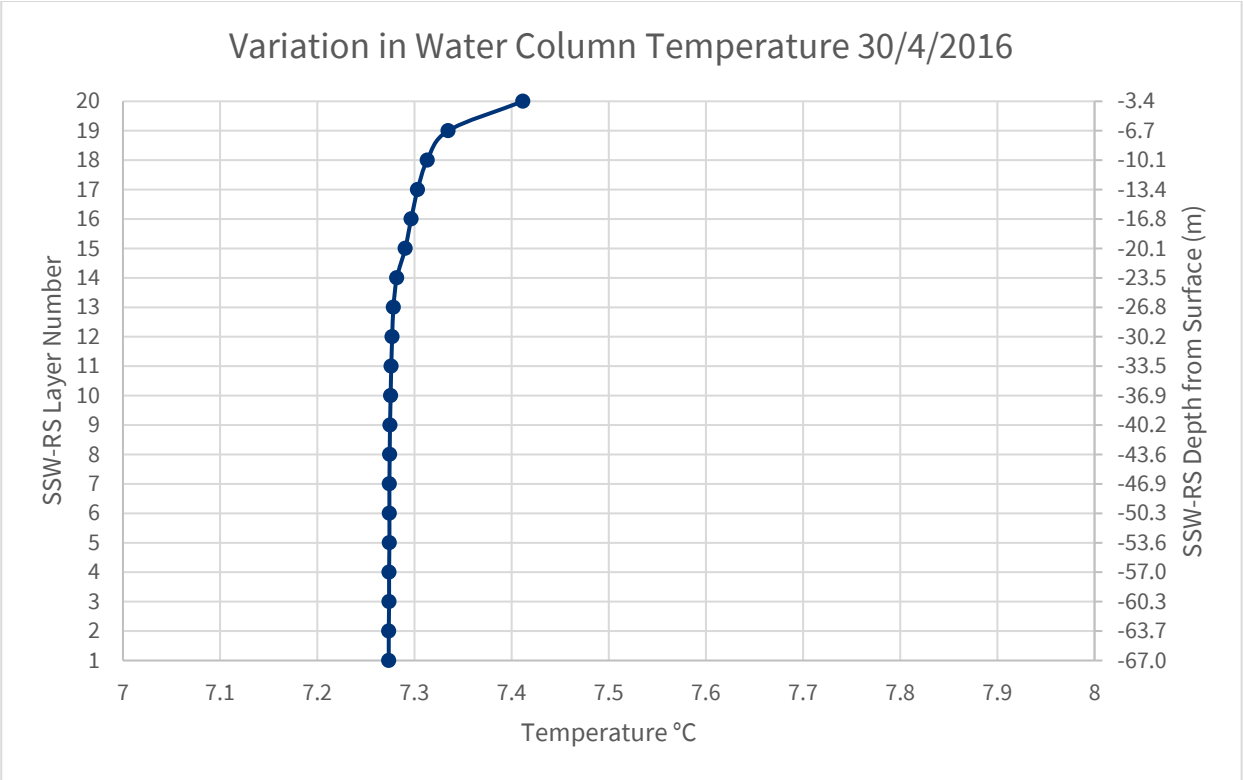

Figure 5.45: Variation in water column temperature at N6 on 30 April 2016 (Barton *et al.*, 2022)

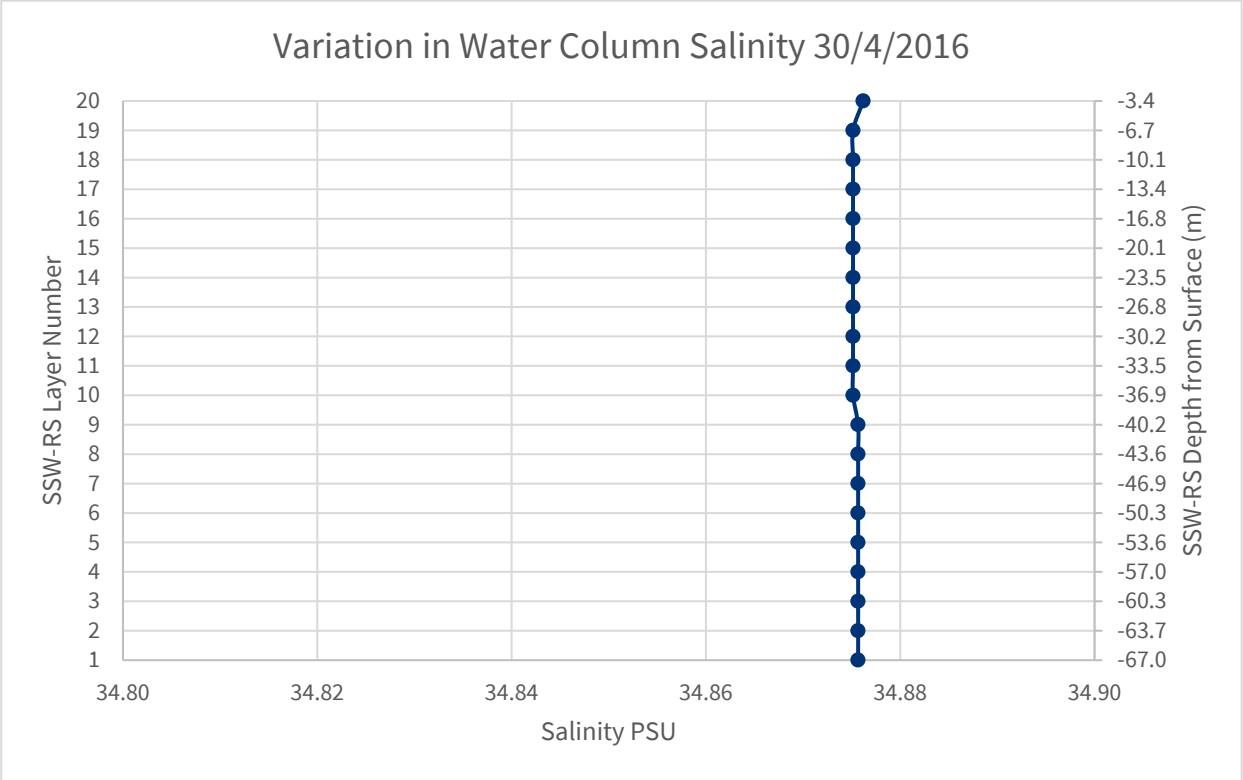

Figure 5.46: Variation in water column salinity at N6 on 30 April 2016 (Barton *et al.*, 2022)

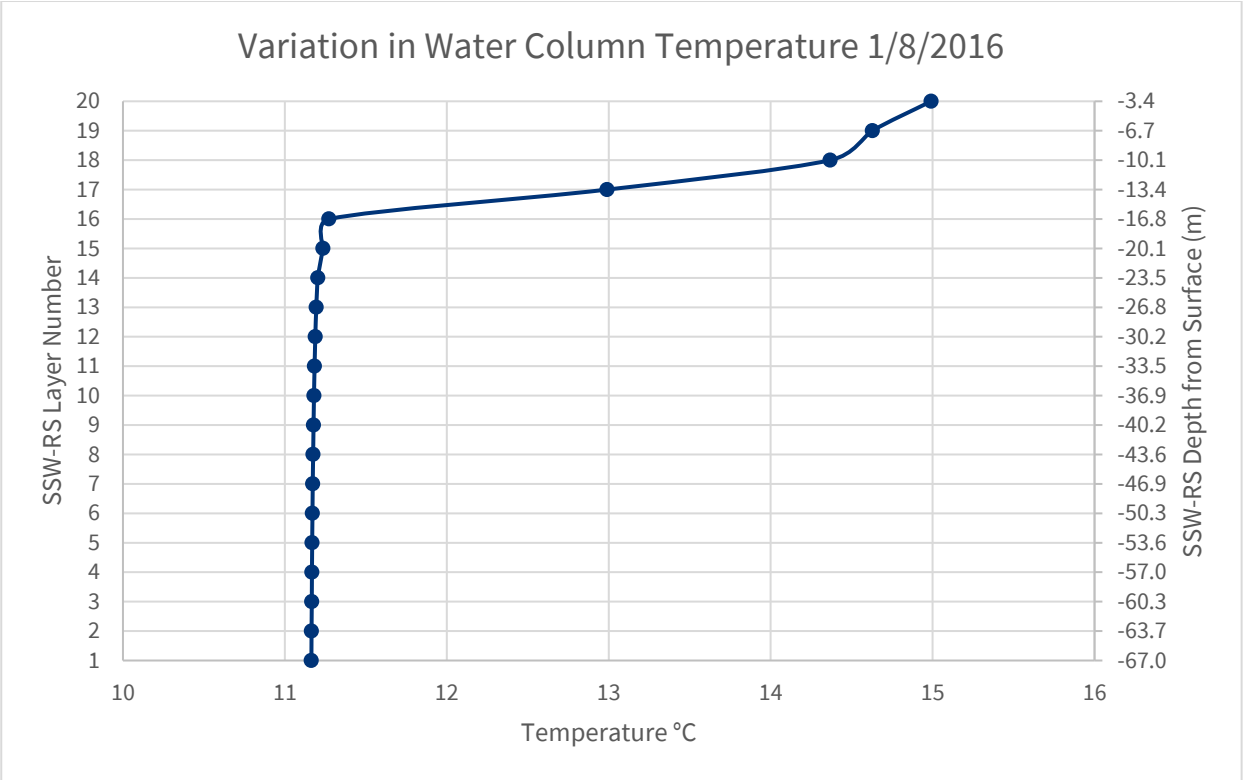

Figure 5.47: Variation in water column temperature at N6 on 01 August 2016 (Barton *et al.*, 2022)

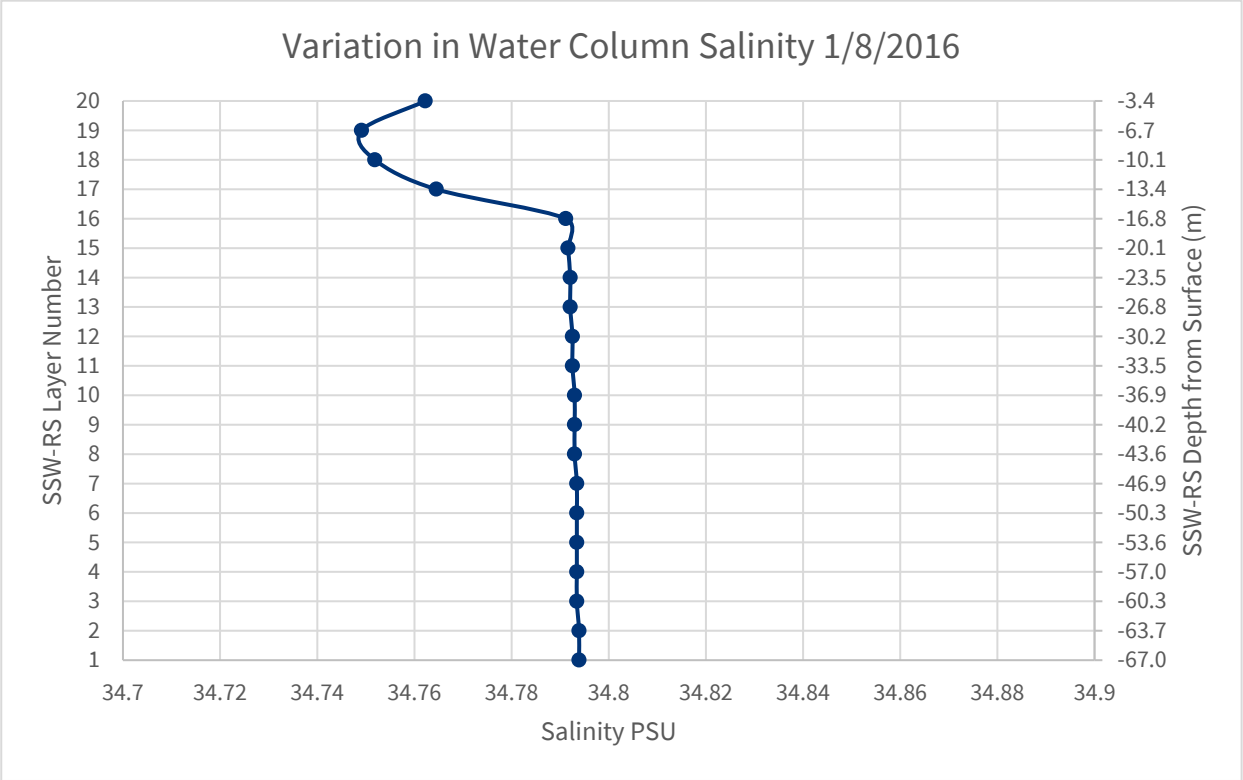

Figure 5.48: Variation in water column salinity at N6 on 01 August 2016 (Barton *et al.*, 2022)

5.2.4.12 Following the simulation of the baseline and post-construction scenarios for the onset and peak stratification periods, a series of difference plots were created to present the proposed infrastructure minus the baseline condition. A range of scenarios have been presented to provide insight into the

impact upon stratification at both the onset and peak stratification periods and at different stages within each period. For each set of difference plots, the relevant water column vertical layers have been provided, with layer 20 referring to the near-surface layer, and subsequent layer numbers decreasing with distance from the surface, with layer 1 being associated with the near-bed. Results have been extracted at a consistent tidal state throughout this assessment, with the ebb tide selected as the point of greatest current speed, although differences in temperature and salinity do not vary significantly over the tidal phase. Log scales have been introduced to accentuate the values for clarity.

5.2.4.13 Figure 5.49 to Figure 5.58 show the difference in temperature due to the combined presence of the Morven North and Morven South foundations during the onset of stratification at model day four, whilst Figure 5.59 to Figure 5.72 show the temperature difference after a spring neap cycle at day 17. Figure 5.73 to Figure 5.78 show the difference in salinity after a spring neap cycle at day 17.

5.2.4.14 Figure 5.79 to Figure 5.89 show the difference in temperature due to the combined presence of the Morven North and Morven South foundations during the peak summer period of stratification at model day four, whilst Figure 5.90 to Figure 5.104 show the temperature difference after a spring neap cycle at day 17. Figure 5.105 to Figure 5.120 show the difference in salinity after a spring neap cycle at day 17.

Change in temperature at onset of stratification – Day four ebb tide

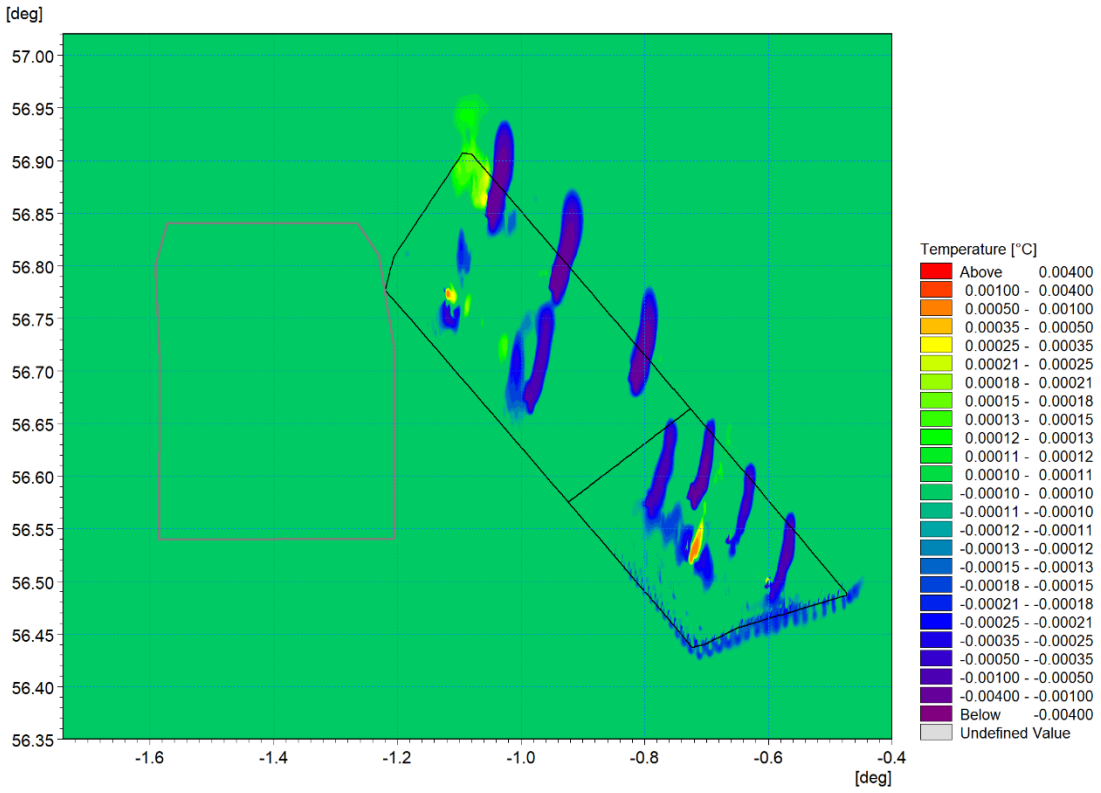

Figure 5.49: Change in temperature at onset of stratification – Day four ebb tide (post-construction Morven North and Morven South minus baseline) – Layer 20

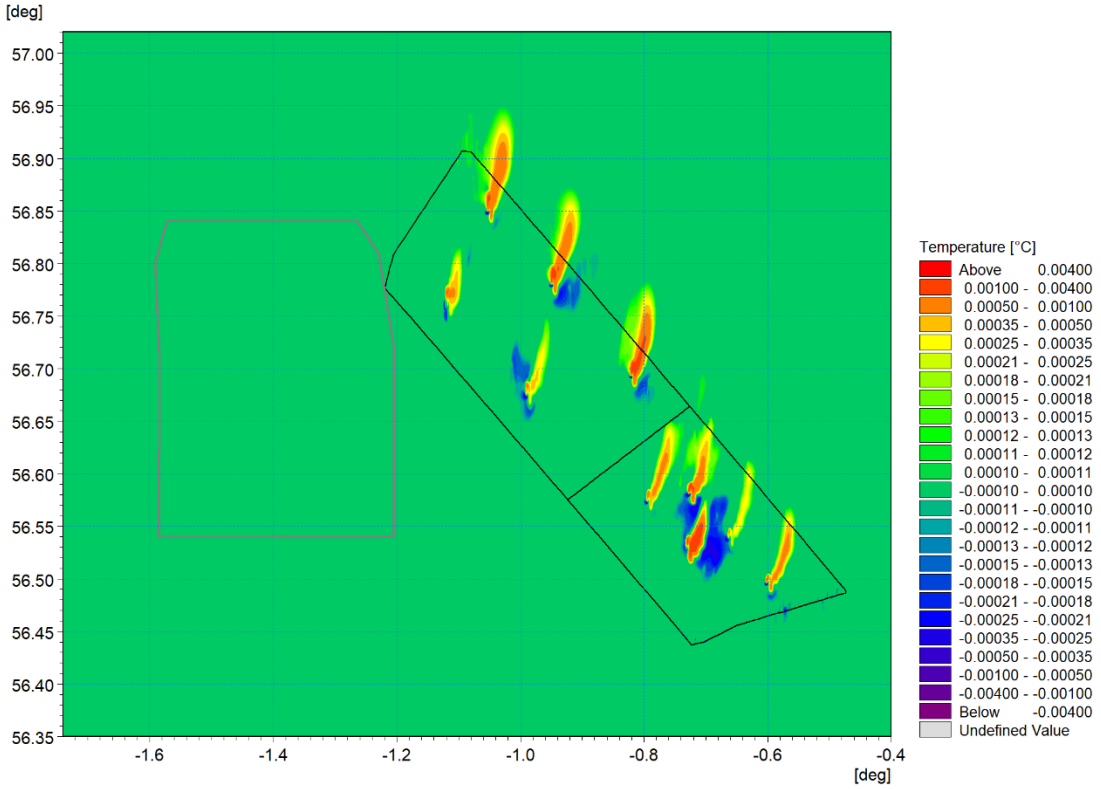

Figure 5.50: Change in temperature at onset of stratification – Day four ebb tide (post-construction Morven North and Morven South minus baseline) – Layer 19

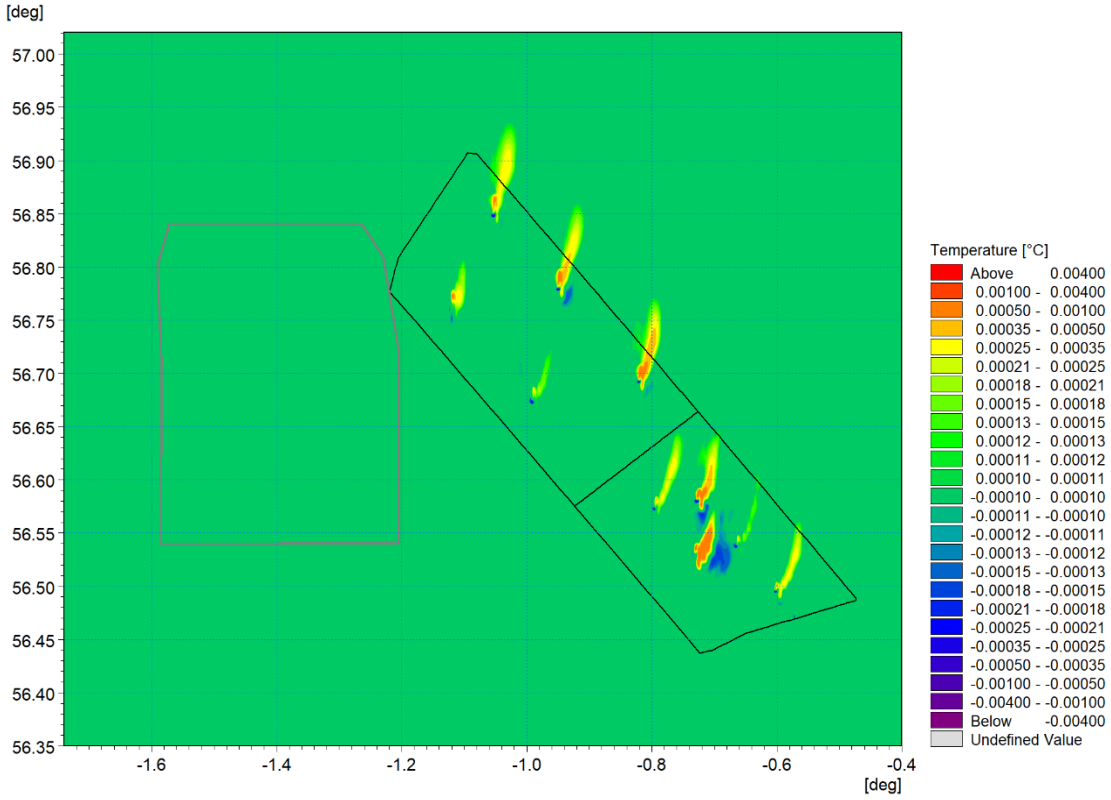

Figure 5.51: Change in temperature at onset of stratification – Day four ebb tide (post-construction Morven North and Morven South minus baseline) – Layer 18

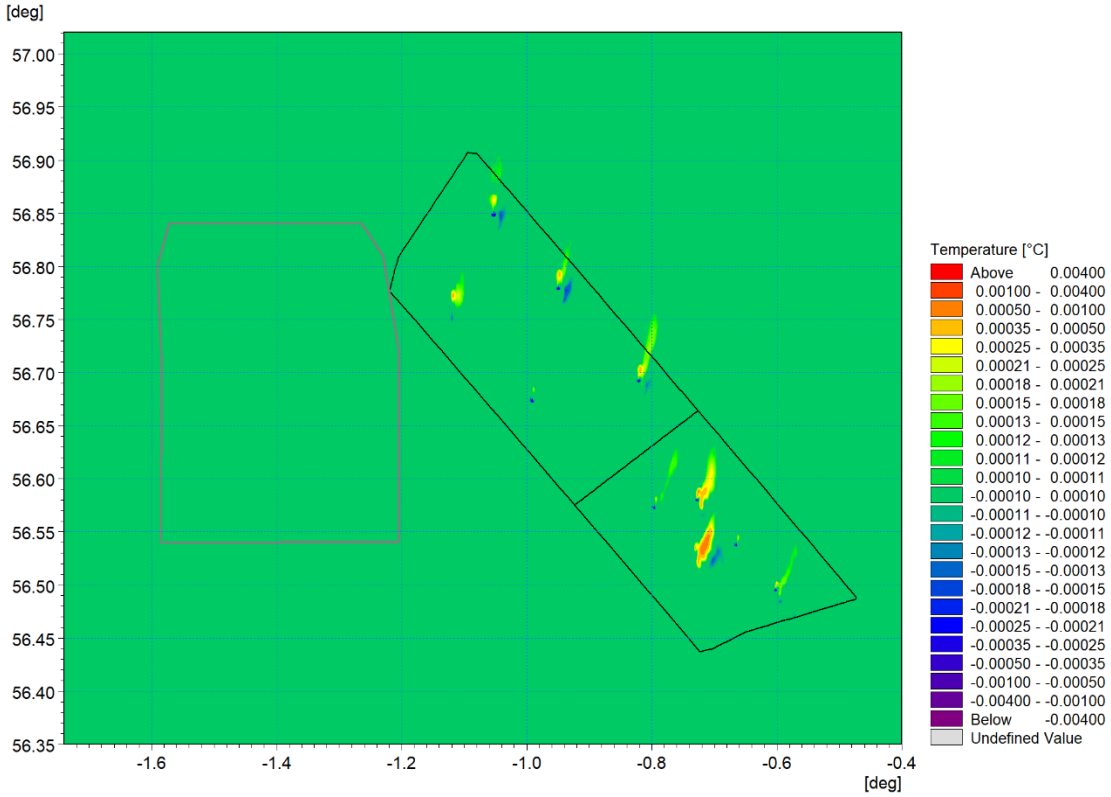

Figure 5.52: Change in temperature at onset of stratification – Day four ebb tide (post-construction Morven North and Morven South minus baseline) – Layer 17

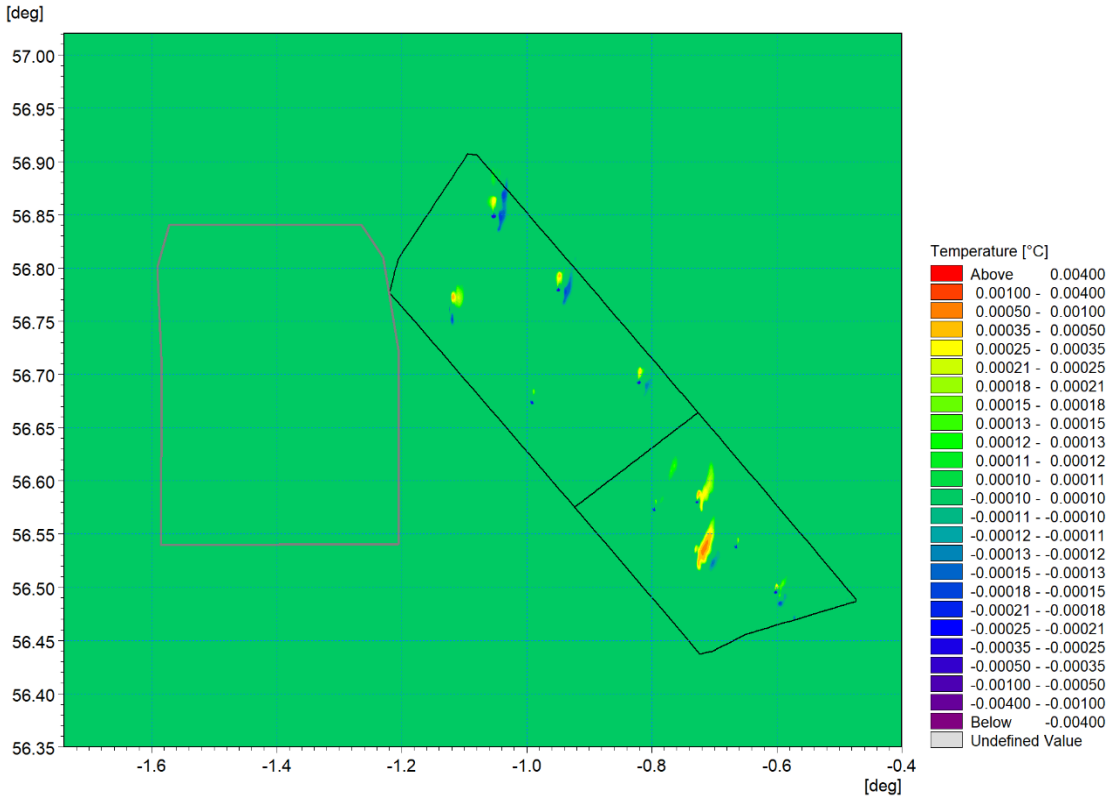

Figure 5.53: Change in temperature at onset of stratification – Day four ebb tide (post-construction Morven North and Morven South minus baseline) – Layer 16

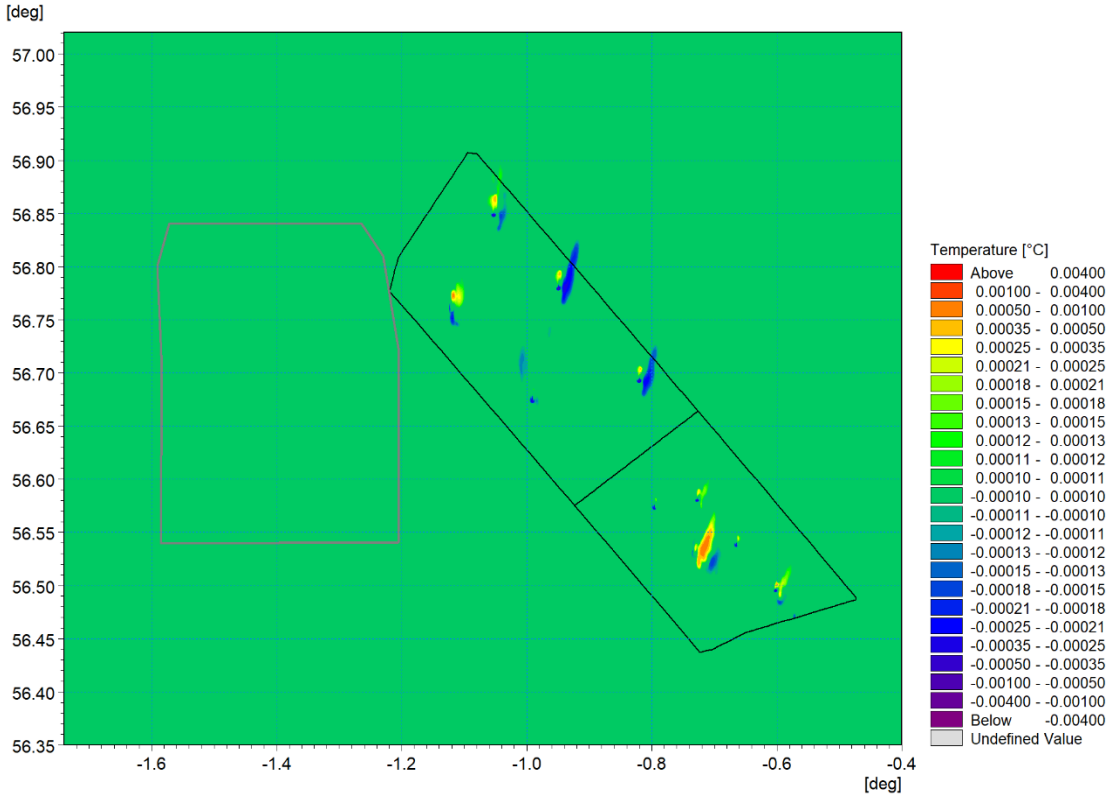

Figure 5.54: Change in temperature at onset of stratification – Day four ebb tide (post-construction Morven North and Morven South minus baseline) – Layer 15

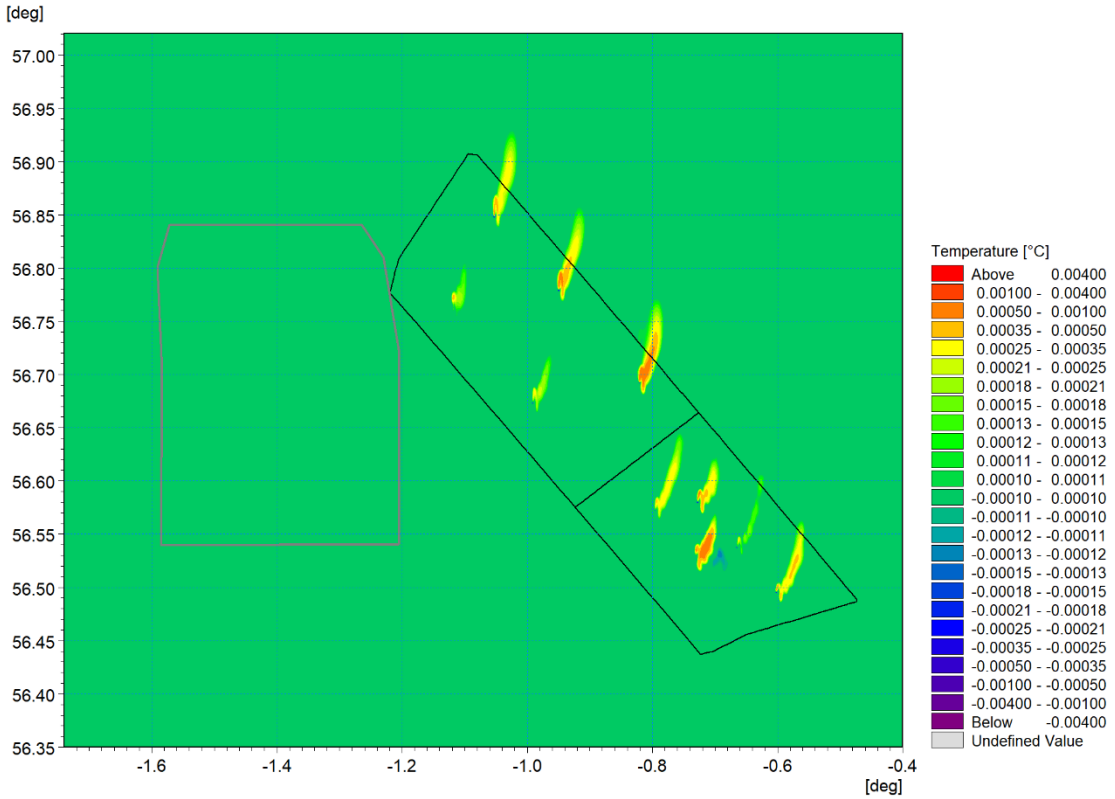

Figure 5.55: Change in temperature at onset of stratification – Day four ebb tide (post-construction Morven North and Morven South minus baseline) – Layer 14

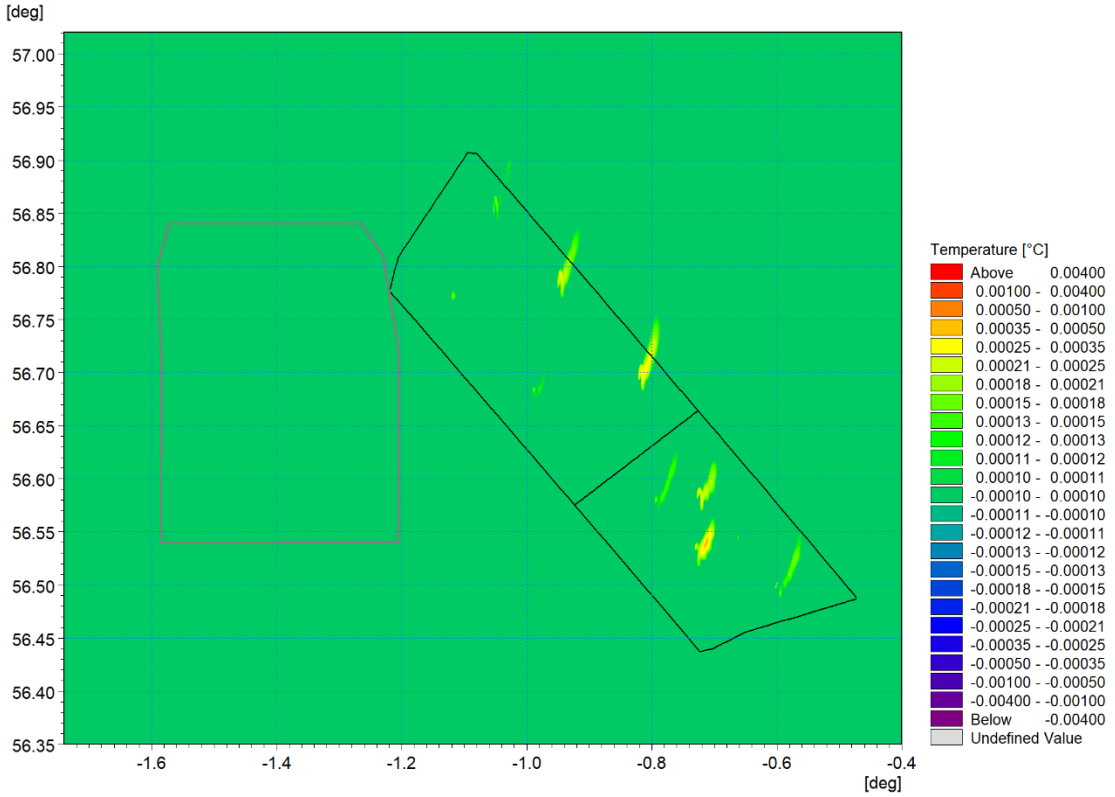

Figure 5.56: Change in temperature at onset of stratification – Day four ebb tide (post-construction Morven North and Morven South minus baseline) – Layer 13

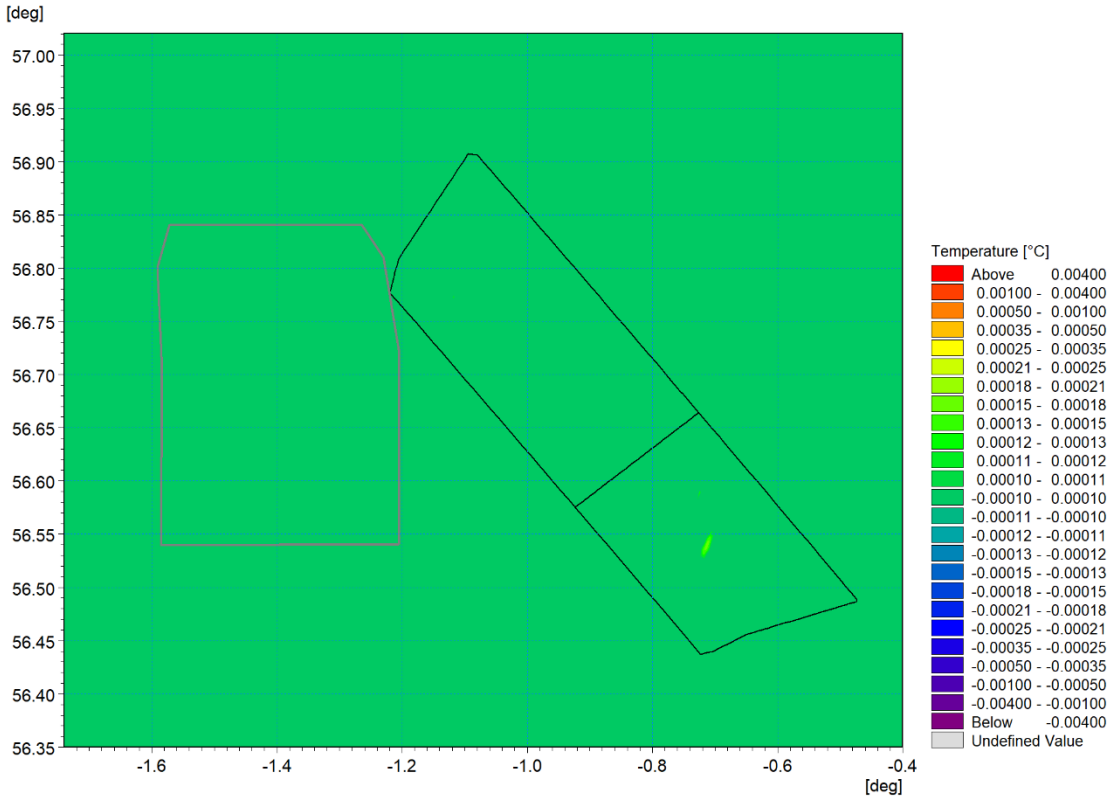

Figure 5.57: Change in temperature at onset of stratification – Day four ebb tide (post-construction Morven North and Morven South minus baseline) – Layer 12

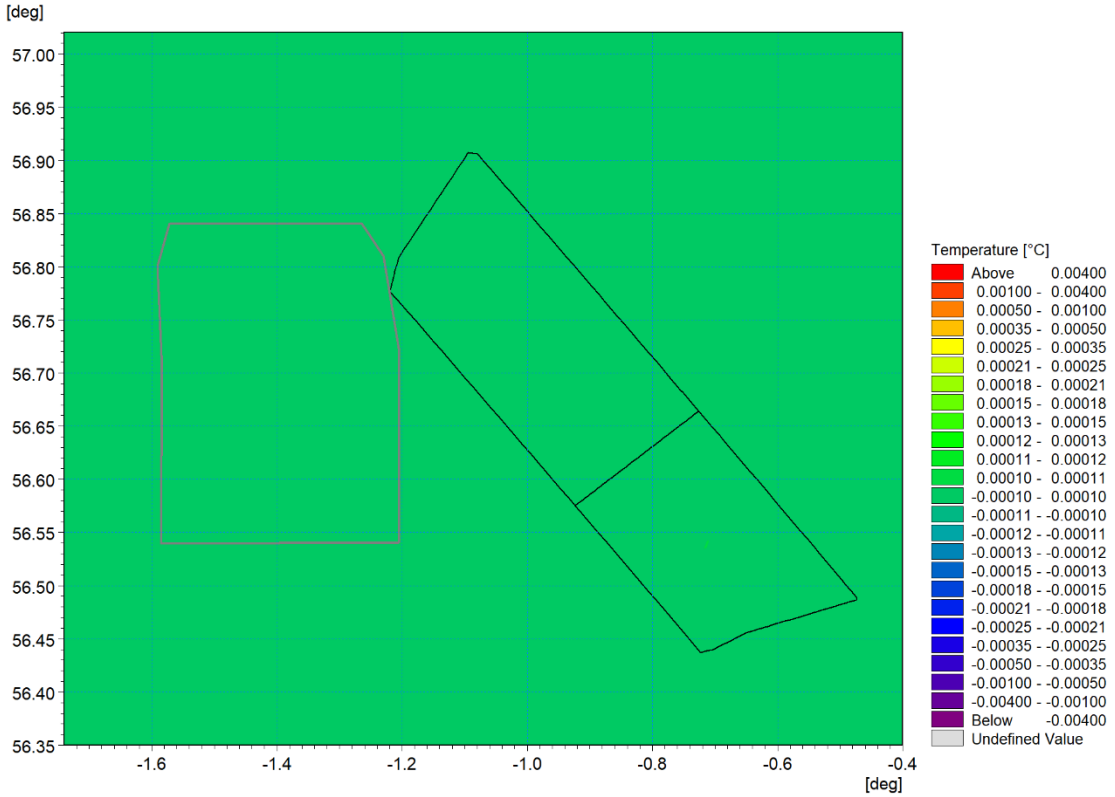

Figure 5.58: Change in temperature at onset of stratification – Day four ebb tide (post-construction Morven North and Morven South minus baseline) – Layer 11

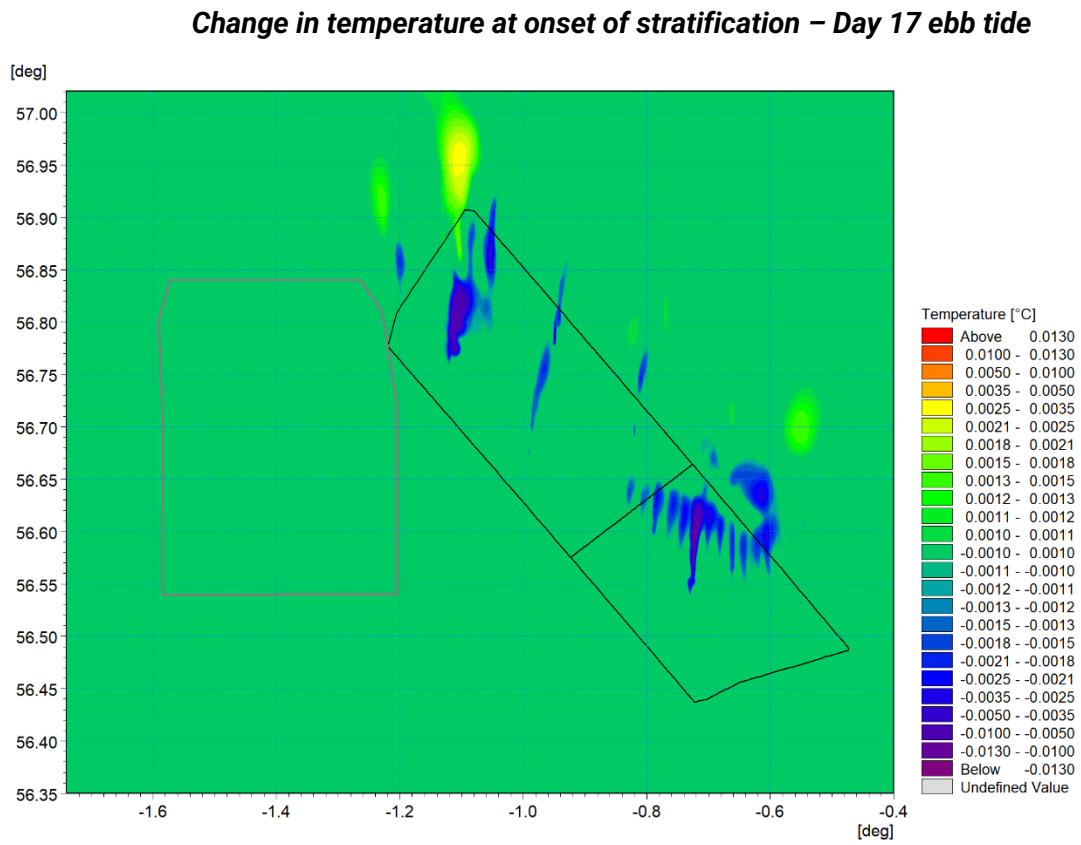

Figure 5.59: Change in temperature at onset of stratification – Day 17 ebb tide (post-construction Morven North and Morven South minus baseline) – Layer 20

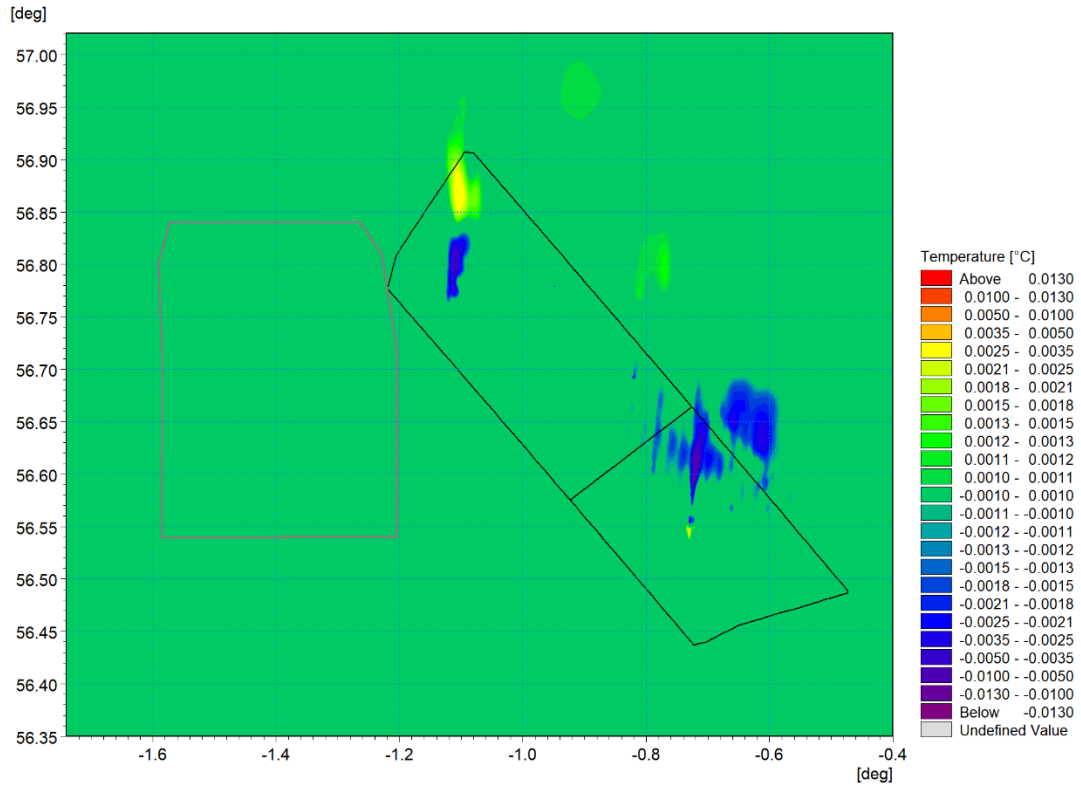

Figure 5.60: Change in temperature at onset of stratification – Day 17 ebb tide (post-construction Morven North and Morven South minus baseline) – Layer 19

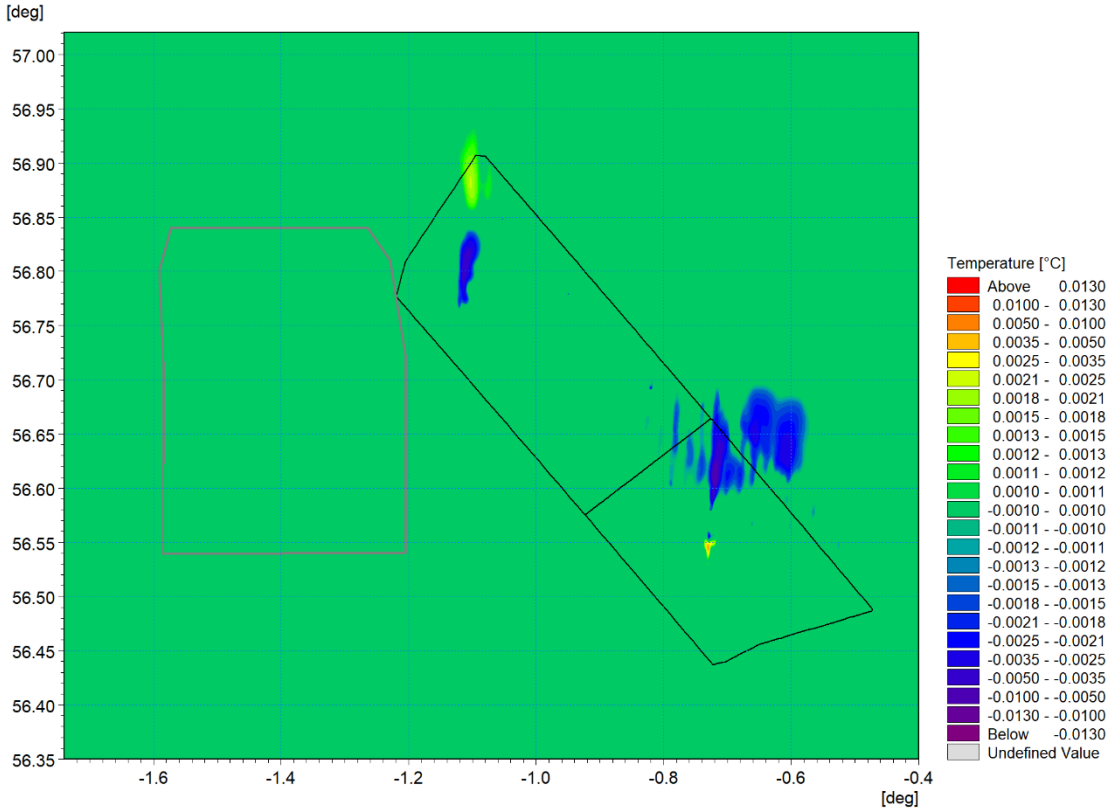

Figure 5.61: Change in temperature at onset of stratification – Day 17 ebb tide (post-construction Morven North and Morven South minus baseline) – Layer 18

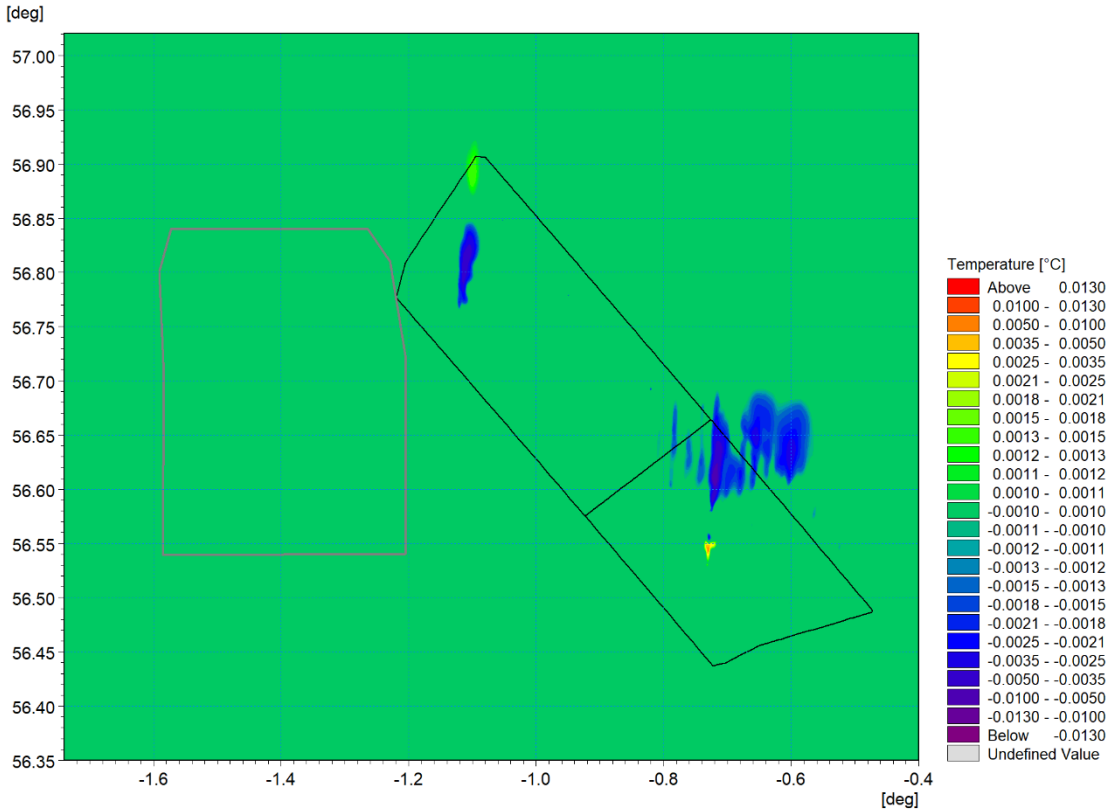

Figure 5.62: Change in temperature at onset of stratification – Day 17 ebb tide (post-construction Morven North and Morven South minus baseline) – Layer 17

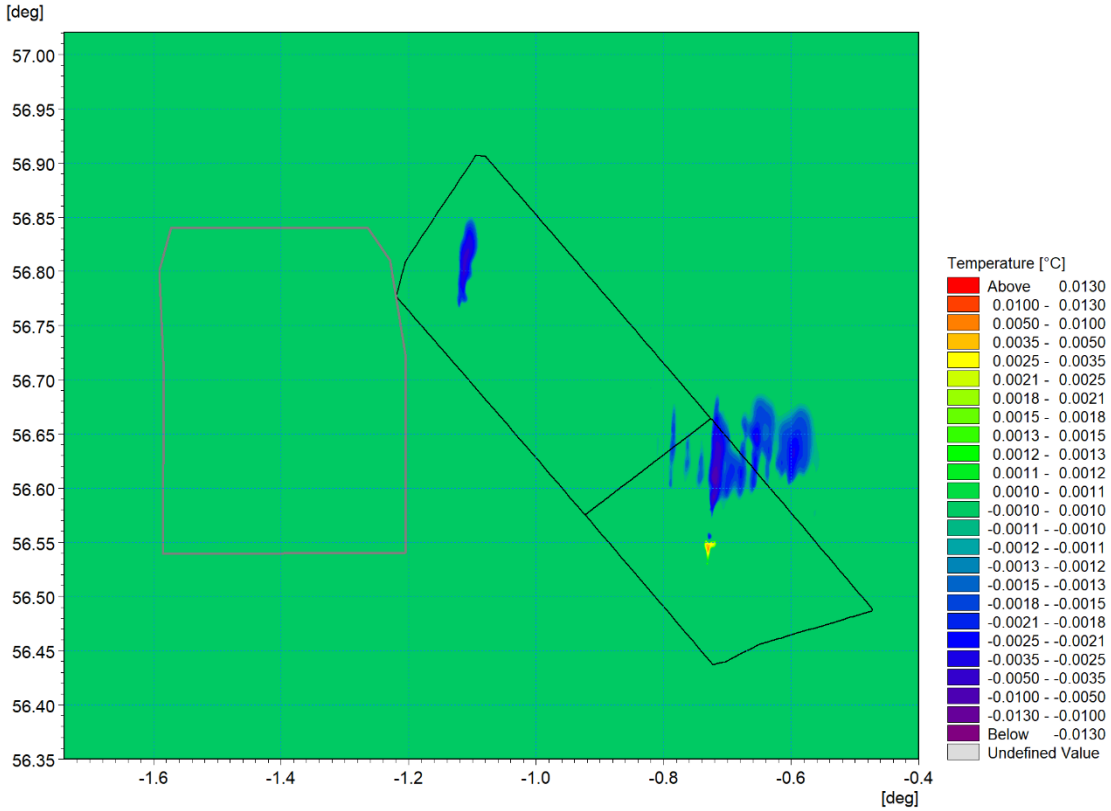

Figure 5.63: Change in temperature at onset of stratification – Day 17 ebb tide (post-construction Morven North and Morven South minus baseline) – Layer 16

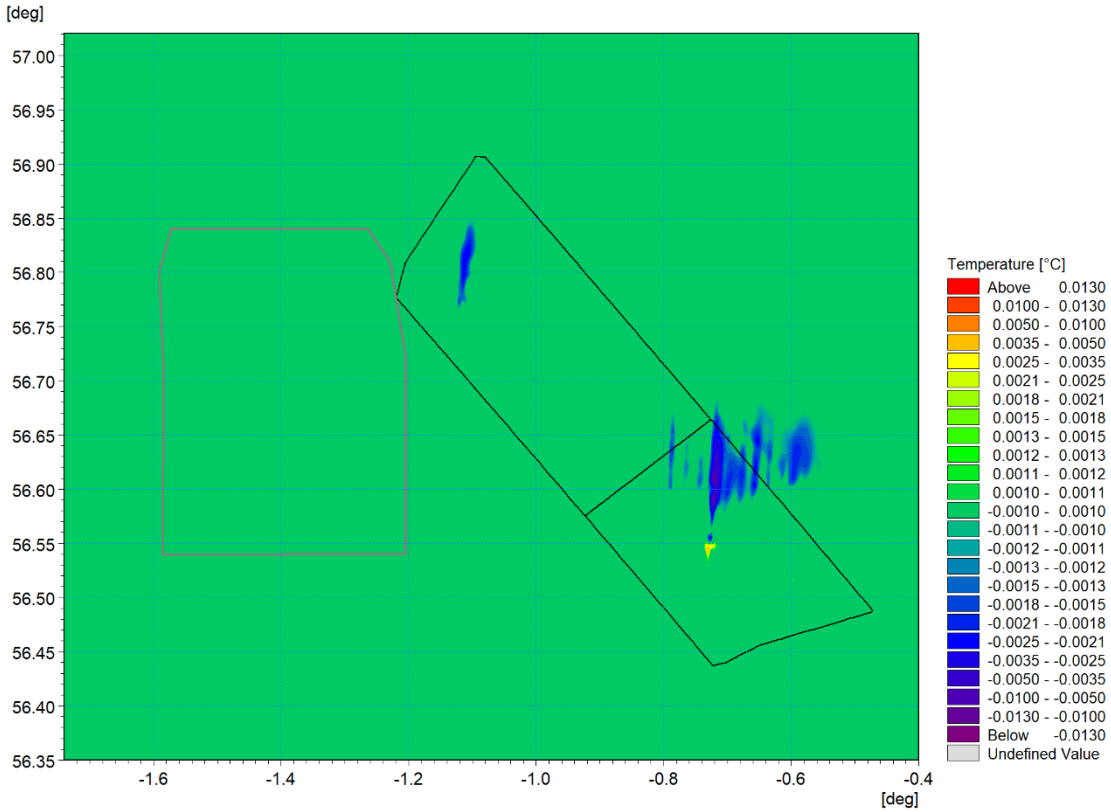

Figure 5.64: Change in temperature at onset of stratification – Day 17 ebb tide (post-construction Morven North and Morven South minus baseline) – Layer 15

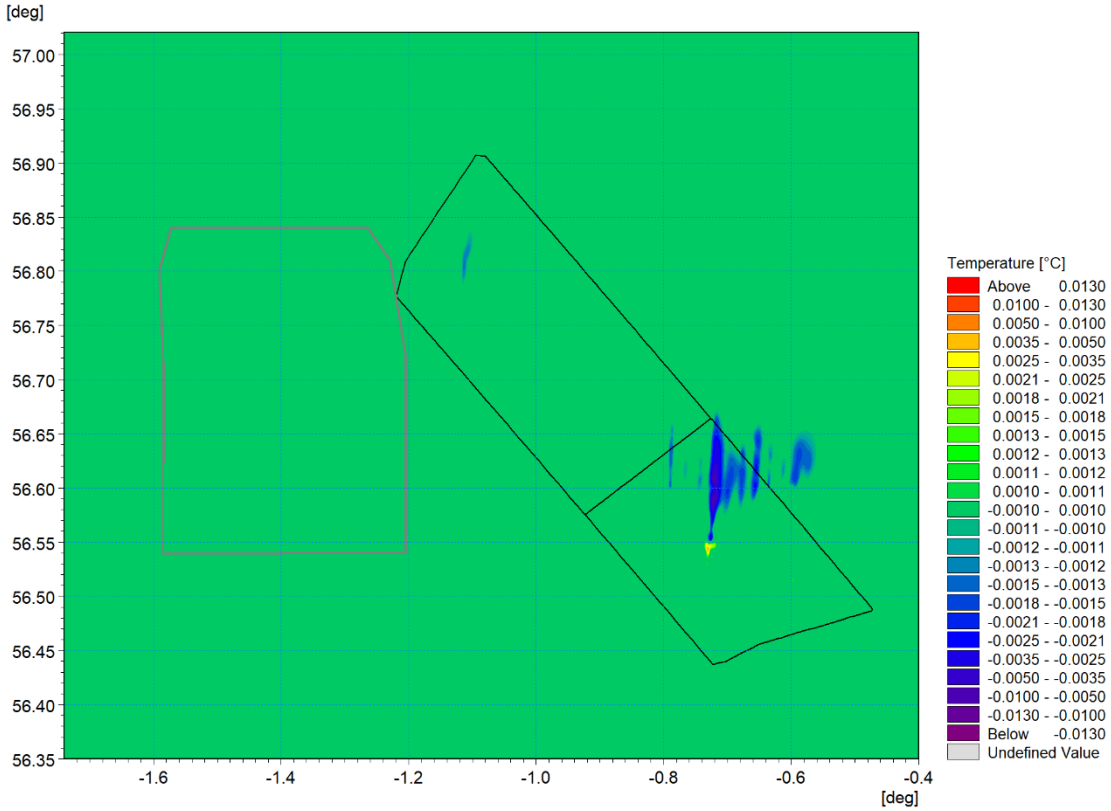

Figure 5.65: Change in temperature at onset of stratification – Day 17 ebb tide (post-construction Morven North and Morven South minus baseline) – Layer 14

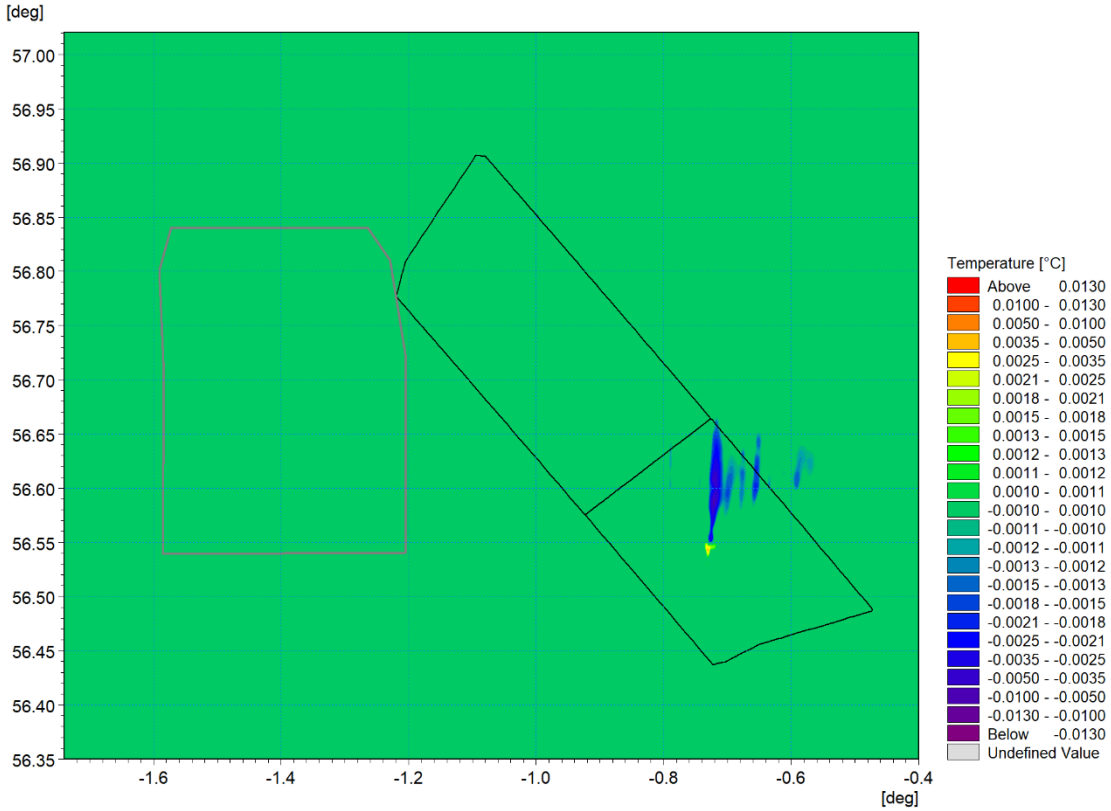

Figure 5.66: Change in temperature at onset of stratification – Day 17 ebb tide (post-construction Morven North and Morven South minus baseline) – Layer 13

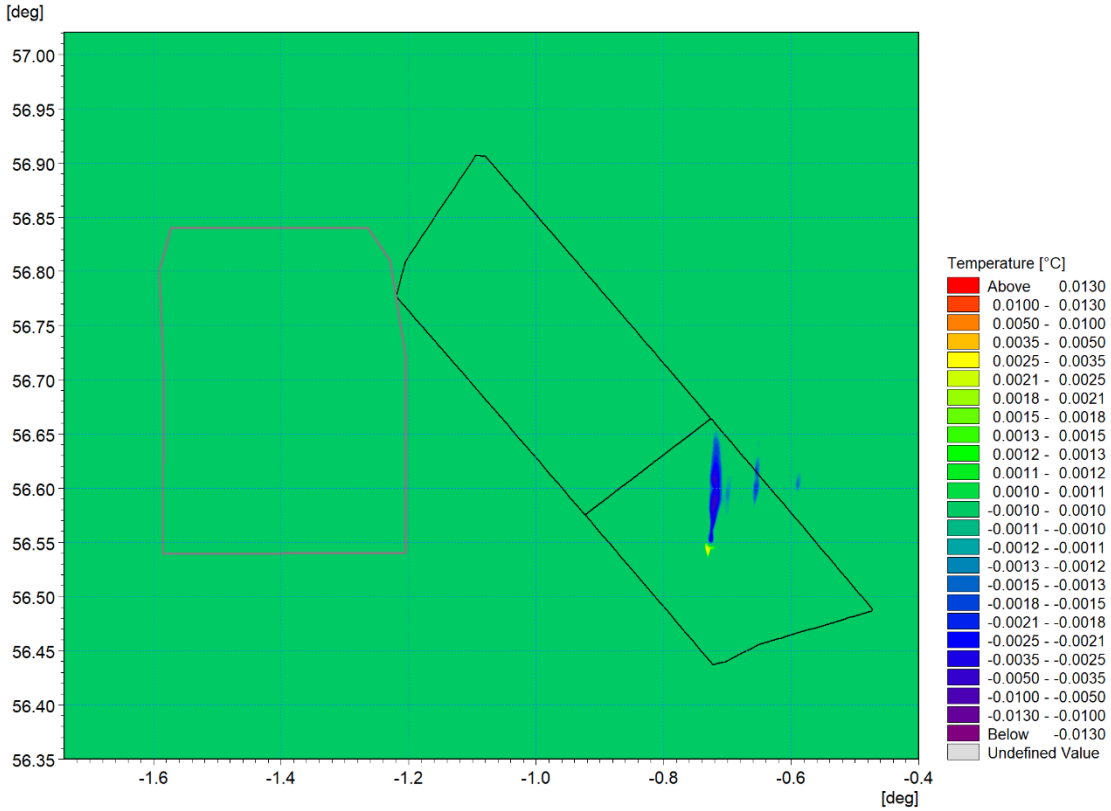

Figure 5.67: Change in temperature at onset of stratification – Day 17 ebb tide (post-construction Morven North and Morven South minus baseline) – Layer 12

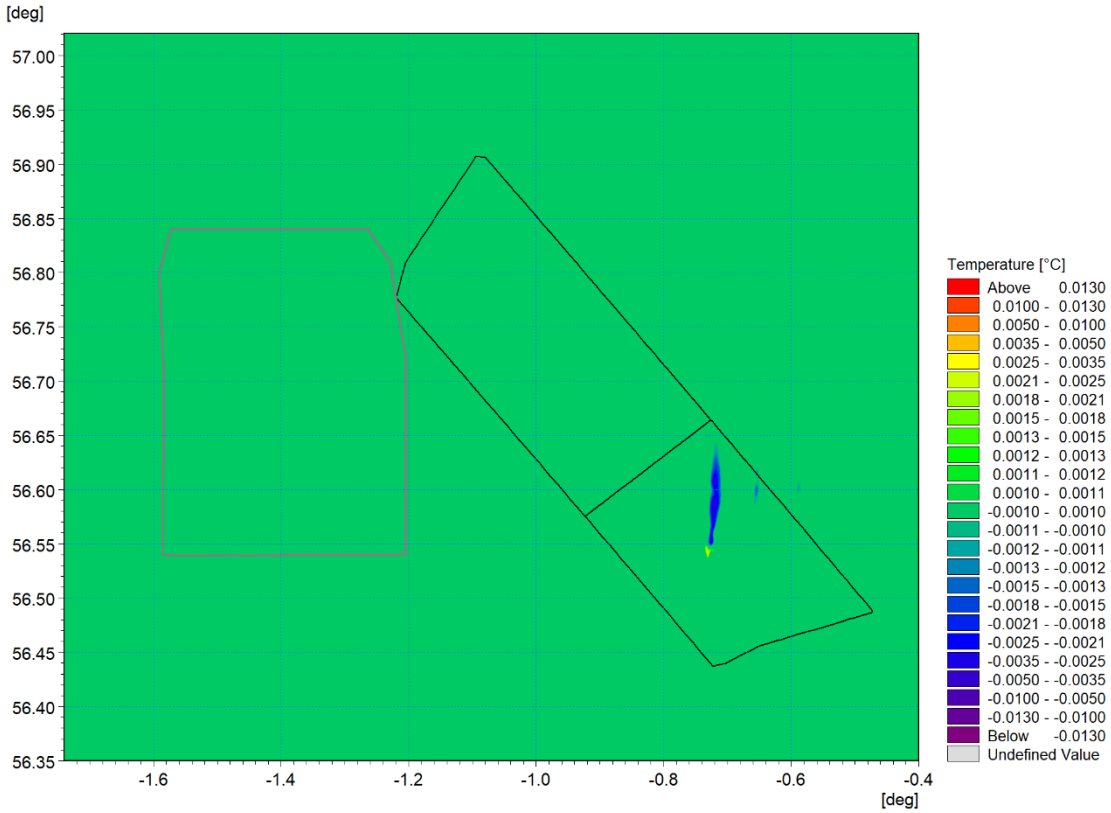

Figure 5.68: Change in temperature at onset of stratification – Day 17 ebb tide (post-construction Morven North and Morven South minus baseline) – Layer 11

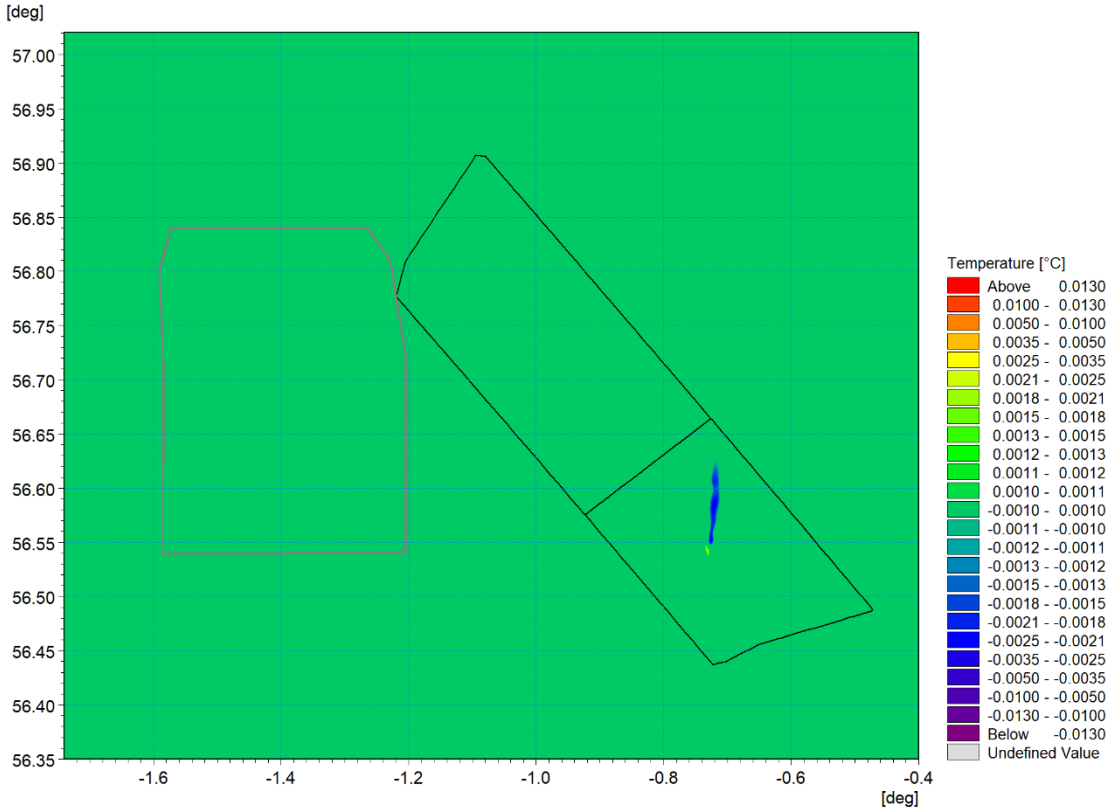

Figure 5.69: Change in temperature at onset of stratification – Day 17 ebb tide (post-construction Morven North and Morven South minus baseline) – Layer 10

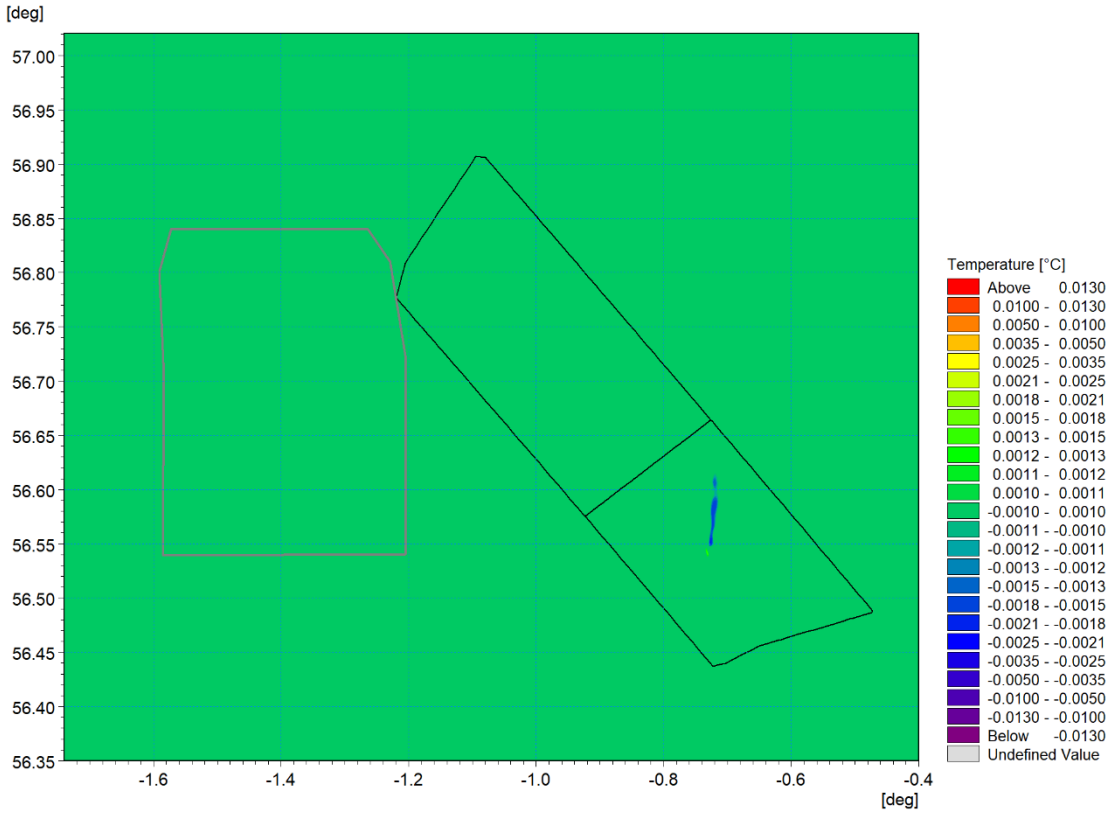

Figure 5.70: Change in temperature at onset of stratification – Day 17 ebb tide (post-construction Morven North and Morven South minus baseline) – Layer 9

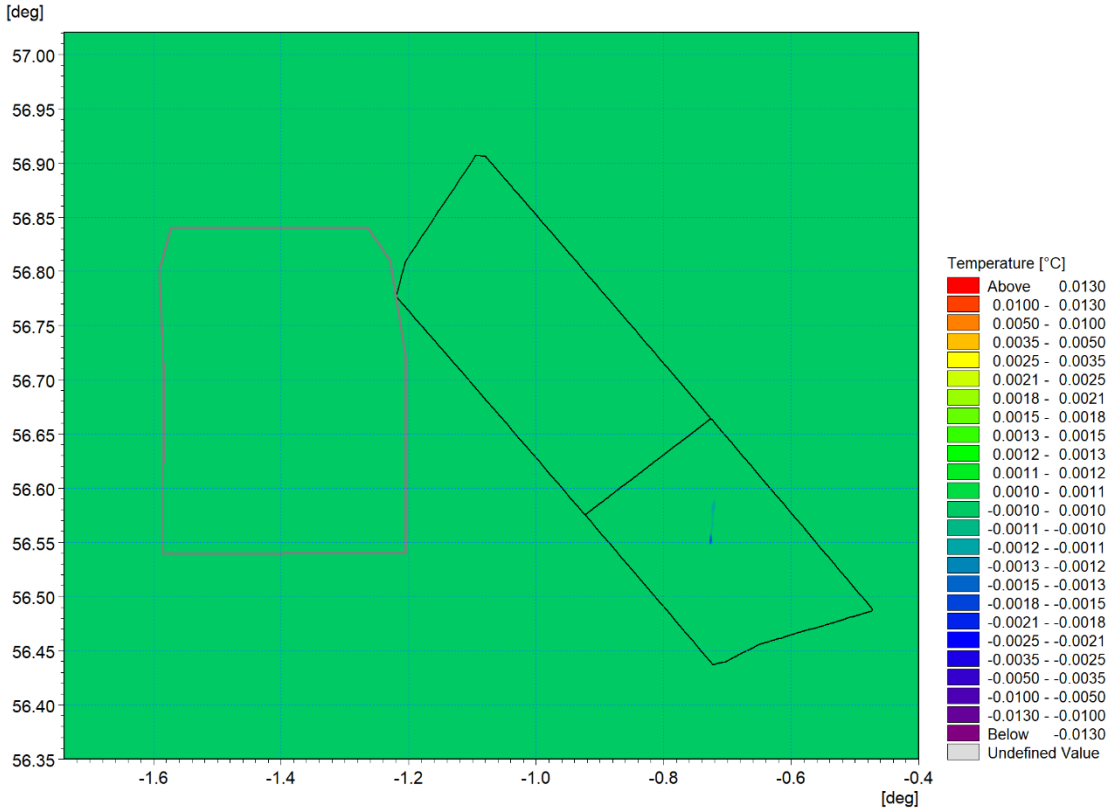

Figure 5.71: Change in temperature at onset of stratification – Day 17 ebb tide (post-construction Morven North and Morven South minus baseline) – Layer 8

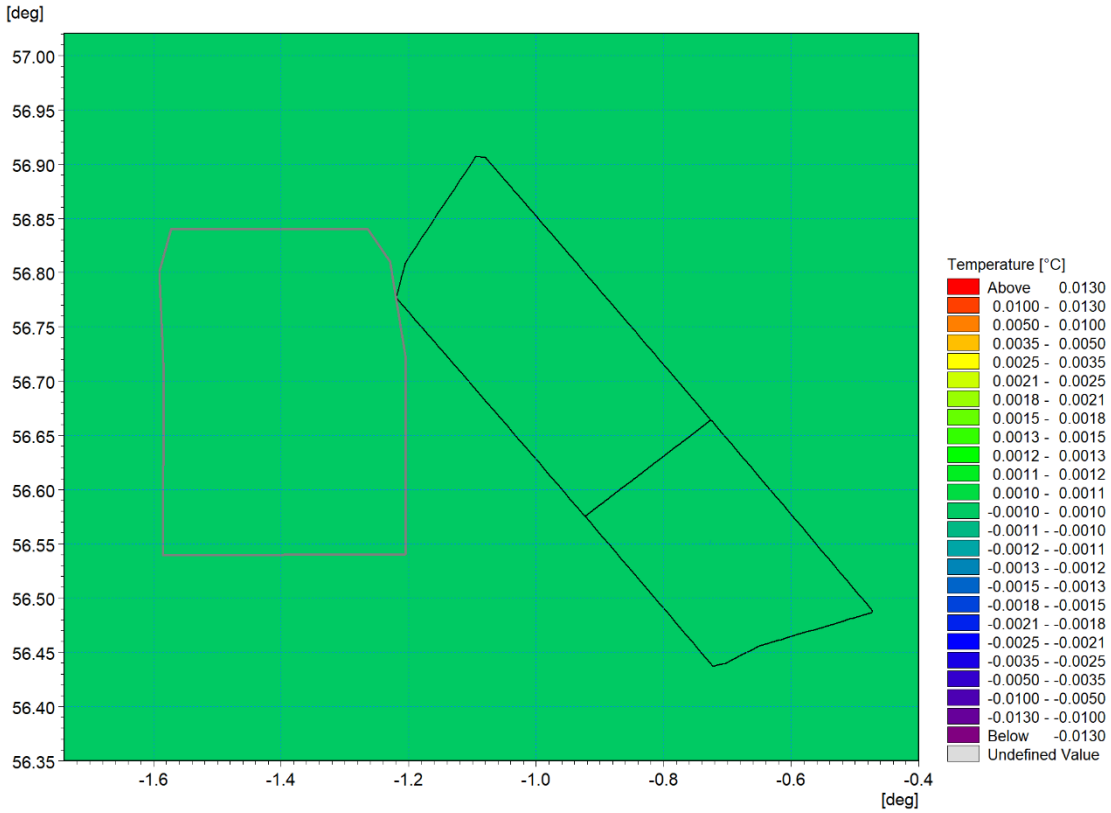

Figure 5.72: Change in temperature at onset of stratification – Day 17 ebb tide (post-construction Morven North and Morven South minus baseline) – Layer 7

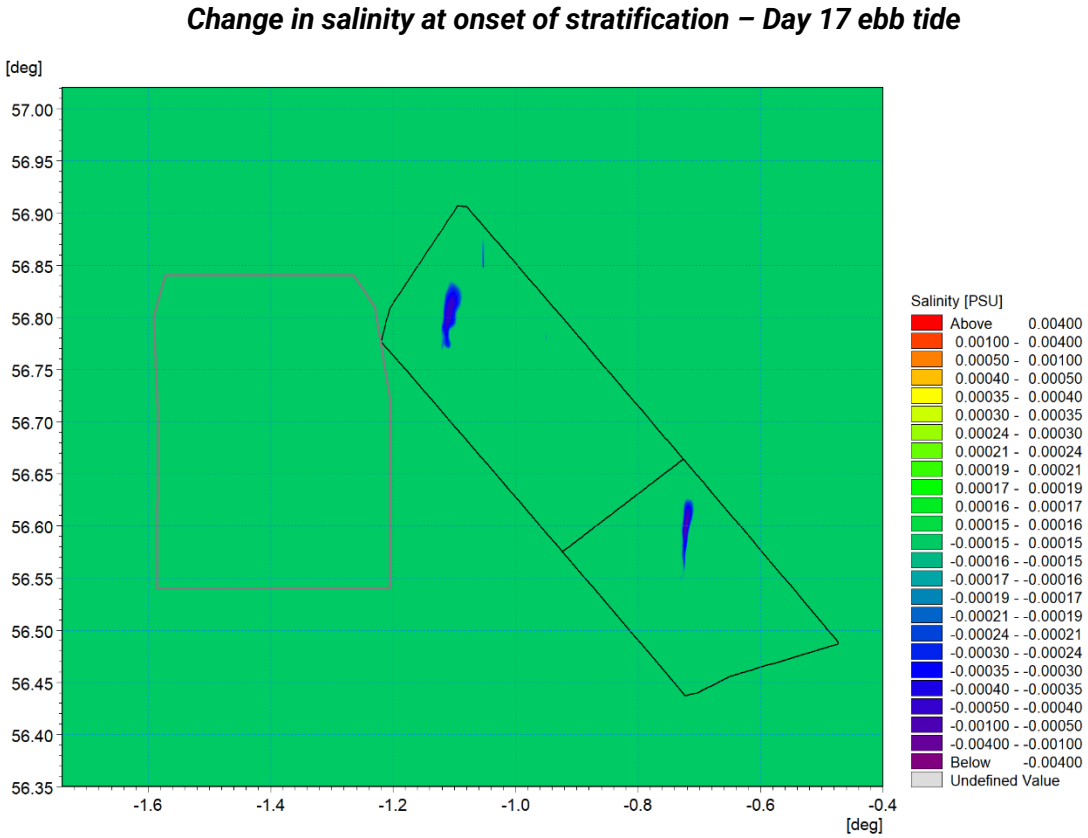

Figure 5.73: Change in salinity at onset of stratification – Day 17 ebb tide (post-construction Morven North and Morven South minus baseline) – Layer 20

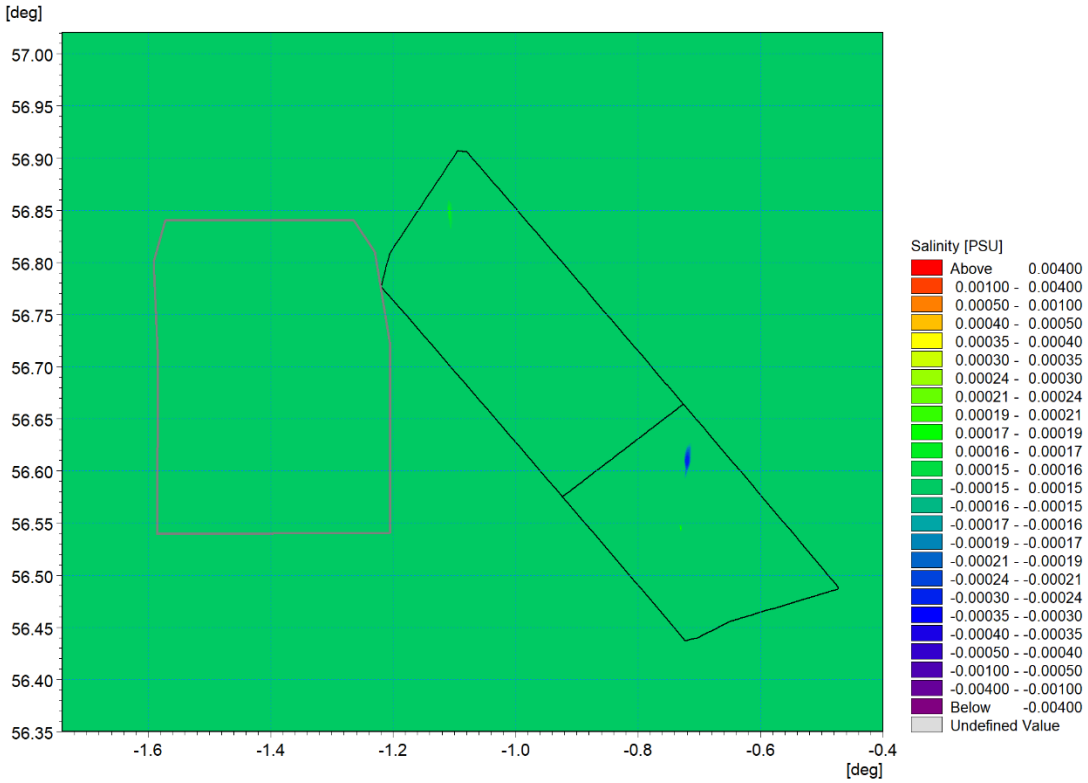

Figure 5.74: Change in salinity at onset of stratification – Day 17 ebb tide (post-construction Morven North and Morven South minus baseline) – Layer 19

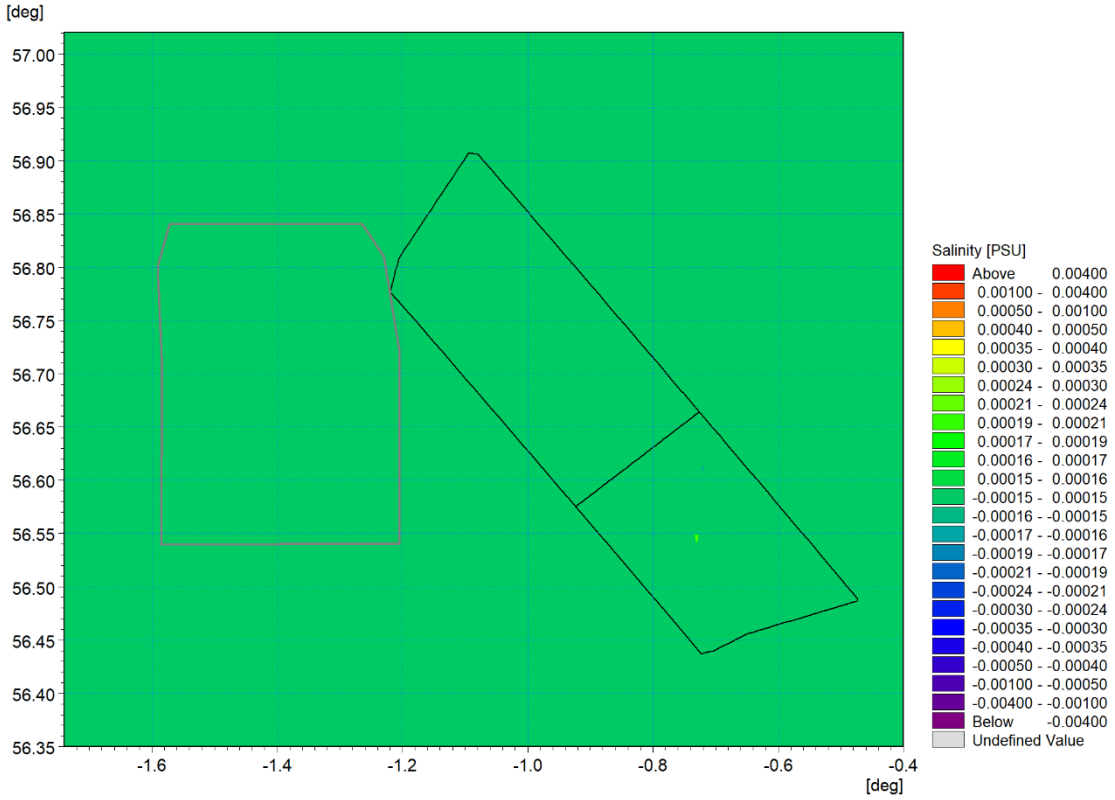

Figure 5.75: Change in salinity at onset of stratification – Day 17 ebb tide (post-construction Morven North and Morven South minus baseline) – Layer 18

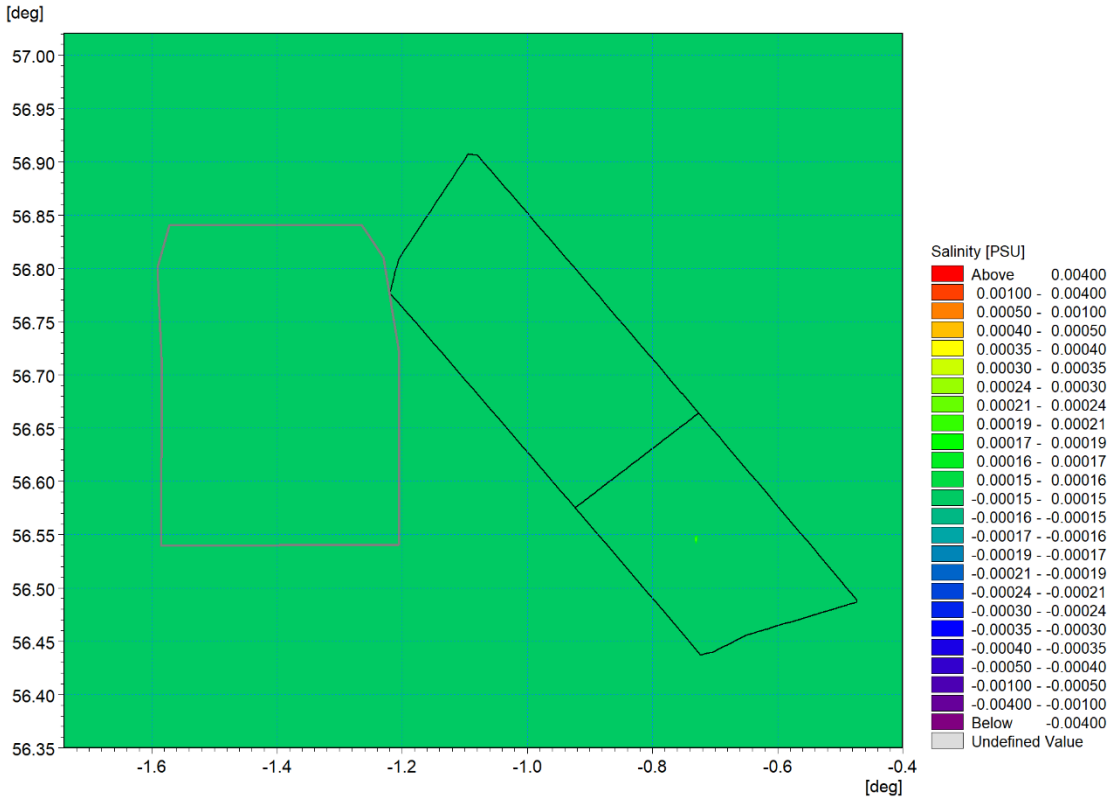

Figure 5.76: Change in salinity at onset of stratification – Day 17 ebb tide (post-construction Morven North and Morven South minus baseline) – Layer 17

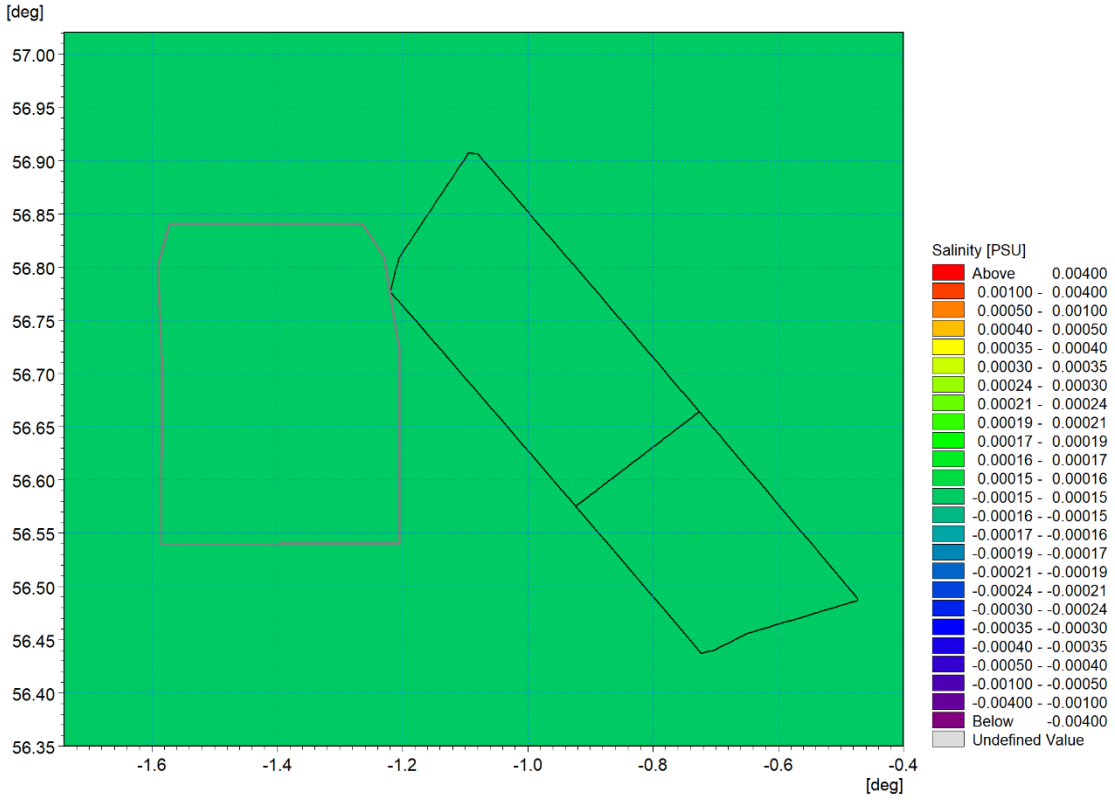

Figure 5.77: Change in salinity at onset of stratification – Day 17 ebb tide (post-construction Morven North and Morven South minus baseline) – Layer 16

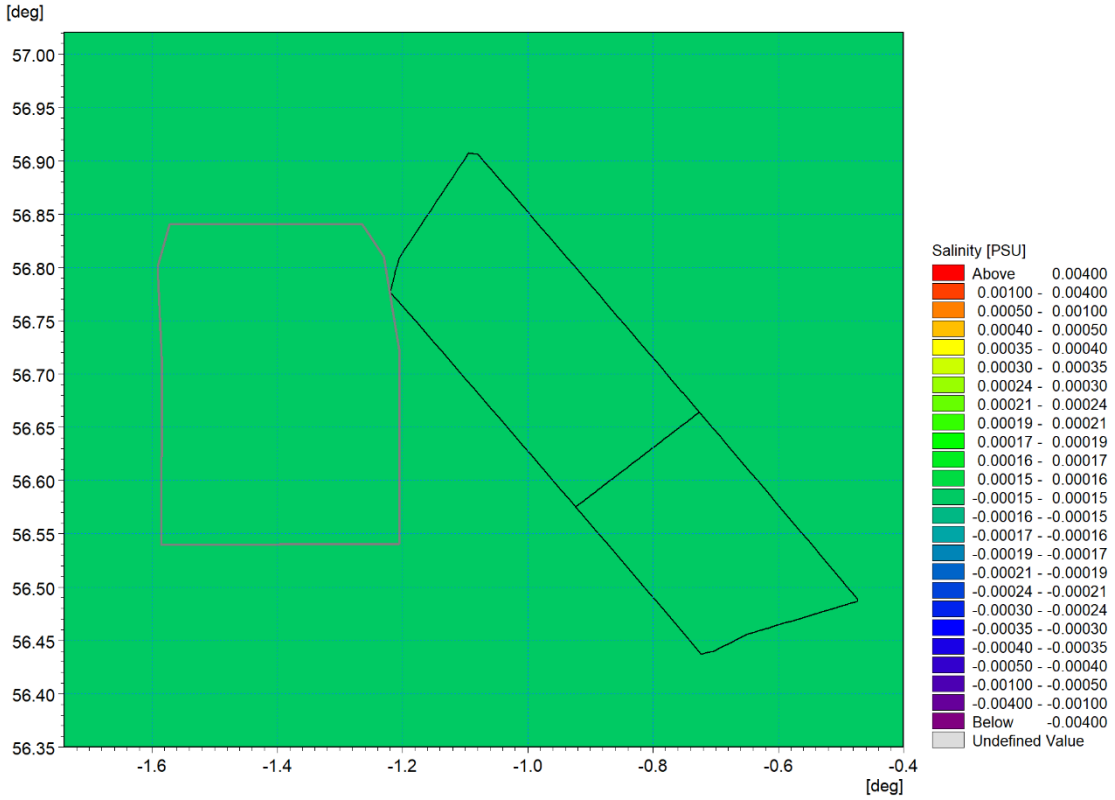

Figure 5.78: Change in salinity at onset of stratification – Day 17 ebb tide (post-construction Morven North and Morven South minus baseline) – Layer 15

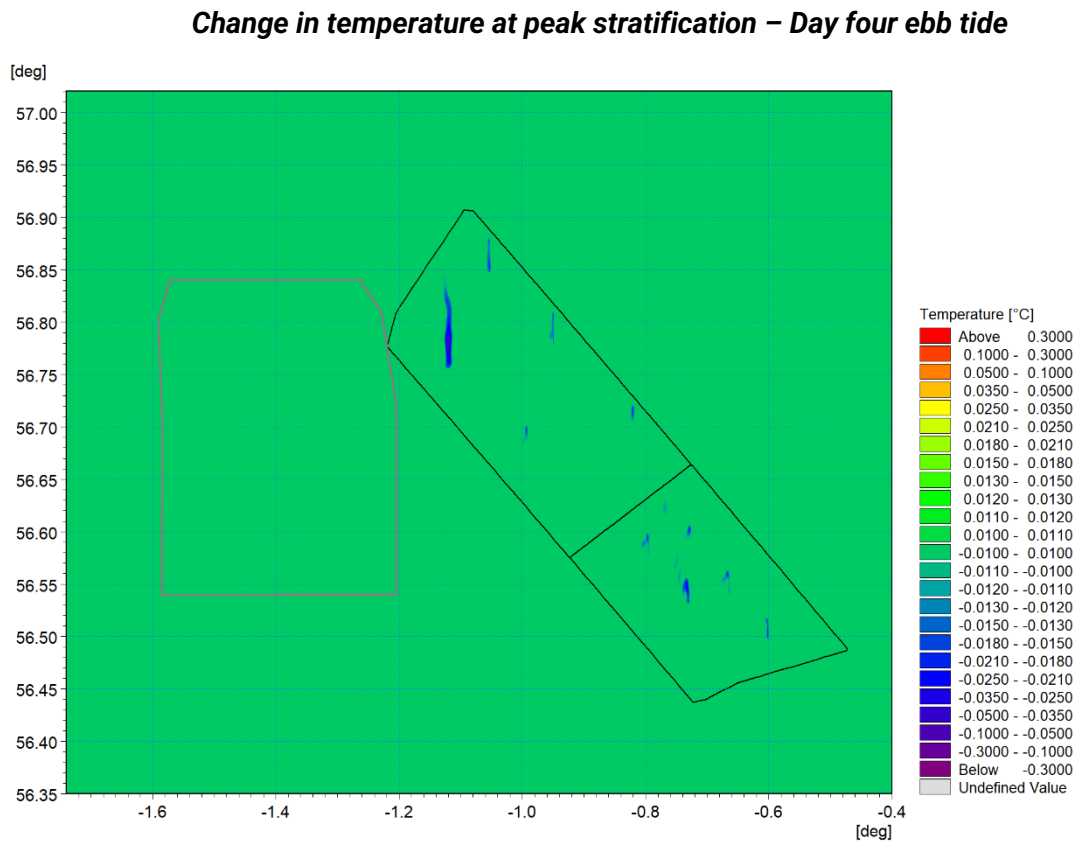

Figure 5.79: Change in temperature at peak stratification – Day four ebb tide (post-construction Morven North and Morven South minus baseline) – Layer 20

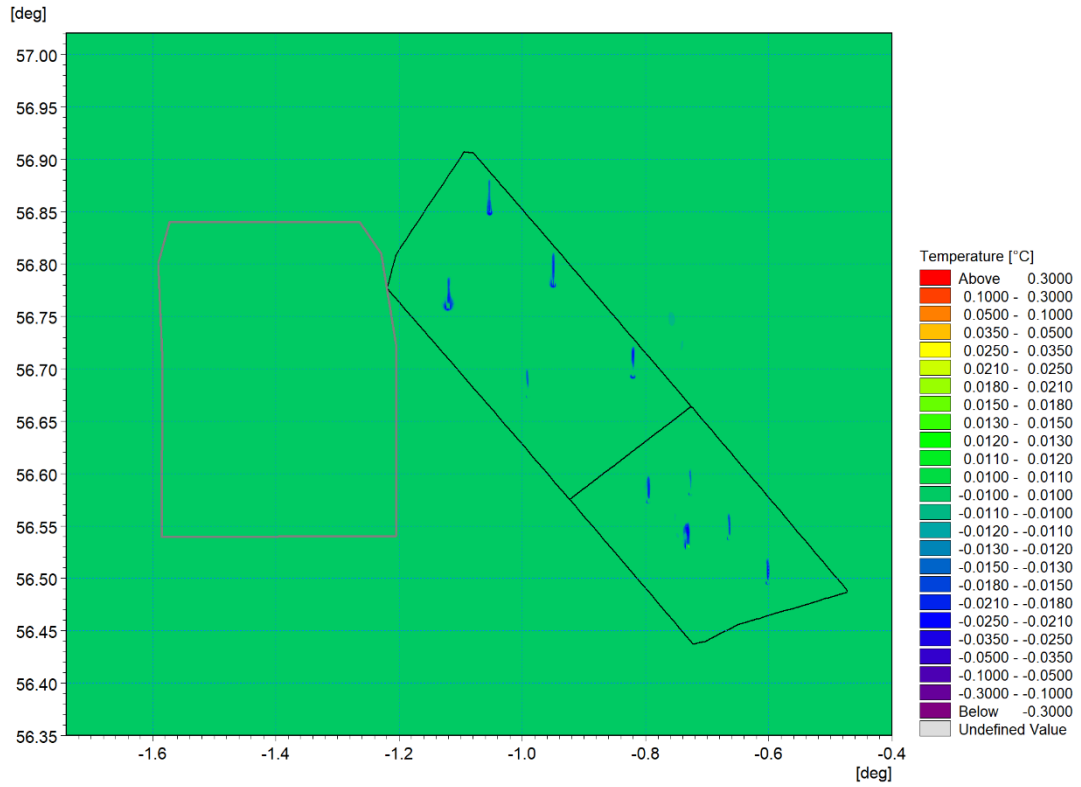

Figure 5.80: Change in temperature at peak stratification – Day four ebb tide (post-construction Morven North and Morven South minus baseline) – Layer 19

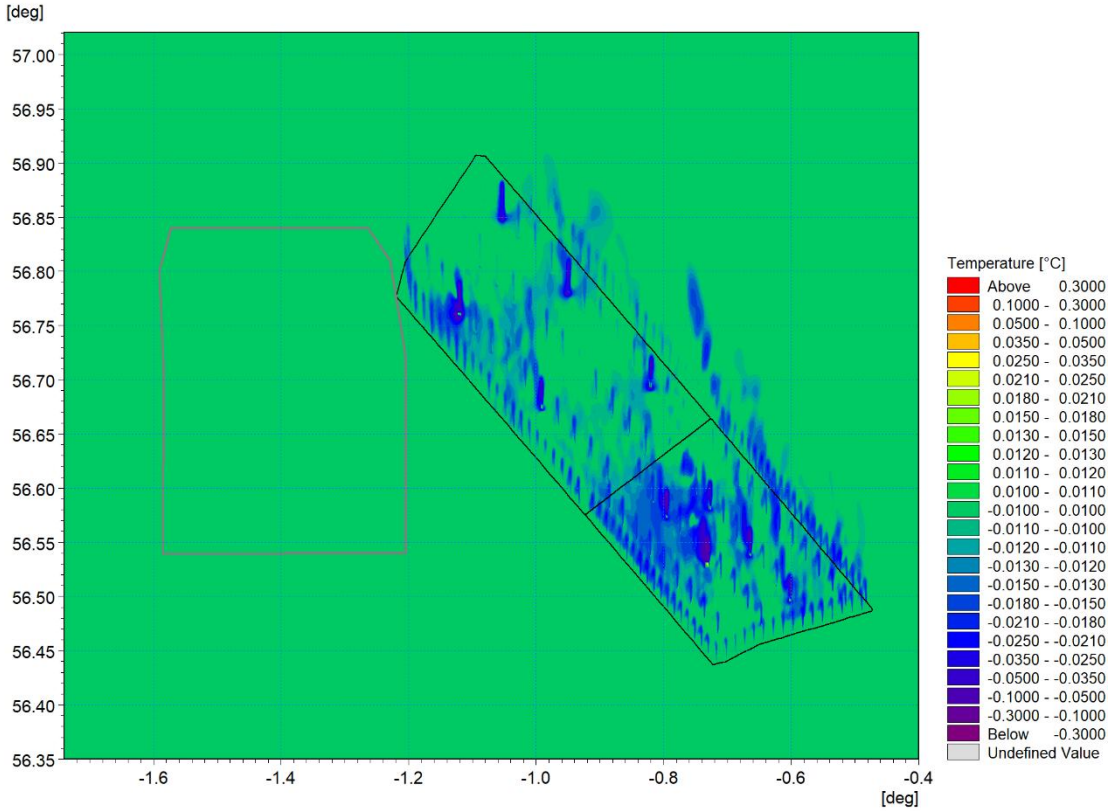

Figure 5.81: Change in temperature at peak stratification – Day four ebb tide (post-construction Morven North and Morven South minus baseline) – Layer 18

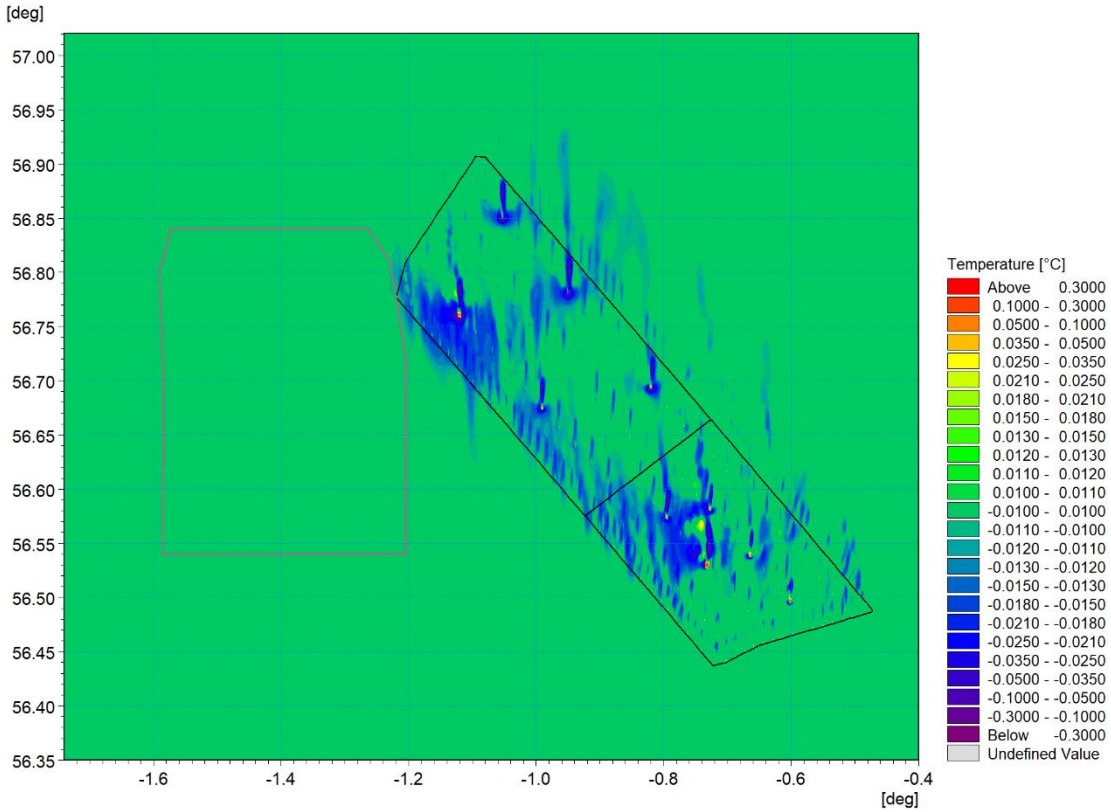

Figure 5.82: Change in temperature at peak stratification – Day four ebb tide (post-construction Morven North and Morven South minus baseline) – Layer 17

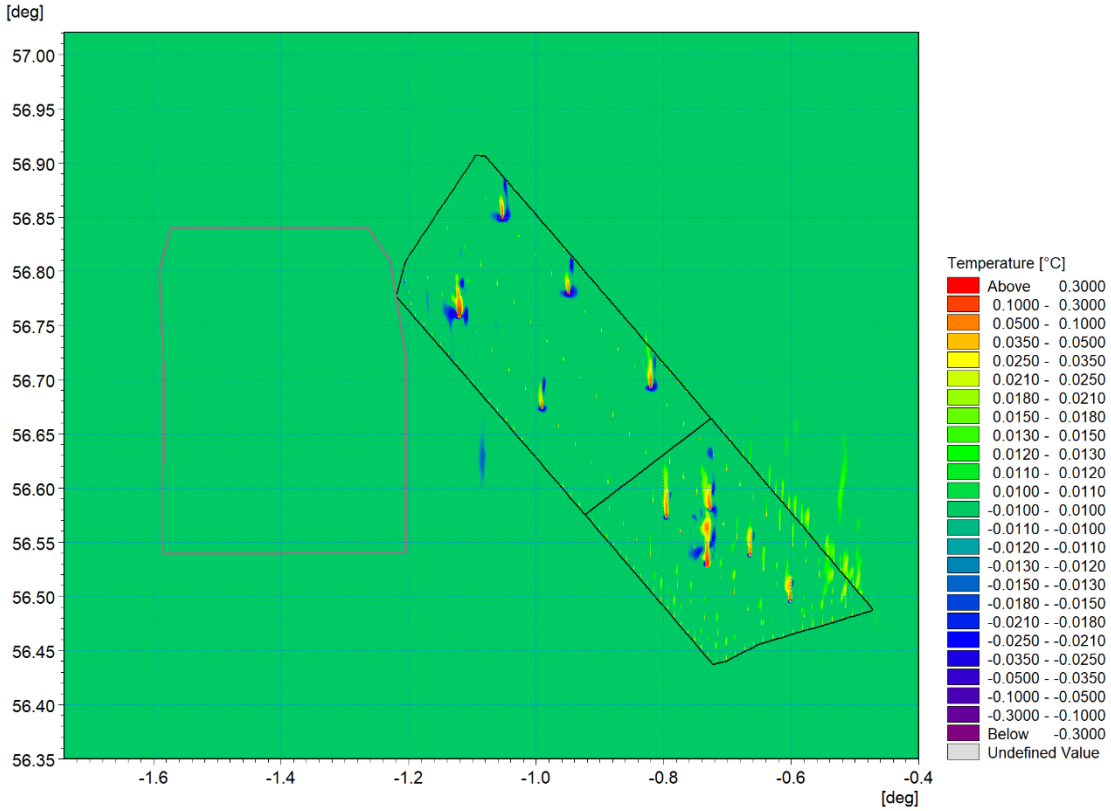

Figure 5.83: Change in temperature at peak stratification – Day four ebb tide (post-construction Morven North and Morven South minus baseline) – Layer 16

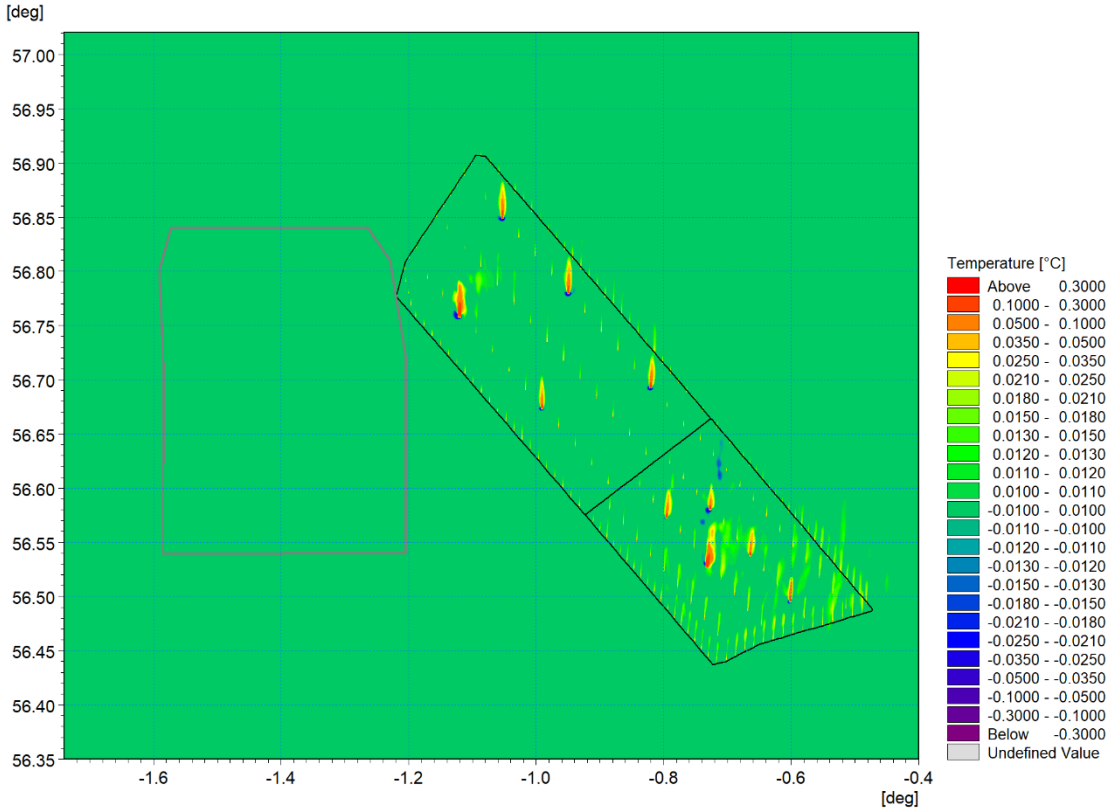

Figure 5.84: Change in temperature at peak stratification – Day four ebb tide (post-construction Morven North and Morven South minus baseline) – Layer 15

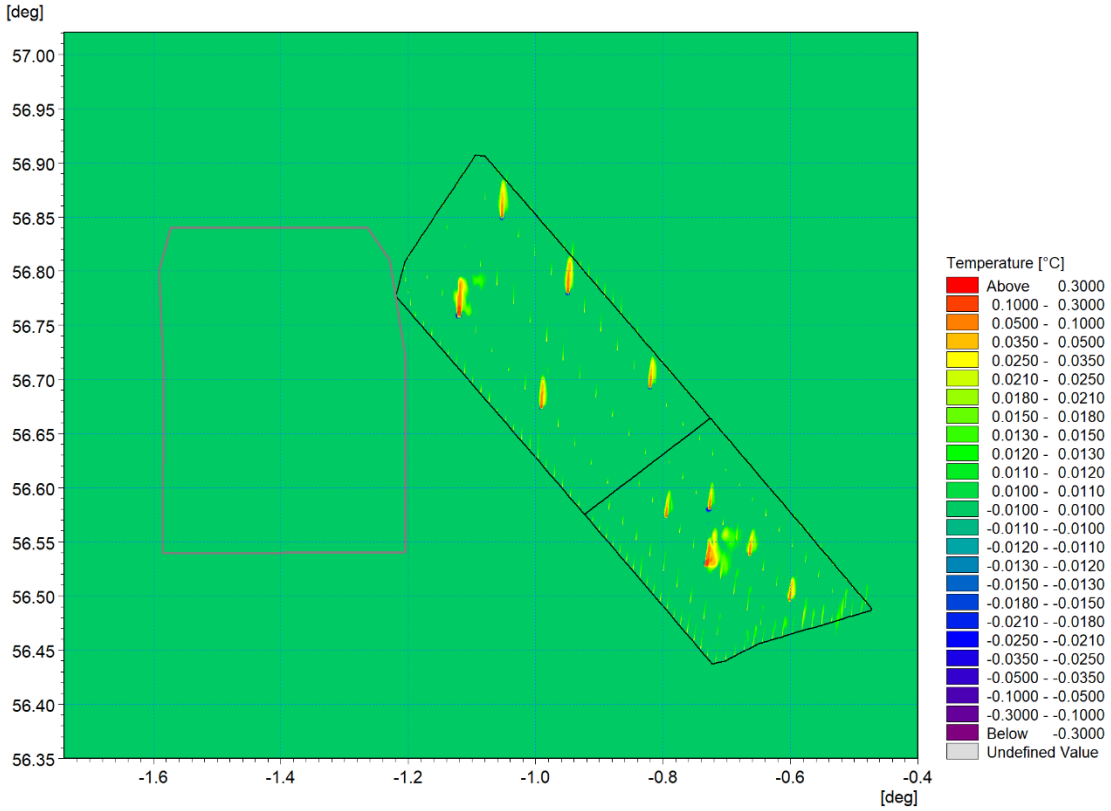

Figure 5.85: Change in temperature at peak stratification – Day four ebb tide (post-construction Morven North and Morven South minus baseline) – Layer 14

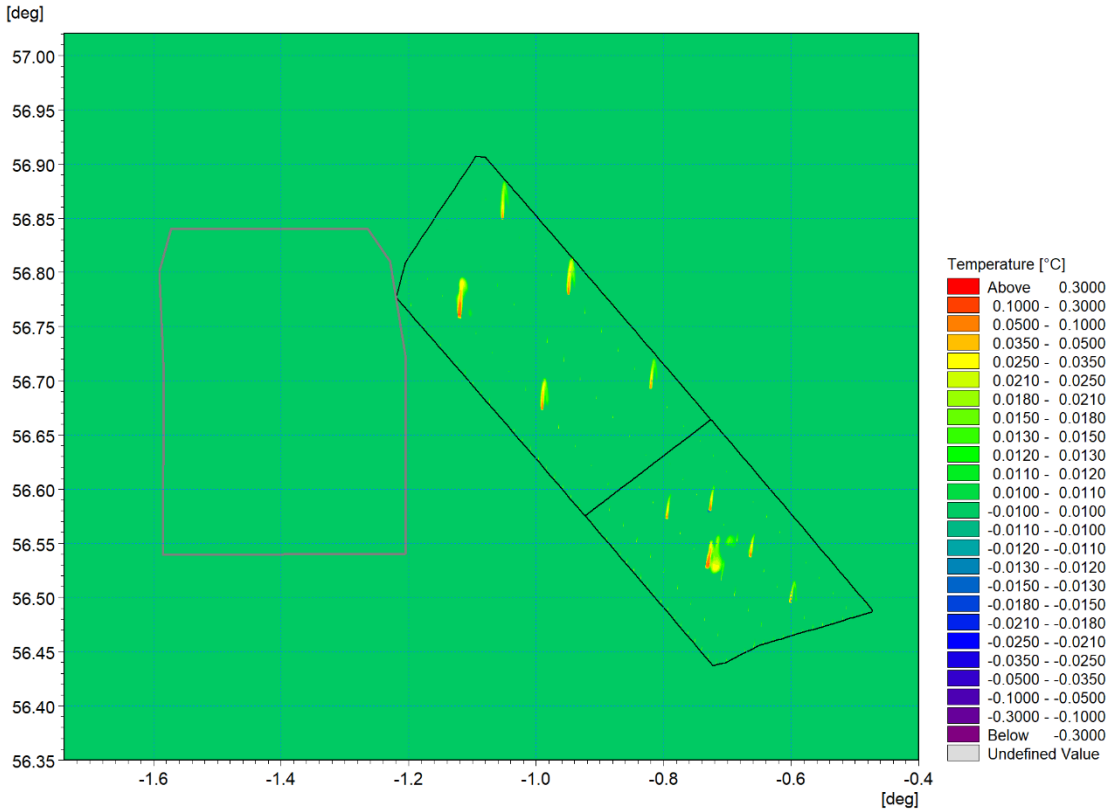

Figure 5.86: Change in temperature at peak stratification – Day four ebb tide (post-construction Morven North and Morven South minus baseline) – Layer 13

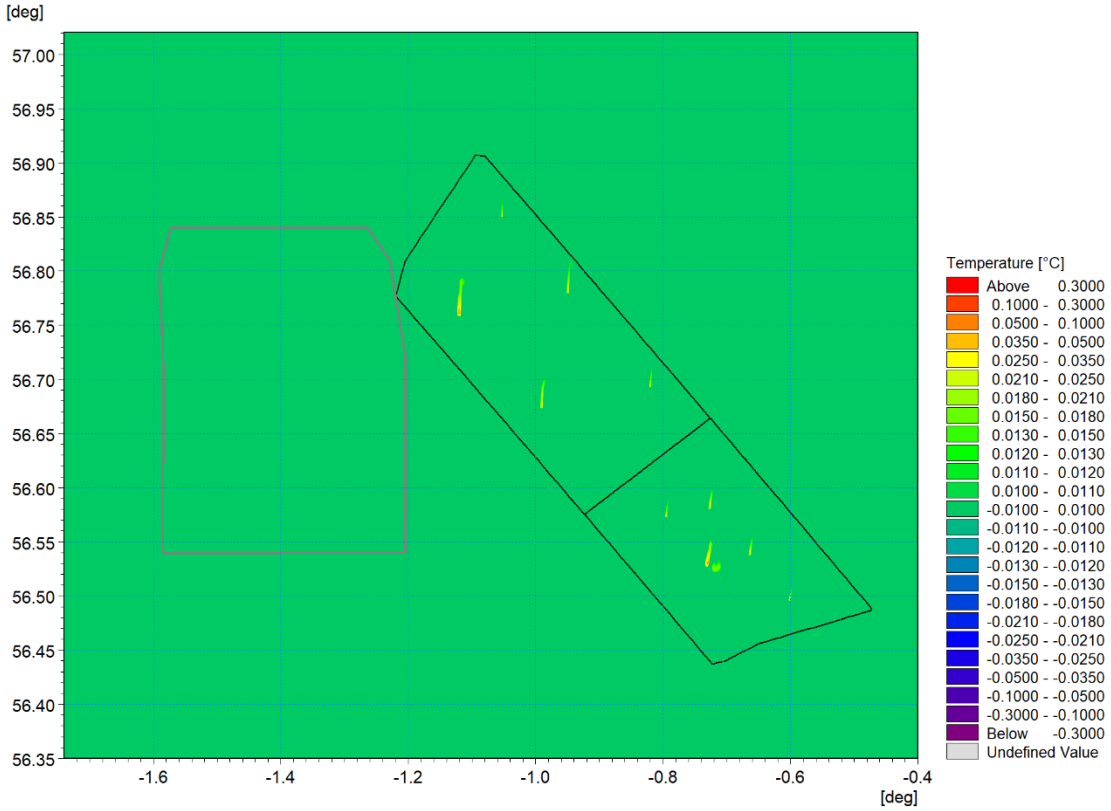

Figure 5.87: Change in temperature at peak stratification – Day four ebb tide (post-construction Morven North and Morven South minus baseline) – Layer 12

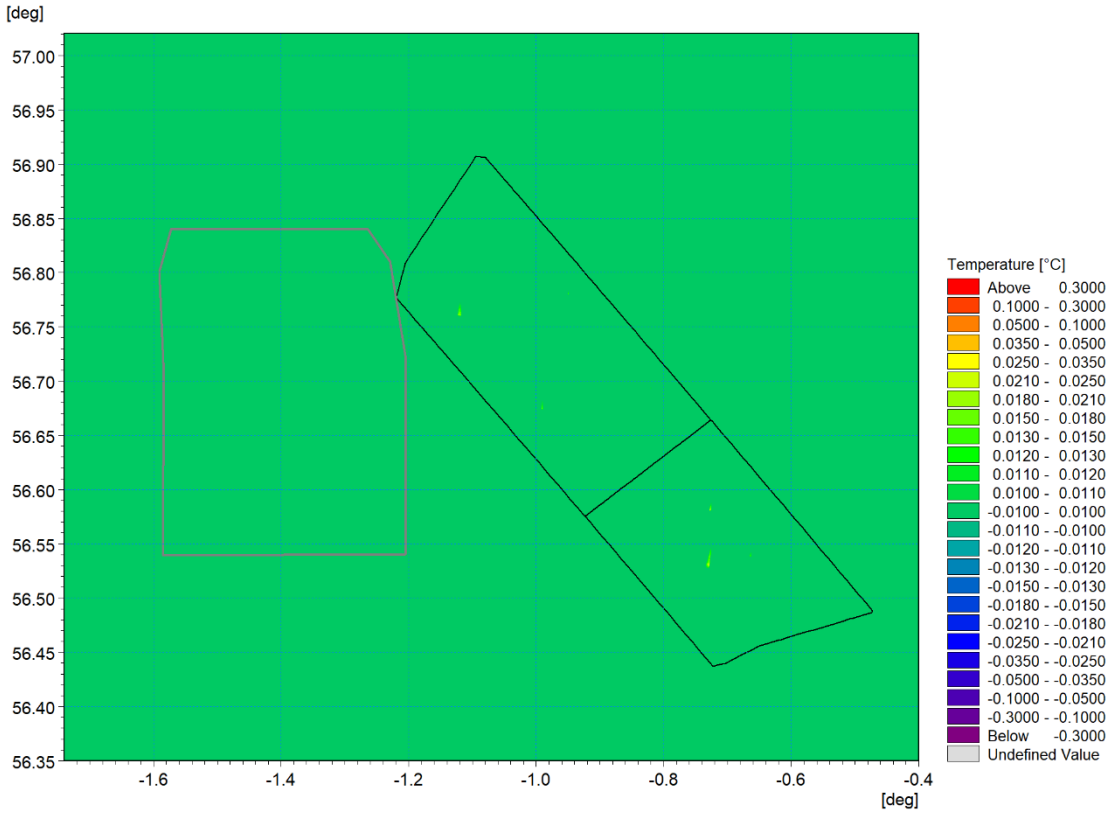

Figure 5.88: Change in temperature at peak stratification – Day four ebb tide (post-construction Morven North and Morven South minus baseline) – Layer 11

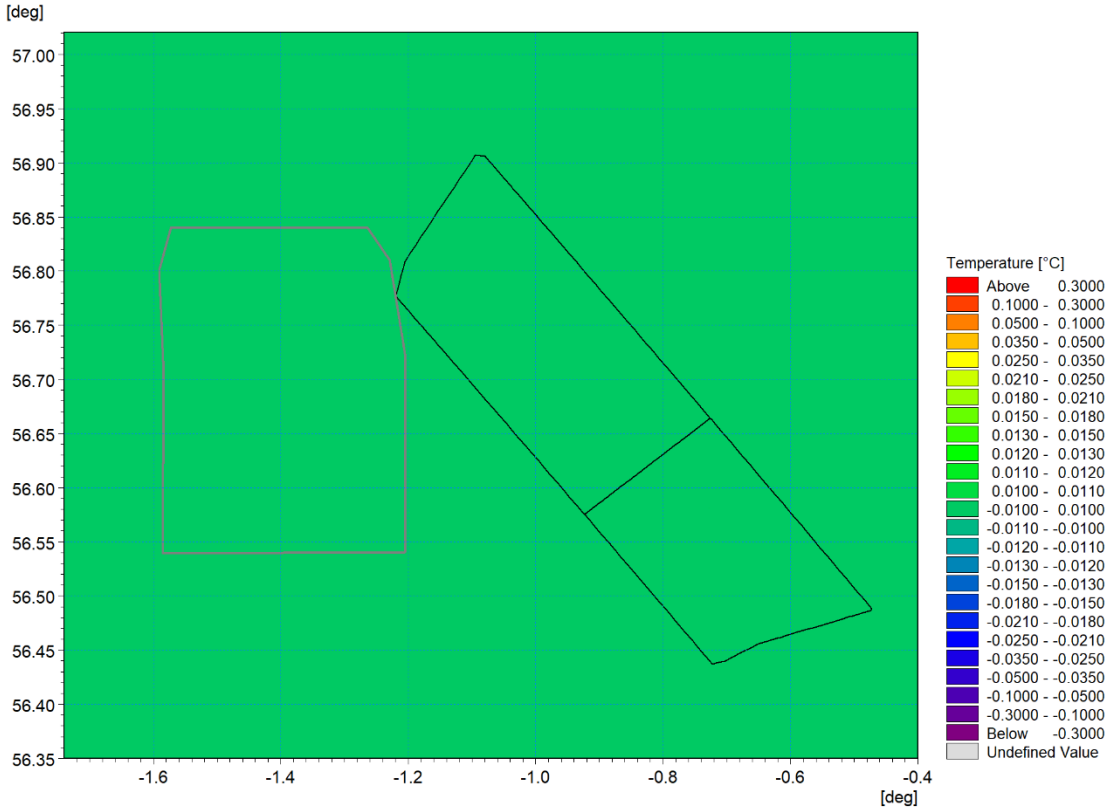

Figure 5.89: Change in temperature at peak stratification – Day four ebb tide (post-construction Morven North and Morven South minus baseline) – Layer 10

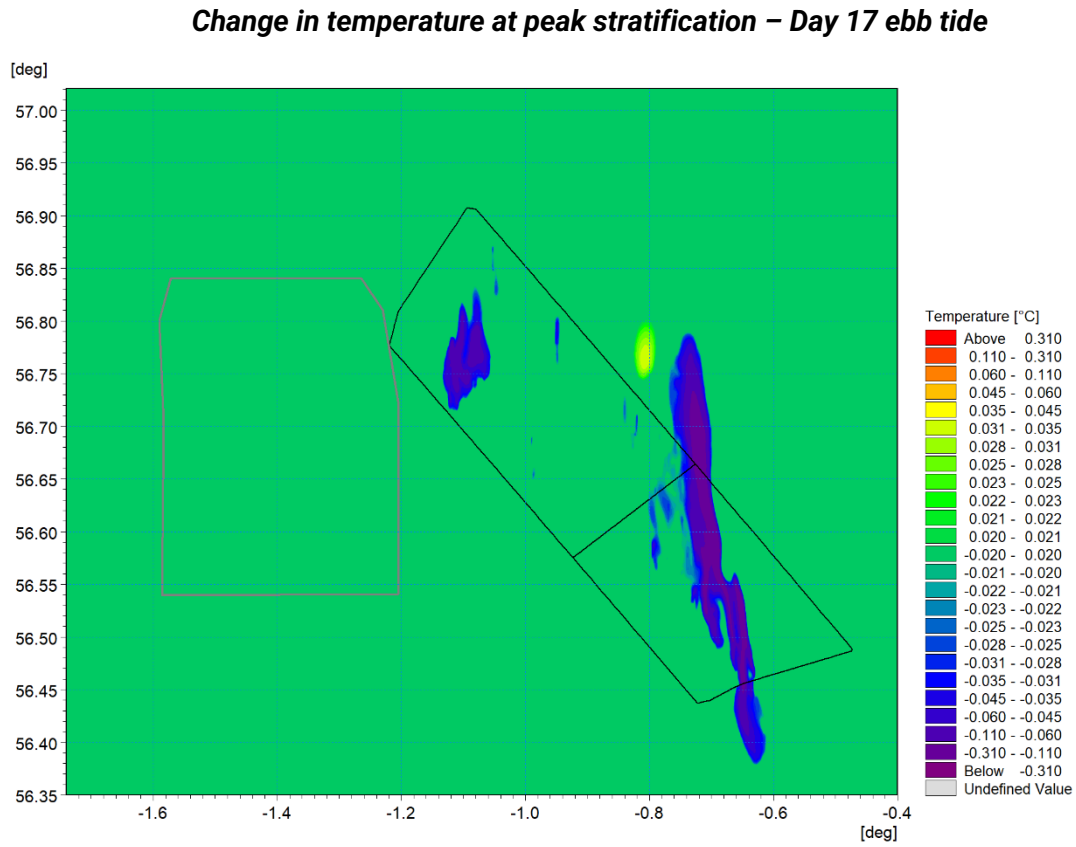

Figure 5.90: Change in temperature at peak stratification – Day 17 ebb tide (post-construction Morven North and Morven South minus baseline) – Layer 20

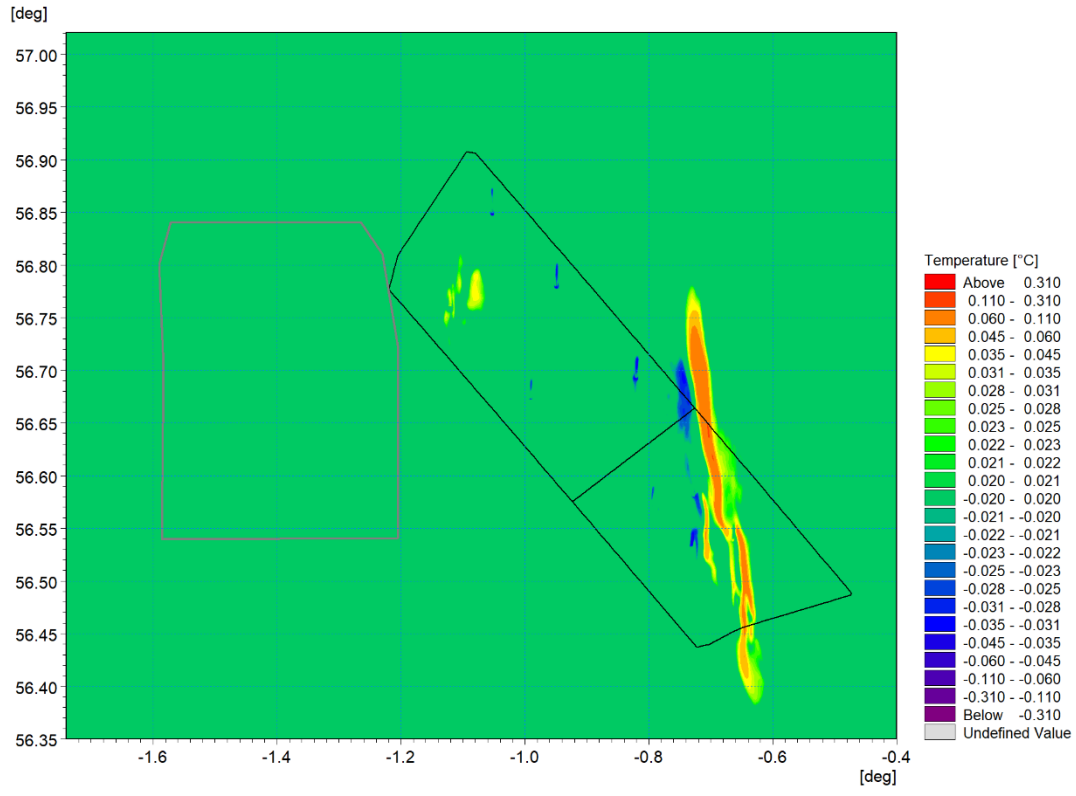

Figure 5.91: Change in temperature at peak stratification – Day 17 ebb tide (post-construction Morven North and Morven South minus baseline) – Layer 19

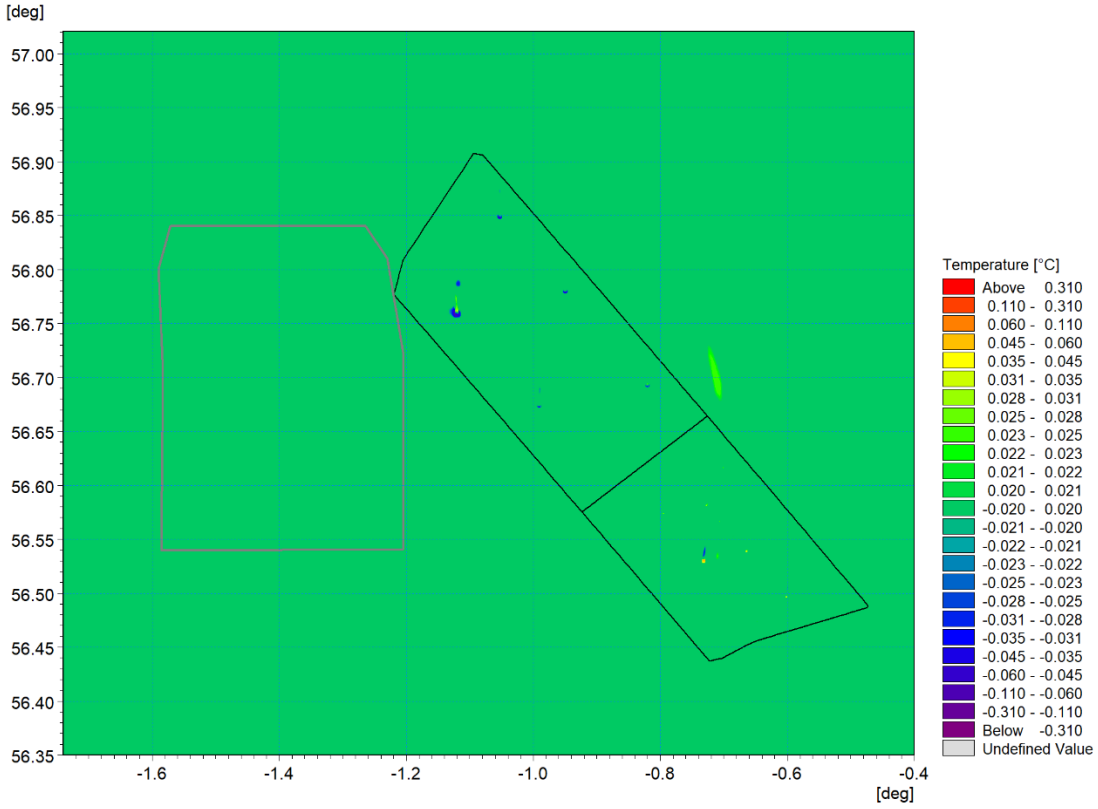

Figure 5.92: Change in temperature at peak stratification – Day 17 ebb tide (post-construction Morven North and Morven South minus baseline) – Layer 18

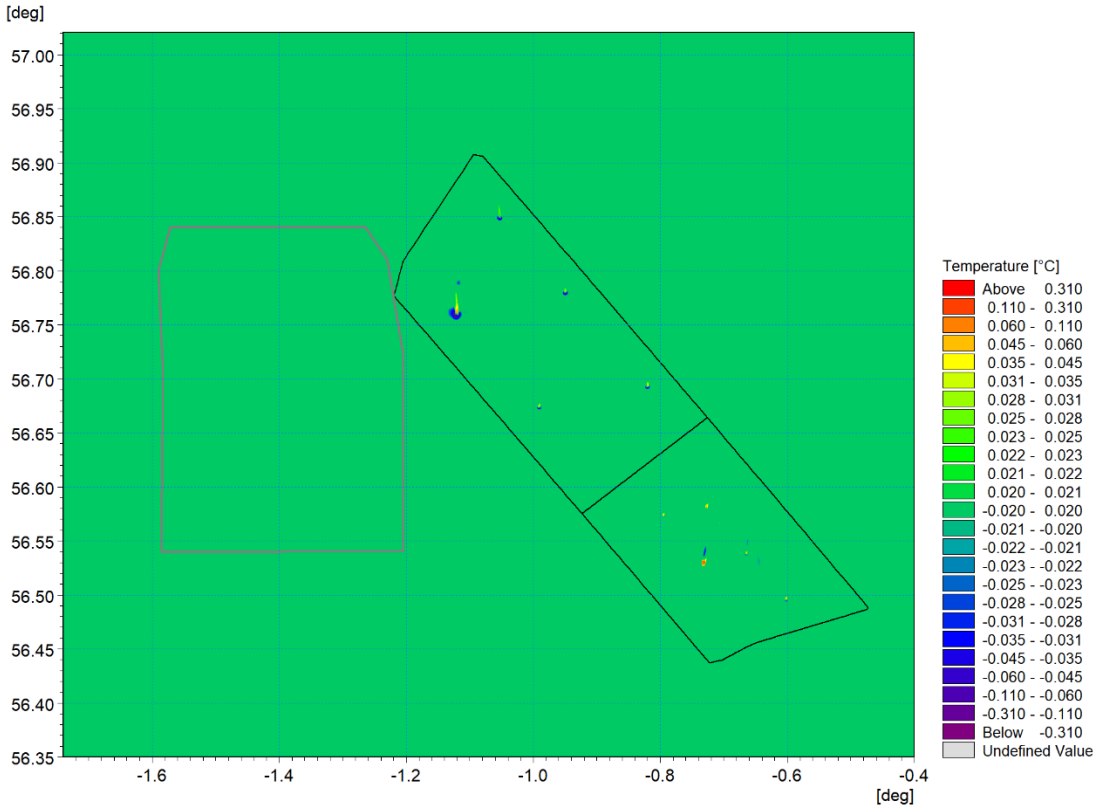

Figure 5.93: Change in temperature at peak stratification – Day 17 ebb tide (post-construction Morven North and Morven South minus baseline) – Layer 17

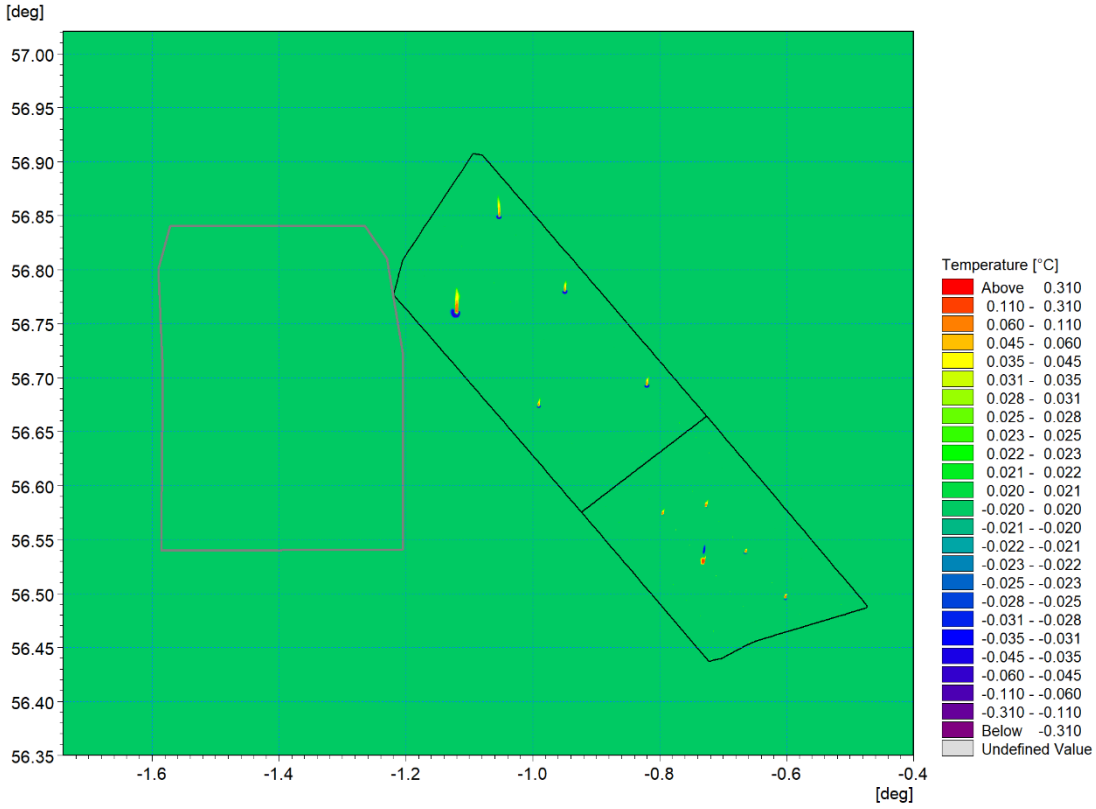

Figure 5.94: Change in temperature at peak stratification – Day 17 ebb tide (post-construction Morven North and Morven South minus baseline) – Layer 16

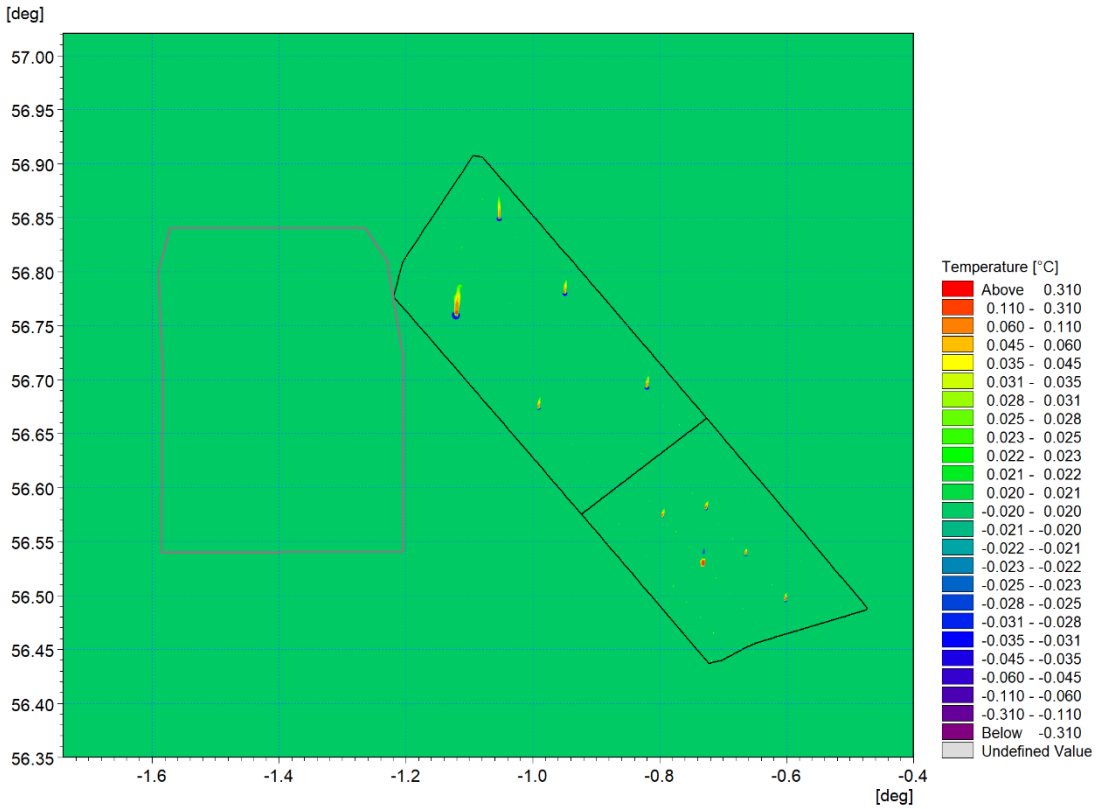

Figure 5.95: Change in temperature at peak stratification – Day 17 ebb tide (post-construction Morven North and Morven South minus baseline) – Layer 15

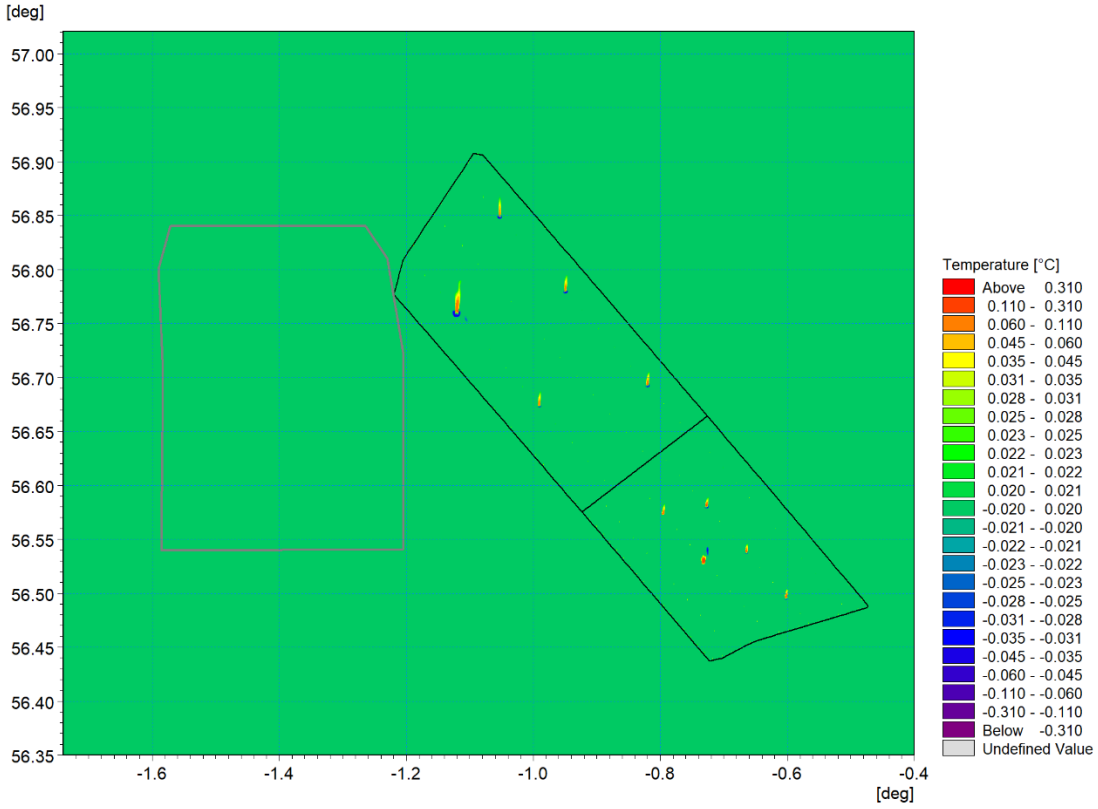

Figure 5.96: Change in temperature at peak stratification – Day 17 ebb tide (post-construction Morven North and Morven South minus baseline) – Layer 14

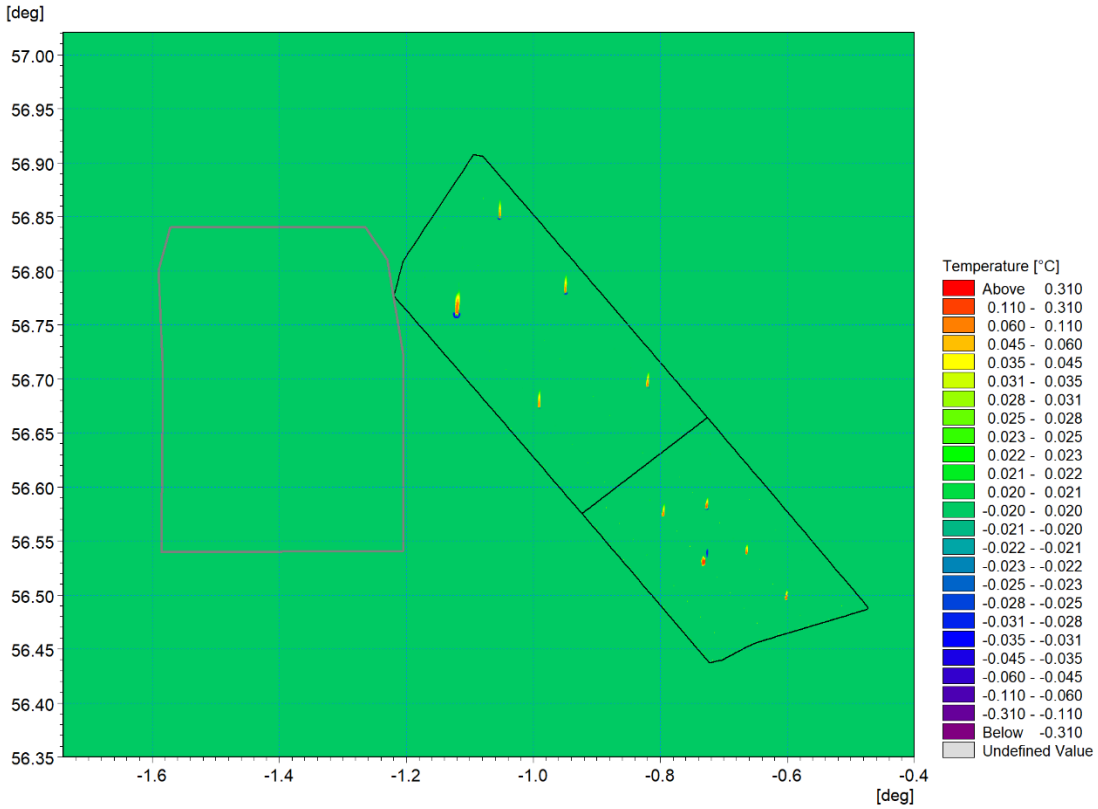

Figure 5.97: Change in temperature at peak stratification – Day 17 ebb tide (post-construction Morven North and Morven South minus baseline) – Layer 13

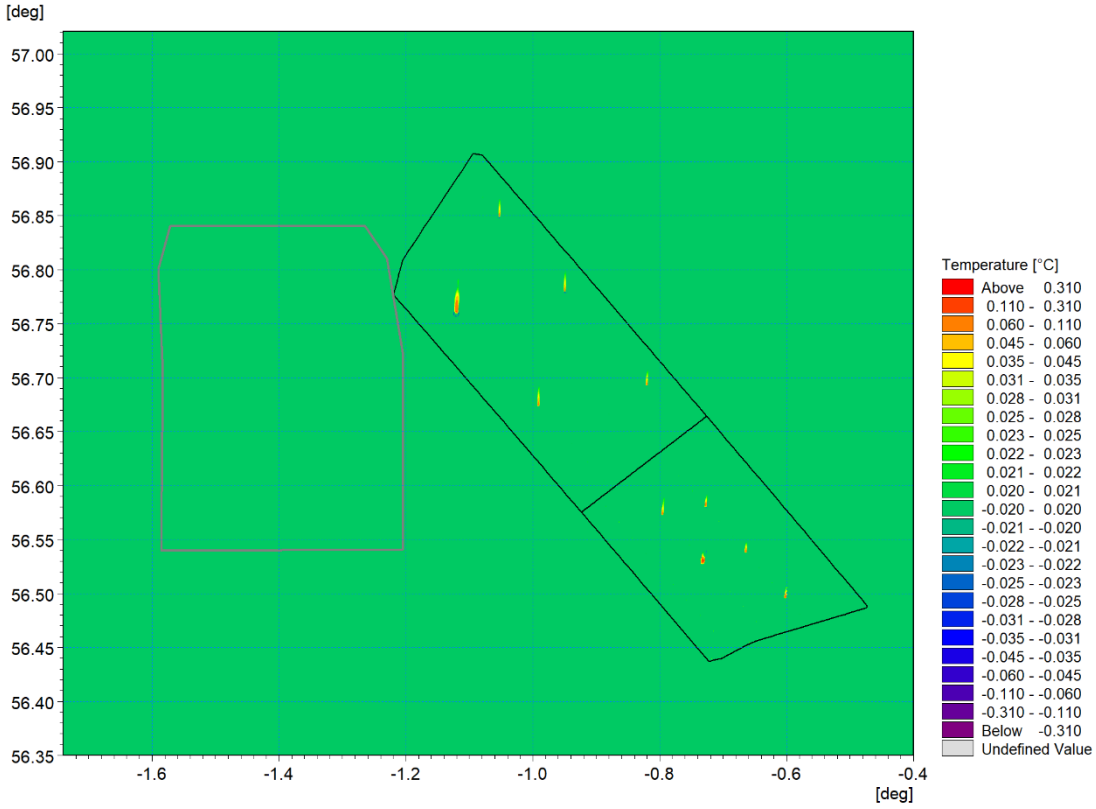

Figure 5.98: Change in temperature at peak stratification – Day 17 ebb tide (post-construction Morven North and Morven South minus baseline) – Layer 12

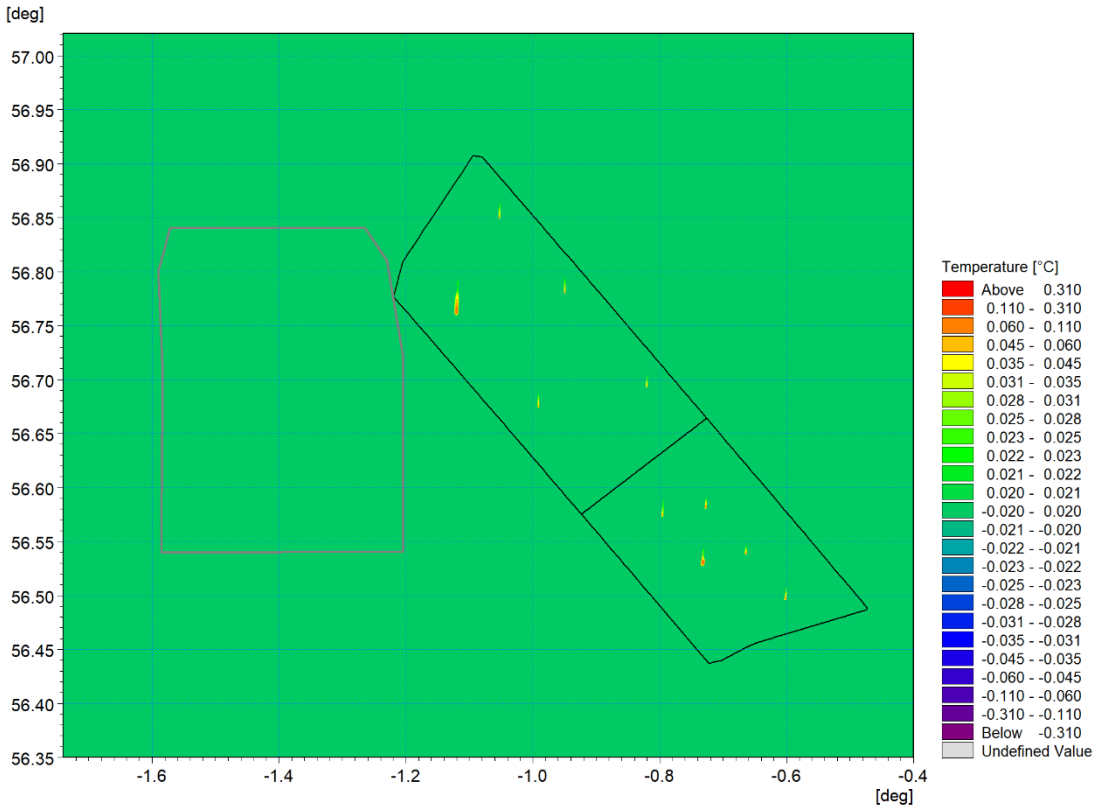

Figure 5.99: Change in temperature at peak stratification – Day 17 ebb tide (post-construction Morven North and Morven South minus baseline) – Layer 11

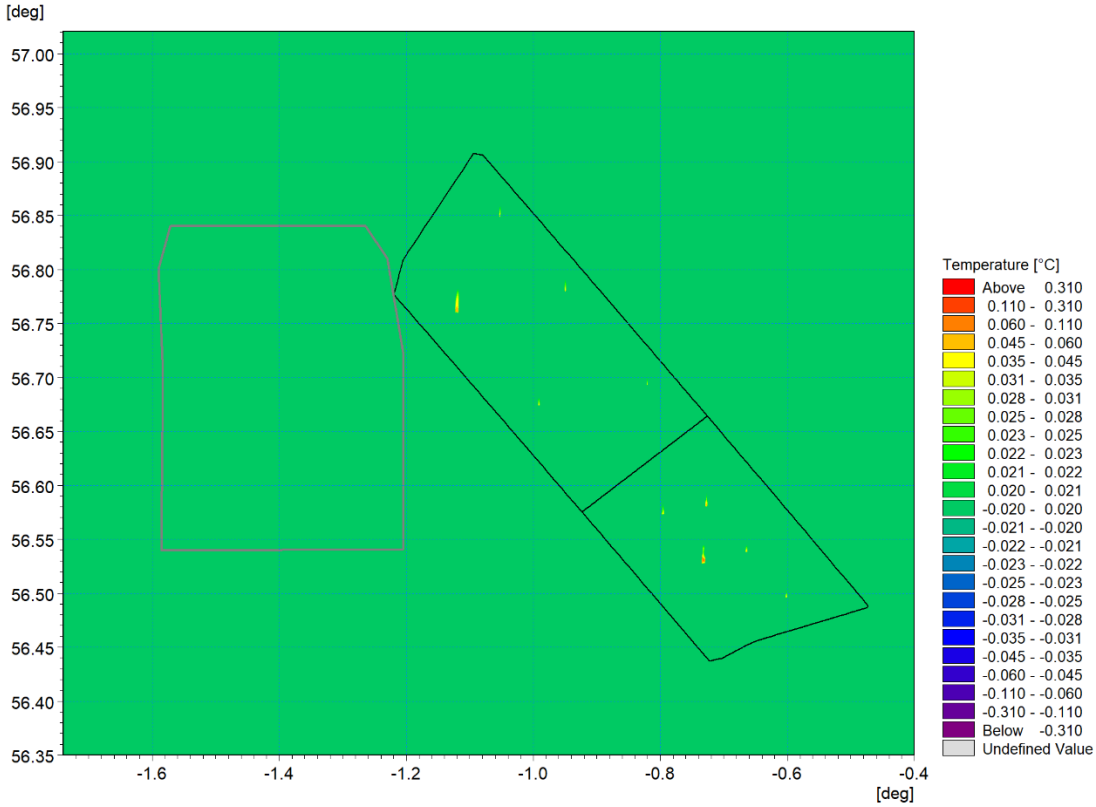

Figure 5.100: Change in temperature at peak stratification – Day 17 ebb tide (post-construction Morven North and Morven South minus baseline) – Layer 10

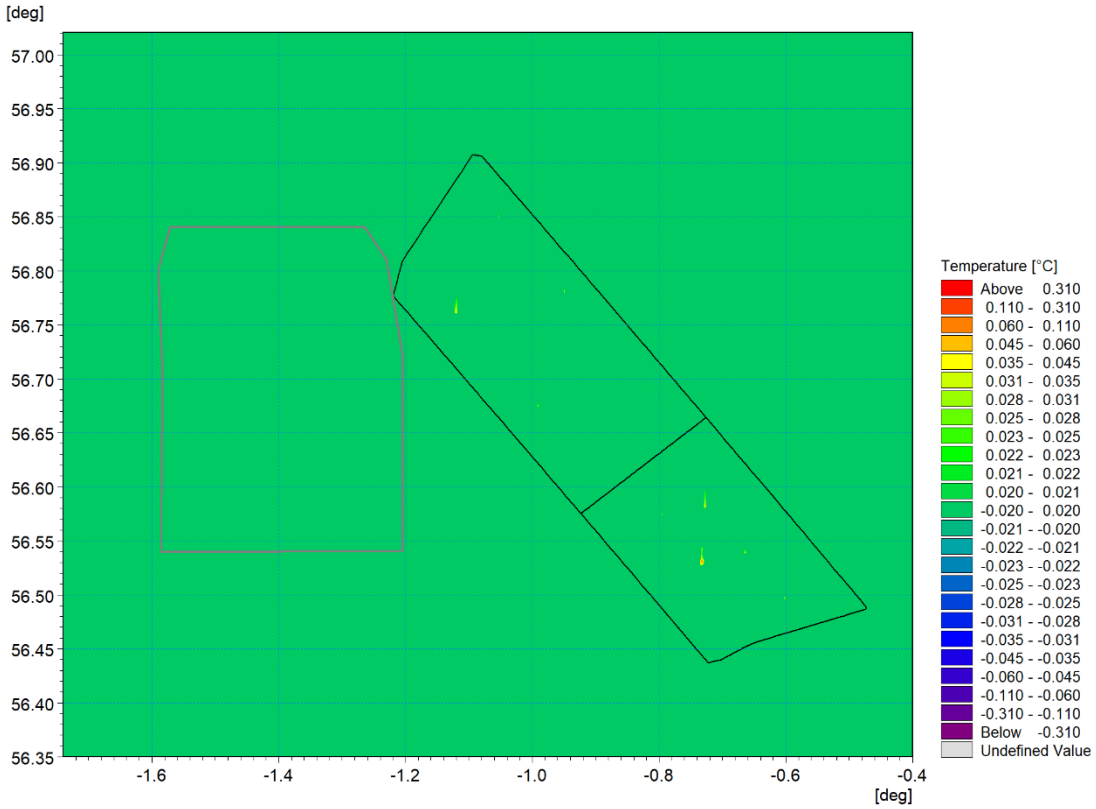

Figure 5.101: Change in temperature at peak stratification – Day 17 ebb tide (post-construction Morven North and Morven South minus baseline) – Layer 9

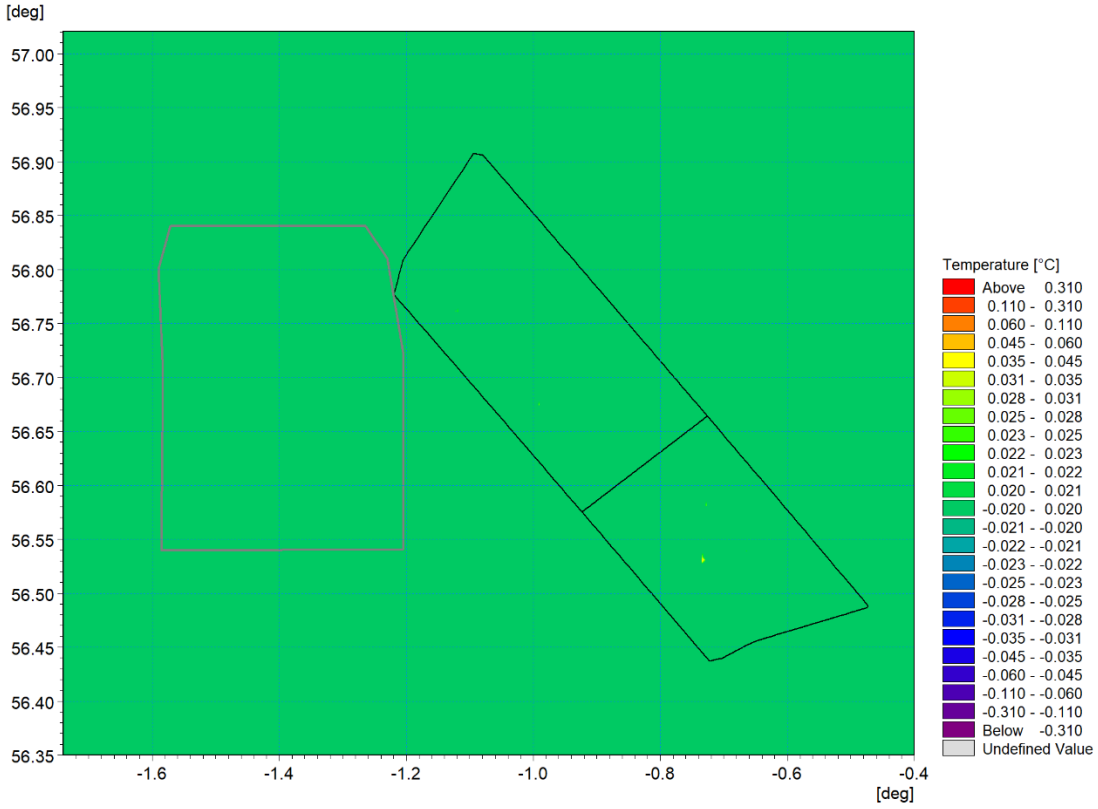

Figure 5.102: Change in temperature at peak stratification – Day 17 ebb tide (post-construction Morven North and Morven South minus baseline) – Layer 8

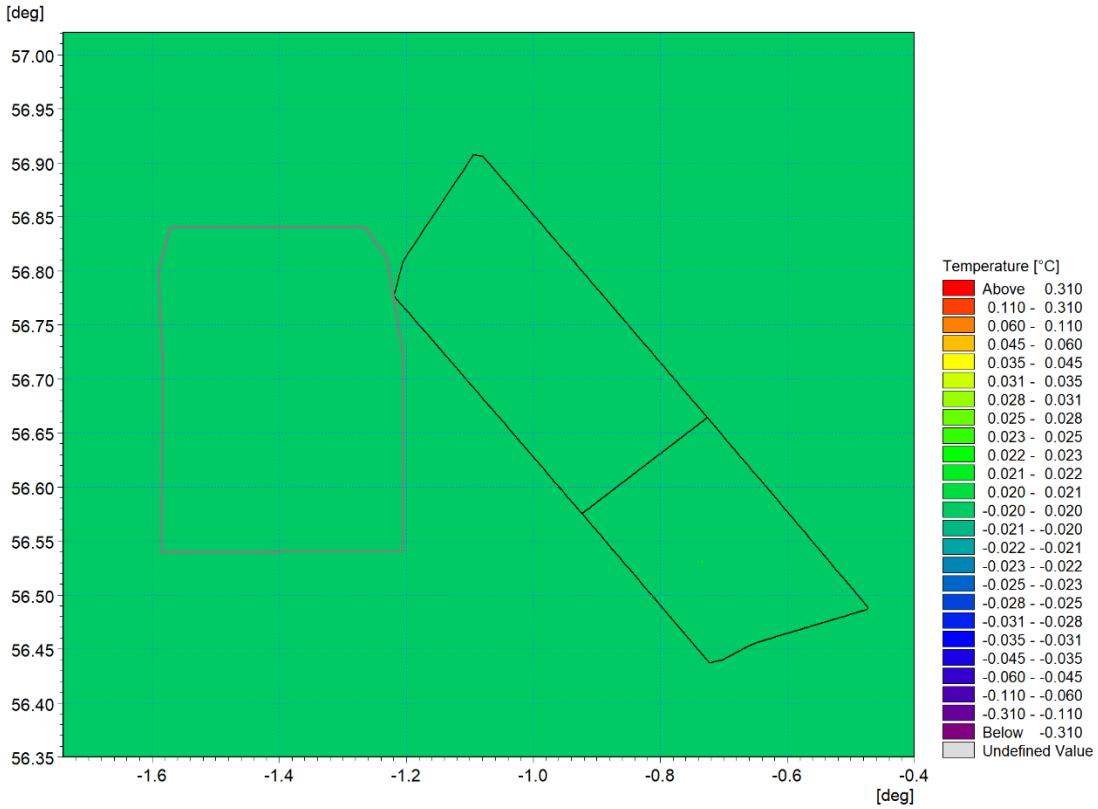

Figure 5.103: Change in temperature at peak stratification – Day 17 ebb tide (post-construction Morven North and Morven South minus baseline) – Layer 7

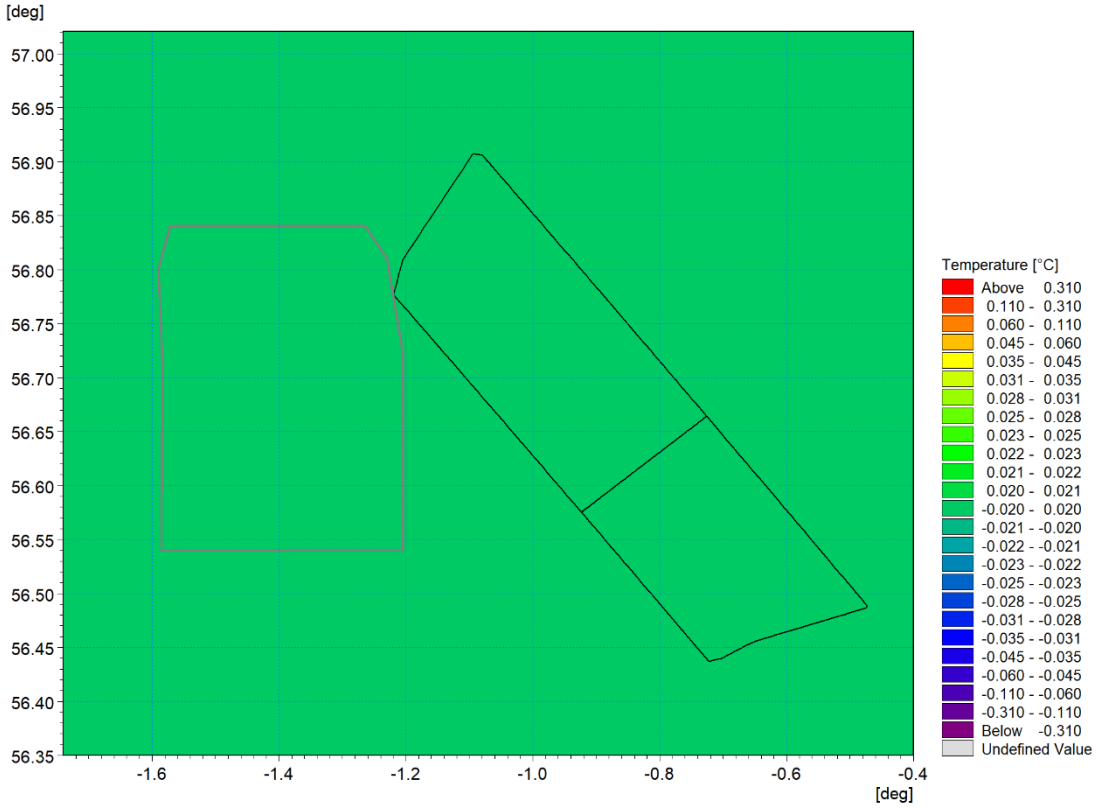

Figure 5.104: Change in temperature at peak stratification – Day 17 ebb tide (post-construction Morven North and Morven South minus baseline) – Layer 6

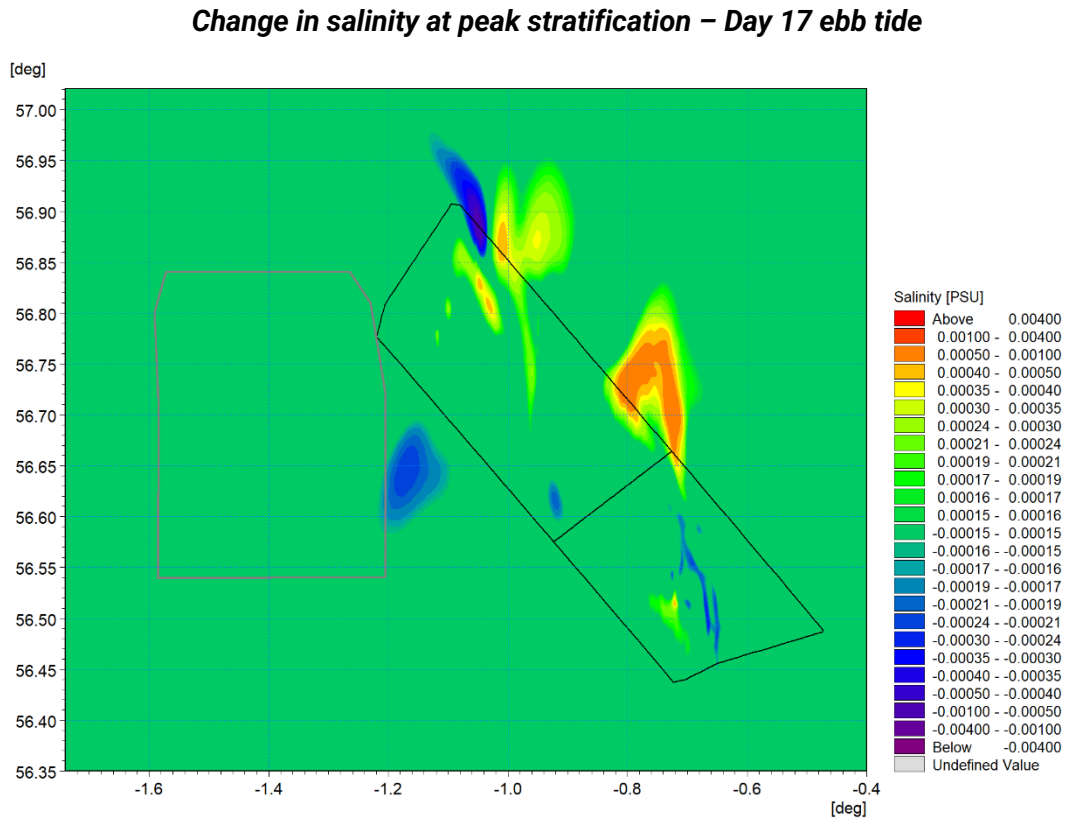

Figure 5.105: Change in salinity at peak stratification – Day 17 ebb tide (post-construction Morven North and Morven South minus baseline) – Layer 20

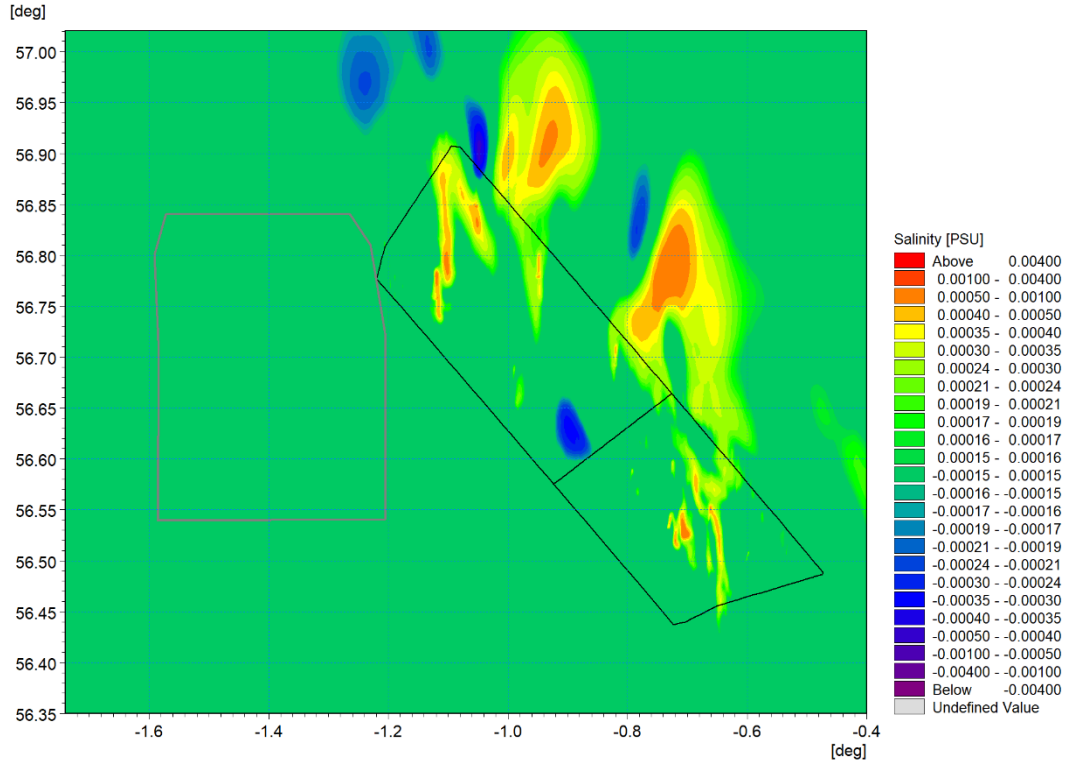

Figure 5.106: Change in salinity at peak stratification – Day 17 ebb tide (post-construction Morven North and Morven South minus baseline) – Layer 19

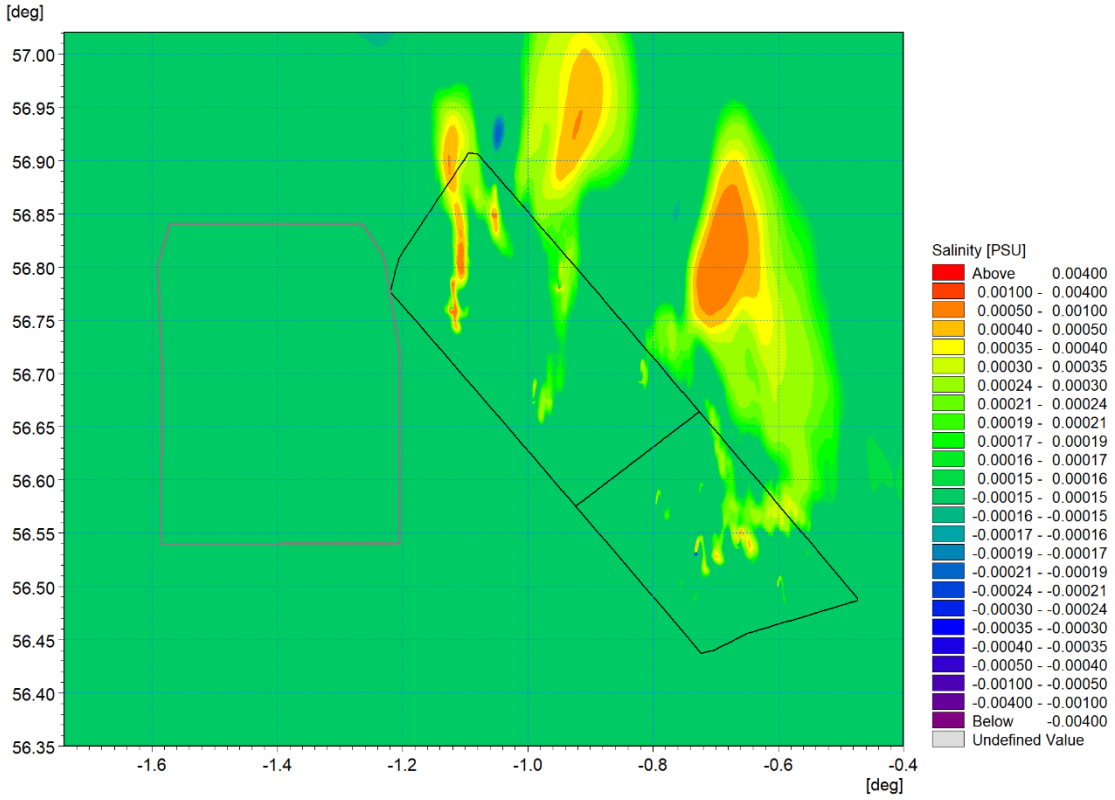

Figure 5.107: Change in salinity at peak stratification – Day 17 ebb tide (post-construction Morven North and Morven South minus baseline) – Layer 18

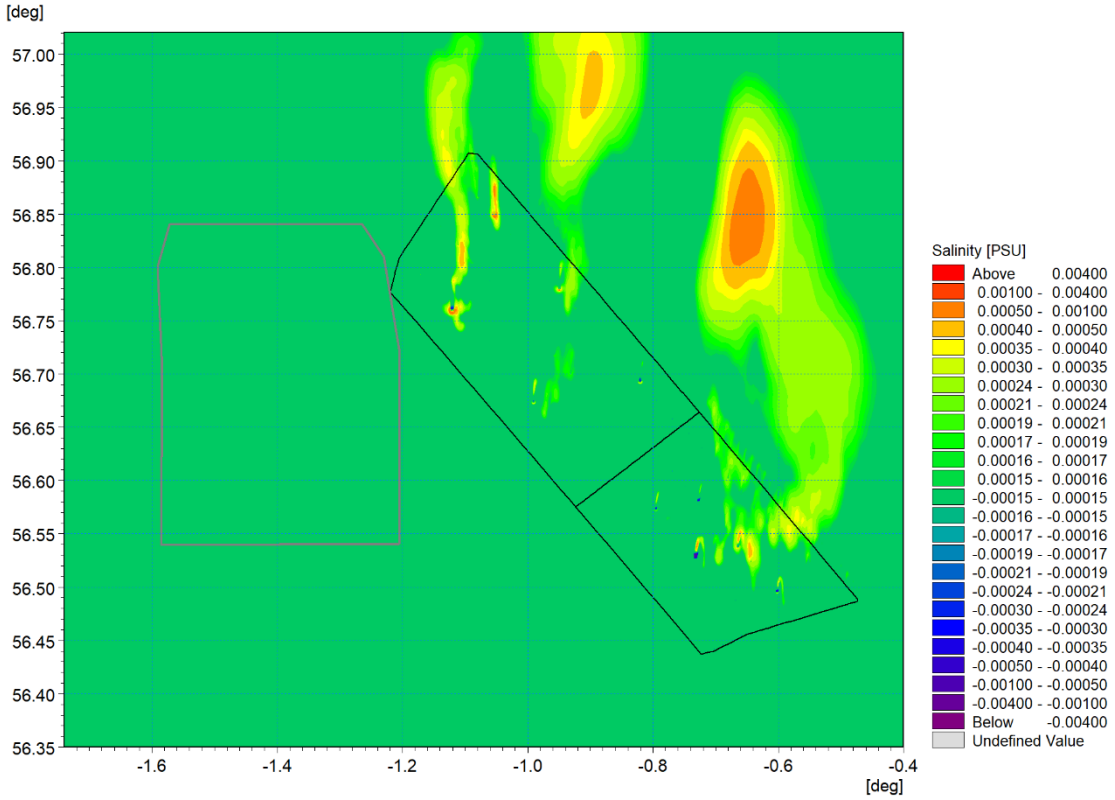

Figure 5.108: Change in salinity at peak stratification – Day 17 ebb tide (post-construction Morven North and Morven South minus baseline) – Layer 17

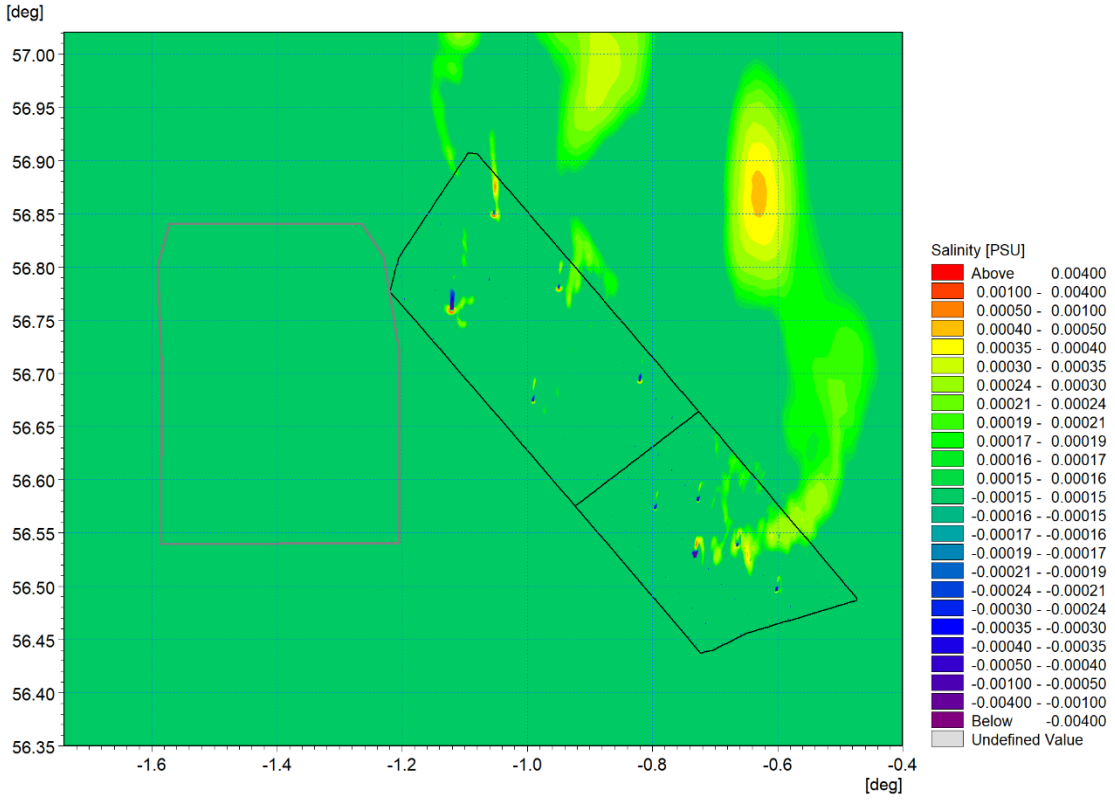

Figure 5.109: Change in salinity at peak stratification – Day 17 ebb tide (post-construction Morven North and Morven South minus baseline) – Layer 16

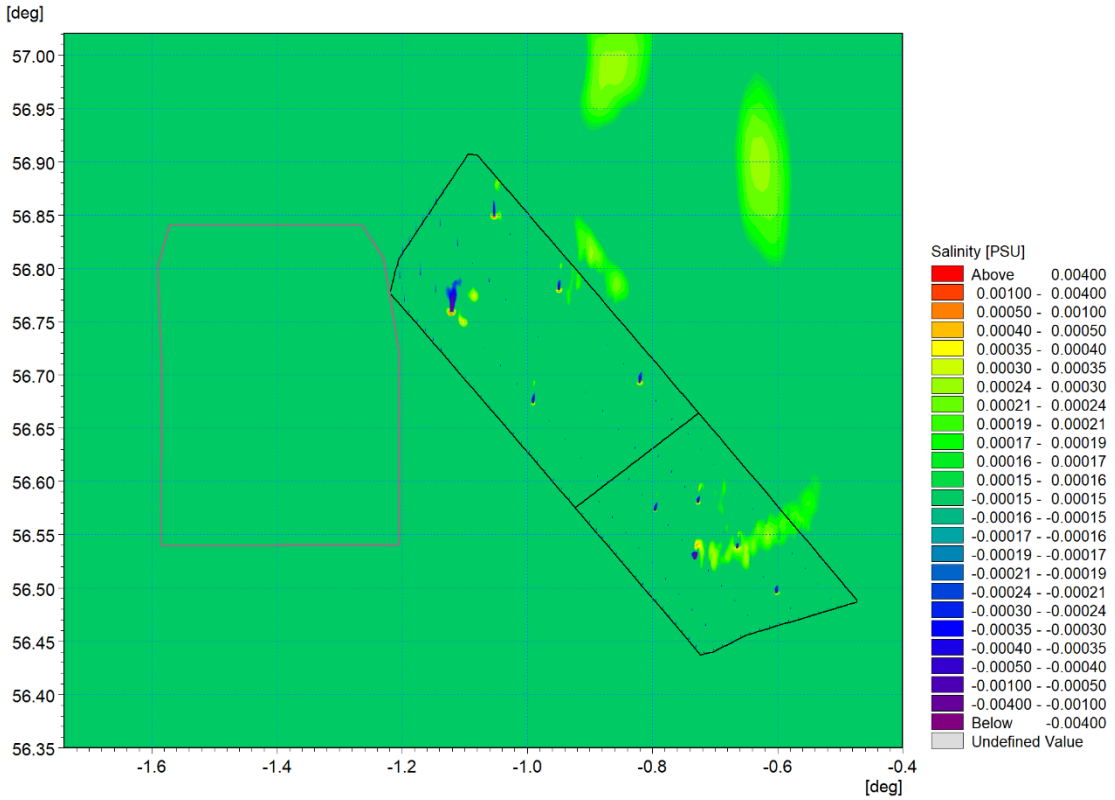

Figure 5.110: Change in salinity at peak stratification – Day 17 ebb tide (post-construction Morven North and Morven South minus baseline) – Layer 15

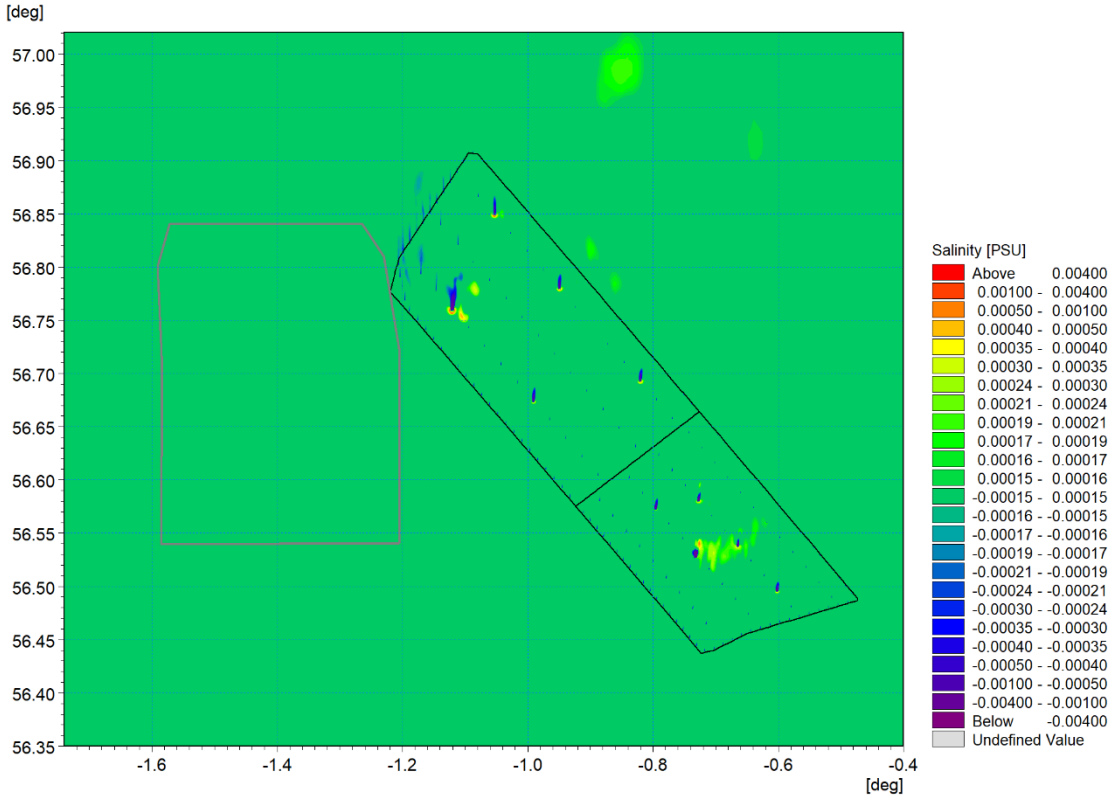

Figure 5.111: Change in salinity at peak stratification – Day 17 ebb tide (post-construction Morven North and Morven South minus baseline) – Layer 14

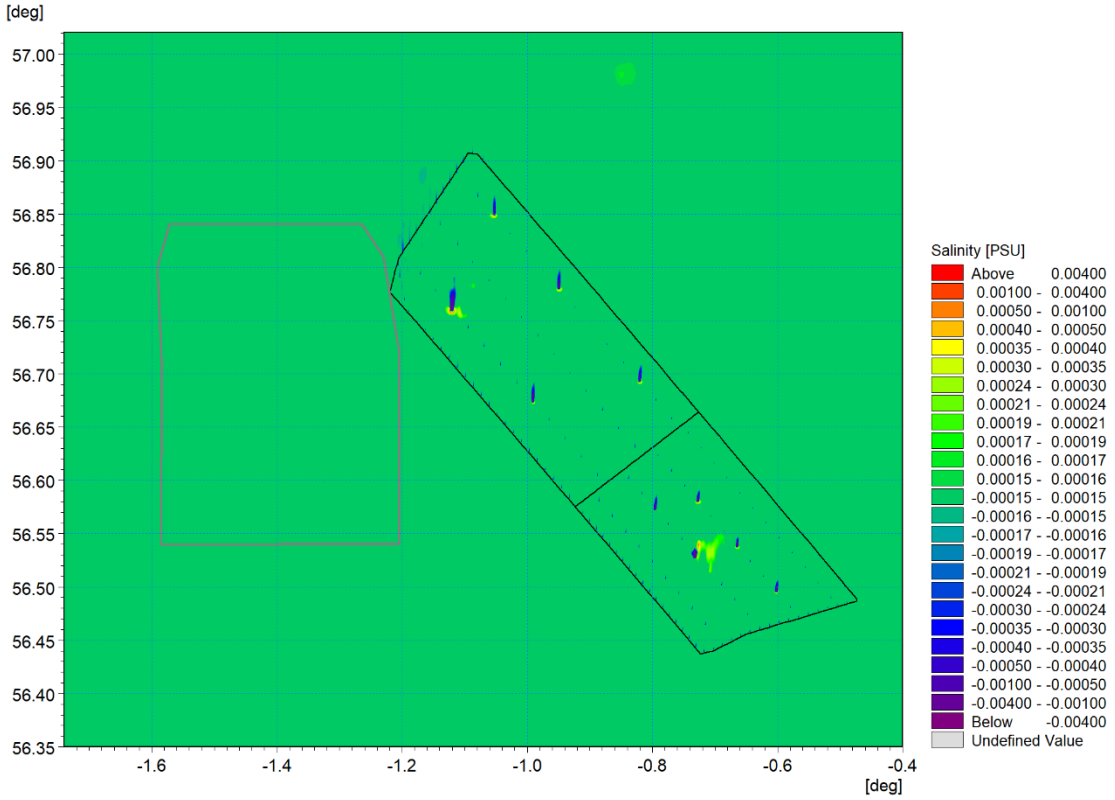

Figure 5.112: Change in salinity at peak stratification – Day 17 ebb tide (post-construction Morven North and Morven South minus baseline) – Layer 13

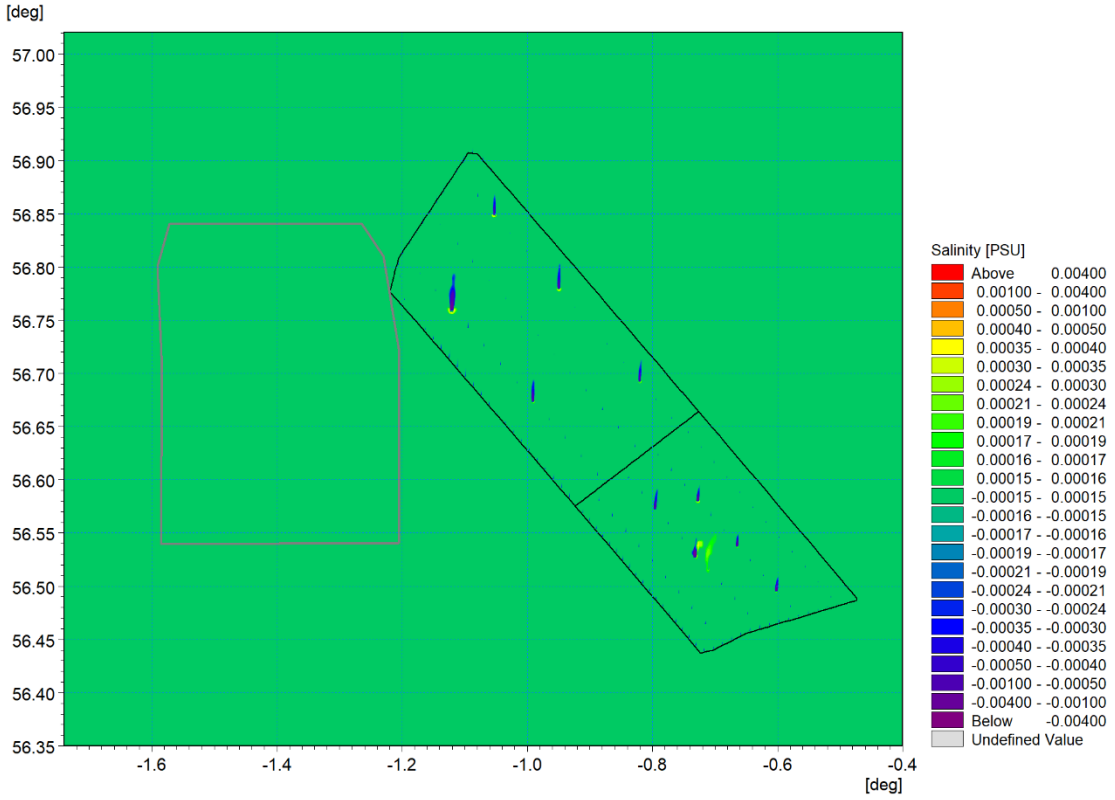

Figure 5.113: Change in salinity at peak stratification – Day 17 ebb tide (post-construction Morven North and Morven South minus baseline) – Layer 12

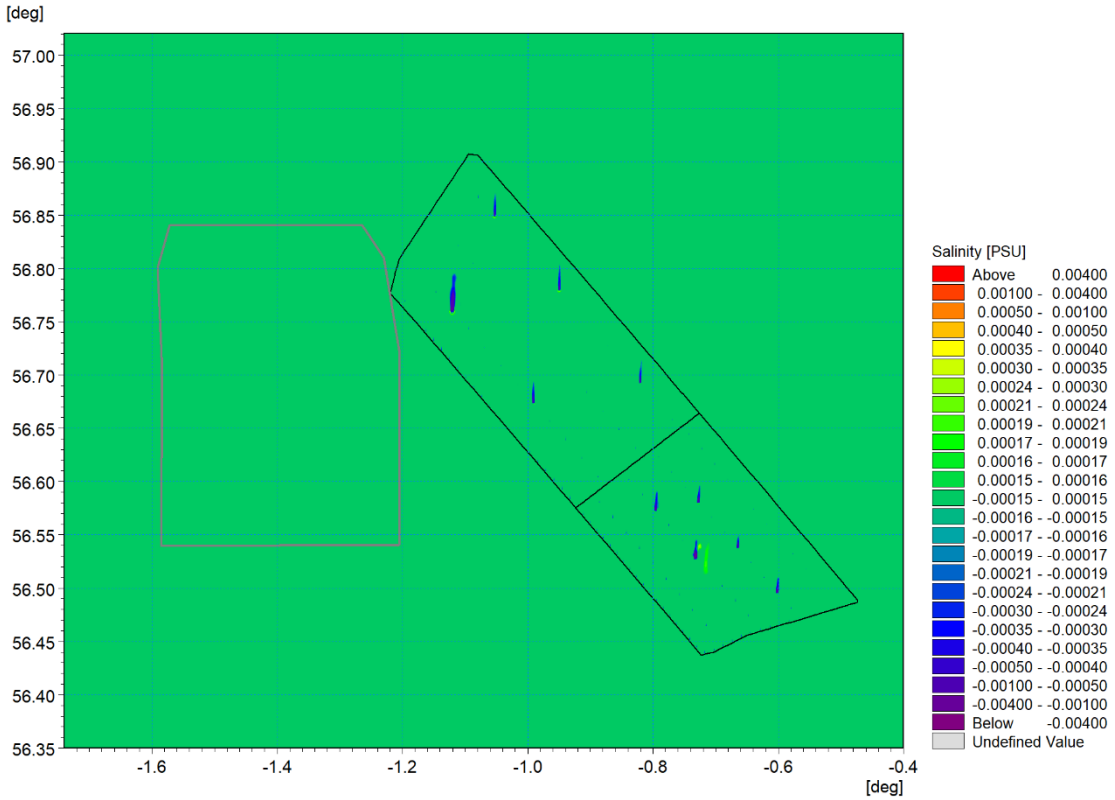

Figure 5.114: Change in salinity at peak stratification – Day 17 ebb tide (post-construction Morven North and Morven South minus baseline) – Layer 11

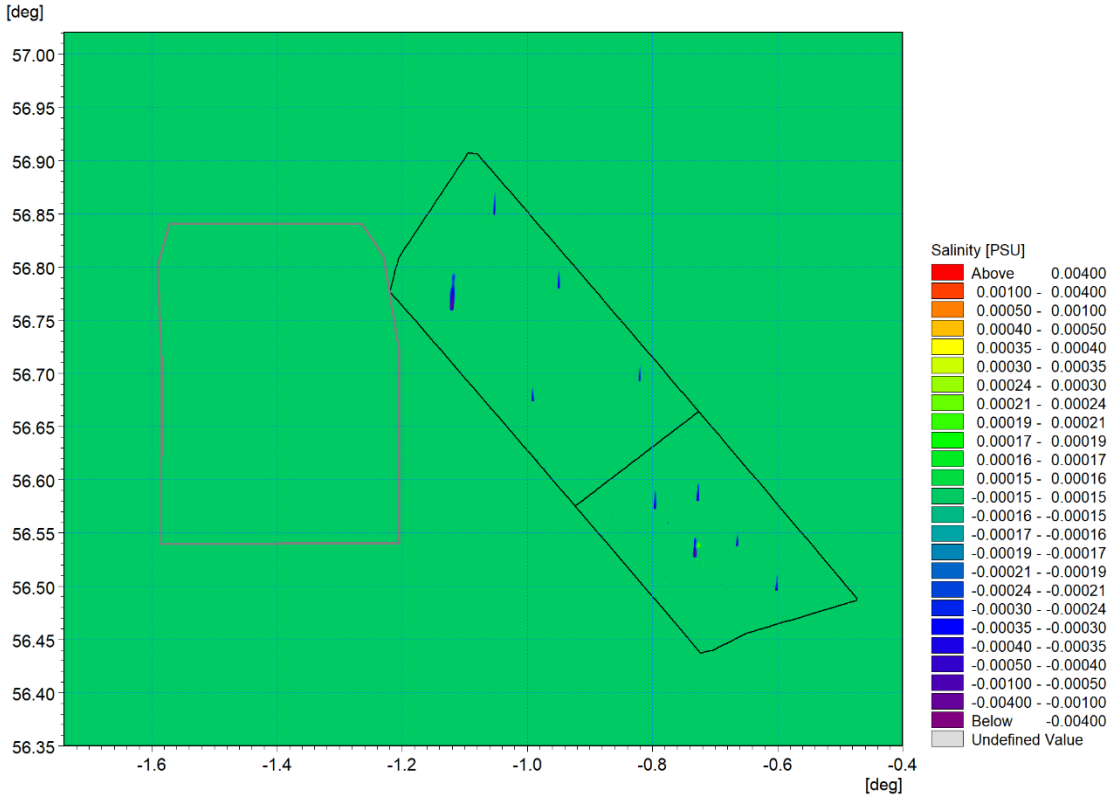

Figure 5.115: Change in salinity at peak stratification – Day 17 ebb tide (post-construction Morven North and Morven South minus baseline) – Layer 10

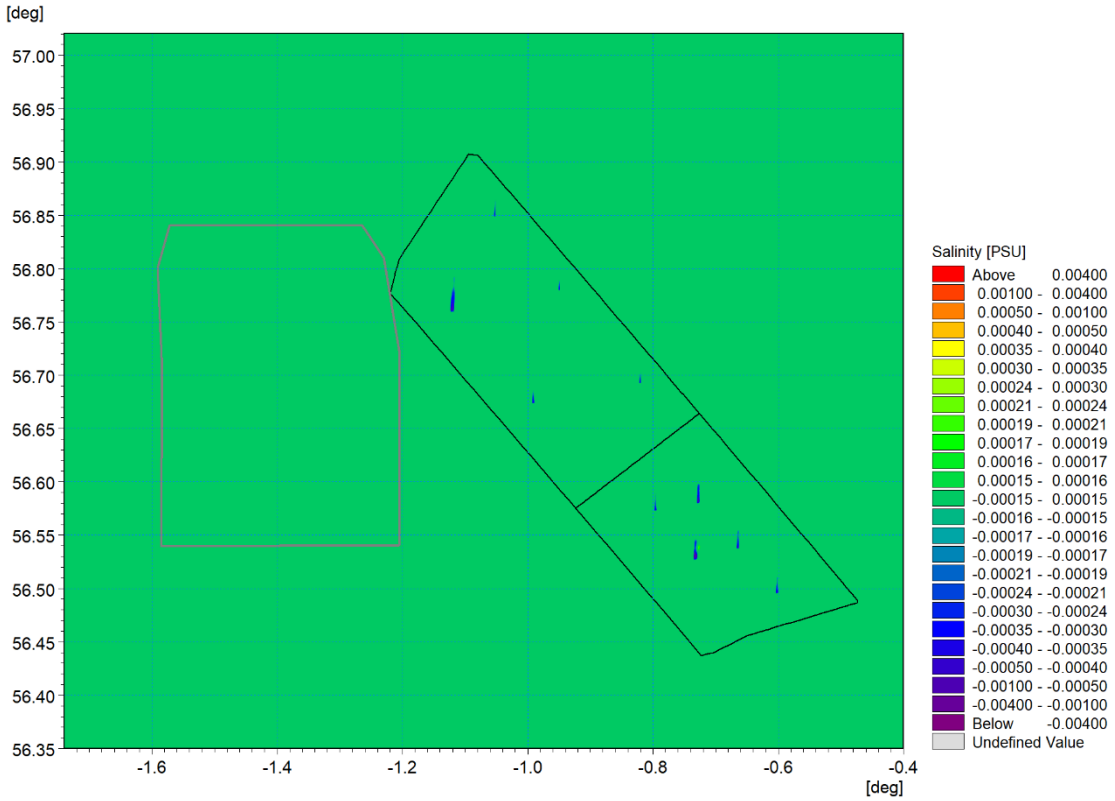

Figure 5.116: Change in salinity at peak stratification – Day 17 ebb tide (post-construction Morven North and Morven South minus baseline) – Layer 9

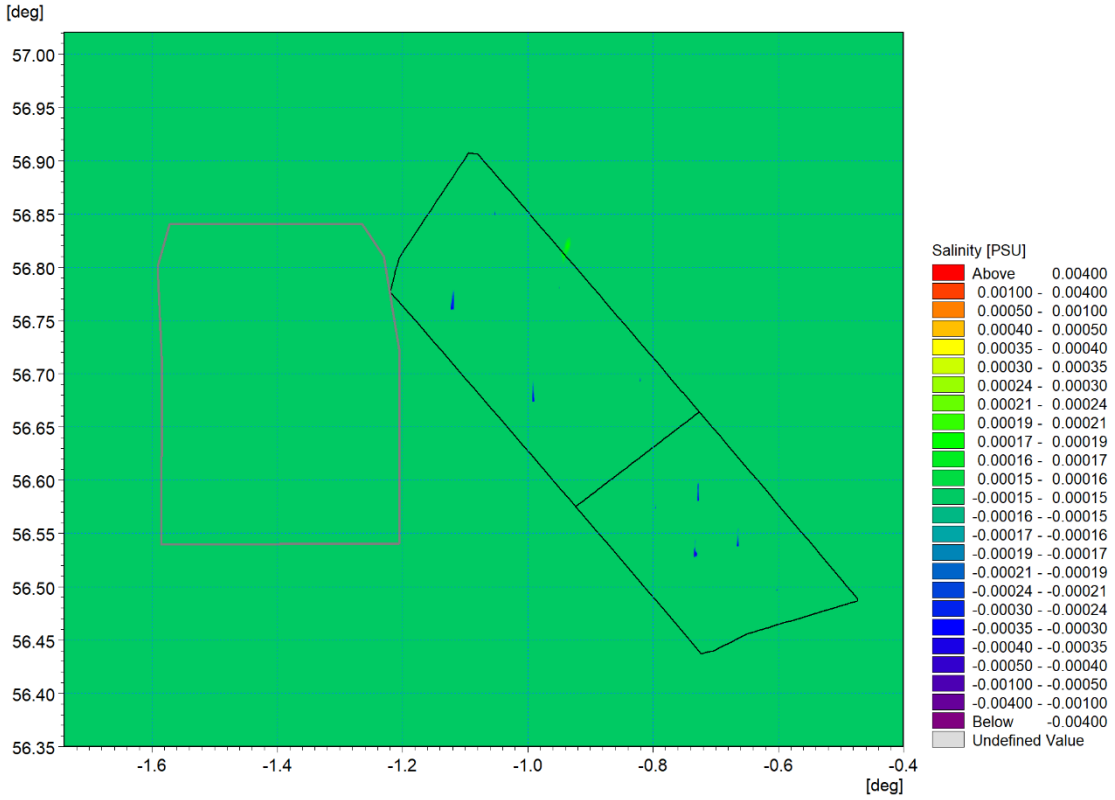

Figure 5.117: Change in salinity at peak stratification – Day 17 ebb tide (post-construction Morven North and Morven South minus baseline) – Layer 8

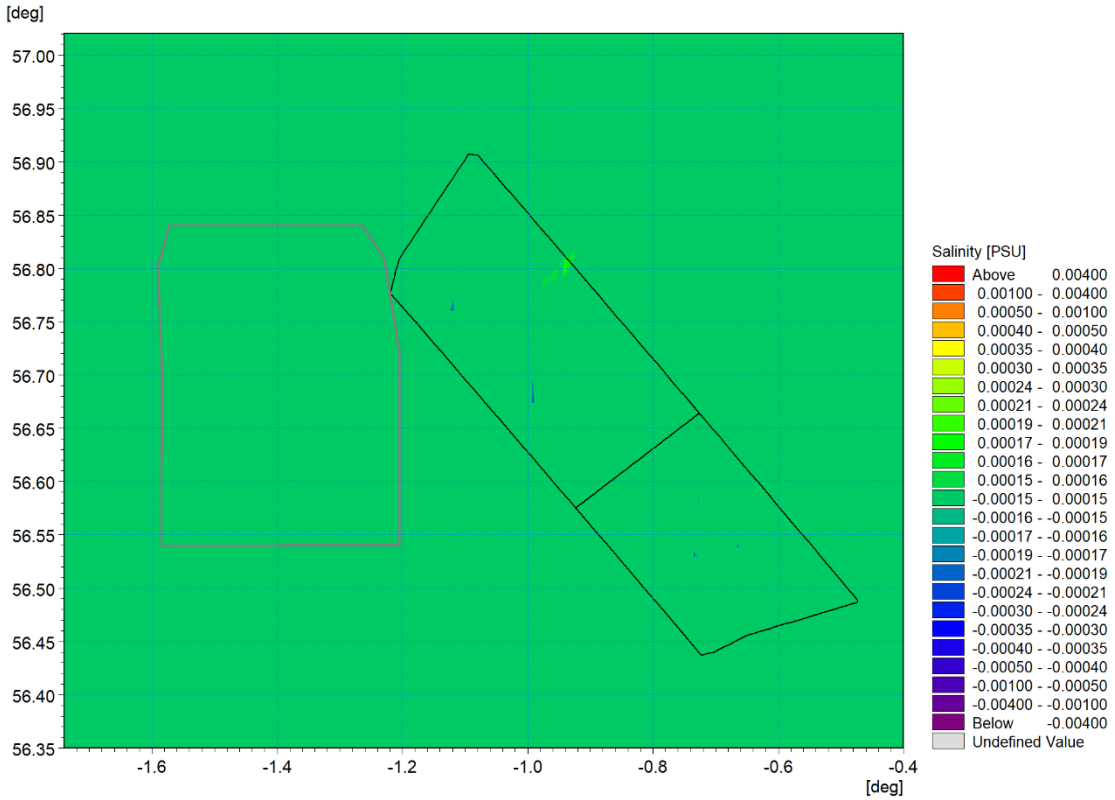

Figure 5.118: Change in salinity at peak stratification – Day 17 ebb tide (post-construction Morven North and Morven South minus baseline) – Layer 7

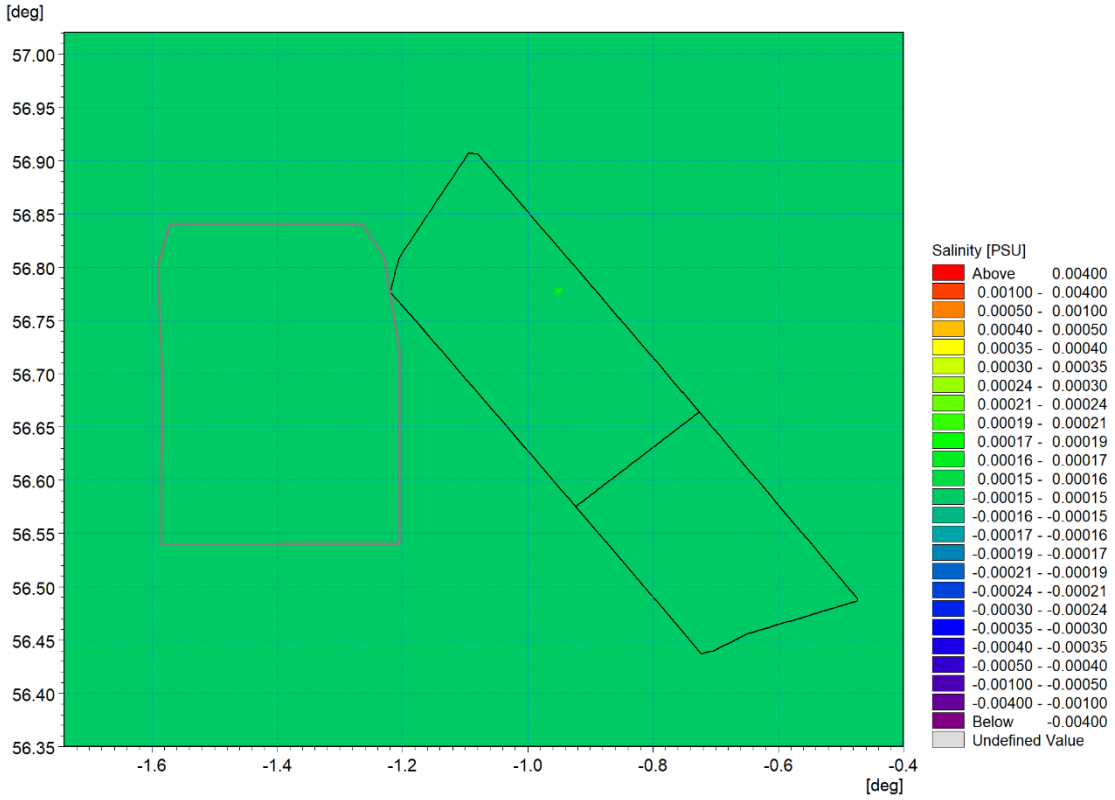

Figure 5.119: Change in salinity at peak stratification – Day 17 ebb tide (post-construction Morven North and Morven South minus baseline) – Layer 6

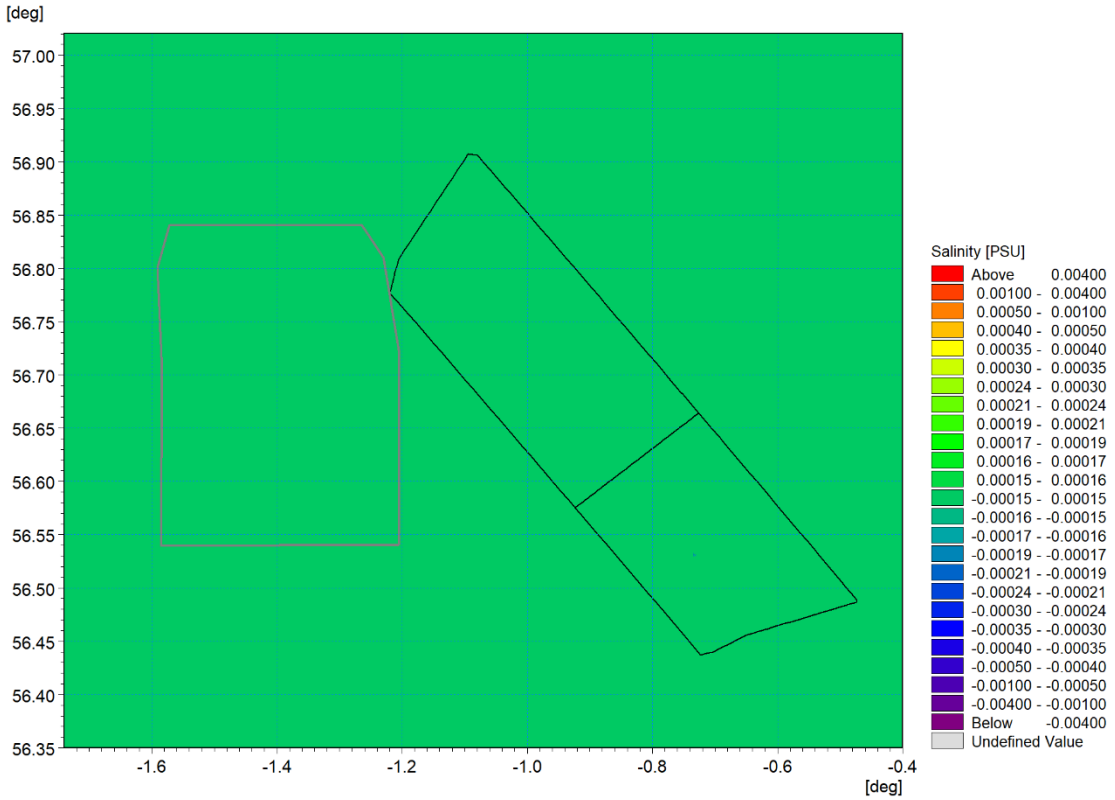

Figure 5.120: Change in salinity at peak stratification – Day 17 ebb tide (post-construction Morven North and Morven South minus baseline) – Layer 5

Morven North and Morven South discussion

5.2.4.15 As shown by the plots in Figure 5.49 to Figure 5.58, there is a perceived difference in temperature in surface layers due to Morven North and Morven South at the onset of stratification. These figures allow the effects of individual structures to be more clearly observed towards the commencement of the simulations, whereas Figure 5.59 to Figure 5.72 show the temperature difference after a spring neap cycle when more time has been allowed for mixing processes to occur. At the early stage of the simulation, it can be seen that the largest temperature differences can be attributed to the OSP structures due to the size of the obstruction within the water column. The surface layer presents a small decrease in temperatures due to the infrastructure, however below the surface layer, at layer 19 (circa 3.4m to 6.7m at point N6), this is largely countered by a small increase in temperatures, as the warmer surface temperatures are seen to disperse through the water column. The increased temperatures are generally seen to persist through the layers to a depth of circa 26.8m at point N6, showing that mixing is evident just below the thermocline presented in Figure 5.45, but does not persist through the remainder of the water column to the seabed. Fundamentally, it is noted that although the anticipated pattern of mixing is evident in the model simulations, results show that the values are very small, with changes in temperatures due to the infrastructure less than 0.005°C. Baseline temperatures were observed in the SSW-RS dataset as 7.27°C to 7.41°C, of which this is less than 0.07%.

5.2.4.16 Figure 5.59 to Figure 5.72 show a similar reduction in surface waters following a spring neap cycle, with temperature difference up to 0.016°C, showing that the impact on seasonal stratification increases with time. However, once again, these differences are minimal at less than 0.22% of baseline values. Changes are not seen to penetrate throughout the water column, thus there is evidence of stratification remaining in the water column at the end of this period, and thus the infrastructure is not seen to delay the onset of stratification but only cause minimal differences to approximately the upper half of the water column.

5.2.4.17 As noted in paragraph 0, temperature is the dominant and most critical factor of the stratification within the Morven Site, however for completeness, Figure 5.73 to Figure 5.78 provide insight into the changes in salinity due to Morven North and Morven South after a spring neap cycle. A reduction in salinity values is seen to occur in the surface layer, which is countered by an increase in salinity through the water column. Changes are not seen to extend beyond circa 13.4m depth at point N6. The maximum change observed is negligible at 0.00084PSU, which is 0.0024% of the background range at point N6 of 34.876PSU to 34.880PSU.

5.2.4.18 During peak stratification, there is a more notable change in temperature due to Morven North and Morven South than during the onset of stratification, as shown in Figure 5.79 to Figure 5.89 at day four and Figure 5.90 to Figure 5.104 at the end of a spring neap cycle. Temperature changes reach up to 0.3°C during peak stratification, which is less than 2.7% of the baseline values at point N6 (11.16°C to 14.99°C). At day four, there is a reduction in surface temperatures observed within the results of the modelling, which transitions to a dominance of temperature increases by layer 16 (16.8m depth at point N6 and coinciding with the thermocline). The temperature increases are seen to gradually reduce down to a depth of circa 33.5m at point N6, within the cooler sub-thermocline layer.

5.2.4.19 A similar pattern is observed following a spring neap cycle, with temperature changes again reaching up to 0.3°C, however more widescale horizontal disruption is seen to occur within the surface layers. Nonetheless, the changes of this magnitude remain within the Regional Physical Processes Study Area. Following the spring neap period, the changes are seen to penetrate deeper within the water column compared to day four, reaching circa 43.6m at point N6. Note that the difference in background warmer surface waters and the cooler waters below the thermocline is circa 3.83°C at N6 at this point in time, as assumed in the modelling. A change in temperature due to Morven North and Morven South of 0.3°C, is significantly less than the background temperature difference between the stratified layers, and thus a potential change of this magnitude would not breakdown stratification by allowing the water column to become fully mixed. The position of the thermocline is also unlikely to be significantly impacted, as seen by the dominance of temperature decreases within the thermocline and above, and temperature increases below the thermocline. This is further evidenced by the sample post-construction vertical slice plot in Figure 5.121 taken at one of the

areas seen to be subject to greatest change, to the north of the bridge-linked HVDC converter OSP gravity base foundations within the Morven South Boundary. This vertical slice extends approximately 290m to the north of the structure. The strong presence of the thermocline can be seen at circa 10m to 20m depth, where the contours are closer together due to the rapid change of temperature. The equivalent plot has been provided for the baseline scenario in Figure 5.122, which presents a very similar profile.

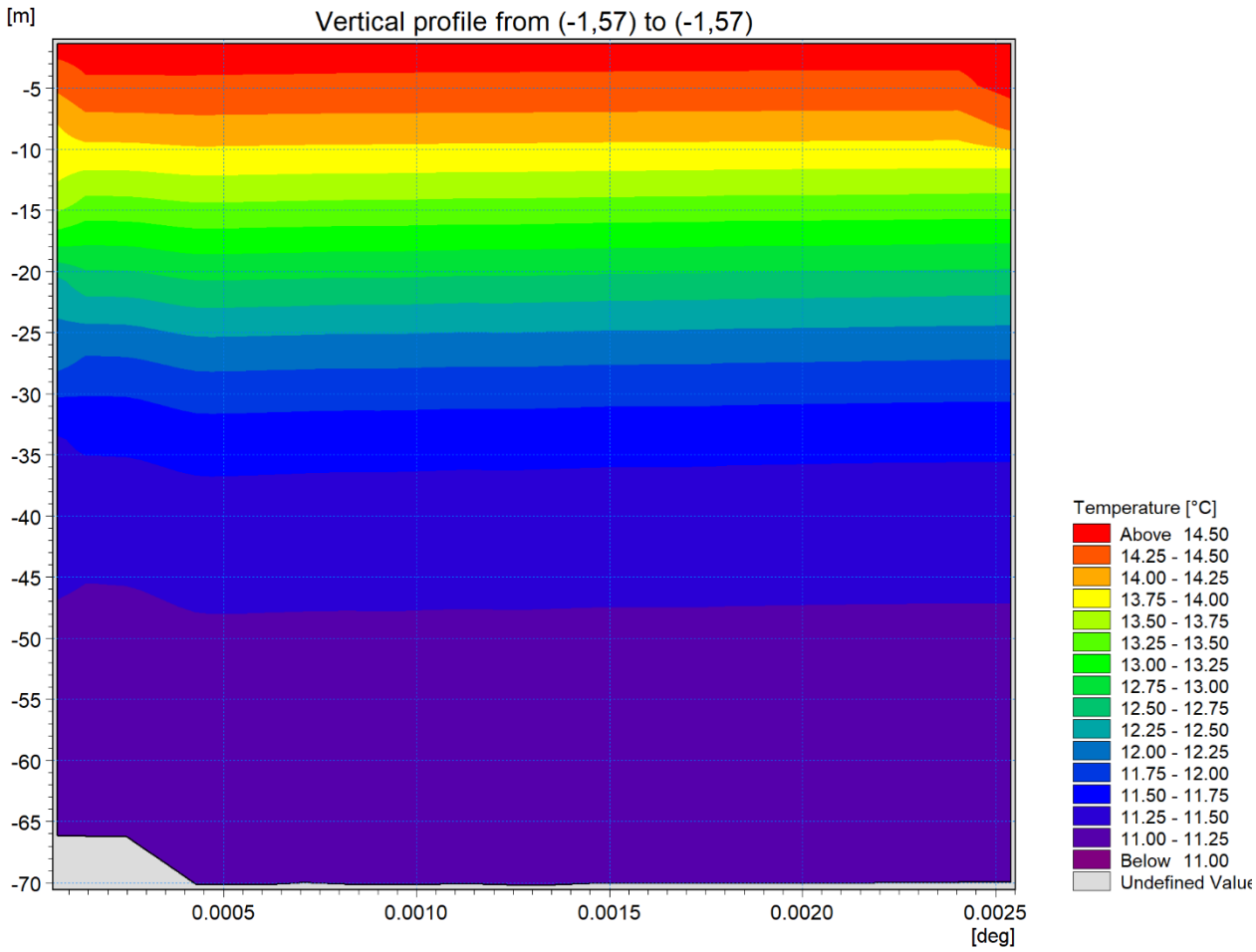

Figure 5.121: Vertical slice to the north of Morven South High Voltage Direct Current converter Offshore Substation Platform foundations – post-construction during peak stratification period, following spring neap cycle

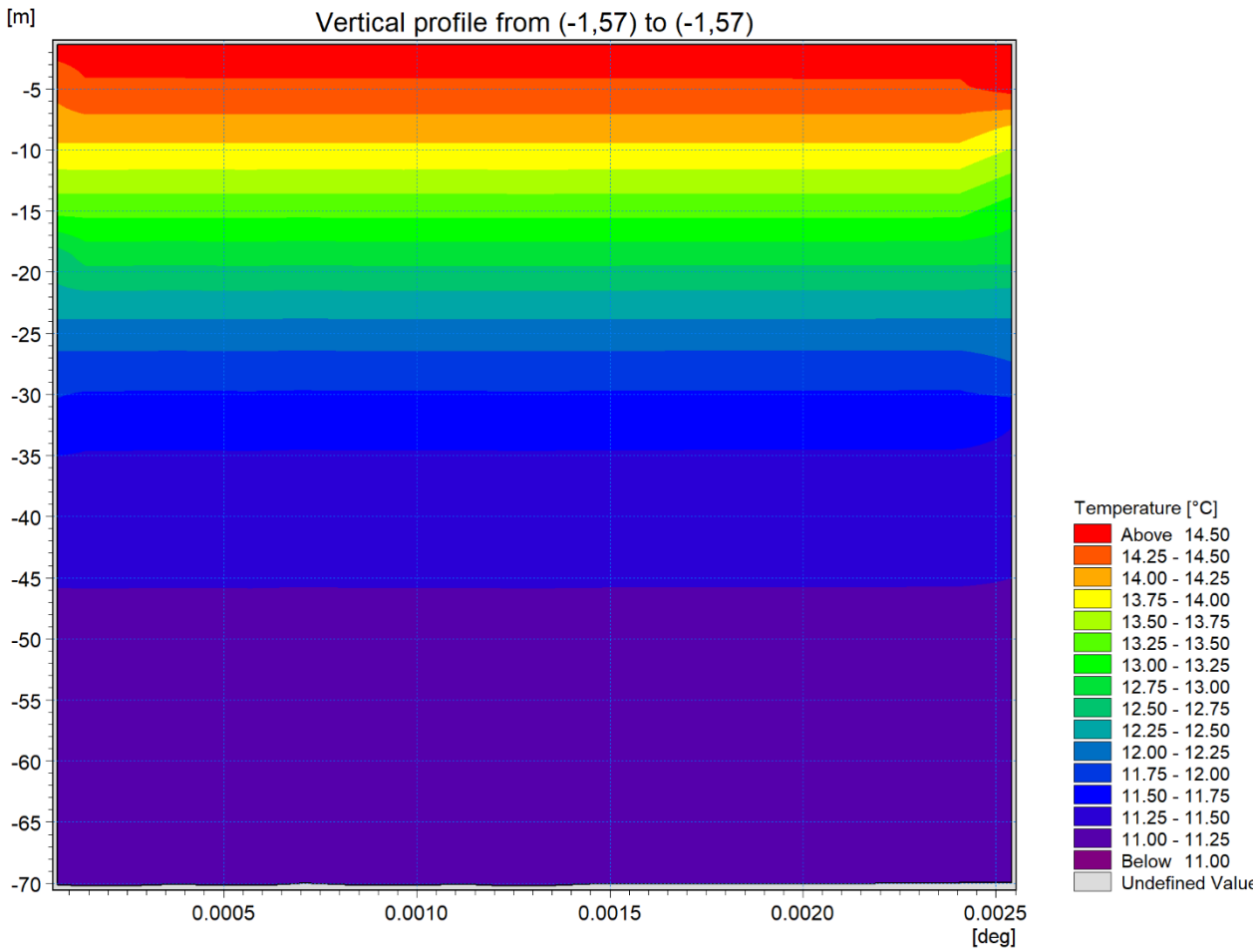

Figure 5.122: Vertical slice to the north of Morven South High Voltage Direct Current Offshore Substation Platform foundations – baseline during peak stratification period, following spring neap cycle

5.2.4.20 Finally, in Figure 5.105 to Figure 5.120, increases in salinity are predominantly seen to occur in the upper layers, decreasing with depth, with a maximum change of 0.003PSU observed in the results, which is not expected to disrupt the halocline. The baseline salinity range at N6 was 34.762PSU to 34.794PSU and therefore the maximum change equates to 0.0086% of the baseline values, which is negligible.

5.2.4.21 In summary, the high level modelling study on the impact on seasonal stratification due to the presence of Morven North and Morven South has shown that changes have the potential to occur. However, these changes are limited in magnitude, with the largest percentage temperature changes from baseline occurring during the peak summer stratification period when the potential energy anomaly is at its greatest and up to a maximum of 2.7% change. The potential energy anomaly in the peak summer period would require more energy to fully mix the water column, in comparison to the lower energy required to potentially break up stratification at its onset. Note the maximum percentage change in temperature at the onset is 0.22%. It is anticipated that there will be no significant impact on the position of the thermocline or breakdown in seasonal stratification due to the infrastructure, although there may be marginally more mixing within the water column. To provide context to these changes, it is noted that in terms of water column obstruction within the Morven North Boundary which has an area of 510.881km^2, the infrastructure may cover 0.03% of the Morven North Boundary at a maximum. This is calculated using the largest diameters of each of the types of infrastructure within the water column, which results in a maximum area of 0.131km^2 of water column obstruction. Similarly, the 0.130km^2 of water column obstruction within the Morven South Boundary covers 0.04% of the 347.635km^2 area. It is thus anticipated that there will be a negligible

effect on the overall pattern of seasonal stratification within the Regional Physical Processes Study Area due to Morven North and Morven South.

5.2.4.22 It is noted that in addition to the impact to seasonal stratification due to the physical obstruction within the water column, a further impact to stratification may arise due to downstream reductions in the wind field and subsequent effect on waves and tides. Wind turbines operate by converting kinetic energy from the wind into electricity with a generator. This process results in less kinetic energy in the atmosphere and a localised reduction in wind speed behind the wind turbine rotor. This reduction in wind speed is known as a "wake".

5.2.4.23 A recent study funded by the European Union Horizon 2020 project, made use of satellite-borne Synthetic Aperture Radar (SAR) to conclude that this reduction in downstream wind speeds was in the region of 2% to 10% at 10m above MSL with average wakes persisting for 20km to 40km (Owda and Badger, 2022). This study was based upon offshore wind farms or clusters of offshore wind farms with between 80 and 240 wind turbines in operation (Owda and Badger, 2022). A further study using SAR on two large offshore wind farms (circa 80 wind turbines) showed a decrease in wind speed in the lee of the wind turbines, with a velocity deficit of 8% to 9% immediately downstream of the wind turbines, recovering to within 2% over a distance of 5km to 20km (Christiansen and Hasager, 2005). This was validated using results from wake modelling and in situ measurements (Christiansen and Hasager, 2005).

5.2.4.24 As would be expected, these wakes vary in both intensity and dimensions, and are highly dependent on a variety of project and location-specific factors, such as ambient wind speed, wind turbine size and layout (i.e. direction and spacing) of the wind turbine array (Barthelmie *et al*. 2010). Typically, reductions in wind speed increase with the number of wind turbines within an offshore wind farm up to a certain threshold (Christiansen and Hasager, 2005) and wakes will persist further in more stable atmospheric conditions (Platis *et al*., 2018). In the majority of weather situations, where unstable conditions are present, wind turbine wakes are typically localised within the offshore wind farm (Platis *et al*., 2018). This is due to the atmospheric turbulence aiding the recovery of the wake from vertical layers (Platis *et al*., 2018).

5.2.4.25 The MDS for stratification included up to 96 wind turbines within the Morven North Boundary and 95 wind turbines within the Morven South Boundary, with hub height at 168m above LAT and a maximum rotor diameter of 250m. It is assumed for the purposes of this assessment that there could be a reduction in downstream wind speeds by up to 10% at 10m above MSL due to the large number of wind turbines within the MDS, however designed-in measures such as wind turbine spacing will in reality likely yield a lesser reduction at this altitude. Furthermore, the percentage reduction in wind speed will reduce further at the water surface. Wake distances are anticipated to extend beyond the Morven North and Morven South Boundaries due to the offshore location and stable atmospheric conditions, however, as outlined in paragraph 5.2.4.23, wake effects beyond 5km to 20km are considered to be very limited. This is even more applicable at the sea surface, where the effect of turbulence is greater.

5.2.4.26 Assuming a maximum of circa 10% reduction in wind speeds at 10m above the sea surface, this will be further reduced at the water surface. Studies in the North Sea have shown wind speed reductions at the surface due to these wakes in the order of 0.1m/s to 0.5m/s, depending on a range of factors including but not limited to the season and density of wind turbines (Akhtar *et al*., 2021; Christiansen *et al*., 2022). Christiansen *et al*. (2022) noted that "as a result of constantly changing wind directions, pronounced wake patterns disappear when averaging over time". In context of prevailing physical processes at the site boundary, speed reductions of 0.1m/s to 0.5m/s within the surface layer would be considered to be of low magnitude, particularly given that these patterns would likely disappear when averaging over time owing to naturally varying wind speeds and directions across the Morven North Boundary and Morven South Boundary. Thus, the limited reduction in wind speed due to the presence of the infrastructure is not considered to have the potential to result in a marked effect on waves and currents within the Morven Site, which are predominantly determined from other factors, such as swell (as evidenced from the long period waves in the baseline environment) and the large scale tidal regime.

5.2.4.27 In conclusion, when holistically assessing the potential impact on seasonal stratification, any reduction to stratification due to the presence of Morven North and Morven South within the water

column, may also be countered by any potential increase to stratification caused by a decrease in wind speeds, as the two impacts would likely have opposing, though not equal, effects. Furthermore, any increase in seasonal stratification due to climate change, as evident from a recent Intergovernmental Panel on Climate Change (IPCC) Special Report (Bindoff *et al*., 2019), may counteract the stratification reduction due to water column infrastructure, although it is recognised that there is uncertainty in how these two opposing effects may interact.

5.3 Post-construction sedimentology

5.3.1.1 The numerical modelling methodology for sediment transport was described in Section 4.8, which indicated how the baseline information was discretised to form the basis of the modelled scenarios. For the post-construction scenarios, in addition to the Morven North or Morven South structures being included in the tide and wave models, the bed material map was updated to include the proposed additional scour and cable protection for each of the three post-construction scenarios (Morven North, Morven South and with Morven North and Morven South together). In each case an area of fixed bed was applied overlain with a thin layer of sand to initialise the model and avoid instabilities. The models were then re-run for a spring tide under calm conditions and also for a 1 in 1 year storm from 000°.

5.3.2 Sediment transport under calm conditions

5.3.2.1 There are a number of approaches for quantifying potential sediment transport, given that transport rates vary both across the area and due to tidal state and climate conditions. For this analysis, the residual current was calculated over the course of two tidal cycles (one day) with the Morven North and Morven South structures in place and compared with that for the baseline (Figure 4.75) for the calm condition. The combined Morven North and Morven South post-construction residual current and changes are shown in Figure 5.123 and Figure 5.124 respectively, with Figure 5.125 and Figure 5.126 showing the changes due to Morven North and Morven South independently. The change in residual currents were seen to be represented by an increase in the immediate vicinity of the structures, in addition to localised decreases.

5.3.2.2 The corresponding sediment transport was simulated over the course of one day where the equivalent baseline daily sediment transport rate was shown in Figure 4.80. The Morven North and Morven South post-construction daily sediment transport rates are shown in Figure 5.127, with Figure 5.128, Figure 5.129 and Figure 5.130 showing the differences from baseline for the combined Morven North and Morven South infrastructure, the Morven North infrastructure and the Morven South infrastructure respectively.

5.3.2.3 It should be noted that both the sediment transport and difference plots use a log scale as there is a large range in sediment transport potential across the domain and even so the changes in sediment transport rates are very small.

Morven North

5.3.2.4 The change in sediment transport due to the infrastructure over the course of a day is a maximum of 0.13m^3/m within the Morven North Boundary. The sediment load was seen to increase immediately in the vicinity of the structures and decrease to the northeast of the structures for a distance of circa 5km from the bridge-linked HVDC converter OSP gravity base foundations within the Morven North Boundary. An area of increase was also observed to the southwest of the Morven North structures up to a distance of 3.5km from the same structures. Note these results are representative of the flood tide at the point at which they are extracted, with the dominant flow direction from northwest to southeast.

Morven South

5.3.2.5 The change in sediment transport due to the infrastructure over the course of a day is a maximum of 0.04m^3/m within the Morven South Boundary. This is less than the changes observed within the Morven North Boundary, although the same pattern is observed as outlined in paragraph 5.3.2.4.

Morven North and Morven South

5.3.2.6 There is no discernible difference observed from the modelling results to sediment transport rates under calm conditions due to the combined presence of Morven North and Morven South, in comparison to Morven North and Morven South independently.

5.3.3 Sediment transport under storm conditions

5.3.3.1 The modelling outlined in Section 5.3.2 was repeated for the 1 in 1 year storm. The baseline residual current (Figure 4.79) and daily potential sediment transport (Figure 4.80) were compared with the equivalent Morven North and Morven South post-construction residual current pattern as shown in Figure 5.131; with the difference in Figure 5.132 and Figure 5.133 for Morven North independently and Figure 5.134 for Morven South independently. A similar comparison of the potential sediment transport is shown in Figure 5.135, with differences provided in Figure 5.136, Figure 5.137 and Figure 5.138 for Morven North and Morven South, Morven North or Morven South respectively.

5.3.3.2 This analysis shows that although there are changes as a result of the presence of the Morven North and Morven South structures and associated scour and cable protection, the magnitude is limited in nature and log scales were required to illustrate values.

Morven North

5.3.3.3 As anticipated, in areas of reduced residual current in the lee of Morven North structures the sediment transport rate is also reduced and vice versa. Within the context of this comparative study, the maximum change in residual current and sediment transport occurs during storm conditions within the Morven North Boundary, rather than the calm conditions discussed under Section 5.3.2. The maximum changes in residual current and sediment transport within the Morven North Boundary are largely sited within close proximity to the bridge-linked HVDC OSP gravity base foundations, extending up to 2km elongated in the orientation of principal tidal currents and is not widespread. The remainder of the proposed infrastructure within the Morven North Boundary is observed to have a much smaller impact on residual currents and sediment transport.

5.3.3.4 It is also important to note, that although changes observed within the Morven North Boundary may be large, the baseline sediment transport rates are low (up to circa 0.15m^3/d/m in the vicinity of the Morven North bridge-linked HVDC OSP gravity base foundations). These low rates are therefore sensitive to any change in magnitude, which will result in a large proportional difference. Structures located within the water column will have a direct impact on sediment transport at the location in which they are installed, by acting as a physical barrier to sediment transport in that location, where previously sediment transport was able to take place. Therefore, it is important to contextualise this impact within the wider sediment transport regime. It is noted that areas of reduced residual current and sediment transport are often accompanied by a similar increase in close proximity. This indicates that the residual current and resulting sediment transport paths are adjusted to accommodate the structures rather than transport pathways being cut off and the overall regime being affected.

Morven South

5.3.3.5 Areas of reduced residual current in the lee of Morven South structures the sediment transport rate is also reduced and vice versa. Within the context of this comparative study, the maximum change in residual current and sediment transport occurs during storm conditions within the Morven South Boundary, rather than the calm conditions discussed under Section 5.3.2. The maximum changes in residual current and sediment transport within the Morven South Boundary are attributed to the bridge-linked HVDC converter OSP gravity base foundations, occurring in close proximity, with peak changes extending up to 1.5km elongated in the orientation of principal tidal currents. The remainder of the proposed infrastructure within the Morven South Boundary is observed to have a much smaller impact on residual currents and sediment transport.

5.3.3.6 It is also important to note, that although changes observed within the Morven South Boundary may be large, the impacts must be contextualised within the wider sediment transport regime. With low baseline sediment transport rates (up to circa 0.15m^3/d/m in the vicinity of the Morven South bridge-

linked HVDC converter OSP gravity base foundations) these will be sensitive to any change in magnitude. Due to increases and decreases within the locality, residual current and resulting sediment transport paths are adjusted to accommodate the structures rather than transport pathways being cut off and the overall regime being affected, as further detailed within paragraph 5.3.3.4.

Morven North and Morven South

5.3.3.7 There is no discernible difference observed from the modelling results to sediment transport rates under storm conditions due to the combined presence of Morven North and Morven South, in comparison to Morven North and Morven South independently.

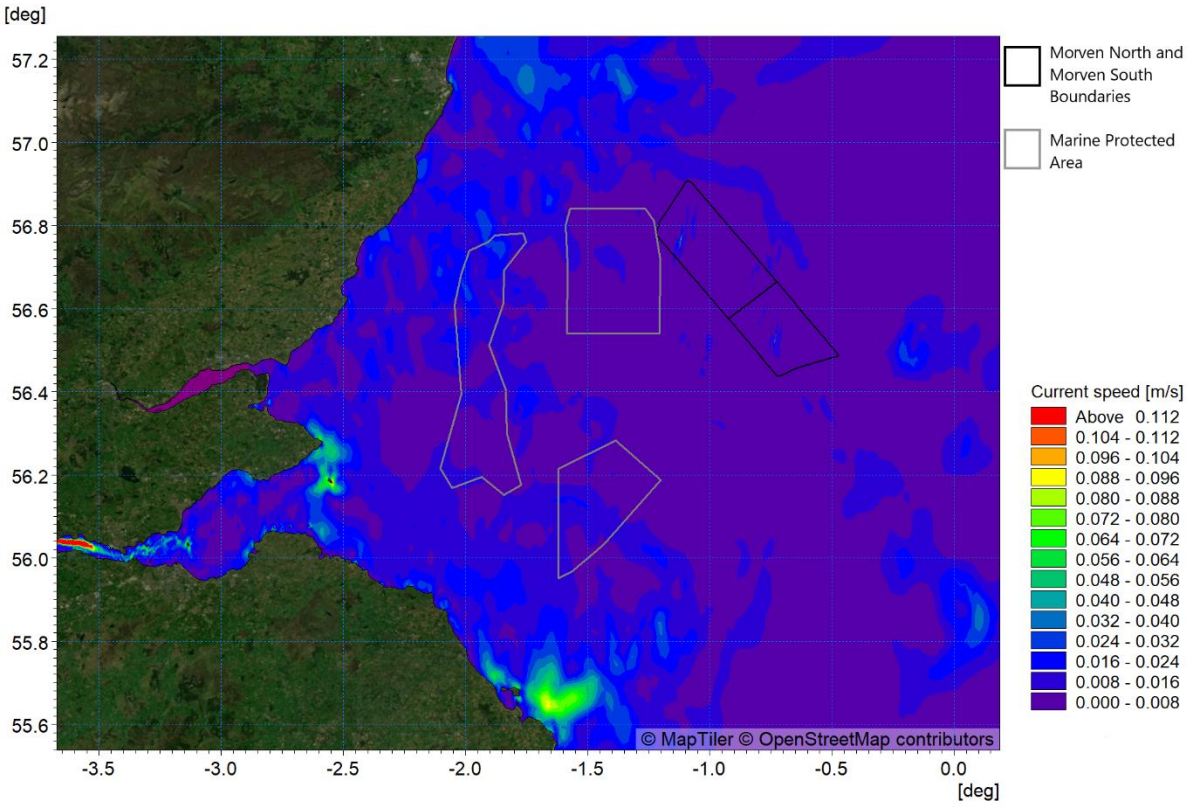

Figure 5.123: Post-construction (Morven North and Morven South) residual current spring tide

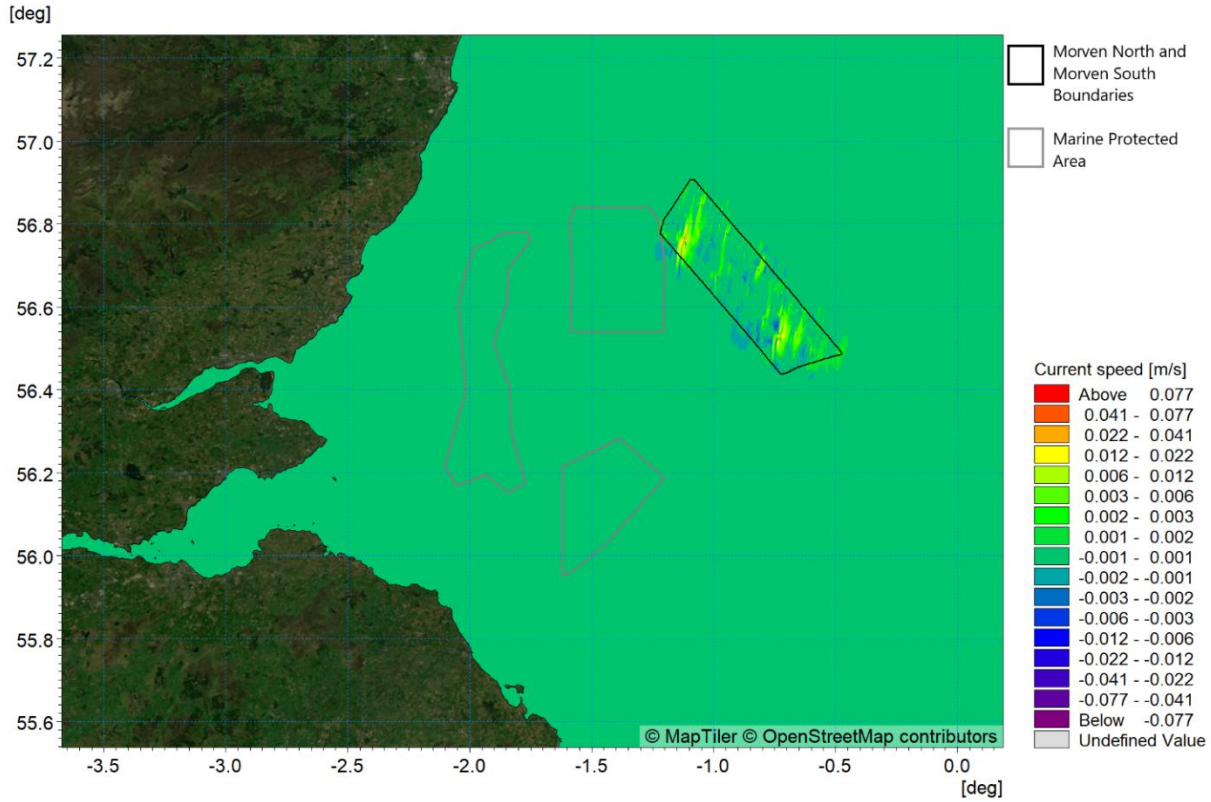

Figure 5.124: Change in residual current spring tide (post-construction Morven North and Morven South minus baseline)

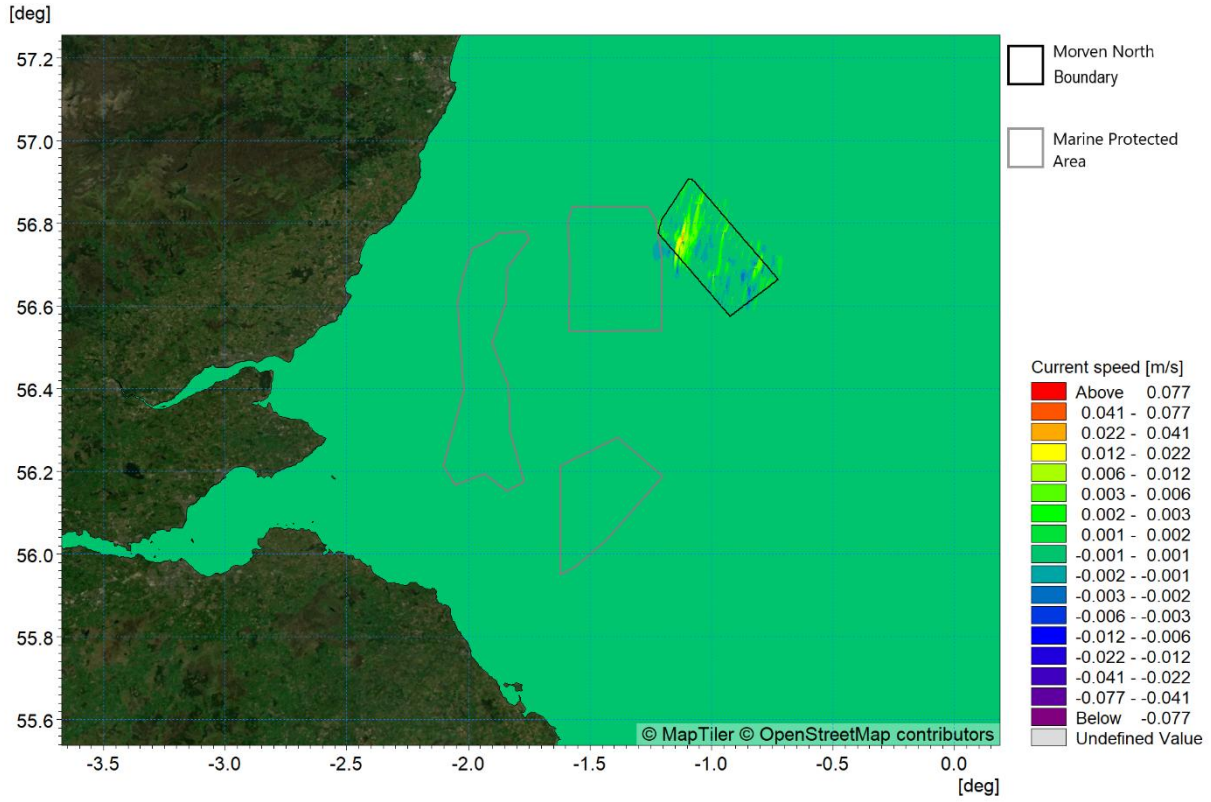

Figure 5.125: Change in residual current spring tide (post-construction Morven North minus baseline)

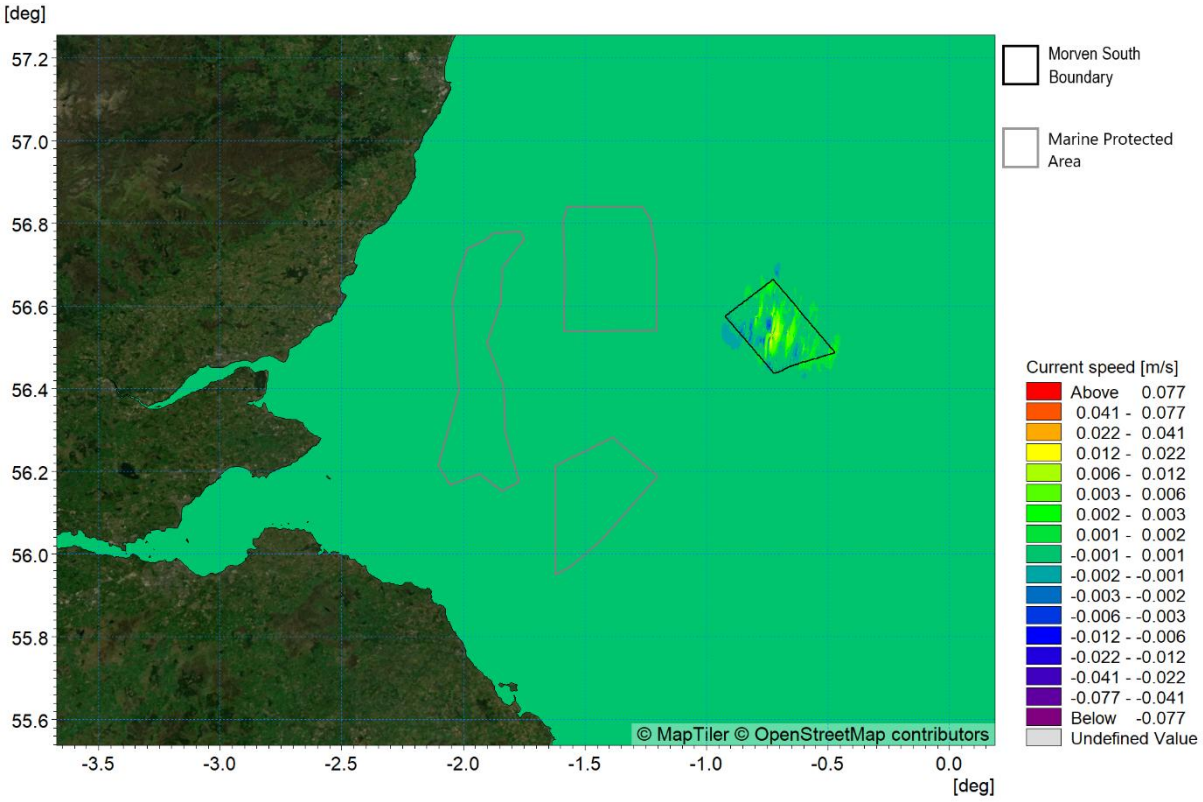

Figure 5.126: Change in residual current spring tide (post-construction Morven South minus baseline)

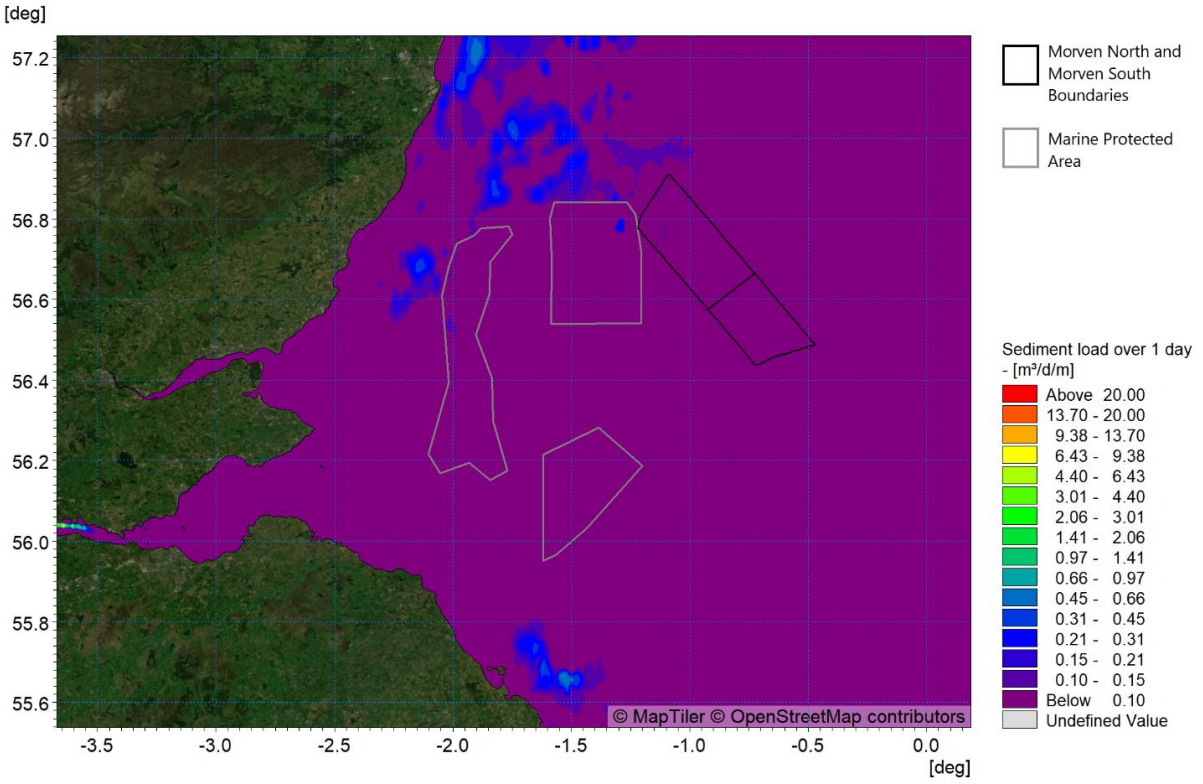

Figure 5.127: Post-construction (Morven North and Morven South) potential sediment transport over the course of one day (two tide cycles)

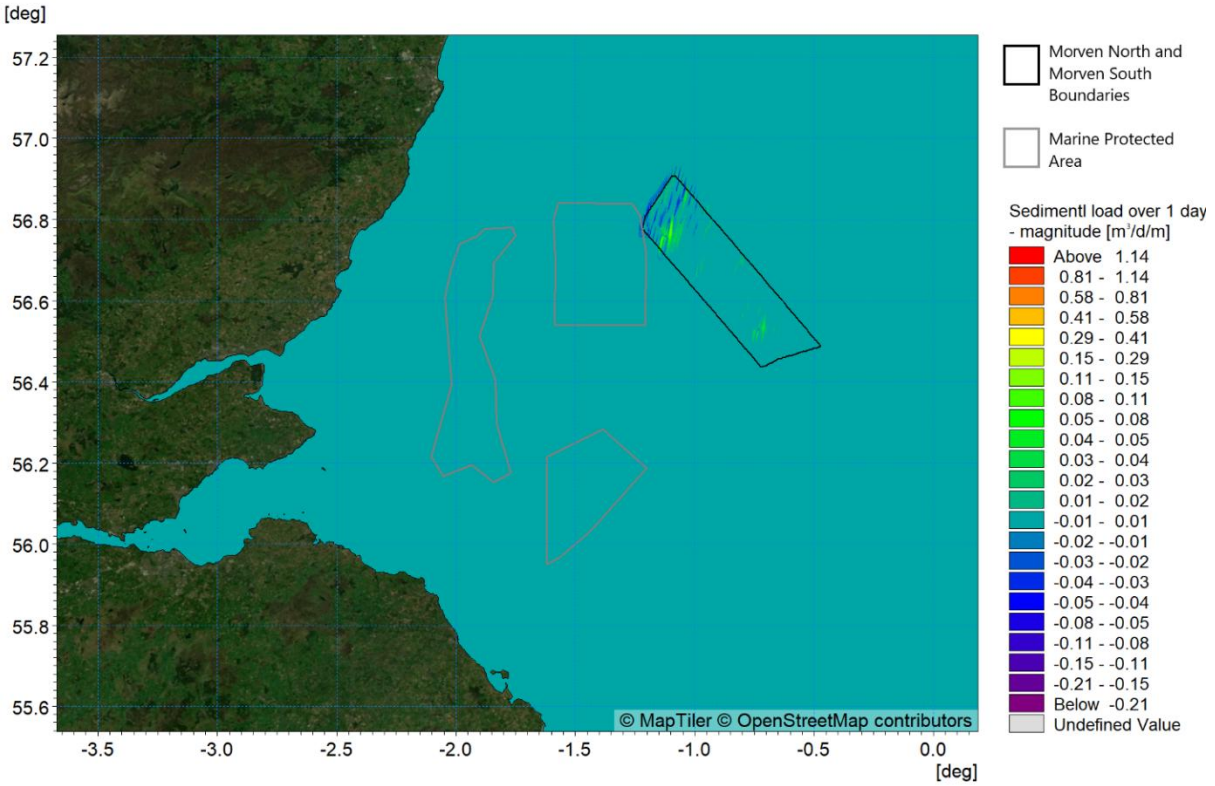

Figure 5.128: Difference in potential sediment transport over the course of one day (post-construction Morven North and Morven South minus baseline)

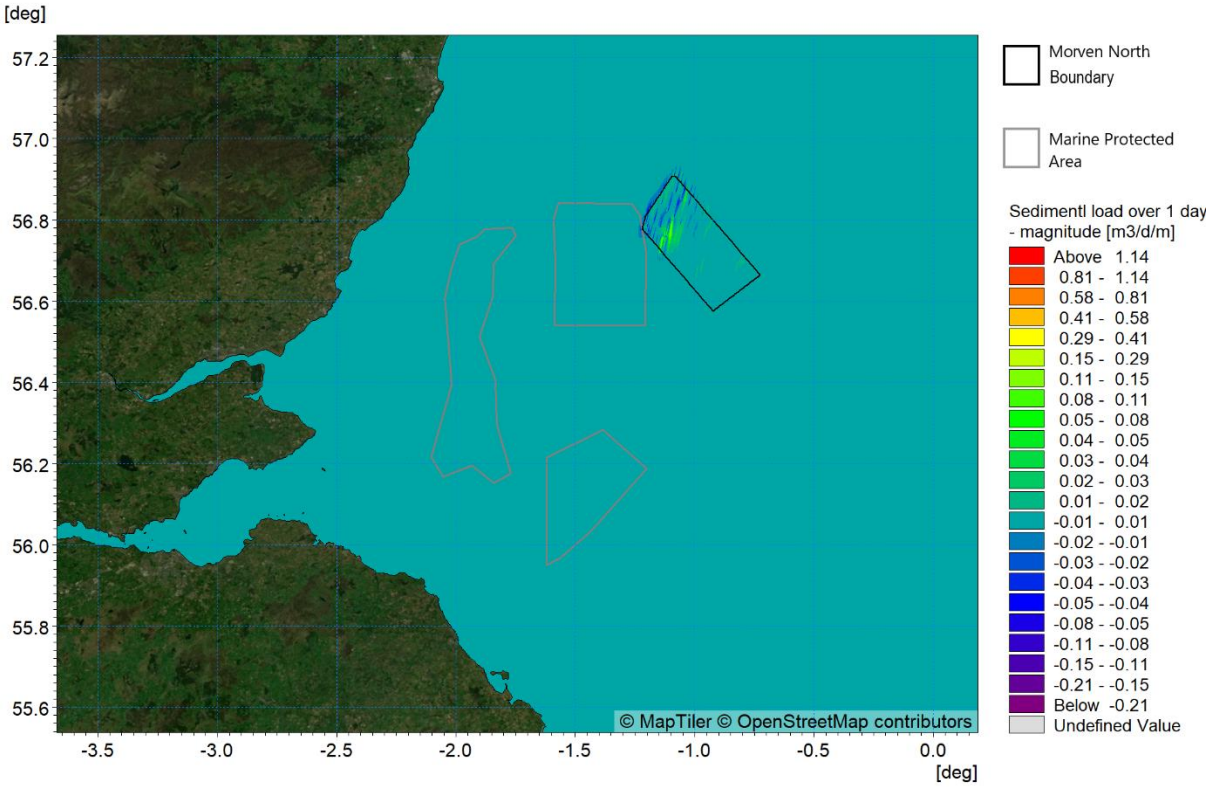

Figure 5.129: Difference in potential sediment transport over the course of one day (post-construction Morven North minus baseline)

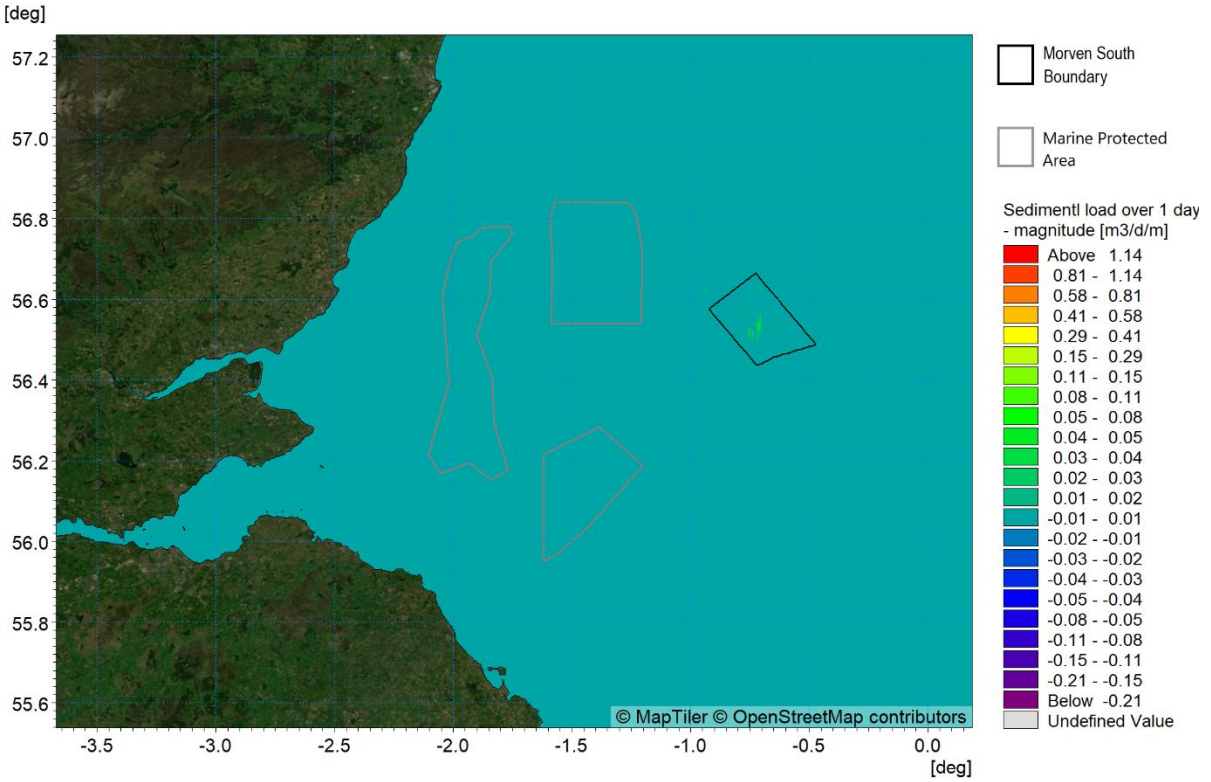

Figure 5.130: Difference in potential sediment transport over the course of one day (post-construction Morven South minus baseline)

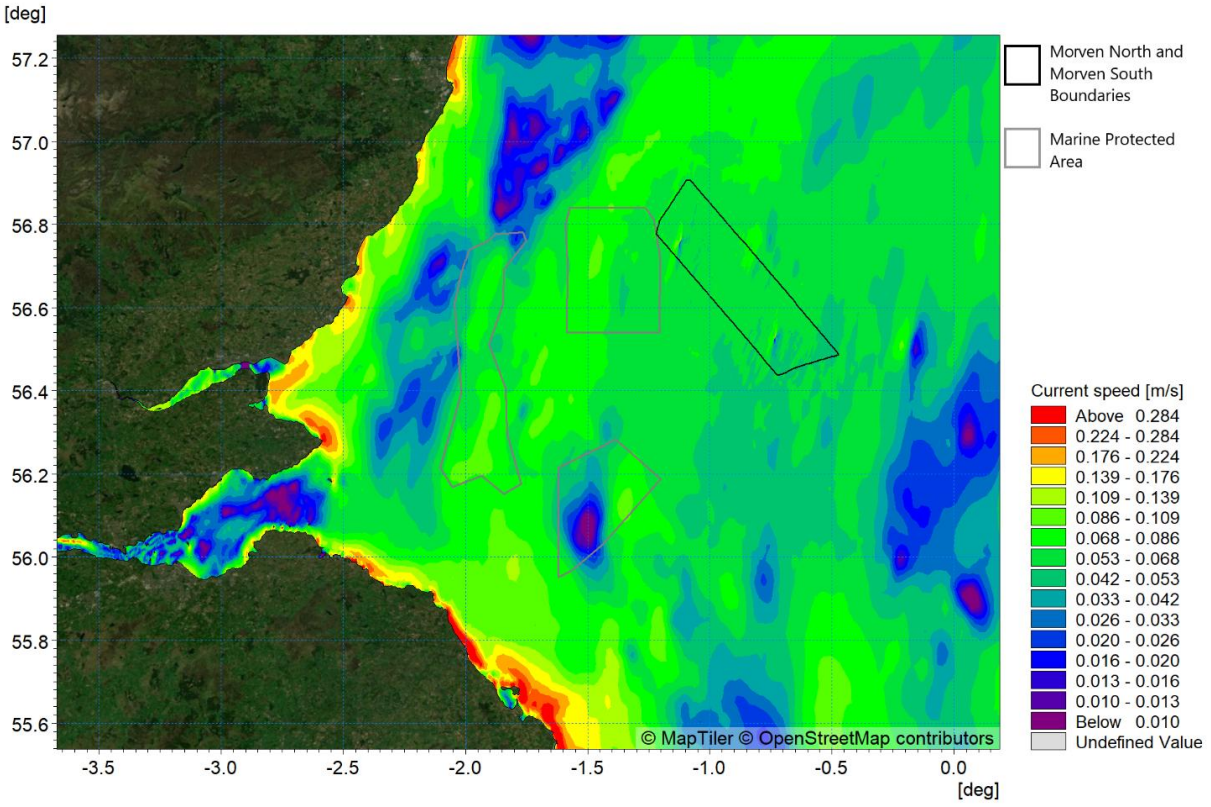

Figure 5.131: Post-construction (Morven North and Morven South) residual current spring tide with 1:1 year storm from 000°

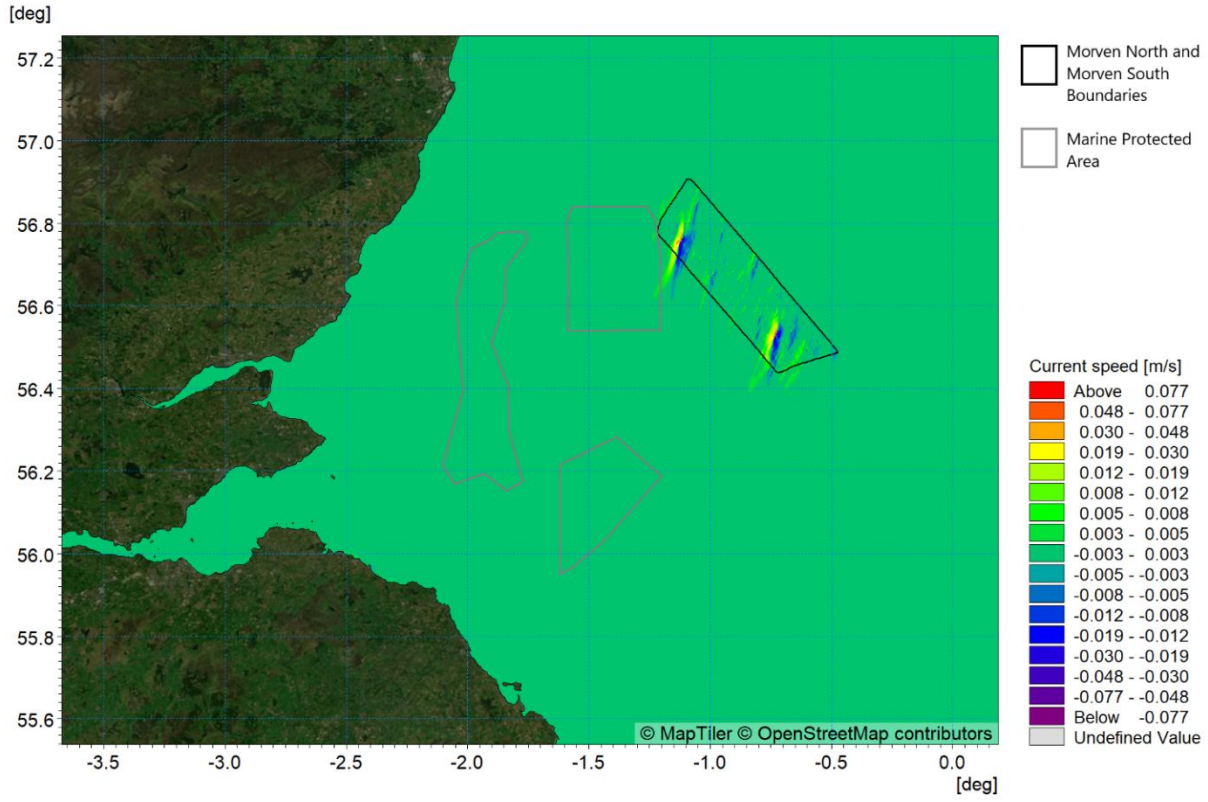

Figure 5.132: Change in residual current spring tide with 1:1 year storm from 000° (post-construction Morven North and Morven South minus baseline)

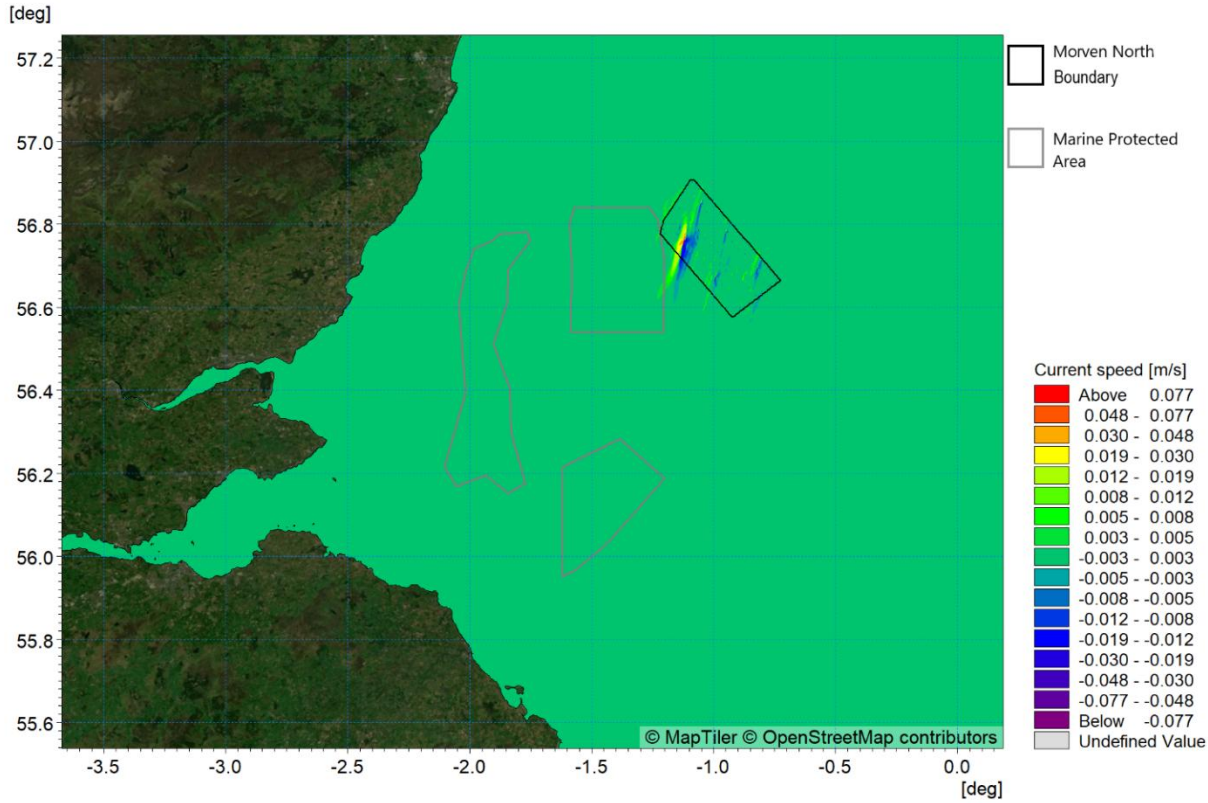

Figure 5.133: Change in residual current spring tide with 1:1 year storm from 000° (post-construction Morven North minus baseline)

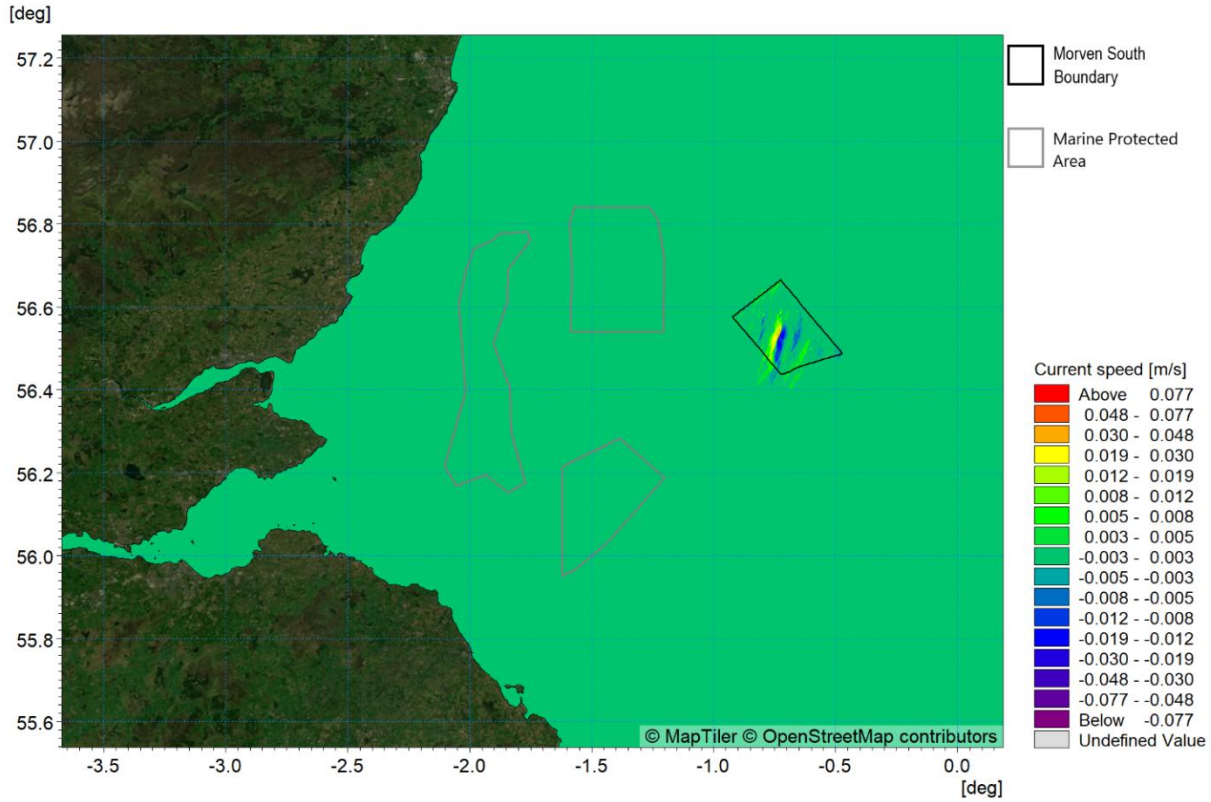

Figure 5.134: Change in residual current spring tide with 1:1 year storm from 000° (post-construction Morven South minus baseline)

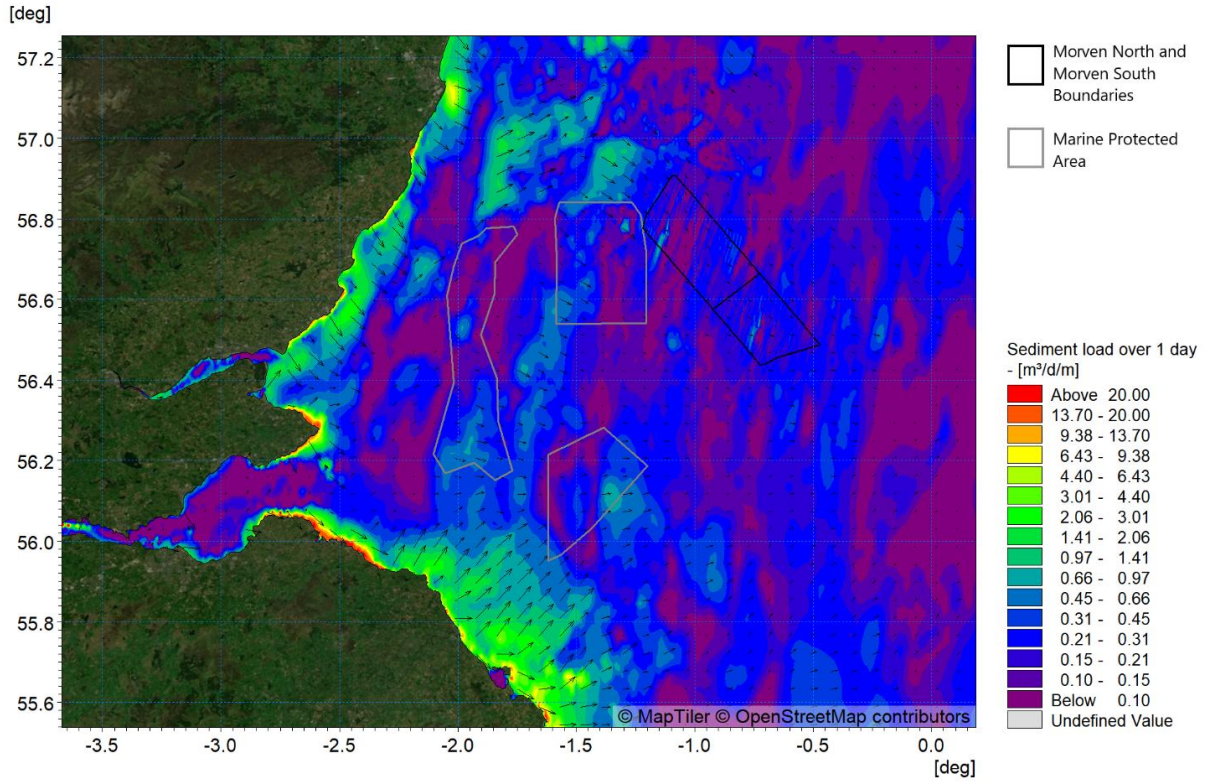

Figure 5.135: Post-construction (Morven North and Morven South) potential sediment transport over the course of one day with 1:1 year storm from 000°

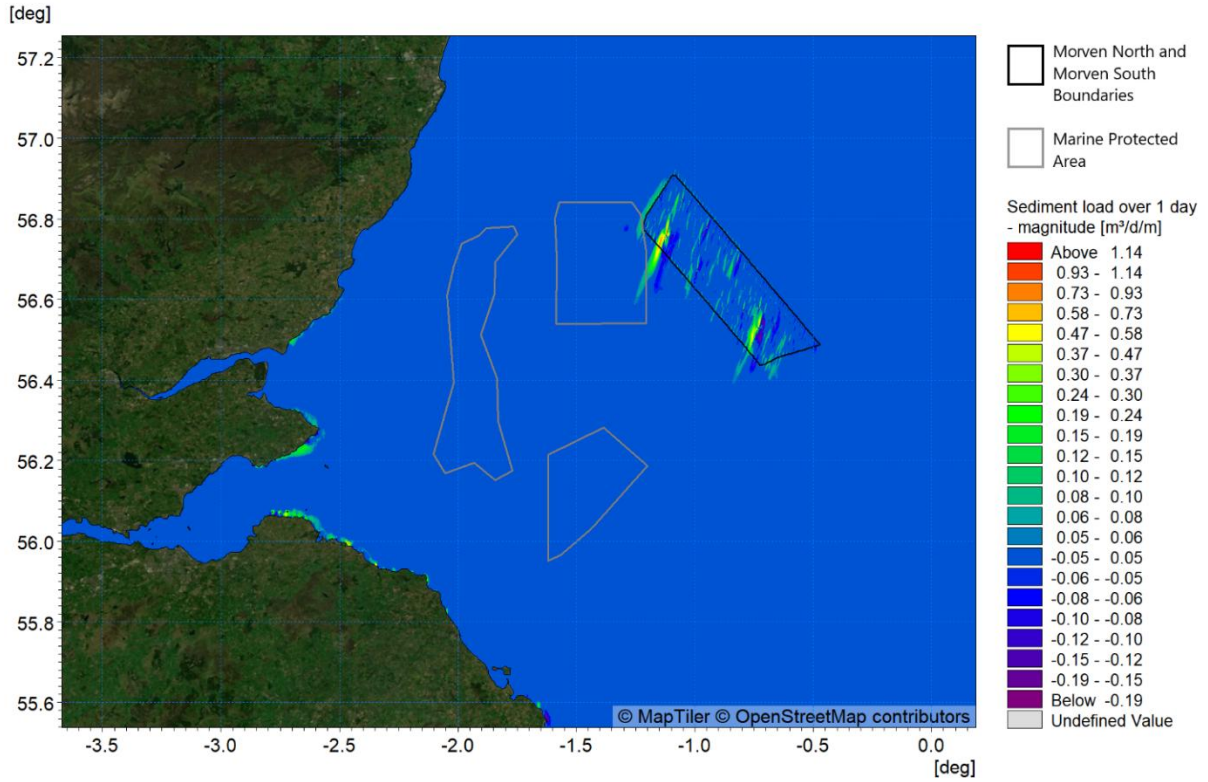

Figure 5.136: Difference in potential sediment transport over the course of one day (post-construction Morven North and Morven South minus baseline) 1:1 year storm from 000°

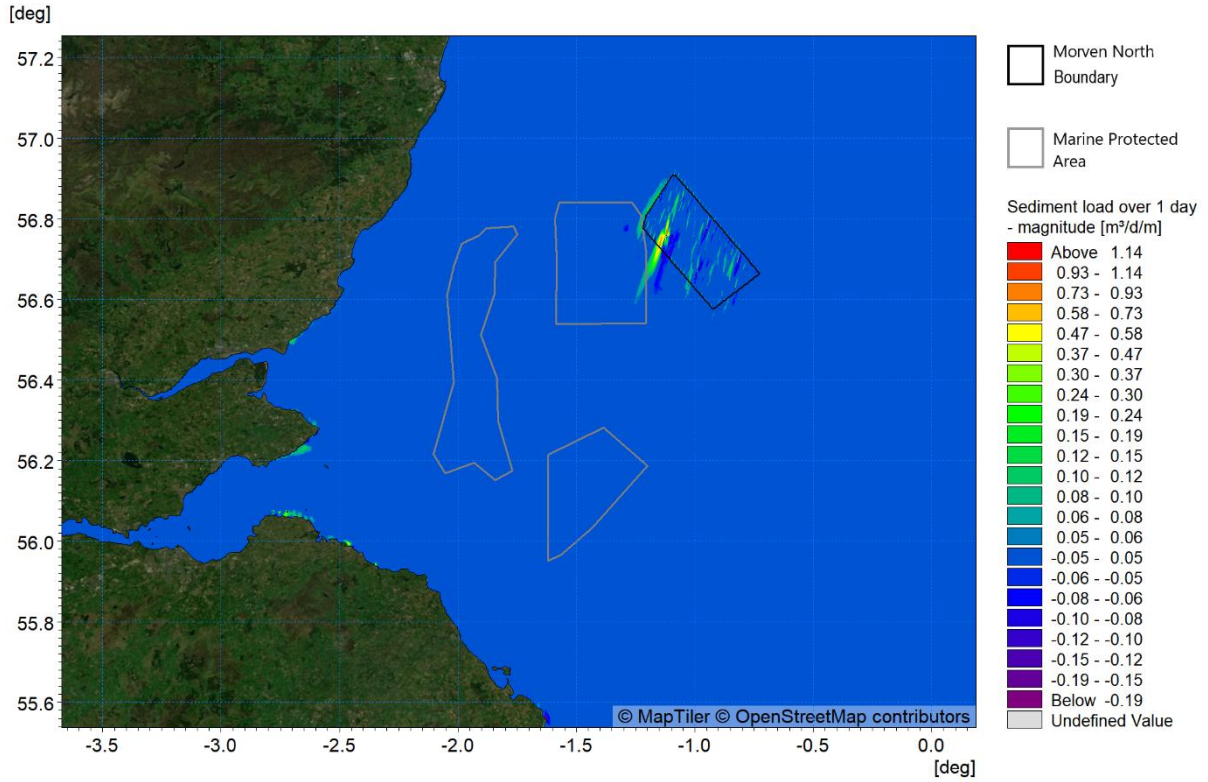

Figure 5.137: Difference in potential sediment transport over the course of one day (post-construction Morven North minus baseline) 1:1 year storm from 000°

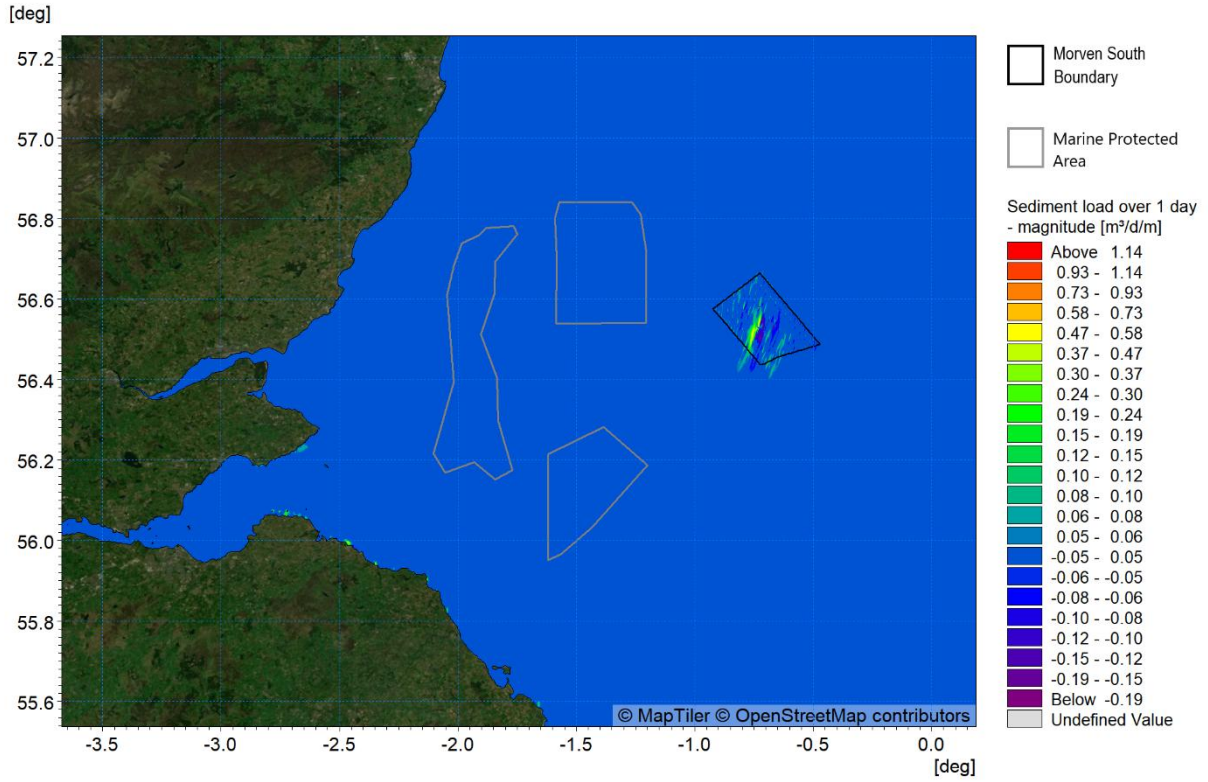

Figure 5.138: Difference in potential sediment transport over the course of one day (post-construction Morven South minus baseline) 1:1 year storm from 000°

6 Potential changes during construction

6.1.1.1 In addition to the changes in physical processes resulting from the presence of Morven North and Morven South, the construction phase influences were quantified. The principal construction elements relate to the transport and fate of sediment brought into suspension due to seabed preparation, the installation of the foundation structures and the laying of inter-array and interconnector cables between the wind turbines and OSPs. An overview of the modelling techniques implemented is provide in Table 3.1.

6.1.1.2 As with the post-construction aspects, the approach was to examine the construction technique which represents the MDS in terms of physical processes. In practice, these changes are therefore likely to be of lesser magnitude. In each scenario the modelling examined excess SSC arising from the proposed activities (i.e. ambient SSC were not included). Baseline studies outlined in Section 4.8 and Section 4.9 indicate that turbidity levels are generally low, particularly in deep water areas, however sediment transport mechanisms are active with the associated bedload. Sedimented material arising from the construction phase activities would therefore be amalgamated into the sediment transport regime. The numerical modelling of SSC provides depth average values and does not therefore differentiate between bed load and water column suspended sediment.

6.1.1.3 During each phase of the assessment the transport of suspended sediment was modelled by undertaking simulations which released sediment at a rate and location appropriate to each type of construction (sandwave clearance, foundation installation or cable installation). The sediment released was defined according to the characteristics of grab samples collected within the site specific survey by Gardline in 2022.

6.2 Seabed preparation

6.2.1.1 Due to the nature of the seabed within the Morven North Boundary and Morven South Boundary, the foundation and cable installation will require seabed preparation in the form of sandwave clearance.

6.2.2 Wind turbine and offshore substation platform foundation sandwave clearance

6.2.2.1 The Project Description outlined in Volume 1, Chapter 3, of the Morven North and Morven South EIA Reports indicates that sandwaves may be cleared for up to 80% of foundations, with a total sandwave clearance area of 3,753,226m^2 and volume of 11,259,679m^3 within each of the Morven North and Morven South Boundaries, assuming sandwaves 3m in height. The total area and volume are based on 58 locations supporting the three-legged suction bucket wind turbine foundations and five locations supporting gravity base OSP foundations.

6.2.2.2 The MDS for physical processes has been selected based on the greatest potential volume of suspended sediments at an individual sandwave clearance location, rather than the total sandwave clearance to be undertaken within the Morven North Boundary or Morven South Boundary. The potential spoil volume per foundation type was calculated to determine the infrastructure likely to cause the greatest potential volume of suspended sediments during sandwave clearance activities.

6.2.2.3 The single greatest sandwave clearance area may occur due to the bridge-linked HVDC OSP gravity base foundations, with a clearance area up to 597,800m^2 or volume of up to 1,793,400m^3. Note that the MDS for this activity is the same for both Morven North and Morven South, due to the same quantity and type of proposed infrastructure, (i.e. one bridge-linked HVDC OSP with gravity base foundations). This does not correspond to the MDS selected for potential impacts to hydrography and sedimentation due to the presence of the infrastructure, whereby the MDS differs for both Morven North and Morven South due to the comprised presence of the infrastructure within Morven North and Morven South.

6.2.2.4 The modelling undertaken to quantify the potential increases in SSC and sedimentation simulated the use of a suction hopper dredger to remove material from the crest of sandwaves and deposit material in the adjacent area. In practice, plough dredging may be undertaken, however this type of operation would have less impact in terms of both SSC and sedimentation footprint.

6.2.2.5 Two representative clearance operations were assessed, one relating to the bridge-linked HVDC converter OSP gravity base foundations within the Morven North Boundary, and the other related to the bridge-linked HVDC OSP gravity base foundations within the Morven South Boundary, as shown in Figure 6.1. As noted previously, there will be a maximum of one bridge-linked HVDC converter OSP within the Morven Site, however the modelling has accounted for one HVDC converter OSP within both the Morven North Boundary and Morven South Boundary, in order to provide a representation of potential impact due to each separate project. In each case, the clearance was undertaken in a north south orientation with a dredging rate of 20,000m^3/h with a spill of 3%, prior to being dumped at the northerly or southerly ends of the clearance areas. The dredging route was considered to have a clearance width of 6.7m and a spill at a rate of 600m^3/h, taking one hour for the hopper to travel the length of the clearance site, prior to releasing material at a rate of 39,007m^3/h at the disposal sites over a period of 30 minutes. The modelled route represents a sandwave clearance operation of 5.6 days in duration.

6.2.2.6 The redistributed material was classified based on the properties identified from the Particle Size Analysis (PSA) of sediment grab samples undertaken as part of the site specific sampling during 2022 (Gardline, 2023). This was comprised of 7.8% silts, 91.7% sands and 0.5% gravels at the Morven North bridge-linked HVDC OSP gravity base foundations. Similarly, the composition at the Morven South bridge-linked HVDC OSP gravity base foundations was 7.0% silts, 92.8% sands and 0.2% gravels.

Morven North

6.2.2.7 The SSC vary greatly during the course of the dredge and disposal campaign. During the dredging phase when only 3% of the material is released the plume is very small with concentrations less than 170mg/l within the Morven North Boundary, as shown in Figure 6.2. During the disposal phase, the plume is larger (Figure 6.3) with concentrations reaching 14,500mg/l at the release site within the Morven North Boundary. However, the most extensive increases are seen as the deposited material is redistributed on the successive tides, where sedimentation occurs on the slack tide reducing the SSC completely and resuspension and transport occurs when the tidal currents increase. Under these circumstances, large areas with concentrations in the order of 500mg/l are observed, as illustrated in Figure 6.4, which shows SSC during peak current speed. The average SSC within the Morven North Boundary during the course of the dredge and disposal campaign is presented in Figure 6.5 with values <1mg/l with a plume length of circa 28km in a north northeast, south southwest orientation and width of 4km. Thus, wherever the sandwave clearance activity is undertaken within the Morven North Boundary, the increases will be limited to within 14km from the activity and hence elevated SSC plumes will remain within the Morven North Physical Processes Study Area. SSC would be increased for a limited period in the vicinity of the sandwave clearance activity and would not become widespread throughout the Morven North Boundary.

6.2.2.8 The average sedimentation depth is shown in Figure 6.6 for Morven North and illustrates how the deposited material is focussed within circa 200m of the site of release with a maximum depth 0.5m to 2.0m, whilst the finer sediment fractions are distributed in the vicinity at much smaller depths, circa 5mm to 50mm. The dispersion of the released material would continue on successive tides and be incorporated into the baseline sediment transport regime. The sedimentation one day following the cessation of the clearance operation is presented in Figure 6.7 and is consistent with this mechanism.

Morven South

6.2.2.9 The SSC vary greatly during the course of the dredge and disposal campaign. During the dredging phase when only 3% of the material is released the plume is very small with concentrations less than 210mg/l within the Morven South Boundary, as shown in Figure 6.2. During the disposal phase, the plume is larger (Figure 6.3) with concentrations reaching 17,200mg/l at the release site within the Morven South Boundary. As per Morven North, as discussed under paragraph 6.2.2.7, the most extensive increases are seen as the deposited material is redistributed on the successive tides. Under these circumstances, large areas with concentrations in the order of 500mg/l are observed, as illustrated in Figure 6.4, which shows SSC during peak current speed. The average SSC within the Morven South Boundary during the course of the dredge and disposal campaign is presented in

Figure 6.5 with values <1mg/l with a plume length of circa 26km in a north northeast, south southwest orientation and width of 4.5km. Thus, wherever the sandwave clearance activity is undertaken within the Morven South Boundary, the increases will be limited to within 13km from the activity and hence elevated SSC plumes will remain within the Morven South Physical Processes Study Area. SSC would be increased for a limited period in the vicinity of the sandwave clearance activity and would not become widespread throughout the Morven South Boundary.

6.2.2.10 The average sedimentation depth is shown in Figure 6.6 for Morven South and is in line with the depths discussed for Morven North under paragraph 6.2.2.8. The sedimentation one day following the cessation of the clearance operation is presented in Figure 6.7.

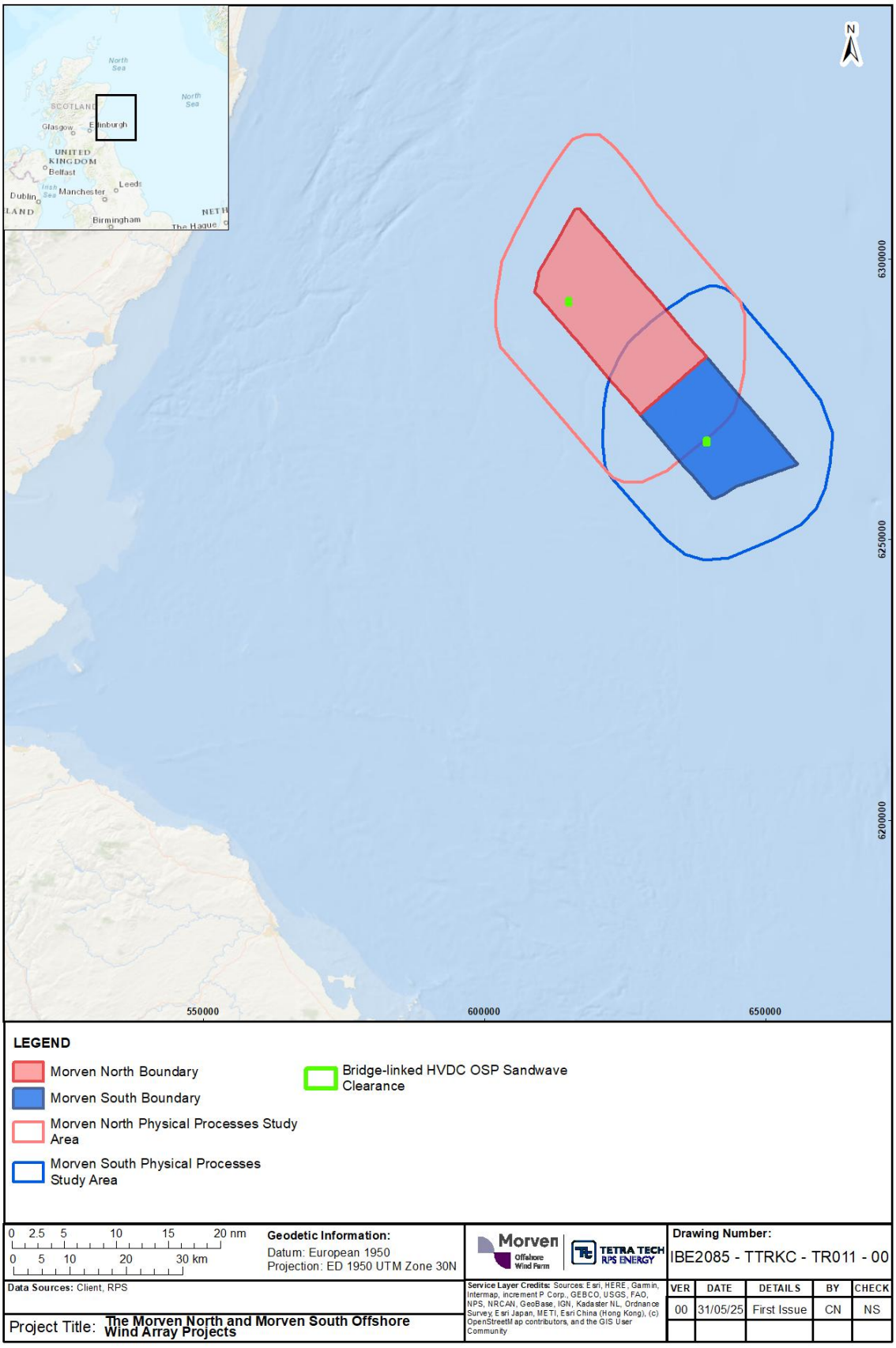

Figure 6.1: Sandwave clearance area modelled (Morven North/Morven South)

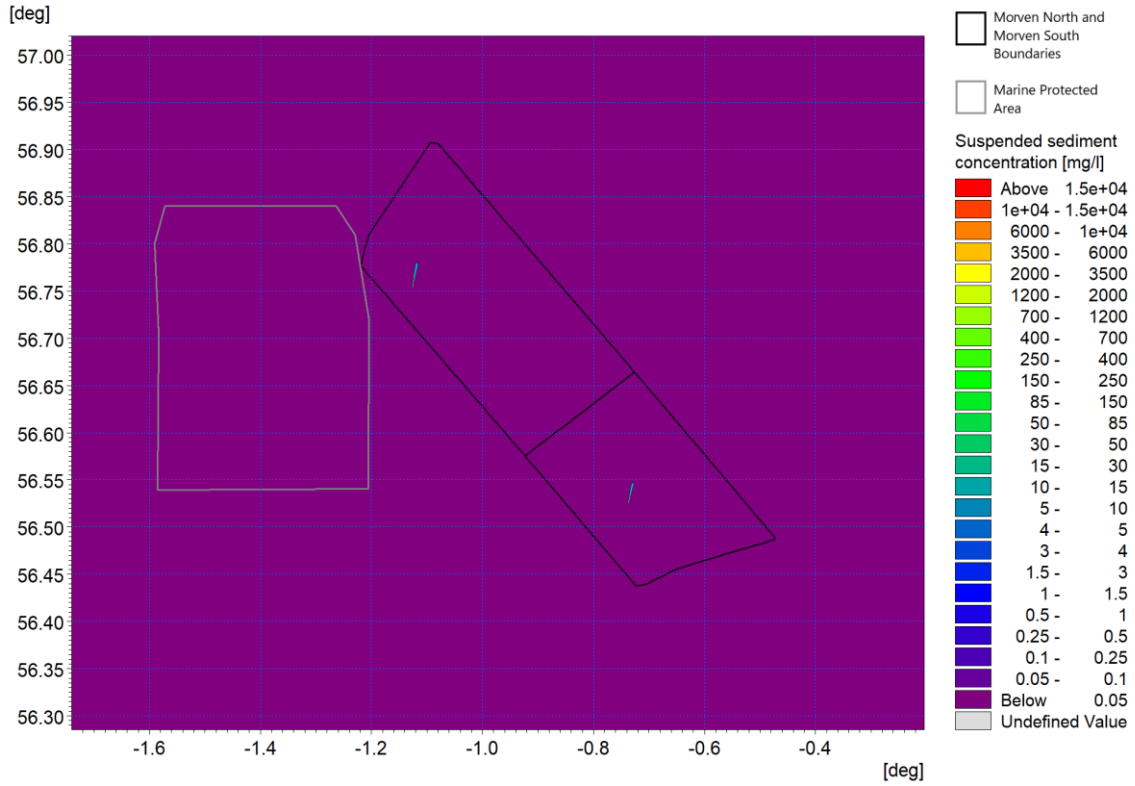

Figure 6.2: Suspended Sediment Concentrations resulting from dredging phase of sandwave clearance activity at the High Voltage Direct Current Offshore Substation Platform foundation location (Morven North/Morven South)

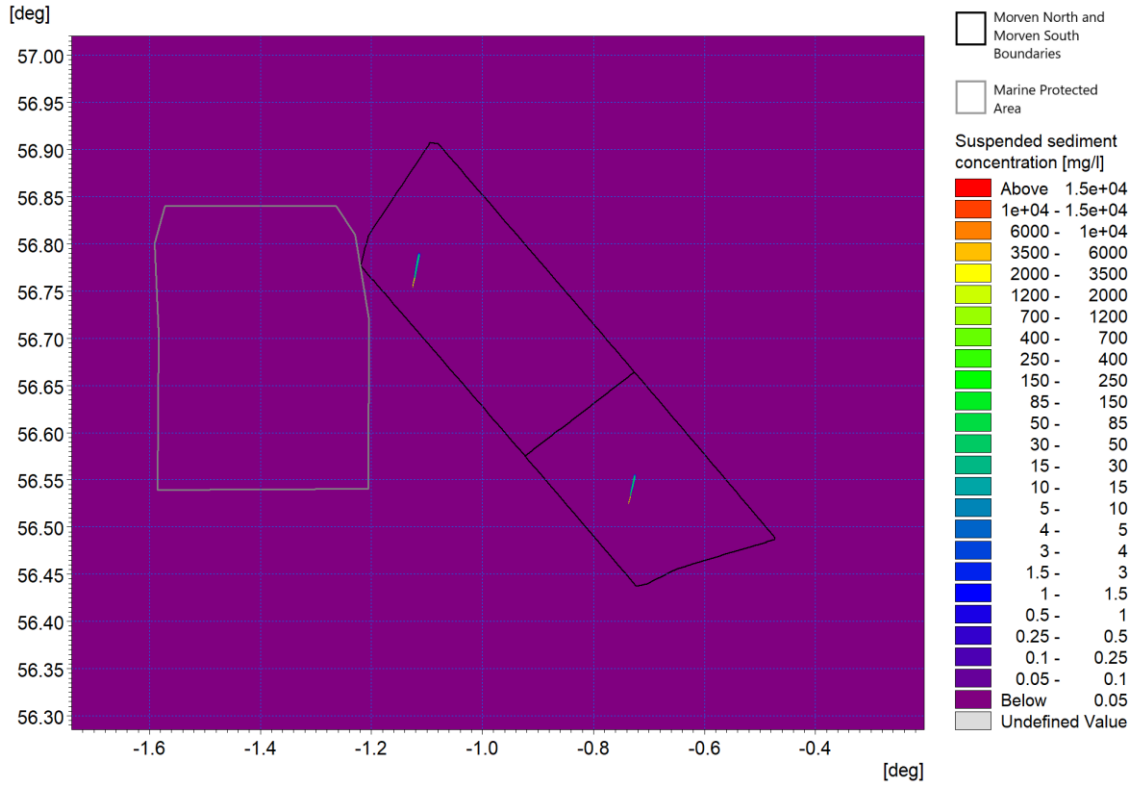

Figure 6.3: Suspended Sediment Concentrations resulting from disposal phase of sandwave clearance activity at the High Voltage Direct Current Offshore Substation Platform foundation location (Morven North/Morven South)

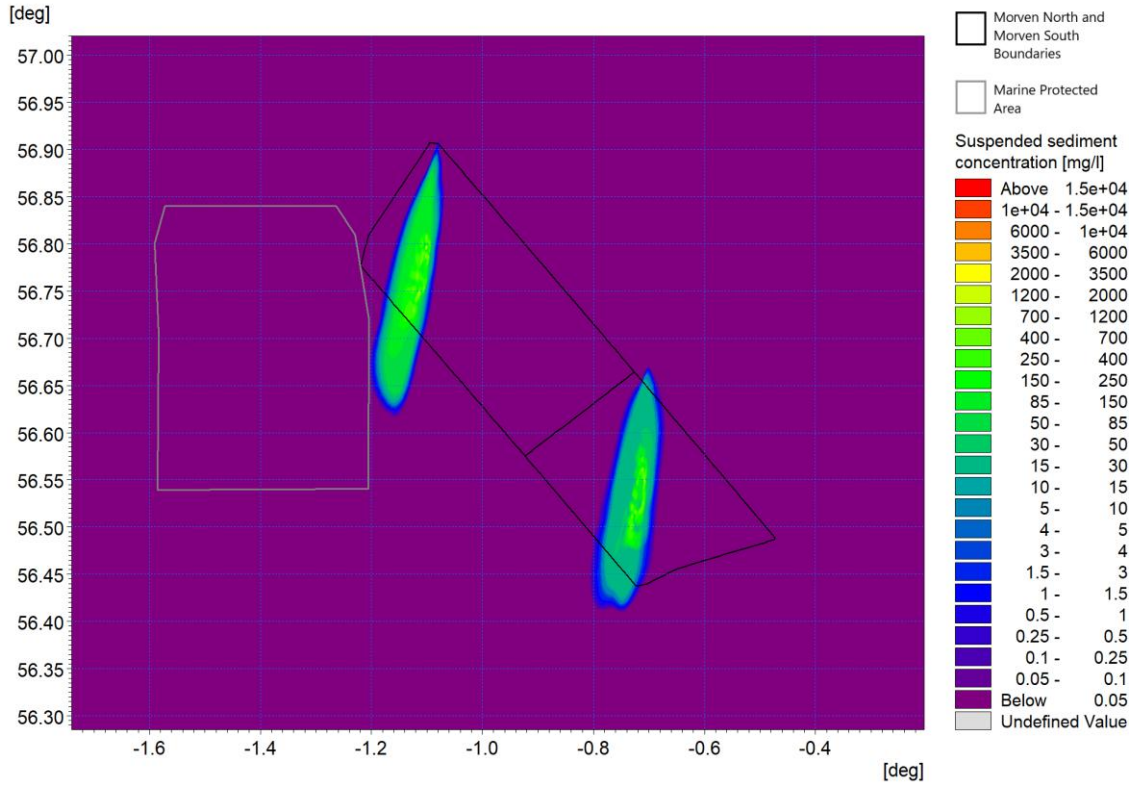

Figure 6.4: Suspended Sediment Concentrations resulting from sediment remobilisation associated with sandwave clearance at the High Voltage Direct Current Offshore Substation Platform foundation location (Morven North/Morven South)

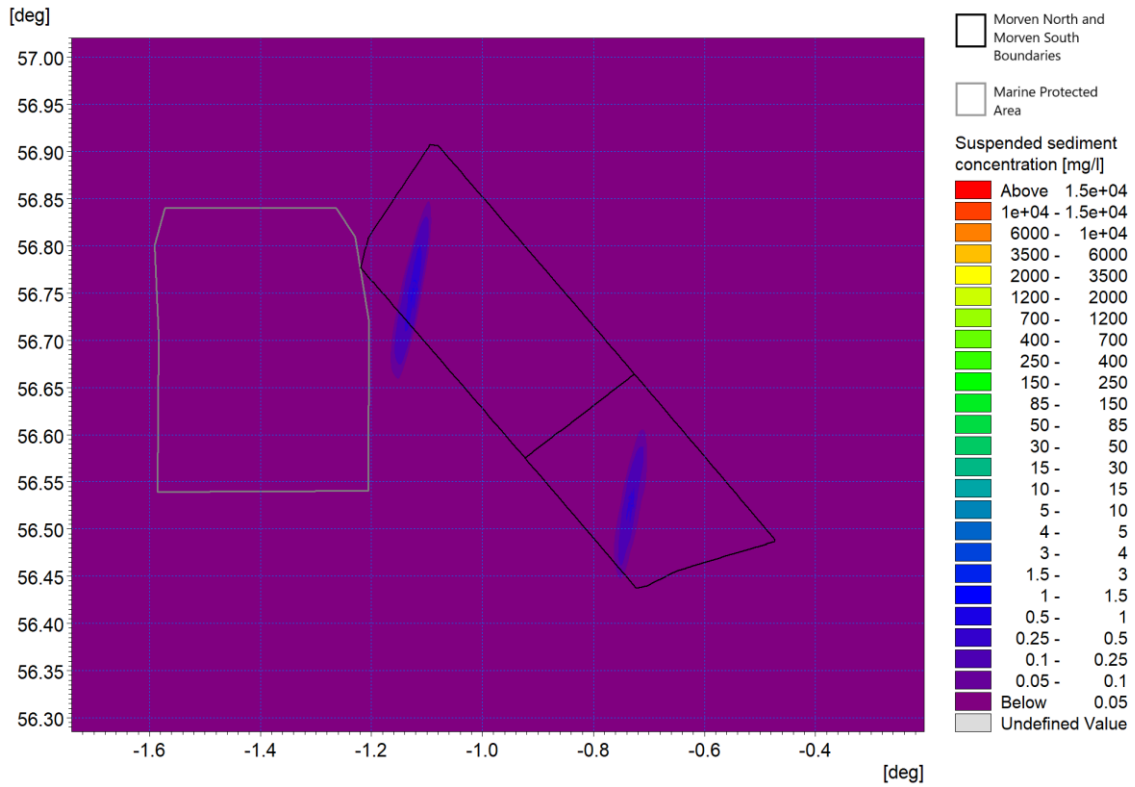

Figure 6.5: Average Suspended Sediment Concentrations during modelled sandwave clearance activity at the High Voltage Direct Current Offshore Substation Platform foundation location (Morven North/Morven South)

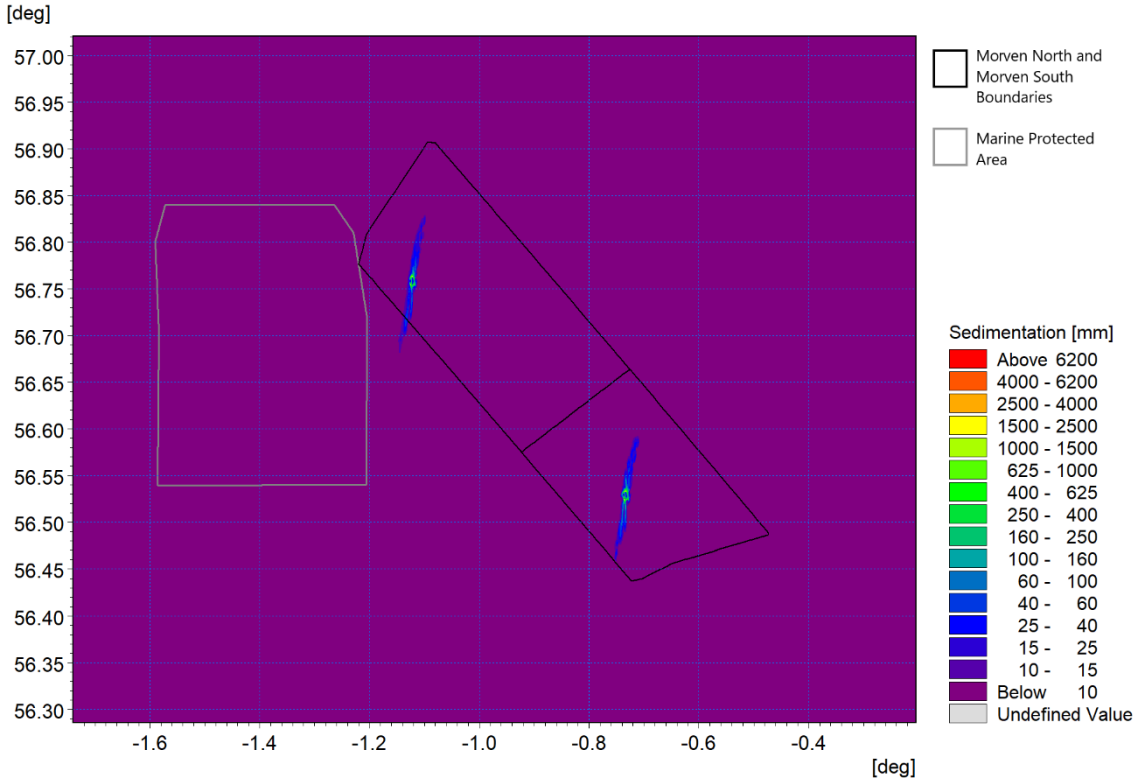

Figure 6.6: Average sedimentation during modelled sandwave clearance activity at the High Voltage Direct Current Offshore Substation Platform foundation location (Morven North/Morven South)

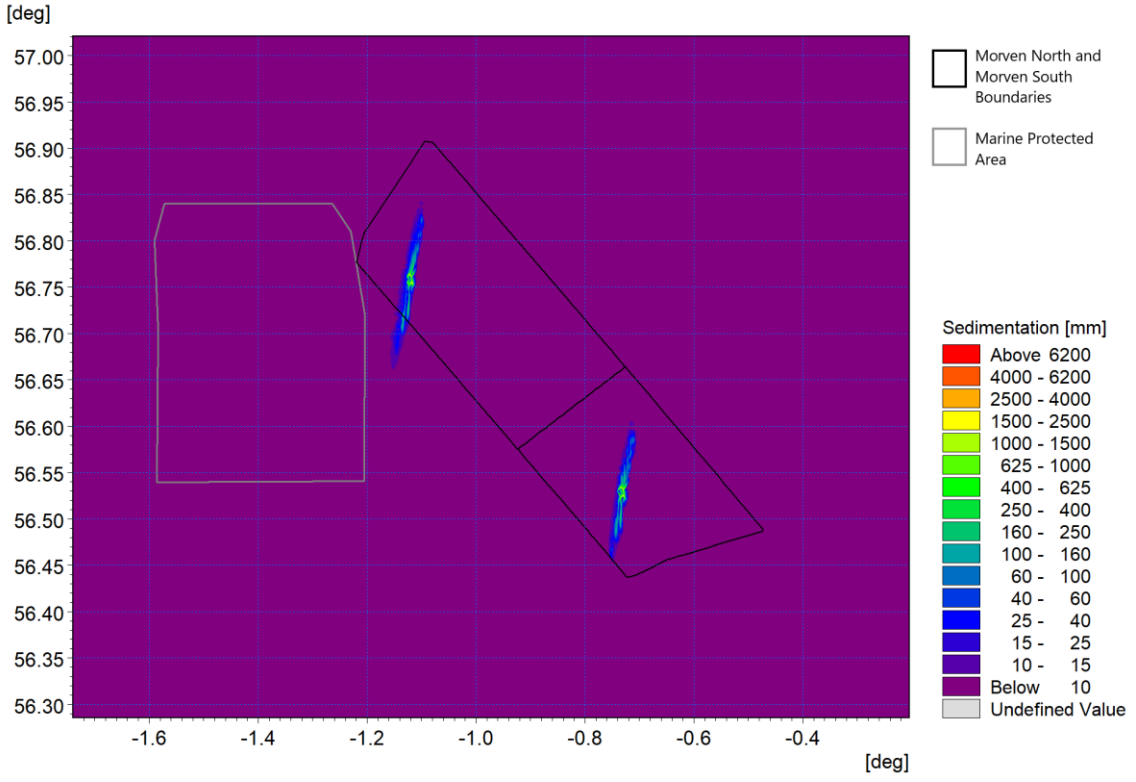

Figure 6.7: Sedimentation one day following cessation of sandwave clearance at the High Voltage Direct Current Offshore Substation Platform foundation location (Morven North/Morven South)

6.2.3 Inter-array cable sandwave clearance

6.2.3.1 The Project Description outlined in Volume 1, Chapter 3 of the Morven North and Morven South EIA Reports indicates that sandwaves may be cleared for the inter-array and interconnector cabling along up to a 20m wide corridor within both Morven North and Morven South. Clearance activities may extend along circa 63.6km of inter-array cabling and 72.6km of interconnector cabling within the Morven North Boundary, equating to total spoil volumes of 6,102,000m^3 and 6,969,600m^3 respectively across the Morven North Boundary when considering sandwaves 3m in height. Similarly, within the Morven South Boundary, the MDS for this activity is considered to be sandwave clearance along 63.0km of inter-array cable, and along 39.6km of interconnector cable, resulting in a total spoil volume of 6,048,000m^3 and 3,801,600m^3 respectively.

6.2.3.2 The modelling undertaken to quantify the potential increases in SSC and sedimentation simulated the use of plough dredging or similar mechanism, whereby all of the material being cleared is considered to be disturbed and mobilised into the water column. This occurs across the 20m wide corridor during the dredging process.

6.2.3.3 Two representative interconnector cable clearance operations were assessed within both the Morven North Boundary and Morven South Boundary, as shown in Figure 6.8. The geophysical survey data was used to identify areas of sandwaves and megaripples where the operations are most likely to be required. The clearance routes were selected so that different orientations would be modelled within both Morven North and Morven South, so that the potential magnitude of SSC and associated deposition within various states of the tide could be fully understood. A dredging rate of 20,000m^3/h was selected as a feasible rate based on the size of the clearance area and typical clearance activities of this nature.

6.2.3.4 The dredging routes were considered to have a clearance depth of 3m and width of 5.5m and a spill at a rate of 611m^3/h, with each hopper manoeuvring from side to side of the 20m wide clearance path required along each cable route. The modelled routes of 14.6km represent a sandwave clearance operation of 12 hours in duration.

6.2.3.5 The redistributed material was classified based on the properties identified from the site specific sampling in line with the foundation sandwave clearance as outlined in the previous section.

Morven North

6.2.3.6 The resulting SSC for Morven North showed similar characteristics to the foundation sandwave clearance (Section 6.2.2) in terms of the dredging operation, although the plumes were more concentrated due to the 100% displacement of the material. As shown in Figure 6.9, concentrations of up to 750mg/l were found in the vicinity of the releases, with narrow plumes (with width circa 200m) of up to 40mg/l extending up to 8km in a north northeasterly direction within the Morven North Boundary. Plume widths increase with distance from the activity due to dispersion.

6.2.3.7 The greatest area of increased SSC, extending a tidal excursion circa 9km from the releases within the Morven North Boundary is also associated with remobilisation of the deposited material on subsequent tide (Figure 6.10) with concentrations of up to 800mg/l, but typically in the order of 20mg/l to 50mg/l over greater areas. Average SSC over the campaign were typically <100mg/l as illustrated in Figure 6.11.

6.2.3.8 The average sedimentation over the sandwave clearance activity is shown in Figure 6.12, whilst the sedimentation one day following the cessation of the clearance operation is presented in Figure 6.13. The average sedimentation is seen to be below 10mm within the Morven North Boundary and returns to less than 2mm one day following the cessation of activity. Average sedimentation is shown to occur over a distance of 25km for this activity due to the locations of the two concurrent clearance operations, however, remains within the Morven North Physical Processes Study Area.

6.2.3.9 It can be inferred from the Morven North modelled routes that sandwave clearance operations of the scale presented in the Project Description (Volume 1, Chapter 3 of the Morven North EIA Report) will produce elevated SSC and an increase in sedimentation which will be limited to the extent of the Morven South Physical Processes Study Area for any selected sandwave clearance route required during the construction stage.

Morven South

6.2.3.10 The resulting SSC for Morven South showed similar characteristics to the foundation sandwave clearance (Section 6.2.2) in terms of the dredging operation, although the plumes were more concentrated due to the 100% displacement of the material. As shown in Figure 6.9, concentrations of up to 650mg/l were found in the vicinity of the releases, with narrow plumes (with width circa 200m) of up to 50mg/l extending up to 6.5km in a north northeasterly direction within the Morven South Boundary.

6.2.3.11 The greatest area of increased SSC, extending a tidal excursion circa 8km from the releases within the Morven South Boundary is also associated with remobilisation of the deposited material on subsequent tide (Figure 6.10) with concentrations of up to 400mg/l, but typically in the order of 20mg/l to 50mg/l over greater areas. Average SSC over the campaign were typically <100mg/l as illustrated in Figure 6.11.

6.2.3.12 The average sedimentation over the sandwave clearance activity is shown in Figure 6.12, whilst the sedimentation one day following the cessation of the clearance operation is presented in Figure 6.13. The average sedimentation is seen to be below 20mm within the Morven South Boundary and returns to less than 2mm one day following the cessation of activity. The extent of the sedimentation for these concurrent sample routes is less than the Morven North samples outlined in paragraph 6.2.3.8 due to their close locality and varied orientations. Sedimentation occurs over a distance of circa 15km due to the two modelled clearance routes and remains within the Morven South Boundary.

6.2.3.13 It can be inferred from the Morven South modelled routes that sandwave clearance operations of the scale presented in the Project Description (Volume 1, Chapter 3 of the Morven South EIA Report) will produce elevated SSC and an increase in sedimentation which will be limited to the extent of the Morven South Physical Processes Study Area for any selected sandwave clearance route required during the construction stage.

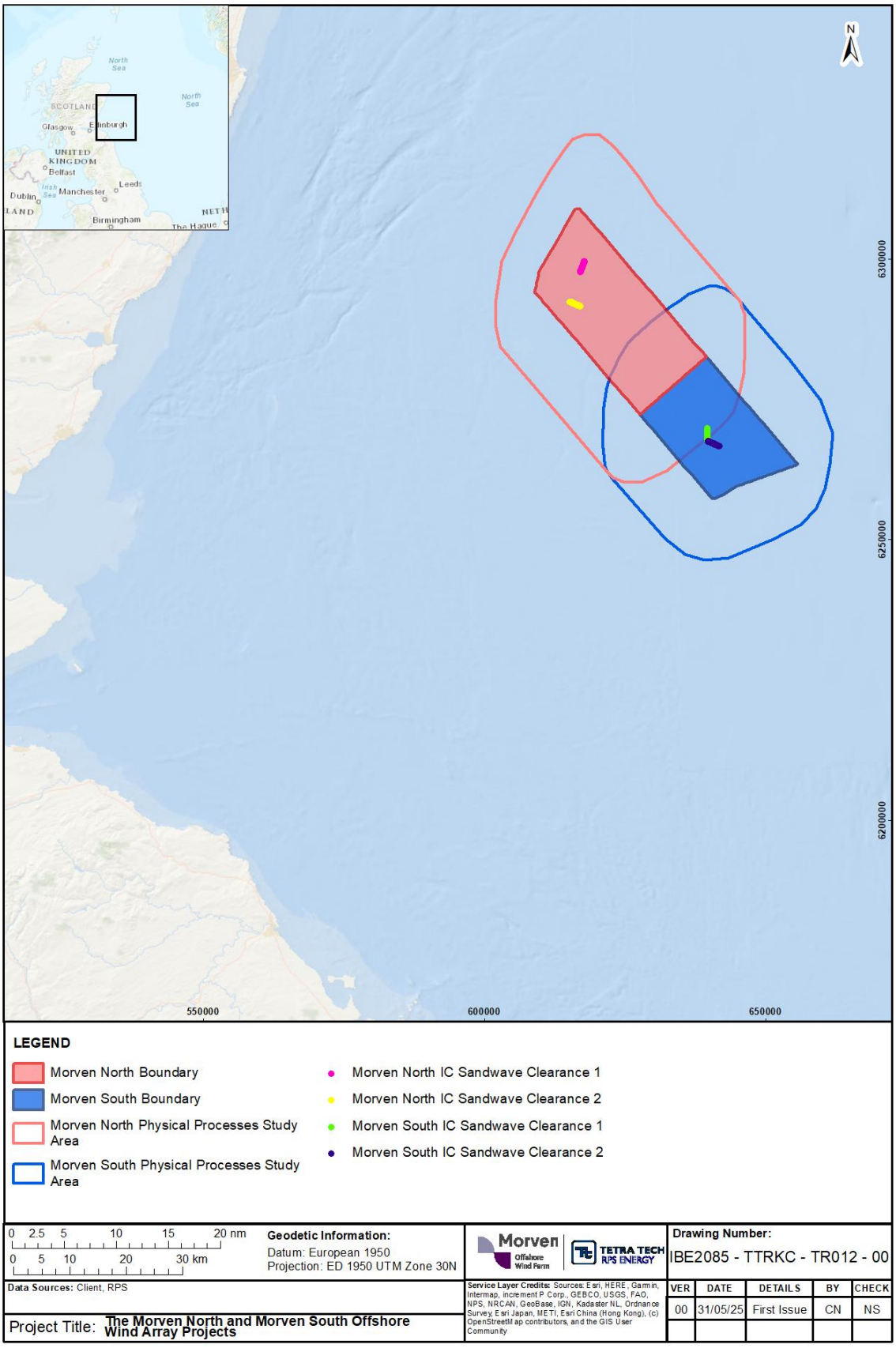

Figure 6.8: Modelled interconnector cable sandwave clearance (Morven North/Morven South)

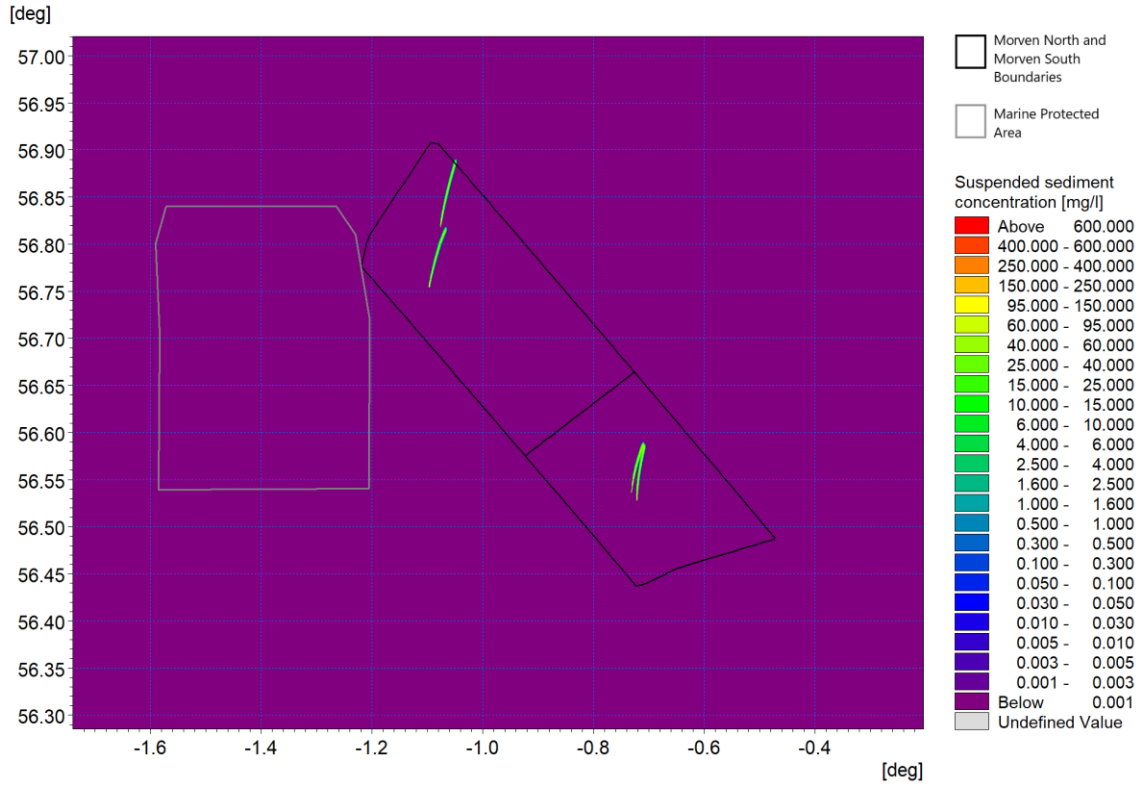

Figure 6.9: Suspended Sediment Concentrations resulting from dredging phase of sandwave clearance activity at sample interconnector cable locations (Morven North/Morven South)

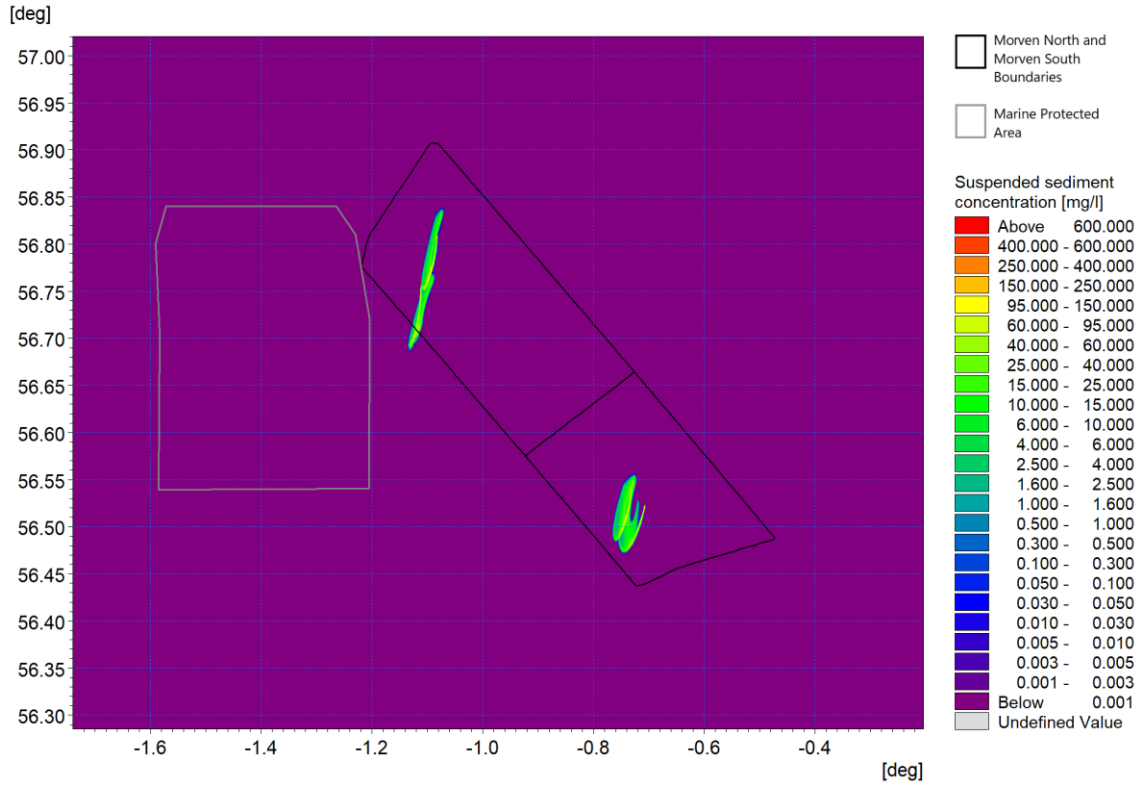

Figure 6.10: Suspended Sediment Concentrations resulting from sediment re-mobilisation associated with sandwave clearance at sample interconnector cable locations (Morven North/Morven South)

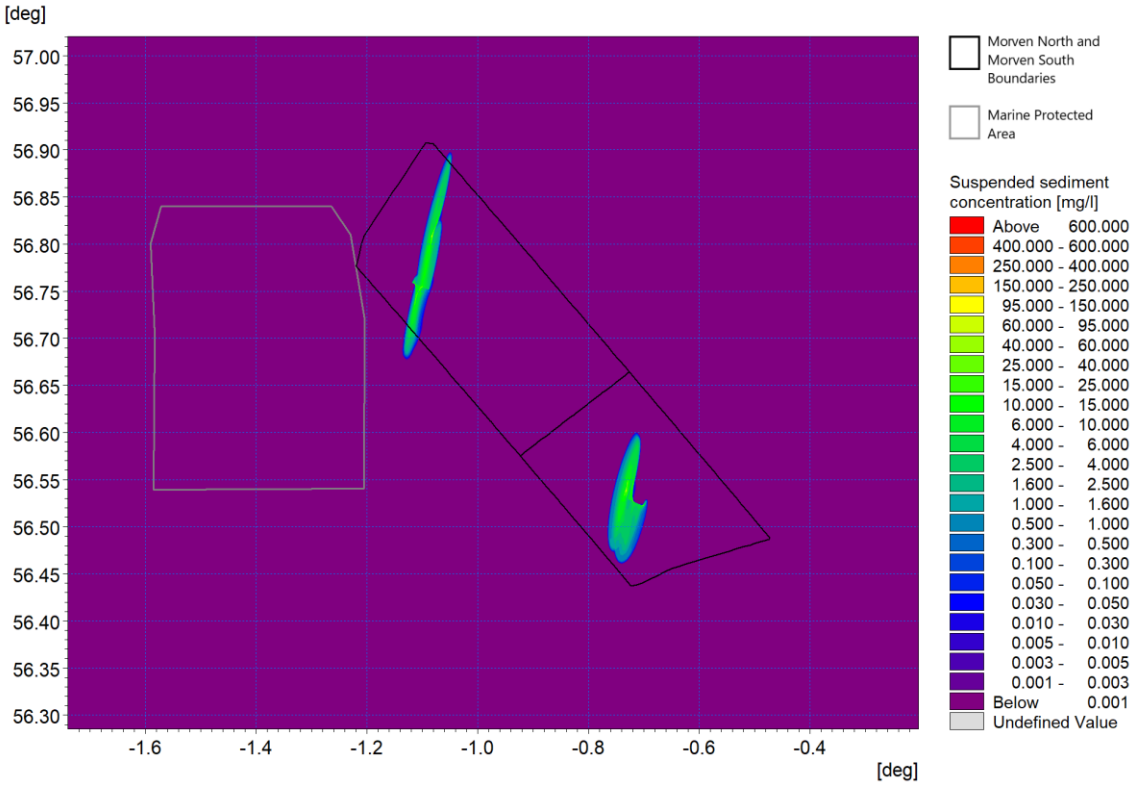

Figure 6.11: Average Suspended Sediment Concentrations during modelled sandwave clearance activity at sample interconnector cable locations (Morven North/Morven South)

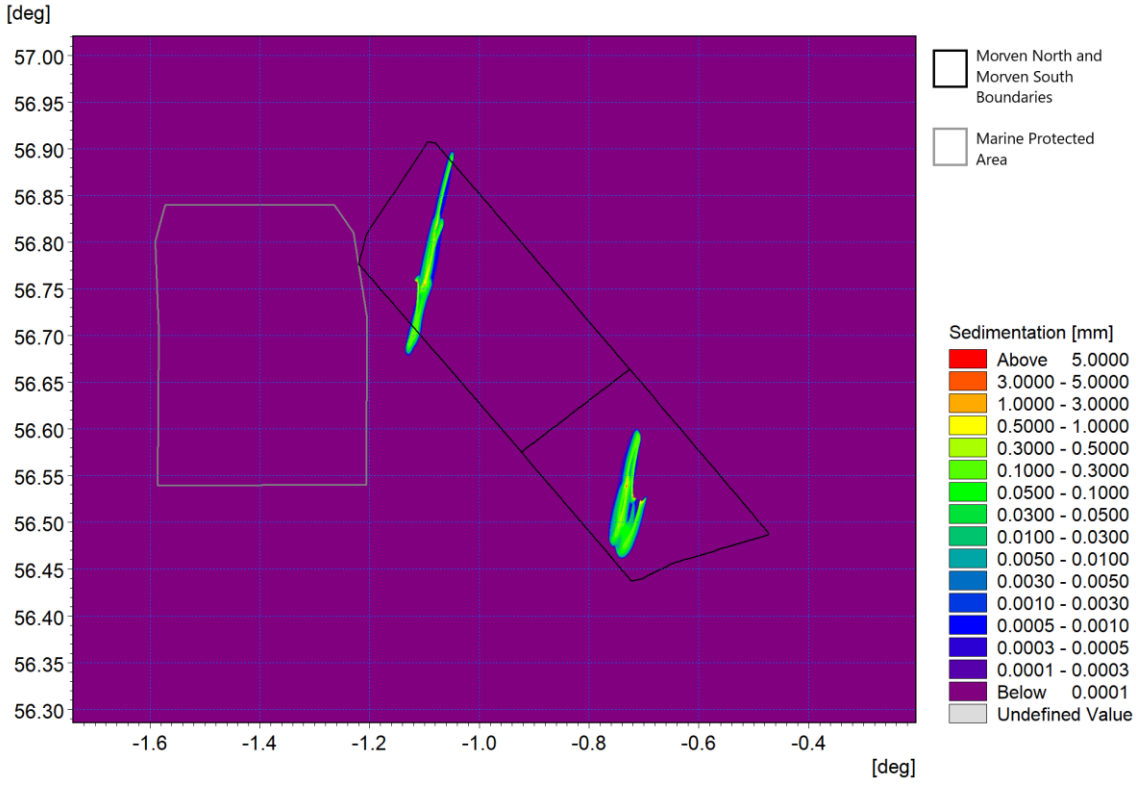

Figure 6.12: : Average sedimentation during modelled sandwave clearance activity at sample interconnector cable locations (Morven North/Morven South)

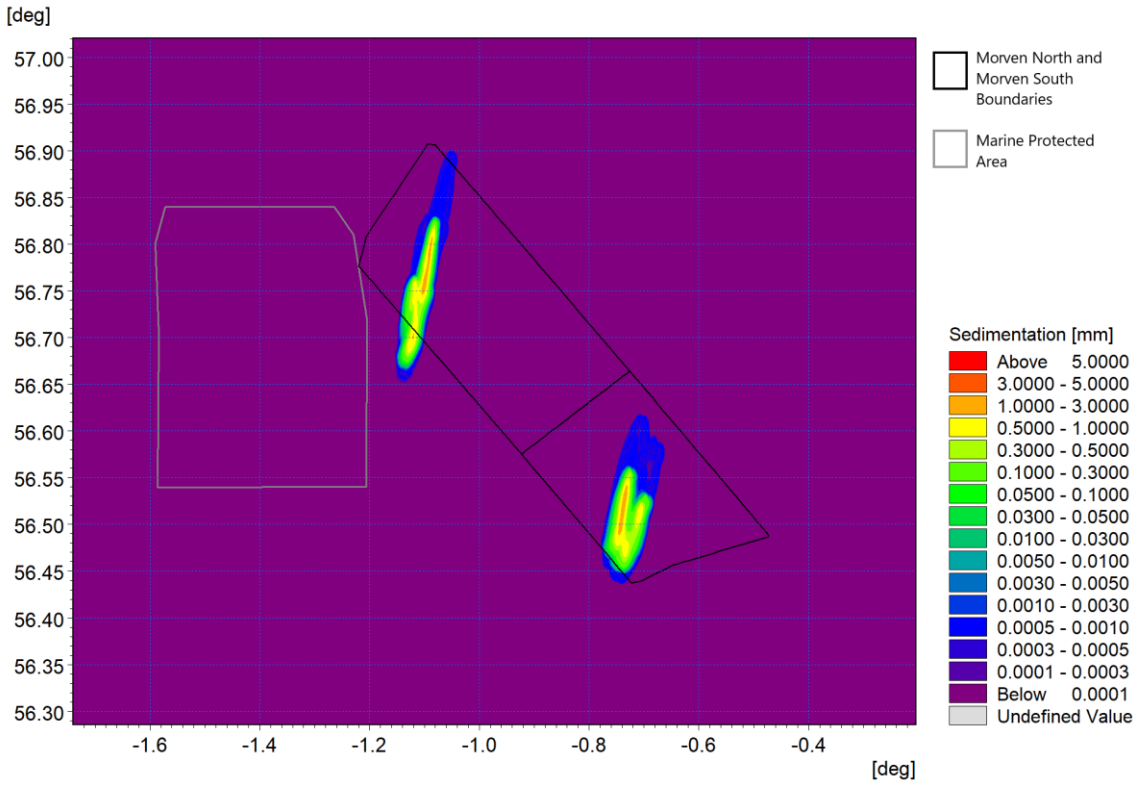

Figure 6.13: Sedimentation one day following cessation of sandwave clearance at sample interconnector cable locations (Morven North/Morven South)

6.3 Installation activities

6.3.1 Foundation installation

6.3.1.1 The Project Description outlined in Volume 1, Chapter 3 of the Morven North and Morven South EIA Reports includes a range of potential foundation types for wind turbines and OSPs. The largest potential release from foundation installation would be from augured (drilled) piles relating to the wind turbine monopile foundations or HVAC collector OSP monopile foundations, where the material would be jetted and released to the water column as a plume. It is anticipated that 34 wind turbine piles and four HVAC collector OSP piles may require drilling to a depth of 64m across the Morven North Boundary, with the same number of each across the Morven South Boundary. Also included within the MDS for this activity is one HVDC converter OSP with six-legged jacket foundations which may require drilling to a depth of 80m. The monopiles were selected for the modelling process as the source of the largest potential release at one location. As noted previously, there will be a maximum of one bridge-linked HVDC converter OSP within the Morven Site, however the modelling has accounted for one HVDC converter OSP within both the Morven North Boundary and Morven South Boundary, in order to provide a representation of potential impact due to each separate project.

6.3.1.2 A sample of six representative wind turbine pile installations were simulated to cover the range of conditions across the Morven North Boundary and Morven South Boundary, in terms of water depth, tidal currents and sediment grading. The three locations within the Morven North Boundary and three locations within the Morven South Boundary are shown on an indicative layout in Figure 6.14. The sites were also selected based on their outer positions within the Morven North Boundary and Morven South Boundary to allow the greatest potential plume and sedimentation distances from the Morven North Boundary or Morven South Boundary to be realised. The modelling was undertaken using the MIKE MT module which allows the modelling of erosion, transport and deposition of

cohesive and cohesive/granular sediments. This model is suited to sediment releases in the water column and allows sediment sources which may vary spatially and temporally. In this case, the cohesive functions were not utilised as the material released comprised sand. The sediment grading was defined for each location and assumed three concurrent drilling operations of adjacent monopile foundations within each of the Morven North Boundary and Morven South Boundary.

6.3.1.3 The modelling assumed that at each site the material which is released has a similar composition to the sampled sediment. In reality, to require drilling (rather than driving) the sediments are generally less granular and augured material would be less easily brought into suspension therefore the modelled scenario provides a conservative assessment in terms of SSC.

6.3.1.4 At each location the MDS assumed that the auguring was required to the 64m pile depth for an assumed 16m diameter pile (i.e. 14,356m^3 per pile). The drilling rate was 1.5m/h, as described in the Project Description (Volume 1, Chapter 3, of the Morven North and Morven South EIA Reports) and this allowed the release to cover the full range of tidal conditions (i.e. the auguring was undertaken continuously over a 43 hour period with material released throughout the water column). The drilled material was classified based on the properties identified from the site specific sampling in line with the foundation sandwave clearance, as outlined in Section 6.2.2.

6.3.1.5 The average suspended sediment plumes during the course of the installations are shown in Figure 6.15. Due to the temporal variation in suspended sediment levels, instantaneous plots of the sediment plumes are also presented during peak flood and ebb tides on each of the first two days when SSC has the potential to be at its greatest. Figure 6.16, Figure 6.17, Figure 6.18 and Figure 6.19 show the SSC during peak ebb on day one, peak flood on day one, peak ebb on day two and peak flood on day two respectively. It should be noted that all the plots require the use of a log scale to cover this range and provide clarity. During slack water SSC decrease to background levels, when material is sedimented before being resuspended on the returning tide.

Morven North

6.3.1.6 It can be seen that within the Morven North Boundary, where current speeds are higher in comparison to within the Morven South Boundary, the extent of the SSC plumes are greater, as dispersion potential is higher. The average suspended sediment plot shown in Figure 6.16, shows concentrations <0.2mg/l at the discharge locations within the Morven North Boundary and the instantaneous concentrations on the peak ebb and flood tides are below 0.15mg/l. Some small areas of increased suspended sediment can be seen where material has been deposited on slack tides and subsequently re-suspended.

6.3.1.7 The average sedimentation during the course of the installations within the Morven North Boundary is also provided in Figure 6.20, with Figure 6.21 showing the sedimentation one day following the cessation of the installations. Due to the fine sandy nature of the material, it is clear that the sediment will be dispersed. It will be transported mid-tide, settle on slack water and be re-suspended and further dispersed on the resumption of tidal flow. For all locations, sediment levels after the cessation of construction would not be discernible from the background sediments due to the limited magnitude of deposition and the similar nature of the material.

Morven South

6.3.1.8 The average suspended sediment plot shown in Figure 6.16, shows concentrations <0.2mg/l at the discharge locations within the Morven South Boundary. The instantaneous concentrations on the peak ebb and flood tides are below 0.16mg/l. Some small areas of increased suspended sediment can be seen where material has been deposited on slack tides and subsequently re-suspended.

6.3.1.9 The average sedimentation during the course of the installations within the Morven South Boundary is also provided in Figure 6.20, with Figure 6.21 showing the sedimentation one day following the cessation of the installations. Sediment levels after the cessation of construction would not be discernible from the background sediments, as outlined in paragraph 6.3.1.7 for Morven North.

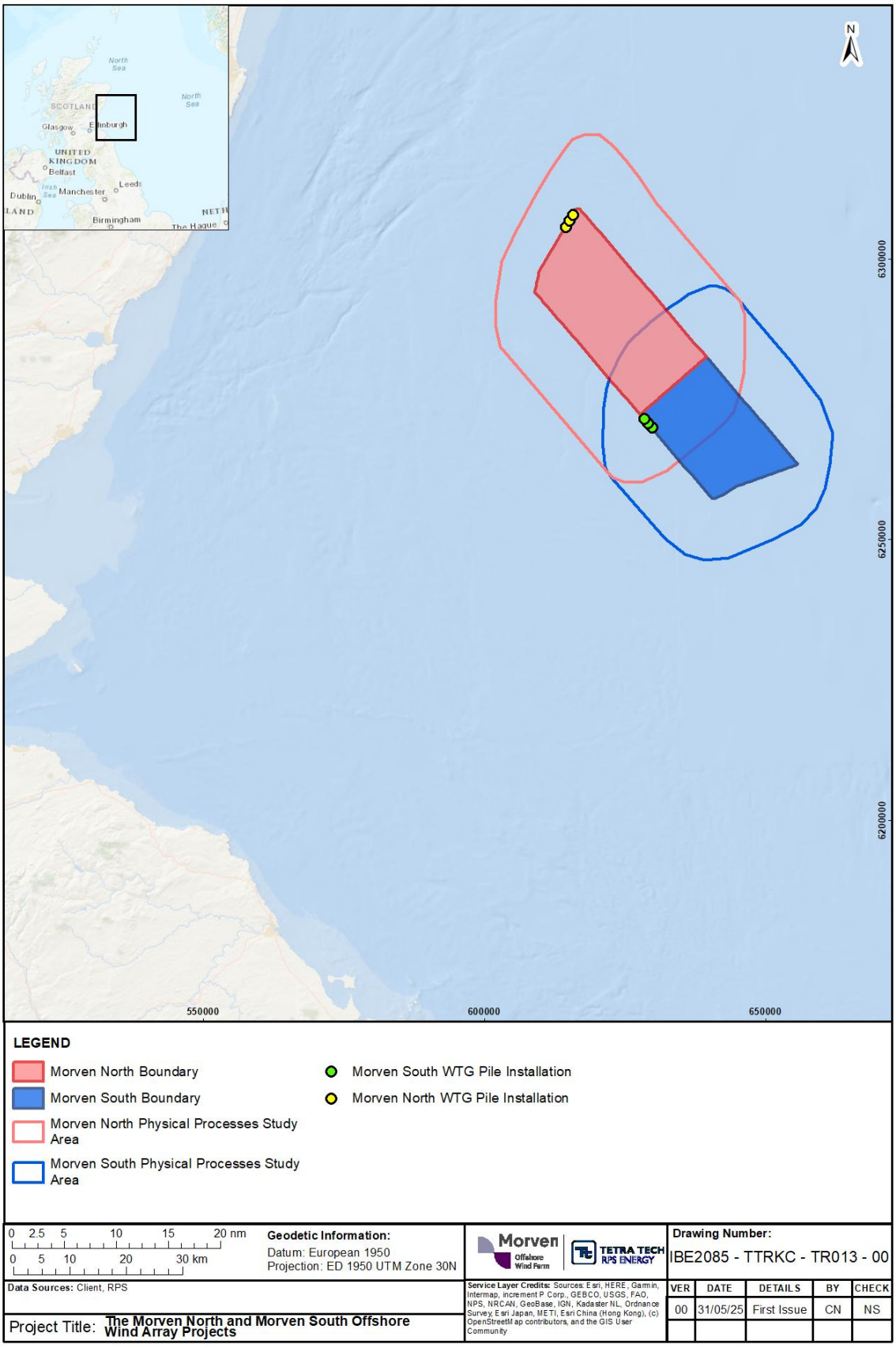

Figure 6.14: Locations of modelled piled installations (Morven North and Morven South)

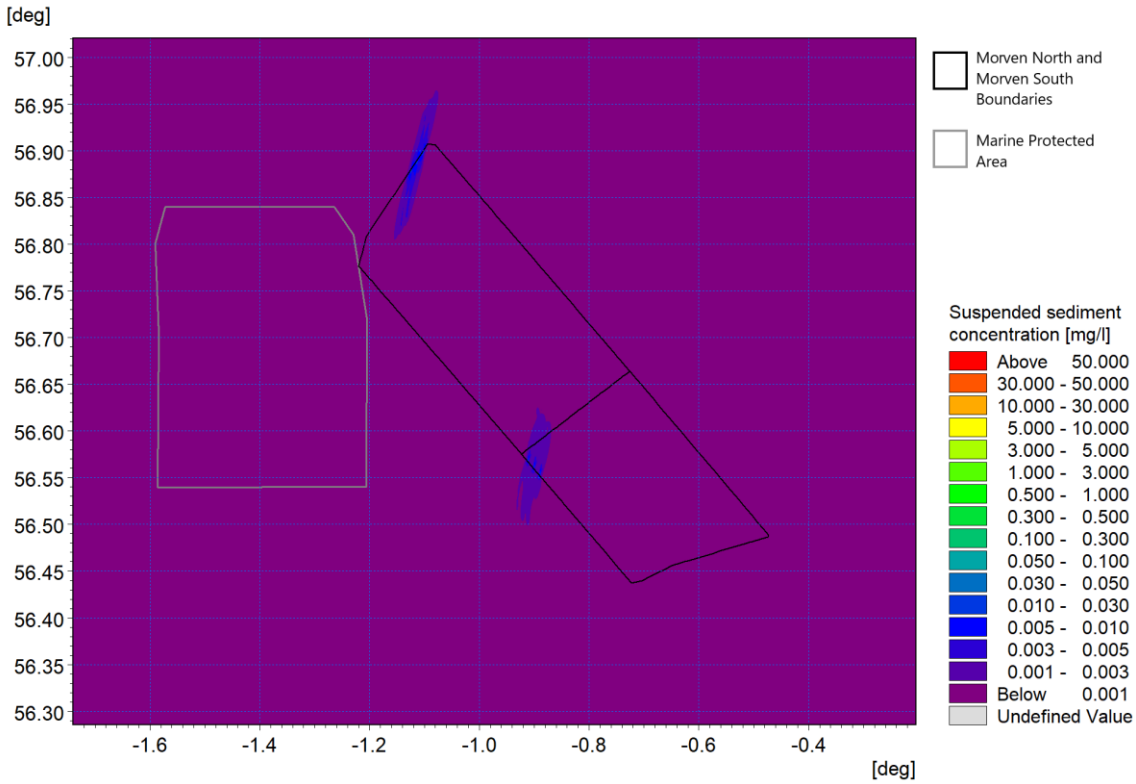

Figure 6.15: Average Suspended Sediment Concentrations during modelled pile installation at the sample wind turbine monopile foundation locations (Morven North/Morven South)

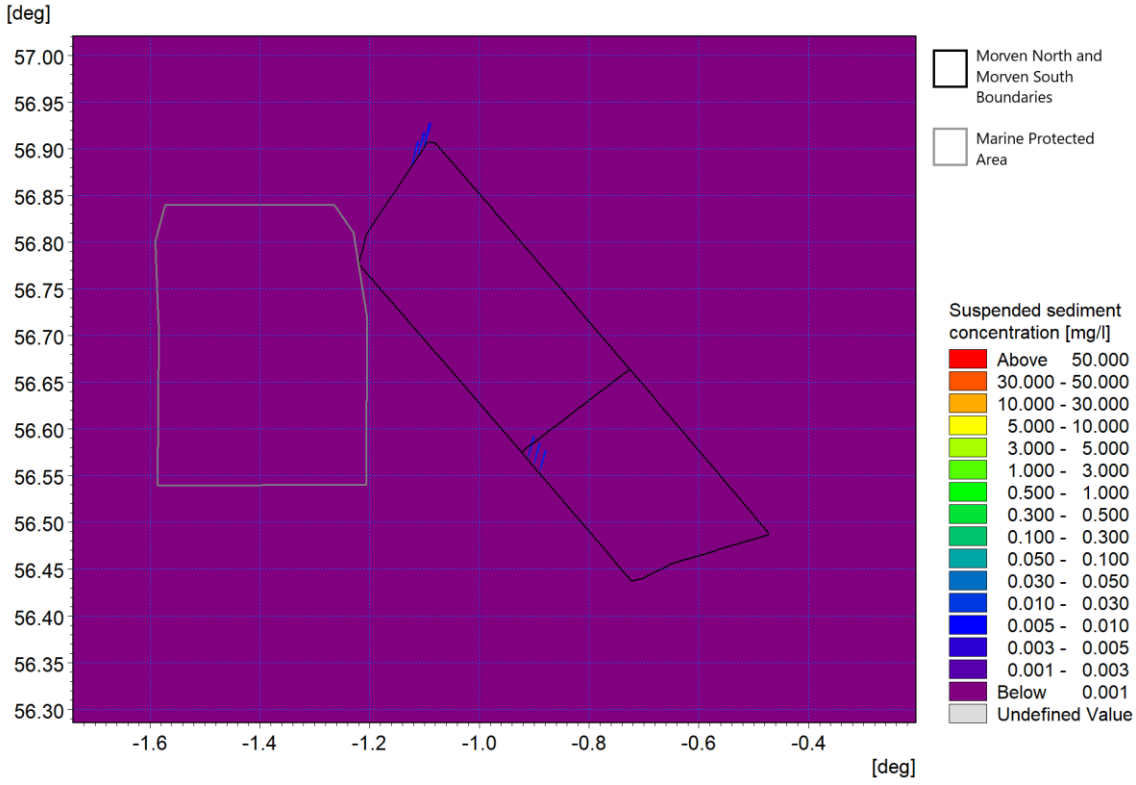

Figure 6.16: Suspended Sediment Concentrations resulting from pile installation during peak ebb on day one at the sample wind turbine monopile foundation locations (Morven North/Morven South)

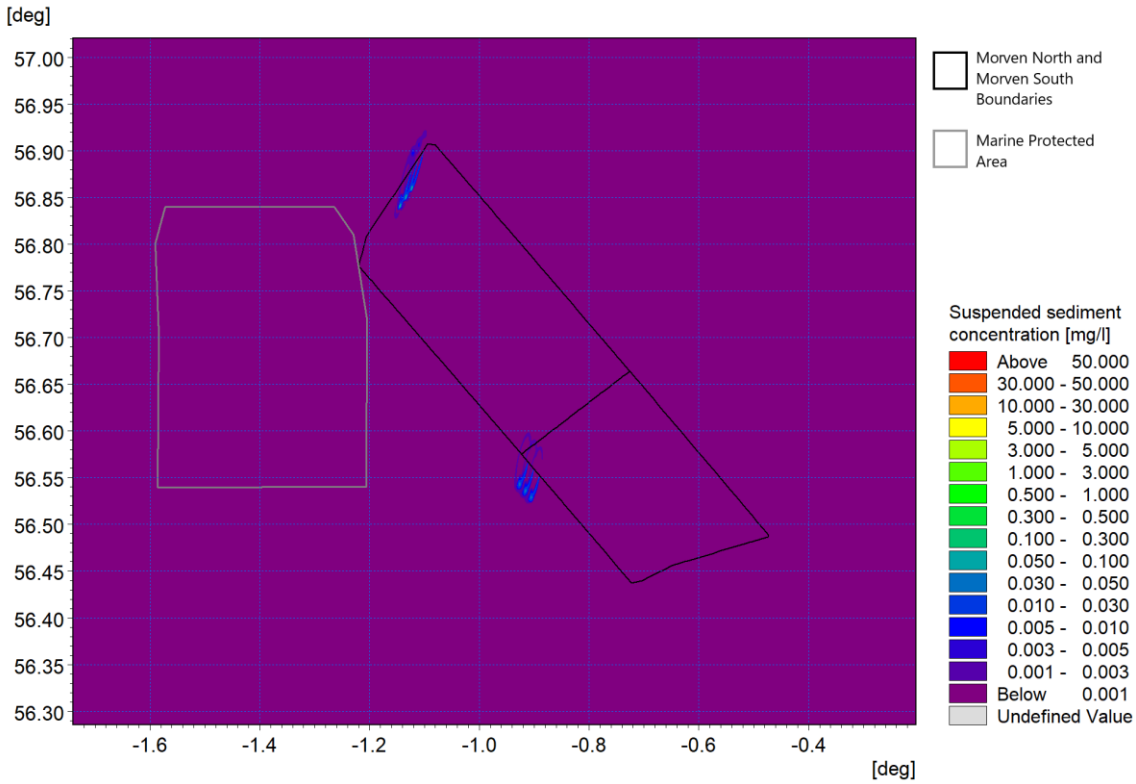

Figure 6.17: Suspended Sediment Concentrations resulting from pile installation during peak flood on day one at the sample wind turbine monopile foundation locations (Morven North/Morven South)

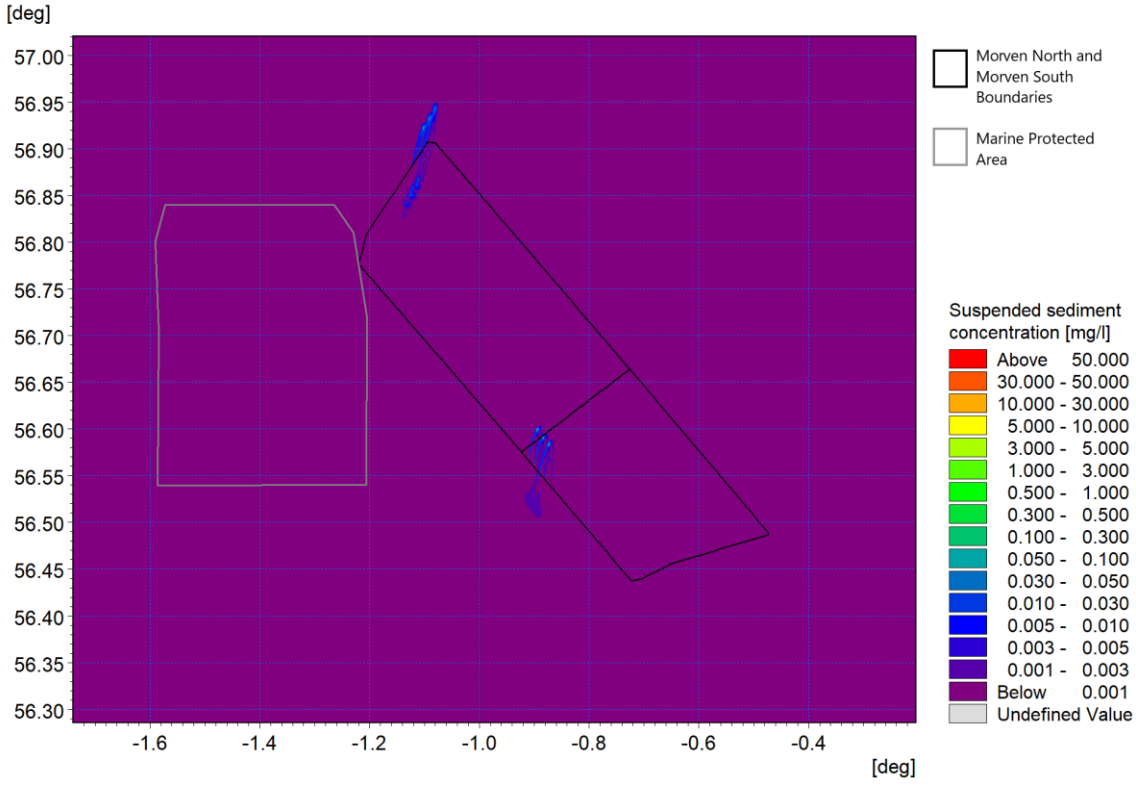

Figure 6.18: Suspended Sediment Concentrations resulting from pile installation during peak ebb on day two at the sample wind turbine monopile foundation locations (Morven North/Morven South)

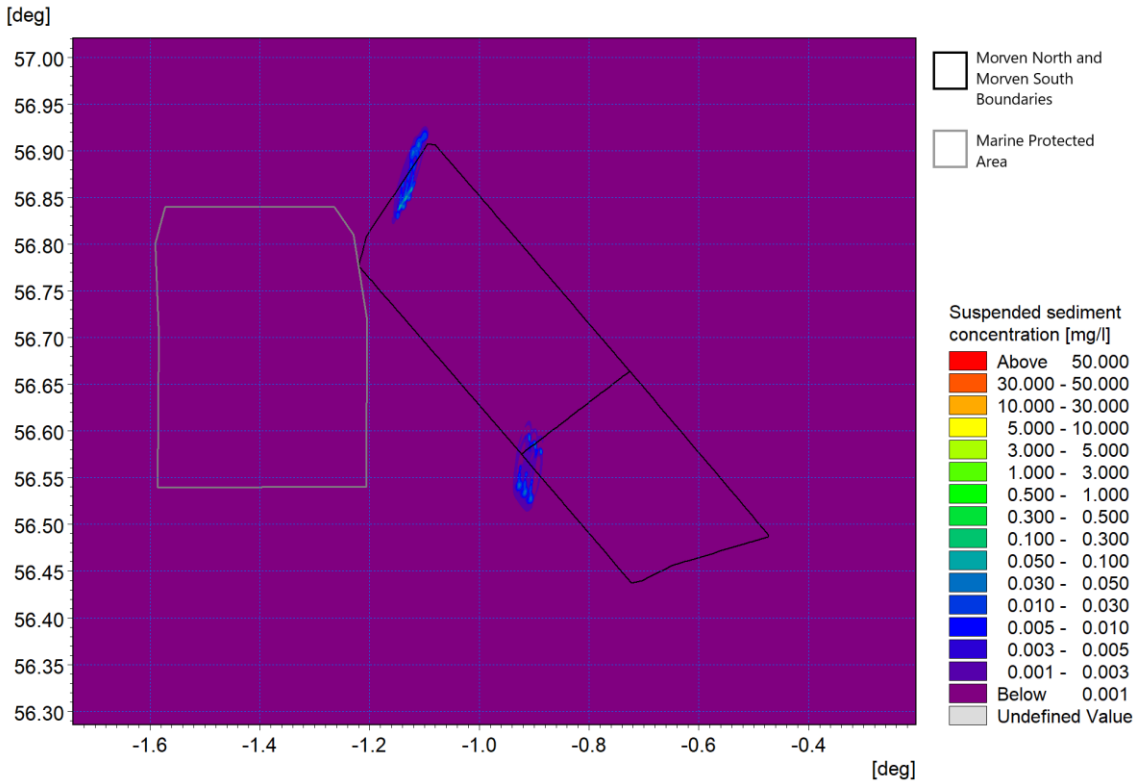

Figure 6.19: Suspended Sediment Concentrations resulting from pile installation during peak flood on day two at the sample wind turbine monopile foundation locations (Morven North/Morven South)

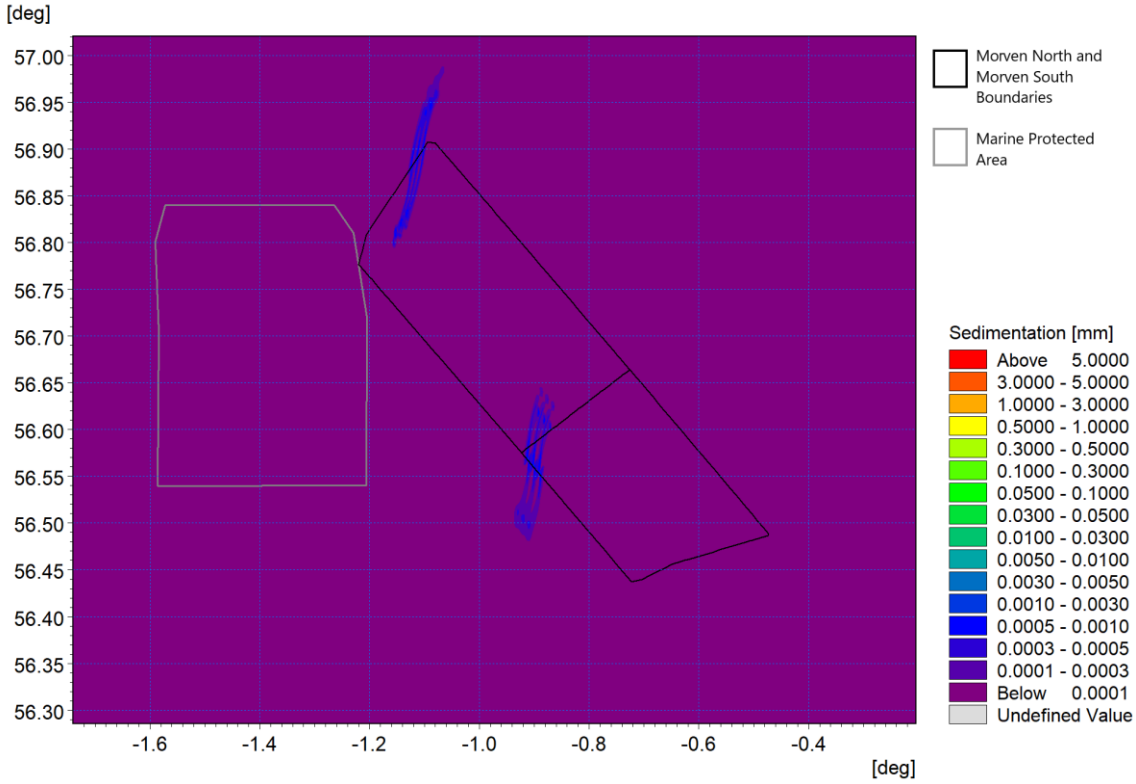

Figure 6.20: Average sedimentation during modelled pile installation at the sample wind turbine monopile foundation locations (Morven North/Morven South)

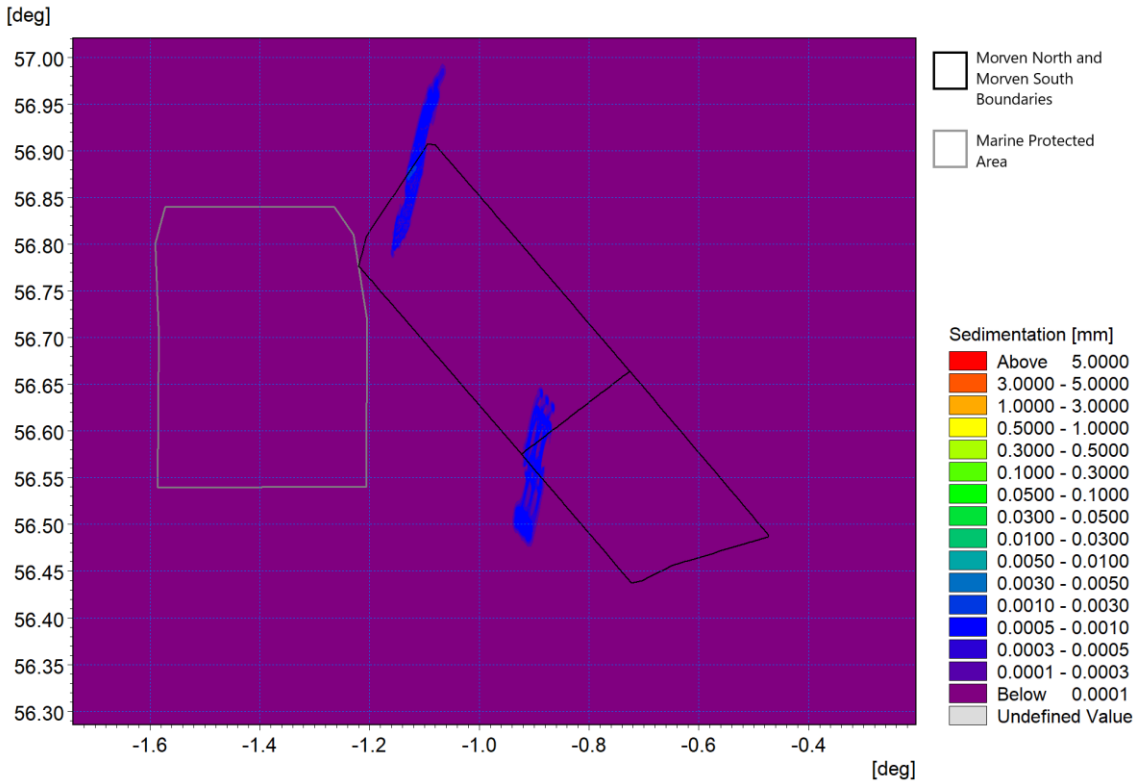

Figure 6.21: Sedimentation one day following cessation of pile installation at the sample wind turbine monopile foundation locations (Morven North/Morven South)

6.3.2 Cable installation

6.3.2.1 Another aspect of the construction phase is cable installation, including the inter-array cables and interconnector cables. Inter-array and interconnector cable installation will be undertaken along a number of routes which connect groups of wind turbines to each other or to the OSPs, or which connect two OSPs to each other.

6.3.2.2 For the MDS in terms of release of sediment into the water column, cables were assumed to be trenched. A number of trenching techniques may be suited to the ground conditions; however, it was assumed within the modelling that a trench of material of the maximum depth presented in Volume 1, Chapter 3: Project Description, of the Morven North and Morven South EIA Reports, was mobilised into the water column as a result of the cable burial process. In reality, the preferred scenario may be jet trenching, and the maximum depth may not always be required, which would result in a corresponding reduction in the amount of material mobilised. It is noted that the MDS for inter-array and interconnector cables is the same for this activity in terms of maximum burial depth and maximum width of the cable trench and thus potential release of material into the water column.

6.3.2.3 Similar to the foundation installation discussed in Section 6.3.1, the model simulations used the sediment grading determined from sediment sampling and the modelling was undertaken using the MIKE MT module.

6.3.2.4 Trenching rates can vary widely depending on the bed material and equipment used; typically, rates are between 25m/h and 780m/h. For the simulation, a rate of 200m/h was used in line with the typical cable burial rate suggested by the Kingfisher Information Service – Offshore Renewable and Cable Awareness (KIS-ORCA) project (KIS-ORCA, 2025).

6.3.2.5 Sample trenching modelling was undertaken along two sample inter-array cable routes within the Morven North Boundary and two sample inter-array cable routes within the Morven South Boundary, to provide a range of orientations, water depths and flow velocities. Each sample route is circa 5km

in length, with a burial depth of 3m and trench width of 3m. This equates to circa 21,885m^3 material released through the water column along each route over a duration of 15 hours. Figure 6.22 shows the indicative concurrent routes of the sample modelled inter-array cable routes within the Morven North Boundary and Morven South Boundary.

6.3.2.6 The model results presented follow the same format as those for the wind turbine foundation installation described in paragraphs 6.3.1.5 to 6.3.1.7. Figure 6.23 shows the average suspended sediment concentration over the course of the trenching phase with peak values up to 0.1mg/l.

Morven North

6.3.2.7 Figure 6.24 and Figure 6.25 shows the suspended sediment patterns over the course of the trenching operation for cable installation on peak ebb and peak flood tides respectively. Elevated tidal currents disperse the material giving rise to concentrations of up to 0.2mg/l during the peak ebb tide within the Morven North Boundary. As was evident in the previous operations for seabed preparation (Section 6.2) and foundation installation (Section 6.3.1), the material settles during slack water and then is re-suspended to form an amalgamated plume, with concentrations of up to 0.6mg/l. This is further illustrated in Figure 6.26 and Figure 6.27 which show the average sedimentation and the sedimentation at slack water one day following cessation. The average sedimentation during the modelled trenching operation is greatest at the location of the trenching and is up to 0.003mm in depth, reducing rapidly, as shown by the sedimentation one day following cessation. Due to the low magnitude of sedimentation, the impact would not be detectible in reality.

Morven South

6.3.2.8 Figure 6.24 and Figure 6.25 shows the suspended sediment patterns over the course of the trenching operation for cable installation on peak ebb and peak flood tides respectively. Elevated tidal currents disperse the material giving rise to concentrations of up to 0.2mg/l during the peak ebb tide within the Morven South Boundary. As was evident in the previous operations for seabed preparation (Section 6.2) and foundation installation (Section 6.3.1), the material settles during slack water and then is re-suspended to form an amalgamated plume, with concentrations of up to 0.7mg/l. This is further illustrated in Figure 6.26 and Figure 6.27 which show the average sedimentation and the sedimentation at slack water one day following cessation. The average sedimentation during the modelled trenching operation is greatest at the location of the trenching and is up to 0.004mm in depth, reducing rapidly, as shown by the sedimentation one day following cessation. Due to the low magnitude of sedimentation, the impact would not be detectible in reality.

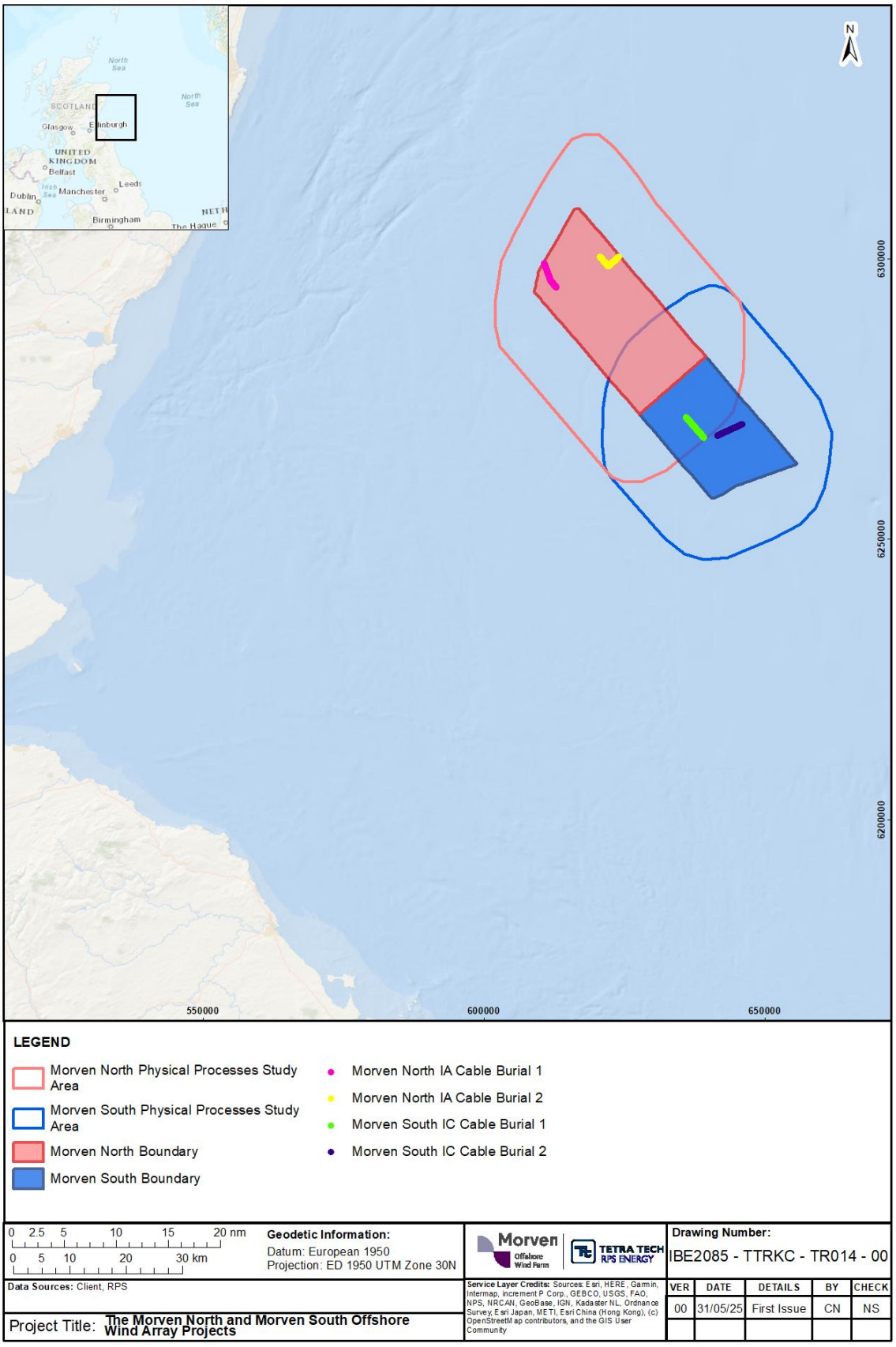

Figure 6.22: Modelled inter-array cable routes (Morven North/Morven South)

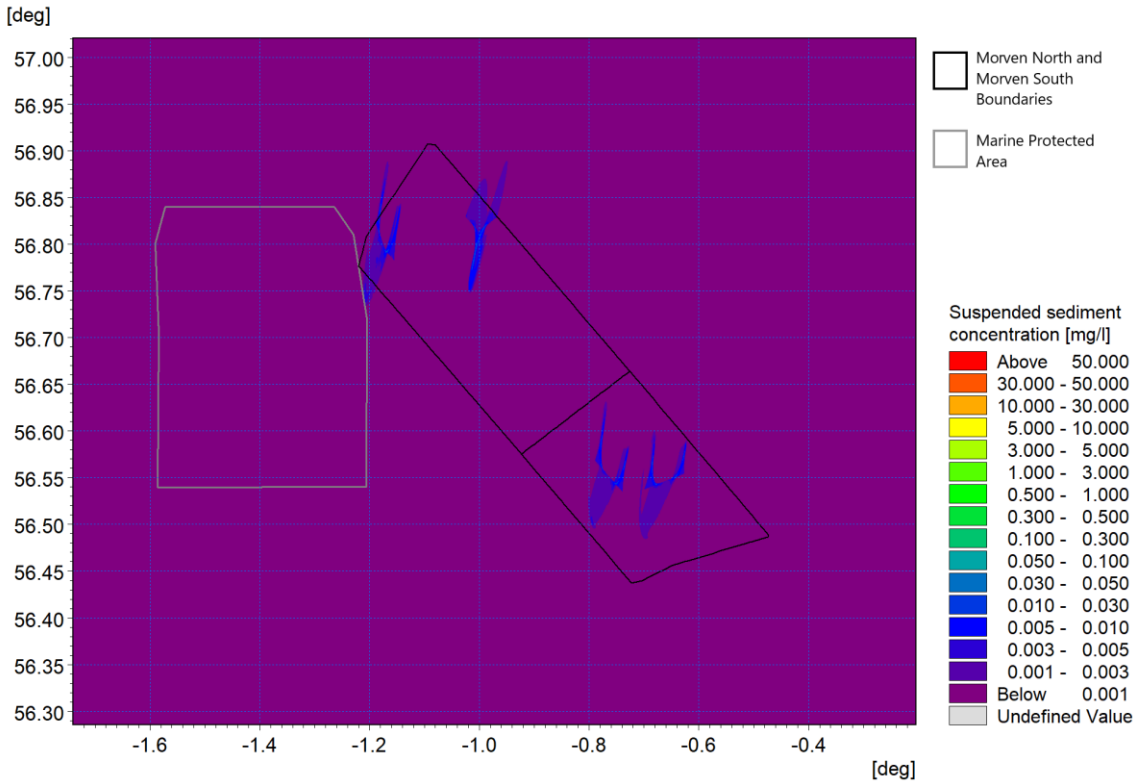

Figure 6.23: Average Suspended Sediment Concentrations during modelled cable trenching at the sample inter-array cable locations (Morven North/Morven South)

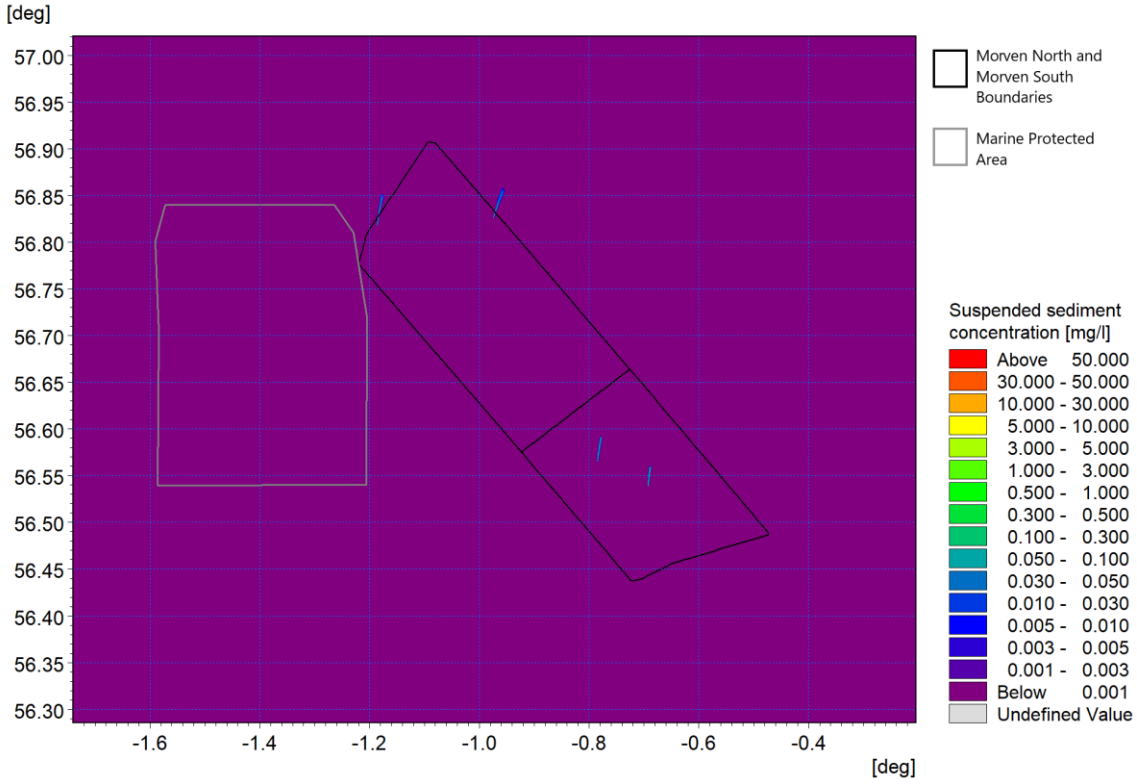

Figure 6.24: Suspended Sediment Concentrations resulting from cable trenching during peak ebb at the sample inter-array cable locations (Morven North/Morven South)

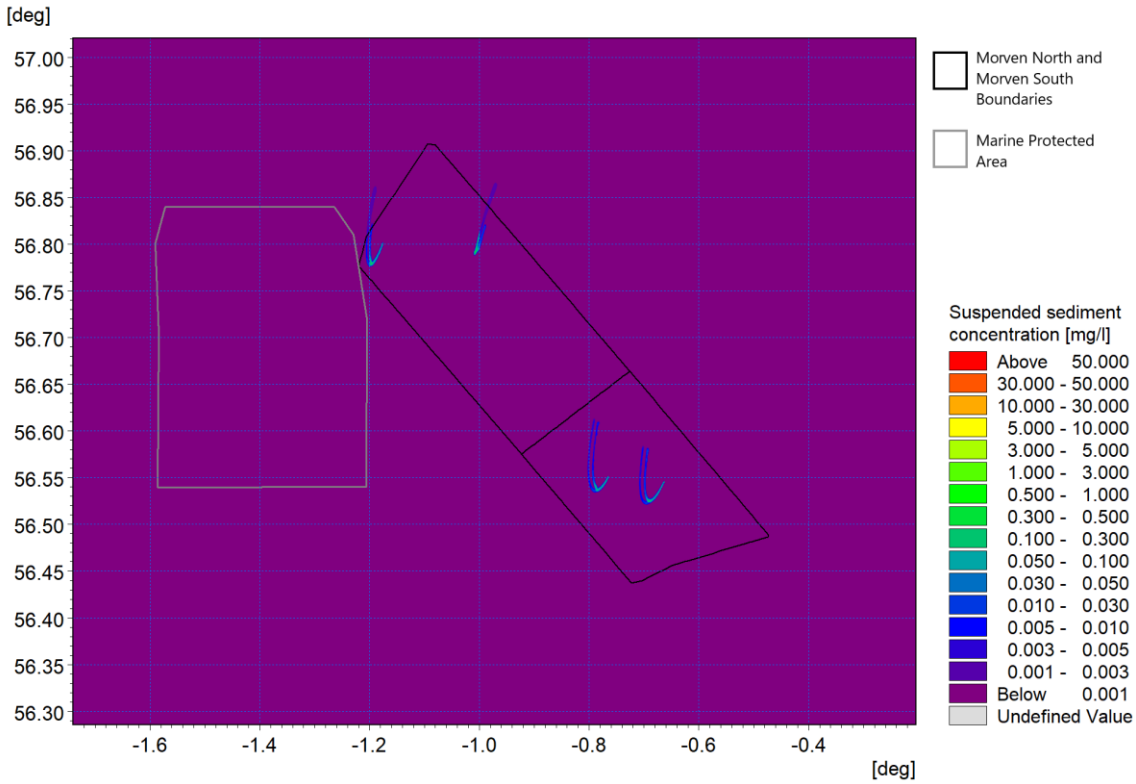

Figure 6.25: Suspended Sediment Concentrations resulting from cable trenching during peak flood at the sample inter-array cable locations (Morven North/Morven South)

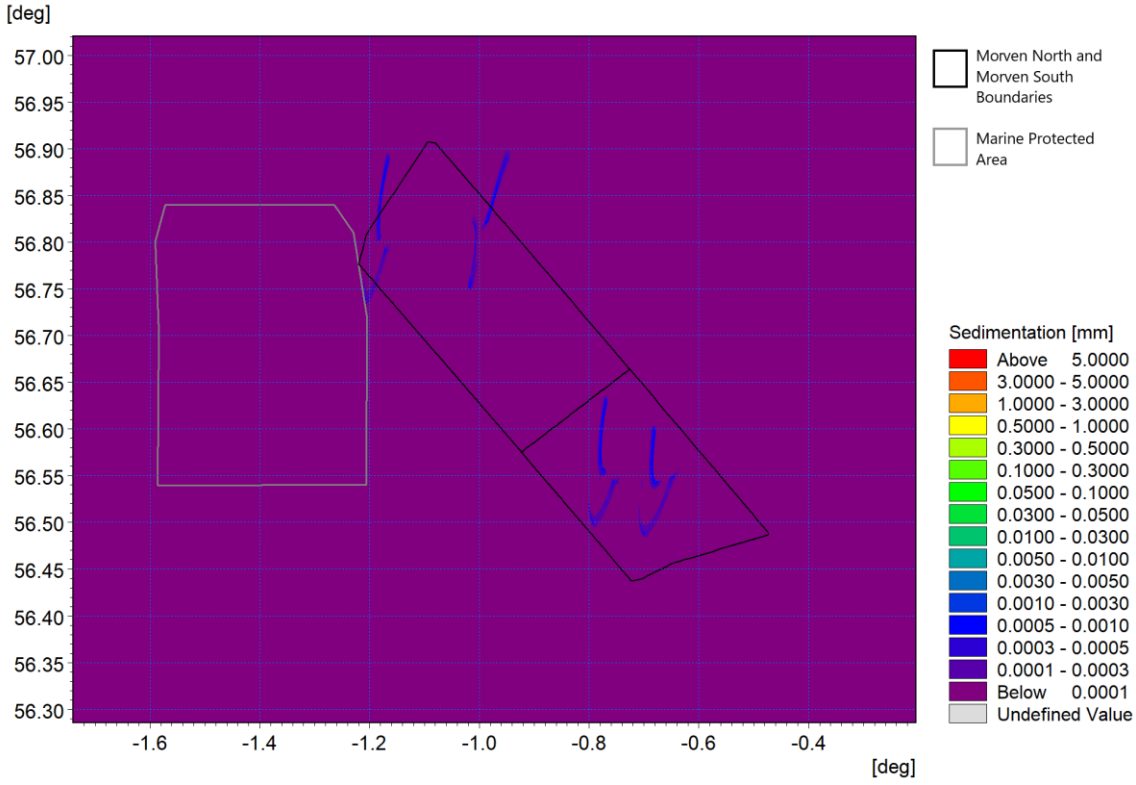

Figure 6.26: Average sedimentation during modelled cable trenching at the sample inter-array cable locations (Morven North/Morven South)

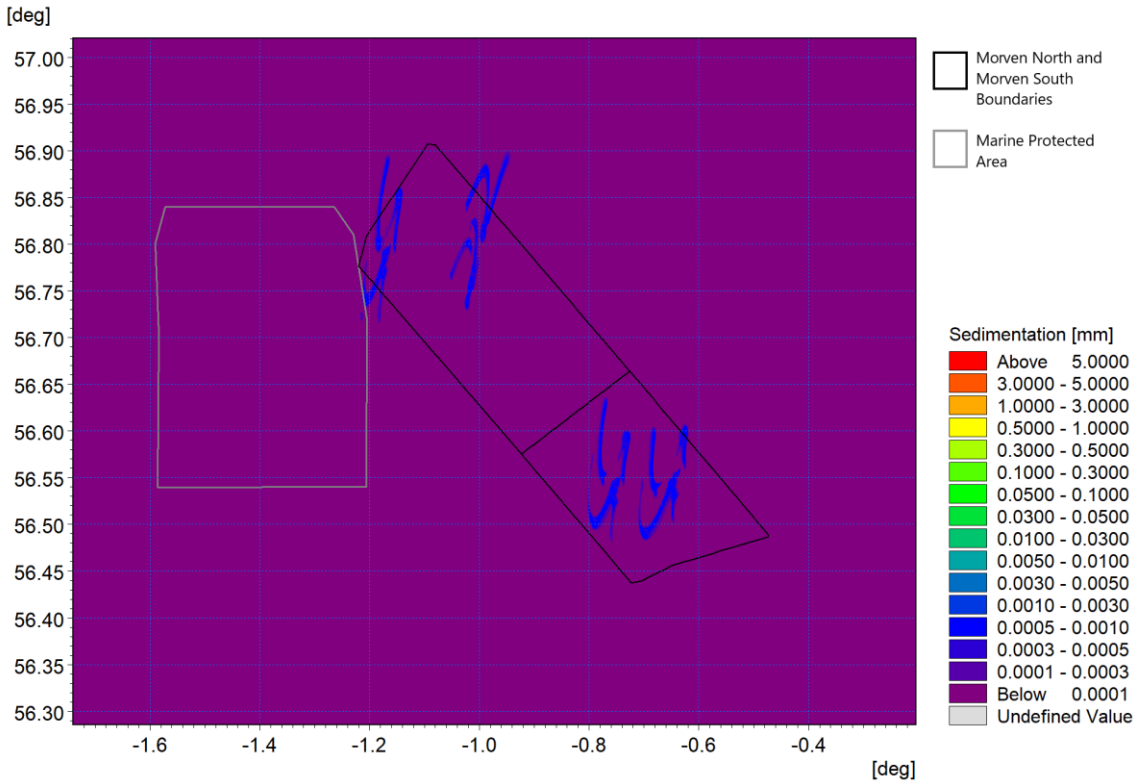

Figure 6.27: Sedimentation one day following cessation of cable installation at the sample inter-array cable locations (Morven North/Morven South)

7 Summary

7.1.1.1 Morven North and Morven South are located within a region which encompasses the Firth of Forth Banks Complex MPA, therefore the impact on physical processes is important in the assessment of the potential environmental impact. This report has outlined the baseline characteristics of the region in terms of physical processes. This includes tidal current, wave climate and sediment transport under both calm and storm conditions. Numerical modelling has been used to quantify the changes in physical processes due to the presence of Morven North and Morven South, including high level 3D modelling to determine the impact on seasonal stratification.

7.1.1.2 The presence of the wind turbine foundations redirects both waves and tidal flow and although some changes in sediment transport were revealed, these were limited in magnitude and represented an adjustment in the transport path alignment. The presence of Morven North and Morven South was seen to marginally reduce wave heights in the lee of the structures whilst a marginal increase was noted at the periphery, however during larger storm events these effects were less marked. Any considerable changes in tidal currents and wave climate would not extend to the coastline and there would be no change in physical processes in this area.

7.1.1.3 There is evidence of potential changes to seasonal stratification due to Morven North and Morven South, however modelling has determined that any changes are likely to be small, with a maximum change in temperature of 2.7% during the peak summer stratification period and thus it is anticipated that there will be a negligible effect on the overall pattern of seasonal stratification and position of the thermocline.

7.1.1.4 Finally, suspended sediment plumes for construction activities were quantified. In all cases, it is assumed that the material released will be native to the bed sediments due to the nature of the activities and, although there are short periods of increased turbidity, the material is expected to be subsequently assimilated into the existing sediment transport regime.

8 References

ABPmer (2017). Atlas of UK Marine Renewable Energy Resources. Available at: http://www.renewables-atlas.info/. (Accessed: May 2025).

Admiralty Marine Data Portal https://www.admiralty.co.uk/access-data. (Accessed: March 2025).

Akhtar, N., B. Geyer, B. Rockel, P. S. Sommer, and C. Schrum (2021). Accelerating deployment of offshore wind energy alter wind climate and reduce future power generation potentials. Scientific Reports 11:11826.

Barthelmie, R. J., S. C. Pryor, S. T. Frandsen, K. S. Hansen, J. G. Schepers, K. Rados, W. Schlez, A. Neubert, L. E. Jensen, and S. Neckelmann (2010). Quantifying the impact of wind turbine wakes on power output at offshore wind farms. Journal of Atmospheric and Oceanic Technology 27:1302-1317.

Barton, B., De Dominicis, M., O'Hara Murray, R., Campbell, L. (2022). Scottish Shelf Model 3.02 - 27 Year Reanalysis. https://doi.org/10.7489/12423-1. (Accessed: May 2025).

Bindoff, N. L. *et al*. (2019) Changing Ocean, Marine Ecosystems, and Dependent Communities. IPCC Special Report on the Ocean and Cryosphere in a Changing Climate.

Cefas (2016). Suspended sediment climatologies around the UK. Report for the UK Department for Business, Energy & Industrial Strategy Offshore Energy Strategic Environmental Assessment Programme.

Christiansen, M.B., Hasager, C.B. (2005). Wake effects of large offshore wind farms identified from satellite SAR. Remote Sensing of Environment 98(2-3):251-268.

Christiansen, N., Daewel, U., Djath, B. and Schrum, C. 2022. Emergence of large-scale hydrodynamic structures due to atmospheric offshore wind farm wakes. Frontiers in Marine Science 9:818501.

De Dominicis, M., O'Hara Murray, R., Wolf, J., Gallego, A. (2018). The Scottish Shelf Model 1990 – 2014 climatology version 2.01. doi: 10.7489/12037-1.

European Centre for Medium-Range Weather Forecasts (2021) European Wave Model. Available at: https://www.ecmwf.int/en/forecasts/dataset/operational-archive. (Accessed: June 2025).

European Marine Observation and Data Network (EMODnet) (2021) Seafloor Geomorphology https://emodnet.ec.europa.eu/geoviewer/#!/. (Accessed: May 2025).

European Marine Observation and Data Network (EMODnet) (2016) Seabed Substrate https://emodnet.ec.europa.eu/geoviewer/#!/. (Accessed: May 2025).

Gardline (2022). Interpretation Report for bp Alternative Energy Investments Limited. Project Morven Integrated Site Survey. Offshore Wind Farm Site Survey. April to August 2022.

Gardline (2023). Morven Offshore Wind Farm Integrated Survey UKCS Quads 26 and 27. Environmental Baseline Survey Report.

Joint Nature Conservation Committee (2023). Marine Protected Area (MPA) Mapper. Available at: https://jncc.gov.uk/mpa-mapper/. (Accessed: May 2025).

Kingfisher Information Service – Offshore Renewable & Cable Awareness (KIS-ORCA) project, 2025. Cable Burial https://kis-orca.org/subsea-cables/cable-burial/.

Marine Scotland (2017). BGS – Seabed geology layers. Available: https://marine.gov.scot/node/12813. (Accessed: May 2025).

Owda, A. and Badger, M. (2022). Wind speed variation mapped using SAR before and after commissioning offshore wind farms. Remote Sens. 2022, 14(6), 1464.

Partrac (2024). Morven Metocean Measurement Campaign – Recovery BP/EnBW Final Data Report M5061 V02

Platis, A., Siedersleben, S.K., Bange, J., Lampert, A., Bärfuss, K., Hankers, R., Cañadillas, B., Foreman, R., Schulz-Stellenfeth, J., Djath, B., Neumann, T., Emeis, S. (2018). First in situ evidence of wakes in the far field behind offshore wind farms. Scientific Reports, 8:2163.

Royal HaskoningDHV (2012). Seagreen Wind Energy: Appendix E3 – Geomorphological Assessment. Environmental Statement – Volume 3 – Technical Appendices – Seagreen Alpha and Bravo Offshore Wind Farms. Available at: https://marine.gov.scot/sites/default/files/appendix_e3.pdf (Accessed: September 2025)

Silva, T. (2016). Monthly average non-algal Suspended Particulate Matter concentrations. Cefas, UK. V1. doi: https://data.cefas.co.uk/view/18133. (Accessed: December 2024).

United Kingdom Hydrographic Office (2023). Published Charts and Tide tables.

Vindenes, H., Orvik, K. A., Søiland, H., and Wehde, H. (2018). Analysis of tidal currents in the North Sea from shipboard acoustic Doppler current profiler data. Continental Shelf Research, 162, 1-12.

Whitehouse, R., 2006. Scour at coastal structures (Invited lecture). Proceedings Third International Conference on Scout and Erosion, November 1-3, pp.52-59,©CURNET, Gouda, The Netherlands [CD-ROM].